Tool Compounds to Study Proteolytic Events: Development of von Hippel-Lindau (VHL) Ligands and Combinatorial Generation of Serine Protease Inhibitors

Dissertation

zur

Erlangung des Doktorgrades (Dr. rer. nat.)

der

Mathematisch-Naturwissenschaftlichen Fakultät

der

Rheinischen Friedrich-Wilhelms-Universität Bonn

vorgelegt von

Lan Phuong Vu

aus

Bremen

Bonn 2023

Angefertigt mit Genehmigung der Mathematisch-Naturwissenschaftlichen Fakultät
der Rheinischen Friedrich-Wilhelms-Universität Bonn

1. Gutachter: Prof. Dr. Michael Gütschow
2. Gutachter: Prof. Dr. Gerd Bendas

Tag der Promotion: 31.08.2023
Erscheinungsjahr: 2023

Die vorliegende Arbeit wurde in der Zeit von November 2018 bis April 2023 unter Leitung von Herrn Prof. Dr. Michael Gütschow am Pharmazeutischen Institut der Rheinischen Friedrich-Wilhelms-Universität Bonn angefertigt.

Table of Contents

List of Abbreviations

AbTAC	antibody-targeting chimera
Ac	acetyl
ADC	antibody-drug conjugate
ADKM	aminolyzed diketomorpholine
ALI	acute lung injury
AMD	age-related macular degeneration
APC	aptamer-PROTAC conjugate
ApDC	aptamer-drug conjugate
AR	androgen receptor
ARDS	acute respiratory distress syndrome
Asp	aspartic acid
AUTOTAC	autophagy-targeting chimeras
BCA	bicinchoninic acid
BET	bromodomain and extraterminal domain
BMP	bone morphogenetic protein
Bn	benzyl
Boc	*tert*-butyloxycarbonyl
BRD4	bromodomain-containing protein 4
bRo5	beyond Rule of Five
CatG	cathepsin G
cIAP1	cellular inhibitor of apoptosis protein 1
COPD	chronic obstructive pulmonary disease
CRBN	cereblon
$CRL2^{VHL}$	Cullin2 RING VHL E3 ubiquitin ligase complex
CuAAC	copper-catalyzed azide-alkyne cycloaddition
CUB	C1s/C1r, urchin embryonic growth factor, bmp-1 domain
DAD	diode-array detection
DBCO	dibenzylcyclooctyne
DESC	differentially expressed in squamous cell carcinoma

DFHBI	3,5-difluoro-4-hydroxybenzylidene imidazolinone
DIPEA	*N,N*-diisopropylethylamine
DKM	diketomorpholine
DMA	4-(*N*,*N*-dimethylamino)pyridine
DMEM	Dulbecco's modified Eagle's medium
DMF	*N*,*N*-dimethylformamide
DMSO	dimethyl sulfoxide
DOAC	direct oral anticoagulant
DTT	dithiothreitol
E1	ubiquitin-activating enzyme
E2	ubiquitin-conjugating enzyme
E3	ubiquitin ligase
EC	enzyme commission
EDC	1-ethyl-3-(3-dimethylaminopropyl)carbodiimide
EDTA	ethylenediaminetetraacetic acid
EloB	Elongin B
EloC	Elongin C
ER	estrogen receptor
ERRα	estrogen-related receptor-α
Et	ethyl
Et_3N	triethylamine
F	factor
FAM	5,6-carboxyfluorescein
FBS	fetal bovine serum
FDA	Food and Drug Administration
FKBP12	FK506 binding protein 12
FP	fluorescence polarization
GFP	green fluorescent protein
HAT	human airway trypsin-like protease
HATU	*O*-(7-azabenzotriazol-1-yl)-*N*,*N*,*N*′,*N*′-tetramethyluronium hexafluorophosphate
HEK	human embryonic kidney

HEPES	4-(2-hydroxyethyl)-1-piperazineethanesulfonic acid
HER2	human epidermal growth factor receptor 2
HIF	hypoxia-inducible factor
His	histidine
HIV-1	human immunodeficiency virus 1
HLE	human leukocyte elastase
HRE	hypoxia-responsive elements
HRMS	high resolution mass spectrometry
Hyp	hydroxyproline
IMiD	immunomodulatory imide drugs
IR	infrared
IRIDA	iron-refractory iron deficiency anemia
ITC	isothermal titration calorimetry
IUBMB	International Union for Biochemistry and Molecular Biology
LC-MS	liquid chromatography-mass spectrometry
LDLA	low-density lipoprotein receptor class A
LHS	left-hand side
logD	distribution coefficient
LYTAC	lysosome-targeting chimera
MDM2	mouse double minute 2 homologue
Me	methyl
MetAP-2	methionine aminopeptidase 2
miRNA	micro RNA
MoA	mode of action
mp	melting point
MUC1	mucin 1
MW	molecular weight
NanoBRET	nano-bioluminescence resonance energy transfer
NET	neutrophil extracellular trap
NMR	nuclear magnetic resonance
PBS	phosphate-buffered saline

Pd/C	palladium on activated carbon
PDB	protein data bank
PEG	polyethylene glycol
Ph	phenyl
PHD	prolyl hydroxylase domain
POI	protein of interest
PPB	plasma protein binding
PPI	protein-protein interaction
PROTAC	proteolysis-targeting chimera
PSMA	prostate-specific membrane antigen
PTK7	protein tyrosine kinase 7
Rbx1	RING-box protein 1
R_f	retention factor
RHS	right-hand side
RIBOTAC	ribonuclease-targeting chimera
RING	really interesting new gene
RIPK2	receptor-interacting serine/threonine-protein kinase 2
rt	room temperature
SAR	structure-activity relationship
SARS-CoV-2	targeting severe acute respiratory syndrome coronavirus 2
$SCF^{\beta\text{-TRCP}}$	Skp1-Cul1-F-box protein containing the F-box protein β-TRCP
SEA	sea urchin sperm protein/enteropeptidase/agrin domain
SELEX	systematic evolution of ligands by exponential enrichment
Ser	serine
shRNA	small hairpin RNA
siRNA	small interfering RNA
SMAD	sons of mothers against decapentaplegic
S_NAr	nucleophilic aromatic substitution
SPR	surface plasmon resonance
TBAF	tetrabutylammonium fluoride
TBAHS	tetrabutylammonium hydrogen sulfate

TBDPSCl	*tert*-butyldiphenylsilyl chloride
TBS-T	tris-buffered saline with Tween
TBTU	*O*-(benzotriazol-1-yl)-*N*,*N*,*N*',*N*'-tetramethyluronium tetrafluoroborate
TCEP	tris(2-carboxyethyl)phosphine
TF	tissue factor
TFA	trifluoroacetic acid
THF	tetrahydrofuran
TLC	thin layer chromatography
Tle	*tert*-leucine
TMPRSS	transmembrane serine protease
TPD	targeted protein degradation
TPSA	topological polar surface area
TR-FRET	time-resolved Förster resonance energy transfer
TsCl	*p*-toluenesulfonyl chloride
TTSP	type II transmembrane serine protease
Ub	ubiquitin
UPS	ubiquitin-proteasome system
VBC	VHL:ElonginC:ElonginB complex
VEGF	vascular endothelial growth factor
VHL	von Hippel-Lindau

List of Figures

List of Schemes

List of Tables

List of Appendices

1 Introduction

1.1 Von Hippel-Lindau (VHL) E3 Ligase

More than over 600 E3 ubiquitin ligases are encoded in the human genome, each with a distinct specificity for a particular subset of proteins.[1] Among these ligases, the von Hippel-Lindau (VHL) ligase has gained significant attention due to its central role in regulating the degradation of hypoxia-inducible factors (HIFs).[2–4] The VHL protein is a substrate recognition component of the Cullin2, really interesting new gene (RING) E3 ubiquitin ligase complex ($CRL2^{VHL}$). In addition to VHL, the $CRL2^{VHL}$ complex is constituted of further subunits, *i.e.* the central scaffold Cullin2, the adaptor subunits Elongin B (EloB) and Elongin C (EloC), and the RING-box protein 1 (Rbx1).[5–7] As the largest superfamily of E3 ubiquitin ligases, CRLs are responsible for ~20% of all ubiquitination events executed by the ubiquitin-proteasome system (UPS),[7] a cellular machinery which is involved in the degradation of intracellular protein targets, such as short-lived, damaged, misfolded, and also oxidized proteins.[7,8] Protein degradation by the UPS is initiated by the conjugation of the small protein ubiquitin (Ub), a highly conserved 76 amino-acid residue polypeptide with a size of eight kDa, to the target protein.[9–12] This process involves three types of enzymes and consists of the following three-step cascade mechanism: In the first step, the C-terminal carboxyl group of Gly76 of ubiquitin is ATP-dependently attached to a cysteine of a ubiquitin-activating enzyme (E1), forming an Ub-E1 thioester product (Figure 1). The activated ubiquitin is then transferred by a transacylation reaction to a cysteine residue of the ubiquitin-conjugating enzyme (E2), leading to the production of the Ub-E2 intermediate. In the final step, the covalent transfer of the ubiquitin from the E2 enzyme to a lysine residue of a specific target protein is catalyzed by a ubiquitin ligase (E3). Since ubiquitin has seven lysine residues, further ubiquitin molecules can be transferred to the target-bound ubiquitin.[9] This polyubiquitin chain serves as a tag for target recognition, allowing the target to be degraded by the 26S proteasome.[11,12]

Dysregulation of both CRLs and the UPS pathway are associated with numerous of human diseases, such as cancer, neurodegenerative disorders, and inflammation.[13] The development of proteasome inhibitors and the extensively exploration of their inhibition activity indicated the importance of therapeutic interventions. However, such inhibitors have several limitations and suffer from drawbacks due to their lack of specificity and potential to cause accumulation of a variety of cellular proteins.[7,13] To overcome these inherent limitations, E3 ligases represent

attractive therapeutic targets upstream of the proteasome. By targeting the E3 ligase, the respective drugs can disrupt or modulate the interaction between the E3 ligase and their natural substrates.[12]

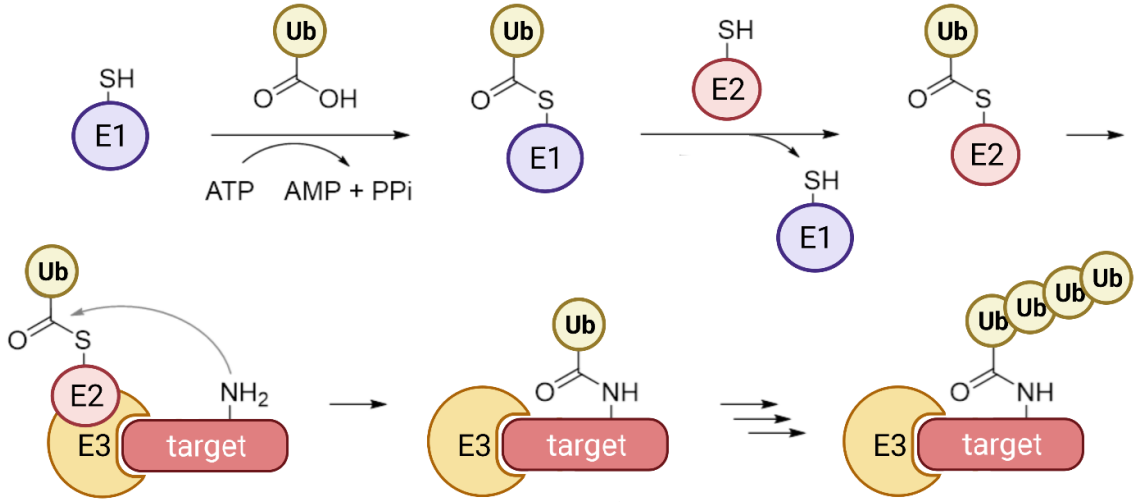

Figure 1. Schematic overview of the ubiquitination mechanism.

In recent years, several E3 ligases received much attention in drug discovery, particularly the E3 ubiquitin ligase VHL has attracted wide interest due to its crucial role in oxygen and hypoxia sensing.[2–4] One of the most well-characterized substrates of VHL is the hypoxia-inducible factor-1α (HIF-1α), a transcription factor that regulates various human genes, in particular those involved in the maintenance of oxygen homeostasis. HIFs, the master regulators of hypoxic signaling, function as heterodimeric protein and consist of the oxygen-dependent HIF-α subunit, of which three isoforms (HIF-1α, HIF-2α, and HIF-3α) are known in humans, and the oxygen-independent HIF-β subunit, which is constitutively expressed. Under normal oxygen levels (normoxia), two proline residues of HIF-1α (Pro402 and Pro564) are hydroxylated by oxygen- and iron-dependent prolyl hydroxylase domain (PHD) enzymes, which belong to the EglN family of dioxygenases.[6,14,15] This post-translational hydroxylation of HIF-1α triggers the recognition and binding by VHL, resulting in ubiquitination and degradation of HIF-1α *via* the proteasomal pathway.[2,3] In contrast, at low oxygen levels (hypoxia), the PHD activity is diminished and the HIF-1α subunits remain unhydroxylated. Consequently, they are no longer recognized by VHL, which entail the accumulation of HIF-1α molecules. The stabilized HIF-1α is able to translocate to the nucleus and form a heterodimeric complex with the HIF-1β subunit. By binding of the α/β heterodimer to specific hypoxia-responsive elements (HREs), the transcription of the hypoxia-responsive target genes is induced (Figure 2).[4,6,16–18] Upon this

mechanism, further opportunities for therapeutic intervention could be provided by the stabilization of HIF-1α and concomitant alterations in gene expression, which can be achieved through the use of PHD inhibitors preventing the HIF hydroxylation. Such drugs are already in clinical use for the treatment of renal anemia. Recently, the U.S. Food and Drug Administration (FDA) have approved the use of the PHD inhibitor daprodustat for the treatment of anemia caused by chronic kidney disease.[6,16]

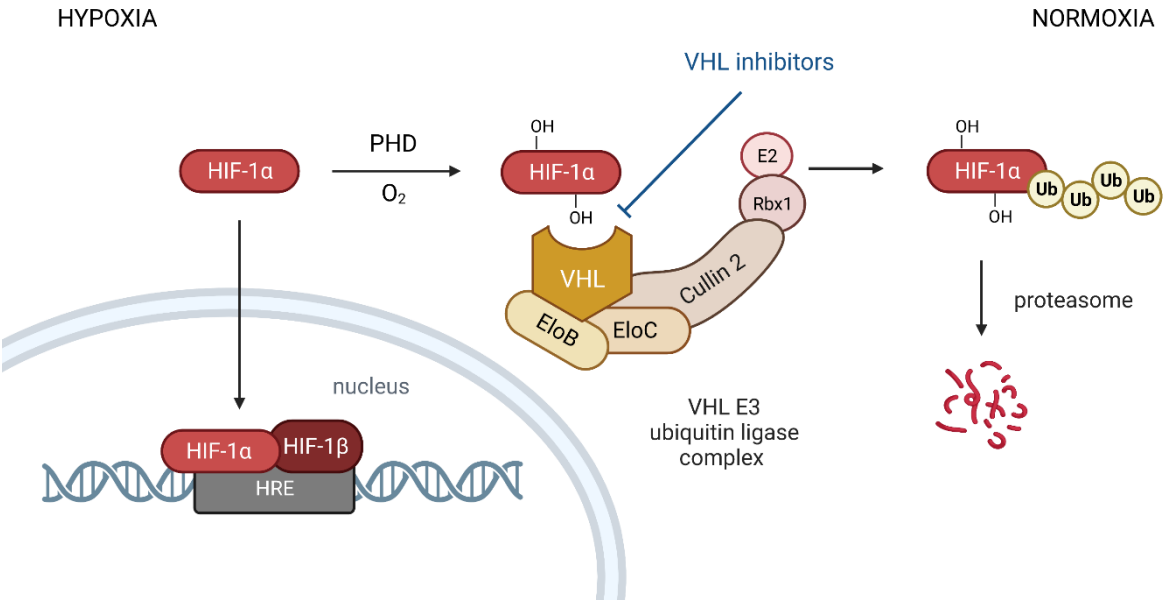

Figure 2. Mechanism of the oxygen-regulated HIF-1α activity. Under normoxia, PHDs use oxygen to hydroxylate HIF-1α, which is recognized by the $CRL2^{VHL}$ complex, followed by ubiquitination and proteasomal degradation. Under hypoxia, non-hydroxylated HIF-1α accumulates and dimerizes with HIF-1β, forming a transcriptionally active complex that binds to the HREs to activate the transcription of target genes.

Germline mutations in the VHL gene can be the genetic cause of the VHL disease, which is a hereditary autosomal dominant genetic disease that is often linked to various tumors, such as retinal angiomatosis and haemangioblastomas.[19–21] Although the VHL gene was first discovered in 1993 by a positional cloning strategy, the symptoms associated with the disease had already been observed long before.[19–21] In 1894, Treacher Collins initially described patients with familial retinal hemangioblastomas,[22] while in 1904, Eugene von Hippel studied independently the clinical appearance and progression of retinal lesions, which are now known as hemangioblastomas.[23] In 1927, Arvid Lindau found a link between the central nervous system angiomatosis and the previously reported retinal hemangioblastomas and visceral tumors.[24] Since then, the term von Hippel-Lindau disease was coined to described patients with

loss or mutation of the VHL wild-type allele exhibiting retinal angiomatosis and cerebellar hemangioblastomas. In addition to these tumors, VHL disease is also associated with clear-cell renal cell carcinomas, phaeochromocytomas, and tumors affecting the kidney, epididymis, and pancreas.[20,21,25]

The VHL gene is located on the chromosome 3p25 and encodes two VHL proteins, which is due to the presence of two internal translational initiation sites separated by the AUG codon (Met54) within the VHL open reading frame. The larger isoform ($VHL_{1–213}$) consist of 213 amino acids, the shorter isoform ($VHL_{54–213}$) contains of 160 amino acids. Based on their apparent molecular masses of 30 kDa or 19 kDa, they are often referred to as pVHL30 and pVHL19, respectively.[26–28] Despite their difference in size, both isoforms are functionally active and exhibit the same mechanism of tumor suppression activity. Likewise, they possess E3 ligase activity, which enables them to target HIFs for oxygen-dependent degradation.[29]

Several chemical strategies to affect the redox homeostasis have already been developed.[30–32] However, these strategies, such as using proteasome inhibitors or iron chelators, have often result in broad-spectrum activities and off-target effects, necessitating an alternative approach. The approach to infer the binding of HIF-1α to VHL was achieved by small molecule VHL binders, which can directly block the VHL:HIF-α protein-protein interaction (PPI).[5,33] Downstream of HIF-α hydroxylation by PHD enzymes but upstream of proteasomal degradation, VHL binders compete with the native substrate HIF-1α and enhance the stabilization of HIF-1α levels, resulting in the upregulation of genes involved in the hypoxic response, thus affecting hypoxia signaling.[5,33] The successful development of such VHL inhibitors has highlighted the significance of VHL as a therapeutic target for treating conditions such as anemia, ischemia, inflammation, and mitochondrial diseases.[5,33]

The rational design of breakthrough VHL inhibitors was based on the structure of the native HIF-1α substrate and its molecular recognition by VHL.[34–36] The first co-crystal structure of a 20-residue HIF-1α peptide bound to the VHL:EloC:EloB complex (PDB 1LM8)[14] revealed that HIF-1α was in an extended β strand-like conformation, with hydroxyproline Hyp564 inserted into a groove in a hydrophobic core composed of buried, mostly aromatic residues.[14] As crucial element for the recognition by VHL, Hyp564 served as a central motif for designing new VHL ligands. From this starting point, the design of the molecular scaffold of such ligands were extended to both sides of the central hydroxyproline by appending left-hand side (LHS) fragments at the N-terminus and right-hand side (RHS) fragments at the C-terminus (Figure 3).[5]

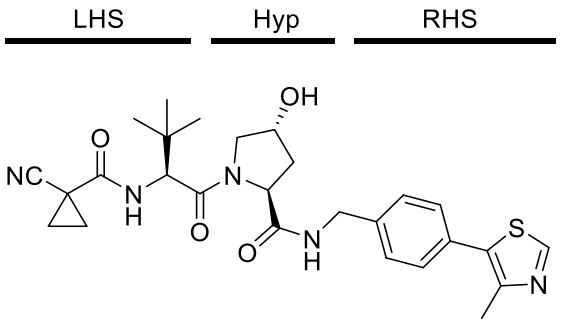

Figure 3. Chemical structure of an exemplary VHL inhibitor with its characteristic subsections, *i.e.*, the left-hand side (LHS), the key hydroxyproline (Hyp), and the right-hand side (RHS) fragments.

Representative compounds, which were developed over time and that bind to and inhibit VHL, are depicted in Figure 4. The RHS benzylamine moiety, which is equipped with a five-membered heteroaromatic ring, was already realized in ligands **I** and **II** and maintained in the course of further structural optimizations.[34,35] In the case of ligand **II**, an anilinic LHS fragment and a methylthiazole were introduced, whereas the latter was found as characteristic RHS moiety in several potent VHL inhibitors.[35,37] Further structure-activity relationship (SAR) studies revealed that a neopentyl residue within the LHS fragment was advantageous, while acetylated amino acids other than *tert*-leucine in **III** (VH032) resulted in reduced binding affinity to VHL.[38] A constrained cyclopropyl ring bearing a cyano or fluoro group at the α

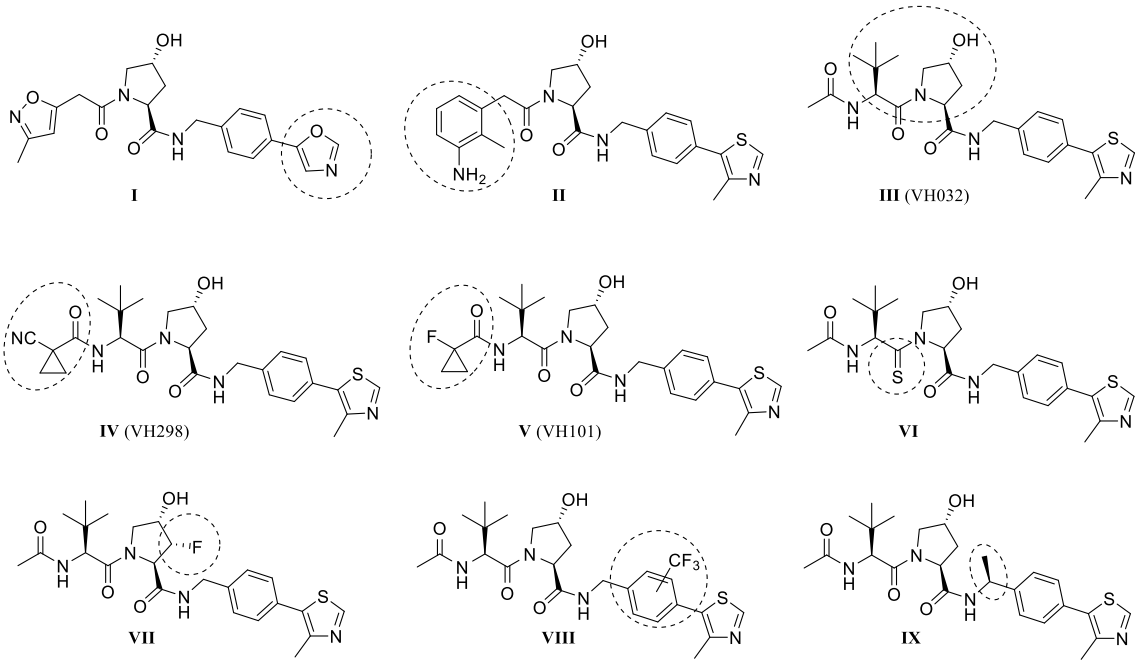

Figure 4. Structures of exemplary VHL inhibitors. Characteristic structural features of inhibitors **I**-**IX** are highlighted.

position was employed, leading to the VHL inhibitors **IV** (VH298) and **V** (VH101), respectively. While VH298 is widely used as a benchmark compound, the application of VH101 is restricted due to its cytotoxicity.[33,39] To explore the impact of bioisoteric O-to-S replacements, the thioamide derivative **VI** was synthesized, which exhibited reduced VHL affinity VHL compared to its counterpart **III**.[40] By introducing fluorohydroxyprolines, the influence of hydroxyproline fluorination on VHL binding was studied using all four 3-fluoro-4-hydroxyproline stereoisomers, including the (3*R*,4*S*)-configured derivative **VII**.[41] Trifluoromethyl groups were strategically attached to the inhibitor scaffold at various positions, as present in reporters **VIII**. These modifications allowed for the utilization of ^{19}F NMR spy molecules to track the hydroxyproline binding site of VHL.[42] Furthermore, the stereoselective methylation at the benzylic position within the RHS fragment provided an additional advantage, resulting in a two-fold improved IC_{50} value for **IX** compared to the parent **III**.[43–45]

These VHL inhibitors exemplify an avenue for ongoing enhancement through an SAR-based optimization. The emerged compounds have proven to be effective and applicable as chemical probes and have been successfully utilized in the development of heterobifunctional proteolysis-targeting chimeras (PROTACs), which exploit the UPS machinery for targeted protein degradation.[46–49]

1.2 Proteolysis-Targeting Chimeras (PROTACs)

The genomic revolution has revealed a large number of novel protein targets that are linked to various diseases, which has driven the search for small molecules that can selectively modulate these targets.[50,51] However, the development of such classical small-molecule inhibitor strategies faces significant challenges in targeting proteins that lack accessible binding sites or require high systemic drug exposure to achieve sufficient target inhibition, thus increasing the risk of undesirable off-target effects. As a result, many proteins remain “undruggable” by small molecule inhibitors, making it difficult to develop effective treatments for a wide range of diseases. While new biologic modalities such as monoclonal antibodies and oligonucleotide therapies offer opportunities to address previously undruggable targets, they still have limitations, such as poor cell membrane permeability.[10,50,51] To overcome these limitations, a new approach called proteolysis-targeting chimeras (PROTACs) has emerged as a promising and innovative technology in the field of targeted protein degradation (TPD) and has rapidly gained increasing attention in the drug discovery landscape in recent years.[52,53]

PROTACs are bifunctional small molecules that engage an E3 ubiquitin ligase to a protein of interest (POI) and thus induce a proteasomal degradation cascade. Such compounds are typically composed of three parts: a target-binding moiety, an E3 ubiquitin ligase recruiting ligand and a variable linker portion that connects these two ligands. By simultaneous binding of the PROTAC molecule to the POI and the E3 ubiquitin ligase, a ternary complex is assembled. Due to the resulting spatial proximity between the target protein and the E3 ligase, ubiquitin can be transferred to the POI, which can be recognized and degraded by the UPS (Figure 5). Once the process is completed, the degrader molecule dissociates from the complex and is accessible for another binding event. For this strategy to selectively degrade target proteins *via* the UPS, E3 ubiquitin ligases such as cereblon (CRBN) and VHL become a key part in the PROTAC field.[53–56]

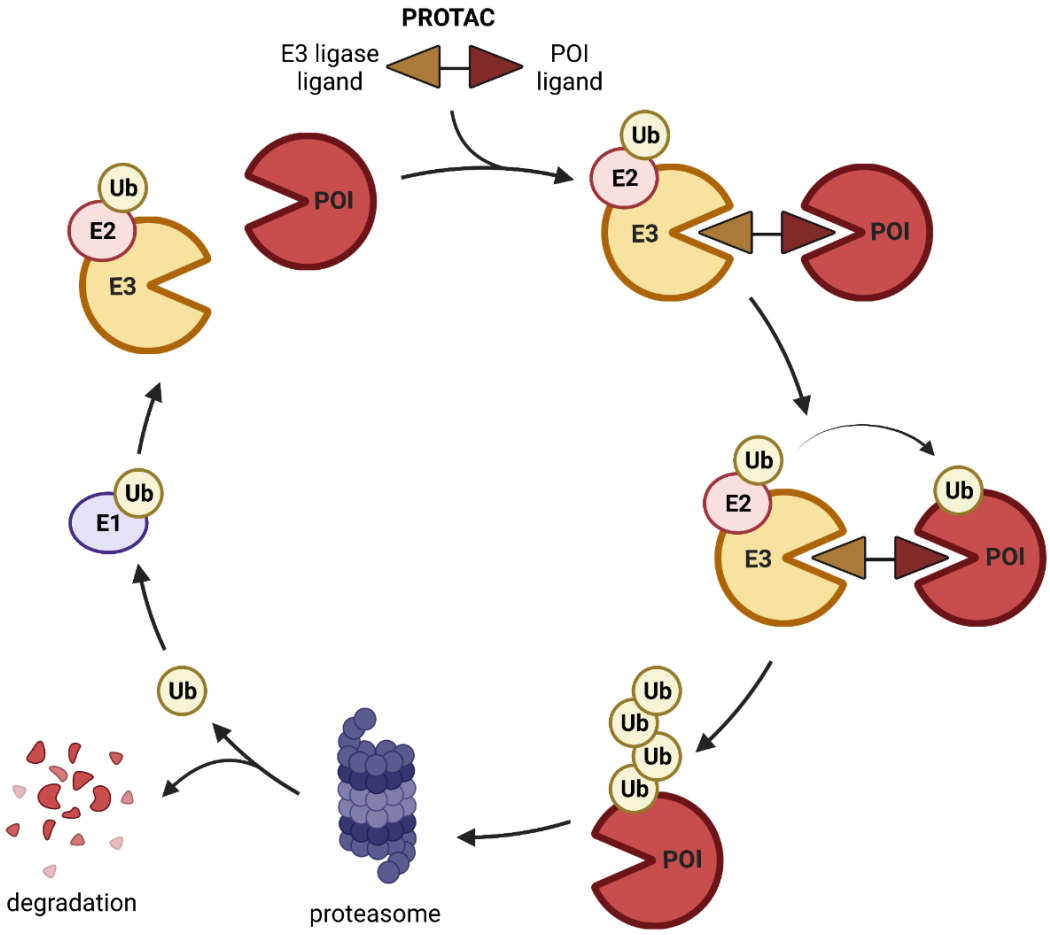

Figure 5. Mode of action of targeted protein degradation by PROTACs. A PROTAC molecule simultaneously binds to an E3 ubiquitin ligase complex and a protein of interest (POI), inducing the ubiquitination and degradation of the POI *via* the UPS.

By considering the properties of PROTACs, many advantages over traditional small-molecule inhibitors are observed. In contrast to classical occupancy-driven inhibitors, which are based on a competitive principle and therefore requiring constant presence, PROTACs provide a long-lasting effect by the degradation of the target. Additionally, PROTACs are effective at significantly lower concentrations for the degradation of the target protein, as they act *via* a catalytic mechanism and therefore PROTAC molecules can be recycled for multiple rounds of the ubiquitination and degradation process. This catalytic and event-driven mode of action (MoA) distinguishes PROTACs from classical drugs and is among the most remarkable advantages of this technology.[57]

The first proof-of-concept PROTAC was developed by the Crews and Deshaies laboratories in 2001.[58] This PROTAC was designed to recruit the enzyme methionine aminopeptidase 2 (MetAP-2) to the E3 ligase complex consisting of the F-box protein β-transducin repeat-containing protein ($SCF^{\beta\text{-}TRCP}$), leading to the ubiquitination and subsequent degradation of MetAP-2.[58] A few years later, PROTACs targeting steroid hormone receptor proteins, such as androgen receptors (ARs) and estrogen receptors (ERs), were successfully employed.[59] However, these peptide-based PROTACs were applied by microinjection since they had limited cell permeability and hence suffered from low cellular activity. In 2004, the development of the first cell-permeable PROTAC, which utilized a seven amino acid recognition sequence derived from HIF-1α, the endogenous substrate of VHL, was reported to demonstrate degradation activity against FK506 binding protein 12 (FKBP12).[60] These pioneering first-generation PROTACs represented a major step forward in the field of PROTAC technology and led to the development of numerous small molecule-based PROTACs to overcome poor cell permeability and stability (Figure 6). The first small molecule PROTAC based on the mouse double minute 2 homologue (MDM2) E3 ligand was developed in 2008. This PROTAC utilized nutlin-3a, a well-known inhibitor of the MDM2-p53 PPI, as an E3 ligase ligand and was able to degrade the androgen receptor (AR) at micromolar concentration.[61] Two years later, in 2010, the first cellular inhibitor of apoptosis protein 1 (cIAP1) recruiting PROTAC using methyl bestatin as a ligand to induce degradation of cellular retinol-and retinoic acid-binding proteins I and II was described.[62] In the same year, the primary target of the drug thalidomide, which is the E3 ligase cereblon (CRBN), and later its analogues lenalidomide and pomalidomide were identified, leading to the discovery of CRBN-recruiting PROTACs. Due to their effects on immune cells, CRBN ligands are known as immunomodulatory imide drugs (IMiDs) in cancer therapy.[63–67] In 2012, the first small-molecule ligands for VHL were developed and improved by the Crews and Ciulli laboratory on the basis of a peptide fragment of HIF-1α obtained through *in silico*

and fragment-based screening.[34–36] The crystal structure of VHL in complex with its inhibitors has been established as a starting point for further ligand optimization and led to the most utilized VHL ligands, VH032 and VH298, these days.[33,39] The VHL E3 ligase ligand was initially used to degrade HaloTag7 fusion proteins by its incorporation into HaloPROTACs.[68,69] HaloTag7 is an artificial modified bacterial dehalogenase that bind covalently to chloroalkanes. By conjugating the VHL E3 ligand to different chloroalkanes, these HaloPROTACs are able to recruit VHL to promote the degradation of the green fluorescent protein (GFP)-HaloTag7 fusion protein.[68,69] In 2015, the first small molecule-based, VHL-recruiting PROTACs that target estrogen-related receptor-α (ERRα) and receptor-interacting serine/threonine-protein kinase 2 (RIPK2) inducing endogenous protein degradation were developed.[70] Further targets such as bromodomain-containing protein 4 (BRD4) were successfully degraded by MZ1, a PROTAC consisting of VH032 as the E3 recruiting ligand and JQ1, a bromodomain and extraterminal domain (BET) inhibitor.[71] During the same time, the CRBN-recruiting PROTACs ARV-825 and dBET1, composed of the BRD4 addressing inhibitor JQ1 and a phthalimide moiety hijacking the CRBN E3 ligase complex, were also reported. Furthermore, *in vivo* studies have demonstrated the ability of such PROTACs to degrade proteins in various tissues, including solid tumors.[66,67] In 2019, two heterobifunctional targeted degraders, ARV-110 and ARV-471, were introduced as human therapeutics into the first-in-human trials. These orally bioavailable PROTAC protein degraders were designed to selectively target and degrade AR and ER, and have now moved on to clinical phase II trials.[72,73]

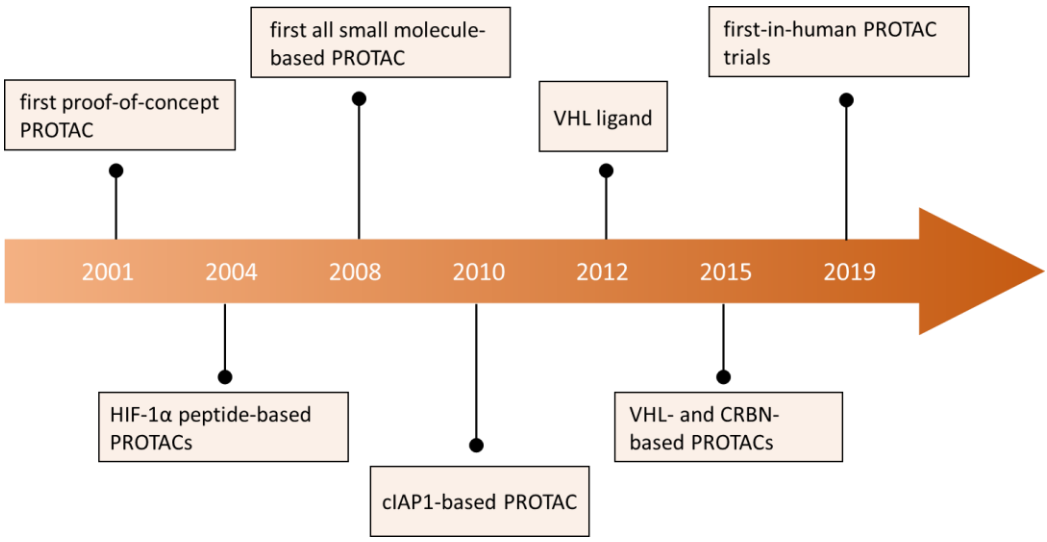

Figure 6. Timeline of the early PROTAC discoveries with highlighted milestones in the evolution of PROTACs.

Overall, the research on TPD has revolutionized the field of drug discovery over the last decades. TPD molecules have advanced from the initial peptide-based compounds to rationally designed small molecules, providing a promising alternative to traditional small molecule drugs (Figure 7). This development has opened up new therapeutic possibilities and paved the way for future scientific advancements. As the research in TPD continues to progress, it is expected that this innovative modality will increase significantly in the development of novel drugs.[56,73]

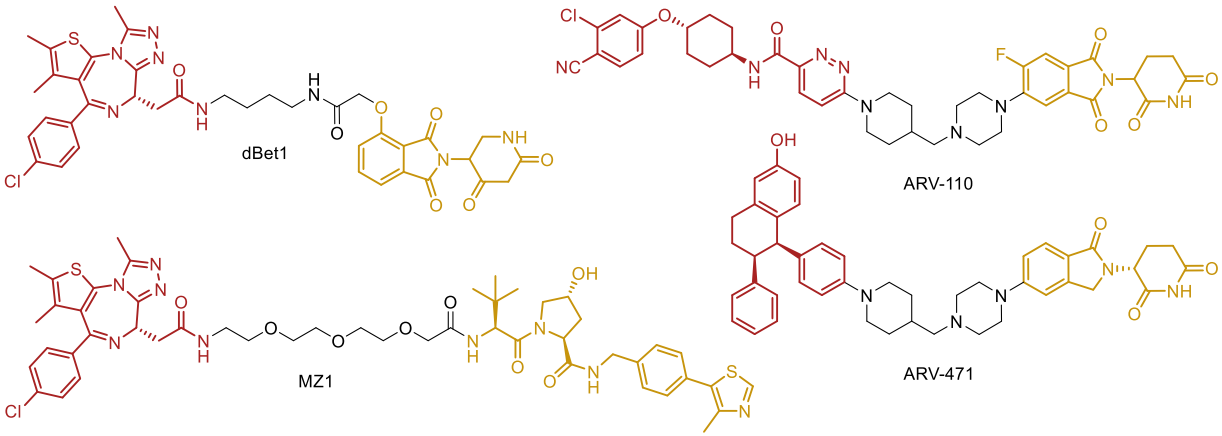

Figure 7. Structures of exemplary PROTACs. They are composed of a target-binding moiety (red), a linker (black) and an E3 ligase-binding moiety (yellow).

To understand the correlation between the target binding affinity and the PROTAC degradation profile, researchers have investigated the underlying mechanisms more closely, in particular in terms of the thermodynamics of the ternary complex formation. Bifunctional PROTAC molecules have the ability to interact with their protein binding partners as binary complexes. However, for their functional activity to degrade target proteins, it is essential that both partners are engaged simultaneously in a POI:PROTAC:E3 ternary complex. The propensity for such ternary complex formation can be quantified by the cooperativity (α) factor, which reflects the affinity between the binary and ternary complexes and is defined by ratio of their dissociation constants for PROTAC binding.[74–76] By applying different biophysical methods such as isothermal titration calorimetry (ITC), fluorescence polarisation (FP), or surface plasmon resonance (SPR), but also proximity-based assays, which includes AlphaLISA, time-resolved Förster resonance energy transfer (TR-FRET), and nano-bioluminescence resonance energy transfer (NanoBRET), the binding affinities can be measured and the successful assembly of ternary complex can be proved.[75,77] The presence of thermodynamically favorable interactions between the POI and the E3 ligase result in positive cooperativity ($\alpha > 1$), whereas unfavorable

repulsive interactions lead to negative cooperativity ($\alpha < 1$), hindering the formation of a ternary complex. These results emphasize the crucial role of positive cooperativity in the formation of a productive ternary complex. An example of positive cooperativity was provided by the first crystal structure of the PROTAC MZ1 in complex with its target BRD4 and the E3 ligase VHL.[76]

The formation of PROTAC-mediated ternary complexes relies on established mathematical models, which predict a bell-shaped relationship between the PROTAC concentration and its formation to ternary complexes.[78,79] At high concentrations, ineffective binary complexes such as PROTAC-POI or PROTAC-E3 ligase are observed and compete with effective ternary complexes. This phenomenon is referred to as the "hook effect",[79,80] which negatively impacts the potency of PROTACs in a concentration-dependent manner (Figure 8). The hook effect can be affected by various factors, including POI and E3 ligase concentrations, PROTAC binary binding affinity, and cooperativity. Hence, the hook effect is an intrinsic event in PROTAC pharmacology that is difficult to avoid. However, since positive cooperativity is more favourable for ternary complex formation than for unproductive binary complexes, a strategy to reduce the hook effect can be afforded by improving the cooperative-binding PPIs in order to stabilize the PPI between the POI and E3 ligase.[80]

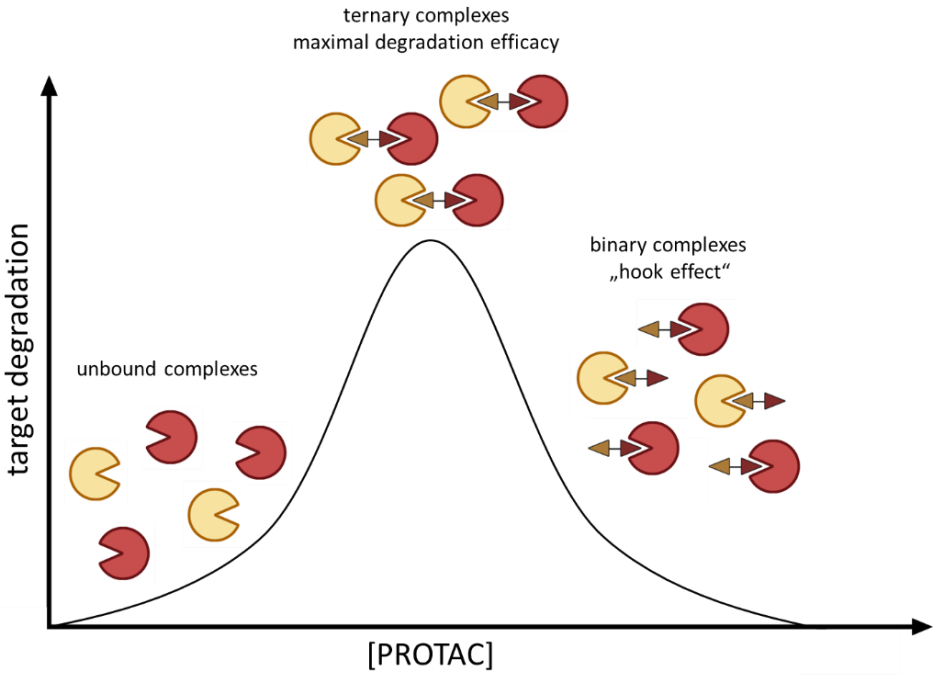

Figure 8. PROTAC-mediated ternary complex formation and “hook effect”.

1.3 Aptamers

Aptamers are short single-stranded DNA or RNA molecules with a length of about 25 to 80 oligonucleotides. Their flexible three-dimensional structures confer them the ability to bind specifically to a broad range of target molecules with high specificity and affinity, which is comparable to antibodies.[81,82] However, in contrast to monoclonal antibodies, aptamers provide several superior advantages and, therefore, overcome some of the limitations of antibodies. They benefit from their high stability, short generation time, high target potential ranging from ions and small molecules to *in vitro* complexes, low manufacturing cost, little batch-to-batch differences, facile modifiability, and very low immunogenicity.[82] Nucleic acid aptamers are generated by an *in vitro* technique known as systematic evolution of ligands by exponential enrichment (SELEX).[83,84] The mechanism involves the following steps: The SELEX process begins with the production of a random nucleic acid library containing up to 10^{16} single-stranded oligonucleotides, which are incubated with the target molecules of interest (Figure 9).

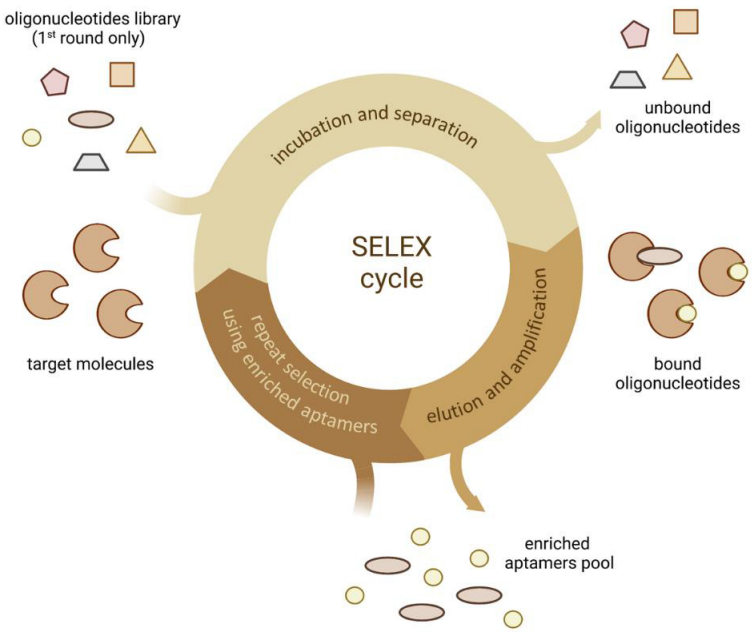

Figure 9. Schematic representation of SELEX. A library of single-stranded oligonucleotides is incubated with the target of interest. Bound oligonucleotides are partitioned from the unbound ones and amplified by PCR. The resulting enriched aptamer pool is used for the next selection cycle.

Subsequently, the target-bound sequences are separated from the unbound oligonucleotides by removing the unbound ones through washing steps. After elution, the bound oligonucleotides are amplified by polymerase chain reaction (PCR) for DNA aptamers or a reverse transcription

PCR (RT-PCR) for RNA aptamers. By following these steps, a selection cycle is completed and a new enhanced library of selected oligonucleotides is generated to be incubated with the target in the next SELEX round. The iterative protocol of binding, washing, recovery, and amplification is repeated for several rounds until the sequence is enriched with the desired high affinity. Finally, the aptamers obtained through SELEX are characterized by sequencing and are analyzed to confirm their specificity and affinity for the target. To date, SELEX has been a widely-used method to identify numerous of aptamers and several variations of SELEX have been established over the past years. These include, *e.g.*, magnetic bead-based SELEX, cell-SELEX, and *in vivo* SELEX.[85,86]

The high affinity and specificity of aptamers account for their usage as an ideal tool for diagnostics and therapeutics, particularly in biotechnological and biomedical areas. Analogously to monoclonal antibodies, aptamers are exploited for their highly specific molecular recognition of their targets, thus, gaining importance as biosensors and biomarkers. A variety of applications have been successfully developed ranging from monitoring environmental contaminants to pathogen and cancer recognition.[87]

Since inhibitory aptamers can interfere with the function of a target protein, they can be applied directly as therapeutic antagonists.[88] For instance, such therapeutic aptamers have been developed for the treatment of infectious diseases like the human immunodeficiency virus 1 (HIV-1).[89] Furthermore, the vascular endothelial growth factor (VEGF) targeting aptamer pegaptanib was the first therapeutic aptamer being approved by the U.S. FDA for its clinical use as anti-VEGF antagonist in the treatment of neovascular ocular diseases, such as age-related macular degeneration (AMD).[90] In addition to serving as stand-alone therapeutics, aptamers have also been widely studied to be used as targeted drug delivery system. These aptamer-drug conjugates (ApDCs), composed of an aptamer ligand, which is linked *via* a covalent conjugation to a drug warhead, present several potential advantages compared to their antibody-drug conjugate (ADC) counterparts (Figure 10).[82,91] One of these advantages is the facile chemical modification of aptamers with versatile functional groups, enhancing their resistance to nuclease degradation and optimizing their biostability, functionality and pharmacokinetic properties.[92–94] Various ApDCs have already been successfully applied to target disease-related biomarkers such as protein tyrosine kinase 7 (PTK7), prostate-specific membrane antigen (PSMA), mucin 1 (MUC1), and human epidermal growth factor receptor 2 (HER2), in cancer cells.[94] The profound exploration of ApDCs allows for their application in multiple modalities of therapy, including chemotherapy, gene therapy, immunotherapy, radiotherapy and

phototherapy. In the last years, ApDC-mediated gene therapy has been explored in transcriptome approaches, where DNA/RNA aptamers can be conjugated with nucleic acid gene therapeutics, for example with small interfering RNA (siRNA), small hairpin RNA (shRNA), or micro RNA (miRNA).[94] Recently, a wide range of anti-viral aptamers have been identified and approaches of aptamers targeting severe acute respiratory syndrome coronavirus 2 (SARS-CoV-2) have emerged as a promising tool to fight against COVID-19.[95–97]

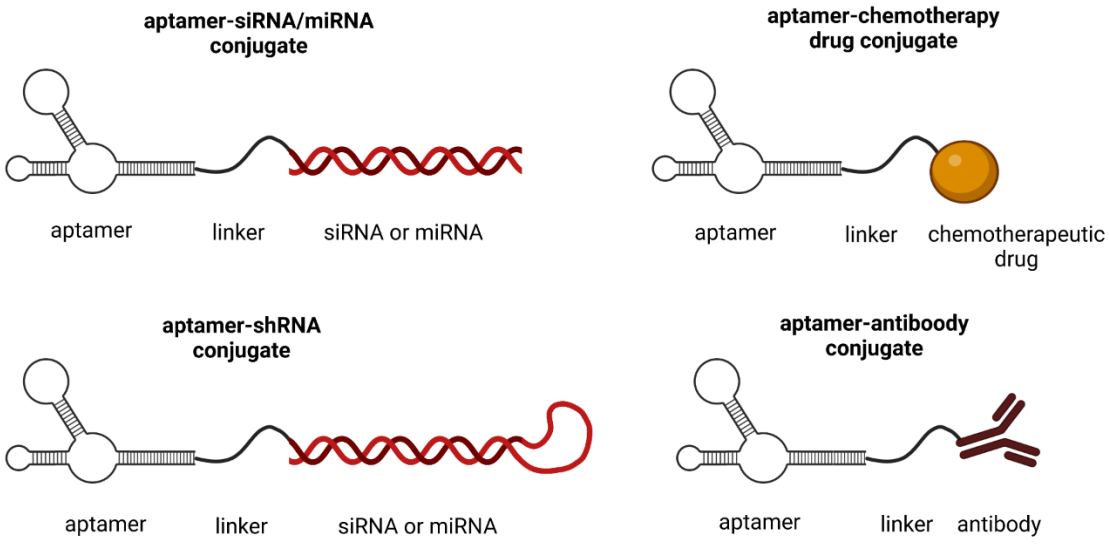

Figure 10. Schematic examples of ApDCs.

1.4 Serine Proteases

The International Union for Biochemistry and Molecular Biology (IUBMB) categorizes enzymes into seven main classes based on the type of chemical reaction they catalyze.[98] The classification system is known as the Enzyme Commission (EC) number, which imply a code consisting of four numbers. Those numbers represent the catalyzed reaction with an increasing finer classification of the enzyme. Proteases are enzymes that catalyzed the hydrolysis of peptide bonds and, therefore, categorized into the class of hydrolases (EC 3) or more precisely, into the subclass of hydrolyses that act on peptide bonds (EC 3.4). Sequencing of the human genome has identified over 500 proteases, which can be further classified into clans based on catalytic mechanism and families on basis of common ancestry.[99–101] According to their catalytic mechanism, they can be classified into these categories: aspartic acid proteases, cysteine proteases, serine proteases, threonine proteases, and metalloproteases. However,

almost one-third of all proteases are covered by serine proteases (or serine endopeptidases; EC 3.4.21), found ubiquitously in eukaryotes, prokaryotes, archaea and viruses.[102] As indicated by their name, they possess a nucleophilic serine residue at the active site and their proteolytic activity is driven by the recognition of the substrates' amino acid residues (P) by the enzymes' specificity pockets (S). According to Schechter and Berger, the amino acid residues of the substrate starting from the scissile bond to direction of the N-terminus are defined as non-prime sites (P1, P2, P3, etc.) and the residues towards the C-terminus are labeled as primed sites (P1', P2', P3', etc.). The corresponding subsites of the enzyme are termed S1, S2, S3 and S1', S2', S3, respectively (Figure 11).[103]

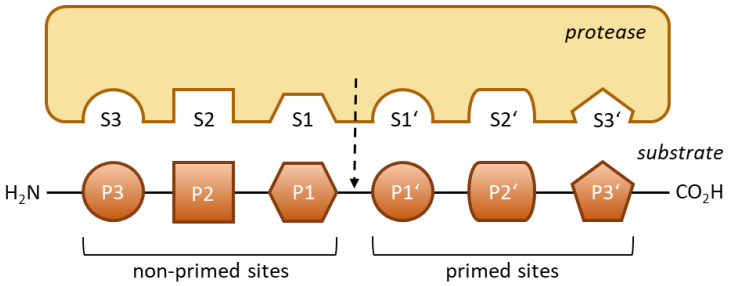

Figure 11. Schematic representation of an active site of a substrate-bound protease. The enzyme subsites S3 to S3' and the corresponding amino acid residues P3 to P3' are referred to the Schlechter and Berger nomenclature.[103] The scissile bond is highlighted by a dashed arrow.

Serine proteases utilize the catalytic triad consisting of a specific spatial arrangement of aspartic acid (Asp), histidine (His), and serine (Ser) to induce the proteolytic cleavage (Figure 12).[102,104] The initial step of the reaction is a nucleophilic attack by the serine residue on the scissile carbonyl carbon, forming an oxyanion tetrahedral intermediate, which is stabilized by an oxyanion hole formed by additional two amide groups of the main chain. Subsequently, the tetrahedral intermediate collapses, followed by the release of the C-terminal peptide and the generation of an acyl-enzyme intermediate. A second nucleophilic attack by an activated water molecule leads to hydrolysis of the acyl-enzyme and gives rise to the second tetrahedral intermediate. By collapsing of this intermediate, the N-terminal portion of the peptide is released and the catalytic serine residue is restored to its initial state. In each step of the reaction, the histidine side chain serves either as a base for activating the nucleophilic character of serine or as an acid for the transfer of a proton to the leaving group. The role of aspartic acid is

expected to stabilized the imidazole ring of histidine in its orientation and also the positive charge accumulating on histidine in the transition states.[102,105–107]

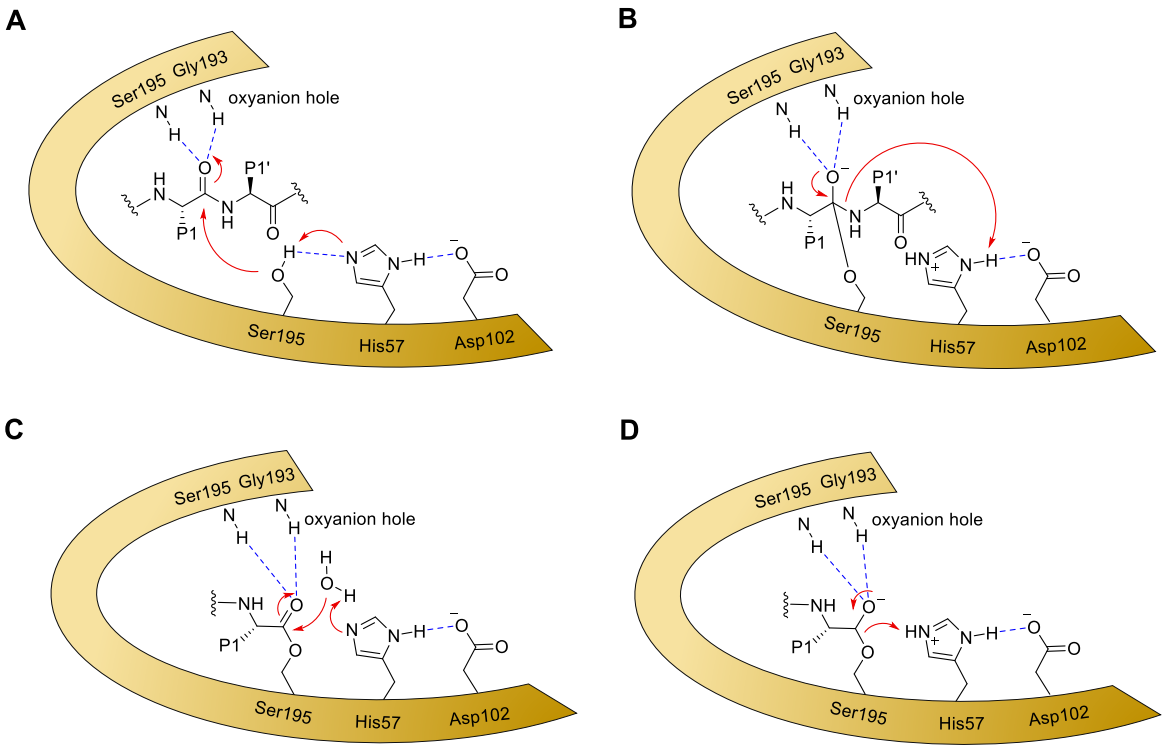

Figure 12. Proteolytic mechanism of serine proteases. The steps in the catalytic mechanism includes: (A) The nucleophilic attack by the serine residue on the carbonyl carbon, (B) the formation of a first tetrahedral intermediate, (C) the release of the C-terminal peptide and generation of an acyl-enzyme intermediate, followed by a second nucleophilic attack, leading to (D) a second tetrahedral intermediate, which collapses into the N-terminal product and the free enzyme.

The importance of proteases in almost every biological process has indicated them as relevant targets for drug development. These enzymes play a crucial role in a variety of physiological processes such as hemostasis, inflammation, and blood coagulation.[108] Due to the crucial role of proteases in these processes, a detailed understanding of these enzymes can aid in the development of new drugs to treat various diseases. In the following, five selected serine proteases will be further described.

1.4.1 Thrombin

Thrombosis is a main issue of cardiovascular diseases and a leading cause of mortality, accounting for one in four deaths worldwide.[109,110] It arises due to the formation of unwanted blood clots (thrombus) inside blood vessels, which disrupt the normal blood flow and lead to diseases causing myocardial infarction, stroke, heart attacks, deep venous thrombosis or pulmonary embolism.[110,111] Thrombin, a key enzyme in the blood coagulation, is a trypsin-like protease, which originates from its inactive precursor prothrombin. Upon activation by factor Xa in presence of an anionic phospholipid surface, factor Va and calcium ions, thrombin cleaves fibrinogen to produce fibrin, promotes platelet activation and is responsible for the activation of protein C as well as the coagulation factors V, XI, XIII, which are involved in generating cross-linked fibrin clots. An imbalance between these factors and their activators causes dysregulated hemostasis and is associated with thrombotic diseases.[112–114] Hence, there is ongoing search for a potent, selective, and bioavailable inhibitor of thrombin, which could regulate these disease states. Indirect thrombin inhibitors such as heparins and vitamin K antagonists have been widely used in anticoagulation therapy to prevent and treat thromboembolic disorders.[115,116] These inhibitors catalyze the function of antithrombin, a natural anticoagulant of the coagulation cascade, which binds to an exosite of thrombin, generating a ternary complex consisting of thrombin, antithrombin and the indirect thrombin inhibitor.[116] However, indirect thrombin inhibitors have several limitations, accounting for the development of direct thrombin inhibitors, which can bind directly to the active site of thrombin and act independently of antithrombin. Bivalent direct thrombin inhibitors, such as hirudin and bivalirudin, block the thrombin activity at both its active site and at one exosite, whereas univalent direct thrombin inhibitors, which include argatroban, melagatran, and dabigatran (Figure 13), bind only to the active site of thrombin.[116] However, melagatran and its prodrug ximelagatran were withdrawn from the market due to liver toxicity.[117] Dabigatran is the only approved oral direct thrombin inhibitor and has been shown to reduce the risk of stroke and systemic embolism in patients with nonvalvular atrial fibrillation.[118]

The Merck Research Laboratories identified comparable low molecular thrombin inhibitors which contain the common P1, P2, P3 structural motif found in many potential thrombin inhibitors (Figure 13).[119–121] These compounds consist of a P1 benzylic amine, a P2 proline and a varying P3 group, comprising of either a *tert*-butyl side chain or a fluorenyl group or an acyl pyrrole. All these compounds originated from mimicking fibrinogen, thrombin's natural substrate, which contains the sequence D-Phe-Pro-Arg.[122,123]

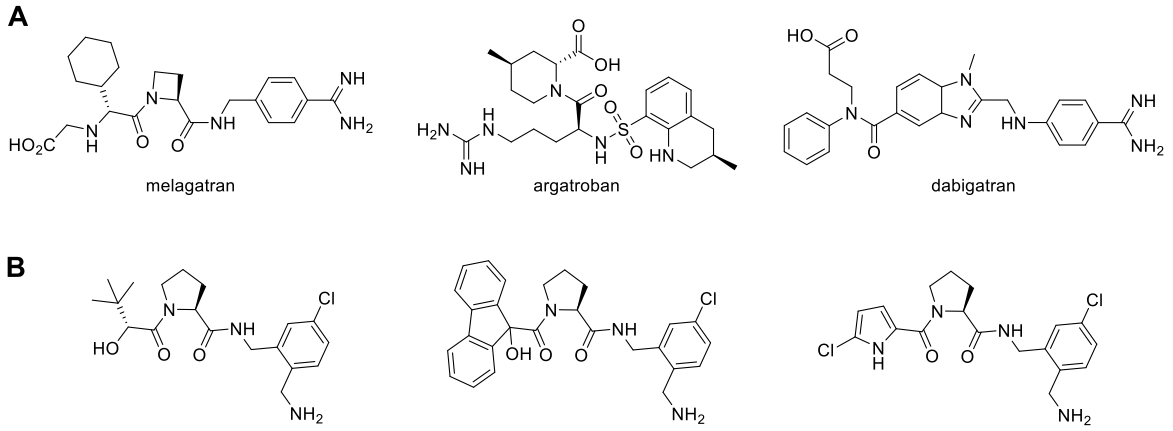

Figure 13. Examples of direct thrombin inhibitors. (A) Structures of the inhibitors melagatran, argatroban, and dabigatran. (B) Inhibitors developed by the Merck Research Laboratories.[119–121]

1.4.2 Factor Xa

Factor (F) Xa is a trypsin-like protease, also involve in the blood coagulation cascade. The coagulation is regulated by two parallel pathways, the extrinsic and the intrinsic pathways, which converge at the point of activation of FXa (Figure 14).[124,125] The initiation of the extrinsic pathway occurs upon injury to the endothelial tissue, which leads to the exposure of tissue factor (TF), a transmembrane protein that serves as receptor for FVII/FVIIa, in the bloodstream. Upon binding with calcium and FVIIa, TF-FVIIa complex triggers the activation of FX to FXa. Meanwhile, the intrinsic pathway is initiated when coagulation FXII, prekallikrein, and high molecular weight kininogen are exposed to a negatively charged surface, leading to the activation of FXII to FXIIa. Once activated, FXIIa converts FXI into FXIa, which subsequently cleaves and activates FIX. The activated FIXa subsequently forms a complex with FVIIIa, phospholipid, and calcium that activates FX. The common pathway results when FX is activated at the end of either the intrinsic or extrinsic pathway. Upon activation, FXa combines with FVa and calcium ions to form a prothrombinase complex. This complex promotes the conversion of prothrombin (FII) to thrombin (FIIa), which in turn cleaves fibrinogen (FI) into fibrin (FIa). Additionally, thrombin cleaves the stabilizing FXIII into FXIIIa, which forms fibrin crosslinks and produces a stable clot at the site of injury. Due to its key responsibility for the propagation of the coagulation process by generating thrombin, FXa plays a crucial amplifying role in the coagulation cascade.[126–128] An increased activation of this system can lead to various thromboembolic disorders (see chapter 1.4.1). To prevent arterial thrombosis in patients with cardiovascular diseases, antiplatelet drugs were used, while anticoagulants play a

critical role in preventing and treating venous thromboembolism by reducing the formation of fibrin.[129] Compared to direct inhibition of thrombin, inhibiting FXa may be more effective due to its position upstream of thrombin in the coagulation cascade.[130] Thus, FXa inhibitors have emerged as a potential target for anticoagulation therapy.[129] Several direct oral FXa inhibitors, such as rivaroxaban, apixaban and edoxaban, have been approved by the FDA for the prevention of stroke in nonvalvular atrial fibrillation patients.[131–134]

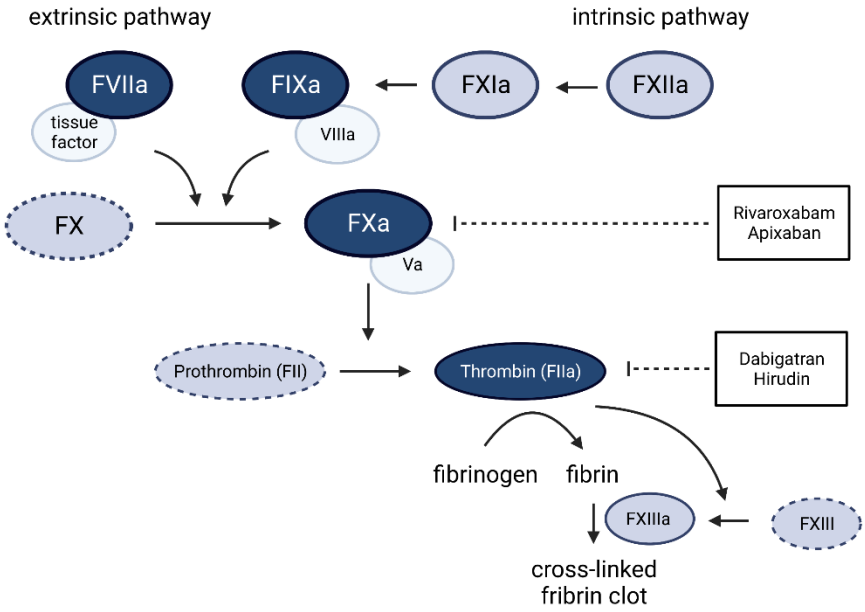

Figure 14. Schematic illustration of the blood coagulation cascade with focus on thrombin and FXa and their inhibition through direct oral anticoagulants (DOACs). The dashed circles indicate inactive states of the blood coagulation factors, whereas normal circles represent the active states of the blood coagulation factors. Drugs are shown in boxes, including direct inhibitors of FXa and thrombin.

1.4.3 Matriptase-2

Matriptase-2, a member of the type II transmembrane serine proteases (TTSPs), is a cell surface protease encoded by the *TMPRSS6* gene. The structural features of TTSPs are defined by a short intracellular N-terminal domain, a transmembrane domain, a large extracellular stem region that contains various functional domains, and a C-terminal extracellular serine protease domain with a highly conserved chymotrypsin fold harboring the catalytic triad.[135–137] The human TTSP family comprises 17 members, and based on their stem region, they are divided into the following four subfamilies: (i) human airway trypsin-like protease/differentially expressed in squamous cell carcinoma (HAT/DESC), (ii) transmembrane protease/serine (hepsin/TMPRSS), (iii) matriptase, and (iv) corin. Matriptase-2, as well as matriptase,

matriptase-3, and the unique polyserase-1, belong to the matriptase subfamily. All matriptases share common features of TTSPs, including a stem region, which consist of a sea urchin sperm protein/enteropeptidase/agrin (SEA) domain, two C1s/C1r, urchin embryonic growth factor, bone morphogenetic protein-1 (CUB) domains, and three to four low-density lipoprotein receptor class A (LDLA) domains (Figure 15).[138–140] In general, TTSPs are produced as inactive single-chain proenzyme, also known as zymogens, and thus, require activation. The activation can be triggered by cleaving a conserved activation motif that includes a basic amino acid residue such as arginine or lysine.[140,141] After cleavage, a disulfide bond attaches the protease domain's cleaved portion to the stem region, keeping the TTSPs connected to the cell membrane. A second autocatalytic cleavage in the stem region results in an activated two-chain form.[140,141]

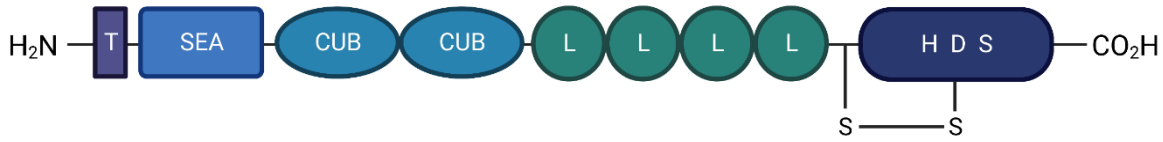

Figure 15. Schematic representation of matriptase-2 with its domains and disulfide bridge connecting the protease domain to the stem region after autocatalytic cleavage.

Matriptase-2 plays an important role in the regulation of iron homeostasis in humans. It is primarily expressed on the cell surface of hepatocytes, the major parenchymal cell in the liver, and acts as a suppressor of hepcidin expression.[142–144] Hepcidin, a systemic iron regulatory hormone, controls the cellular plasma iron levels and the iron tissue distribution by promoting the internalization and degradation of the iron exporter ferroportin, which are located on the surface of enterocytes, hepatocytes, and macrophages. By targeting ferroportin for its degradation, hepcidin inhibits the release of iron, leading to a reduced supply of iron into plasma.[145,146] Thus, chronic excess of hepcidin may lead to the development of iron-restricted anemia.[147] Conversely, a deficiency in hepcidin results in the increase of iron transfer to plasma, which causes systemic iron overload with iron deposits in the liver and other parenchymal organs and increases the risk of developing severe iron overload disorders such as hemochromatosis and β-thalassemia.[148] The cell surface serine protease matriptase-2 exerts its regulatory effect on the expression of the hepcidin-encoding gene *HAMP* by cleaving the membrane-bound bone morphogenetic protein (BMP) co-receptor hemojuvelin from the plasma membrane. This restrains the complex formation of the endogenous ligand BMP6 and

the BMP receptor, and thus, suppressing the phosphorylation of the sons of mothers against decapentaplegic (SMAD) complex, which would translocate to the nucleus to activate the gene transcription under normal conditions.[149–151] Hence, hemojuvelin is an essential component, as it is required for the signaling cascade. The hydrolytic cleavage of hemojuvelin by matriptase-2 leads to a down-regulation of *HAMP* expression, thus impeding the synthesis of hepcidin.[149,152] Due to its significant role in such a critical physiological process, matriptase-2 has emerged as a potential therapeutic target for the treatment of diseases arising from iron overload. Furthermore, it has been found that mutations in the *TMPRSS6* gene lead to severe iron-refractory iron deficiency anemia (IRIDA), a rare autosomal recessive disorder.[142–144] Typical features of the disease are congenital hypochromic and microcytic anemia, low mean corpuscular erythrocyte volume, low transferrin saturation, and defects in iron absorption and utilization.[143] Patients that suffer from IRIDA are not amenable to oral iron treatment, but partially responsive to parental iron therapy.[153] Therefore, several attempts were made to develop peptidic substrates for matriptase-2 in order to design potent and selective low-molecular-weight inhibitors. Along with arginine in P1 position, further basic amino acids in P4-P2 positions have been observed to be highly preferred.[154] This was also confirmed by a combinatorial approach which identified the sequence Ile-Arg-Ala-Arg as the preferred P4-P1 substrate sequence.[155] In recent years, various small molecule matriptase-2 inhibitors have been developed, allowing a thorough analysis of their SAR, proving basic substructures to be advantageous in the S1 specificity pocket, and further basic or hydrophobic substructures in the S4-S2 pocket.[156–160]

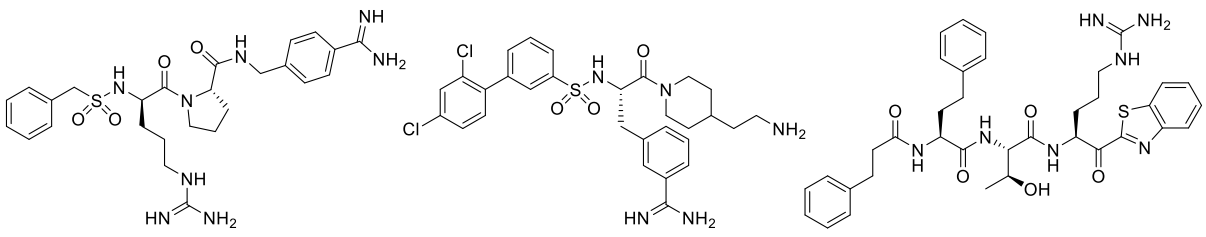

Figure 16. Exemplary structures of synthetic low-molecular-weight matriptase-2 inhibitors.

1.4.4 Elastase

Human leukocyte elastase (HLE), a member of the chymotrypsin superfamily of serine proteases, is one of the major enzymes stored in azurophilic granules of the human polymorphonuclear neutrophils. It is capable of cleaving several structural proteins including compounds of the extracellular matrix such as elastin, fibronectin, laminin, collagens and proteoglycans, as well as a variety of plasma proteins such as complement factors and cytokines.[161–165]

Intracellular HLEs exhibit antimicrobial functions and contribute to the defense against bacterial infection at inflammatory sites by phagocytosis. During the phagocytosis process, HLEs act intracellularly within phagolysosomes in combination with various microbicidal peptides and the oxygen metabolites producing membrane-associated NADPH oxidase system to destruct those phagocytized microorganisms at the initial stage of infection. This oxidative pathway is also referred to as "respiratory burst".[166,167] In addition, HLEs provide also an extracellular antimicrobial mechanism *via* neutrophil extracellular traps (NETs).[168] NETs are complex web-like structures, made of extracellular DNA fibers, which comprise histone and neutrophil serine proteases. Acting as a physical barrier to destruct pathogens extracellularly, they prevent virulent factors and bacteria, such as gram-negative bacteria, from escaping from phagolysosomes and surviving in the cytoplasm. Additionally to their antimicrobial capacity, HLEs are important regulators in inflammatory response and can control cellular signaling by proteolytic modification of chemokines and the cytokine network, and activating specific cell surface receptors.[165,169] Their proteolytic activity is controlled by their endogenous inhibitors including α1-proteinase inhibitor, α2-macroglobulin, secretory leukocyte protease inhibitor, and elafin. However, an out-of-balance activity between HLE und these inhibitors can lead to a variety of pathologies. These include diseases such as acute respiratory distress syndrome (ARDS), acute lung injury (ALI), chronic obstructive pulmonary disease (COPD), cystic fibrosis, rheumatoid arthritis, atherosclerosis and other inflammatory-related disorders.[165,170–172]

To combat these neutrophil serine protease-related human diseases, various strategies have been established for the development of HLE inhibitors as potential treatment. During the last years, several types of HLE inhibitors have been reported ranging from natural products to low-molecular-weight compounds that mimic the natural substrate cleavage site with small hydrophobic residues in P1 position.[173–175] Currently, the small molecule sivelestat is the only synthetic HLE inhibitor that has reached the market for the treatment of the elastase-mediated diseases ARDS and ALI, and has only been approved in Japan and the Republic of Korea.[174,176]

1.4.5 Cathepsin G

The serine protease cathepsin G (CatG), among two other neutrophil serine proteases, HLE and proteinase 3, is stored in neutrophil azurophilic granules. In comparison to HLE, CatG has a dual substrate specificity, with both trypsin and chymotrypsin-like properties, allowing it to cleave peptide bonds formed by positively charged (arginine, lysine) and aromatic (phenylalanine, tyrosine) amino acid residues. The main source of CatG expression is in polymorphonuclear neutrophils.[171,177]

Similar to HLEs, CatG possesses strong antimicrobial properties and is involved in the pathway of intracellular and extracellular pathogen destruction. While HLE is required for the intracellular clearance of gram-negative bacteria, cathepsin G is crucial for resistance against gram-positive infection.[178,179] As crucial element of neutrophil proteolytic machinery, CatG is also responsible for the regulation of inflammatory processes by promoting the production of cytokines and chemokines, which in turn activate and mobilize immune cells to the site of pathogen or tissue damage. However, the activity of CatG, along with HLE and proteinase 3, is tightly regulated in the extracellular and pericellular space by their natural inhibitors in order to prevent degradation of connective tissue proteins. In contrast to HLE and proteinase 3, CatG is inhibited by α1-antichymotrypsin in addition to the common inhibitors α1-proteinase inhibitor, α2-macroglobulin, and secretory leukocyte protease inhibitor.[171] If the levels of CatG exceed their inhibitors, an imbalance can occur which is associated with chronic inflammatory disorders, such as COPD, bronchiectasis, and lung cystic fibrosis. Therefore, the development of inhibitors of CatG represents a promising therapeutic pathway for the treatment of these chronic inflammatory disorders.[165,171]

2 Objectives

Over the last decades, PROTACs have emerged as a promising approach for targeted protein degradation. The VHL E3 ligase is one of the most extensively investigated and commonly utilized E3 ligases for the establishment of novel PROTACs. Therefore, this work aims at synthesizing an alternative and optimized route towards functional VHL E3 ligase ligands in the first step. By addressing the limitations of the reaction procedures from the current literature, the PROTAC community would benefit from an optimized strategy with facile accessibility, enabling an easier development of new PROTACs. Secondly, this work aims to improve the binding affinity of VHL ligands by exploring the largely unexplored SAR of the RHS phenylene core. To achieve this, a library of VHL ligands with high structural diversity at the phenylene core will be combinatorially generated and subsequently evaluated using several biophysical methods. By a structure-guided and bioactivity-driven design, the chemical space of VHL ligands will be explored in order to identify novel compounds with improved binding affinity, offering new avenues for the development of PROTACs.

A further focus of this work is the generation of novel PROTACs that exploit the features of aptamers, thereby constituting a combination of two highly effective technologies. The assembly of such aptamer-addressing PROTACs will involve the incorporation of a GFP-type dye, which becomes fluorescent upon binding to an RNA aptamer. Although fluorogenic RNA aptamers have traditionally been used as imaging tools for genetically encoded domains in living cells, modified aptamers can be employed to target a wide range of proteins and subsequently degrade them by applying the PROTAC technology. Therefore, new aptamer-based PROTACs as a versatile tool for targeted protein degradation will be developed.

In a further project, a combinatorial approach will be conceived to identify substrate-analogue inhibitors for therapeutically relevant serine proteases, including thrombin, factor Xa, matriptase, elastase, and cathepsin G. The approach will utilize diketomorpholines as key intermediates, which will be generated using solid-phase synthesis. By cleaving them with primary amines under bioassay-compatible conditions, a library of compounds will be produced that can be directly subjected to *in situ* evaluation, enabling a rapid identification of hit compounds. The identified potent compounds will then be synthesized as authentic compounds and screened for their inhibitory effect *via* enzyme kinetic studies. This project will contribute to the establishment of an innovative method for accessing new potential drug candidates.

3 A Facile Synthesis of Ligands for the von Hippel-Lindau E3 Ligase

Christian Steinebach, Sabine Anna Voell, Lan Phuong Vu, Aleša Bricelj, Izidor Sosič, Gregor Schnakenburg, Michael Gütschow

Synthesis **2020**, *52*, 2521−2527. doi: 10.1055/s-0040-1707400

Please refer to Appendix I for the publication's full text and supporting information.

Publication Summary

Proteolysis-targeting chimeras (PROTACs) constitute an emerging technology that gained increasing importance in drug development in recent years.[73,180,181] These heterobifunctional small molecules consist of the target binding moiety and the E3 ubiquitin ligase recruiting ligand, connected by a chemical linker. Besides the remarkable achievements in academic PROTACs research,[182–185] this innovative approach is increasingly gaining traction in clinic and industry.[186,187] For this strategy to selectively degrade target proteins *via* ubiquitin-proteasome system, E3 ubiquitin ligases such as the VHL are key parts in the PROTAC field.[33,39–42,44,188]

In this project, the focus was on developing an efficient and optimized synthetic route to various VHL ligands.[189] At the same time, a synthetic protocol for producing multigram quantities of the essential PROTAC building block was envisaged. In the last years, numerous access points for the attachment of linkers to a VHL ligand have been unveiled by the extensive exploration of the E3 ligase.[5,190] Among them, two linker connection points have been successfully established and were widely used in the PROTAC community.[191–193] On the one hand, several VHL ligand portions were connected *via* an amino bond after the amino acid *tert*-leucine to the linker. This type of ligand is based on the prototypical ligand VH032. On the other hand, a linkage *via* a phenolic group at the RHS phenylene core of the VHL ligands was introduced, demonstrating an alternative option. The synthesis towards the ligands of type VH032 of previously published literature started with the palladium-catalyzed Heck coupling reaction between 4-bromobenzonitrile and 4-methylthiazole.[38] Sodium borohydride and cobalt chloride were then used to reduce the resulting aromatic nitrile to the benzylamine. However, both critical steps were proven to be cumbersome since cobalt chloride, an additive to coordinate nitriles and activate them towards the reduction by sodium borohydride,[194] led to black

precipitate which could not be removed by filtration, thus impeding the extraction and purification steps. In addition, the excess usage of sodium borohydride as reducing agent causes an enormous release of hydrogen gas, making it difficult to handle large reaction scales. To overcome these limitations, a new route starting from commercially available 4-bromobenzaldehyde was established. The reductive amination reactions were carried out using *tert*-butyl carbamate as nitrogen source and triethylsilane as the hydrogen source.[195] This key step, performed under very mild conditions, enabled the development of a scalable synthetic approach for the preparation of protected benzylamines with desired substitution patterns. The next step comprised a Heck coupling with 4-methylthiazole, whereby the Boc-amino group was demonstrated to be compatible as the respective biaryl building block was obtained. Both steps, *i.e.* the reductive amination and Heck coupling, resulted in fair to excellent yields. The Boc-amino groups were then deprotected and used in further steps for the synthesis of VHL ligands as described previously. To avoid side reactions that occur in amide coupling reactions as an undesired acylation of the phenolic moiety,[68,191] a protecting group was introduced. *tert*-Butyldiphenylsilyl chloride (TBDPSCl) was utilized as an appropriate protecting group since it is stable under a variety of conditions and yet labile for deprotection. This orthogonally protecting strategy allowed for HATU-promoted amide coupling reactions leading to VHL precursors that can be utilized for the design of PROTACs using exit vectors at the phenolic position.[184] The silyl protecting group can be easily removed by fluorine reagents, such as tetrabutylammonium fluoride (TBAF),[196] leading to the envisaged phenolic VHL ligands. Despite requiring two additional steps, this new route improved the synthesis by avoiding side reactions and yet giving good to excellent yields.

In conclusion, a highly efficient protocol for synthesizing large quantities of VHL ligands has been established. This synthetic route was developed to prepare several precursors to assemble both established and new VHL ligands and provided various advantages over previous procedures. Due to its facile and straightforward synthesis, this strategy allows for a high level of structural diversity within new tailored VHL ligands, thereby enhancing further advancements in this growing field. In addition to the key entry steps towards VHL ligands, a new protecting group strategy was devised for the synthesis of phenolic VHL ligands.

Author Contribution

For this publication, my main contribution was dedicated to the synthesis of around half of the precursors and final compounds. Apart from the design of each compound to be synthesized, I analyzed the data, evaluated the NMR spectra, and compiled my results for insertion into this publication. Additionally, I supervised the internship students Hannes Buthmann, Deborah Schlipphack, and Nicole Schmitt for parts of this projects.

4 Expanding the Structural Diversity at the Phenylene Core of Ligands for the VHL E3 Ubiquitin Ligase Development of Highly Potent HIF-1α Stabilizers

Over the past few years, numerous VHL inhibitors have been developed and have shown continuous improvement through structure- and SAR-based optimization. However, the SAR of the RHS phenylene core has not been explored to its full potential, providing motivation to investigate the chemical space of VHL ligands and enhance their binding affinity. This has been achieved through the generation of a library of VHL ligands with high structural diversity at the phenylene core. The development of such new VHL ligands is described within this chapter.

In the beginning, the cocrystal structure of the ligand VH298 bound to the VCB complex (PDB 5LLI)[33] was utilized for analyzing its binding mode and deriving a 3D structure-based pharmacophore (Figure 17A). This analysis was performed by Dr. Andrej Perdih (University of Ljubljana) and indicated that the RHS region of the ligand exhibited favorable interactions with the hydrophobic probe, and the buriedness contour also demonstrated the capability of this

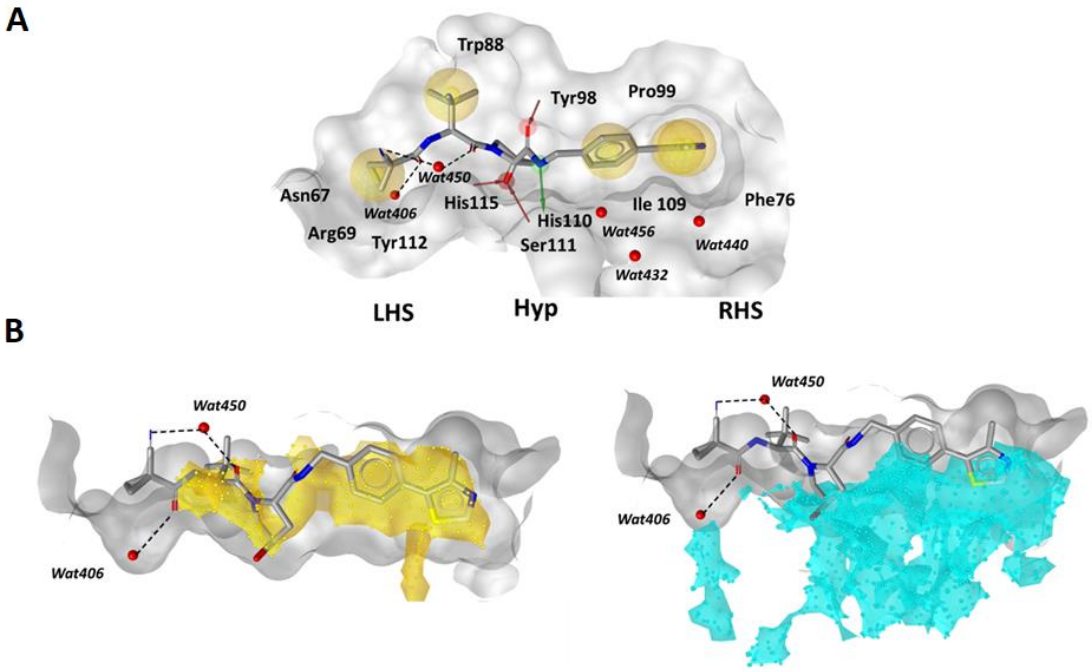

Figure 17. Binding mode of VH298 bound to the VCB complex. (A) Structure-based pharmacophore of the VH298 ligand bound to VCB complex. Red and green arrows denote hydrogen bond acceptors and donors, respectively, and yellow spheres indicate areas that enter into hydrophobic interactions (PDB 5LLI). (B) Calculated hydrophobic molecular interaction field (yellow) and buriedness area (cyan) in the active site. These docking experiments were performed by Dr. Andrej Perdih (University of Ljubljana).

region to accommodate larger moieties (Figure 17B). Based on these findings, it was intended to introduce structural variability at the phenylene core of VHL ligands, either by incorporating additional substituents or replacing it with bicyclic moieties.

Synthesis of the First Series of VHL Inhibitors

Based on the molecular docking analysis, a first series of new VHL ligands with different substituents at the phenylene core was conceived. To ensure comparability with the parent compound VH298 (**1**) and within the series, the cyanocyclopropyl group on the LHS was maintained. Scheme 1 represents the convergent synthetic route to final compounds **1**-**23**. These ligands were accessed using 4-bromobenzaldehyde derivatives **40**, which were subjected to a triethylsilane-promoted reductive amination with *tert*-butyl carbamate (**39**). This synthetic approach pursued our newly developed protocol described in chapter 3, since the utilized reagents of previous described procedures are limited in structural variability.[189] The resulting intermediates **41** underwent a Heck coupling to generate protected benzylamine derivatives **42**. A broad substitution pattern and thus structural diversity of the first series of VHL ligands was realized by incorporating one or two residues at different positions of the arene and by replacing the benzene moiety with naphthalene or quinoline, which led to compounds **22** and **23** with a bicyclic aromatic substructure. For the LHS part of the ligands, benzyl-protected hydroxyproline (**43**) was converted first to dipeptide **44**, then to intermediate **45** *via* two uronium salt-mediated coupling reactions. After hydrogenolytic cleavage of the benzyl ester, the resulting free acid **46** was combined through an amide bond coupling reaction with the varying RHS building blocks of type **42** to assemble VHL ligands **1**-**23** (Table 1).

However, to access specific precursors of type **42**, extended routes needed to be elaborated (Scheme 2). In order to obtain chloro groups at the 2- and 5-position of the phenylene core, 4-bromo-2,5-dichlorobenzoic acid (**47**) was first subjected to a cross-coupling reaction, resulting in biaryl carboxylic acid **48**. After submitting to a carbodiimide-assisted conversion with *N*,*O*-dimethylhydroxylamine, Weinreb amide **49** was produced. Reductive cleavage with lithium aluminum hydride gave aldehyde **50**, which was then converted in a reductive amination to intermediate **42q** and in a subsequent amide coupling reaction to the corresponding VHL ligand **17**. To achieve a vicinal hydroxy-fluoro disubstitution, 3-bromo-2-fluorophenol (**51**) was coupled with 4-methylthiazole to yield biaryl compound **52**. *Ortho*-formylation of the phenol using magnesium chloride, triethylamine, and paraformaldehyde resulted in salicylaldehyde **53**. Compared to the Reimer-Tiemann reaction, which uses chloroform and a strong base to form a reactive dichlorocarbene,[197] the protocol of Skattebøl and co-workers reported regioselective

Scheme 1. Synthesis of the first series of VHL ligands[a]

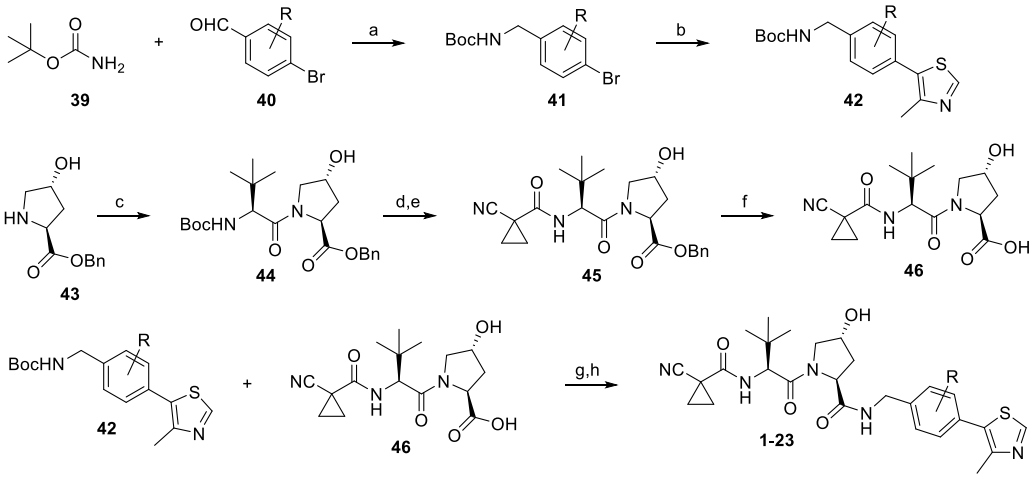

[a]Reagents and conditions: (a) Et_3SiH, TFA, CH_2Cl_2, MeCN, rt, 18 h; (b) 4-methylthiazole, KOAc, $PdCl_2(PPh_3)_2$, dimethylacetamide, 130 °C, 4 h; (c) Boc-Tle-OH, *O*-(7-azabenzotriazol-1-yl)-*N*,*N*,*N*′,*N*′-tetramethyluronium hexafluorophosphate (HATU), DIPEA, DMF, rt, 18 h; (d) TFA, CH_2Cl_2, rt, 2 h; (e) 1-cyano-1-cyclopropanecarboxylic acid, HATU, DIPEA, DMF, rt, 18 h; (f) 10% Pd/C, H_2, EtOH, rt, 18 h; (g) **42**, TFA, CH_2Cl_2, rt, 2 h; (h) **46**, HATU, DIPEA, DMF, rt, 18 h.

Scheme 2. Generation of three precursors for VHL ligands[a]

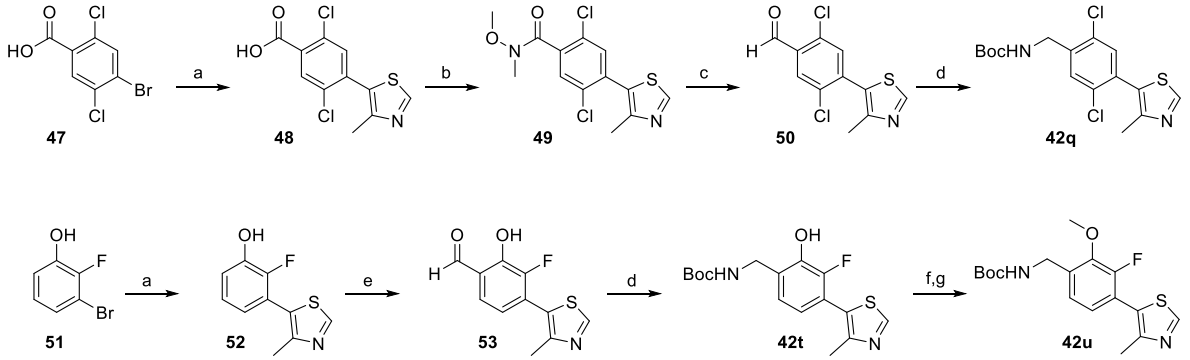

[a]Reagents and conditions: (a) 4-methylthiazole, KOAc, $PdCl_2(PPh_3)_2$, dimethylacetamide, 130 °C, 4 h; (b) *N*,*O*-dimethylhydroxylamine, EDC × HCl, Et_3N, CH_2Cl_2, rt, 18 h; (c) $LiAlH_4$, THF, 0 °C, 1 h; (d) *tert*-butyl carbamate, Et_3SiH, TFA, CH_2Cl_2, MeCN, rt, 18 h; (e) $(CH_2O)_n$, Et_3N, $MgCl_2$, THF, reflux, 18 h; (f) Cs_2CO_3, DMF, 45 °C, 1 h; (g) MeI, DMF, rt, 18 h.

ortho-formylation of substituted phenols using the $MgCl_2$-Et_3N base system *via* a phenoxymagnesium chloride intermediate to give higher yields and fewer by-products.[198,199] After subjecting salicylaldehyde **53** to a reductive amination, the desired intermediate **42t** was obtained, which was reacted in the presence of cesium carbonate *via* an *O*-methylation to the second required intermediate **42u**. Both RHS fragments, **42t** and **42u**, were incorporated into VHL ligands, leading to **20** and **21**. However, alternative attempts to prepare **42q** and **42t** involved the interchanged reaction sequence, where the Heck coupling was performed as last

step, turned out to be unsuccessful and terminated the stage of corresponding bromo-benzylamine of type **41**. In general, the majority of the envisaged first-series VHL ligands were synthesized successfully, with the exception of four substitution patterns (Scheme 3).

Scheme 3. Unsuccessful transformations of 4-bromobenzylamine derivatives to Heck coupling products of type **42** because of low conversions (functional group tolerance) or limited starting material[a]

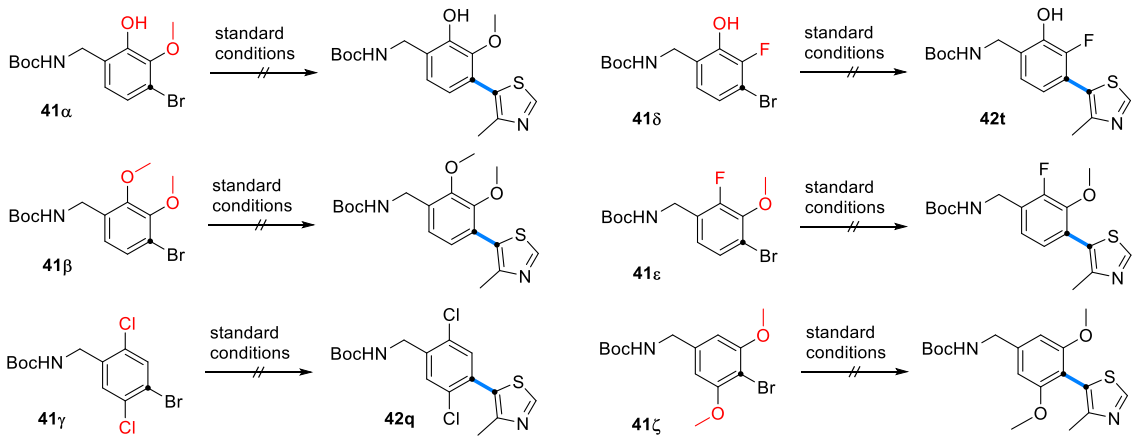

[a]Standard conditions: 4-methylthiazole, KOAc, $PdCl_2(PPh_3)_2$, dimethylacetamide, 130 °C, 4 h.

Biophysical Evaluation of the First-Series VHL Inhibitors

With the obtained VHL inhibitors **1**-**23** in hands, first biophysical experiments were performed to determine the binding affinities. Competitive fluorescence polarization (FP) assay with the first-series VHL inhibitors were carried out by Dr. Adam Bond (University of Dundee). This assay is based on the principle that binding of a ligand to the HIF binding site of VHL leads to the displacement of a fluorescein-labeled, 19-mer HIF-1α oligopeptide, causing a change in polarization of emitted light upon excitation of the competing fluorescent probe. The FP measurements (Table 1) revealed that ligand **8** exhibited the highest binding affinity to VHL (K_d = 97 nM). Interestingly, the binding affinity of **8**, which have a fluorine atom at the R^2 position, was increased by 1.5-fold when compared to the established VHL inhibitor VH298 (**1**). However, the binding affinity of other substituents at this position, such as those present in compounds **6**, **7**, and **9**, which are larger than fluorine, were reduced. Compounds **2**-**5**, which are monosubstituted at the R^1 position, resulted in K_d values below 300 nM, with the methyl derivative **2** showing the highest potency (K_d = 149 nM) in this row. As the R^1 position is a suitable linker attachment point in VHL-addressing PROTACs, the R^1 substitution was expected to be tolerated.[5,68,190,191] In contrast, compounds **10**-**13** bearing two residues, R^1 and R^3 at positions adjacent to the benzylic moiety, exhibited the weakest binding among the series, potentially due to reduced molecular flexibility. Compounds **14**-**17**, which have substitutions

in R^2 and R^3 *para* to each other on the phenylene core, showed an unfavorable effect, which might be due to a steric clash of R^2 with the methylthiazole, thereby preventing the optimal dihedral angle for the bioactive conformation. In this context, it is important to note that when two substituents (R^1 and R^3 or R^2 and R^3) are positioned on opposite sides of the arene, one of them would point towards the protein and potentially induce a clash with amino acid residues that form the pocket. Upon comparing the ligands **10**-**17**, we observed that the difluoro derivative **16**, which had the smallest substituents, was better tolerated than ligands with larger substituents. This suggests that steric hindrance resulting from larger substituents may impact the optimal conformation of the ligand and its ability to interact with the protein effectively. However, the correlation between the affinity of ligands **18**-**21** and their R^1-R^2 disubstitution pattern was not clear. Ligands with fluorine at the R^2 position but varying substituents at R^1 showed unexpected differences in their affinities, with ligands **19**, **20**, and **21** exhibiting lower affinities compared to ligand **8**. Upon further analysis, we hypothesized that the vicinal difluoro substitution in **19** may have caused an unfavorable electron withdrawing effect, leading to reduced efficiency of a T-stacking with Tyr98. In protein-ligand binding events, a T-stacking edge-to-face interaction is favored, where the hydrogen of one aromatic system is oriented perpendicular to the center of another aromatic plane.[200,201] The ligands **22** and **23** featuring bicyclic arylidene cores exhibited similar moderate affinity to VHL since it is likely that their additional aryl ring is pointing out towards the solvent.

Overall, these results revealed that the modifications at the phenylene core did not significantly improve affinity, encouraging for the design of a second series of VHL ligands. Since fluorine appeared to be the most promising among the introduced substituents, this substituent was considered in the second series. Furthermore, compound **2** and **8** from the first series were selected as promising structure to be investigated for their ability to stabilize HIF-1α in a cellular context (see below).

In addition to the kinetic data of the FP measurements, Table 1 provides parameters on physicochemical properties (lipophilicity at physiological pH, $logD_{7.4}$) and pharmacokinetic properties (plasma protein binding, PPB), which were experimentally obtained by means of HPLC-based protocols.[202,203] These experiments were performed by Dr. Christian Steinebach (University of Bonn). The data were provided to estimate the drug-likeness of the VHL ligands. As expected, compounds **13** and **17** comprising two chloro substituents showed the highest lipophilicity, while replacing naphthalene of compound **22** with quinoline leading to compound **23** reduced the lipophilicity.

Table 1. Chemical structures, dissociation constants, distribution coefficients, plasma protein binding properties, and HIF-1α stabilization capabilities of VHL inhibitors **1**-**23**.

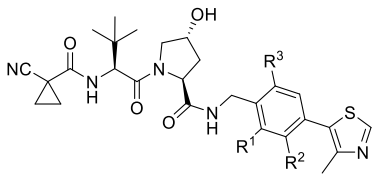

Inhibitor	R^1	R^2	R^3	K_d FP (nM)[a]	e log$D_{7.4}$[b]	PPB (%)[c]
1	H	H	H	129 ± 7[d]	2.3	88
2	Me	H	H	149 ± 28	2.0	90
3	OMe	H	H	183 ± 22	1.9	88
4	F	H	H	297 ± 34	1.9	88
5	Cl	H	H	245 ± 20	2.2	91
6	H	Me	H	496 ± 62	2.0	89
7	H	OMe	H	163 ± 22	1.9	87
8	H	F	H	97 ± 11	1.9	88
9	H	Cl	H	220 ± 11	2.1	91
10	Me	H	Me	4110 ± 560	2.2	90
11	OMe	H	OMe	6240 ± 620	2.0	88
12	F	H	F	2130 ± 150	1.9	86
13	Cl	H	Cl	8150 ± 680	2.4	91
14	H	Me	Me	528 ± 16	2.2	90
15	H	OMe	OMe	1270 ± 150	1.9	86
16	H	F	F	281 ± 46	2.0	88
17	H	Cl	Cl	883 ± 68	2.5	93
18	Me	Me	H	322 ± 38	2.3	91
19	F	F	H	1450 ± 180	2.2	89
20	OH	F	H	141 ± 8	1.9	89
21	OMe	F	H	305 ± 59	2.1	89
22	-CH=CH-CH=CH-		H	397 ± 70	2.3	93
23	-N=CH-CH=CH-		H	330 ± 93	1.7	88

[a] Dissociation constant, determined by FP. Values are mean ± S.E.M. from 3 independent repeats. [b] Experimental distribution coefficient at *p*H 7.4. [c] Plasma protein binding; experimentally determined percentage of compound bound to human serum albumin. [d] Value is the mean ± S.E.M. from 5 independent repeats.

Synthesis of the Second Series of VHL Inhibitors

To achieve an enhanced binding affinity, two additional points of diversity were incorporated into the VHL ligand structure. As the (*S*)-methyl group at the benzylic position VHL-based PROTACs have previously shown to improve VHL binding affinity and also increase target protein degradation potency, a stereochemically defined (*S*)-configured methyl group was added at the benzylic position in the course of the second series.[43–45,185,204] Furthermore, an α-fluoro substituent at the cyclopropyl moiety was included in addition to the cyano group at the LHS terminus, as this modification has already been employed in PROTAC technology, showing improved binding affinity to VHL.[39,185,187,192] These modifications were integrated into our second series of VHL ligands, starting with compounds **2** and **8** as basis for further structural diversification.

A preparative strategy for introducing a (*S*)-configured methyl group at the benzylic position of multisubstituted benzylamine was established in the laboratory of our collaborator, Dr. Izidor Sosič (University of Ljubljana). This strategy started either from the 4-bromobenzoic acids **54** or directly from the corresponding ketones **55** (Scheme 4). When starting from **54**, the acids were converted *via* a Weinreb ketone synthesis by using methylmagnesium iodide to the ketones **55**. For the introduction of the chiral center, a subsequent condensation reaction with Ellman's sulfinamide as chiral ammonia equivalent and with Ti(O*i*Pr)$_4$ as additive, was conducted.[205] The resulting *N*-sulfinyl imines **56** were then subjected to L-selectride-mediated asymmetric reduction, which produced the (*R*,*S*)-configured sulfinamides **57**. In contrast to $NaBH_4$, L-selectride was selected as reducing agent since an opposite sense of inducing is endowed by L-selectride.[206,207]

Scheme 4. Stereoselective introduction of the benzylic methyl group into VHL ligand precursors[a]

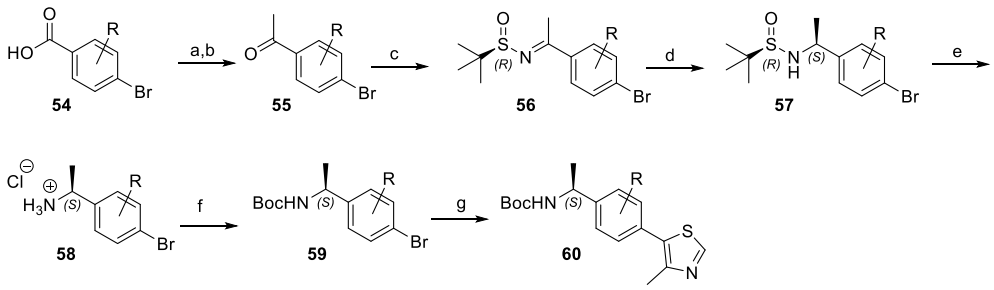

[a]Reagents and conditions: (a) *N*,*O*-dimethylhydroxylamine, *O*-(benzotriazol-1-yl)-*N*,*N*,*N*',*N*'-tetramethyluronium tetrafluoroborate (TBTU), Et_3N, CH_2Cl_2, 0 °C to rt, 18 h; (b) MeMgI, THF, -20 °C to rt, 18 h; (c) (*R*)-(+)-2-methyl-2-propanesulfinamide, Ti(O*i*Pr)$_4$, THF, reflux, 24-48 h; (d) L-selectride, THF, 0 °C, 3 h; (e) HCl in dioxane, rt, 2 h; (f) Boc_2O, $NaHCO_3$, EtOAc, H_2O, 0 °C, 2 h; (g) 4-methylthiazole, KOAc, $PdCl_2(PPh_3)_2$, dimethylacetamide, 130 °C, 4 h.

The auxiliary in **57** was easily removed under mildly acidic conditions and resulted in ammonium chlorides **58**. After Boc-protected and Heck coupling with 4-methylthiazole, building blocks **60** were generated. An exemplary compound of type **59** was submitted to X-ray crystallography, which confirmed the (*S*)-configuration at the benzylic position. Particular representatives of type **60** (Scheme 5) were conceived, which contain a fused cycloaliphatic ring in order to induce structural rigidity in these compounds. To preserve the stereogenic center in the part of a fused ring, the same enantioselective synthetic strategy was applied. Finally, the five-step route, starting from the partially hydrogenated indenone (n = 1) or naphthalenone (n = 2) derivatives **55e-g**, gave the bicyclic building blocks **60e-g**. This approach allowed an efficient introduction of the desired (*S*)-configured methyl group, and enabled the insertion of particular substitution pattern at the phenylene core.

Scheme 5. Synthesis of enantiopure bicyclic VHL ligand precursors[a]

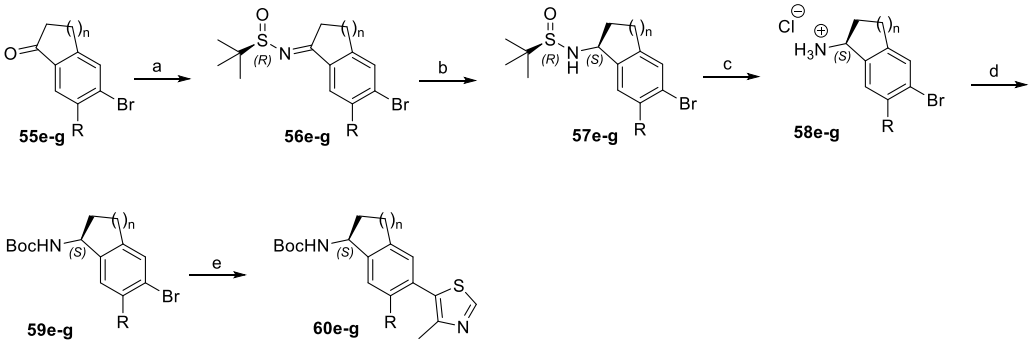

[a]Reagents and conditions: (a) (*R*)-(+)-2-methyl-2-propanesulfinamide, $Ti(OiPr)_4$, THF, reflux, 24-48 h; (b) L-selectride, THF, 0 °C, 3 h; (c) HCl in dioxane, rt, 2 h; (d) Boc_2O, $NaHCO_3$, EtOAc, H_2O, 0 °C, 2 h; (e) 4-methylthiazole, KOAc, $PdCl_2(PPh_3)_2$, dimethylacetamide, 130 °C, 4 h.

For the modification of the LHS, where the cyanocyclopropyl is replaced by fluorocyclopropyl group, dipeptide **44** was couple to 1-fluoro-1-cyclopropanecarboxylic acid (Scheme 6). After deprotection of ester **61**, the free acid **62** was afforded. The last step included the convergent synthesis of the LHS and the RHS fragment to the second-series VHL ligands, which led to the final compounds **24**-**38**. These ligands were generated through a combinatorial approach using either RHS fragments **42** (23 examples) or **60** (8 examples), and LHS fragments **46** or **62**.

Scheme 6. Synthesis of the second series of VHL ligands[a]

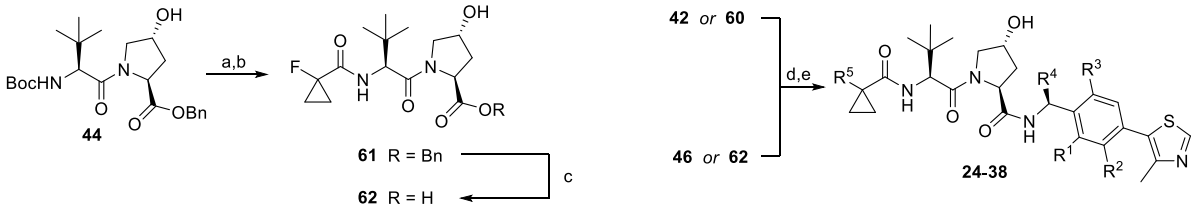

[a]Reagents and conditions: (a) TFA, CH_2Cl_2, rt, 2 h; (b) 1-fluoro-1-cyclopropanecarboxylic acid, HATU, DIPEA, DMF, rt, 18 h; (c) 10% Pd/C, H_2, EtOH, rt, 18 h; (d) **42** *or* **60**, TFA, CH_2Cl_2, rt, 2 h; (e) **46** *or* **62**, HATU, DIPEA, DMF, rt, 18 h.

Biophysical Evaluation of the Second-Series VHL Inhibitors

To investigate whether the second-series VHL inhibitors demonstrated improved binding affinity, FP measurement was conducted with compounds **24**-**38** (Table 2). The replacement of the terminal cyano group with a fluoro substituent led to an improvement in VHL affinity in most cases (**26** *versus* **2**, **30** *versus* **24**, **31** *versus* **25**), even in case of the reference compounds (**38** *versus* **1**). Only compound **27** containing a fluoro substituent at the R^2 position showed unfavorable effects (**27** *versus* **8**). Compounds **24** and **25** featured a (*S*)-configured methyl group at the benzylic carbon and thus are the methylated analogs to **2** and **8**. However, only **24** exhibited an increase in binding affinity (**24** *versus* **2**). By comparing the FP data of **30**-**33** with those of their non-methylated analogs **26**-**29**, the positive effect of (*S*)-methylation was consistent in all four cases and revealed VHL ligands with K_d values lower than 80 nM. Notably, based on the results of FP assays,[38,39,44] compound **30**, exhibiting a K_d value of 37 nM, was found to be one of the most potent VHL ligands discovered to date (Figure 18A). The compounds **34**-**37**, which contained an alkyl bridge from the benzylic carbon to the adjacent phenylene carbon, displayed reduced affinity with K_d values higher than 1 µM, resulting from the structural rigidity induced by the bridge (**36** and **37** *versus* **31**).

In the subsequent step of our study, we decided to perform an orthogonal approach to access the VHL-ligand interaction of eight chosen compounds (**26**-**33**). To do so, a direct binding assay, surface plasmon resonance (SPR), was employed (Table 2). The biotinylated VCB protein was immobilized on a sensor chip that was functionalized with streptavidin, which enabled the real-time measurements of the changes in the refractive index upon ligand binding to the protein.[39] The measured SPR data were basically consistent with the results from the FP assay. Among the eight compounds, ligand **30** exhibited the highest affinity to VHL with an SPR-derived K_d value of 25 nM (Figure 18B).

Table 2. Chemical structures, dissociation constants, distribution coefficients, plasma protein binding properties, and HIF-1α stabilization capabilities of VHL inhibitors **1**, **2**, **8** and **24**-**38**.

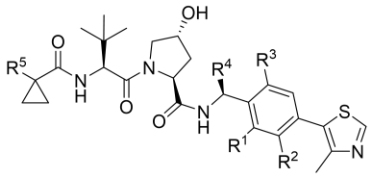

Inhibitor	R^1	R^2	R^3	R^4	R^5	K_d FP (nM)[a]	K_d SPR (nM)[b]	HIF-1α stabilization (%)[c]		HIF-1α-OH stabilization (%)[d]		e log$D_{7.4}$[e]	PPB (%)[f]
								HeLa	HEK293	HeLa	HEK293		
1	H	H	H	H	CN	129 ± 7	52[g]	100	100	100	100	2.3	88
2	Me	H	H	H	CN	149 ± 28	n.d.[h]	89	78	88	66	2.0	90
8	H	F	H	H	CN	97 ± 11	n.d.	83	18	74	20	1.9	88
24	Me	H	H	Me	CN	86 ± 20	n.d.	155	90	221	110	2.3	88
25	H	F	H	Me	CN	186 ± 40	n.d.	105	48	123	52	2.2	88
26	Me	H	H	H	F	112 ± 29	41 ± 10	116	78	120	69	2.2	89
27	H	F	H	H	F	162 ± 45	66 ± 3	107	89	108	75	2.1	88
28	H	F	Me	H	F	80 ± 23	72 ± 8	124	110	153	76	2.3	90
29	H	F	OMe	H	F	134 ± 35	34 ± 3	95	73	98	68	2.2	88
30	Me	H	H	Me	F	37 ± 10	25 ± 5	182	224	263	208	2.5	88
31	H	F	H	Me	F	73 ± 19	45 ± 6	120	92	177	102	2.3	88
32	H	F	Me	Me	F	53 ± 7	41 ± 1	155	152	217	137	2.5	89
33	H	F	OMe	Me	F	63 ± 9	44 ± 6	128	145	179	137	2.5	89

34	H	H	-$(CH_2)_2$-	CN	3920 ± 420	n.d.	n.d.	n.d.	n.d.	n.d.	2.2	90
35	H	F	-$(CH_2)_2$-	CN	4040 ± 530	n.d.	n.d.	n.d.	n.d.	n.d.	2.3	90
36	H	F	-$(CH_2)_2$-	F	2550 ± 510	n.d.	n.d.	n.d.	n.d.	n.d.	2.3	92
37	H	F	-$(CH_2)_3$-	F	1040 ± 240	n.d.	n.d.	n.d.	n.d.	n.d.	2.6	92
38	H	H	H	H	F	90 ± 10[f]	16[g]	98	104	105	92	1.8	86

[a] Dissociation constant, determined by FP. Values are mean ± S.E.M. from 3 independent repeats. [b] Dissociation constant, determined by SPR. Values are mean ± S.E.M. from 2 independent repeats. [c] HeLa or HEK293 cells were treated with 50 μM of the respective inhibitor, and HIF-1α stabilization levels were detected by Western blotting after 2 h treatment. HIF-1α/tubulin protein ratios were normalized to those observed with inhibitor **1** (100%). Mean values of 2 biologically independent experiments are noted. In the absence of inhibitors, HIF-1α values of 24% (HeLa) and 16% (HEK293) were obtained. [d] HeLa or HEK293 cells were treated with 50 μM of the respective inhibitor, and HIF-1α-OH stabilization levels were detected by Western blotting after 2 h treatment. HIF-1α-OH/tubulin protein ratios were normalized to those observed with inhibitor **1** (100%). Mean values of 2 biologically independent experiments are noted. In the absence of inhibitors, HIF-1α-OH values of 11% (HeLa) and 9% (HEK293) were obtained. [e] Experimental distribution coefficient at *p*H 7.4. [f] Plasma protein binding; experimentally determined percentage of compound bound to human serum albumin. [g] Data from ref.[36] [h] Not determined.

Our investigation revealed that these eight selected compounds exhibited strong affinity as demonstrated by second-order rate constants for the association of the binary complexes, which ranged from 1.0×10^6 $M^{-1}s^{-1}$ to 1.7×10^6 $M^{-1}s^{-1}$ (Table 3). The similarly high association rate constants and dissociation half-lives between 8 to 20 s further reflected the potency of these ligands. These kinetic data were consistent with previously investigated structurally related VHL ligands, further emphasizing the robustness and accuracy of our approach.[33,39]

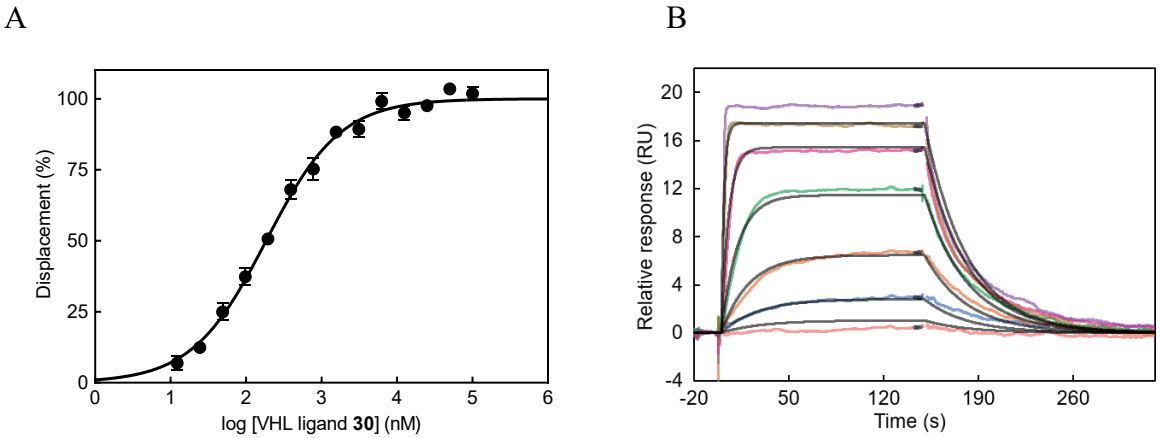

Figure 18. Biophysical characterization of binary complex formation between inhibitor **30** and VCB. (A) Competitive FP binding assay curve, monitoring the displacement of the labeled HIF-1α peptide from VCB by inhibitor **30**. Data show mean ± S.E.M. from one representative experiment in triplicate. (B) SPR sensorgrams monitoring real-time interaction of immobilized biotin-VCB protein with **30** (from top to bottom, 1000 nM, 330 nM, 110 nM, 37 nM, 12.3 nM, 4.12 nM, 1.37 nM). Association and dissociation rate constants are listed in Table S1. Data was fitted to a 1:1 binding model.

Table 3. Second-order on-rate constants for association (k_{on}), and first-order off-rate constants for dissociation (k_{off}) for selected VHL ligands determined by SPR. Data are means of duplicate measurements.

Inhibitor	k_{on} ($M^{-1}s^{-1}$)	k_{off} (s^{-1})
26	1.68×10^6	6.15×10^{-2}
27	1.29×10^6	8.00×10^{-2}
28	1.32×10^6	4.19×10^{-2}
29	1.00×10^6	7.08×10^{-2}
30	1.41×10^6	3.55×10^{-2}
31	1.69×10^6	8.75×10^{-2}
32	1.12×10^6	5.54×10^{-2}
33	1.38×10^6	6.72×10^{-2}

In addition to the above-mentioned biophysical assays, Table 2 presents also the results of cellular, physicochemical, and pharmacokinetic assays obtained with **1**, **2**, **8**, and **24**-**38**. According to the logD values, the bicyclic derivative **37** displayed the highest lipophilicity among the tested compounds, which was already expected based on its structure. The cellular assays will be discussed within the next sections.

X-ray Crystallographic Analyses of Selected VHL Inhibitors

By considering our docking approach and previously reported studies, the substitution of the cyano group with fluorine did not significantly affect the binding mode, as both groups occupied a similar position in the LHS subpocket. Moreover, high affinity VHL ligands with both terminal cyanocyclopropyl and fluorocyclopropyl moiety were reported. Regarding the contribution of (*S*)-configured methyl group, our results, which demonstrated the methylated derivatives to be more potent than the desmethylated counterparts, were in line with other studies.[43–45] Nonetheless, certain VHL ligands with an unmodified benzylic position also exhibited high affinity for VHL,[33,38,39,190] leading to the assumption that a tailored combination of diverse structural features is necessitated to optimize ligand affinity.

Table 2 presents a range of potent VHL ligands, all featuring either hydrogen or fluorine as R^2 moiety. This led to the hypothesis that bulky and sterically demanding substituents may not be well tolerated at this position, potentially hindering rotation around the aryl-aryl axis. Notably, the R^1 methyl group of **24**, the R^2 fluoro substituent of **32**, and the R^3 methoxy group of **33** were found to be solvent exposed, while the R^3 methyl group of **32** and the R^2 fluoro substituent of **33** were directed toward the protein. However, to gain insight into the binding mode of these high-affinity ligands, X-ray crystallographic analyses were performed.

Three compounds, **30**, **33**, and **37**, were selected to be co-crystalized with the VCB complex. Ligands **30** and **33** were two of the most potent ones, while **37**, featuring a bicyclic moiety, showed a significant decreased affinity. The compounds were soaked into VCB crystals and ligand-bound crystals were successfully generated. The structures were obtained at 2.6 Å (**30**), 2.4 Å (**33**), and 2.9 Å (**37**) resolutions (Figure 19) and were solved by molecular replacement and refined by Dr. Ryan Casement (University of Dundee). In addition to the generation of the high-resolution crystal structures, one- and two-dimensional dihedral angle coordinate scans of these three compounds (Figure 20) were performed by Dr. Ryan Casement (University of Dundee) using MacroModel.

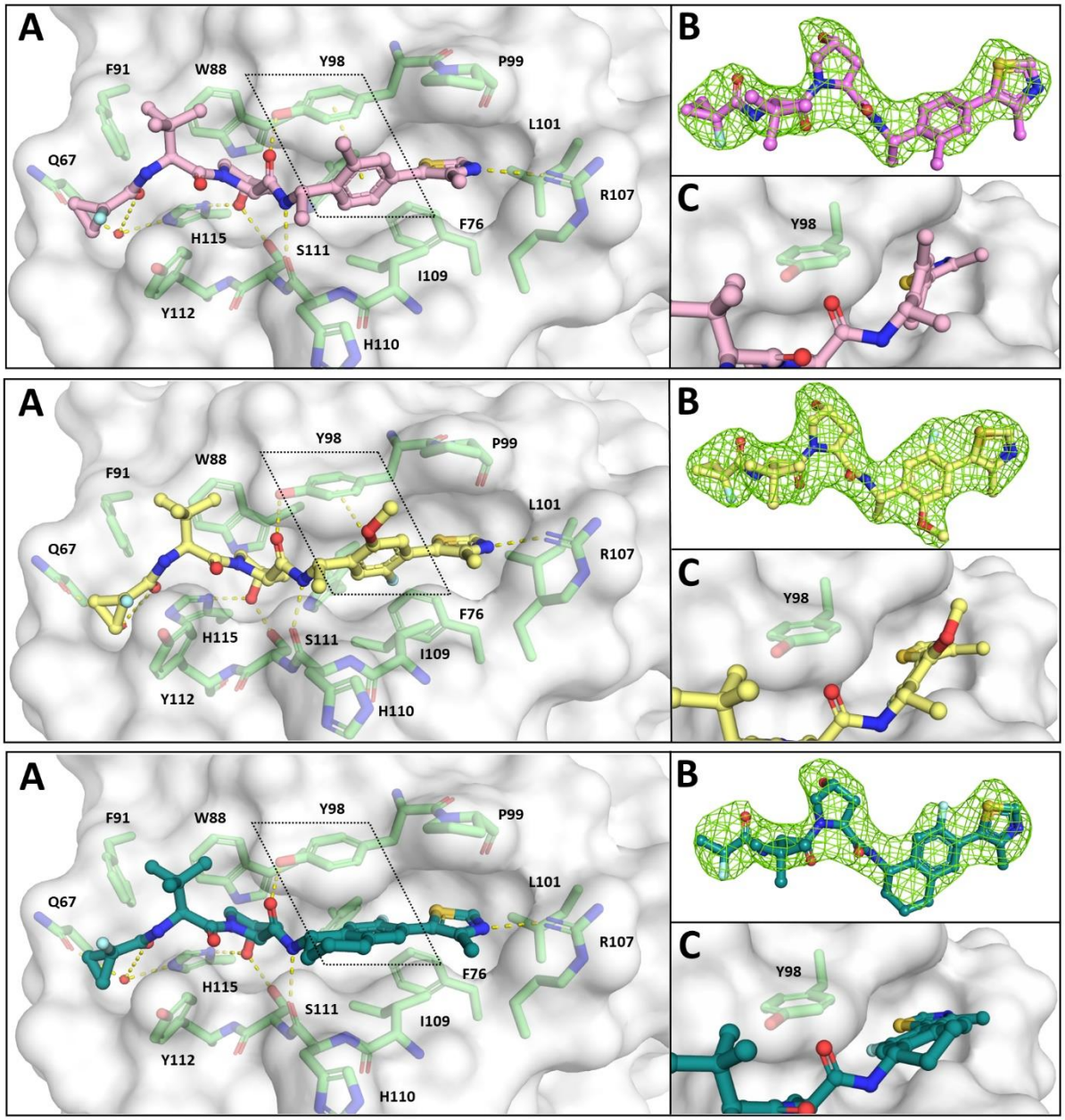

Figure 19. Crystal structures of VCB in complex with ligands **30** (top), **33** (middle) and **37** (bottom). (A) Overall binding mode with VHL shown as a white surface and green sticks, the key π-π interaction of the RHS is highlighted. (B) A polder OMIT map (F_o-F_c) is shown in green contoured at 3σ around each ligand. (C) A close-up view of the phenylene core and Tyr98, highlighting the relative positions of both aromatic rings. These co-crystal structure analyses have been performed by Dr. Ryan Casement (University of Dundee).

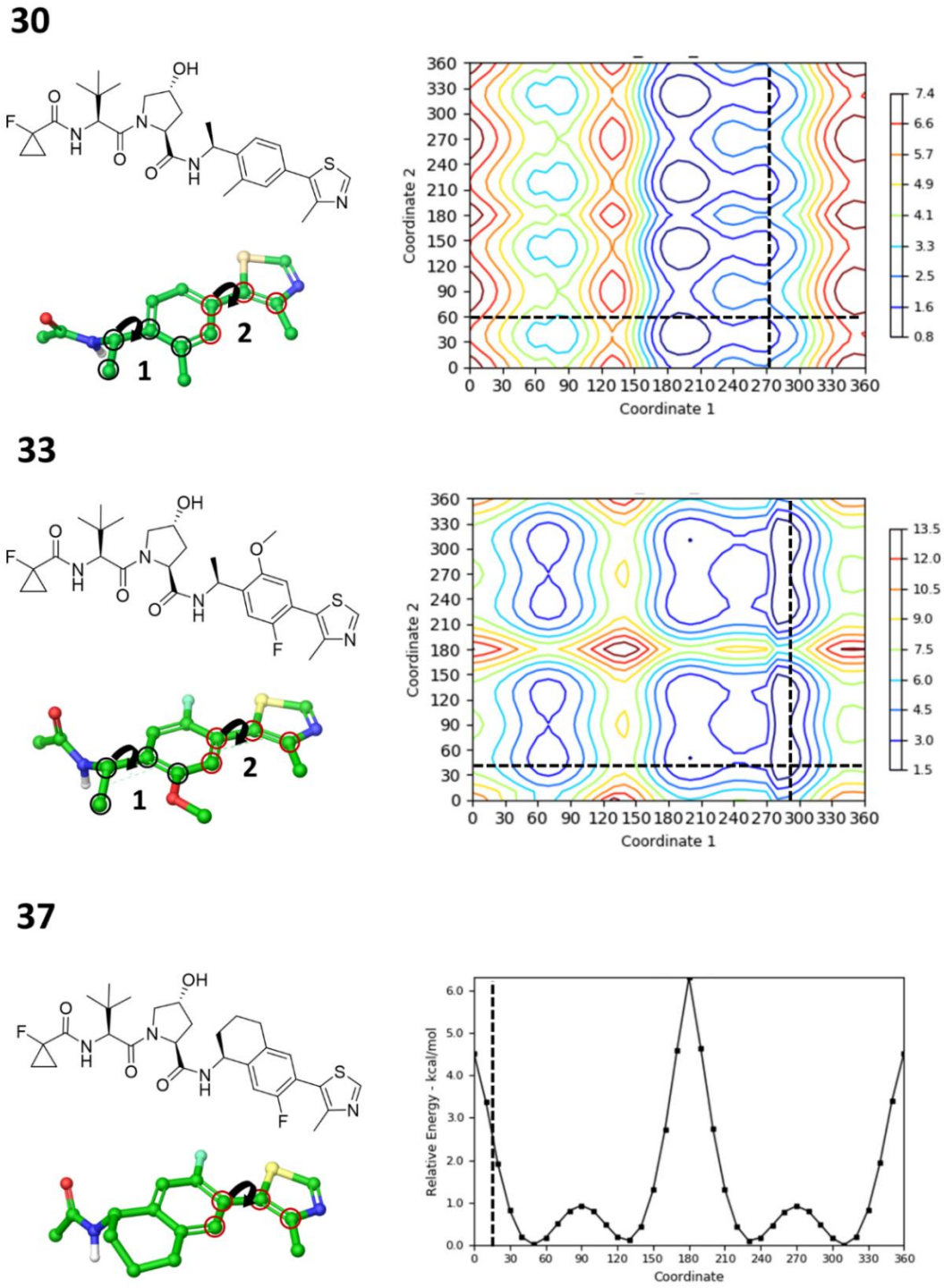

Figure 20. Two- and one-dimensional dihedral angle coordinate scans (MacroModel) compared to measured experimental dihedrals around the phenylene core. The color code of the 2D scans refers to relative energy (kcal/mol). The average of experimental values from the 4 protomers in each asymmetric unit is depicted by a dashed line. Viewing direction is from right to left. The direction of rotation is counterclockwise for a given dihedral. For both rotations (1 and 2), the front part of the structure is the rotator, the back part the stator. At 0°, the indicated atoms are in one plane. Average dihedral values: compound **30** (271°, 60°), compound **33** (290°, 41°), compound **37** (15°). These experiments have been performed by Dr. Ryan Casement (University of Dundee).

All of these compounds followed the expected binding mode for hydroxyproline-based VHL ligands and maintained key interactions with the protein at the LHS. Furthermore, the co-crystal structures revealed that phenylene core of the best compound **30** (Figure 19, top) was positioned perpendicular to Tyr98, allowing for an optimal T-shaped π-π interaction.[200,201] The three methyl groups of **30** were found to be oriented towards the solvent and did not participate in any specific interactions with the binding site of the protein. This observation suggested that they did not influence the dihedral angles significantly. As a result, the measured dihedral angles around the phenylene connection to both the benzylic carbon (271°) and the thiazole carbon (60°) were very similar to the calculated minima (Figure 20). Consequently, it can be inferred that this particular region of the ligand had been preorganized optimally into a conformation that facilitated T-stacking with Tyr98, while still maintaining the binding mode of the methylthiazole moiety. The crystallographic complex obtained with **33** revealed dihedral angles at the phenylene core, which were similarly to the experimentally obtained dihedral angles (290° and 41°) and were also within the same range as in the complex with **30**. Additionally, the crystal complexes with both **30** and **33** were found to be located at the minimum energy regions (Figure 20). However, the T-stacking angle of **33** was slightly offset, likely due to the fluorine atom pointing towards the protein surface, preventing a more perpendicular orientation. Noteworthy, the methoxy group located opposite to the fluoro substituent was orientated in the same direction as the methyl group of compound **30**. On the other hand, compound **37** was found to be a much weaker binder with 17 and 28 times less binding affinity than compounds **33** and **30**, respectively. This was reflected in the crystal structure (Figure 19, bottom), where the T-stacking interaction was entirely absent, attributing to the rigid structure of the bicyclic ring system. The methylthiazole and phenylene planes were almost coplanar with a dihedral angle of 15° that was determined to be energetically unfavorable. Thus, these results highlight the crucial role of T-stacking interaction with Tyr98 and the advantages that can be achieved by preorganizing the protein-bound ligand in a low-energy conformation.

Determination of the HIF-1α Stabilization by VHL Inhibitors

The last experiments of this project aimed to determine whether selected ligands could inhibit the activity of VHL in a cellular environment. In total, 14 ligands were tested, all of which had an FP-derived K_d value lower than 200 nM. The cellular assay was based on blocking the HIF-1α-OH binding site of VHL by using a synthetic ligand, which competes with endogenous HIF-1α-OH protein and prevents ubiquitination, resulting in an accumulation of HIF-1α-OH.

The ability of the inhibitors to stabilize HIF-1α was evaluated in HeLa and HEK293 cells by determination of the remaining HIF-1α protein levels through Western blotting analysis. The cells were treated with an inhibitor concentration of 50 μM for 2 hours, and the results were normalized to reference compound **1** (VH298). These conditions were adapted from previous studies with related VHL inhibitors.[33,39] Primary antibodies against HIF-1α and HIF-1α-OH were used, however, the HIF-1α antibody used in the experiment was not specific to Pro564 hydroxylation, and therefore could bind to both HIF-1α and HIF-1α-OH.[33] Since the cells were exposed to normoxic conditions, Pro564 hydroxylation continued to occur, generating HIF-1α-OH, which will accumulated when VHL inhibitors block the binding site at VHL. On the other hand, the HIF-1α-OH antibody interacts only with HIF-1α-OH.[33]

All of the investigated compounds showed HIF-1α stabilization activity when compared to the DMSO control, with the majority of them outperforming the reference compound **1** (Table 2). A clear SAR could be derived from this study, which were consistent with the results obtained from FP and SPR studies. Notably, ligand **30** emerged as the most promising candidate, as it caused a maximum increase in HIF-1α and HIF-1α-OH protein levels in both HeLa and HEK293 cells (Figure 21). Among the four best HIF stabilizers, three inhibitors, **30**, **32**, and **33**, stood out. These inhibitors were 1.3- to 2.6-fold more potent than reference compound **1**, which indicated the excellent cellular activity of the new inhibitors. Since the used anti-HIF-1α antibody did not distinguish between hydroxylated and non-hydroxylated HIF-1α species, an increase of overall HIF-1α abundance was observed in the immunoblotting data. However, when the specific anti-HIF-1α-OH antibody was employed, consistent data were obtained (Figure 21). The increase in HIF-1α-OH level can be attributed to two interconnected events, on the one hand, the inhibition of VHL-catalyzed ubiquitination and subsequent proteasomal degradation, and on the other hand, the ongoing generation of HIF-1α-OH by PHD under normoxic conditions. In general, the capability of a compound to stabilize HIF-1α is influenced by their cell permeability. However, in most of the inhibitors, there was a strong correlation between binding affinity and cellular potency, which indicated that permeability was not significantly affected by subtle structural changes (Figure 22A). In a previous report, it was observed that the phenylene-unsubstituted compound **38** (VH101) was a highly effective inhibitor of VHL.[39] In order to compare the cellular activity of the ligands, this benchmark compound was taken into consideration. Compound **30** was demonstrated to be 2 times more potent than **38**, in both HeLa and HEK293 cells, as well as in terms of HIF-1α and HIF-1α-OH stabilization. Consequently, VHL inhibitor **30** constitutes the most efficient low-molecular-weight HIF-1α stabilizer to date.

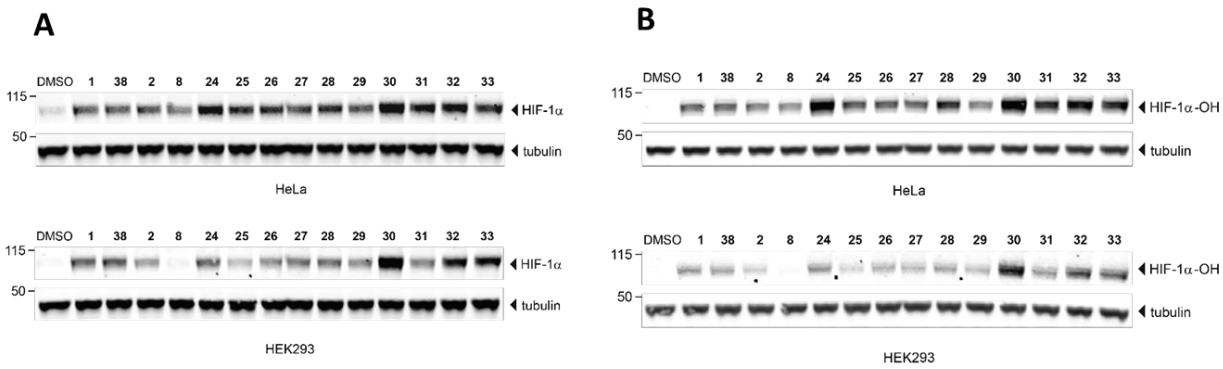

Figure 21. (A) Representative immunoblots of HIF-1α stabilization in HeLa and HEK293 cells treated with 50 μM of selected VHL inhibitors and 1% DMSO for 2 h. A primary antibody against HIF-1α was used. (B) Representative immunoblots of HIF-1α-OH stabilization in HeLa and HEK293 cells treated with 50 μM of selected VHL inhibitors and 1% DMSO for 2 h. A primary antibody against HIF-1α-OH (Pro564) was used. The Western Blot experiment of HIF-1α stabilization has been performed by Dr. Claudia Diehl (University of Dundee).

Conclusions

In this research project, we aimed at exploring the chemical space of VHL by designing new ligands, with a particular focus on the RHS phenylene part of VH298 analogs. Computational insights into specific VHL-ligand interactions and biodata were obtained to optimize the ligand structures. However, the attempts to modify the substitution pattern at the phenylene core, resulting in the first-series VHL ligands, were not particularly successful, indicating limited potential for structural alterations at this site. Therefore, we extended the points of diversity, which involved replacing the LHS cyano groups with the fluorine groups and introducing (*S*)-configured methyl groups at the benzylic position of the VHL ligand. The approach was not only focused on the ligands' affinity to VHL, as monitored by biophysical techniques, but also on their cellular activity, which was measured by their ability to stabilize the level of HIF-1α.

On basis of the monofluoro substitution pattern of compound **8**, the compounds **25** and **27**, which included either a benzylic (*S*)-methylation or cyano-to-fluoro replacement, were synthesized. These modifications led to lower affinity, but higher capability for HIF-1α stabilization (Figure 22B), suggesting that these compounds may have better cell permeability. By readjusting the second point of diversity, compound **31** was developed with improved properties. In the second design pathway (Figure 22C), we found that both structural modifications were additive and advantageous for both VHL affinity and cellular HIF-1α stabilization. Compound **30**, which exhibited both of these structural features, turned out to be an exceptional VHL inhibitor. This inhibitor has the potential to increase the intracellular level

of HIF-1α, which is a critical regulator in the hypoxia signaling pathway. As such, this inhibitor will be an invaluable tool for the study of this pathway. Moreover, compound **30** could serve as a lead compound for the development of drugs for the treatment of conditions where an adaptive cellular response against hypoxia is needed.

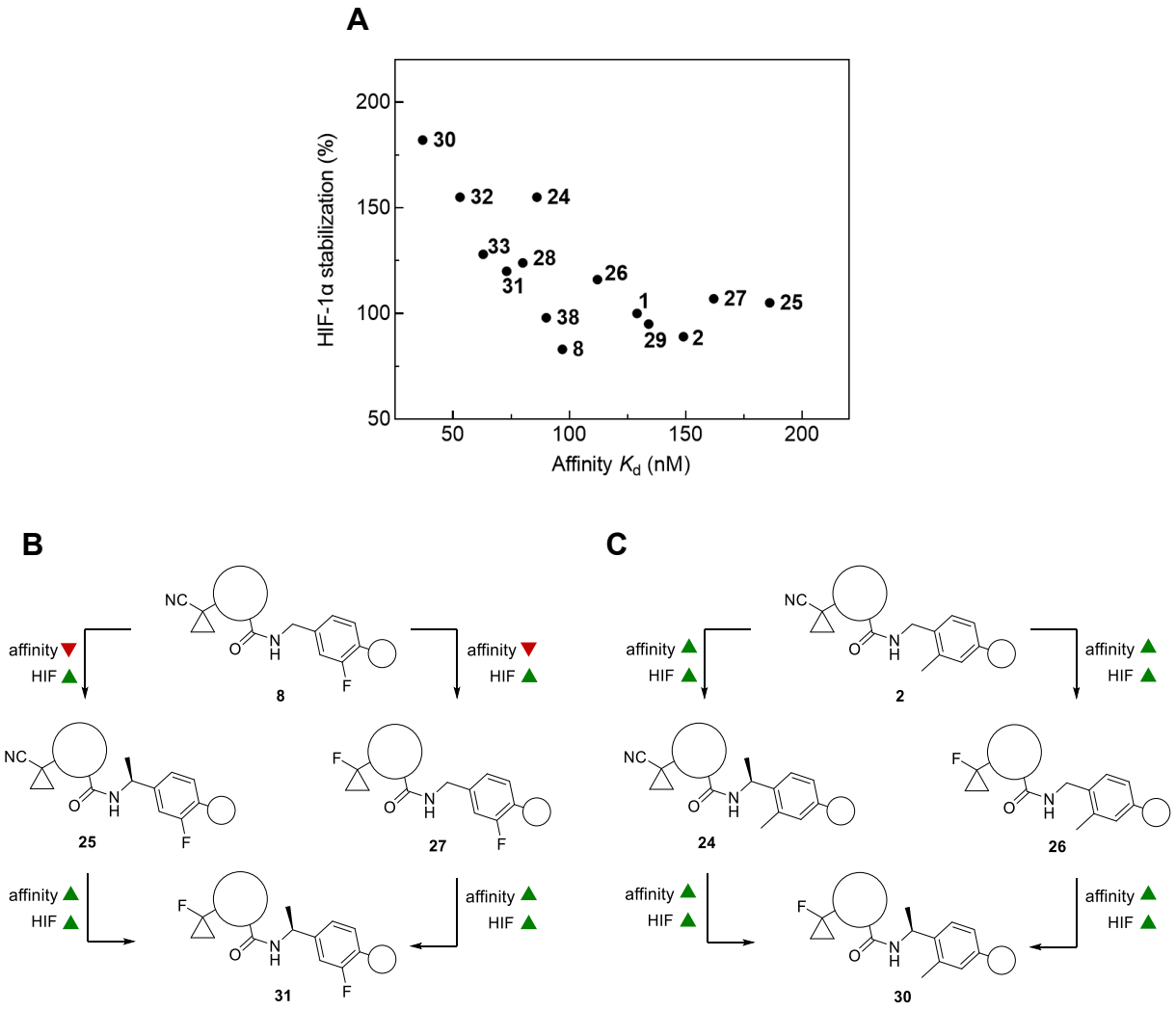

Figure 22. Correlation between the VHL ligands' structure and its binding affinity and HIF stabilization. (A) Correlation of the compounds' binding affinity to VHL as determined by FP and their ability to stabilize HIF-1α in HeLa cells as determined by immunoblotting. (B, C) Bioactivity-driven design pathways to VHL ligands gave rise to (B) compound **31** and (C) compound **30**. Structural optimization is shown regarding (i) FP-derived affinity to VHL and (ii) HIF-1α and HIF-1α-OH stabilization. Circles exemplify the unaltered substructures. Green and red triangles indicate improvement and deterioration, respectively.

In conclusion, we have developed a new VHL ligands with high affinity. In addition to their primary function as inhibitor, such ligands with high structural variability can be utilized to expand the repertoire of VHL-recruiting PROTACs. Since the SAR of ligands that contain a fluoro- or cyanocyclopropyl capping group that blocks the LHS-terminal amino moiety were included in the study, other exit vectors on VHL ligands might be used for the linker attachment, such as a thioether connection at the side chain of *tert*-leucine or an extension of the benzylic methyl group *via* an acetamide portion.[5,190,208] Such approaches have recently emerged as attractive strategies to efficiently hijack VHL and might be pursued in the future PROTAC design by utilizing the structure of the optimized VHL ligand **30**.

Major results of this chapter are included in the following publication: Lan Phuong Vu, Ryan Casement, Adam G. Bond, Christian Steinebach, Nika Strašek, Aleša Bricelj, Andrej Perdih, Claudia J. Diehl, Gregor Schnakenburg, Izidor Sosič, Alessio Ciulli, and Michael Gütschow, Expanding the Structural Diversity at the Phenylene Core of Ligands for the von Hippel-Lindau (VHL) E3 Ubiquitin Ligase: Development of Highly Potent Hypoxia-Inducible Factor-1α (HIF-1α) Stabilizers, submitted.

5 Aptamer-based PROTACs

TPD have emerged as promising technology for both biomedical research and drug discovery. The most representative TPD technique is the PROTAC approach, which hijacks the UPS to degrade targeted proteins. In addition to PROTACs, further TPD-based strategies, such as lysosome-targeting chimeras (LYTACs),[209–211] antibody-based PROTACs (AbTACs),[212] RNA-degrading ribonuclease-targeting chimera (RIBOTAC),[213–216] and autophagy-targeting chimeras (AUTOTACs),[217] have also been demonstrated as successful technologies in degrading a wider range of target proteins, including membrane proteins, extracellular proteins, and protein aggregates. This expanded range of targets offer great potential for further advancement in TPD strategies. Since nucleic acids have various possibilities of biomedical applications, such as gene regulation or drug delivery, nucleic-acid-based drugs have arisen as a new class of therapeutic agents due to their low toxicity, high specificity, and efficiency.[82,218,219] Recently, the development of nucleic-acid-based TPD have emerged as attractive strategies and has gained broad interest.[220] Such PROTACs utilize nucleic acid motifs as warheads and have successfully shown to degraded proteins which lack an accessible ligand-binding pocket, such as RNA-binding proteins and transcription factors.[221–223]

Among these newly introduced TPD strategies based on nucleic acids, several aptamer-based approaches have been developed. Aptamer-PROTAC conjugates (APCs) utilize the properties of aptamers, such as high specificity and affinity, to improve their targeting ability and efficacy compared to conventional PROTACs.[224,225] APCs consist of three components: a PROTAC element that enables the interactions between an E3 ligase and a POI, an aptamer element that aids in selective targeting, and a cleavable linker that releases the original PROTAC intracellularly. A first proof of concept was realized by a tumor-targeting APC, which conjugated a VHL-based BET-targeting PROTAC to the nucleolin-targeting aptamer AS1411 by using an ester-disulfide linker.[224] In addition to the target-specific recognition and drug delivery function of aptamers by fusing them into PROTACs, aptamers were also utilizable as warhead of aptamer-constructed PROTACs. A first nucleolin degrader was developed by conjugating dibenzylcyclooctyne (DBCO)-labeled AS1411 to an VHL-binding ligand, which was demonstrated to be internalized into MCF-7 breast cancer cells and to degrade nucleolin in a VHL-dependent manner.[225] This study revealed that aptamers are feasible to construct PROTACs.

Within this project, the development of a new modality of aptamer-based PROTACs was conceived by utilizing 3,5-difluoro-4-hydroxybenzylidene imidazolinone (DFHBI), a green fluorescent protein (GFP)-mimicking dye (Figure 23). The membrane-permeable, non-fluorescent DFHBI resembles the fluorophore of the GFP and emits green fluorescence when it is bound to the genetically encoded RNA aptamer called Spinach.[226,227] In addition to Spinach, other DFHBI-binding aptamers have also been developed, including the superfolding Spinach2,[228,229] whose fluorescence is brighter in living cells, and iSpinach,[230] which was developed for *in vitro* studies. By analyzing the crystal structure of the Spinach RNA in complex with DFHBI, non-essential regions of the sequence were reduced, which led to truncated versions of Spinach, such as Baby Spinach and the even smaller Broccoli.[231–235] These techniques have been successfully implemented for cellular imaging, including visualization of ribosomal RNA in living mammalian cells, monitoring gene expression, and sensing of intracellular metabolites.[229,236,237]

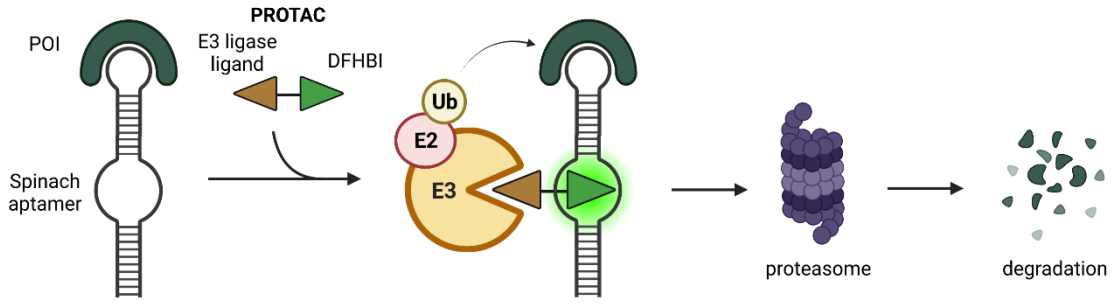

Figure 23. Principle of the mode of action of the envisage aptamer-based PROTAC.

Synthesis of the DFHBI Derivative

Inspired by the features of Spinach fusion RNAs and their broad application spectrum, we envisaged PROTACs with both VHL- and CRBN-recruiting E3 ligase ligands and a DFHBI-labeled warhead. The co-crystalized structure of the Spinach RNA with DFHBI revealed a cleft,[231,238] which is suited as an exit vector for linker attachment. The synthesis of the DFHBI portion was proceeded similarly to the previously described.[226] In a first step, the commercially available 4-hydroxy-3,5-difluorobenzaldehyde (**63**) was reacted with *N*-acetylglycine in the presence of sodium acetate *via* an Erlenmeyer-Plöchl reaction. The cyclization resulted in an oxazolone derivative, which was followed by an acetylation of the hydroxy group generating compound **64** (Scheme 7). The next step involved a nucleophilic attack by the nitrogen of

propargylamine, which induced a ring-opening reaction followed by recyclization to give the clickable compound **65**. Instead of using methylamine, which would lead to the actual DFBHI molecule, propargylamine was employed to introduce a functionalized linker moiety. Such functionalities have often been exploited in the field of medicinal chemistry to perform connecting operations in order to join small molecular building blocks.[239,240] The emerging technique is based on the bioorthogonal labeling method called "click chemistry". Of all the bioorthogonal click reactions that have been developed, the most widely applied is the copper-catalyzed azide-alkyne cycloaddition reaction (CuAAC), which is also referred as to the azide-alkyne Huisgen cycloaddition reaction.[241,242] With regard to the PROTAC development, this reaction has proven effective for a straightforward generation of a PROTAC library with triazole-based linkers by employing an alkyne-functionalized moiety in one ligand and an azide-functionalized moiety in the other.[243]

Scheme 7. Synthesis of a DFHBI derivative[a]

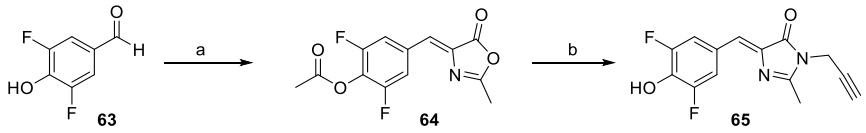

[a]Reagents and conditions: (a) *N*-acetylglycine, NaOAc, Ac_2O, 110 °C, 2 h, 70%; (b) progargylamine, K_2CO_3, EtOH, reflux, 3 h, 10%.

Upon analysis of the overall yield, it was notably low at 7%, arguing for devising an optimized procedure or an alternative route. Since optimization of the conditions, *e.g.* adjusting the solvent, temperature and reaction time, did not improve the reaction, we turned our attention to other potential routes. A four-step synthesis was envisaged, starting from commercially available propargylamine (Scheme 8). After nucleophilic substitution at the carbonyl carbon of acetylchloride, which led to **67**, two further nucleophilic substitution reactions were performed successively. Compound **68** was then subjected to a Staudinger reaction, where the resulting amine underwent an intramolecular carbonyl-amine condensation to **69**. In a last step, 3,5-difluoro-4-hydroxybenzaldehyde was inserted in an aldol condensation with piperidine as a catalyst, leading to the DFHBI derivative **65**. Overall, this route was more laborious than the first one as it contains four steps and, except of the last step, the detection of the product fractions during the chromatographic purification was intricate and required the use of appropriate TLC staining reagents. Additionally, the compounds could only be identified *via* nuclear magnetic resonance (NMR), whereby the identification of compound **68** demonstrated

to be complicated, since the only evidence which distinguished **68** from the its chlorine intermediate was the signal of its α position. Therefore, infrared (IR) spectroscopy was performed to obtain vibrations, which can be unambiguously assigned to an azide or chlorine. The wavenumbers of the absorption of azides are in the range of 2160-2120 cm^{-1} and appears as a strong resonance, whereas halo compounds such as carbon-chlorine absorb strongly at 800-600 cm^{-1}.[244] Despite the increased complexity *en route* to the final compound, this alternative route offered some advantages. The most advantageous argument for proceeding through this route is economical. The most costly material is installed in the last step of the route which delivered the product in an acceptable yield, whereas the preceding steps employ relatively inexpensive starting materials allowing these reactions to be performed in a large scale.

Scheme 8. Alternative route to DFHBI derivative **65**[a]

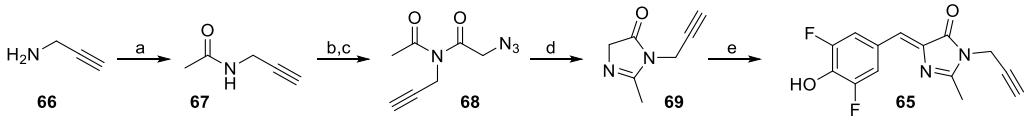

[a]Reagents and conditions: (a) acetylchloride, Et_3N, CH_2Cl_2, 0 °C, 18 h, 66%; (b) (i) 2-chloroacetyl chloride, Et_3N, CH_2Cl_2, rt, 2 h; (ii) NaN_3, DMSO, 40 °C, 12 h, 12% over two steps; (c) PPh_3, $PhCH_3$, rt, 18 h, 33%; (d) 3,5-difluoro-4-hydroxybenzaldehyde, piperidine, $PhCH_3$, rt, 18 h, 67%.

Synthesis of the First Aptamer-addressing PROTACs

For the synthesis of linker tethered E3 ligands, two different E3 ligases, *i.e.* VHL and CRBN ligands, were combined with linkers of different lengths. This approach was conceived, since it was not clear which E3 ligase and which linker length will be appropriate for such aptamer-based PROTACs to trigger selective ubiquitination and a proteasomal degradation event.

To generate VHL-addressing linker conjugates, clickable polyethylene glycol (PEG) linkers of four lengths were synthesized (Scheme 9). The synthesis started either with commercially available PEG-based chloro alcohols **70** or diols **71**. When starting with the diols **71**, the transformation of the alcohol group into sulfonate esters **72** and **73** was achieved by using *p*-toluenesulfonyl chloride (TsCl). Since alcohols have limited reactivity as substrates in nucleophilic substitution reactions, their conversion to tosylate groups significantly enhances their leaving ability due to the possible resonance stabilization, making them an excellent leaving group. To ensure that only the monotosylation of the symmetrical diol occurred, the reaction was performed at the expense of two equivalents of the diol. The sulfonate esters were

then subjected to a S_N2 reaction using sodium azide to provide **76** and **77**. The linker intermediates **74** and **75** comprising of shorter PEG units were generated from compounds **70** *via* nucleophilic substitution using sodium azide in DMF. To convert the azido alcohol into the corresponding *tert*-butyl ester, a Steglich esterification with *tert*-butanol was performed to give the final azide to carboxylate linkers **78**-**81**.

Scheme 9. Convergent synthesis of VHL-addressing linker conjugates[a]

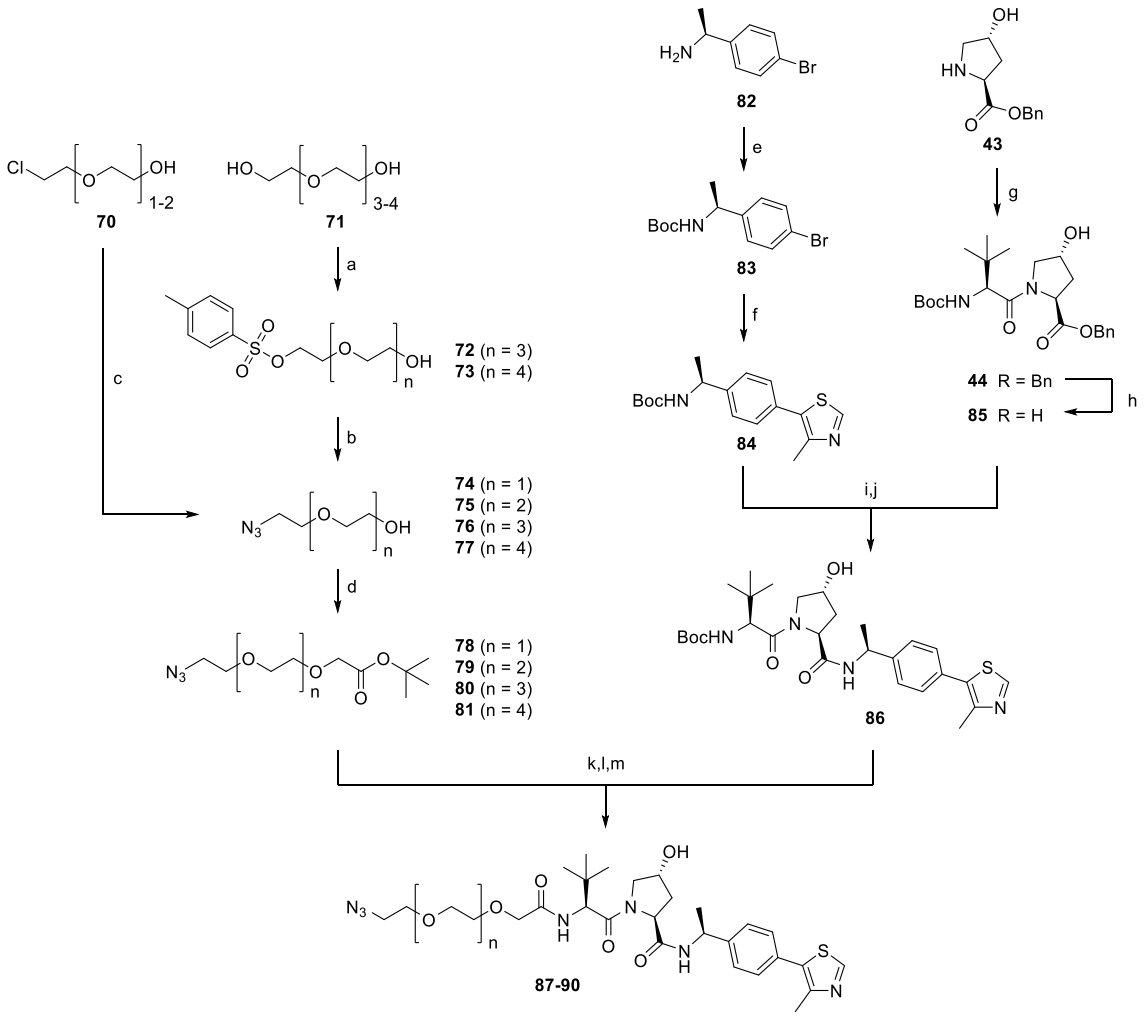

[a]Reagents and conditions: (a) TsCl, Et_3N, CH_2Cl_2, 0 °C to rt, 18 h; (b) NaN_3, DMF, 80 °C, 18 h; (c) NaN_3, DMF, 100 °C, 48 h; (d) *tert*-butyl bromoacetate, TBAHS, NaOH, $PhCH_3$, 0 °C to rt, 18 h; (e) Boc_2O, $NaHCO_3$, H_2O, EtOAc, 0 °C, 2 h; (f) 4-methylthiazole, KOAc, $PdCl_2(PPh_3)_2$, dimethylacetamide, 130 °C, 4 h; (g) Boc-Tle-OH, HATU, DIPEA, DMF, rt, 18 h; (h) **44**, 10% Pd/C, H_2, EtOH, rt, 18 h; (i) **84**, TFA, CH_2Cl_2, rt, 2 h; (j) HATU, DIPEA, DMF, rt, 18 h; (k) **78**-**81**, TFA, CH_2Cl_2, rt, 2 h; (l) **86**, TFA, CH_2Cl_2, rt, 2 h; (m) HATU, DIPEA, DMF, rt, 18 h.

The synthesis of VHL ligand commenced with the usage of (*S*)-1-(4-bromophenyl)ethan-1-amine (**82**) as starting material. After protection with di-*tert*-butyldicarbonate, Boc-protected amine **83** was obtained, which was subsequently subjected to a Heck reaction with 4-methylthiazole, affording the biaryl intermediate **84**. The left-hand side dipeptide moiety was assembled *via* an amide coupling of benzyl-protected hydroxyproline (**43**) with Boc-protected *tert*-leucine, followed by selective cleavage of the benzyl group by a hydrogenolysis using palladium immobilized on charcoal as a catalyst, which produced the free acid of **44**. Convergent HATU-mediated coupling of dipeptide **85** and **84**, yielded VHL ligand **86**. The last step included the Boc-deprotection of both ligand **86** and linkers **78**-**81** and a further amide coupling, giving linker-fused VHL ligands **87**-**90**, which were ready for PROTAC assembly *via* a CuAAC.

The preparation of CRBN-addressing linker conjugates also followed a convergent synthesis strategy (Scheme 10). The four linker building blocks for the CRBN ligands pursued a similar protocol to these described before. In contrast to the synthesis of the linkers for the VHL ligands, the first step involved the ditosylation of the diol which was achieved by adding an excess amount of the tosyl chloride. After performing an azidolysis, reduction to an amine was achieved *via* a Staudinger reaction. Once the linker building blocks were obtained, they were reacted with a fluorinated thalidomide analogue *via* a nucleophilic aromatic substitution (S_NAr) to the linker-fused CRBN ligands **91**-**94**, which were analogous to the linker-conjugated VHL ligand. Compounds **91**-**94** were synthesized and provided by Tim Keuler (University of Bonn).

With the successful generated linker-conjugated VHL- and CRBN ligands, alkyne-azide Huisgen reaction was caried out using sodium ascorbate as a reduction reagent to release catalytically reactive Cu(I) ions from copper(II) sulfate (Scheme 11).

Scheme 10. Convergent synthesis of CRBN-addressing linker conjugates[a]

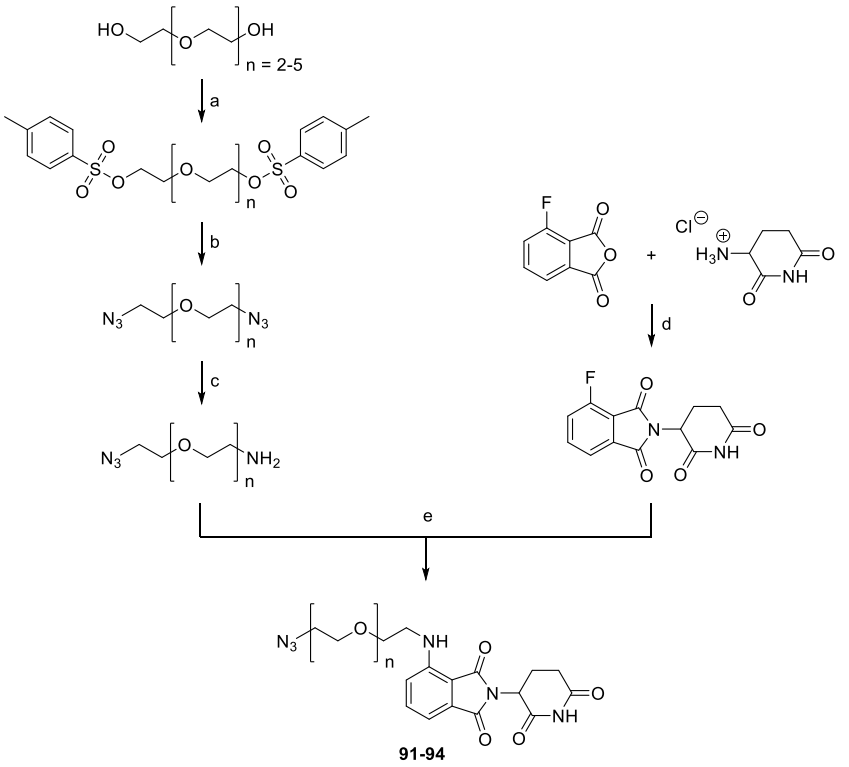

[a]Reagents and conditions: (a) TsCl, Et_3N, CH_2Cl_2, 0 °C to rt, 18 h; (b) NaN_3, DMF, 80 °C, 18 h; (c) PPh_3, THF, H_2O, rt, 18 h; (d) NaOAc, AcOH, 120 °C (reflux), 4 h; (e) DIPEA, DMF, 90 °C, 18 h.

Scheme 11. Final assembly of aptamer-addressing PROTACs[a]

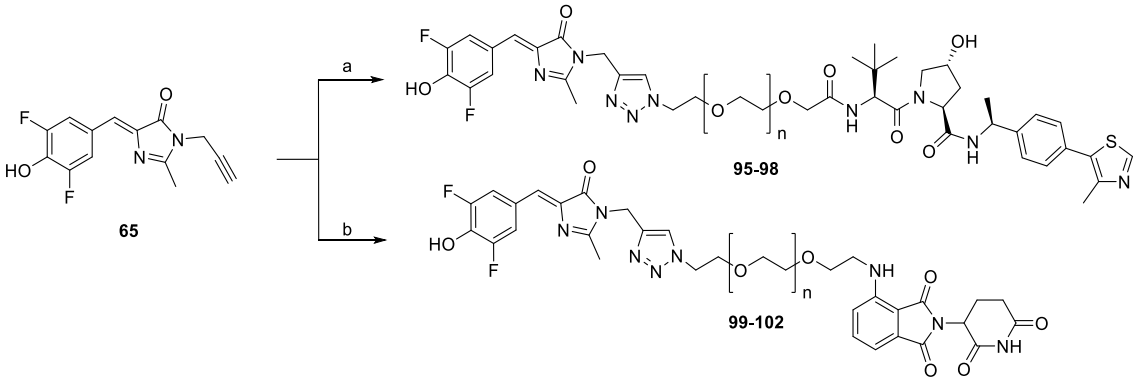

[a]Reagents and conditions: (a) **87-90**, sodium ascorbate, $CuSO_4$, H_2O, THF, rt, 18 h; (b) **99-102**, sodium ascorbate, Cu_2SO_4, H_2O, TFA, rt, 18 h.

Conclusions

In summary, the present study describes the design and synthesis of eight novel VHL- and CRBN-recruiting PROTACs with a DFHBI warhead. The efficacy of these constructs can be assessed through the use of a fluorescent-based assay, wherein an increase in fluorescence is indicative of successful binding to Spinach RNA. This initial validation step would pave the way for further experiments, such as western blot analysis, in order to demonstrate the capability of such a PROTAC molecule to form a quaternary complex and to promote a degradation event. Furthermore, it is essential to synthesize negative controls for the biochemical evaluations to ensure the validity of the results. A common strategy is to modify the ligand of the E3 ligase, for example by inverting the stereocenter of the hydroxyproline of the VHL ligand, which would lead to a decrease in affinity for VHL, or by introducing a *N*-methylated glutarimide portion of the CRBN ligand, which would disrupt the necessary hydrogen-bond network. Overall, valuable PROTAC have been developed, which might have the capability of exploiting aptamers as targets for a directed protein degradation. These novel modalities have the potential to expand the toolbox of chemical degraders and may open new avenues for drug development.

6 Diketomorpholines: Synthetic Accessibility and Utilization

Lan Phuong Vu and Michael Gütschow
ACS Omega **2022**, *7*, 48−54. doi: 10.1021/acsomega.1c05964

Please refer to Appendix II for the publication's full text. This publication, assigned as a mini-review article, provides a summary and gives insights into this thesis' research area based on the contributions of other researchers.

Publication Summary

The family of cyclodepsipeptides, which encompasses a large group of peptide-related natural products, are characterized by the presence of hydroxy and amino acids linked by amide and ester bonds in their molecular structure.[245] Among these compounds, diketomorpholines (DKMs), which are also referred to as cyclodepsidipeptides, represent the simplest members and consist of a six-membered ring bearing both a lactam and a lactone moiety.[245] They exhibit a wide range of biological activities, such as antimicrobial,[246,247] antioxidant,[245,246] immunomodulatory,[245,246] antiproliferative,[245,246] insecticidal,[248] and anti-inflammatory activities.[249] Since the pharmacological potential of these compounds is of particular interest, this review article aimed at providing a comprehensive summary of their structure, synthesis, reactivity and biological properties.

The review article starts out with a general introduction into DKMs, with a main focus on its structure and functional groups within its scaffold.[250] Since numerous methods have been developed for the synthesis of DKMs in recent years, the synthetic approaches were subdivided into solution-phase preparations and polymer-supported methods. For each of the approaches, generalized synthetic routes were described in brief with reference to the original literature. Among the solution-phase synthesis, DKMs are dominantly shown to be accessible through cyclative lactonizations using precursors that already contain a central amide bond. This ring-closure reaction can be either initiated through proton-catalyzed condensations or in the presence of coupling reagents or under Mitsunobu conditions, thereby forming the lactone bond from the free acid.[247,251–257] A further common possibility to achieve DKMs was the lactamization of precursors containing a central ester group.[258–261] Apart from these exemplary solution-phase preparations, there were also various methods to access DKMs by solid-phase

syntheses. One of them is the cyclization of resin-bound precursors, which was treated with trifluoroacetic acid (TFA) leading to the cleavage from the Wang resin and subsequent ring closure to the DKM.[262,263] By considering their reactivity, DKMs have been primarily employed as monomers in ring-opening polymerization reactions to generate polydepsipeptides. These copolymers consist of alternating α-amino and α-hydroxy acids and have desirable attributes like biodegradability and non-toxicity, making them suitable for various applications, such as tissue engineering and drug delivery.[264–267] Unlike polypeptides, polydepsipeptides can be degraded without the requirement of enzymes due to the hydrolytic susceptibility of the ester groups. The carboxamide portions in polydepsipeptides contribute to strong intramolecular hydrogen bond interactions, which influence their mechanical and thermal properties. These properties can be fine-tuned by varying the amino acid components.[264–267] The last section of the review article refers to the occurrence of the DKM scaffold in natural products. DKMs have been reported as natural products, at which monocyclic DKMs from natural sources, but also DKMs as substructures of naturally occurring polycyclic indole alkaloids were found. Several monocyclic DKMs are comprised of two building blocks of enniatin B, a cyclic hexadepsipeptides found in *Fusarium* fungi.[268] Polycyclic natural products typically feature a diketopiperazine ring fused to the five-membered ring of the pyrrolidinoindoline system.[256] However, DKMs have also been observed in certain natural products, where DKM unit has replaced the diketopiperazine core, resulting in tetracyclic compounds, such as mollenines A and B,[269] javanicunines A and B,[270,271] shornephine A,[254,255] and clonorosin A.[272]

Despite its simple structure, DKMs have not received as much attention as expected. Overall, this review highlights a variety of possibilities to synthesize DKMs and their chemical reactivity, particularly in generation of tailored polymers through ring-opening reactions. Additionally, DKM scaffolds are found in natural products, particularly fungal metabolites. These naturally occurring DKMs range from small, monocyclic compounds to complex alkaloids containing a fused DKM structure. However, there is still much to be explored and discovered in the class of DKMs, providing ample opportunities for further research and application.

Author Contribution

For this publication, the literature was scanned to find relevant information for the synthetic accessibility and utilization of diketomorpholines. I designed the outline of the review, analyzed the literature, summarized the synthetic approaches and biological data, and wrote the main text. All schemes and figures were prepared by myself.

7 Combinatorial Assembly, Traceless Generation and *In Situ* Evaluation of Inhibitors for Therapeutically Relevant Serine Proteases

Lan Phuong Vu, Maria Zyulina, Alexandra Hingst, Gregor Schnakenburg, Michael Gütschow
Bioorg. Chem. **2022**, *121*, 105676. doi: 10.1016/j.bioorg.2022.105676

Please refer to Appendix III for the publication's full text and supplementary materials.

Publication Summary

Serine proteases are proteolytic enzymes that play a crucial role in various physiological and pathological processes, such as blood coagulation, hemostasis, immune response, and cell signaling. They have become attractive targets for drug development due to their involvement in numerous diseases. The precise control of serine protease activity is therefore essential for maintaining normal physiological functions. A variety of peptidomimetic serine protease inhibitors, acting both covalently and non-covalently, have already been developed for therapeutic applications.[273–276]

In this study, a combinatorial approach that allows for immediate access to bioactive compounds was devised.[277] These compounds can be directly subjected to biochemical *in situ* evaluation providing a fast prediction of hit compounds. For this approach, DKMs were expected to be appropriate educts for generating bioactive compounds since they are prone to be cleaved with primary amines,[250] resulting in substrate-analogue inhibitors of serine proteases.[156,278–283] The first DKM was assembled from (*S*)-leucic acid and protected (*S*)-proline, which underwent a uronium salt-mediated coupling. The key step to the envisaged DKM was the proton-catalyzed lactonization. Subsequently, test reactions were performed with benzylamine to define the optimal reaction conditions. An exemplary reaction in acetonitrile at 45 °C for 24 h was performed, which generated an aminolyzed diketomorpholine (ADKM) as a first potential inhibitor. X-ray crystallography confirmed the structures of DKM and ADKM, and also revealed the expected *cis* configuration of the amide bond in the DKM structure,[284] which turned to the *trans* configuration when converting into the ADKM structure. To facilitate the reaction and generate a broad range of DKMs a solid phase approach was introduced. Thus, a small library of 18 DKMs were prepared using six different hydroxyl acids and three different

resins, a polymer-bound 2-chlorotrityl proline, a polymer-bound 2-chlorotrityl homoproline, and a Fmoc-protected sarcosine, which was loaded on a Wang resin. These compounds were purified by preparative chromatography and due to their instability in a nucleophilic environment, their purity was confirmed by GC-MS. In order to introduce a third point of diversity, the 18 DKMs were reacted with a selection of 11 primary amines in a further combinatorial approach by using the conditions defined before, resulting in a library of 198 members. These generated AKDMs were designed to constitute the envisaged substrate-analogue inhibitors of serine proteases with a hydroxy acid at P3, an imino acid at P2, and a primary amine with both aliphatic, aromatic, and basic residues at the P1 position. By using equal amounts of both reactants, a traceless ring cleavage reaction with almost complete product conversion was achieved, which allowed the ADKMs to be immediately subjected to enzyme kinetic assays without purification of each compound, enabling an efficient high throughput screening. With this generated library in hand, a screening campaign was carried out on the following five human serine proteases of therapeutic importance: thrombin, factor Xa, matriptase 2, elastase, and cathepsin G. The initial step involved the evaluation of *in situ* generated ADKMs at an apparent concentration of 50 μM. Promising ADKMs were then screened at an apparent concentration of 10 μM, and based on the results, their concentration-dependent inhibition was determined. Guided by these biochemical data, selected ADKMs were synthesized, purified, and characterized as authentic compounds. Following this procedure, a total of eight authentic ADKMs were obtained, which were then subjected to further in-depth kinetic analysis. Among these inhibitors, one demonstrated high activity as a dual inhibitor with a binding affinity of 23.9 nM to thrombin and 32.8 nM to factor Xa.[277]

In summary, this work delineated an innovative combinatorial approach which led to a fast identification of potential drug candidates. By preparing and utilizing DKMs, a bioassay-compatible one-step traceless reaction was accomplishable. Furthermore, this study implies that the approach of the *in situ* evaluation of ADKMs could also be used to identify further candidates with high affinity to other targets than serine proteases. For instance, DKMs could be employed with an electrophilic warhead, such as a nitrile group,[285] by using defined cleaving primary amines. Such a compound library would include members resembling PF-07321332, an inhibitor of the SARS-CoV-2 main cysteine protease, which was developed for COVID-19 treatment.[286]

Author Contribution

Within this project, I took the lead on the investigation including the synthesis of test compounds and the kinetic measurements of human serine proteases, *i.e.* thrombin, factor Xa, matriptase 2, elastase and cathepsin G. All synthetic experiments were performed by myself, whereas the kinetic evaluation comprising of the screening of the combinatorial assembled compounds and the determination of IC_{50} values, was either conducted by myself, or by Maria Zyulina and Alexandra Hingst, both mainly under my supervision. X-ray crystallography to identify the molecular structure of DKM 12 and ADKM 12C was executed by Dr. Gregor Schnakenburg. All other figures and schemes were generated by myself. Finally, I was responsible for the summary of all data and the writing of the manuscript.

8 Summary and Perspective

Many protein functions in cells were regulated by the proteolytic activity of proteases. The process of such proteolysis involves the cleavage of proteins, which leads to protein activation or degradation, resulting in the alteration or impairment of the functionality of cellular proteins. This feature can be exploited to affect specific pathways and to provide valuable insights into the biological function of target proteins in cells. While proteases are known to be the primary enzymes responsible for protein degradation, studies have shown that E3 ligases were utilized to induce proteasomal degradation of target proteins through the UPS. Despite the abundance of E3 ligases, VHL have demonstrated wide applicability for PROTACs. Thus, this thesis was aimed at the development of new VHL ligands for targeted protein degradation, the assembly of novel functional PROTACs, and also the identification of serine protease inhibitors.

The first step of this work was the establishment of a new synthetic route towards VHL ligands. Such an optimized route was realized by introducing the key entry steps of reductive amination and subsequent Heck coupling, allowing for the introduction of attractive substitution patterns. Due to the facile synthesis and purification with a rather good yield, the generation of multigram scales of VHL ligands was enabled. This synthetic route showed clear advantages over previously reported procedures, and a number of precursors for valuable VHL ligands were successfully prepared. It is also highly adaptable for the generation of a wide variety of tailored VHL ligands.

With this highly efficient protocol in hand, new VHL ligands were designed and developed. The strategy for improving the VHL ligand structure was based on the prototypical ligand VH298. To introduce chemical variability into the unexplored RHS phenylene moiety of the VHL ligand structure, thereby providing further adjustable points of diversity, an iterative and combinatorial approach was employed. By combining tailored phenylene fragments with the (*S*)-configured methyl group at the benzylic position, VHL ligands were generated that demonstrated superior binding affinity compared to VH298. To further investigate these ligands, three high-resolution crystal structures of VHL in complex with three new ligands were solved to explore their bioactive conformations. One of the ligands, compound **30**, exhibited the most potent inhibition with dissociation constants (K_d) lower than 40 nM, as independently determined by FP and SPR. The improved binding affinity of compound **30** to VHL was

associated with increased cellular potency, which surpassed the stabilization of HIF-1α by established VHL inhibitors.

As the biophysical and chemical properties of the newly synthesized compounds are characterized in full and exhaustive detail, future research could be expanded by investigating dose-dependent HIF-1α and HIF-1α-OH stabilization for further biological characterization of these molecules. Furthermore, the compounds' ability to promote HIF transcriptional activity can be evaluated by using a luciferase reporter assay, which would demonstrate HIF-dependent luciferase activity and allow monitoring of mRNA levels of HIF-target genes.

Overall, we have developed optimized ligands that represent a promising starting point for the design of PROTACs with VHL as the target protein (Figure 24). Future research may consider the incorporation of ligand **30** into PROTACs equipped with JQ1 for targeting bromodomains.[71] This would result in a PROTAC analogous to MZ1, and potentially a more effective degradation effect could be achieved through improved binding affinity. Although the generation of such a PROTAC would require the replacement of the fluoro capping group of the VHL ligand **30**, a direct comparison to a well-established PROTAC molecule will be enabled. However, it is important to note, that the correlation between binding affinity and degradation efficacy is not clearly proved, since the interplay between the PROTAC and its target proteins, as well as the molecular mechanism of ternary complex formation, is complex and not yet fully understood. Moreover, PROTACs are characterized by their large and flexible molecular structure, which are accompanied with several physicochemical features such as high molecular weight (MW), high topological polar surface area (TPSA), high number of rotatable bonds, and limited solubility and permeability.[287] These properties contradict the Lipinski's Rule of Five, which is a set of physicochemical property guidelines to assess the drug-likeness of a compound.[288] Thus, such degraders were categorized beyond the conventional small-molecule property space into the so-called beyond Rule of Five (bRo5) space.[289] Among these physicochemical properties, MW, logP, and TPSA are considered as key determinants of drug-like properties. However, since PROTACs do not exhibit optimal properties in terms of these parameters, the optimization of the ligand structure may be a viable strategy to enhance the desired properties. For instance, further optimization the VHL ligand, such as reducing the size of the ligand structure, might affect the physicochemical properties of the compound. Furthermore, recent discoveries have identified a new exit vector located at the thiazole that can be utilized for PROTAC design.[49] This discovery might provide new opportunities to modify the VHL ligand at other points. However, it is yet to be investigated whether this exit

vector offers any additional benefits over the traditional approaches in terms of selectivity, degradation activity, and other related properties.

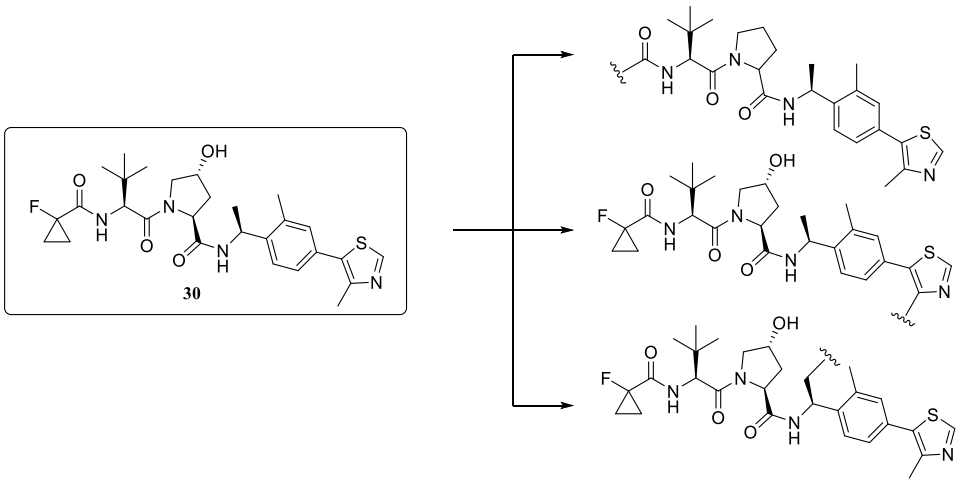

Figure 24. Structure of the optimized VHL ligand **30** and possibilities for its incorporation into a PROTAC molecule with different linker attachment points.

In the subsequent project, a set of eight aptamer-based PROTACs were designed and synthesized. These PROTACs are comprise of either a VHL- or CRBN-recruiting E3 ligase ligand, which is connected by various linkers to the DFHBI fluorophore. Since it is still challenging to find the right E3 ligase for a defined protein of interest, the inclusion of both most commonly used E3 ligases increases the likelihood of identifying the appropriate E3 ligase. Additionally, four different linker lengths ranging from 8 to 17 linear atoms were incorporated to explore the effects of linker length on the complex formation, thereby determining the optimal linker length for this specific type of PROTAC. If the distance between the targeted proteins falls below a certain minimum, it may prevent the formation of a ternary complex and consequently, ubiquitination may not be induced. On the other hand, an oversized linker would lead to an entropically unfavorably higher degree of freedom in the ternary complex formation, which is attributed to its flexibility.[290,291]

In order to further explore this area, future research will involve a series of experimental assays. Firstly, the concept of the newly generated PROTACs should be evaluated using a fluorescence-based technique. Subsequently, immunoblot analysis should be performed to ascertain the degradation activity of these PROTACs. The binding of the PROTAC to the RNA aptamer can be confirmed by observing an increase in fluorescence upon attachment to the Spinach aptamer. As RNA aptamers can be expressed in living cells, an increase in fluorescence would verify their successful intracellular expression, thereby allowing visualization of cellular processes.

To optimize the experimental assay, substitution of the chromophore and Spinach aptamer with the Pepper aptamer could be considered. The Pepper aptamer is known for its brightness and stability as a fluorescent RNA, exhibiting a broad range of emission mission maxima from cyan to red, that can be fine-tuned through a precise choice of excitation wavelengths.[292–294] However, the application of the Pepper aptamer for the proposed approach is currently limited due to its relatively recent development, and may be considered in the later stages of the study. In general, such aptamer-based PROTACs might have promising potential for their application in gene therapeutics.

In the last project, a combinatorial approach was developed for the design and identification of substrate-analogue inhibitors of therapeutically relevant serine proteases. By using solid-phase synthesis, 18 DKMs were generated. These key intermediates were cleaved with primary amines in a traceless manner, producing a compound set of 198 ADKMs by means of the combinatorial approach. The library was generated under bioassay-compatible conditions, which allowed for fast prediction of hit compounds through direct *in situ* evaluation. After performance of a screening campaign with thrombin, factor Xa, matriptase 2, elastase and cathepsin G and in-depth kinetic studies, we successfully identified highly effective serine proteases inhibitors, with the most potent dual inhibitor showing a binding affinity of 23.9 nM to thrombin and 32.8 nM to factor Xa. This project did not only lead to the identification of new serine protease inhibitors, but also introduced a novel approach for identifying drug candidates by using DKMs. These molecules can be easily and efficiently converted into bioactive compounds through a traceless one-step reaction. This approach might be expected to make a valuable contribution to the field of combinatorial methods for drug discovering and identifying bioactive compounds.

9 Experimental Section

9.1 General Methods and Materials

Commercially available starting reagents for each reaction were purchased from ABCR, Acros Organics, BLDpharm, Fischer Scientific, Fluorochem, Merck, Sigma Aldrich, or TCI and used without further purification. All reactions were carried out using anhydrous solvents. Preparative column chromatography was performed on Acros Oragnics silica gel (0.060-0.200 mm, 60 Å) or using an automated flash column chromatography system puriFlash XS520Plus (Interchim, Montluçon, France) with diode-array detection (DAD) from 200 to 400 nm. Thin-layer chromatography was carried out on Merck aluminum sheets, silica gel 60 F_{254}. Detection was performed with UV light at 254 nm or 366 nm. Retention factors (R_f) are indicated. Uncorrected melting points were determined on a Büchi (Essen, Germany) 510 oil bath apparatus. IR spectra were recorded on a Bruker (Ettlingen, Germany) ALPHA-T instrument. ^{1}H NMR and ^{13}C NMR spectra were recorded on a Bruker Avance DRX 500 MHz NMR spectrometer or on a Bruker Avance III 600 MHz NMR spectrometer. NMR spectra were processed and analyzed in MestReNova. Chemical shifts are given in parts per million (ppm), coupling constants *J* are given in hertz (Hz), and standard abbreviations are used to indicate spin multiplicities. In case of rotamers, only the peaks for the major rotamer are given. Assignments were made based on one and two-dimensional NMR techniques, which include ^{1}H, ^{13}C, DEPT, HSQC, and HMBC experiments. LC-MS analyses were carried out on an API 2000 mass spectrometer (AB Sciex, Darmstadt, Germany) coupled with an Agilent HPLC HP 1100 (Santa Clara, CA, USA) using an EC50/2 Nucleodur C18 Gravity 3 µm column (Macherey-Nagel, Düren, Germany) or on an Agilent Infinity Lab LC/MSD-system (Santa Clara, CA, USA) coupled with an Agilent HPLC 1260 Infinity II (Santa Clara, CA, USA) using an EC50/2 Nucleodur C18 Gravity 3 µm column (Macherey-Nagel, Düren, Germany). Samples (1 mg/mL) were dissolved in MeOH containing 2 mM ammonium acetate or H_2O or MeOH or acetonitrile. A volume of 8 µL or 2 µL was injected into the column at 25 °C or 40 °C. Flow rate was 0.3 mL/min or 0.5 mL/min. Unless stated otherwise, the mobile phase was a gradient of 90% H_2O to 100% MeOH containing 2 mM ammonium acetate in 10 min, then 100% MeOH containing 2 mM ammonium acetate to 20 min. The purity was determined by HPLC-DAD. High resolution mass spectrometry (HRMS) spectra were recorded on a Thermo Scientific Q Exactive Plus mass spectrometer (Thermo Fisher Scientific, Dreieich, Germany).

9.2 Fluorescence Polarization Binding Assay

FP competitive binding assays were performed using a PHERAstar FS (BMG LABTECH) with fluorescence excitation and emission wavelengths of λ = 485 and λ = 520 nm, respectively. Assays were run in triplicates of three independent experiments using 384-well plates (Corning 3820), with each well solution containing 15 nM VCB protein, 10 nM 5,6-carboxyfluorescein (FAM)-labeled HIF-1α peptide (FAM-Asp-Glu-Ala-Leu-Ala-Hyp-Tyr-Ile-Pro-Met-Asp-Asp-Asp-Phe-Gln-Leu-Arg-Ser-Phe-NH_2, "JC9"), and decreasing concentrations of VHL ligands (14-point, 2-fold serial dilution starting from 100 μM VHL ligand). All components were dissolved from stock solutions using 100 mM Bis-Tris, 100 mM NaCl, 1 mM DTT, pH 7.0, to yield a final assay volume of 15 μL. DMSO was added as appropriate to ensure a final concentration of 2% (v/v). Control wells containing VCB and JC9 with no compound (zero displacement), or JC9, in the absence of protein (maximum displacement) were also included to allow for normalization. Percentage displacement values were obtained by normalization of controls and were plotted against log[compound]. The IC_{50} values were determined for each titration using nonlinear regression analysis with Prism GraphPad. Dissociation constants K_d were calculated by using a displacement binding model.[16,64]

9.3 Surface Plasmon Resonance

To perform SPR measurements, 10 mM stock solution of VHL inhibitors were diluted 100-fold in DMSO to achieve a 100 μM final stock concentration. The ligand stock solution was diluted in SPR buffer (20 mM HEPES, 150 mM NaCl, 1 mM TCEP, 0.005% Tween 20, pH 7.0) to obtain the final concentration of 2% (v/v) DMSO. Final concentrations from 1 μM to 1.4 nM of the VHL inhibitors were prepared on a 96-well plate (7-point, 3-fold serial dilution starting from 1 μM VHL ligand). The experiments were performed at 20 °C on a Biacore T100 (GE Healthcare, Biacore, Uppsala, Sweden) equipped with a streptavidin-functionalized sensor chip (Series S Sensor Chip SA, Cytiva). The system was flushed with running buffer (20 mM HEPES, 150 mM NaCl, 1 mM TCEP, 0.005% Tween20, 2% DMSO, pH 7.0). Biotinylated VCB protein (50 nM) was immobilized onto the sensor chip at 10 μL/min for using the automated wizard in the T200 control software to reach the required immobilization levels. The solutions were injected individually using 60 and 160 s association and dissociation times, respectively. Reference flow-cell response was subtracted from the sample response with immobilized VCB protein to correct for systematic noise and baseline drift. Data were solvent

corrected by an 8-point solvent correction, and the response from the blank injections was used to double reference the binding data. For determination of binding constants, processed kinetic data were fitted to a 1:1 interaction model using the Biacore Insight Evaluation Software (version 3.0.12.15655).

9.4 Cell Culture and Cell Treatment

HeLa and HEK293 cell lines, purchased from ATCC, were cultured in Dulbecco's modified Eagle's medium (DMEM, Gibco) supplemented with 10% fetal bovine serum (FBS, Gibco), L-glutamine (2 mM, Gibco) and 100 μg mL^{-1} of penicillin/streptomycin (Gibco). All cell lines were maintained in a humidified incubator at 37 °C and 5% CO_2 for no more than 30 passages. Cells were routinely tested for mycoplasma contamination using MycoAlert kit from Lonza. For compound treatment experiments, cells were seeded at 5×10^5 cells/mL (HeLa) and 4.8×10^5 cells/mL (HEK293) in 6-well plates 42 h before treatment. Cells were treated with the indicated compounds at 50 μM concentration or with DMSO as control for 2 h, with a final DMSO concentration of 1% (v/v). After compound treatment, the medium was removed, and the cells were washed with ice-cold phosphate-buffered saline (PBS) and lysed on ice with 100 μL RIPA lysis and extraction buffer (Thermo Fisher Scientific) supplemented with complete EDTA-free protease inhibitor cocktail (Roche). Cells were incubated for 15 min on ice and then detached from the surface by scraping. After removal of the insoluble fraction by centrifugation at 15,000 g at 4 °C for 15 min, supernatants were stored at −80 °C. Protein concentration was determined by bicinchoninic acid (BCA) assay (Pierce).

9.5 Quantitative Immunoblotting

Cell lysates containing a quarter of a volume of 4× NuPAGE LDS sample buffer (NP0007) supplemented with 10% β-mercaptoethanol were heated at 95 °C for 5 min. Samples (30 μg) were loaded onto precast 4–12% bis–tris midi 26W gels (Thermo Fisher Scientific) and resolved at 90 V for 10 min and then 130 V for 1.5 h with a NuPAGE MOPS SDS running buffer (Thermo Fisher Scientific). Proteins were electrophoretically transferred onto a 0.45 μm nitrocellulose membrane (GE Healthcare, Amersham Protran Supported 0.45 mm NC) at 90 V for 90 min on ice in a transfer buffer (48 mM tris base and 39 mM glycine supplemented with 20% ethanol). The transferred membrane was blocked with 5% (w/v) skim milk powder dissolved in tris-buffered saline with Tween (TBS-T) (50 mM tris base, 150 mM sodium

chloride (NaCl), 0.1% (v/v) Tween-20) at rt for 1 h. Western blot images were obtained through detection with anti-HIF-1α (BD Biosciences, #610959, clone 54, 1:1,000) and anti-hydroxy-HIF-1α (Hyp564) (Cell Signaling Technology; #3434, 1:1,000) antibodies. Following overnight incubation with the primary antibodies at 4 °C, the membranes were washed two times for 10 min with TBS-T and then incubated with secondary antibodies (IRDye 800CW donkey anti-rabbit secondary antibody (LI-COR #926-32213, 1:5,000) or IRDye 800CW donkey anti-mouse secondary antibody, (Li-COR #926-32212, 1:5,000) and hFABTM rhodamine anti-tubulin antibody (Biorad, 12004165, 1:10,000)) for 1 h at rt and protected from light. Thereafter, the membranes were washed with TBS-T three times for 10 min, and protein bands were acquired using a ChemiDoc MP imaging system (Bio-Rad). Band quantification was performed using Image Lab software and reported as relative amount as ratio of each protein band relative to the lane's loading control. The values obtained were then normalized to VH298 vehicle control.

9.6 LogD 7.4 Measurement

The determination of the $logD_{7.4}$ values was performed by a chromatographic method as described previously.[41,62] The system was calibrated by plotting the retention times of six different drugs (atenolol, metoprolol, labetalol, diltiazem, triphenylene, permethrin) *versus* their literature known $logD_{7.4}$ values ($R^2 = 0.99$). Subsequently, the mean retention times (n = 2) of the analytes were taken to calculate their $logD_{7.4}$ values.

These experiments were performed by Dr. Christian Steinebach, University of Bonn.

9.7 Plasma Protein Binding Studies

PPB was estimated by correlating the logarithmic retention times of the analytes on a CHIRALPAK HSA 50 × 3 mm, 5 µm column with the literature known %PPB values (converted into logK values) of the following drugs: warfarin, ketoprofen, budesonide, nizatidine, indomethacin, acetylsalicylic acid, carbamazepine, piroxicam, nicardipine, and cimetidine.[63] Samples were dissolved in MeCN/DMSO 9:1 to achieve a final concentration of 0.5 mg/mL. The mobile phase A was 50 mM ammonium acetate adjusted to pH 7.4 with 10% NaOH, while mobile phase B was *i*PrOH. The flow rate was set to 1.0 mL/min, the UV detector was set to 254 nm, and the column temperature was kept at 30 °C. After injecting 3 µL of the

sample, a linear gradient from 100% A to 30% *i*PrOH in 5.4 min was applied. From 5.4 to 18 min, 30% *i*PrOH was kept, followed by switching back to 100% A in 1.0 min and a re-equilibration time of 6 min. With the aid of the calibration line ($R^2 = 0.94$), the logK values of new substances were calculated and converted to their %PPB values.

These experiments were performed by Dr. Christian Steinebach, University of Bonn.

9.8 Crystallization

For VCB crystals, 2 µL of VCB (~5 mg/mL) were mixed with2 µL of liquor solution and grown at rt using a hanging-drop vapour diffusion method. The liquor solutions were composed of 0.1 M sodium cacodylate, pH 6.0-6.3, 15-20% polyethylene glycol 3350, 0.2 M magnesium acetate and 10 mM DTT. Crystals were soaked overnight in 1.25 mM solutions of ligand in 1-10% DMSO, 4-40% isopropanol and 50-95% liquor solution. Crystals did not require further cryoprotection and were flash frozen in liquid nitrogen.

9.9 X-ray Data Collection and Structure Determination

All X-ray data were collected at 100 K at the Diamond (beamline I04) synchrotron facilities. Outputs from the autoPROC pipeline (indexing, integration, scaling, merging) were taken forward for molecular replacement. Molecular replacement, refinement and small molecule restraint generation was carried out using the PHENIX software package.

These experiments were performed by Dr. Ryan Casement, University of Dundee.

9.10 Dihedral Angle Calculations

Torsional energy profiles of the phenylene core of ligands 30, 33 and 37 were calculated with MacroModel (Schrödinger package, version 13.1, OPLS4) using an aqueous solvation model.

These experiments were performed by Dr. Ryan Casement, University of Dundee.

9.11 Illustrations

Figures 1, 2, 5, 8, 9,10, 14, 23 were created using BioRender (http://www.biorender.com).

9.12 Chemistry

9.12.1 General Procedures

General Procedure A. Reductive Amination[189]

tert-Butyl carbamate (**39**, 3 equiv) and the corresponding benzaldehyde derivative **40** (1 equiv) were dissolved in CH_2Cl_2 (2 mL/mmol) and MeCN (6 mL/mmol). Et_3SiH (3 equiv) was added, followed by the dropwise addition of TFA (2 equiv). After stirring for 18 h at rt, the mixture was quenched with saturated aqueous $NaHCO_3$ (10 mL/mmol) and the aqueous layer was extracted with CH_2Cl_2 (3 × 10 mL/mmol). The combined organic phases were washed with brine (10 mL/mmol), dried over Na_2SO_4, filtered, and concentrated *in vacuo*.

General Procedure B. Heck Coupling[183,189]

The corresponding bromoaryl compound **41** (1 equiv), $PdCl_2(PPh_3)_2$ (0.1 equiv), and KOAc (4 equiv) were dissolved in *N*,*N*-dimethylacetamide (5 mL/mmol). 4-Methylthiazole (4 equiv) was added, and the mixture was heated to 130 °C under argon atmosphere for 4 h. Subsequently, the mixture was allowed to cool to rt, diluted with H_2O (25 mL/mmol), and extracted with CH_2Cl_2 (3 × 25 mL/mmol). The combined organic layers were washed with brine (25 mL/mmol), dried over Na_2SO_4, filtered, and concentrated *in vacuo*.

General Procedure C. Boc-deprotection and HATU-promoted Amide Coupling[183,189]

The corresponding Boc-protected amine (1 equiv) was dissolved in anhydrous CH_2Cl_2 (5 mL/mmol), and TFA (5 mL/mmol) was added. The mixture was stirred at rt for 2 h, and then concentrated under high vacuum. The deprotected amine was dissolved in anhydrous DMF (5 mL/mmol), and the appropriate acid (1 equiv) was added. DIPEA (4 equiv) was added, followed by the addition of HATU (1.1 equiv) after 5 min. The mixture was stirred at rt for 18 h, after which H_2O (50 mL/mmol) was added, and extracted with EtOAc (3 × 25 mL/mmol). The combined organic phases were washed with brine (50 mL/mmol), dried over Na_2SO_4, filtered, and concentrated *in vacuo*.

General Procedure D. Preparation of *N*-sulfinyl Imines

The corresponding ketone (1 equiv) and (*R*)-(+)-2-methyl-2-propanesulfinamide (1.5 equiv) were dissolved in dry THF. $Ti(OiPr)_4$ was added, and the mixture was stirred under reflux for 1-2 days. Reactions were monitored by LC-MS. After the reaction was complete, saturated

aqueous NH_4Cl (25 mL/mmol) and EtOAc (25 mL/mmol) were added to the mixture, and phases were separated. After extraction with EtOAc (3 × 25 mL/mmol), the organic phases were combined, washed with brine (25 mL/mmol), dried over Na_2SO_4, filtered, and concentrated *in vacuo*.

General Procedure E. L-selectride-promoted Reduction[206]

The corresponding *N*-sulfinyl imine (1 equiv) was dissolved in dry THF (10 mL/mmol) and was cooled to 0 °C. L-selectride (1.0 M in THF, 3 equiv) was slowly added and the solution was allowed to warm to rt over a 3 h period. The solution was then concentrated under high vacuum. CH_2Cl_2 (25 mL/mmol) and 10% aqueous citric acid (25 mL/mmol) were added to the residue, and after separation of the phases, the organic phase was washed with brine (25 mL/mmol), dried over Na_2SO_4, filtered, and concentrated *in vacuo*.

General Procedure F. Deprotection of Sulfinamides

The corresponding sulfinamide (1 equiv) was dissolved in dry dioxane and HCl (4 M in dioxane, 3 equiv) was added. After stirring for 2 h at rt, the suspension was concentrated *in vacuo*. Then, Et_2O (25 mL/mmol) was added to the residue, the product was filtered off and washed with Et_2O.

General Procedure G. *N*-Boc Protection

The corresponding amine (1 equiv) was dissolved in H_2O (5 mL/mmol). $NaHCO_3$ (1.1 equiv) and a solution of Boc_2O (1.6 equiv) in EtOAc and H_2O (1:1) were added to the mixture at 0°C. After stirring for 2 h at 0°C, the phases were separated, and the organic phase was washed with saturated aqueous $NaHCO_3$ (25 mL/mmol) and brine (25 mL/mmol), dried over Na_2SO_4, filtered and concentrated *in vacuo*. The product was used in the next step without further purification.

General Procedure H. Click Reaction

The linker-conjugated E3 ligase ligand (1 equiv) was weighted into a 10 mL vial and sodium-L-ascorbate (0.2 equiv), copper(II) sulfate × 5 H_2O (0.2 mmol), DFHBI derivative 65 were added. The reaction mixture was treated with THF (1 mL/0.1 mmol) and H_2O (1 mL/0.1 mmol) and vigorously stirred under argon atmosphere for 16 h at rt. After concentration under high vacuum, the crude product was purified *via* flash column chromatography using a gradient from 0 to 20% MeOH in CH_2Cl_2.

9.12.2 Compounds

(2*S*,4*R*)-1-((*S*)-2-(1-Cyanocyclopropane-1-carboxamido)-3,3-dimethylbutanoyl)-4-hydroxy-*N*-(4-(4-methylthiazol-5-yl)benzyl)pyrrolidine-2-carboxamide (1)

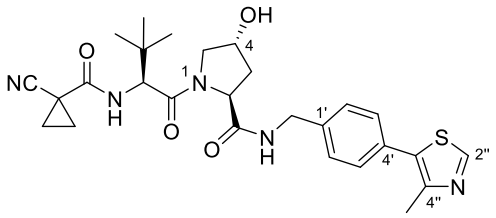

This compound was synthesized and provided by Dr. Christian Steinebach, University of Bonn.

(2*S*,4*R*)-1-((*S*)-2-(1-Cyanocyclopropane-1-carboxamido)-3,3-dimethylbutanoyl)-4-hydroxy-*N*-(2-methyl-4-(4-methylthiazol-5-yl)benzyl)pyrrolidine-2-carboxamide (2)

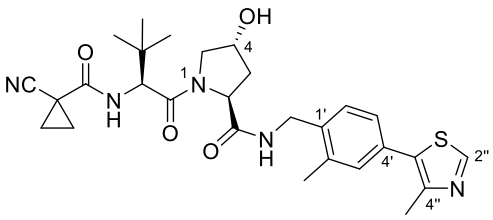

Following General Procedure C, compound **2** was obtained using Boc-protected amine **42b** (type **42**, R = 2-Me; 127 mg, 0.4 mmol) and acid **46** (135 mg, 0.4 mmol). The residue was purified by flash column chromatography using a gradient from 0 to 10% MeOH in CH_2Cl_2 to afford **2** as a white solid (48 mg, 22%).

mp 164-166 °C; R_f = 0.50 (CH_2Cl_2/MeOH 9:1); ^{1}H NMR (600 MHz, DMSO-d_6) δ 0.95 (s, 9H, $C(CH_3)_3$), 1.46 – 1.53 (m, 2H, CH_2CCN), 1.58 – 1.66 (m, 2H, CH_2CCN), 1.88 – 1.94 (m, 1H, 3-H), 2.03 – 2.10 (m, 1H, 3-H), 2.30 (s, 3H, CH_3), 2.44 (s, 3H, CH_3), 3.12 – 3.16 (m, 1H, 5-H), 3.60 – 3.65 (m, 1H, 5-H), 4.22 (dd, J = 15.5, 5.4 Hz, 1H), 4.31 – 4.37 (m, 2H), 4.47 – 4.54 (m, 2H) (2-H, 4-H, NHC<u>H</u>, NHC<u>H</u>$_2$), 5.14 (d, J = 3.7 Hz, 1H, OH), 7.23 (dd, J = 7.9, 1.9 Hz, 1H), 7.28 (d, J = 2.0 Hz, 1H), 7.35 (d, J = 8.9 Hz, 1H), 7.41 (d, J = 7.8 Hz, 1H) (Ar-H, CONH), 8.49 (t, J = 5.7 Hz, 1H, CONH), 8.97 (s, 1H, 2″-H); ^{13}C NMR (126 MHz, DMSO-d_6) δ 12.4, 13.7

(C̲H2CCN), 15.9 (CH2C̲CN), 16.7 (CH3), 18.1 (CH3), 26.1 (C(C̲H3)3), 36.2 (C̲(CH3)3), 37.9 (C-3), 41.8 (NHCH2), 56.6, 57.3, 58.7 (C-2, C-5, NHCH), 68.9 (C-4), 120.1 (CN), 126.1, 127.9, 129.8, 130.3, 131.1 (C-3′, C-4′, C-5′, C-6′, C-5″), 136.4 (C-2′), 136.9 (C-1′), 147.6 (C-4″), 151.3 (C-2″), 164.4, 168.6, 171.4 (CO). LC-MS (ESI) (90% H_2O to 100% MeOH in 10 min, then 100% MeOH to 20 min, DAD 220-400 nm), t_R = 10.70 min, 95% purity, *m/z* calcd for $C_{28}H_{35}N_5O_4S$ $[M + H]^+$, 538.25; found, 538.6. HRMS (ESI) *m/z* calcd for $C_{28}H_{35}N_5O_4S$ $[M + H]^+$, 538.2482; found, 538.2482.

(2*S*,4*R*)-1-((*S*)-2-(1-Cyanocyclopropane-1-carboxamido)-3,3-dimethylbutanoyl)-4-hydroxy-*N*-(2-methoxy-4-(4-methylthiazol-5-yl)benzyl)pyrrolidine-2-carboxamide (3)

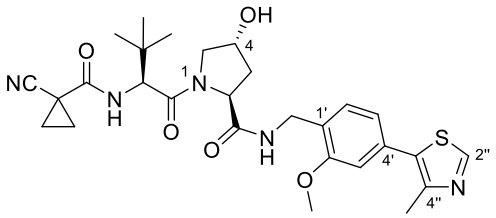

Following General Procedure C, compound **3** was obtained using Boc-protected amine **42c** (type **42**, R = 2-OMe; 100 mg, 0.3 mmol) and acid **46** (101 mg, 0.3 mmol). The residue was purified by flash column chromatography using a gradient from 0 to 10% MeOH in CH_2Cl_2 to afford **3** as a white solid (23 mg, 14%).

mp 168-170 °C; R_f = 0.50 (CH_2Cl_2/MeOH 9:1); ^{1}H NMR (600 MHz, DMSO-d_6) δ 0.95 (s, 9H, C(CH3)3), 1.46 – 1.53 (m, 2H, CH2CCN), 1.59 – 1.66 (m, 2H, CH2CCN), 1.89 – 1.94 (m, 1H, 3-H), 2.05 – 2.10 (m, 1H, 3-H), 2.47 (s, 3H, CH3), 3.56 (d, *J* = 10.8 Hz, 1H, 5-H), 3.63 (dd, *J* = 10.8, 3.9 Hz, 1H, 5-H), 3.85 (s, 3H, OCH3), 4.18 – 4.30 (m, 2H), 4.31 – 4.36 (m, 1H), 4.48 – 4.54 (m, 2H) (2-H, 4-H, NHC̲H, NHC̲H2), 5.14 (d, *J* = 3.6 Hz, 1H, OH), 6.96 (dd, *J* = 7.7, 1.6 Hz, 1H), 7.01 – 7.04 (m, 1H), 7.38 (dd, *J* = 23.8, 8.3 Hz, 2H (Ar-H, CONH), 8.48 (t, *J* = 6.0 Hz, 1H, CONH), 8.98 (s, 1H, 2″-H); ^{13}C NMR (151 MHz, DMSO-d_6) δ 13.7 (CH2C̲CN), 16.0 (CH3), 16.6, 16.8 (C̲H2CCN), 26.1 (C(C̲H3)3), 36.2 (C̲(CH3)3), 37.1 (C-3, NHCH2), 37.8, 55.5, 56.6, 57.3, 58.8 (OCH3, C-2, C-5, NHCH), 68.9 (C-4), 110.9 (C-3′), 120.1 (C-5′), 120.7 (CN), 126.8 (C-1′), 127.9 (C-6′), 131.0, 131.3 (C-4′, C-5″), 147.9 (C-4″), 151.4 (C-2″), 156.5 (C-2′), 164.4, 168.7, 171.7 (CO). LC-MS (ESI) (90% H_2O to 100% MeOH in 10 min, then 100%

MeOH to 20 min, DAD 220-400 nm), t_R = 10.48 min, 95% purity, *m/z* calcd for $C_{28}H_{35}N_5O_5S$ $[M + H]^+$, 554.24; found, 554.6. HRMS (ESI) *m/z* calcd for $C_{28}H_{35}N_5O_5S$ $[M + H]^+$, 554.2432; found, 554.2431.

(2*S*,4*R*)-1-((*S*)-2-(1-Cyanocyclopropane-1-carboxamido)-3,3-dimethylbutanoyl)-*N*-(2-fluoro-4-(4-methylthiazol-5-yl)benzyl)-4-hydroxypyrrolidine-2-carboxamide (4)

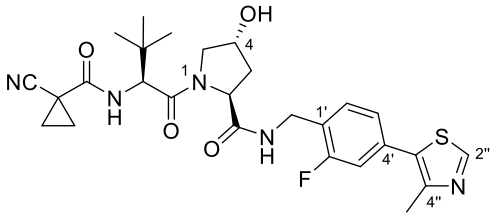

Following General Procedure C, compound **4** was obtained using Boc-protected amine **42d** (type **42**, R = 2-F; 97 mg, 0.3 mmol) and acid **46** (101 mg, 0.3 mmol). The residue was purified by flash column chromatography using a gradient from 0 to 10% MeOH in CH_2Cl_2 to afford **4** as a pale brown solid (32 mg, 20%).

mp 136-138 °C; R_f = 0.27 (CH_2Cl_2/MeOH 9:1); ^{1}H NMR (600 MHz, DMSO-d_6) δ 0.94 (s, 9H, $C(CH_3)_3$), 1.45 – 1.53 (m, 2H, CH_2CCN), 1.58 – 1.67 (m, 2H, CH_2CCN), 1.86 – 1.92 (m, 1H, 3-H), 2.04 – 2.09 (m, 1H, 3-H), 2.46 (s, 3H, CH_3), 3.57 (dt, *J* = 11.0, 1.7 Hz, 1H, 5-H), 3.63 (dd, *J* = 10.8, 3.9 Hz, 1H, 5-H), 4.26 – 4.40 (m, 3H), 4.46 – 4.54 (m, 2H) (2-H, 4-H, NHC<u>H</u>, NHC<u>H</u>$_2$), 5.15 (d, *J* = 3.7 Hz, 1H, OH), 7.22 (dd, *J* = 7.9, 1.8 Hz, 1H), 7.27 – 7.40 (m, 2H), 7.54 (t, *J* = 8.0 Hz, 1H) (Ar-H, CONH), 8.64 (t, *J* = 5.9 Hz, 1H, CONH), 9.02 (s, 1H, 2″-H); ^{13}C NMR (151 MHz, DMSO-d_6) δ 13.7 (CH_2<u>C</u>CN), 15.9 (CH_3), 16.6, 16.8 (<u>C</u>H_2CCN), 26.0 (C(<u>C</u>H_3)$_3$), 35.9 (d, $^3J_{F,C}$ = 4.1 Hz, $NHCH_2$), 36.2 (<u>C</u>$(CH_3)_3$), 37.8 (C-3), 56.6, 57.3, 58.7 (C-2, C-5, NHCH), 68.9 (C-4), 115.2 (d, $^2J_{F,C}$ = 22.5 Hz, C-3′), 120.1 (CN), 124.7 (d, $^4J_{F,C}$ = 2.4 Hz, C-5′), 125.7 (d, $^2J_{F,C}$ = 14.3 Hz, C-1′), 129.8 (d, $^3J_{F,C}$ = 5.2 Hz, C-6′), 132.0, 132.0 (C-4′, C-5″), 148.5 (C-4″), 152.0 (C-2″), 159.7 (d, $^1J_{F,C}$ = 245.4 Hz, C-2′), 164.4, 168.7, 171.8 (CO). LC-MS (ESI) (90% H_2O to 100% MeOH in 10 min, then 100% MeOH to 20 min, DAD 220-400 nm), t_R = 10.58 min, 99% purity, *m/z* calcd for $C_{27}H_{32}FN_5O_4S$ $[M + H]^+$, 542.65; found, 542.4. HRMS (ESI) *m/z* calcd for $C_{27}H_{32}FN_5O_4S$ $[M + H]^+$, 542.2232; found, 542.2232.

(2*S*,4*R*)-*N*-(2-Chloro-4-(4-methylthiazol-5-yl)benzyl)-1-((*S*)-2-(1-cyanocyclopropane-1-carboxamido)-3,3-dimethylbutanoyl)-4-hydroxypyrrolidine-2-carboxamide (5)

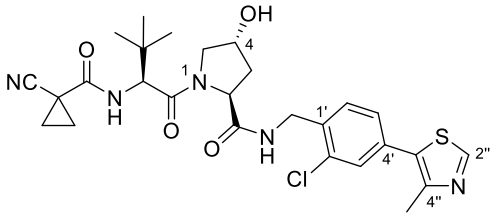

Following General Procedure C, compound **5** was obtained using Boc-protected amine **42e** (type **42**, R = 2-Cl; 101 mg, 0.3 mmol) and acid **46** (101 mg, 0.3 mmol). The residue was purified by flash column chromatography using a gradient from 0 to 10% MeOH in CH_2Cl_2 to afford **5** as a white solid (13 mg, 8%).

mp 160-162 °C; R_f = 0.55 (CH_2Cl_2/MeOH 9:1); ^{1}H NMR (600 MHz, DMSO-d_6) δ 0.94 (s, 9H, C(CH_3)$_3$), 1.47 – 1.54 (m, 2H, CH_2CCN), 1.59 – 1.67 (m, 2H, CH_2CCN), 1.92 (ddd, J = 13.1, 9.0, 4.5 Hz, 1H, 3-H), 2.06 – 2.12 (m, 1H, 3-H), 2.45 (s, 3H, CH_3), 3.55 – 3.59 (m, 1H, 5-H), 3.64 (dd, J = 10.8, 3.9 Hz, 1H, 5-H), 4.30 (dd, J = 16.4, 5.7 Hz, 1H), 4.34 – 4.37 (m, 1H), 4.39 (dd, J = 16.5, 6.2 Hz, 1H), 4.49 – 4.55 (m, 2H) (2-H, 4-H, NHC<u>H</u>, NHC<u>H</u>$_2$), 5.16 (d, J = 3.6 Hz, 1H, OH), 7.34 – 7.40 (m, 2H), 7.54 (d, J = 1.9 Hz, 1H), 7.61 (d, J = 8.0 Hz, 1H) (Ar-H, CONH), 8.72 (t, J = 6.0 Hz, 1H, CONH), 9.03 (s, 1H, 2″-H); ^{13}C NMR (151 MHz, DMSO-d_6) δ 13.7 (CH_2<u>C</u>CN), 15.9 (CH_3), 16.6, 16.8 (<u>C</u>H_2CCN), 26.1 (C(<u>C</u>H_3)$_3$), 36.2 (<u>C</u>(CH$_3$)$_3$), 37.8 (C-3), 56.6, 57.3, 58.8 (C-2, C-5, NHCH), 68.9 (C-4), 120.1 (CN), 127.5, 128.9, 129.1, 129.5, 131.7, 132.2 (C-1′, C-3′, C-4′, C-5′, C-5″, C-6′), 136.0 (C-2′), 148.6 (C-4″), 152.1 (C-2″), 164.4, 168.8, 171.9 (CO); the signal for $NHCH_2$ is missing (overlapping solvent peak). LC-MS (ESI) (90% H_2O to 100% MeOH in 10 min, then 100% MeOH to 20 min, DAD 220-400 nm), t_R = 10.92 min, 97% purity, *m/z* calcd for $C_{27}H_{32}ClN_5O_4S$ $[M + H]^+$, 558.19; found, 558.5. HRMS (ESI) *m/z* calcd for $C_{27}H_{32}ClN_5O_4S$ $[M + H]^+$, 558.1936; found, 558.1936.

(2*S*,4*R*)-1-((*S*)-2-(1-Cyanocyclopropane-1-carboxamido)-3,3-dimethylbutanoyl)-4-hydroxy-*N*-(3-methyl-4-(4-methylthiazol-5-yl)benzyl)pyrrolidine-2-carboxamide (6)

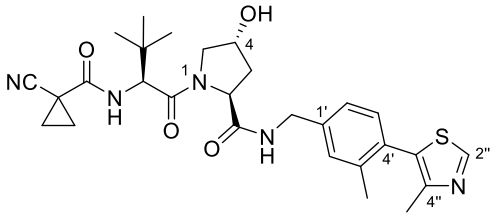

Following General Procedure C, compound **6** was obtained using Boc-protected amine **42f** (type **42**, R = 3-Me; 95 mg, 0.3 mmol) and acid **46** (101 mg, 0.3 mmol). The residue was purified by flash column chromatography using a gradient from 0 to 10% MeOH in CH_2Cl_2 to afford **6** as a white solid (25 mg, 16%).

mp 88-90 °C; R_f = 0.40 (CH_2Cl_2/MeOH 9:1); ^{1}H NMR (600 MHz, DMSO-d_6) δ 0.95 (s, 9H, C(CH_3)$_3$), 1.46 – 1.52 (m, 2H, CH_2CCN), 1.58 – 1.65 (m, 2H, CH_2CCN), 1.88 – 1.93 (m, 1H, 3-H), 2.05 – 2.10 (m, 1H, 3-H), 2.12 (s, 3H, CH_3), 2.17 (s, 3H, CH_3), 3.55 – 3.59 (m, 1H, 5-H), 3.64 (dd, *J* = 10.8, 3.9 Hz, 1H, 5-H), 4.18 – 4.22 (m, 1H), 4.35 (ddt, *J* = 6.1, 4.2, 2.3 Hz, 1H), 4.41 (dd, *J* = 15.7, 6.5 Hz, 1H), 4.46 – 4.50 (m, 1H), 4.52 (d, *J* = 8.9 Hz, 1H) (2-H, 4-H, NHC<u>H</u>, NHC<u>H</u>$_2$), 5.15 (d, *J* = 3.6 Hz, 1H, OH), 7.14 – 7.20 (m, 2H), 7.33 (dd, *J* = 5.3, 3.6 Hz, 2H) (Ar-H, CONH), 8.59 (t, *J* = 6.0 Hz, 1H, CONH), 9.04 (s, 1H, 2″-H); ^{13}C NMR (151 MHz, DMSO-d_6) δ 13.6 (CH_2<u>C</u>CN), 15.2 (CH_3), 16.6, 16.8 (<u>C</u>H_2CCN), 19.7 (CH_3), 26.1 (C(<u>C</u>H_3)$_3$), 36.3 (<u>C</u>(CH$_3$)$_3$), 37.8 (C-3), 41.7 (NHCH_2), 56.6, 57.3, 58.9 (C-2, C-5, NHCH), 68.9 (C-4), 120.0 (CN), 124.5, 128.7, 128.9, 129.6, 130.8 (C-3′, C-4′, C-5′, C-6′, C-5″), 136.9 (C-2′), 140.1 (C-1′), 149.0 (C-4″), 152.2 (C-2″), 164.3, 168.6, 171.6 (CO). LC-MS (ESI) (90% H_2O to 100% MeOH in 10 min, then 100% MeOH to 20 min, DAD 220-400 nm), t_R = 11.05 min, 97% purity, *m/z* calcd for $C_{28}H_{35}N_5O_4S$ $[M + H]^+$, 538.25; found, 538.5. HRMS (ESI) *m/z* calcd for $C_{28}H_{35}N_5O_4S$ $[M + H]^+$, 538.2486; found, 538.2482.

(2*S*,4*R*)-1-((*S*)-2-(1-Cyanocyclopropane-1-carboxamido)-3,3-dimethylbutanoyl)-4-hydroxy-*N*-(3-methoxy-4-(4-methylthiazol-5-yl)benzyl)pyrrolidine-2-carboxamide (7)

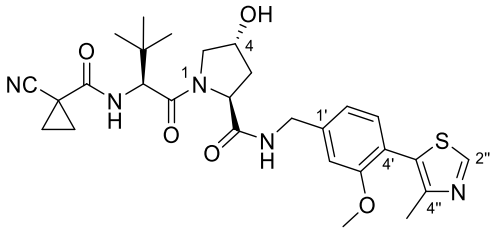

Following General Procedure C, compound **7** was obtained using Boc-protected amine **42g** (type **42**, R = 3-OMe; 100 mg, 0.3 mmol) and acid **46** (101 mg, 0.3 mmol). The residue was purified by flash column chromatography using a gradient from 0 to 10% MeOH in CH_2Cl_2 to afford **7** as a white solid (17 mg, 10%).

mp 105-106 °C; R_f = 0.25 (CH_2Cl_2/MeOH 9:1); ^{1}H NMR (600 MHz, DMSO-d_6) δ 0.95 (s, 9H, $C(CH_3)_3$), 1.45 – 1.53 (m, 2H, CH_2CCN), 1.59 – 1.67 (m, 2H, CH_2CCN), 1.87 – 1.94 (m, 1H, 3-H), 2.06 – 2.12 (m, 1H, 3-H), 2.27 (s, 3H, CH_3), 3.57 (d, J = 10.9 Hz, 1H, 5-H), 3.64 (dd, J = 10.9, 3.8 Hz, 1H, 5-H), 3.84 (s, 3H, OCH_3), 4.19 (dd, J = 15.8, 5.1 Hz, 1H), 4.33 – 4.38 (m, 1H), 4.46 – 4.53 (m, 3H) (2-H, 4-H, NHC<u>H</u>, NHC<u>H</u>$_2$), 5.16 (d, J = 3.6 Hz, 1H, OH), 6.93 – 6.97 (m, 1H), 7.14 – 7.17 (m, 1H), 7.22 (d, J = 7.7 Hz, 1H), 7.28 (d, J = 8.9 Hz, 1H) (Ar-H, CONH), 8.64 (dd, J = 6.9, 5.1 Hz, 1H, CONH), 8.98 (s, 1H, 2″-H); ^{13}C NMR (151 MHz, DMSO-d_6) δ 13.6 (CH_2<u>C</u>CN), 15.9 (CH_3), 16.6, 16.8 (<u>C</u>H_2CCN), 26.1 (C(<u>C</u>H_3)$_3$), 36.4 (<u>C</u>$(CH_3)_3$), 37.8, 41.8 (C-3, $NHCH_2$), 55.6, 56.7, 57.4, 59.0 (OCH_3, C-2, C-5, NHCH), 68.9 (C-4), 110.2 (C-2′), 117.9, 118.9 (C-5′, C-6′), 120.1 (CN), 126.7 (C-1′), 131.1 (C-4′), 142.0 (C-5″), 149.3 (C-4″), 151.9 (C-2″), 156.6 (C-3′), 164.3, 168.7, 171.5 (CO). LC-MS (ESI) (90% H_2O to 100% MeOH in 10 min, then 100% MeOH to 20 min, DAD 220-400 nm), t_R = 10.64 min, 99% purity, *m/z* calcd for $C_{28}H_{35}N_5O_5S$ $[M + H]^+$, 554.24; found, 554.5. HRMS (ESI) *m/z* calcd for $C_{28}H_{35}N_5O_5S$ $[M + H]^+$, 554.2432; found, 554.2430.

(2*S*,4*R*)-1-((*S*)-2-(1-Cyanocyclopropane-1-carboxamido)-3,3-dimethylbutanoyl)-*N*-(3-fluoro-4-(4-methylthiazol-5-yl)benzyl)-4-hydroxypyrrolidine-2-carboxamide (8)

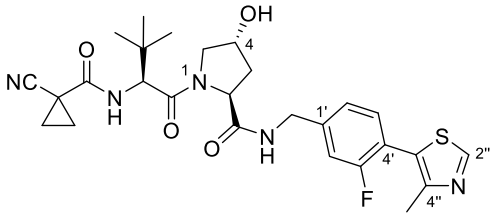

Following General Procedure C, compound **8** was obtained using Boc-protected amine **42h** (type **42**, R = 3-F; 97 mg, 0.3 mmol) and acid **46** (101 mg, 0.3 mmol). The residue was purified by flash column chromatography using a gradient from 0 to 10% MeOH in CH_2Cl_2 to afford **8** as a white solid (23 mg, 17%).

mp 98-100 °C; R_f = 0.38 (CH_2Cl_2/MeOH 9:1); ^{1}H NMR (600 MHz, DMSO-d_6) δ 0.95 (s, 9H, C(CH_3)$_3$), 1.46 – 1.53 (m, 2H, CH_2CCN), 1.58 – 1.66 (m, 2H, CH_2CCN), 1.88 – 1.94 (m, 1H, 3-H), 2.05 – 2.11 (m, 1H, 3-H), 2.32 (d, J = 1.1 Hz, 3H, CH_3), 3.56 – 3.59 (m, 1H, 5-H), 3.64 (dd, J = 10.8, 3.8 Hz, 1H, 5-H), 4.24 (dd, J = 16.1, 5.6 Hz, 1H), 4.34 – 4.37 (m, 1H), 4.43 – 4.54 (m, 3H) (2-H, 4-H, NHC<u>H</u>, NHC<u>H</u>$_2$), 5.16 (d, J = 3.6 Hz, 1H, OH), 7.22 – 7.24 (m, 1H), 7.31 – 7.36 (m, 2H), 7.40 (t, J = 7.8 Hz, 1H) (Ar-H, CONH), 8.70 (t, J = 6.1 Hz, 1H, CONH), 9.09 (s, 1H, 2″-H); ^{13}C NMR (151 MHz, DMSO-d_6) δ 13.7 (CH_2<u>C</u>CN), 15.7 (CH_3), 16.6, 16.8 (<u>C</u>H_2CCN), 26.0 (C(<u>C</u>H_3)$_3$), 36.2 (<u>C</u>(CH$_3$)$_3$), 37.8, 41.4 (C-3, NHCH_2), 56.6, 57.3, 58.9 (C-2, C-5, NHCH), 68.9 (C-4), 114.4 (d, $^2J_{F,C}$ = 23.0 Hz, C-2′), 116.9 (d, $^2J_{F,C}$ = 15.3 Hz, C-4′), 120.1 (CN), 123.1 (d, $^3J_{F,C}$ = 2.9 Hz, C-5′), 123.8 (C-5″), 131.7 (d, $^4J_{F,C}$ = 2.3 Hz, C-6′), 143.2 (d, $^3J_{F,C}$ = 7.6 Hz, C-1′), 150.1 (C-4″), 153.1 (C-2″), 158.9 (d, $^1J_{F,C}$ = 246.6 Hz, C-3′), 164.4, 168.7, 171.9 (CO). LC-MS (ESI) (90% H_2O to 100% MeCN in 10 min, then 100% MeCN to 15 min, DAD 200-600 nm), t_R = 8.28 min, 97% purity, *m/z* calcd for $C_{27}H_{23}FN_5O_4S$ [M + H]$^+$, 542.22; found, 542.4. HRMS (ESI) *m/z* calcd for $C_{27}H_{23}FN_5O_4S$ [M + H]$^+$, 542.2232; found, 542.2233.

(2*S*,4*R*)-*N*-(3-Chloro-4-(4-methylthiazol-5-yl)benzyl)-1-((*S*)-2-(1-cyanocyclopropane-1-carboxamido)-3,3-dimethylbutanoyl)-4-hydroxypyrrolidine-2-carboxamide (9)

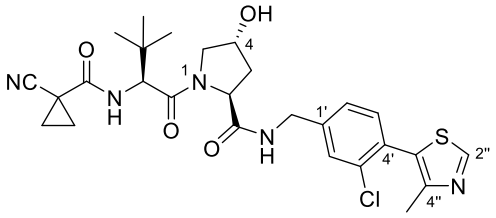

Following General Procedure C, compound **9** was obtained using Boc-protected amine **42i** (type **42**, R = 3-Cl; 135 mg, 0.4 mmol) and acid **46** (135 mg, 0.4 mmol). The residue was purified by flash column chromatography using a gradient from 0 to 10% MeOH in CH_2Cl_2 to afford **9** as a white solid (12 mg, 5%).

mp 157-159 °C; R_f = 0.44 (CH_2Cl_2/MeOH 9:1); ^{1}H NMR (600 MHz, DMSO-d_6) δ 0.95 (s, 9H, C(CH_3)$_3$), 1.46 – 1.54 (m, 2H, CH_2CCN), 1.58 – 1.66 (m, 2H, CH_2CCN), 1.90 (ddd, J = 13.1, 9.1, 4.4 Hz, 1H, 3-H), 2.05 – 2.11 (m, 1H, 3-H), 2.23 (s, 3H, CH_3), 3.54 – 3.58 (m, 1H, 5-H), 3.64 (dd, J = 10.8, 3.8 Hz, 1H, 5-H), 4.24 (dd, J = 16.0, 5.4 Hz, 1H), 4.33 – 4.38 (m, 1H), 4.43 – 4.53 (m, 3H) (2-H, 4-H, NHC<u>H</u>, NHC<u>H</u>$_2$), 5.15 (d, J = 3.6 Hz, 1H, OH), 7.31 – 7.40 (m, 3H), 7.60 (d, J = 1.6 Hz, 1H) (Ar-H, CONH), 8.69 (t, J = 6.1 Hz, 1H, CONH), 9.09 (s, 1H, 2″-H); ^{13}C NMR (151 MHz, DMSO-d_6) δ 13.6 (CH_2<u>C</u>CN), 15.5 (CH_3), 16.6, 16.8 (<u>C</u>H_2CCN), 26.1 (C(<u>C</u>H_3)$_3$), 36.3 (<u>C</u>(CH_3)$_3$), 37.8 (C-3), 41.3 (NHCH_2), 56.6, 57.3, 58.9 (C-2, C-5, NHCH), 68.9 (C-4), 120.0 (CN), 125.9, 127.3, 128.0, 128.2, 132.4, 133.3 (C-1′, C-2′, C-4′, C-5′, C-5″, C-6′), 142.6 (C-3′), 150.2 (C-4″), 152.9 (C-2″), 164.3, 168.7, 171.8 (CO). LC-MS (ESI) (90% H_2O to 100% MeOH in 10 min, then 100% MeOH to 20 min, DAD 220-400 nm), t_R = 10.64 min, 98% purity, *m/z* calcd for $C_{27}H_{32}ClN_5O_4S$ $[M + H]^+$, 558.19; found, 558.3. HRMS (ESI) *m*/*z* calcd for $C_{27}H_{32}ClN_5O_4S$ $[M + H]^+$, 558.1936; found, 558.1938.

(2*S*,4*R*)-1-((*S*)-2-(1-Cyanocyclopropane-1-carboxamido)-3,3-dimethylbutanoyl)-*N*-(2,6-dimethyl-4-(4-methylthiazol-5-yl)benzyl)-4-hydroxypyrrolidine-2-carboxamide (10)

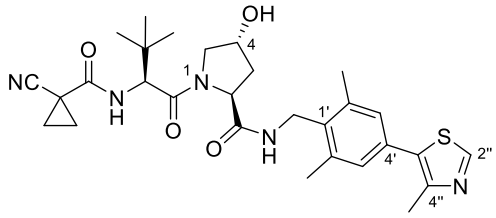

Following General Procedure C, compound **10** was obtained using Boc-protected amine **42j** (type **42**, R = 2-Me, 6-Me; 100 mg, 0.3 mmol) and acid **46** (101 mg, 0.3 mmol). The residue was purified by flash column chromatography using a gradient from 0 to 10% MeOH in CH_2Cl_2 to afford **10** as a white solid (28 mg, 17%).

mp 106-110 °C; R_f = 0.42 (CH_2Cl_2/MeOH 9:1); ^{1}H NMR (600 MHz, DMSO-d_6) δ 0.96 (s, 9H, C(CH_3)$_3$), 1.44 – 1.52 (m, 2H, CH_2CCN), 1.56 – 1.66 (m, 2H, CH_2CCN), 1.82 – 1.89 (m, 1H, 3-H), 1.96 – 2.03 (m, 1H, 3-H), 2.35 (s, 6H, Ar-CH_3), 2.46 (s, 3H, CH_3), 3.51 – 3.56 (m, 1H, 5-H), 3.64 (dd, *J* = 10.8, 4.0 Hz, 1H, 5-H), 4.24 (dd, *J* = 14.0, 4.5 Hz, 1H), 4.30 – 4.34 (m, 1H), 4.38 – 4.42 (m, 2H), 4.51 (d, *J* = 8.9 Hz, 1H) (2-H, 4-H, NHC<u>H</u>, NHC<u>H</u>$_2$), 5.10 (d, *J* = 3.6 Hz, 1H, OH), 7.16 (s, 2H, Ar-H), 7.28 (d, *J* = 8.9 Hz, 1H, CONH), 8.08 (t, *J* = 5.0 Hz, 1H, CONH), 8.97 (s, 1H, 2″-H); ^{13}C NMR (151 MHz, DMSO-d_6) δ 13.7 (CH_2<u>C</u>CN), 16.0 (CH_3), 16.6, 16.8 (<u>C</u>H_2CCN), 19.3 (Ar-CH_3), 26.1 (C(<u>C</u>H_3)$_3$), 36.2 (<u>C</u>(CH_3)$_3$), 36.7, 37.9 (C-3, $NHCH_2$), 56.6, 57.3, 58.6 (C-2, C-5, NHCH), 68.8 (C-4), 120.1 (CN), 128.3, 130.3, 131.1, 134.7, 138.2 (C-1′, C-2′, C-3′, C-4′, C-5′, C-5″, C-6′), 147.7 (C-4″), 151.4 (C-2″), 164.4, 168.5, 170.9 (CO). LC-MS (ESI) (90% H_2O to 100% MeOH in 10 min, then 100% MeOH to 20 min, DAD 220-400 nm), t_R = 11.23 min, 99% purity, *m/z* calcd for $C_{29}H_{37}N_5O_4S$ $[M + H]^+$, 552.26; found, 552.6. HRMS (ESI) *m/z* calcd $C_{29}H_{37}N_5O_4S$ $[M + H]^+$, 552.2639; found, 552.2634.

(2*S*,4*R*)-1-((*S*)-2-(1-Cyanocyclopropane-1-carboxamido)-3,3-dimethylbutanoyl)-*N*-(2,6-dimethoxy-4-(4-methylthiazol-5-yl)benzyl)-4-hydroxypyrrolidine-2-carboxamide (11)

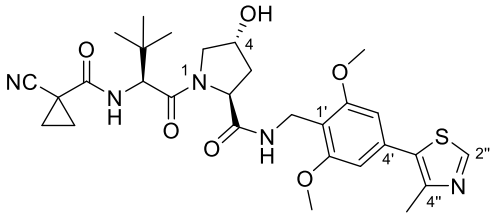

Following General Procedure C, compound **11** was obtained using Boc-protected amine **42k** (type **42**, R = 2-OMe, 6-OMe; 109 mg, 0.3 mmol) and acid **46** (101 mg, 0.3 mmol). The residue was purified by flash column chromatography using a gradient from 0 to 10% MeOH in CH_2Cl_2 to afford **11** as a yellow solid (90 mg, 51%).

mp 102-104 °C; R_f = 0.42 (CH_2Cl_2/MeOH 9:1); ^{1}H NMR (500 MHz, DMSO-d_6) δ 0.94 (s, 9H, $C(CH_3)_3$), 1.43 – 1.52 (m, 2H, CH_2CCN), 1.55 – 1.67 (m, 2H, CH_2CCN), 1.84 – 1.99 (m, 2H, 3-H), 3.51 (d, *J* = 9.7 Hz, 1H, 5-H), 3.61 (dd, *J* = 10.8, 4.3 Hz, 1H, 5-H), 3.82 (s, 6H, OCH_3), 4.20 (dd, *J* = 13.1, 3.8 Hz, 1H), 4.27 – 4.32 (m, 1H), 4.35 (dd, *J* = 13.1, 5.6 Hz, 1H), 4.44 (t, *J* = 7.9 Hz, 1H), 4.50 (d, *J* = 8.9 Hz, 1H) (2-H, 4-H, NHC<u>H</u>, NHC<u>H</u>$_2$), 5.06 (d, *J* = 3.8 Hz, 1H, OH), 6.72 (s, 2H, Ar-H), 7.26 (d, *J* = 8.9 Hz, 1H, CONH), 7.65 (t, *J* = 4.7 Hz, 1H, CONH), 9.00 (s, 1H, 2″-H); ^{13}C NMR (126 MHz, DMSO-d_6) δ 13.6 (CH_2<u>C</u>CN), 16.0 (CH_3), 16.6, 16.7 (<u>C</u>H_2CCN), 26.0 (C(<u>C</u>H_3)$_3$), 31.4 ($NHCH_2$), 36.1 (<u>C</u>$(CH_3)_3$), 37.5 (C-3), 56.0, 57.3, 58.4 (C-2, C-5, NHCH), 68.7 (C-4), 105.1, 113.5 (C-3′, C-4’, C-5′), 120.0 (CN), 131.4, 132.2 (C-1′, C-5″), 148.2 (C-4″), 151.6 (C-2″), 158.5 (C-2′, C-6′), 164.3, 168.6, 170.5 (CO); the signal for CH_3 is missing (overlapping solvent peak). LC-MS (ESI) (90% H_2O to 100% MeOH in 10 min, then 100% MeOH to 20 min, DAD 220-400 nm), t_R = 10.91 min, 96% purity, *m/z* calcd for $C_{29}H_{37}N_5O_4S$ $[M + H]^+$, 584.25; found, 584.7. HRMS (ESI) *m/z* calcd for $C_{29}H_{37}N_5O_4S$ $[M + H]^+$, 584.2537; found, 584.2531.

(2*S*,4*R*)-1-((*S*)-2-(1-Cyanocyclopropane-1-carboxamido)-3,3-dimethylbutanoyl)-*N*-(2,6-difluoro-4-(4-methylthiazol-5-yl)benzyl)-4-hydroxypyrrolidine-2-carboxamide (12)

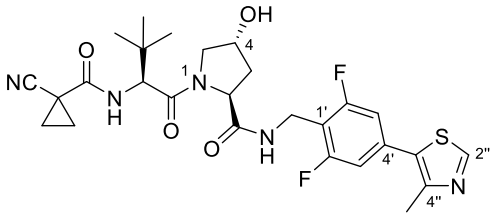

Following General Procedure C, compound **12** was obtained using Boc-protected amine **42l** (type **42**, R = 2-F, 6-F; 102 mg, 0.3 mmol) and acid **46** (101 mg, 0.3 mmol). The residue was purified by flash column chromatography using a gradient from 0 to 10% MeOH in CH_2Cl_2 to afford **12** as a white solid (83 mg, 49%).

mp 84-86 °C; R_f = 0.42 (CH_2Cl_2/MeOH 9:1); ^{1}H NMR (500 MHz, DMSO-d_6) δ 0.92 (s, 9H, C(CH_3)$_3$), 1.43 – 1.53 (m, 2H, CH_2CCN), 1.56 – 1.67 (m, 2H, CH_2CCN), 1.79 – 1.87 (m, 1H, 3-H), 1.94 – 2.01 (m, 1H, 3-H), 2.48 (s, 3H, CH_3), 3.52 (d, J = 10.8 Hz, 1H, 5-H), 3.61 (dd, J = 10.8, 4.0 Hz, 1H, 5-H), 4.23 – 4.32 (m, 2H), 4.37 – 4.46 (m, 2H), 4.49 (d, J = 8.9 Hz, 1H) (2-H, 4-H, NHC<u>H</u>, NHC<u>H</u>$_2$), 5.09 (d, J = 3.7 Hz, 1H, OH), 7.21 – 7.29 (m, 3H) (Ar-H, CONH), 8.38 (t, J = 5.3 Hz, 1H, CONH), 9.06 (s, 1H, 2″-H); ^{13}C NMR (126 MHz, DMSO-d_6) δ 13.6 (CH_2<u>C</u>CN), 16.0 (CH_3), 16.6, 16.7 (<u>C</u>H_2CCN), 26.1 (C(<u>C</u>H_3)$_3$), 30.4 (NHCH_2), 36.1 (<u>C</u>(CH_3)$_3$), 37.6 (C-3), 56.5, 57.3, 58.5 (C-2, C-5, NHCH), 68.7 (C-4), 111.9 (d, $^2J_{F,C}$ = 14.1 Hz), 111.9 (d, $^2J_{F,C}$ = 27.3 Hz, C-3′, C-5′), 113.6 (t, $^2J_{F,C}$ = 19.8 Hz, C-1′), 120.0 (CN), 128.8 (C-4″), 133.2 (t, $^3J_{F,C}$ = 11.0 Hz, C-4′), 149.3 (C-5″), 152.6 (C-2″), 160.9 (dd, $^1J_{F,C}$ = 248.7 Hz, $^3J_{F,C}$ = 9.7 Hz, C-2′, C-6′), 164.3, 168.5, 170.9 (CO). LC-MS (ESI) (90% H_2O to 100% MeOH in 10 min, then 100% MeOH to 20 min, DAD 220-400 nm), t_R = 10.73 min, 98% purity, *m/z* calcd for $C_{27}H_{31}F_2N_5O_4S$ $[M + H]^+$, 560.21; found, 560.4. HRMS (ESI) *m/z* calcd for $C_{27}H_{31}F_2N_5O_4S$ $[M + H]^+$, 560.2138; found, 560.2135.

(2*S*,4*R*)-1-((*S*)-2-(1-Cyanocyclopropane-1-carboxamido)-3,3-dimethylbutanoyl)-*N*-(2,6-dichloro-4-(4-methylthiazol-5-yl)benzyl)-4-hydroxypyrrolidine-2-carboxamide (13)

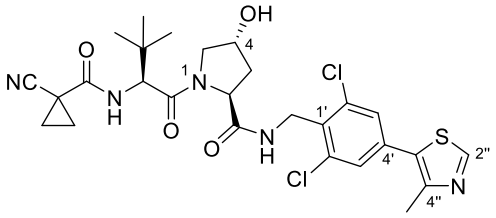

Following General Procedure C, compound **13** was obtained using Boc-protected amine **42m** (type **42**, R = 2-Cl, 6-Cl; 112 mg, 0.3 mmol) and acid **46** (101 mg, 0.3 mmol). The residue was purified by flash column chromatography using a gradient from 0 to 10% MeOH in CH_2Cl_2 to afford **13** as a white solid (66 mg, 37%).

mp 138-140 °C; R_f = 0.49 (CH_2Cl_2/MeOH 9:1); ^{1}H NMR (500 MHz, DMSO-d_6) δ 0.96 (s, 9H, C(CH_3)$_3$), 1.45 – 1.53 (m, 2H, CH_2CCN), 1.57 – 1.65 (m, 2H, CH_2CCN), 1.85 – 1.92 (m, 1H, 3-H), 1.96 – 2.03 (m, 1H, 3-H), 2.48 (s, 3H, CH_3), 3.51 – 3.55 (m, 1H, 5-H), 3.63 (dd, J = 10.7, 4.1 Hz, 1H, 5-H), 4.29 – 4.34 (m, 1H), 4.41 – 4.52 (m, 3H), 4.63 (dd, J = 13.8, 5.8 Hz, 1H) (2-H, 4-H, NHC<u>H</u>, NHC<u>H</u>$_2$), 5.09 (d, J = 3.7 Hz, 1H, OH), 7.27 (d, J = 8.8 Hz, 1H, CONH), 7.61 (s, 2H, Ar-H), 8.20 (dd, J = 5.7, 3.7 Hz, 1H, CONH), 9.08 (s, 1H, 2″-H); ^{13}C NMR (126 MHz, DMSO-d_6) δ 13.6 (CH_2<u>C</u>CN), 15.9 (CH_3), 16.6, 16.8 (<u>C</u>H_2CCN), 26.1 (C(<u>C</u>H_3)$_3$), 36.1 (<u>C</u>(CH_3)$_3$), 37.8, 38.4 (C-3, NHCH_2), 56.5, 57.3, 58.5 (C-2, C-5, NHCH), 68.7 (C-4), 120.0 (CN), 128.0, 128.4, 132.9, 133.5, 135.9 (C-1′, C-2′, C-3′, C-4′, C-5′, C-5″, C-6′), 149.6 (C-4″), 152.9 (C-2″), 164.3, 168.5, 170.8 (CO). LC-MS (ESI) (90% H_2O to 100% MeOH in 10 min, then 100% MeOH to 20 min, DAD 220-400 nm), t_R = 11.47 min, 100% purity, *m/z* calcd for $C_{27}H_{32}Cl_2N_5O_4S$ $[M + H]^+$, 592.15; found, 592.2. HRMS (ESI) *m/z* calcd for $C_{27}H_{32}Cl_2N_5O_4S$ $[M + H]^+$, 592.1547; found, 592.1540.

(2*S*,4*R*)-1-((*S*)-2-(1-Cyanocyclopropane-1-carboxamido)-3,3-dimethylbutanoyl)-*N*-(2,5-dimethyl-4-(4-methylthiazol-5-yl)benzyl)-4-hydroxypyrrolidine-2-carboxamide (14)

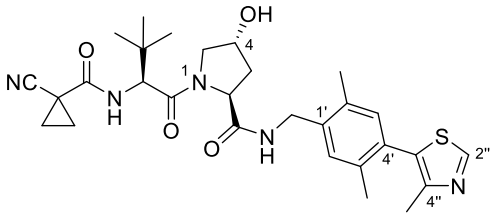

Following General Procedure C, compound **14** was obtained using Boc-protected amine **42n** (type **42**, R = 2-Me, 5-Me; 98 mg, 0.3 mmol) and acid **46** (101 mg, 0.3 mmol). The residue was purified by flash column chromatography using a gradient from 0 to 10% MeOH in CH_2Cl_2 to afford **14** as a white solid (78 mg, 47%).

mp 96-98 °C; R_f = 0.47 (CH_2Cl_2/MeOH 9:1); ^{1}H NMR (500 MHz, DMSO-d_6) δ 0.95 (s, 9H, C(CH_3)$_3$), 1.46 – 1.53 (m, 2H, CH_2CCN), 1.58 – 1.67 (m, 2H, CH_2CCN), 1.91 (ddd, J = 13.2, 9.0, 4.5 Hz, 1H, 3-H), 2.05 – 2.08 (m, 1H, 3-H), 2.09 (s, 3H, CH_3), 2.17 (s, 3H, CH_3), 2.22 (s, 3H, CH_3), 3.56 (d, J = 10.7 Hz, 1H, 5-H), 3.64 (dd, J = 10.8, 3.9 Hz, 1H, 5-H), 4.15 (dd, J = 15.6, 5.2 Hz, 1H), 4.32 – 4.38 (m, 2H), 4.48 – 4.53 (m, 2H) (2-H, 4-H, NHC<u>H</u>, NHC<u>H$_2$</u>), 5.13 (d, J = 3.6 Hz, 1H, OH), 7.04 (s, 1H, Ar-H), 7.32 (d, J = 8.8 Hz, 1H, CONH), 7.36 (s, 1H, Ar-H), 8.47 (t, J = 5.8 Hz, 1H, CONH), 9.02 (s, 1H, 2″-H); ^{13}C NMR (126 MHz, DMSO-d_6) δ 13.6 (CH_2<u>C</u>CN), 15.2 (CH_3), 16.6, 16.8 (<u>C</u>H_2CCN), 17.8, 19.1 (Ar-CH_3), 26.0 (C(<u>C</u>H_3)$_3$), 36.3 (<u>C</u>(CH$_3$)$_3$), 37.9 (C-3), 56.6, 57.3, 58.9 (C-2, C-5, NHCH), 68.9 (C-4), 120.0 (CN), 128.6, 129.3, 129.6, 132.1, 132.9, 134.1 (C-2′, C-3′, C-4′, C-5′, C-5″, C-6′), 137.5 (C-1′), 148.8 (C-4″), 152.0 (C-2″), 164.3, 168.6, 171.4 (CO); the signal for $NHCH_2$ is missing (overlapping solvent peak). LC-MS (ESI) (90% H_2O to 100% MeOH in 10 min, then 100% MeOH to 20 min, DAD 220-400 nm), t_R = 11.14 min, 99% purity, *m/z* calcd for $C_{29}H_{37}N_5O_4S$ $[M + H]^+$, 552.26; found, 552.6. HRMS (ESI) *m/z* calcd for $C_{29}H_{37}N_5O_4S$ $[M + H]^+$, 552.2639; found, 552.2637.

(2*S*,4*R*)-1-((*S*)-2-(1-Cyanocyclopropane-1-carboxamido)-3,3-dimethylbutanoyl)-*N*-(2,5-dimethoxy-4-(4-methylthiazol-5-yl)benzyl)-4-hydroxypyrrolidine-2-carboxamide (15)

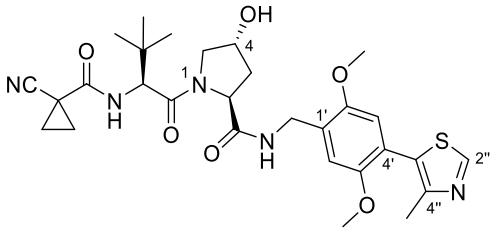

Following General Procedure C, compound **15** was obtained using Boc-protected amine **42o** (type **42**, R = 2-OMe, 5-OMe; 110 mg, 0.3 mmol) and acid **46** (101 mg, 0.3 mmol). The residue was purified by flash column chromatography using a gradient from 0 to 10% MeOH in CH_2Cl_2 to afford **15** as a white solid (52 mg, 30%).

mp 104-106 °C; R_f = 0.38 (CH_2Cl_2/MeOH 9:1); ^{1}H NMR (500 MHz, DMSO-d_6) δ 0.93 (s, 9H, $C(CH_3)_3$), 1.46 – 1.52 (m, 2H, CH_2CCN), 1.59 – 1.67 (m, 2H, CH_2CCN), 1.88 – 1.95 (m, 1H, 3-H), 2.07 – 2.13 (m, 1H, 3-H), 2.31 (s, 3H, CH_3), 3.57 (d, J = 10.9 Hz, 1H, 5-H), 3.64 (dd, J = 10.9, 3.7 Hz, 1H, 5-H), 3.78 (s, 3H, OCH_3), 3.83 (s, 3H, OCH_3), 4.13 (dd, J = 16.5, 5.0 Hz, 1H), 4.34 – 4.37 (m, 1H), 4.41 (dd, J = 16.6, 7.0 Hz, 1H), 4.49 – 4.55 (m, 2H) (2-H, 4-H, NHC<u>H</u>, NHC<u>H</u>$_2$), 5.15 (d, J = 3.6 Hz, 1H, OH), 6.90 (s, 1H, Ar-H), 7.23 (s, 1H, Ar-H), 7.25 (d, J = 8.9 Hz, 1H, CONH), 8.55 (dd, J = 7.0, 5.1 Hz, 1H, CONH), 8.98 (s, 1H, 2″-H); ^{13}C NMR (126 MHz, DMSO-d_6) δ 13.5 (CH_2<u>C</u>CN), 15.9 (CH_3), 16.6, 16.9 (<u>C</u>H_2CCN), 26.0 (C(<u>C</u>H_3)$_3$), 36.4 (<u>C</u>$(CH_3)_3$), 36.9, 37.8 (C-3, $NHCH_2$), 55.9, 56.2, 56.7, 57.4, 59.1 (OCH_3, C-2, C-5, NHCH), 68.9 (C-4), 111.7, 113.6 (C-3′, C-6′), 118.0, 120.0, 126.8, 128.9 (C-1′, C-4′, C-5″, CN), 149.4, 149.9, 150.6, 151.9 (C-2′, C-2″, C-4″, C-5′), 164.2, 168.7, 171.6 (CO). LC-MS (ESI) (90% H_2O to 100% MeOH in 10 min, then 100% MeOH to 20 min, DAD 220-400 nm), t_R = 10.92 min, 98% purity, *m/z* calcd for $C_{29}H_{37}N_5O_6S$ $[M + H]^+$, 584.25; found, 584.5. HRMS (ESI) *m/z* calcd for $C_{29}H_{37}N_5O_6S$ $[M + H]^+$, 584.2537; found, 584.2531.

(2*S*,4*R*)-1-((*S*)-2-(1-Cyanocyclopropane-1-carboxamido)-3,3-dimethylbutanoyl)-*N*-(2,5-difluoro-4-(4-methylthiazol-5-yl)benzyl)-4-hydroxypyrrolidine-2-carboxamide (16)

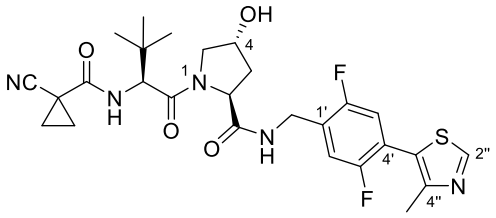

Following General Procedure C, compound **16** was obtained using Boc-protected amine **42p** (type **42**, R = 2-F, 5-F; 102 mg, 0.3 mmol) and acid **46** (101 mg, 0.3 mmol). The residue was purified by flash column chromatography using a gradient from 0 to 10% MeOH in CH_2Cl_2 to afford **16** as a white solid (79 mg, 47%).

mp 129-130 °C; R_f = 0.50 (CH_2Cl_2/MeOH 9:1); ^{1}H NMR (600 MHz, DMSO-d_6) δ 0.93 (s, 9H, C(CH_3)$_3$), 1.46 – 1.53 (m, 2H, CH_2CCN), 1.58 – 1.66 (m, 2H, CH_2CCN), 1.87 – 1.93 (m, 1H, 3-H), 2.05 – 2.10 (m, 1H, 3-H), 2.34 (d, J = 1.0 Hz, 3H, CH_3), 3.55 – 3.59 (m, 1H, 5-H), 3.64 (dd, J = 10.8, 3.9 Hz, 1H, 5-H), 4.23 (dd, J = 16.3, 5.3 Hz, 1H), 4.34 – 4.38 (m, 1H), 4.41 – 4.53 (m, 3H) (2-H, 4-H, NHC<u>H</u>, NHC<u>H</u>$_2$), 5.17 (d, J = 3.6 Hz, 1H, OH), 7.35 (d, J = 8.9 Hz, 1H), 7.38 (dd, J = 9.9, 6.0 Hz, 1H), 7.49 (dd, J = 10.4, 6.2 Hz, 1H) (Ar-H, CONH), 8.76 (t, J = 6.0 Hz, 1H, CONH), 9.12 (s, 1H, 2″-H); ^{13}C NMR (151 MHz, DMSO-d_6) δ 13.7 (CH_2<u>C</u>CN), 15.7 (d, $^5J_{F,C}$ = 2.0 Hz, CH_3), 16.6, 16.8 (<u>C</u>H_2CCN), 26.0 (C(<u>C</u>H_3)$_3$), 35.9 (d, $^3J_{F,C}$ = 3.6 Hz, NHCH_2), 36.2 (<u>C</u>(CH_3)$_3$), 37.7 (C-3), 56.6, 57.3, 58.9 (C-2, C-5, NHCH), 68.9 (C-4), 116.1 (d, $^3J_{F,C}$ = 5.1 Hz), 116.3 (d, $^3J_{F,C}$ = 4.9 Hz, C-5′, C-6′), 117.7 (dd, J = 25.1, 2.2 Hz), 118.4 (dd, $^2J_{F,C}$ = 18.2 Hz, $^3J_{F,C}$ = 9.1 Hz, C-4′), 120.1 (CN), 122.7 (C-5″), 129.0 (dd, $^2J_{F,C}$ = 17.2 Hz, $^3J_{F,C}$ = 7.9 Hz, C-1′), 150.7 (C-4″), 153.6 (C-2″), 155.2 (dd, $^1J_{F,C}$ = 242.5 Hz, $^2J_{F,C}$ = 25.9 Hz, C-2′, C-3′), 164.4, 168.8, 172.2 (CO). LC-MS (ESI) (90% H_2O to 100% MeOH in 10 min, then 100% MeOH to 20 min, DAD 220-400 nm), t_R = 10.78 min, 100% purity, *m/z* calcd for $C_{27}H_{31}F_2N_5O_4S$ $[M + H]^+$, 560.21; found, 560.4. HRMS (ESI) *m/z* calcd for $C_{27}H_{31}F_2N_5O_4S$ $[M + H]^+$, 560.2138 found, 560.2134.

(2*S*,4*R*)-1-((*S*)-2-(1-Cyanocyclopropane-1-carboxamido)-3,3-dimethylbutanoyl)-*N*-(2,5-dichloro-4-(4-methylthiazol-5-yl)benzyl)-4-hydroxypyrrolidine-2-carboxamide (17)

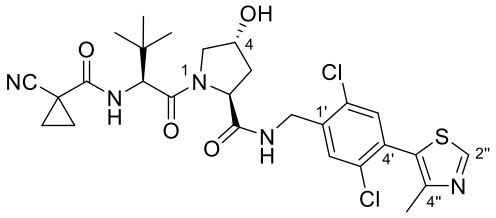

Following General Procedure C, compound **17** was obtained using Boc-protected amine **42q** (type **42**, R = 2-Cl, 5-Cl; 110 mg, 0.3 mmol) and acid **46** (101 mg, 0.3 mmol). The residue was purified by flash column chromatography using a gradient from 0 to 10% MeOH in CH_2Cl_2 to afford **17** as a white solid (59 mg, 33%).

mp 188-190 °C; R_f = 0.38 (CH_2Cl_2/MeOH 9:1); ^{1}H NMR (600 MHz, DMSO-d_6) δ 0.93 (s, 9H, C(CH_3)$_3$), 1.45 – 1.52 (m, 2H, CH_2CCN), 1.58 – 1.66 (m, 2H, CH_2CCN), 1.87 – 1.94 (m, 1H, 3-H), 2.06 – 2.13 (m, 1H, 3-H), 2.24 (s, 3H, CH_3), 3.57 (d, J = 10.8 Hz, 1H, 5-H), 3.64 (dd, J = 10.9, 3.7 Hz, 1H, 5-H), 4.22 (dd, J = 16.7, 5.2 Hz, 1H), 4.34 – 4.39 (m, 1H), 4.44 – 4.54 (m, 3H) (2-H, 4-H, NHC<u>H</u>, NHC<u>H</u>$_2$), 5.18 (d, J = 3.5 Hz, 1H, OH), 7.33 (d, J = 8.9 Hz, 1H, CONH), 7.59 (s, 1H, Ar-H), 7.87 (s, 1H, Ar-H), 8.82 (dd, J = 6.8, 5.3 Hz, 1H, CONH), 9.12 (s, 1H, 2″-H); ^{13}C NMR (151 MHz, DMSO-d_6) δ 13.6 (CH_2<u>C</u>CN), 15.4 (CH_3), 16.6, 16.8 (<u>C</u>H_2CCN), 26.1 (C(<u>C</u>H_3)$_3$), 36.4 (<u>C</u>(CH_3)$_3$), 37.7 (C-3), 56.6, 57.3, 59.1 (C-2, C-5, NHCH), 69.0 (C-4), 119.9 (CN), 126.0, 129.5, 129.9, 130.1, 132.4, 132.5 (C-2′, C-3′, C-4′, C-5′, C-5″, C-6′), 139.0 (C-1′), 150.7 (C-4″), 153.4 (C-2″), 164.3, 168.7, 172.2 (CO); the signal for $NHCH_2$ is missing (overlapping solvent peak). LC-MS (ESI) (90% H_2O to 100% MeCN in 10 min, then 100% MeCN to 15 min, DAD 200-600 nm), t_R = 6.10 min, 98% purity, *m/z* calcd for $C_{27}H_{31}Cl_2N_5O_4S$ $[M + H]^+$, 592.15; found, 592.3. HRMS (ESI) *m/z* calcd for $C_{27}H_{31}Cl_2N_5O_4S$ $[M + H]^+$, 592.1547; found, 592.1536.

(2*S*,4*R*)-1-((*S*)-2-(1-Cyanocyclopropane-1-carboxamido)-3,3-dimethylbutanoyl)-*N*-(2,3-dimethyl-4-(4-methylthiazol-5-yl)benzyl)-4-hydroxypyrrolidine-2-carboxamide (18)

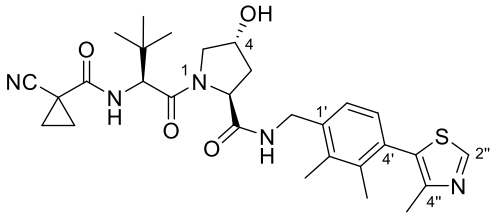

Following General Procedure C, compound **18** was obtained using Boc-protected amine **42r** (type **42**, R = 2-Me, 3-Me; 98 mg, 0.3 mmol) and acid **46** (101 mg, 0.3 mmol). The residue was purified by flash column chromatography using a gradient from 0 to 10% MeOH in CH_2Cl_2 to afford **18** as a white solid (60 mg, 36%).

mp 131-132 °C; R_f = 0.58 (CH_2Cl_2/MeOH 9:1); ^{1}H NMR (500 MHz, DMSO-d_6) δ 0.95 (s, 9H, C(CH_3)$_3$), 1.43 – 1.54 (m, 2H, CH_2CCN), 1.58 – 1.66 (m, 2H, CH_2CCN), 1.87 – 1.94 (m, 1H, 3-H), 2.03 – 2.09 (m, 4H, 3-H, CH_3), 2.15 (s, 3H, CH_3), 2.20 (s, 3H, CH_3), 3.56 (d, *J* = 10.8 Hz, 1H, 5-H), 3.64 (dd, *J* = 10.8, 3.9 Hz, 1H, 5-H), 4.28 (dd, *J* = 15.4, 5.5 Hz, 1H), 4.31 – 4.38 (m, 2H), 4.50 (dd, *J* = 16.1, 8.4 Hz, 2H) (2-H, 4-H, NHC<u>H</u>, NHC<u>H</u>$_2$), 5.12 (d, *J* = 3.6 Hz, 1H, OH), 7.02 (d, *J* = 7.9 Hz, 1H), 7.24 (d, *J* = 7.9 Hz, 1H), 7.32 (d, *J* = 8.8 Hz, 1H) (Ar-H, CONH), 8.43 (t, *J* = 5.8 Hz, 1H, CONH), 9.03 (s, 1H, 2″-H); ^{13}C NMR (126 MHz, DMSO-d_6) δ 13.6 (CH_2<u>C</u>CN), 14.9 (CH_3), 15.1 (CH_3), 16.5, 16.7 (<u>C</u>H_2CCN), 16.8 (CH_3), 26.0 (C(<u>C</u>H_3)$_3$), 36.2 (<u>C</u>(CH$_3$)$_3$), 37.9 (C-3), 41.1 (NHCH_2), 56.6, 57.3, 58.7 (C-2, C-5, NHCH), 68.8 (C-4), 120.0 (CN), 125.3, 128.0, 129.1, 130.7, 135.2, 135.78 (C-2′, C-3′, C-4′, C-5′, C-5″, C-6′), 137.4 (C-1′), 148.9 (C-4″), 152.0 (C-2″), 164.3, 168.6, 171.2 (CO). LC-MS (ESI) (90% H_2O to 100% MeCN in 10 min, then 100% MeCN to 15 min, DAD 200-600 nm), t_R = 5.96 min, 100% purity, *m/z* calcd for $C_{29}H_{37}N_5O_4S$ $[M + H]^+$, 552.26; found, 552.4. HRMS (ESI) *m/z* calcd for $C_{29}H_{37}N_5O_4S$ $[M + H]^+$, 552.2639; found, 552.2638.

(2*S*,4*R*)-1-((*S*)-2-(1-Cyanocyclopropane-1-carboxamido)-3,3-dimethylbutanoyl)-*N*-(2,3-difluoro-4-(4-methylthiazol-5-yl)benzyl)-4-hydroxypyrrolidine-2-carboxamide (19)

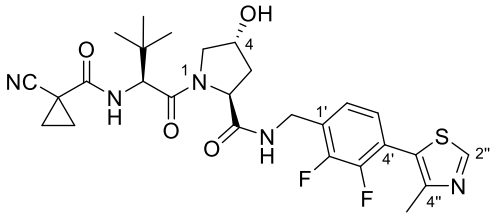

Following General Procedure C, compound **19** was obtained using Boc-protected amine **42s** (type **42**, R = 2-F, 3-F; 102 mg, 0.3 mmol) and acid **46** (101 mg, 0.3 mmol). The residue was purified by flash column chromatography using a gradient from 0 to 10% MeOH in CH_2Cl_2 to afford **19** as a white solid (57 mg, 34%).

mp 159-162 °C; R_f = 0.58 (CH_2Cl_2/MeOH 9:1); ^{1}H NMR (600 MHz, DMSO-d_6 δ 0.93 (s, 9H, C(CH_3)$_3$), 1.45 – 1.54 (m, 2H, CH_2CCN), 1.58 – 1.66 (m, 2H, CH_2CCN), 1.86 – 1.93 (m, 1H, 3-H), 2.04 – 2.10 (m, 1H, 3-H), 2.35 (s, 3H, CH_3), 3.54 – 3.58 (m, 1H, 5-H), 3.63 (dd, J = 10.8, 3.9 Hz, 1H, 5-H), 4.30 – 4.39 (m, 2H), 4.42 (dd, J = 15.9, 6.1 Hz, 1H), 4.45 – 4.54 (m, 2H) (2-H, 4-H, NHC<u>H</u>, NHC<u>H</u>$_2$), 5.15 (d, J = 3.6 Hz, 1H, OH), 7.17 – 7.25 (m, 1H), 7.30 – 7.39 (m, 2H) (Ar-H, CONH), 8.70 (t, J = 6.0 Hz, 1H, CONH), 9.14 (s, 1H, 2″-H); ^{13}C NMR (151 MHz, DMSO-d_6) δ 13.7 (CH_2<u>C</u>CN), 15.7 (CH_3), 16.6, 16.8 (<u>C</u>H_2CCN), 26.0 (C(<u>C</u>H_3)$_3$), 35.9 (NHCH_2), 36.1 (<u>C</u>(CH_3)$_3$), 37.7 (C-3), 56.6, 57.3, 58.7 (C-2, C-5, NHCH), 68.85 (C-4), 119.4 (d, $^2J_{F,C}$ = 11.7 Hz, C-4′), 120.1 (CN), 122.6 (d, $^3J_{F,C}$ = 2.3 Hz, C-5″), 124.1 (d, $^3J_{F,C}$ = 3.6 Hz), 126.0 (d, $^3J_{F,C}$ = 2.9 Hz, C-5′, C-6′), 129.0 (d, $^2J_{F,C}$ = 11.8 Hz, C-1′), 146.5 (dd, $^1J_{F,C}$ = 189.9 Hz, $^2J_{F,C}$ = 13.2 Hz, C-2′), 148.1 (dd, $^1J_{F,C}$ = 189.2 Hz, $^2J_{F,C}$ = 13.3 Hz, C-3′), 150.7 (C-4″), 153.8 (C-2″), 164.4, 168.7, 171.9 (CO). LC-MS (ESI) (90% H_2O to 100% MeCN in 10 min, then 100% MeCN to 15 min, DAD 200-600 nm), t_R = 5.63 min, 100% purity, *m/z* calcd for $C_{27}H_{31}F_2N_5O_4S$ [M + H]$^+$, 560.21; found, 560.5. HRMS (ESI) *m/z* calcd for $C_{27}H_{31}F_2N_5O_4S$ [M + H]$^+$, 560.2138; found, 560.2130.

(2*S*,4*R*)-1-((*S*)-2-(1-Cyanocyclopropane-1-carboxamido)-3,3-dimethylbutanoyl)-*N*-(3-fluoro-2-hydroxy-4-(4-methylthiazol-5-yl)benzyl)-4-hydroxypyrrolidine-2-carboxamide (20)

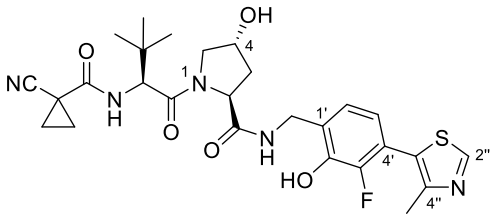

Following General Procedure C, compound **20** was obtained using Boc-protected amine **42t** (type **42**, R = 2-OH, 3-F; 135 mg, 0.4 mmol) and acid **46** (135 mg, 0.4 mmol). The residue was purified by flash column chromatography using a gradient from 0 to 10% MeOH in CH_2Cl_2 to afford **20** as a white solid (33 mg, 15%).

mp 152-154 °C; R_f = 0.53 (CH_2Cl_2/MeOH 9:1); ^{1}H NMR (600 MHz, DMSO-d_6) δ 0.93 (s, 9H, C(CH_3)$_3$), 1.45 – 1.53 (m, 2H, CH_2CCN), 1.57 – 1.65 (m, 2H, CH_2CCN), 1.86 – 1.94 (m, 1H, 3-H), 2.02 – 2.09 (m, 1H, 3-H), 2.32 (s, 3H, CH_3), 3.52 – 3.58 (m, 1H, 5-H), 3.62 (dd, J = 10.8, 3.9 Hz, 1H, 5-H), 4.20 – 4.29 (m, 2H), 4.31 – 4.36 (m, 1H), 4.45 – 4.53 (m, 2H) (2-H, 4-H, NHC<u>H</u>, NHC<u>H</u>$_2$), 5.14 (d, J = 3.7 Hz, 1H, OH), 6.78 (dd, J = 7.9, 6.6 Hz, 1H), 7.14 (d, J = 8.0 Hz, 1H), 7.32 (d, J = 8.9 Hz, 1H) (Ar-H, CONH), 8.64 (t, J = 6.1 Hz, 1H, CONH), 9.07 (s, 1H, 2″-H), 9.95 (s, 1H, Ar-OH); ^{13}C NMR (151 MHz, DMSO-d_6) δ 13.7 (CH_2<u>C</u>CN), 15.8 (CH_3), 16.6, 16.8 (<u>C</u>H_2CCN), 26.0 (C(<u>C</u>H_3)$_3$), 36.2 (<u>C</u>(CH$_3$)$_3$), 37.4, 37.8 (C-3, NHCH_2), 56.6, 57.3, 58.7 (C-2, C-5, NHCH), 68.9 (C-4), 117.8 (d, $^2J_{F,C}$ = 13.2 Hz, C-4′), 120.1 (CN), 120.7 (C-5″), 123.3 (d, $^3J_{F,C}$ = 2.6 Hz, C-5′), 124.2 (C-6′), 129.26 (d, $^3J_{F,C}$ = 1.7 Hz, C-1′), 142.6 (d, $^2J_{F,C}$ = 14.4 Hz, C-2′), 148.3 (d, $^1J_{F,C}$ = 241.3 Hz, C-3′), 149.9 (C-4″), 152.94 (C-2″), 164.4, 168.7, 172.2 (CO). LC-MS (ESI) (90% H_2O to 100% MeCN in 10 min, then 100% MeCN to 15 min, DAD 200-600 nm), t_R = 5.34 min, 95% purity, *m/z* calcd for $C_{27}H_{32}FN_5O_5S$ [M + H]$^+$, 558.22; found, 558.4. HRMS (ESI) *m/z* calcd for $C_{27}H_{32}FN_5O_5S$ [M + H]$^+$, 558.2181; found, 558.2176.

(2*S*,4*R*)-1-((*S*)-2-(1-Cyanocyclopropane-1-carboxamido)-3,3-dimethylbutanoyl)-*N*-(3-fluoro-2-methoxy-4-(4-methylthiazol-5-yl)benzyl)-4-hydroxypyrrolidine-2-carboxamide (21)

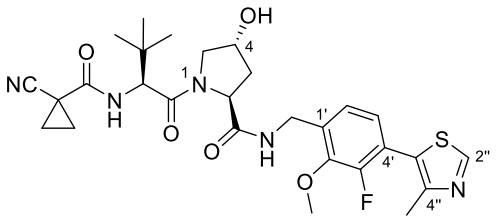

Following General Procedure C, compound **21** was obtained using Boc-protected amine **42u** (type **42**, R = 2-OMe, 3-F; 105 mg, 0.3 mmol) and acid **46** (101 mg, 0.3 mmol). The residue was purified by flash column chromatography using a gradient from 0 to 10% MeOH in CH_2Cl_2 to afford **21** as a pale orange solid (57 mg, 33%).

mp 82-83 °C; R_f = 0.40 (CH_2Cl_2/MeOH 9:1); ^{1}H NMR (600 MHz, DMSO-d_6) δ 0.94 (s, 9H, C(CH_3)$_3$), 1.46 – 1.54 (m, 2H, CH_2CCN), 1.58 – 1.65 (m, 2H, CH_2CCN), 1.87 – 1.94 (m, 1H, 3-H), 2.04 – 2.10 (m, 1H, 3-H), 2.34 (s, 3H, CH_3), 3.55 – 3.59 (m, 1H, 5-H), 3.63 (dd, J = 10.8, 3.9 Hz, 1H, 5-H), 3.90 (s, 3H, OCH_3), 4.27 – 4.40 (m, 3H), 4.46 – 4.54 (m, 2H) (2-H, 4-H, NHC<u>H</u>, NHC<u>H</u>$_2$), 5.14 (d, J = 3.7 Hz, 1H, OH), 7.07 – 7.11 (m, 1H), 7.27 (d, J = 8.1 Hz, 1H), 7.34 (d, J = 8.9 Hz, 1H) (Ar-H, CONH), 8.57 (t, J = 6.0 Hz, 1H, CONH), 9.11 (s, 1H, 2′′-H); ^{13}C NMR (151 MHz, DMSO-d_6) δ 13.7 (CH_2<u>C</u>CN), 15.7 (CH_3), 16.6, 16.8 (<u>C</u>H_2CCN), 26.0 (C(<u>C</u>H_3)$_3$), 36.2 (<u>C</u>(CH_3)$_3$), 36.9, 37.8 (C-3, NHCH_2), 56.6, 57.3, 58.8 (C-2, C-5, NHCH), 61.3 (d, $^4J_{F,C}$ = 4.8 Hz, OCH_3), 68.9 (C-4), 118.7 (C-5′′), 120.1 (CN), 123.6 (d, $^2J_{F,C}$ = 10.2 Hz, C-4′), 123.6, 125.5, 134.5 (C-1′, C-5′, C-6′), 145.1 (d, $^2J_{F,C}$ = 11.4 Hz, C-2′), 150.3 (C-4′′), 151.8 (d, $^1J_{F,C}$ = 248.1 Hz, C-3′) 153.3 (C-2′′), 164.4, 168.7, 171.7 (CO). LC-MS (ESI) (90% H_2O to 100% MeCN in 10 min, then 100% MeCN to 15 min, DAD 200-600 nm), t_R = 5.49 min, 99% purity, *m/z* calcd for $C_{28}H_{34}FN_5O_5S$ $[M + H]^+$, 571.23; found, 572.5. HRMS (ESI) *m/z* calcd for $C_{28}H_{34}FN_5O_5S$ $[M + H]^+$, 572.2337; found, 572.2330.

(2*S*,4*R*)-1-((*S*)-2-(1-Cyanocyclopropane-1-carboxamido)-3,3-dimethylbutanoyl)-4-hydroxy-*N*-((4-(4-methylthiazol-5-yl)naphthalen-1-yl)methyl)pyrrolidine-2-carboxamide (22)

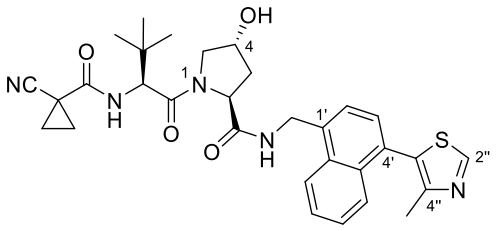

Following General Procedure C, compound **22** was obtained using Boc-protected amine **42v** (type **42**, subst. phenylene = 1,4-naphthylene; 106 mg, 0.3 mmol) and acid **46** (101 mg, 0.3 mmol). The residue was purified by flash column chromatography using a gradient from 0 to 10% MeOH in CH_2Cl_2 to afford **22** as a pale brown solid (65 mg, 38%).

mp 127-129 °C; R_f = 0.40 (CH_2Cl_2/MeOH 9:1); ^{1}H NMR (500 MHz, DMSO-d_6) δ 0.96 (s, 9H, C(CH_3)$_3$), 1.45 – 1.56 (m, 2H, CH_2CCN), 1.57 – 1.66 (m, 2H, CH_2CCN), 1.91 – 2.00 (m, 1H, 3-H), 2.03 – 2.10 (m, 1H, 3-H), 2.17 (s, 3H, CH_3), 3.55 – 3.60 (m, 1H, 5-H), 3.66 (dd, J = 10.8, 4.0 Hz, 1H, 5-H), 4.34 – 4.41 (m, 1H), 4.48 – 4.58 (m, 2H), 4.76 – 4.85 (m, 2H) (2-H, 4-H, NHC<u>H</u>, NHC<u>H</u>$_2$), 5.13 (d, J = 3.7 Hz, 1H, OH), 7.33 (d, J = 8.9 Hz, 1H), 7.46 (d, J = 7.2 Hz, 1H), 7.54 – 7.69 (m, 4H), 8.13 – 8.19 (m, 1H) (Ar-H, CONH), 8.68 (t, J = 5.8 Hz, 1H, CONH), 9.16 (s, 1H, 2′′-H); ^{13}C NMR (126 MHz, DMSO-d_6) δ 13.7 (CH_2<u>C</u>CN), 15.4 (CH_3), 16.6, 16.8 (<u>C</u>H_2CCN), 26.1 (C(<u>C</u>H_3)$_3$), 36.2 (<u>C</u>(CH$_3$)$_3$), 37.9 (C-3), 56.6, 57.3, 58.8 (C-2, C-5, NHCH), 68.9 (C-4), 120.0 (CN), 124.1, 124.5, 125.5, 126.4, 126.7, 127.7, 128.4, 128.7, 131.0, 131.8, 135.9 (C-Ar, C-5′′), 150.0 (C-4′′), 152.8 (C-2′′), 164.4, 168.6, 171.5 (CO); the signal for $NHCH_2$ is missing (overlapping solvent peak). LC-MS (ESI) (90% H_2O to 100% MeOH in 10 min, then 100% MeOH to 20 min, DAD 220-600 nm), t_R = 6.21 min, 97% purity, *m/z* calcd for $C_{31}H_{35}N_5O_4S$ $[M + H]^+$, 574.24; found, 574.4. HRMS (ESI) *m/z* calcd for $C_{31}H_{35}N_5O_4S$ $[M + H]^+$, 574.2485; found, 574.2477.

(2*S*,4*R*)-1-((*S*)-2-(1-Cyanocyclopropane-1-carboxamido)-3,3-dimethylbutanoyl)-4-hydroxy-*N*-((5-(4-methylthiazol-5-yl)quinolin-8-yl)methyl)pyrrolidine-2-carboxamide (23)

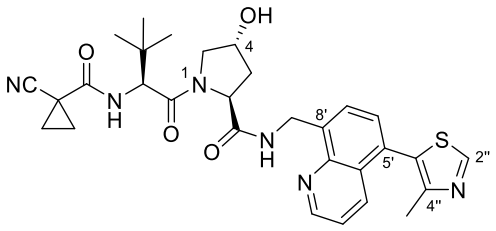

Following General Procedure C, compound **23** was obtained using Boc-protected amine **42w** (type **42**, subst. phenylene = quinoline-5,8-diyl; 107 mg, 0.3 mmol) and acid **46** (101 mg, 0.3 mmol). The residue was purified by flash column chromatography using a gradient from 0 to 10% MeOH in CH_2Cl_2 to afford **23** as a pale brown solid (61 mg, 36%).

mp 116-118 °C; R_f = 0.40 (CH_2Cl_2/MeOH 9:1^{1}H NMR (500 MHz, DMSO-d_6) δ 0.93 (s, 9H, C(CH_3)$_3$), 1.45 – 1.56 (m, 2H, CH_2CCN), 1.58 – 1.66 (m, 2H, CH_2CCN), 1.95 – 2.01 (m, 1H, 3-H), 2.07 – 2.15 (m, 1H, 3-H), 2.18 (s, 3H, CH_3), 3.58 (d, J = 10.8 Hz, 1H, 5-H), 3.65 (dd, J = 10.9, 3.9 Hz, 1H, 5-H), 4.34 – 4.39 (m, 1H), 4.53 (d, J = 8.9 Hz, 1H), 4.59 (t, J = 8.2 Hz, 1H), 4.90 – 5.03 (m, 2H) (2-H, 4-H, NHC<u>H</u>, NHC<u>H</u>$_2$), 5.15 (d, J = 3.6 Hz, 1H, OH), 7.36 (d, J = 8.9 Hz, 1H), 7.54 (d, J = 7.4 Hz, 1H), 7.61 (dd, J = 8.5, 4.1 Hz, 1H), 7.88 (d, J = 7.4 Hz, 1H), 8.03 (dd, J = 8.6, 1.7 Hz, 1H), 8.68 (t, J = 6.1 Hz, 1H) (Ar-H, CONH), 9.00 (dd, J = 4.2, 1.7 Hz, 1H, CONH), 9.19 (s, 1H, 2′′-H); ^{13}C NMR (126 MHz, DMSO-d_6) δ 13.7 (CH_2<u>C</u>CN), 15.5 (CH_3), 16.6, 16.7 (<u>C</u>H_2CCN), 26.0 (C(<u>C</u>H_3)$_3$), 36.2 (<u>C</u>(CH_3)$_3$), 37.8 (C-3), 56.6, 57.3, 58.9 (C-2, C-5, NHCH), 68.9 (C-4), 120.1 (CN), 122.1, 126.2, 126.5, 127.1, 127.3, 129.2, 133.7, 137.9 (C-Ar, C-5′′), 145.4, 149.9 (C-2′, C-8a′), 150.3 (C-4′′), 153.2 (C-2′′), 164.4, 168.8, 171.9 (CO); the signal for $NHCH_2$ is missing (overlapping solvent peak). LC-MS (ESI) (90% H_2O to 100% MeOH in 10 min, then 100% MeOH to 20 min, DAD 220-400 nm), t_R = 10.61 min, 98% purity, *m/z* calcd for $C_{30}H_{34}N_6O_4S$ $[M + H]^+$, 575.24; found, 575.3. HRMS (ESI) *m/z* calcd for $C_{30}H_{34}N_6O_4S$ $[M + H]^+$, 575.2435; found, 575.2430.

(2*S*,4*R*)-1-((*S*)-2-(1-Cyanocyclopropane-1-carboxamido)-3,3-dimethylbutanoyl)-4-hydroxy-*N*-((*S*)-1-(2-methyl-4-(4-methylthiazol-5-yl)phenyl)ethyl)pyrrolidine-2-carboxamide (24)

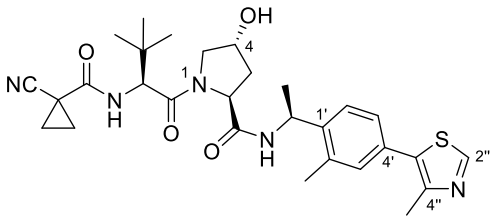

Following General Procedure C, compound **24** was obtained using Boc-protected amine **60a** (type **60**; R = 2-Me; 100 mg, 0.3 mmol) and acid **46** (101 mg, 0.3 mmol). The residue was purified by flash column chromatography using a gradient from 0 to 10% MeOH in CH_2Cl_2 to afford **24** as a white solid (58 mg, 35%).

mp 110-112 °C; R_f = 0.40 (CH_2Cl_2/MeOH 9:1); ^{1}H NMR (600 MHz, DMSO-d_6) δ 0.95 (s, 9H, C(CH_3)$_3$), 1.35 (d, J = 6.9 Hz, 3H, CHC<u>H</u>$_3$), 1.47 – 1.53 (m, 2H, CH_2CCN), 1.59 – 1.67 (m, 2H, CH_2CCN), 1.70 – 1.77 (m, 1H), 2.01 – 2.06 (m, 1H, 3-H), 2.33 (s, 3H, CH_3), 2.45 (s, 3H, Ar-CH_3), 3.49 – 3.59 (m, 2H, 5-H), 4.24 – 4.28 (m, 1H), 4.46 (t, J = 8.3 Hz, 1H), 4.50 (d, J = 8.9 Hz, 1H) (2-H, 4-H, NHC<u>H</u>), 5.02 – 5.09 (m, 1H, C<u>H</u>CH$_3$), 5.11 (d, J = 3.6 Hz, 1H, OH), 7.23 – 7.26 (m, 1H), 7.28 – 7.32 (m, 2H), 7.39 (d, J = 8.0 Hz, 1H) (Ar-H, CONH), 8.43 (d, J = 7.7 Hz, 1H, CONH), 8.97 (s, 1H, 2″-H); ^{13}C NMR (151 MHz, DMSO-d_6) δ 13.6 (CH_2<u>C</u>CN), 16.0 (CH_3), 16.6, 16.8 (<u>C</u>H_2CCN), 18.5 (CH_3), 21.0 (CH<u>C</u>H$_3$), 26.1 (C(<u>C</u>H$_3$)$_3$), 36.2 (<u>C</u>(CH$_3$)$_3$), 37.6 (C-3), 44.4 (<u>C</u>HCH$_3$), 56.6, 57.3, 58.6 (C-2, C-5, NHCH), 68.7 (C-4), 125.3, 126.6, 129.6, 130.5, 131.1 (C-3′, C-4′, C-5′, C-6′, C-5″), 135.5 (C-2′), 142.6 (C-1′), 147.6 (C-4″), 151.3 (C-2″), 164.3, 168.5, 170.1 (CO). LC-MS (ESI) (90% H_2O to 100% MeCN in 10 min, then 100% MeCN to 15 min, DAD 200-600 nm), t_R = 5.98 min, 97% purity, *m/z* calcd for $C_{29}H_{37}N_5O_4S$ $[M + H]^+$, 552.26; found, 552.4. HRMS (ESI) *m/z* calcd for $C_{29}H_{37}N_5O_4S$ $[M + H]^+$, 552.2639; found, 552.2637.

(2*S*,4*R*)-1-((S)-2-(1-Cyanocyclopropane-1-carboxamido)-3,3-dimethylbutanoyl)-*N*-((*S*)-1-(3-fluoro-4-(4-methylthiazol-5-yl)phenyl)ethyl)-4-hydroxypyrrolidine-2-carboxamide (25)

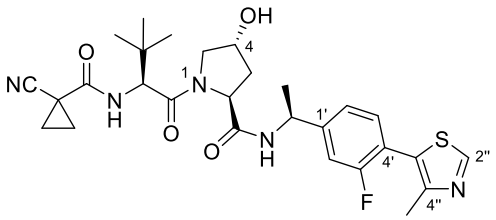

Following General Procedure C, compound **25** was obtained using Boc-protected amine **60b** (type **60**; R = 3-F; 101 mg, 0.3 mmol) and acid **46** (101 mg, 0.3 mmol). The residue was purified by flash column chromatography using a gradient from 0 to 10% MeOH in CH_2Cl_2 to afford **25** as a white solid (62 mg, 37%).

mp 198 °C; R_f = 0.47 (CH_2Cl_2/MeOH 9:1); ^{1}H NMR (600 MHz, DMSO-d_6) δ 0.95 (s, 9H, C(CH_3)$_3$), 1.39 (d, J = 7.0 Hz, 3H, CHC<u>H</u>$_3$), 1.47 – 1.53 (m, 2H, CH_2CCN), 1.59 – 1.67 (m, 2H, CH_2CCN), 1.75 – 1.81 (m, 1H, 3-H), 2.06 – 2.11 (m, 1H, 3-H), 2.33 (s, 3H, CH_3), 3.51 – 3.61 (m, 2H, 5-H), 4.27 – 4.32 (m, 1H), 4.47 (dd, J = 9.0, 7.7 Hz, 1H), 4.51 (d, J = 8.9 Hz, 1H) (2-H, 4-H, NHC<u>H</u>), 4.89 – 4.97 (m, 1H, C<u>H</u>CH_3), 5.13 (d, J = 3.6 Hz, 1H, OH), 7.20 – 7.32 (m, 3H), 7.44 (t, J = 7.8 Hz, 1H) (Ar-H, CONH), 8.50 (d, J = 7.6 Hz, 1H, CONH), 9.10 (s, 1H, 2″-H); ^{13}C NMR (151 MHz, DMSO-d_6) δ 13.7 (CH_2<u>C</u>CN), 15.7 (d, $^5J_{F,C}$ = 1.9 Hz, CH_3), 16.6, 16.8 (<u>C</u>H_2CCN), 22.3 (CH<u>C</u>H_3), 26.1 (C(<u>C</u>H_3)$_3$), 36.2 (<u>C</u>(CH_3)$_3$), 37.7 (C-3), 47.6 (<u>C</u>HCH_3), 56.6, 57.3, 58.7 (C-2, C-5, NHCH), 68.8 (C-4), 113.3 (d, $^2J_{F,C}$ = 22.9 Hz, C-2′), 116.9 (d, $^2J_{F,C}$ = 15.3 Hz, C-4′), 120.1 (CN), 122.1 (d, $^3J_{F,C}$ = 2.8 Hz, C-5″), 123.8 (C-6′), 131.9 (d, $^2J_{F,C}$ = 2.5 Hz, C-5′), 148.5 (d, $^3J_{F,C}$ = 7.3 Hz, C-1′), 150.1 (C-4″), 153.1 (C-2″), 158.8 (d, $^1J_{F,C}$ = 246.4 Hz, C-3′), 164.3, 168.6, 170.5 (CO). LC-MS (ESI) (90% H_2O to 100% MeCN in 10 min, then 100% MeCN to 15 min, DAD 200-600 nm), t_R = 5.80 min, 95% purity, *m/z* calcd for $C_{17}H_{22}N_2O_2S$ [M + H]$^+$, 556.24; found, 556.4. HRMS (ESI) *m/z* calcd for $C_{17}H_{22}N_2O_2S$ [M + H]$^+$, 556.2388; found, 556.2388.

(2*S*,4*R*)-1-((*S*)-2-(1-Fluorocyclopropane-1-carboxamido)-3,3-dimethylbutanoyl)-4-hydroxy-*N*-(2-methyl-4-(4-methylthiazol-5-yl)benzyl)pyrrolidine-2-carboxamide (26)

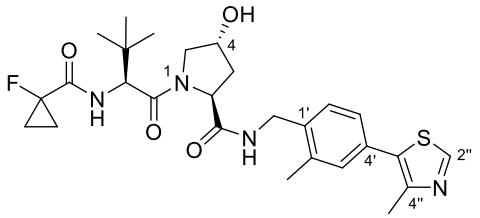

Following General Procedure C, compound **26** was obtained using Boc-protected amine **42b** (type **42**; R = 2-Me; 127 mg, 0.4 mmol) and acid **62** (132 mg, 0.4 mmol). The residue was purified by flash column chromatography using a gradient from 0 to 10% MeOH in CH_2Cl_2 to afford **26** as a yellow solid (137 mg, 66%).

mp 107-108 °C; R_f = 0.48 (CH_2Cl_2/MeOH 9:1); ^{1}H NMR (500 MHz, DMSO-d_6) δ 0.97 (s, 9H, $(CH_3)_3$), 1.17 – 1.26 (m, 2H, CH_2CF), 1.29 – 1.43 (m, 2H, CH_2CF), 1.87 – 1.96 (m, 1H, 3-H), 2.04 – 2.12 (m, 1H, 3-H), 2.30 (s, 3H, CH_3), 2.45 (s, 3H, Ar-CH_3), 3.60 (d, J = 10.8 Hz, 1H, 5-H), 3.66 (dd, J = 10.7, 3.9 Hz, 1H, 5-H), 4.21 (dd, J = 15.6, 5.3 Hz, 1H), 4.31 – 4.38 (m, 2H), 4.50 (t, J = 8.2 Hz, 1H), 4.56 – 4.62 (m, 1H) (2-H, 4-H, NHC<u>H</u>, NHC<u>H</u>$_2$), 5.13 (d, J = 3.7 Hz, 1H, OH), 7.20 – 7.30 (m, 3H), 7.41 (d, J = 7.9 Hz, 1H) (Ar-H, CONH), 8.47 (t, J = 5.7 Hz, 1H, CONH), 8.97 (s, 1H, 2″-H); ^{13}C NMR (126 MHz, DMSO-d_6) δ 12.6 (d, $^2J_{F,C}$ = 10.5 Hz, CH_2CF), 12.9 (d, $^2J_{F,C}$ = 10.1 Hz, CH_2CF), 15.9 (CH_3), 18.4 (Ar-CH_3), 26.1 (C(<u>C</u>H$_3$)$_3$), 36.0 (<u>C</u>(CH$_3$)$_3$), 37.9 (C-3), 54.8 ($NHCH_2$), 56.5, 56.6, 58.7 (C-2, C-5, NHCH), 68.9 (C-4), 78.1 (d, $^1J_{F,C}$ = 232.6 Hz, CF), 126.1, 127.9, 129.0, 130.2, 131.1 (C-3′, C-4′, C-5′, C-5″, C-6′), 136.3, 136.9 (C-1′, C-2′), 147.63 (C-4″), 151.3 (C-2″), 168.0 (d, $^2J_{F,C}$ = 20.1 Hz), 168.8 , 171.4 (CO). LC-MS (ESI) (90% H_2O to 100% MeCN in 10 min, then 100% MeCN to 15 min, DAD 200-600 nm), t_R = 5.77 min, 99% purity, *m/z* calcd for $C_{27}H_{35}FN_4O_4S$ $[M + H]^+$, 531.24; found, 531.3. HRMS (ESI) *m/z* calcd for $C_{27}H_{35}FN_4O_4S$ $[M + H]^+$, 531.2436; found, 531.2430.

(2*S*,4*R*)-*N*-(3-Fluoro-4-(4-methylthiazol-5-yl)benzyl)-1-((S)-2-(1-fluorocyclopropane-1-carboxamido)-3,3-dimethylbutanoyl)-4-hydroxypyrrolidine-2-carboxamide (27)

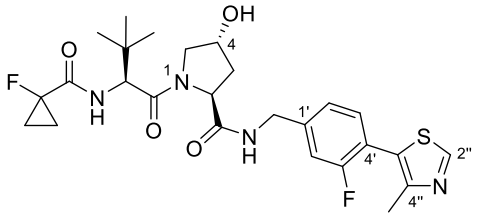

Following General Procedure C, compound **27** was obtained using Boc-protected amine **42h** (type **42**; R = 3-F; 129 mg, 0.4 mmol) and acid **62** (132 mg, 0.4 mmol). The residue was purified by flash column chromatography using a gradient from 0 to 10% MeOH in CH_2Cl_2 to afford **27** as a white solid (155 mg, 74%).

mp 92-94 °C; R_f = 0.48 (CH_2Cl_2/MeOH 9:1 ^{1}H NMR (600 MHz, DMSO-d_6) δ 0.96 (s, 9H, C(CH_3)$_3$), 1.17 – 1.25 (m, 2H, CH_2CF), 1.31 – 1.41 (m, 2H, CH_2CF), 1.88 – 1.94 (m, 1H, 3-H), 2.05 – 2.12 (m, 1H, 3-H), 2.32 (s, 3H, CH_3), 3.58 – 3.63 (m, 1H, 5-H), 3.67 (dd, *J* = 10.8, 3.9 Hz, 1H, 5-H), 4.23 (dd, *J* = 16.1, 5.5 Hz, 1H), 4.33 – 4.38 (m, 1H), 4.44 – 4.51 (m, 2H), 4.55 – 4.61 (m, 1H) (2-H, 4-H, NHC<u>H</u>, NHC<u>H</u>$_2$), 5.16 (d, *J* = 3.6 Hz, 1H, OH), 7.19 – 7.28 (m, 2H), 7.33 (dd, *J* = 11.4, 1.6 Hz, 1H), 7.40 (t, *J* = 7.8 Hz, 1H) (Ar-H, CONH), 8.69 (t, *J* = 6.1 Hz, 1H, CONH), 9.09 (s, 1H, 2″-H); ^{13}C NMR (151 MHz, DMSO-d_6) δ 12.7 (d, $^2J_{F,C}$ = 10.1 Hz, CH_2CF), 12.9 (d, $^2J_{F,C}$ = 10.2 Hz, CH_2CF), 15.7 (CH_3), 26.1 (C(<u>C</u>H_3)$_3$), 36.0 (<u>C</u>(CH_3)$_3$), 37.8 (C-3), 41.4 ($NHCH_2$), 56.5, 56.6, 58.8 (C-2, C-5, NHCH), 68.9 (C-4), 78.1 (d, $^1J_{F,C}$ = 231.9 Hz, CF), 114.4 (d, $^2J_{F,C}$ = 23.0 Hz, C-2′), 116.8 (d, $^2J_{F,C}$ = 15.4 Hz, C-4′), 123.1 (d, $^3J_{F,C}$ = 3.3 Hz, C-5″), 123.8 (C-6′), 131.7 (d, $^3J_{F,C}$ = 2.8 Hz, C-5′), 143.2 (d, $^3J_{F,C}$ = 7.6 Hz, C-1′), 150.1 (C-4″), 153.1 (C-2″), 158.9 (d, $^2J_{F,C}$ = 246.3 Hz, C-3′), 168.0 (d, $^2J_{F,C}$ = 21.0 Hz), 168.9, 171.9 (CO). LC-MS (ESI) (90% H_2O to 100% MeCN in 10 min, then 100% MeCN to 15 min, DAD 200-600 nm), t_R = 5.59 min, 100% purity, *m/z* calcd for $C_{26}H_{32}F_2N_4O_4S$ $[M + H]^+$, 535.22; found, 535.3. HRMS (ESI) *m/z* calcd for $C_{26}H_{32}F_2N_4O_4S$ $[M + H]^+$, 535.2185; found, 535.2179.

(2*S*,4*R*)-*N*-(5-Fluoro-2-methyl-4-(4-methylthiazol-5-yl)benzyl)-1-((*S*)-2-(1-fluorocyclopropane-1-carboxamido)-3,3-dimethylbutanoyl)-4-hydroxypyrrolidine-2-carboxamide (28)

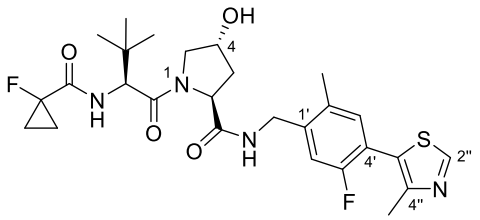

Following General Procedure C, compound **28** was obtained using Boc-protected amine **42x** (type **42**; R = 2-Me, 5-F; 100 mg, 0.3 mmol) and acid **62** (99 mg, 0.3 mmol). The residue was purified by flash column chromatography using a gradient from 0 to 10% MeOH in CH_2Cl_2 to afford **28** as a white solid (111 mg, 67%).

mp 85-86 °C °C; R_f = 0.51 (CH_2Cl_2/MeOH 9:1); ^{1}H NMR (500 MHz, DMSO-d_6) δ 0.95 (s, 9H, C(CH_3)$_3$), 1.18 – 1.28 (m, 2H, CH_2CF), 1.30 – 1.42 (m, 2H, CH_2CF), 1.87 – 1.96 (m, 1H, 3-H), 2.05 – 2.12 (m, 1H, 3-H), 2.26 (s, 3H, CH_3), 2.32 (d, J = 1.2 Hz, 3H, CH_3), 3.61 (d, J = 10.8 Hz, 1H, 5-H), 3.67 (dd, J = 10.8, 3.8 Hz, 1H, 5-H), 4.14 (dd, J = 16.2, 5.2 Hz, 1H), 4.33 – 4.42 (m, 2H), 4.51 (t, J = 8.2 Hz, 1H), 4.56 – 4.62 (m, 1H) (2-H, 4-H, NHC<u>H</u>, NHC<u>H</u>$_2$), 5.16 (d, J = 3.6 Hz, 1H, OH), 7.21 – 7.28 (m, 2H), 7.35 (d, J = 11.3 Hz, 1H) (Ar-H, CONH), 8.62 (t, J = 5.9 Hz, 1H, CONH), 9.08 (s, 1H, 2″-H); ^{13}C NMR (126 MHz, DMSO-d_6) δ 12.6 (d, $^2J_{F,C}$ = 10.2 Hz, <u>C</u>H_2CF), 12.9 (d, $^2J_{F,C}$ = 10.1 Hz, <u>C</u>H_2CF), 15.6 (d, $^5J_{F,C}$ = 2.8 Hz, CH_3), 17.5 (Ar-CH_3), 26.1 (C(<u>C</u>H_3)$_3$), 36.0 (NHCH_2), 37.8 (C-3), 56.5, 56.6, 58.8 (C-2, C-5, NHCH), 68.9 (C-4), 78.1 (d, $^1J_{F,C}$ = 232.3 Hz, CF), 114.4 (d, $^2J_{F,C}$ = 23.7 Hz, C-2′), 116.3 (d, $^2J_{F,C}$ = 15.2 Hz, C-4′), 123.9 (C-6′), 131.5 (d, $^3J_{F,C}$ = 3.4 Hz, C-5″), 132.7 (d, $^3J_{F,C}$ = 2.3 Hz, C-5′), 140.4 (d, $^3J_{F,C}$ = 7.2 Hz, C-1′), 149.9 (C-4″), 152.8 (C-2″), 157.4 (d, $^1J_{F,C}$ = 244.0 Hz, C-3′), 168.0 (d, $^2J_{F,C}$ = 20.2 Hz), 168.9, 171.8 (CO). LC-MS (ESI) (90% H_2O to 100% MeCN in 10 min, then 100% MeCN to 15 min, DAD 200-600 nm), t_R = 5.84 min, 99% purity, *m/z* calcd for $C_{27}H_{34}F_2N_4O_4S$ $[M + H]^+$, 549.23; found, 549.4. HRMS (ESI) *m/z* calcd for $C_{27}H_{34}F_2N_4O_4S$ $[M + H]^+$, 549.2341; found, 549.2334.

(2*S*,4*R*)-*N*-(5-Fluoro-2-methoxy-4-(4-methylthiazol-5-yl)benzyl)-1-((*S*)-2-(1-fluorocyclopropane-1-carboxamido)-3,3-dimethylbutanoyl)-4-hydroxypyrrolidine-2-carboxamide (29)

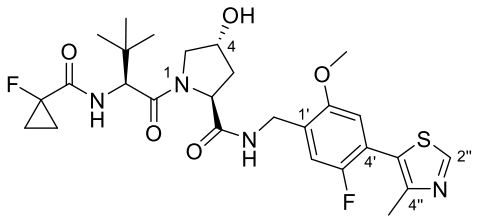

Following General Procedure C, compound **29** was obtained using Boc-protected amine **42y** (type **42**; R = 2-OMe, 5-F; 141 mg, 0.4 mmol) and acid **62** (132 mg, 0.4 mmol). The residue was purified by flash column chromatography using a gradient from 0 to 10% MeOH in CH_2Cl_2 to afford **29** as a white solid (128 mg, 55%).

mp 88-90°C; R_f = 0.44 (CH_2Cl_2/MeOH 9:1); ^{1}H NMR (600 MHz, DMSO-d_6) δ 0.94 (s, 9H, C(CH_3)$_3$), 1.17 – 1.27 (m, 2H, CH_2CF), 1.30 – 1.41 (m, 2H, CH_2CF), 1.87 – 1.96 (m, 1H, 3-H), 2.04 – 2.11 (m, 1H, 3-H), 2.33 (d, J = 1.2 Hz, 3H, CH_3), 3.60 (d, J = 10.8 Hz, 1H, 5-H), 3.65 (dd, J = 10.8, 3.8 Hz, 1H, 5-H), 4.11 (dd, J = 16.8, 5.3 Hz, 1H), 4.25 – 4.39 (m, 2H), 4.49 (t, J = 8.3 Hz, 1H), 4.58 (d, J = 9.2 Hz, 1H) (2-H, 4-H, NHC<u>H</u>, NHC<u>H</u>$_2$), 5.15 (d, J = 3.6 Hz, 1H, OH), 6.97 (d, J = 5.9 Hz, 1H), 7.24 (dd, J = 9.2, 2.8 Hz, 1H), 7.36 (d, J = 10.6 Hz, 1H) (Ar-H, CONH), 8.60 (t, J = 6.0 Hz, 1H, CONH), 9.08 (s, 1H, 2′′-H); ^{13}C NMR (151 MHz, DMSO-d_6) δ 12.7 (d, $^2J_{F,C}$ = 10.4 Hz, <u>C</u>H_2CF), 12.9 (d, $^2J_{F,C}$ = 10.1 Hz, <u>C</u>H_2CF), 15.7 (CH_3), 26.1 (C(<u>C</u>H_3)$_3$), 36.0 (<u>C</u>(CH_3)$_3$), 37.1 (C-3), 37.8 ($NHCH_2$), 56.1, 56.5, 56.6, 58.9 (OCH_3, C-2, C-5, NHCH), 68.9 (C-4), 78.2 (d, $^1J_{F,C}$ = 232.3 Hz, CF), 112.9 (C-5′′), 114.9 (d, $^2J_{F,C}$ = 25.7 Hz, C-2′), 116.7b(d, $^2J_{F,C}$ = 16.7 Hz, C-4′), 124.1 (C-5′), 130.0 (d, $^3J_{F,C}$ = 7.4 Hz, C-1′), 150.2 (C-4′′), 152.3 (C-6′), 153.0 (C-2′′), 153.3 (d, $^1J_{F,C}$ = 238.8 Hz, C-3′), 168.0 (d, $^2J_{F,C}$ = 20.6 Hz), 169.0, 172.1 (CO). LC-MS (ESI) (90% H_2O to 100% MeCN in 10 min, then 100% MeCN to 15 min, DAD 200-600 nm), t_R = 5.82 min, 95% purity, *m/z* calcd for $C_{27}H_{35}F_2N_4O_5S$ $[M + H]^+$, 565.23; found, 565.4. HRMS (ESI) *m/z* calcd for $C_{27}H_{35}F_2N_4O_5S$ $[M + H]^+$, 565.2291; found, 565.2284.

(2*S*,4*R*)-1-((*S*)-2-(1-Fluorocyclopropane-1-carboxamido)-3,3-dimethylbutanoyl)-4-hydroxy-N-((*S*)-1-(2-methyl-4-(4-methylthiazol-5-yl)phenyl)ethyl)pyrrolidine-2-carboxamide (30)

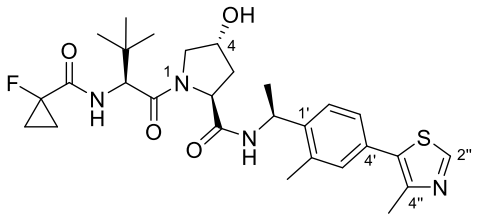

Following General Procedure C, compound **30** was obtained using Boc-protected amine **60a** (type **60**; R = 2-Me; 100 mg, 0.3 mmol) and acid **62** (99 mg, 0.3 mmol). The residue was purified by flash column chromatography using a gradient from 0 to 10% MeOH in CH_2Cl_2 to afford **30** as a white solid (118 mg, 72%).

mp 196 °C; R_f = 0.42 (CH_2Cl_2/MeOH 9:1); ^{1}H NMR (500 MHz, DMSO-d_6) δ 0.97 (s, 9H, C(CH_3)$_3$), 1.19 – 1.28 (m, 2H, CH_2CF), 1.32 – 1.41 (m, 5H, CH_2CF, CHC<u>H</u>$_3$), 1.71 – 1.78 (m, 1H, 3-H), 2.01 – 2.07 (m, 1H, 3-H), 2.33 (s, 3H, CH_3), 2.46 (s, 3H, CH_3), 3.53 – 3.61 (m, 2H, 5-H), 4.24 – 4.30 (m, 1H), 4.46 (t, J = 8.2 Hz, 1H), 4.55 – 4.60 (m, 1H) (2-H, 4-H, NHC<u>H</u>), 5.03 – 5.09 (m, 1H, C<u>H</u>CH$_3$), 5.10 (d, J = 3.6 Hz, 1H, OH), 7.21 – 7.26 (m, 2H), 7.31 (dd, J = 8.0, 2.0 Hz, 1H), 7.39 (d, J = 8.0 Hz, 1H) (Ar-H, CONH), 8.40 (d, J = 7.7 Hz, 1H, CONH), 8.97 (s, 1H, 2″-H); ^{13}C NMR (126 MHz, DMSO-d_6) δ 12.6 (d, $^2J_{F,C}$ = 10.4 Hz, <u>C</u>H$_2$CF), 12.9 (d, $^2J_{F,C}$ = 10.4 Hz, <u>C</u>H$_2$CF), 16.0 (CH_3), 18.5 (CH_3), 21.0 (CH<u>C</u>H$_3$), 26.2 (C(<u>C</u>H$_3$)$_3$), 36.0 (<u>C</u>(CH$_3$)$_3$), 37.6 (C-3), 44.4 (<u>C</u>HCH$_3$), 56.5, 56.5, 58.6 (C-2, C-5, NHCH), 68.7 (C-4), 78.1 (d, $^1J_{F,C}$ = 232.5 Hz, CH$_2$<u>C</u>F), 125.3, 126.5, 129.6, 130.5, 131.1, 135.5 (C-2′, C-3′, C-4′, C-5′, C-5″, C-6′), 142.5 (C-1′), 147.6 (C-4″), 151.3 (C-2″), 167.9 (d, $^2J_{F,C}$ = 20.1 Hz), 168.7, 170.1 (CO). LC-MS (ESI) (90% H_2O to 100% MeCN in 10 min, then 100% MeCN to 15 min, DAD 200-600 nm), t_R = 6.13 min, 98% purity, *m/z* calcd for $C_{28}H_{37}FN_4O_4S$ $[M + H]^+$, 545.26; found, 545.4. HRMS (ESI) *m/z* calcd for $C_{28}H_{37}FN_4O_4S$ $[M + H]^+$, 545.2592; found, 545.2586.

(2*S*,4*R*)-*N*-((S)-1-(3-Fluoro-4-(4-methylthiazol-5-yl)phenyl)ethyl)-1-((*S*)-2-(1-fluorocyclopropane-1-carboxamido)-3,3-dimethylbutanoyl)-4-hydroxypyrrolidine-2-carboxamide (31)

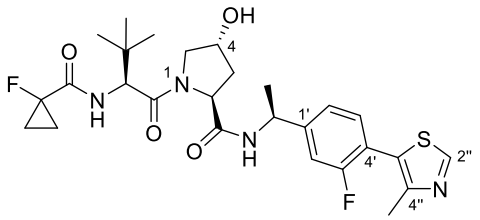

Following General Procedure C, compound **31** was obtained using Boc-protected amine **60b** (type **60**; R = 3-F; 101 mg, 0.3 mmol) and acid **62** (99 mg, 0.3 mmol). The residue was purified by flash column chromatography using a gradient from 0 to 10% MeOH in CH_2Cl_2 to afford **31** as a white solid (129 mg, 78%).

mp 198-200 °C; R_f = 0.42 (CH_2Cl_2/MeOH 9:1); ^{1}H NMR (500 MHz, DMSO-d_6) δ 0.97 (s, 9H, $C(CH_3)_3$), 1.19 – 1.24 (m, 2H, CH_2CF), 1.32 – 1.45 (m, 5H, CH_2CF, $CHC\underline{H}_3$), 1.75 – 1.82 (m, 1H, 3-H), 2.06 – 2.11 (m, 1H, 3-H), 2.34 (d, J = 1.1 Hz, 3H, CH_3), 3.54 – 3.63 (m, 2H, 5-H), 4.28 – 4.32 (m, 1H), 4.47 (t, J = 8.3 Hz, 1H), 4.58 (dd, J = 9.3, 1.3 Hz, 1H) (2-H, 4-H, NHC$\underline{H}$), 4.90 – 4.97 (m, 1H, C$\underline{H}CH_3$), 5.13 (d, J = 3.6 Hz, 1H, OH), 7.17 – 7.29 (m, 3H), 7.42 – 7.47 (m, 1H) (Ar-H, CONH), 8.47 (d, J = 7.6 Hz, 1H, CONH), 9.09 (s, 1H, 2″-H); ^{13}C NMR (126 MHz, DMSO-d_6) δ 12.6 (d, $^2J_{F,C}$ = 10.2 Hz, $\underline{C}H_2CF$), 12.9 (d, $^2J_{F,C}$ = 10.1 Hz, $\underline{C}H_2CF$), 15.7 (d, $^5J_{F,C}$ = 2.6 Hz, CH_3), 22.3 ($CH\underline{C}H_3$), 26.2 ($C(\underline{C}H_3)_3$), 36.0 ($\underline{C}(CH_3)_3$), 37.7 (C-3), 47.5 ($\underline{C}HCH_3$), 56.5, 56.6, 58.6 (C-2, C-5, NHCH), 68.8 (C-4), 78.1 (d, $^1J_{F,C}$ = 232.4 Hz, $CH_2\underline{C}F$), 113.3 (d, $^2J_{F,C}$ = 22.8 Hz, C-2′), 116.9 (d, $^2J_{F,C}$ = 15.4 Hz, C-4′), 122.1 (d, $^3J_{F,C}$ = 3.0 Hz, C-5″), 123.7 (C-6′), 131.9 (d, $^3J_{F,C}$ = 2.8 Hz, C-5′), 148.4 (d, $^3J_{F,C}$ = 7.1 Hz, C-1′), 150.1 (C-4″), 153.1 (C-2″), 158.8 (d, $^1J_{F,C}$ = 246.5 Hz, C-3′), 168.0 (d, $^2J_{F,C}$ = 20.2 Hz), 168.8, 170.5 (CO). LC-MS (ESI) (90% H_2O to 100% MeCN in 10 min, then 100% MeCN to 15 min, DAD 200-600 nm), t_R = 5.94 min, 98% purity, *m/z* calcd for $C_{27}H_{34}F_2N_4O_4S$ $[M + H]^+$, 549.23; found, 549.3. HRMS (ESI) *m/z* calcd for $C_{27}H_{34}F_2N_4O_4S$ $[M + H]^+$, 549.2342; found, 549.2336.

(2*S*,4*R*)-*N*-((*S*)-1-(5-Fluoro-2-methyl-4-(4-methylthiazol-5-yl)phenyl)ethyl)-1-((*S*)-2-(1-fluorocyclopropane-1-carboxamido)-3,3-dimethylbutanoyl)-4-hydroxypyrrolidine-2-carboxamide (32)

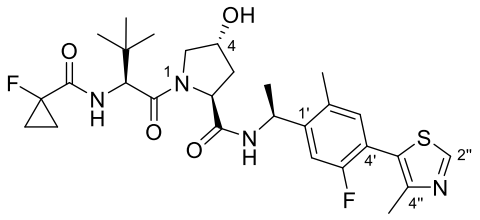

Following General Procedure C, compound **32** was obtained using Boc-protected amine **60c** (type **60**; R = 2-Me, 5-F; 103 mg, 0.3 mmol) and acid **62** (99 mg, 0.3 mmol). The residue was purified by flash column chromatography using a gradient from 0 to 10% MeOH in CH_2Cl_2 to afford **32** as a white solid (122 mg, 72%).

mp 142-145 °C; R_f = 0.40 (CH_2Cl_2/MeOH 9:1); ^{1}H NMR (600 MHz, DMSO-d_6) δ 0.96 (s, 9H, $C(CH_3)_3$), 1.19 – 1.23 (m, 2H, CH_2CF), 1.31 – 1.41 (m, 5H, CH_2CF, $CHC\underline{H}_3$), 1.70 – 1.77 (m, 1H, 3-H), 2.03 – 2.09 (m, 1H, 3-H), 2.30 (s, 3H, CH_3), 2.33 (s, 3H, CH_3), 3.54 – 3.61 (m, 2H, 5-H), 4.26 – 4.31 (m, 1H), 4.44 (t, J = 8.3 Hz, 1H), 4.57 (d, J = 9.3 Hz, 1H) (2-H, 4-H, NHC$\underline{H}$), 5.00 – 5.07 (m, 1H, C$\underline{H}CH_3$), 5.13 (d, J = 3.6 Hz, 1H, OH), 7.20 – 7.29 (m, 3H, Ar-H, CONH), 8.44 (d, J = 7.7 Hz, 1H, CONH), 9.09 (s, 1H, 2″-H); ^{13}C NMR (151 MHz, DMSO-d_6) δ 12.6 (d, $^2J_{F,C}$ = 10.1 Hz, $\underline{C}H_2CF$), 12.9 (d, $^2J_{F,C}$ = 10.4 Hz, $\underline{C}H_2CF$), 15.8 (d, $^5J_{F,C}$ = 3.1 Hz, CH_3), 17.6 (CH_3), 20.8 ($CH\underline{C}H_3$), 26.2 ($C(\underline{C}H_3)_3$), 36.0 ($\underline{C}(CH_3)_3$), 37.6 (C-3), 44.6 ($\underline{C}HCH_3$), 56.5, 56.6, 58.7 (C-2, C-5, NHCH), 68.8 (C-4), 78.1 (d, $^1J_{F,C}$ = 232.4 Hz, $CH_2\underline{C}F$), 112.4 (d, $^2J_{F,C}$ = 23.0 Hz, C-2′), 116.6 (d, $^2J_{F,C}$ = 15.2 Hz, C-4′), 123.8 (C-5″), 131.2 (d, $^4J_{F,C}$ = 3.2 Hz, C-5′), 133.2 (C-6′), 146.0 (d, $^3J_{F,C}$ = 6.5 Hz, C-1′), 150.0 (C-4″), 153.0 (C-2″), 157.5 (d, $^1J_{F,C}$ = 244.1 Hz, C-3′), 168.0 (d, $^2J_{F,C}$ = 19.9 Hz), 168.8, 170.3 (CO). LC-MS (ESI) (90% H_2O to 100% MeCN in 10 min, then 100% MeCN to 15 min, DAD 200-600 nm), t_R = 6.38 min, 98% purity, *m/z* calcd for $C_{28}H_{36}F_2N_4O_4S$ $[M + H]^+$, 563.25; found, 563.4. HRMS (ESI) *m/z* calcd for $C_{28}H_{36}F_2N_4O_4S$ $[M + H]^+$, 563.2498; found, 563.2492.

(2*S*,4*R*)-*N*-((S)-1-(5-Fluoro-2-methoxy-4-(4-methylthiazol-5-yl)phenyl)ethyl)-1-((*S*)-2-(1-fluorocyclopropane-1-carboxamido)-3,3-dimethylbutanoyl)-4-hydroxypyrrolidine-2-carboxamide (33)

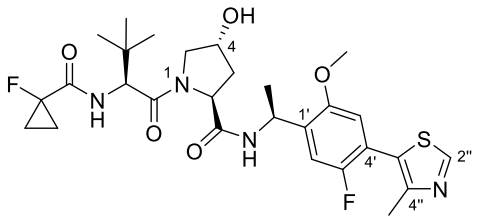

Following General Procedure C, compound **33** was obtained using Boc-protected amine **60d** (type **60**; R= 2-OMe, 5-F; 110 mg, 0.3 mmol) and acid **62** (99 mg, 0.3 mmol). The residue was purified by flash column chromatography using a gradient from 0 to 10% MeOH in CH_2Cl_2 to afford **33** as a white solid (52 mg, 60%).

mp 115-116 °C; R_f = 0.42 (CH_2Cl_2/MeOH 9:1); ^{1}H NMR (600 MHz, DMSO-d_6) δ 0.97 (s, 9H, $C(CH_3)_3$), 1.19 – 1.25 (m, 2H, CH_2CF), 1.28 – 1.40 (m, 5H, CH_2CF, $CHC\underline{H}_3$), 1.74 – 1.81 (m, 1H, 3-H), 2.07 – 2.13 (m, 1H, 3-H), 2.36 (s, 3H, CH_3), 3.54 – 3.62 (m, 2H, 5-H), 3.83 (s, 3H, OCH_3), 4.29 – 4.32 (m, 1H), 4.48 (t, J = 8.3 Hz, 1H), 4.58 (d, J = 9.2 Hz, 1H) (2-H, 4-H, NHC$\underline{H}$), 5.11 – 5.18 (m, 2H, OH, C$\underline{H}CH_3$), 7.01 (d, J = 6.1 Hz, 1H), 7.17 (d, J = 10.6 Hz, 1H), 7.25 (dd, J = 9.3, 2.9 Hz, 1H) (Ar-H, CONH), 8.42 (d, J = 7.9 Hz, 1H, CONH), 9.10 (s, 1H, 2″-H); ^{13}C NMR (151 MHz, DMSO-d_6) δ 12.6 (d, $^2J_{F,C}$ = 10.4 Hz, $\underline{C}H_2CF$), 12.9 (d, $^2J_{F,C}$ = 10.2 Hz, $\underline{C}H_2CF$), 15.8 (d, $^5J_{F,C}$ = 1.9 Hz, CH_3), 21.1 ($CH\underline{C}H_3$), 26.2 ($C(\underline{C}H_3)_3$), 36.1 ($\underline{C}(CH_3)_3$), 37.6 (C-3), 42.7 ($\underline{C}HCH_3$), 56.2, 56.5, 56.6, 58.6 (OCH_3, C-2, C-5, NHCH), 68.8 (C-4), 78.1 (d, $^1J_{F,C}$ = 232.6 Hz, $CH_2\underline{C}F$), 113.0 (d, $^2J_{F,C}$ = 25.1 Hz, C-2′), 113.6 (C-5″), 117.0 (d, $^2J_{F,C}$ = 16.5 Hz, C-4′), 123.9 (C-5′), 135.7 (d, $^3J_{F,C}$ = 6.5 Hz, C-1′), 150.3 (C-4″), 151.9 (C-6′), 153.1 (C-2″), 153.2 (d, $^1J_{F,C}$ = 238.9 Hz, C-3′), 168.0 (d, $^2J_{F,C}$ = 20.2 Hz), 168.8, 170.3 (CO). LC-MS (ESI) (90% H_2O to 100% MeCN in 10 min, then 100% MeCN to 15 min, DAD 200-600 nm), t_R = 6.21 min, 99% purity, *m/z* calcd for $C_{28}H_{36}F_2N_4O_5S$ $[M + H]^+$, 579.24; found, 579.5. HRMS (ESI) *m/z* calcd for for $C_{28}H_{36}F_2N_4O_5S$ $[M + H]^+$, 579.2447; found, 579.2445.

(2*S*,4*R*)-1-((*S*)-2-(1-Cyanocyclopropane-1-carboxamido)-3,3-dimethylbutanoyl)-4-hydroxy-*N*-((*S*)-5-(4-methylthiazol-5-yl)-2,3-dihydro-1H-inden-1-yl)pyrrolidine-2-carboxamide (34)

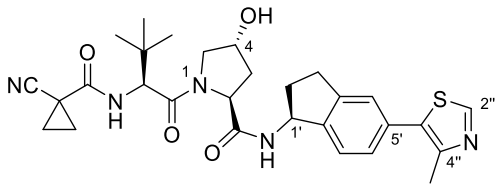

Following General Procedure C, compound **34** was obtained using Boc-protected amine **60e** (type **60**; R = H, n = 1; 99 mg, 0.3 mmol) and acid **46** (101 mg, 0.3 mmol). The residue was purified by flash column chromatography using a gradient from 0 to 10% MeOH in CH_2Cl_2 to afford **34** as a white solid (59 mg, 36%).

mp 102-104 °C; R_f = 0.39 (CH_2Cl_2/MeOH 9:1); ^{1}H NMR (500 MHz, DMSO-d_6) δ 0.97 (s, 9H, C(CH_3)$_3$), 1.45 – 1.53 (m, 2H, CH_2CCN), 1.57 – 1.65 (m, 2H, CH_2CCN), 1.85 – 1.92 (m, 1H, CH_2CH_2), 1.92 – 1.99 (m, 1H, CH_2CH_2), 2.01 – 2.10 (m, 1H, CH_2CH_2), 2.39 – 2.46 (m, 4H, CH_2CH_2, CH_3), 2.80 – 2.89 (m, 1H, 3-H), 2.93 – 3.02 (m, 1H, 3-H), 3.52 – 3.58 (m, 1H, 5-H), 3.65 (dd, *J* = 10.8, 3.9 Hz, 1H, 5-H), 4.31 – 4.37 (m, 1H), 4.38 – 4.45 (m, 1H), 4.52 (d, *J* = 8.9 Hz, 1H) (2-H, 4-H, NHC<u>H</u>), 5.11 (d, *J* = 3.7 Hz, 1H, OH), 5.23 – 5.30 (m, 1H, 1′-H), 7.19 – 7.25 (m, 1H), 7.26 – 7.31 (m, 2H), 7.34 – 7.36 (m, 1H) (Ar-H, CONH), 8.34 (d, *J* = 8.3 Hz, 1H, CONH), 8.96 (d, *J* = 1.8 Hz, 1H, 2′′-H); ^{13}C NMR (126 MHz, DMSO-d_6) δ 13.6 (<u>C</u>CN), 15.9 (CH_3), 16.6, 16.8 (<u>C</u>H_2CCN), 26.1 (C(<u>C</u>H_3)$_3$), 29.6, 32.7 (CH_2CH_2), 36.2 (<u>C</u>(CH_3)$_3$), 38.1 (C-3), 53.4, 56.6, 57.3, 58.7 (<u>C</u>HCH_2CH_2, C-2, C-5, NHCH), 68.8 (C-4), 120.0 (CN), 124.2, 125.1, 127.3, 130.6, 131.4 (C-Ar), 143.8, 144.1 (C-2′, C-4′), 147.7 (C-4′′), 151.3 (C-2′′), 164.3, 168.6, 171.2 (CO). LC-MS (ESI) (90% H_2O to 100% MeCN in 10 min, then 100% MeCN to 15 min, DAD 200-600 nm), t_R = 5.85 min, 95% purity, *m/z* calcd for $C_{29}H_{35}N_5O_4S$ $[M + H]^+$, 550.25; found, 550.4. HRMS (ESI) *m/z* calcd for $C_{29}H_{35}N_5O_4S$ $[M + H]^+$, 550.2486; found, 550.2481.

(2*S*,4*R*)-1-((*S*)-2-(1-Cyanocyclopropane-1-carboxamido)-3,3-dimethylbutanoyl)-*N*-((*S*)-6-fluoro-5-(4-methylthiazol-5-yl)-2,3-dihydro-1*H*-inden-1-yl)-4-hydroxypyrrolidine-2-carboxamide (35)

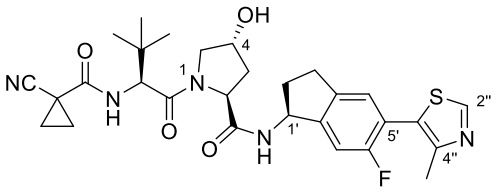

Following General Procedure C, compound **35** was obtained using Boc-protected amine **60f** (type **60**, R = F, n = 1; 104 mg, 0.3 mmol) and acid **46** (99 mg, 0.3 mmol). The residue was purified by flash column chromatography using a gradient from 0 to 10% MeOH in CH_2Cl_2 to afford **35** as a white solid (77 mg, 45%).

mp 163-165 °C; R_f = 0.38 (CH_2Cl_2/MeOH 9:1); ^{1}H NMR (600 MHz, DMSO-d_6) δ 0.97 (s, 9H, C(CH_3)$_3$), 1.47 – 1.53 (m, 2H, CH_2CCN), 1.58 – 1.66 (m, 2H, CH_2CCN), 1.91 – 2.00 (m, 2H, CH_2CH_2), 2.05 – 2.11 (m, 1H, CH_2CH_2), 2.32 (s, 3H, CH_3), 2.41 – 2.47 (m, 1H, CH_2CH_2), 2.79 – 2.86 (m, 1H, 3-H), 2.92 – 2.98 (m, 1H, 3-H), 3.53 – 3.58 (m, 1H, 5-H), 3.66 (dd, *J* = 10.8, 3.9 Hz, 1H, 5-H), 4.34 – 4.37 (m, 1H), 4.42 (dd, *J* = 8.9, 7.7 Hz, 1H), 4.52 (d, *J* = 8.9 Hz, 1H) (2-H, 4-H, NHC<u>H</u>), 5.14 (d, *J* = 3.6 Hz, 1H, OH), 5.23 – 5.28 (m, 1H, 1′-H), 7.06 (d, *J* = 9.7 Hz, 1H), 7.30 – 7.36 (m, 2H) (Ar-H, CONH), 8.43 (d, *J* = 8.0 Hz, 1H, CONH), 9.09 (s, 1H, 2′′-H); ^{13}C NMR (151 MHz, DMSO-d_6) δ 13.7 (CH_2<u>C</u>CN), 15.7 (d, $^5J_{F,C}$ = 3.0 Hz, CH_3), 16.6, 16.8 (<u>C</u>H_2CCN), 26.1 (C(<u>C</u>H_3)$_3$), 29.0, 33.0 (CH_2CH_2), 36.2 (<u>C</u>(CH$_3$)$_3$), 38.0 (C-3), 53.8, 56.6, 57.3, 58.8 (C-1′, C-2, C-5, NHCH), 68.84 (C-4), 111.3 (d, $^2J_{F,C}$ = 23.3 Hz, C-6′), 117.7 (d, $^2J_{F,C}$ = 16.7 Hz, C-4′), 120.1 (CN), 124.3, 127.6 (C-2′, C-5′′), 139.1 (C-4′′), 147.2 (d, $^3J_{F,C}$ = 7.7 Hz, C-1′), 153.0 (C-2′′), 158.1 (d, $^1J_{F,C}$ = 244.4 Hz, C-5′), 164.4, 168.6, 171.3 (CO). LC-MS (ESI) (90% H_2O to 100% MeCN in 10 min, then 100% MeCN to 15 min, DAD 200-600 nm), t_R = 6.00 min, 99% purity, *m/z* calcd for $C_{29}H_{34}FN_5O_4S$ $[M + H]^+$, 568.24; found, 568.4. HRMS (ESI) *m/z* calcd for $C_{29}H_{34}FN_5O_4S$ $[M + H]^+$, 568.2388; found, 568.2382.

(2*S*,4*R*)-*N*-((*S*)-6-Fluoro-5-(4-methylthiazol-5-yl)-2,3-dihydro-1*H*-inden-1-yl)-1-((S)-2-(1-fluorocyclopropane-1-carboxamido)-3,3-dimethylbutanoyl)-4-hydroxypyrrolidine-2-carboxamide (36)

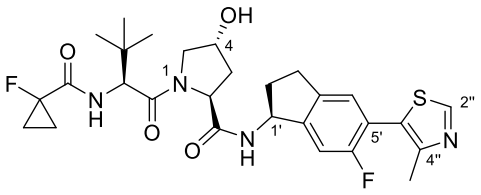

Following General Procedure C, compound **36** was obtained using Boc-protected amine **60f** (type **60**, R = F, n = 1; 105 mg, 0.3 mmol) and acid **62** (99 mg, 0.3 mmol). The residue was purified by flash column chromatography using a gradient from 0 to 10% MeOH in CH_2Cl_2 to afford **36** as a white solid (131 mg, 78%).

mp 109-111 °C; R_f = 0.38 (CH_2Cl_2/MeOH 9:1); ^{1}H NMR (600 MHz, DMSO-d_6) δ 0.98 (s, 9H, C(CH_3)$_3$), 1.16 – 1.25 (m, 2H, CH_2CF), 1.30 – 1.42 (m, 2H, CH_2CF), 1.89 – 2.00 (m, 2H, CH_2CF), 2.05 – 2.11 (m, 1H, CH_2CH_2), 2.32 (s, 3H, CH_3), 2.40 – 2.46 (m, 1H, CH_2CH_2), 2.77 – 2.86 (m, 1H, 3-H), 2.91 – 2.98 (m, 1H, 3-H), 3.56 – 3.61 (m, 1H, 5-H), 3.68 (dd, *J* = 10.8, 3.9 Hz, 1H, 5-H), 4.34 – 4.38 (m, 1H), 4.42 (t, *J* = 8.2 Hz, 1H), 4.57 – 4.61 (m, 1H) (2-H, 4-H, NHC<u>H</u>), 5.14 (d, *J* = 3.6 Hz, 1H, OH), 5.22 – 5.29 (m, 1H, 1′-H), 7.04 – 7.09 (m, 1H), 7.26 (dd, *J* = 9.4, 2.8 Hz, 1H), 7.32 – 7.36 (m, 1H) (Ar-H, CONH), 8.41 (d, *J* = 8.0 Hz, 1H, CONH), 9.09 (s, 1H, 2′′-H); ^{13}C NMR (151 MHz, DMSO-d_6) δ 12.6 (d, $^2J_{F,C}$ = 10.3 Hz, <u>C</u>H_2CF), 12.9 (d, $^2J_{F,C}$ = 9.9 Hz, <u>C</u>H_2CF), 15.7 (d, $^5J_{F,C}$ = 2.6 Hz, CH_3), 26.2 (C(<u>C</u>H_3)$_3$), 29.0, 33.0 (CH_2CH_2), 36.0 (<u>C</u>(CH_3)$_3$), 38.0 (C-3), 53.8, 56.5, 56.6, 58.8 (C-1′, C-2, C-5, NHCH), 68.8 (C-4), 78.1 (d, $^1J_{F,C}$ = 232.7 Hz, CH_2CF), 111.3 (d, $^2J_{F,C}$ = 23.2 Hz, C-6′), 117.7 (d, $^2J_{F,C}$ = 16.3 Hz, C-4′), 124.3, 127.6 (C-3′,C-5′′), 139.1 (d, $^4J_{F,C}$ = 2.6 Hz, C-2′), 147.2 (d, $^3J_{F,C}$ = 7.6 Hz, C-1′), 150.1 (C-4′′), 153.0 (C-2′′), 158.1 (d, $^1J_{F,C}$ = 244.5 Hz, C-5′), 168.0 (d, $^2J_{F,C}$ = 20.2 Hz), 168.8, 171.3 (CO). LC-MS (ESI) (90% H_2O to 100% MeCN in 10 min, then 100% MeCN to 15 min, DAD 200-600 nm), t_R = 6.18 min, 100% purity, *m/z* calcd for $C_{28}H_{34}F_2N_4O_4S$ $[M + H]^+$, 561.23; found, 561.3. HRMS (ESI) *m/z* calcd for $C_{28}H_{34}F_2N_4O_4S$ $[M + H]^+$, 561.2342; found, 561.2337.

(2*S*,4*R*)-*N*-((*S*)-7-Fluoro-6-(4-methylthiazol-5-yl)-1,2,3,4-tetrahydronaphthalen-1-yl)-1-((*S*)-2-(1-fluorocyclopropane-1-carboxamido)-3,3-dimethylbutanoyl)-4-hydroxypyrrolidine-2-carboxamide (37)

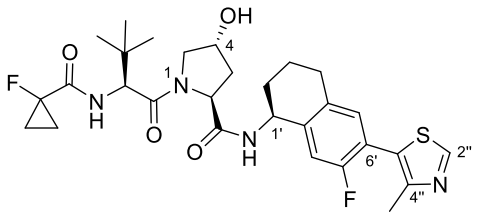

Following General Procedure C, compound **37** was obtained using Boc-protected amine **60g** (type **60**, R = H, n = 2; 103 mg, 0.3 mmol) and acid **62** (99 mg, 0.3 mmol). The residue was purified by flash column chromatography using a gradient from 0 to 10% MeOH in CH_2Cl_2 to afford **37** as a white solid (159 mg, 95%).

mp 78-82 °C; R_f = 0.38 (CH_2Cl_2/MeOH 9:1); ^{1}H NMR (600 MHz, DMSO-d_6) δ 0.98 (s, 9H, C(CH_3)$_3$), 1.13 – 1.28 (m, 4H), 1.30 – 1.41 (m, 2H), 1.68 – 1.78 (m, 2H), 1.87 – 1.94 (m, 2H), 1.95 – 2.00 (m, 1H), 2.04 – 2.11 (m, 1H) (CH_2CF, $CH_2CH_2CH_2$, 3-H), 2.32 (s, 3H, CH_3), 3.55 – 3.61 (m, 1H, 5-H), 3.69 (dd, J = 10.7, 4.0 Hz, 1H, 5-H), 4.34 – 4.39 (m, 1H), 4.43 (t, J = 8.2 Hz, 1H), 4.55 – 4.62 (m, 1H) (2-H, 4-H, NHCH), 4.90 – 4.96 (m, 1H, 1′-H), 5.14 (d, J = 3.6 Hz, 1H, OH), 6.95 – 7.04 (m, 1H), 7.19 – 7.29 (m, 2H) (Ar-H, CONH), 8.41 (d, J = 8.5 Hz, 1H, CONH), 9.09 (s, 1H, 2′′-H); ^{13}C NMR (151 MHz, DMSO-d_6) δ 12.7 (d, $^2J_{F,C}$ = 10.3 Hz, $\underline{C}H_2$CF), 12.9 (d, $^2J_{F,C}$ = 10.4 Hz, $\underline{C}H_2$CF), 15.7 (d, $^5J_{F,C}$ = 2.7 Hz), 26.2 (C($\underline{C}H_3$)$_3$), 27.8, 29.1 (CH_2), 36.0 ($\underline{C}$(CH_3)$_3$), 37.9 (CH_2), 38.2 (C-3), 45.8, 46.6, 56.6 (d, J = 5.3 Hz), 58.9 (C-1′, C-2, C-5, NHCH), 68.8 (C-4), 78.1 (d, $^1J_{F,C}$ = 232.3 Hz, $CH_2\underline{C}$F), 114.6 (d, $^2J_{F,C}$ = 22.0 Hz, C-6′), 117.3 (d, $^2J_{F,C}$ = 15.5 Hz, C-4′), 123.8 (C-5′′), 132.0 (C-3′), 133.6 (d, $^3J_{F,C}$ = 3.2 Hz, C-1′), 140.6 (C-2′), 150.1 (C-4′′), 153.1 (C-2′′), 157.1 (d, $^1J_{F,C}$ = 244.7 Hz, C-5′), 168.0 (d, $^2J_{F,C}$ = 20.1 Hz), 168.8 , 171.0 (CO). LC-MS (ESI) (90% H_2O to 100% MeCN in 10 min, then 100% MeCN to 15 min, DAD 200-600 nm), t_R = 6.51 min, 96% purity, *m/z* calcd for $C_{29}H_{36}F_2N_4O_4S$ $[M + H]^+$, 575.25; found, 575.4. HRMS (ESI) *m/z* calcd for $C_{29}H_{36}F_2N_4O_4S$ $[M + H]^+$, 575.2492; found, 575.2498.

(2*S*,4*R*)-1-((*S*)-2-(1-Fluorocyclopropane-1-carboxamido)-3,3-dimethylbutanoyl)-4-hydroxy-*N*-(4-(4-methylthiazol-5-yl)benzyl)pyrrolidine-2-carboxamide (38)

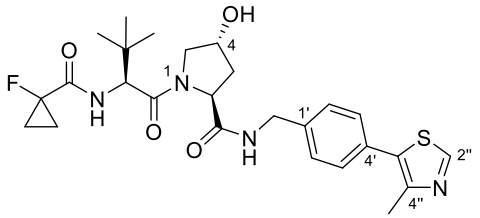

Following General Procedure C, compound **38** was obtained using Boc-protected amine **42a** and acid **62** (99 mg, 0.3 mmol). The residue was purified by flash column chromatography using a gradient from 0 to 10% MeOH in CH_2Cl_2 to afford **38** as a white solid (68 mg, 65%).

mp 87-89 °C; R_f = 0.40 (CH_2Cl_2/MeOH 9:1); ^{1}H NMR (600 MHz, DMSO-d_6) δ 0.97 (s, 9H, $C(CH_3)_3$), 1.18 – 1.25 (m, 2H, CH_2CF), 1.31 – 1.42 (m, 2H, CH_2CF), 1.86 – 1.95 (m, 1H, 3-H), 2.04 – 2.10 (m, 1H, 3-H), 2.45 (s, 3H, CH_3), 3.57 – 3.63 (m, 1H, 5-H), 3.66 (dd, J = 10.8, 3.9 Hz, 1H, 5-H), 4.26 (dd, J = 15.6, 5.6 Hz, 1H), 4.33 – 4.42 (m, 2H), 4.48 (t, J = 8.2 Hz, 1H), 4.58 – 4.62 (m, 1H) (2-H, 4-H, NHC<u>H</u>, NHC<u>H</u>$_2$), 5.15 (d, J = 3.6 Hz, 1H, OH), 7.27 (dd, J = 9.2, 2.8 Hz, 1H), 7.36 – 7.45 (m, 4H) (Ar-H, CONH), 8.60 (t, J = 6.0 Hz, 1H, CONH), 8.98 (s, 1H, 2″-H); ^{13}C NMR (151 MHz, DMSO) δ 12.67 (d, $^2J_{F,C}$ = 10.3 Hz, <u>C</u>H_2CF), 12.94 (d, $^2J_{F,C}$ = 10.1 Hz, <u>C</u>H_2CF), 15.9 (CH_3), 26.2 (C(<u>C</u>H_3)$_3$), 36.0 (<u>C</u>(CH_3)$_3$), 37.9 (C-3), 41.7 (<u>C</u>HCH_3), 56.5, 56.6, 58.8 (C-2, C-5, NHCH), 68.9 (C-4), 78.09 (d, $^1J_{F,C}$ = 232.3 Hz, CH_2<u>C</u>F), 127.5, 128.7, 129.7, 131.1 (C-2′, C-3′, C-4′, C-5′, C-6′, C-5″), 139.4 (C-1′), 147.7 (<u>C</u>HCH_3), 151.4 (C-2″), 168.02 (d, $^2J_{F,C}$ = 20.1 Hz), 168.8, 171.6 (CO). LC-MS (ESI) (90% H_2O to 100% MeCN in 10 min, then 100% MeCN to 15 min, DAD 220-600 nm), t_R = 5.49 min, 97% purity, *m/z* calcd for $C_{26}H_{33}FN_4O_4S$ $[M + H]^+$, 517.23; found, 517.3.

***tert*-Butyl Carbamate (39)**

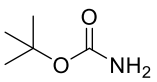

This compound was purchased from TCI Deutschland (Eschborn, Germany).

4-Bromobenzaldehydes (type 40)

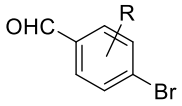

Compounds of type **40** were purchased from abcr GmbH (Karlsruhe, Germany), BLDpharm (Kaiserslautern, Germany), TCI Deutschland (Eschborn, Germany).

4-Bromo-5-fluoro-2-methoxybenzaldehyde (type 40, R = 2-OMe, 5-F)

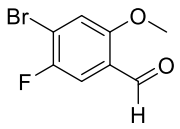

This compound was synthesized and provided by Dr. Christian Steinebach, University of Bonn.

***tert*-Butyl (4-Bromobenzyl)carbamate (41a)**

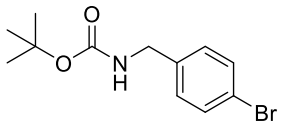

This compound was synthesized and provided by Dr. Christian Steinebach, University of Bonn.

***tert*-Butyl *N*-((4-Bromo-2-methylphenyl)methyl)carbamate (41b)**

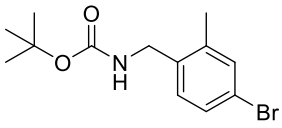

Following General Procedure A, compound **41b** was obtained from **39** and 4-bromobenzaldehyde (type **40**, R = 2-Me; 1.00 g, 5.0 mmol). The crude product was purified by column chromatography (petroleum ether/EtOAc 9:1) to obtain a colorless solid (1.28 g, 86%).

mp 80-82 °C; R_f = 0.30 (petroleum ether/EtOAc 9:1); ^{1}H NMR (600 MHz, DMSO-d_6) δ 1.39 (s, 9H, C(CH$_3$)$_3$), 2.25 (s, 3H, CH$_3$), 4.06 (d, J = 6.0 Hz, 2H, CH$_2$), 7.12 (d, J = 8.0 Hz, 1H, Ar-H), 7.30 (t, J = 5.6 Hz, 1H, NH), 7.33 – 7.36 (m, 2H, Ar-H); ^{13}C NMR (151 MHz, DMSO-d_6) δ 18.15 (CH$_3$), 28.18 (C(CH$_3$)$_3$), 40.80 (CH$_2$), 77.80 (C(CH$_3$)$_3$), 119.42 (C-4), 128.37, 129.07 (C-5, C-6), 132.10 (C-3), 137.27, 138.15 (C-1, C-2), 155.62 (CO). LC-MS (ESI) (90% H$_2$O to 100% MeOH in 10 min, then 100% MeOH to 20 min, DAD 220-400 nm), t_R = 11.63 min, 97% purity, *m/z* calcd for $C_{13}H_{18}{}^{79}BrNO_2$ $[M + H]^+$, 300.06; found, 300.0.

tert-Butyl _N_-((4-Bromo-2-methoxyphenyl)methyl)carbamate (41c)

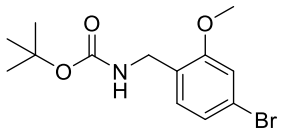

Following General Procedure A, compound **41c** was obtained from **39** and 4-bromobenzaldehyde (type **40**, R = 2-OMe; 1.08 g, 5.0 mmol). The crude product was purified by column chromatography (petroleum ether/EtOAc 9:1) to obtain **41c** as a colorless solid (1.57 g, 99%).

mp 68-70 °C; R_f = 0.30 (petroleum ether/EtOAc 9:1); ^{1}H NMR (600 MHz, DMSO-d_6) δ 1.39 (s, 9H, C(CH$_3$)$_3$), 3.81 (s, 2H, CH$_3$), 4.04 (d, J = 6.0 Hz, 2H, CH$_2$), 7.07 (d, J = 8.0 Hz, 1H), 7.10 – 7.15 (m, 2H, Ar-H), 7.19 (t, J = 5.7 Hz, 1H, NH); ^{13}C NMR (151 MHz, DMSO-d_6) δ 28.21 (C(CH$_3$)$_3$), 38.00 (CH$_2$), 55.78 (OCH$_3$), 77.81 (C(CH$_3$)$_3$), 113.60 (C-3), 120.13 (C-4), 122.85 (C-1), 127.14, 128.64 (C-5, C-6), 155.72 (CO), 157.25 (C-2). LC-MS (ESI) (90% H$_2$O to 100% MeOH in 10 min, then 100% MeOH to 20 min, DAD 220-400 nm), t_R = 11.48 min, 100% purity, *m/z* calcd for $C_{13}H_{18}{}^{79}BrNO_3$ $[M + H]^+$, 316.05; found, 315.9.

tert-Butyl _N_-((4-Bromo-2-fluorophenyl)methyl)carbamate (41d)

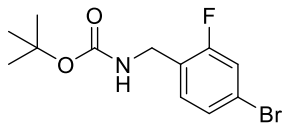

This compound was synthesized and provided by Dr. Christian Steinebach, University of Bonn.

tert-Butyl _N_-((4-Bromo-3-chlorophenyl)methyl)carbamate (41e)

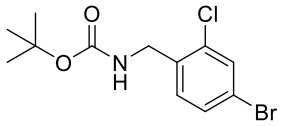

Following General Procedure A, compound **41e** was obtained from **39** and 4-bromobenzaldehyde (type **40**, R = 2-Cl; 0.66 g, 3.0 mmol). The crude product was purified by column chromatography (petroleum ether /EtOAc 9:1) to obtain **41e** as a colorless oil (269 mg, 28%).

R_f = 0.38 (petroleum ether/EtOAc 9:1); ^{1}H NMR (500 MHz, DMSO-d_6) δ 1.40 (s, 9H, C(CH_3)$_3$), 4.15 (d, J = 6.1 Hz, 2H, CH_2), 7.25 (d, J = 8.3 Hz, 1H, Ar-H), 7.43 (t, J = 6.1 Hz, 1H, NH), 7.56 (dd, J = 8.2, 2.1 Hz, 1H, Ar-H), 7.68 (d, J = 1.9 Hz, 1H, Ar-H); ^{13}C NMR (126 MHz, DMSO) δ 28.1 (C(CH_3)$_3$), 40.9 (CH_2), 78.1 (C(CH_3)$_3$), 120.0 (C-4), 130.2, 131.1 (C-5, C-6), 132.8 (C-2), 136.6 (C-1), 155.6 (CO). LC-MS (ESI) (90% H2O to 100% MeOH in 10 min, then 100% MeOH to 20 min, DAD 220-400 nm), t_R = 11.83 min, 89% purity, *m/z* calcd for $C_{12}H_{16}{}^{81}BrClNO_2$ [M - H]$^-$, 320.00; found, 320.1.

tert-Butyl _N_-((4-Bromo-3-methylphenyl)methyl)carbamate (41f)

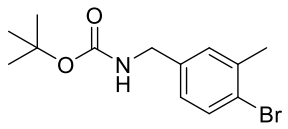

Following General Procedure A, compound **41f** was obtained from **39** and 4-bromobenzaldehyde (type **40**, R = 3-Me; 0.20 g, 1.0 mmol). The crude product was purified by column chromatography (petroleum ether/EtOAc 9:1) to obtain **41f** as a colorless solid (126 mg, 42%).

mp 88-90 °C; R_f = 0.30 (petroleum ether/EtOAc 6:1); ^{1}H NMR (500 MHz, DMSO-d_6) δ 1.38 (s, 9H, C(CH_3)$_3$), 2.31 (s, 3H, CH_3), 4.04 (d, J = 6.2 Hz, 2H, CH_2), 6.98 (dd, J = 2.2, 8.2 Hz, 1H), 7.19 (d, J = 2.5 Hz, 1H, Ar-H), 7.34 (t, J = 6.5 Hz, 1H, NH), 7.49 (d, J = 8.2 Hz, 1H, Ar-H); ^{13}C NMR (126 MHz, DMSO-d_6) δ 22.52 (CH_3), 28.36 (C(CH_3)$_3$), 42.91 (CH_2), 78.00 (C(CH_3)$_3$), 122.17 (C-4), 126.59 (C-6), 129.86 (C-2), 132.01 (C-5), 136.96 (C-1), 140.03 (C-3), 155.88 (CO). LC-MS (ESI) (90% H_2O to 100% MeOH in 10 min, then 100% MeOH to 20 min, DAD 220-400 nm), t_R = 11.65 min, 99% purity, *m/z* calcd for $C_{13}H_{18}{}^{81}BrNO_2$ $[M + H]^+$, 302.05; found, 301.9.

tert-Butyl (4-Bromo-3-methoxybenzyl)carbamate (41g)

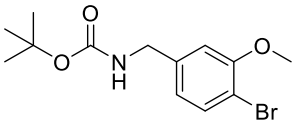

This compound was synthesized and provided by Dr. Izidor Sosič, University of Ljubljana.

***tert*-Butyl *N*-((4-Bromo-3-fluorophenyl)methyl)carbamate (41h)**

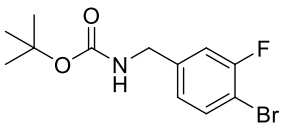

Following General Procedure A, compound **41h** was obtained from **39** and 4-bromobenzaldehyde (type **40**, R = 3-F; 1.76 g, 5.0 mmol). The crude product was purified by flash column chromatography using a gradient from 10 to 40% EtOAc in cyclohexane to give **41h** as a colorless solid (0.49 g, 32%).

mp 92 – 94 °C; R_f = 0.46 (petroleum ether/EtOAc 6:1); ^{1}H NMR (500 MHz, DMSO-d_6) δ 1.38 (s, 9H, CH_3), 4.10 (d, J = 6.1 Hz, 2H, CH_2), 7.03 (dd, J = 1.9, 8.2 Hz, 1H, 2-H), 7.19 (dd, J = 2.0, 9.9 Hz, 1H, 5-H), 7.42 (t, J = 6.4 Hz, 1H, 6-H), 7.63 (t, J = 7.8 Hz, 1H, NH); ^{13}C NMR (126 MHz, DMSO-d_6) δ 28.32 (C($\underline{C}H_3$)$_3$), 42.69 (CH_2), 78.21 ($\underline{C}(CH_3)_3$), 105.83 (d, J = 20.8 Hz, C-4), 115.17 (d, J = 22.3 Hz, C-2), 124.66 (d, J = 3.3 Hz, C-6), 133.39 (C-5), 143.11 (d, J = 6.1 Hz, C-1), 155.90 (CO), 158.23 (d, J = 244.6 Hz, C-3). LC-MS (ESI) (90% H_2O to 100% MeOH in 10 min, then 100% MeOH to 20 min, DAD 220-400 nm), t_R = 11.33 min, 99% purity, *m*/*z* calcd for $C_{12}H_{16}{}^{81}BrFNO_2$ $[M + H]^+$, 306.03; found, 306.1.

***tert*-Butyl *N*-((4-Bromo-3-chloro-phenyl)methyl)carbamate (41i)**

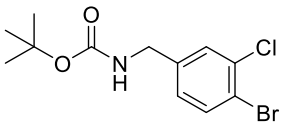

Following General Procedure A, compound **41i** was obtained from **39** and 4-bromobenzaldehyde (type **40**, R = 3-Cl; 0.22 g, 1.0 mmol). The crude product was purified by column chromatography (petroleum ether/EtOAc 9:1) to obtain **41i** as a colorless solid (93 mg, 29%).

mp 98-100 °C; R_f = 0.49 (petroleum ether/EtOAc 6:1); ^{1}H NMR (500 MHz, DMSO-d_6) δ 1.38 (s, 9H, CH_3), 4.08 (d, J = 6.1 Hz, 2H, CH2), 7.13 (dd, J = 2.1, 8.4 Hz, 1H, Ar-H), 7.42 (t, J =

7.2 Hz, 1H, NH), 7.45 (d, J = 2.1 Hz, 1H), 7.70 (d, J = 8.2 Hz, 1H, Ar-H); ^{13}C NMR (126 MHz, DMSO-d_6) δ 28.32 ($C(CH_3)_3$), 42.55 (CH_2), 78.23 ($C(CH_3)_3$), 119.40 (C-4), 127.61, 128.96 (C-3, C-6), 132.95, 133.80 (C-2, C-5), 142.25 (C-1), 155.89 (CO). LC-MS (ESI) (90% H_2O to 100% MeOH in 10 min, then 100% MeOH to 20 min, DAD 220-400 nm), t_R = 11.66 min, 97% purity, m/z calcd for $C_{12}H_{15}{}^{81}BrClNO_2$ $[M + H]^+$, 322.00; found, 321.9.

tert-Butyl (4-Bromo-2,6-dimethylbenzyl)carbamate (41j)

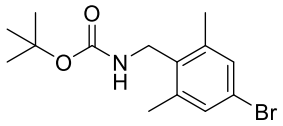

This compound was synthesized and provided by Dr. Izidor Sosič, University of Ljubljana.

tert-Butyl (4-Bromo-2,6-dimethoxybenzyl)carbamate (41k)

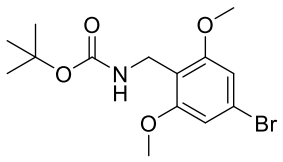

This compound was synthesized and provided by Dr. Izidor Sosič, University of Ljubljana.

tert-Butyl (4-Bromo-2,6-difluorobenzyl)carbamate (41l)

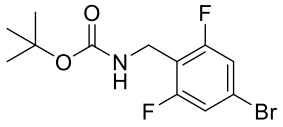

This compound was synthesized and provided by Dr. Izidor Sosič, University of Ljubljana.

***tert*-Butyl (4-Bromo-2,6-dichlorobenzyl)carbamate (41m)**

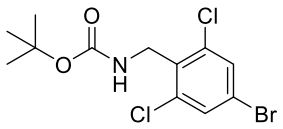

This compound was synthesized and provided by Dr. Izidor Sosič, University of Ljubljana.

***tert*-Butyl (4-Bromo-2,5-dimethylbenzyl)carbamate (41n)**

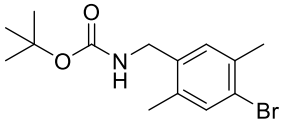

This compound was synthesized and provided by Dr. Izidor Sosič, University of Ljubljana.

***tert*-Butyl *N*-((4-Bromo-2,5-dimethoxyphenyl)methyl)carbamate (41o)**

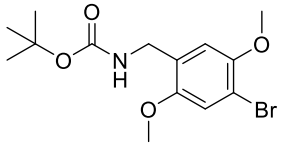

Following General Procedure A, compound **41o** was obtained from **39** and 4-bromobenzaldehyde (type **40**, R = 2-OMe, R = 5-OMe; 0.25 g, 1.0 mmol). The crude product was purified by column chromatography (petroleum ether/EtOAc 9:1) to obtain **41o** as a colorless solid (242 mg, 70%).

mp 74-76 °C; R_f = 0.31 (petroleum ether/EtOAc 6:1); ^{1}H NMR (500 MHz, DMSO-d_6) δ1.39 (s, 9H, CH_3), 3.74 (br s, 6H, OCH_3), 4.05 (d, J = 6.0 Hz, 2H, CH_2), 6.92 (s, 1H), 7.15 (s, 1H, Ar-H), 7.20 (t, J = 6.2 Hz, 1H, NH); ^{13}C NMR (126 MHz, DMSO-d_6) δ 28.35 ($C(CH_3)_3$), 38.38 (CH_2), 56.34, 56.68 (OCH_3), 78.05 ($C(CH_3)_3$), 108.59 (C-4), 112.42, 115.70 (C-3, C-6), 128.45 (C-1), 149.50, 150.93 (C-2, C-5), 155.93 (CO). LC-MS (ESI) (90% H_2O to 100% MeOH in 10

min, then 100% MeOH to 20 min, DAD 220-400 nm), t_R = 11.27 min, 99% purity, *m/z* calcd for $C_{14}H_{20}{}^{79}BrNO_4$ $[M + H]^+$, 346.06; found, 346.1.

tert-Butyl (4-Bromo-2,5-difluorobenzyl)carbamate (41p)

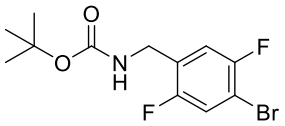

This compound was synthesized and provided by Dr. Izidor Sosič, University of Ljubljana.

tert-Butyl (4-Bromo-2,3-dimethylbenzyl)carbamate (41r)

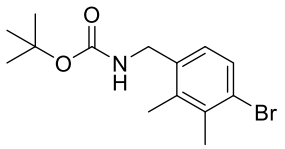

This compound was synthesized and provided by Dr. Izidor Sosič, University of Ljubljana.

tert-Butyl (4-Bromo-2,3-difluorobenzyl)carbamate (41s)

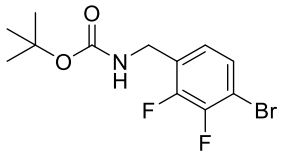

Following General Procedure A, compound **41s** was obtained from **39** and 4-bromobenzaldehyde (type **40**, R = 2-F, 3-F; 0.66 g, 3.0 mmol). The crude product was purified by column chromatography (petroleum ether /EtOAc 9:1) to obtain **41s** as a colorless solid (130 mg, 14%).

mp 78 – 81 °C; R_f = 0.16 (petroleum ether/EtOAc 9:1); ^{1}H NMR (500 MHz, DMSO-d_6) δ 1.38 (s, 9H, C(CH_3)$_3$), 4.17 (d, J = 6.0 Hz, 2H, CH_2), 7.05 – 7.15 (m, 1H, Ar-H), 7.41 – 7.48 (m, 1H, Ar-H), 7.49 – 7.55 (m, 1H, NH); ^{13}C NMR (126 MHz, DMSO-d_6) δ 28.1 (C($\underline{C}H_3$)$_3$), 36.8 (CH_2), 78.2 ($\underline{C}$(CH$_3$)$_3$), 107.3 (d, $^2J_{F,C}$ = 17.5 Hz, C-4), 125.0 (d, $^3J_{F,C}$ = 4.9 Hz, C-6), 127.8 (d, $^3J_{F,C}$ = 4.0 Hz, C-5), 129.2 (d, $^2J_{F,C}$ = 11.8 Hz, C-1), 146.4 (dd, $^1J_{F,C}$ = 136.0 Hz, $^2J_{F,C}$ = 14.0 Hz, C-2), 148.4 (dd, $^1J_{F,C}$ = 140.3 Hz, $^2J_{F,C}$ = 14.0 Hz, C-3), 155.6 (CO). LC-MS (ESI) (90% H_2O to 100% MeCN in 10 min, then 100% MeCN to 15 min, DAD 200-600 nm), t_R = 7.48 min, 95% purity, *m/z* calcd for $C_{12}H_{14}{}^{79}BrF_2NO_2$ [M - H]$^-$, 320.01; found, 320.1. HRMS (ESI) *m/z* calcd for $C_{12}H_{14}{}^{79}BrF_2NO_2$ [M + H]$^+$, 322.0071; found, 322.0069.

tert-Butyl ((4-Bromonaphthalen-1-yl)methyl)carbamate (41v)

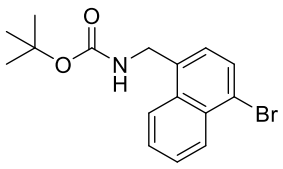

This compound was synthesized and provided by Aleša Bricelj, University of Ljubljana.

tert-Butyl _N_-((5-Bromo-8-quinolyl)methyl)carbamate (41w)

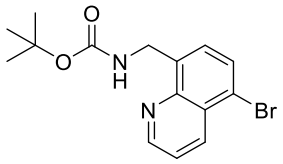

This compound was synthesized and provided by Dr. Christian Steinebach, University of Bonn.

tert-Butyl (4-Bromo-5-fluoro-2-methylbenzyl)carbamate (41x)

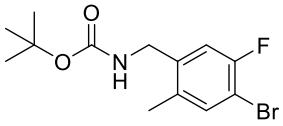

This compound was prepared using the General Procedure A and 4-bromo-5-fluoro-2-methylbenzaldehyde (type **40**, R = 2-Me, 5-F; 0.98 g, 4.5 mmol). The crude product was purified by flash column chromatography (gradient from 10 to 20% EtOAc in petroleum ether) to obtain **41x** as a white solid (0.21 g, 15%).

mp 108 °C; R_f = 0.26 (petroleum ether/EtOAc 9:1); ^{1}H NMR (500 MHz, DMSO-d_6) δ 1.40 (s, 9H, C(CH$_3$)$_3$), 2.23 (s, 3H, CH$_3$), 4.06 (d, J = 6.0 Hz, 2H, CH$_2$), 7.07 (d, J = 10.0 Hz, 1H), 7.34 – 7.40 (m, 1H), 7.48 (d, J = 7.2 Hz, 1H) (3-H, 6-H, NH); ^{13}C NMR (126 MHz, DMSO-d_6) δ 17.3 (CH$_3$), 28.1 (C(<u>C</u>H$_3$)$_3$), 40.8 (CH$_2$), 78.0 (<u>C</u>(CH$_3$)$_3$), 105.0 (d, $^2J_{F,C}$ = 20.5 Hz, C-4), 114.7 (d, $^2J_{F,C}$ = 22.7 Hz, C-6), 133.4 (d, $^3J_{F,C}$ = 3.5 Hz, C-3), 134.0 (C-2), 140.2 (d, $^3J_{F,C}$ = 5.9 Hz, C-1), 155.7 (CO), 156.5 (d, $^1J_{F,C}$ = 241.8 Hz, C-5). LC-MS (ESI) (90% H$_2$O to 100% MeCN in 10 min, then 100% MeCN to 15 min, DAD 200-600 nm), t_R = 7.85 min, 96% purity, *m/z* calcd for C$_{13}$H$_{17}$^{79}BrFNO$_2$ [M - H]$^-$, 316.03; found, 316.0. HRMS (ESI) *m/z* calcd for C$_{13}$H$_{17}$^{79}BrFNO$_2$ [M + H]$^+$, 318.0499; found, 318.0495.

tert-Butyl (4-Bromo-5-fluoro-2-methoxybenzyl)carbamate (41y)

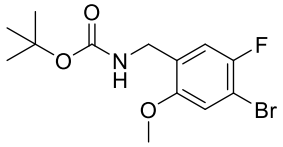

This compound was prepared using the General Procedure A and 4-bromo-5-fluoro-2-methoxybenzaldehyde (type **40**, R = 2-OMe, 5-F; 0.70 g, 3.0 mmol). The crude product was purified by flash column chromatography (gradient from 0 to 10% EtOAc in petroleum ether) to obtain **41y** as a white solid (0.84 g, 84%).

mp 118-220 °C; R_f = 0.38 (petroleum ether/EtOAc 9:1); ^{1}H NMR (500 MHz, DMSO-d_6) δ 1.39 (s, 9H, C(CH$_3$)$_3$), 3.81 (s, 3H, OCH$_3$), 4.04 (d, J = 6.1 Hz, 2H, CH$_2$), 7.05 (d, J = 9.4 Hz, 1H), 7.21 – 7.30 (m, 2H) (3-H, 6-H, NH); ^{13}C NMR (126 MHz, DMSO-d_6) δ 28.1 (C(<u>C</u>H$_3$)$_3$), 37.9 (CH$_2$), 56.3 (OCH$_3$), 78.0 (<u>C</u>(CH$_3$)$_3$), 105.4 (d, $^2J_{F,C}$ = 22.4 Hz, C-4), 114.7 (d, $^2J_{F,C}$ = 24.6 Hz, C-6), 115.0 (C-3), 129.7 (d, $^3J_{F,C}$ = 5.6 Hz, C-1), 152.6 (d, $^1J_{F,C}$ = 236.7 Hz, C-5), 153.1 (C-2), 155.7 (CO). LC-MS (ESI) (90% H$_2$O to 100% MeCN in 10 min, then 100% MeCN to 15 min, DAD 200-600 nm), t_R = 7.58 min, 99% purity, *m/z* calcd for $C_{13}H_{17}{}^{79}BrFNO_3$ [M - H]$^-$, 332.03; found, 331.9. HRMS (ESI) *m/z* calcd for $C_{13}H_{17}{}^{79}BrFNO_3$ [M + H]$^+$, 334.0449; found, 334.0448.

tert-Butyl _N_-((4-Bromo-2-hydroxy-3-methoxyphenyl)methyl)carbamate (41α)

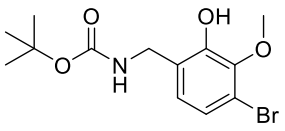

This compound was synthesized and provided by Dr. Christian Steinebach, University of Bonn.

tert-Butyl _N_-((4-Bromo-2,3-dimethoxyphenyl)methyl)carbamate (41β)

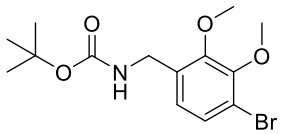

This compound was synthesized and provided by Dr. Christian Steinebach, University of Bonn.

***tert*-Butyl *N*-((4-Bromo-2,5-dichlorophenyl)methyl)carbamate (41γ)**

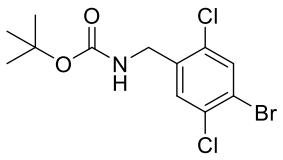

This compound was prepared by using General Procedure A and aldehyde **68** (1.73 g, 6.8 mmol). The crude product was purified by flash chromatography (gradient from 0 to 30% THF in petroleum ether) to give a colorless solid (0.37 g, 15%).

mp 240 – 242 °C; R_f = 0.38 (petroleum ether/THF 9:1); ^{1}H NMR (600 MHz, $CDCl_3$) δ 1.41 (s, 9H, CH_3), 5.64 (s, 2H, CH_2), 6.20 (t, J = 7.8 Hz, 1H, NH), 7.59 (s, 1H, Ar-H), 7.62 (s, 1H, Ar-H); ^{13}C NMR (151 MHz, $CDCl_3$) δ 28.3 (C($\underline{C}H_3)_3$), 59.5 (CH_2), 80.8 ($\underline{C}(CH_3)_3$), 122.5 (C-4), 129.4 (C-5), 131.3 (C-6), 133.3 (C-2), 134.3 (C-1), 137.8 (C-3), 154.3 (CO). LC-MS (ESI) (90% H_2O to 100% MeOH in 10 min, then 100% MeOH to 20 min, DAD 220-400 nm), t_R = 12.33 min, 94% purity, *m*/*z* calcd for $C_{12}H_{15}{}^{79}BrCl_2NO_2$ $[M + H]^+$, 353.97; found, 354.0.

***tert*-Butyl *N*-((4-Bromo-3-fluoro-2-hydroxyphenyl)methyl)carbamate (41δ)**

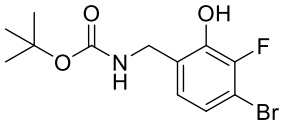

This compound was synthesized and provided by Dr. Christian Steinebach, University of Bonn.

***tert*-Butyl *N*-((4-Bromo-2-fluoro-3-methoxyphenyl)methyl)carbamate (41ε)**

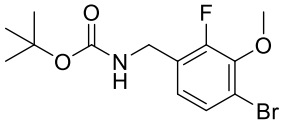

This compound was synthesized and provided by Dr. Christian Steinebach, University of Bonn.

***tert*-Butyl (4-Bromo-3,5-dimethoxybenzyl)carbamate (41ζ)**

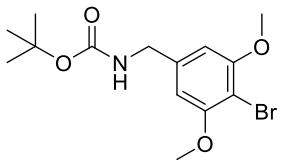

This compound was synthesized and provided by Dr. Christian Steinebach, University of Bonn.

***tert*-Butyl *N*-((4-(4-Methylthiazol-5-yl)phenyl)methyl)carbamate (42a)**

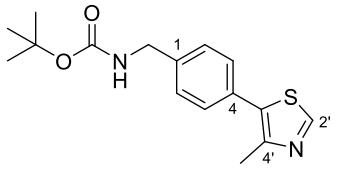

This compound was synthesized and provided by Dr. Christian Steinebach, University of Bonn.

***tert*-Butyl *N*-((2-Methyl-4-(4-methylthiazol-5-yl)phenyl)methyl)carbamate (42b)**

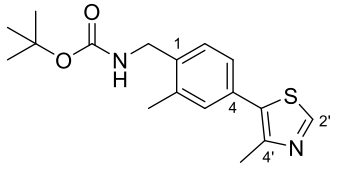

Following General Procedure B, compound **42b** was obtained from **41b** (type **41**, R = 2-Me; 0.60 g, 2.0 mmol). The crude product was purified by column chromatography (gradient of petroleum ether/EtOAc 10:1 to 2:1) to obtain a colorless oil (0.34 g, 53%).

R_f = 0.50 (petroleum ether/EtOAc 1:1); ^{1}H NMR (600 MHz, DMSO-d_6) δ 1.40 (s, 9H, C(CH_3)$_3$), 2.31 (s, 3H, CH_3), 2.45 (s, 3H, CH_3), 4.14 (d, J = 5.9 Hz, 2H, CH_2), 7.25 – 7.30 (m, 3H, Ar-H), 7.34 (t, J = 5.8 Hz, 1H, NH), 8.97 (s, 1H, 2″-H); ^{13}C NMR (151 MHz, DMSO-d_6) δ 15.95 (CH_3), 18.46 (CH_3), 28.23 (C(CH_3)$_3$), 41.05 (CH_2), 77.80 (C(CH_3)$_3$), 126.25 (C-5″), 127.44, 129.73, 130.29, 131.13 (C-3, C-4, C-5, C-6), 136.02 (C-2), 137.76 (C-1), 147.66 (C-4″), 151.30

(C-2″), 155.71 (CO). LC-MS (ESI) (90% H_2O to 100% MeOH in 10 min, then 100% MeOH to 20 min, DAD 220-400 nm), t_R = 11.21 min, 92% purity, *m*/*z* calcd for $C_{17}H_{22}N_2O_2S$ $[M + H]^+$, 319.14; found, 318.9.

tert-Butyl _N_-((2-Methyl-4-(4-methylthiazol-5-yl)phenyl)methyl)carbamate (42c)

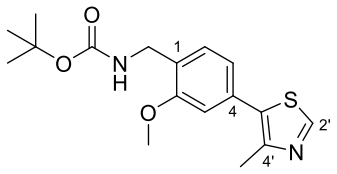

Following General Procedure B, compound **42c** was obtained from **41c** (type **41**, R = 2-OMe; 0.63 g, 2.0 mmol). The crude product was purified by column chromatography (gradient of petroleum ether/EtOAc 10:1 to 2:1) to obtain a colorless oil (0.45 g, 68%).

R_f = 0.50 (petroleum ether/EtOAc 1:1); ^{1}H NMR (600 MHz, DMSO-d_6) δ 1.40 (s, 9H, $C(CH_3)_3$), 2.47 (s, 3H, CH_3), 3.84 (s, 3H, OCH_3), 4.13 (d, *J* = 6.0 Hz, 2H, CH_2), 7.01 (d, *J* = 1.4 Hz, 1H), 7.04 (d, *J* = 7.7 Hz, 1H), 7.19 – 7.24 (m, 2H, Ar-H, NH), 8.98 (s, 1H, 2″-H); ^{13}C NMR (151 MHz, DMSO-d_6) δ 16.00 (CH_3), 28.24 ($C(CH_3)_3$), 38.15 (CH_2), 55.49 (OCH_3), 77.79 ($C(CH_3)_3$), 111.00 (C-3), 120.90 (C-5″), 127.40, 127.58, 131.01, 131.25 (C-1, C-4, C-5, C-6), 147.91 (C-4″), 151.41 (C-2″), 155.79 (CO), 156.48 (C-2′). LC-MS (ESI) (90% H_2O to 100% MeOH in 10 min, then 100% MeOH to 20 min, DAD 220-400 nm), t_R = 11.12 min, 90% purity, *m*/*z* calcd for $C_{17}H_{22}N_2O_3S$ $[M + H]^+$, 335.14; found, 334.9.

***tert*-Butyl (2-Fluoro-4-(4-methylthiazol-5-yl)benzyl)carbamate (42d)**

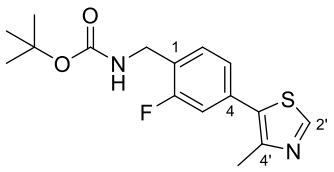

Following General Procedure B, compound **42d** was obtained from **41d** (type **41**, R = 2-F; 0.618 g, 2.0 mmol). The crude product was purified by flash column chromatography (gradient from 10 to 30% EtOAc in petroleum ether) to obtain a colorless oil (233 mg, 36%).

R_f = 0.22 (petroleum ether/EtOAc 4:1). ^{1}H NMR (600 MHz, DMSO-d_6) δ 1.40 (s, 9H, C(CH$_3$)$_3$), 2.46 (s, 3H, CH$_3$), 4.21 (d, J = 6.0 Hz, 2H, CH$_2$), 7.31 (d, J = 9.4 Hz, 2H), 7.38 (t, J = 7.8 Hz, 1H), 7.43 (t, J = 6.1 Hz, 1H) (Ar-H, CONH), 9.02 (s, 1H, 2′-H); ^{13}C NMR (151 MHz, DMSO-d_6) δ 15.9 (CH$_3$), 28.2 (C(<u>C</u>H$_3$)$_3$), 36.9 (CH$_2$), 78.0 (<u>C</u>(CH$_3$)$_3$), 115.3 (d, $^2J_{F,C}$ = 22.6 Hz, C-3), 125.0 (d, $^4J_{F,C}$ = 3.2 Hz, C-5′), 126.5 (d, $^2J_{F,C}$ = 15.1 Hz, C-1), 129.6 (d, $^3J_{F,C}$ = 5.2 Hz, C-6), 129.8 (d, $^4J_{F,C}$ = 1.7 Hz, C-5), 132.0 (d, $^3J_{F,C}$ = 8.5 Hz, C-4), 148.5 (C-4′), 152.0 (C-2′), 155.7 (CO), 159.7 (d, $^1J_{F,C}$ = 245.5 Hz, C-2). LC-MS (ESI) (90% H$_2$O to 100% MeOH in 10 min, then 100% MeOH to 20 min, DAD 220-400 nm), t_R = 11.01 min, 99% purity, *m/z* calcd for C$_{16}$H$_{19}$FN$_2$O$_2$S [M + H]$^+$, 323.12; found, 323.1. HRMS (ESI) *m/z* calcd for C$_{16}$H$_{19}$FN$_2$O$_2$S [M + H]$^+$, 323.1224; found, 323.1222.

***tert*-Butyl (2-Chloro-4-(4-methylthiazol-5-yl)benzyl)carbamate (42e)**

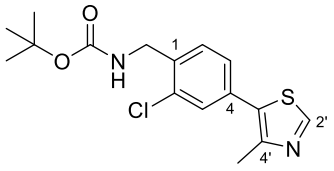

Following General Procedure B, compound **42e** was obtained from **41e** (type **41**, R = 2-Cl; 961 mg, 0.3 mmol). The crude product was purified by column chromatography (gradient of petroleum ether/EtOAc 9:1 to 4:1) to obtain a colorless oil (247 mg, 49%).

R_f = 0.45 (petroleum ether/EtOAc 4:1). ^{1}H NMR (500 MHz, DMSO-d_6) δ 1.41 (s, 9H, C(CH_3)$_3$), 2.46 (s, 3H, CH_3), 4.24 (d, J = 6.1 Hz, 2H, CH_2), 7.40 (d, J = 8.0 Hz, 1H), 7.44 – 7.49 (m, 2H), 7.53 (d, J = 1.8 Hz, 1H) (Ar-H, CONH), 9.02 (s, 1H, 2′-H); ^{13}C NMR (126 MHz, DMSO-d_6) δ 15.9 (CH_3), 28.2 (C($\underline{C}H_3$)$_3$), 41.0 ($NHCH_2$), 78.1 ($\underline{C}(CH_3)_3$), 127.8, 128.6, 128.9, 129.5, 131.7, 132.1 (C-2, C-3, C-4, C-5, C-5′, C-6), 136.7 (C-1), 148.6 (C-4′), 152.1 (C-2′), 155.7 (CO). LC-MS (ESI) (90% H_2O to 100% MeOH in 10 min, then 100% MeOH to 20 min, DAD 220-400 nm), t_R = 11.41 min, 96% purity, *m/z* calcd for $C_{16}H_{19}ClN_2O_2S$ $[M + H]^+$, 339.09; found, 339.1. HRMS (ESI) *m/z* calcd for $C_{16}H_{19}ClN_2O_2S$ $[M + H]^+$, 339.0928; found, 339.0926.

tert-Butyl (3-Methyl-4-(4-methylthiazol-5-yl)benzyl)carbamate (42f)

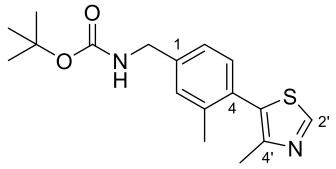

Following General Procedure B, compound **42f** was obtained from **41f** (type **41**, R = 3-Me; 90 mg, 0.3 mmol). The crude product was purified by column chromatography (gradient of petroleum ether/EtOAc 9:1 to 4:1) to obtain a colorless oil (155 mg, 15%).

R_f = 0.25 (petroleum ether/EtOAc 4:1). ^{1}H NMR (500 MHz, DMSO-d_6) δ 1.41 (s, 9H, C(CH_3)$_3$), 2.12 (s, 3H, CH_3), 2.17 (s, 3H, CH_3), 4.15 (d, J = 6.2 Hz, 2H, CH_2), 7.13 (dd, J = 8.0, 1.7 Hz, 1H, Ar-H), 7.19 – 7.22 (m, 2H, Ar-H), 7.38 (t, J = 5.8 Hz, 1H, CONH), 9.04 (s, 1H, 2′-H); ^{13}C NMR (126 MHz, DMSO-d_6) δ 15.2 (CH_3), 19.7 (Ar-CH_3), 28.2 (C($\underline{C}H_3$)$_3$), 43.0 ($NHCH_2$), 77.8 ($\underline{C}(CH_3)_3$), 124.4, 128.7, 128.8, 129.5, 130.9, 136.9 (C-2, C-3, C-4, C-5, C-5′, C-6), 140.8 (C-1), 149.0 (C-4′), 152.1 (C-2′), 155.8 (CO). LC-MS (ESI) (90% H_2O to 100% MeOH in 10 min, then 100% MeOH to 20 min, DAD 220-400 nm), t_R = 11.12 min, 97% purity, *m/z* calcd for $C_{17}H_{22}N_2O_2S$ $[M + H]^+$, 319.15; found, 318.9. HRMS (ESI) *m/z* calcd for $C_{17}H_{22}N_2O_2S$ $[M + H]^+$, 319.1475; found, 319.1472.

tert-Butyl (3-Methoxy-4-(4-methylthiazol-5-yl)benzyl)carbamate (42g)

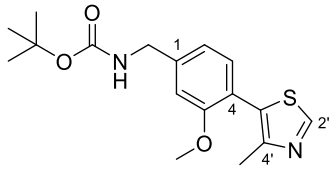

This compound was synthesized and provided by Aleša Bricelj, University of Ljubljana.

tert-Butyl (3-Fluoro-4-(4-methylthiazol-5-yl)benzyl)carbamate (42h)

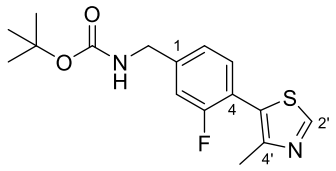

Following General Procedure B, compound **42h** was obtained from **41h** (type **41**, R = 3-F; 91 mg, 0.3 mmol). The crude product was purified by column chromatography (petroleum ether/EtOAc 4:1) to obtain a yellow solid (74 mg, 77%).

mp 106 °C; R_f = 0.26 (petroleum ether/EtOAc 4:1). ^{1}H NMR (600 MHz, DMSO-d_6) δ 1.41 (s, 9H, C(CH$_3$)$_3$), 2.33 (d, J = 1.0 Hz, 3H, CH$_3$), 4.19 (d, J = 6.2 Hz, 2H, CH$_2$), 7.16 – 7.21 (m, 2H), 7.43 – 7.50 (m, 2H) (Ar-H, CONH), 9.10 (s, 1H, 2′-H); ^{13}C NMR (151 MHz, DMSO-d_6) δ 15.7 (CH$_3$), 28.2 (C(<u>C</u>H$_3$)$_3$), 42.7 (NHCH$_2$), 78.0 (<u>C</u>(CH$_3$)$_3$), 114.2 (d, $^2J_{F,C}$ = 22.9 Hz, C-2), 117.0 (d, $^2J_{F,C}$ = 15.3 Hz, C-4), 123.1 (d, $^3J_{F,C}$ = 3.2 Hz, C-5′), 123.7 (C-6), 132.0 (d, $^3J_{F,C}$ = 2.8 Hz, C-5), 143.9 (d, $^3J_{F,C}$ = 7.2 Hz, C-1), 150.2 (C-4′), 153.1 (C-2′), 155.8 (CO), 158.8 (d, $^1J_{F,C}$ = 246.6 Hz, C-3). LC-MS (ESI) (90% H$_2$O to 100% MeOH in 10 min, then 100% MeOH to 20 min, DAD 220-400 nm), t_R = 10.89 min, 98% purity, *m/z* calcd for $C_{16}H_{19}FN_2O_2S$ $[M + H]^+$, 323.12; found, 323.2. HRMS (ESI) *m/z* calcd for $C_{16}H_{19}FN_2O_2S$ $[M + H]^+$, 323.1224; found, 323.1221.

tert-Butyl (3-Chloro-4-(4-methylthiazol-5-yl)benzyl)carbamate (42i)

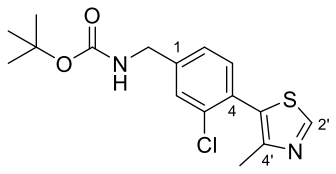

Following General Procedure B, compound **42i** was obtained from **41i** (type **41**, R = 3-Cl; 96 mg, 0.3 mmol). The crude product was purified by column chromatography (gradient of petroleum ether/EtOAc 9:1 to 4:1) to obtain a colorless oil (584 mg, 58%).

R_f = 0.26 (petroleum ether/EtOAc 4:1); ^{1}H NMR (500 MHz, DMSO-d_6) δ 1.41 (s, 9H, C(CH_3)$_3$), 2.23 (s, 3H, CH_3), 4.19 (d, J = 6.2 Hz, 2H, CH_2), 7.27 – 7.31 (m, 1H), 7.42 – 7.50 (m, 3H) (Ar-H, CONH), 9.09 (s, 1H, 2′-H); ^{13}C NMR (126 MHz, DMSO-d_6) δ 15.5 (CH_3), 28.2 (C($\underline{C}H_3$)$_3$), 42.6 ($NHCH_2$), 78.1 ($\underline{C}(CH_3)_3$), 125.9, 127.2, 128.0, 128.1, 132.7, 133.1 (C-2, C-3, C-4, C-5, C-5′, C-6), 143.2 (C-1), 150.2 (C-4′), 152.9 (C-2′), 155.8 (CO). LC-MS (ESI) (90% H_2O to 100% MeOH in 10 min, then 100% MeOH to 20 min, DAD 220-400 nm), t_R = 11.9 min, 96% purity, *m/z* calcd for $C_{16}H_{19}ClN_2O_2S$ $[M + H]^+$, 339.09; found, 339.1. HRMS (ESI) *m/z* calcd for $C_{16}H_{19}ClN_2O_2S$ $[M + H]^+$, 339.0929; found, 339,0927.

tert-Butyl (2,6-Dimethyl-4-(4-methylthiazol-5-yl)benzyl)carbamate (42j)

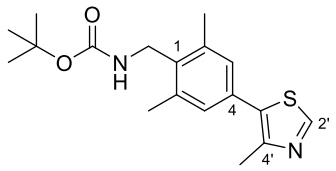

This compound was synthesized and provided by Aleša Bricelj, University of Ljubljana.

tert-Butyl (2,6-Dimethoxy-4-(4-methylthiazol-5-yl)benzyl)carbamate (42k)

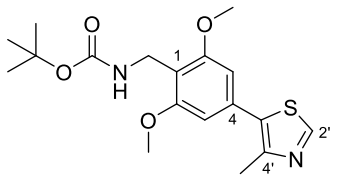

This compound was synthesized and provided by Aleša Bricelj, University of Ljubljana.

tert-Butyl (2,6-Difluoro-4-(4-methylthiazol-5-yl)benzyl)carbamate (42l)

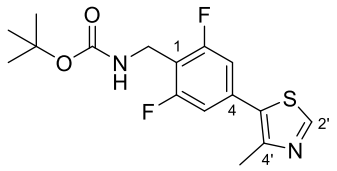

This compound was synthesized and provided by Aleša Bricelj, University of Ljubljana.

tert-Butyl (2,6-Dichloro-4-(4-methylthiazol-5-yl)benzyl)carbamate (42m)

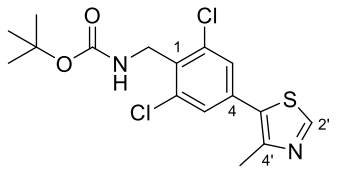

This compound was synthesized and provided by Aleša Bricelj, University of Ljubljana.

tert-Butyl (2,5-Dimethyl-4-(4-methylthiazol-5-yl)benzyl)carbamate (42n)

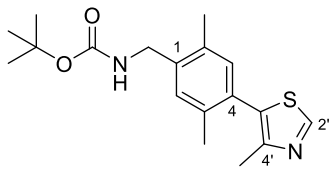

This compound was synthesized and provided by Aleša Bricelj, University of Ljubljana.

tert-Butyl _N_-((2,5-Dimethoxy-4-(4-methylthiazol-5-yl)phenyl)methyl)carbamate (42o)

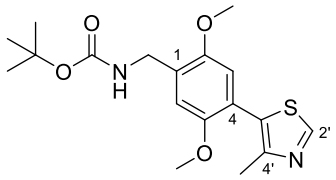

This compound was prepared using the General Procedure B and **41o** (type **41**, R = 2-OMe, 5-OMe; 0.69 g, 2.0 mmol). The crude product was purified by flash chromatography (gradient from 0 to 60% EtOAc in petroleum ether) to give a colorless resin (0.11 g, 16%).

R_f = 0.28 (petroleum ether/EtOAc 2:1); ^{1}H NMR (500 MHz, DMSO-d_6) δ 1.41 (s, 9H, C(CH$_3$)$_3$), 2.30 (s, 3H, CH$_3$), 3.69 (s, 3H), 3.75 (s, 3H, OCH$_3$), 4.13 (d, J = 6.2 Hz, 2H, CH$_2$), 6.89 (s, 1H), 6.95 (s, 1H) (6-H, NH), 7.24 (s, 1H, 3-H), 8.98 (s, 1H, 2′-H); ^{13}C NMR (126 MHz, DMSO-d_6) δ 16.1 (CH$_3$), 28.4 (C(<u>C</u>H$_3$)$_3$), 38.5 (CH$_2$), 56.1, 56.1 (OCH$_3$), 78.0 (<u>C</u>(CH$_3$)$_3$), 111.7 (C-3), 114.1 (C-6), 118.4, 126.8, 129.4 (C-1, C-2, C-4), 149.6, 150.2, 150.5, 152.1 (CO, C-4′, C-5, C-5′), 156.0 (C-2′). LC-MS (ESI) (90% H$_2$O to 100% MeOH in 10 min, then 100% MeOH to 20 min, DAD 220-400 nm), t_R = 11.04 min, 99% purity, m/z calcd for C$_{18}$H$_{25}$N$_2$O$_4$S [M + H]$^+$, 365.15; found, 365.1; HRMS (ESI) m/z calcd for C$_{18}$H$_{25}$N$_2$O$_4$S [M + H]$^+$, 365.1530; found, 365.1527.

tert-Butyl (2,5-Difluoro-4-(4-methylthiazol-5-yl)benzyl)carbamate (42p)

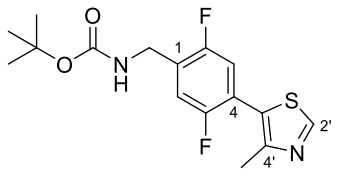

This compound was synthesized and provided by Aleša Bricelj, University of Ljubljana.

tert-Butyl (2,5-Dichloro-4-(4-methylthiazol-5-yl)benzyl)carbamate (42q)

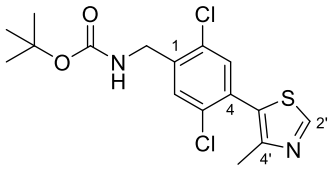

Following General Procedure A, compound **42q** was obtained from **50** (0.22 g, 0.8 mmol). The crude product was purified by column chromatography (gradient of petroleum ether/EtOAc 9:1 to 4:1) to obtain a white solid (0.10 g, 32%).

mp 104 °C; R_f = 0.26 (petroleum ether/EtOAc 4:1). ^{1}H NMR (500 MHz, DMSO-d_6) δ 1.42 (s, 9H, C(CH$_3$)$_3$), 2.25 (s, 3H, CH$_3$), 4.24 (d, J = 6.1 Hz, 2H, CH$_2$), 7.47 (s, 1H, Ar-H), 7.53 (t, J = 6.0 Hz, 1H, CONH), 7.61 (s, 1H, Ar-H), 9.13 (s, 1H, 2′-H); ^{13}C NMR (126 MHz, DMSO-d_6) δ 15.5 (CH$_3$), 28.1 (C(<u>C</u>H$_3$)$_3$), 41.0 (CH$_2$), 78.4 (<u>C</u>(CH$_3$)$_3$), 125.8, 129.0, 130.1, 130.4, 132.1, 132.7 (C-2, C-3, C-4, C-5, C-5′, C-6), 139.6 (C-1), 150.8 (C-4′), 153.5 (C-2′), 155.7 (CO). LC-MS (ESI) (90% H$_2$O to 100% MeCN in 10 min, then 100% MeCN to 15 min, DAD 200-600 nm), t_R = 7.48 min, 99% purity, *m/z* calcd for $C_{16}H_{18}Cl_2N_2O_2S$ $[M + H]^+$, 373.05; found, 373.1. HRMS (ESI) m/z $[M + H]^+$ calcd for $C_{16}H_{18}Cl_2N_2O_2S$, 373.0539; found, 373.0539.

tert-Butyl (2,3-Dimethyl-4-(4-methylthiazol-5-yl)benzyl)carbamate (42r)

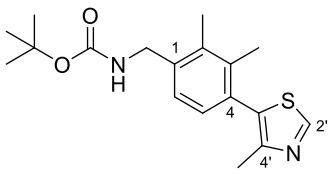

This compound was synthesized and provided by Aleša Bricelj, University of Ljubljana.

tert-Butyl (2,3-Difluoro-4-(4-methylthiazol-5-yl)benzyl)carbamate (42s)

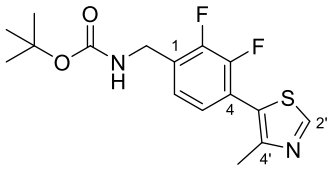

Following General Procedure B, compound **42s** was obtained from bromoaryl compound **41s** (type **41**, R = 2-F, 3-F; 97 mg, 0.3 mmol). The crude product was purified by flash column chromatography (gradient of petroleum ether/EtOAc 4:1 to 1:1) to obtain a colorless oil (0.06 g, 63%).

R_f = 0.15 (petroleum ether/EtOAc 4:1). ^{1}H NMR (600 MHz, DMSO-d_6) δ 1.40 (s, 9H, C(CH_3)$_3$), 2.35 (d, J = 1.2 Hz, 3H, CH_3), 4.25 (d, J = 6.0 Hz, 2H, CH_2), 7.20 (t, J = 7.4 Hz, 1H, Ar-H), 7.31 (t, J = 7.1 Hz, 1H, Ar-H), 7.50 (t, J = 6.0 Hz, 1H, CONH), 9.15 (s, 1H, 2′-H); ^{13}C NMR (151 MHz, DMSO-d_6) δ 15.7 (CH_3), 28.2 (C($\underline{C}H_3$)$_3$), 37.0 (CH_2), 78.2 ($\underline{C}$(CH_3)$_3$), 119.4 (d, $^2J_{F,C}$ = 12.0 Hz, C-4), 122.6, 123.8, 126.4 (d, $^3J_{F,C}$ = 3.0 Hz, C-5, C-5′, C-6), 129.7 (d, $^2J_{F,C}$ = 11.6 Hz, C-1), 146.7 (dd, $^1J_{F,C}$ = 248.3 Hz, $^2J_{F,C}$ = 13.6 Hz, C-2, C-3), 150.8 (C-4′), 153.8 (C-2′), 155.7 (CO). LC-MS (ESI) (90% H_2O to 100% MeCN in 10 min, then 100% MeCN to 15 min, DAD 200-600 nm), t_R = 6.79 min, 98% purity, *m/z* calcd for $C_{16}H_{18}F_2N_2O_2S$ $[M + H]^+$, 341.11; found, 341.4. HRMS (ESI) *m/z* calcd for $C_{16}H_{18}F_2N_2O_2S$ $[M + H]^+$, 341.1130; found, 341.1125.

***tert*-Butyl (3-Fluoro-2-hydroxy-4-(4-methylthiazol-5-yl)benzyl)carbamate (42t)**

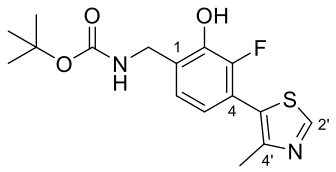

Following General Procedure A, compound **42t** was obtained from **53** (0.19 g, 0.8 mmol). The crude product was purified by flash column chromatography (gradient of petroleum ether/EtOAc 4:1 to 1:1) to obtain a white solid (0.22 g, 81%).

mp 128 °C; R_f = 0.50 (petroleum ether/EtOAc 1:1). ^{1}H NMR (500 MHz, DMSO-d_6) δ 1.41 (s, 9H, C(CH_3)$_3$), 2.33 (s, 3H, CH_3), 4.16 (d, J = 6.1 Hz, 2H, CH_2), 6.87 (t, J = 7.3 Hz, 1H, Ar-H), 7.00 (d, J = 7.9 Hz, 1H, Ar-H), 7.30 (t, J = 5.9 Hz, 1H, CONH), 9.08 (s, 1H, 2′-H), 9.83 (s, 1H, OH); ^{13}C NMR (126 MHz, DMSO-d_6) δ 15.7 (d, $^5J_{F,C}$ = 2.5 Hz, CH_3), 28.2 (C(<u>C</u>H_3)$_3$), 38.3 (CH_2), 78.0 (<u>C</u>(CH_3)$_3$), 117.7 (d, $^2J_{F,C}$ = 13.5 Hz, C-4), 120.9, 122.7, 124.12, 130.1 (C-1, C-5, C-5′, C-6), 142.3 (d, $^2J_{F,C}$ = 14.6 Hz, C-2), 148.2 (d, $^1J_{F,C}$ = 241.2 Hz, C-3), 149.9 (C-4′), 152.9 (C-2′), 156.0 (CO). LC-MS (ESI) (90% H_2O to 100% MeCN in 10 min, then 100% MeCN to 15 min, DAD 200-600 nm), t_R = 6.33 min, 97% purity, *m/z* calcd for $C_{16}H_{19}FN_2O_3S$ $[M + H]^+$, 339.12; found, 339.2. HRMS (ESI) m/z $[M + H]^+$ calcd for $C_{16}H_{19}FN_2O_3S$, 339.1173; found, 339.1172.

***tert*-Butyl (3-Fluoro-2-methoxy-4-(4-methylthiazol-5-yl)benzyl)carbamate (42u)**

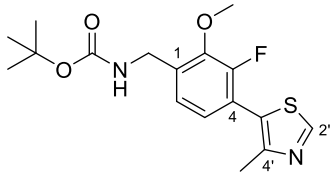

Compound **42t** (0.27 g, 0.8 mmol) and Cs_2CO_3 (0.65 g, 2.0 mmol) were suspended in dry DMF (10 mL). The mixture was stirred at 45 °C for 1 h, after which MeI (0.15 mL, 2.4 mmol) was added. It was further stirred at this temperature for 16 h. The suspension was filtered through a pad of celite and washed with EtOAc (50 mL). The organic layer was washed with H_2O (50 mL) and brine (25 mL), dried over Na_2SO_4, filtered, and evaporated *in vacuo*. The crude product

was purified by flash column chromatography (gradient of petroleum ether/EtOAc 4:1 to 1:1) to obtain a colorless oil (0.18 g, 63%).

R_f = 0.52 (petroleum ether/EtOAc 1:1). ^{1}H NMR (600 MHz, DMSO-d_6) δ 1.40 (s, 9H, C(CH$_3$)$_3$), 2.34 (s, 3H, CH$_3$), 3.88 (s, 3H, OCH$_3$), 4.21 (d, J = 6.1 Hz, 2H, CH$_2$), 7.12 (d, J = 8.1 Hz, 1H, Ar-H), 7.19 (t, J = 7.4 Hz, 1H, Ar-H), 7.38 (t, J = 6.0 Hz, 1H, CONH), 9.11 (s, 1H, 2′-H); ^{13}C NMR (151 MHz, DMSO-d_6) δ 15.8 (CH$_3$), 28.2 (C(<u>C</u>H$_3$)$_3$), 37.9 (CH$_2$), 61.4 (d, $^4J_{F,C}$ = 4.9 Hz, OCH$_3$), 78.0 (<u>C</u>(CH$_3$)$_3$), 118.7 (d, $^2J_{F,C}$ = 14.0 Hz, C-4), 123.2 (d, $^3J_{F,C}$ = 3.5 Hz), 123.5, 125.8 (C-5, C-5′, C-6), 135.3 (C-1), 145.0 (d, $^2J_{F,C}$ = 11.3 Hz, C-2), 150.3 (C-4′), 151.9 (d, $^1J_{F,C}$ = 247.9 Hz, C-3), 153.3 (C-2′), 155.8 (CO). LC-MS (ESI) (90% H$_2$O to 100% MeCN in 10 min, then 100% MeCN to 15 min, DAD 200-600 nm), t_R = 6.80 min, 94% purity, *m/z* calcd for C$_{17}$H$_{21}$FN$_2$O$_3$S [M + H]$^+$, 353.13; found, 353.2. HRMS (ESI) *m/z* calcd for C$_{17}$H$_{21}$FN$_2$O$_3$S [M + H]$^+$, 353.1330; found, 353.1324.

tert-Butyl ((4-(4-Methylthiazol-5-yl)naphthalen-1-yl)methyl)carbamate (42v)

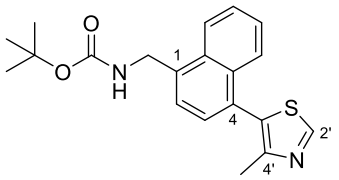

This compound was synthesized and provided by Aleša Bricelj, University of Ljubljana.

tert-Butyl _N_-((5-(4-Methylthiazol-5-yl)-8-quinolyl)methyl)carbamate (42w)

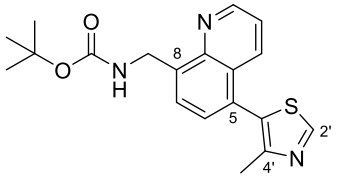

This compound was synthesized and provided by Dr. Christian Steinebach, University of Bonn

***tert*-Butyl (5-Fluoro-2-methyl-4-(4-methylthiazol-5-yl)benzyl)carbamate (42x)**

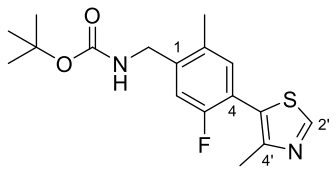

Following General Procedure B, compound **42x** was obtained from bromoaryl compound **41x** (type **41**, R = 2-Me, 5-F; 0.19 g, 0.6 mmol). The crude product was purified by flash column chromatography (gradient from 10 to 20% EtOAc in petroleum ether) to obtain a yellow oil (0.12 g, 58%).

R_f = 0.24 (petroleum ether/EtOAc 4:1).; ^{1}H NMR (500 MHz, DMSO-d_6) δ 1.41 (s, 9H, C(CH$_3$)$_3$), 2.26 (s, 3H, CH$_3$), 2.32 (s, 3H, CH$_3$), 4.13 (d, J = 6.0 Hz, 2H, CH$_2$), 7.07 (d, J = 11.1 Hz, 1H, Ar-H), 7.27 (d, J = 7.6 Hz, 1H, Ar-H), 7.43 (t, J = 5.9 Hz, 1H, NH), 9.09 (s, 1H, 2′-H); ^{13}C NMR (126 MHz, DMSO-d_6) δ 15.6 (d, $^5J_{F,C}$ = 2.6 Hz, CH$_3$), 17.5 (CH$_3$), 28.2 (C(<u>C</u>H$_3$)$_3$), 40.9 (CH$_2$), 78.0 (<u>C</u>(CH$_3$)$_3$), 114.0 (d, $^2J_{F,C}$ = 22.8 Hz, C-6), 116.5 (d, $^2J_{F,C}$ = 15.0 Hz, C-4), 123.8 (C-2), 131.6 (d, $^3J_{F,C}$ = 3.4 Hz, C-3), 132.9 (d, $^3J_{F,C}$ = 2.4 Hz, C-5′), 141.1 (d, $^3J_{F,C}$ = 7.4 Hz, C-3), 150.0 (C-4′), 152.9 (C-2′), 155.7 (CO), 157.2 (d, $^1J_{F,C}$ = 244.2 Hz, C-5). LC-MS (ESI) (90% H$_2$O to 100% MeCN in 10 min, then 100% MeCN to 15 min, DAD 200-600 nm), t_R = 7.10 min, 99% purity, *m/z* calcd for $C_{17}H_{21}FN_2O_2S$ $[M + H]^+$, 337.14; found, 337.2. HRMS (ESI) *m*/*z* calcd for $C_{17}H_{21}FN_2O_2S$ $[M + H]^+$, 337.1380; found, 337.1374.

***tert*-Butyl (5-Fluoro-2-methoxy-4-(4-methylthiazol-5-yl)benzyl)carbamate (42y)**

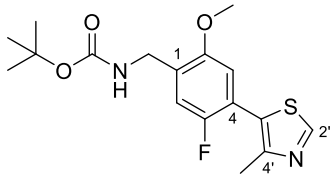

Following General Procedure B, compound **42y** was obtained from **41y** (type **41**, R = 2-OMe, 5-F; 0.20 g, 0.6 mmol). The crude product was purified by flash column chromatography (gradient from 20 to 50% EtOAc in petroleum ether) to obtain colorless oil (0.14 g, 67%).

R_f = 0.51 (petroleum ether/EtOAc 1:1); ^{1}H NMR (500 MHz, DMSO-d_6) δ 1.41 (s, 9H, C(CH$_3$)$_3$), 2.36 (s, 3H, CH$_3$), 3.82 (s, 3H, OCH$_3$), 4.13 (d, J = 6.3 Hz, 2H, CH$_2$), 7.00 (d, J = 6.0 Hz, 1H), 7.05 (d, J = 10.5 Hz, 1H) (3-H, 6-H), 7.31 (t, J = 6.3 Hz, 1H, NH), 9.10 (s, 1H, 2′-H); ^{13}C NMR (126 MHz, DMSO-d_6) δ 15.7 (d, $^5J_{F,C}$ = 2.5 Hz, CH$_3$), 28.2 (C(<u>C</u>H$_3$)$_3$), 38.1 (CH$_2$), 56.1 (OCH$_3$), 78.0 (<u>C</u>(CH$_3$)$_3$), 113.3 (d, $^3J_{F,C}$ = 2.5 Hz, C-3), 114.3 (d, $^2J_{F,C}$ = 25.2 Hz, C-6), 117.0 (d, $^2J_{F,C}$ = 16.5 Hz, C-4), 123.9 (C-5′), 130.7 (d, $^3J_{F,C}$ = 6.8 Hz, C-1), 150.3 (C-4′), 152.4 (C-2′), 153.0 (d, $^1J_{F,C}$ = 238.8 Hz, C-5), 153.0 (C-2), 155.8 (CO). LC-MS (ESI) (90% H$_2$O to 100% MeCN in 10 min, then 100% MeCN to 15 min, DAD 200-600 nm), t_R = 7.02 min, 97% purity, *m/z* calcd for C$_{17}$H$_{21}$FN$_2$O$_3$S [M + H]$^+$, 353.13; found, 353.2. HRMS (ESI) *m/z* calcd for C$_{17}$H$_{21}$FN$_2$O$_3$S [M + H]$^+$, 353.1330; found, 353.1325.

Benzyl (2*S*,4*R*)-4-Hydroxypyrrolidine-2-carboxylate hydrochloride (43)

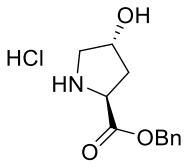

This compound was purchased from abcr GmbH (Karlsruhe, Germany).

Benzyl (2*S*,4*R*)-1-((*S*)-2-((*tert*-Butoxycarbonyl)amino)-3,3-dimethylbutanoyl)-4-hydroxypyrrolidine-2-carboxylate (44)[202]

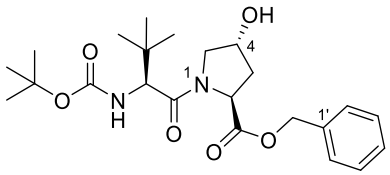

Boc-Tle-OH (4.63 g, 20 mmol) was dissolved in dry DMF (18 mL) and H-Hyp-OBzl × HCl (**43**, 5.15 g, 20 mmol) was added. DIPEA (14 mL, 80 mmol) was added, followed by the addition of HATU (8.36 g, 22 mmol) after 5 min. The mixture was stirred at rt for 18 h. The reaction was quenched by the addition of H$_2$O (150 mL) and extracted with EtOAc (3 × 150 mL). The combined organic layers were washed with saturated NaHCO$_3$ (150 mL)

and brine (150 mL), dried over Na_2SO_4, filtered and concentrated. The residue was purified by column chromatography (petroleum ether/EtOAc 1:1) to yield **44** as a white solid (5.91 g, 68%).

mp. 118-120 °C; R_f = 0.33 (petroleum ether/EtOAc 1:1); ^{1}H NMR (500 MHz, DMSO-d_6) δ 0.89 (s, 9H, C(CH$_3$)$_3$), 1.38 (s, 9H, OC(CH$_3$)$_3$), 1.87 – 1.96 (m, 1H, 3-H), 2.09 – 2.18 (m, 1H, 3-H), 3.59 – 3.63 (m, 1H, 5-H), 3.67 (dd, J = 10.7, 4.1 Hz, 1H, 5-H), 4.15 (d, J = 9.4 Hz, 1H), 4.32 – 4.36 (m, 1H), 4.42 (t, J = 8.4 Hz, 1H) (2-H, 4-H, NHCH), 5.07 – 5.15 (m, 2H, Ar-CH$_2$), 5.20 (d, J = 3.7 Hz, 1H, OH), 6.47 (d, J = 9.4 Hz, 1H, CONH), 7.29 – 7.39 (m, 5H, Ar-H); ^{13}C NMR (126 MHz, DMSO-d_6) δ 26.1 (C(CH$_3$)$_3$), 28.1 (OC(CH$_3$)$_3$), 35.2 (C(CH$_3$)$_3$), 37.2 (C-3), 55.9, 57.8, 58.2, 65.8, 68.8 (C-2, C-4, C-5, NHCH, Ar-CH$_2$), 78.1 (OC(CH$_3$)$_3$), 127.8 (C-2′, C-6′), 127.9 (C-4′), 128.3 (C-3′, C-5′), 135.9 (C-1′), 155.3 (CONH), 170.2, 171.6 (CO). LC-MS (ESI) (90% H_2O to 100% MeOH in 10 min, then 100% MeOH to 20 min, DAD 220-400 nm), t_R = 11.26 min, 99% purity, *m/z* calcd for $C_{23}H_{34}N_2O_6$ $[M + H]^+$, 435.25, found 435.3.

Benzyl (2*S*,4*R*)-1-((*S*)-2-(1-Cyanocyclopropane-1-carboxamido)-3,3-dimethylbutanoyl)-4-hydroxypyrrolidine-2-carboxylate (45)

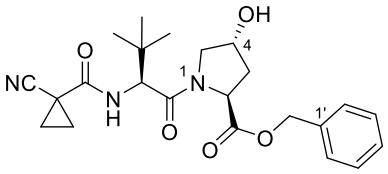

Following General Procedure C, compound **45** was obtained using Boc-protected amine **44** (1.30 mg, 3.0 mmol) and 1-cyano-1-cyclopropanecarboxylic acid (0.33 mg, 3.0 mmol). The residue was purified by flash column chromatography using a gradient from 0 to 10% MeOH in CH_2Cl_2 to afford **45** as a white solid (0.81 mg, 63%).

mp 112-114 °C; R_f = 0.37 (CH_2Cl_2/MeOH 9:1); ^{1}H NMR (500 MHz, DMSO-d_6) δ 0.91 (s, 9H, C(CH$_3$)$_3$), 1.44 – 1.54 (m, 2H, CH$_2$CCN), 1.57 – 1.65 (m, 2H, CH$_2$CCN), 1.89 – 1.97 (m, 1H, 3-H), 2.12 – 2.19 (m, 1H, 3-H), 3.56 – 3.60 (m, 1H, 5-H), 3.65 (dd, J = 10.9, 3.9 Hz, 1H, 5-H), 4.31 – 4.36 (m, 1H), 4.46 (dd, J = 9.2, 7.8 Hz, 1H), 4.52 (d, J = 8.9 Hz, 1H) (2-H, 4-H, NHCH), 5.13 (s, 2H, Ar-CH$_2$), 5.21 (d, J = 3.9 Hz, 1H, OH), 7.29 – 7.41 (m, 6H, CONH, Ar-H); ^{13}C NMR (126 MHz, DMSO-d_6) δ 13.7 (CH$_2$CCN), 16.6, 16.7 (CH$_2$CCN), 25.9 (C(CH$_3$)$_3$), 36.0

($\underline{C}(CH_3)_3$), 37.1 (C-3), 56.2, 57.2, 57.9, 66.0, 68.7 (C-2, C-4, C-5, NHCH, Ar-CH_2), 120.0 (CN), 127.9 (C-2′, C-6′), 128.0 (C-4′), 128.3 (C-3′, C-5′), 135.7 (C-1′), 164.5, 169.1, 171.4 (CO). LC-MS (ESI) (90% H_2O to 100% MeOH in 10 min, then 100% MeOH to 20 min, DAD 220-400 nm), t_R = 10.76 min, 93% purity, *m/z* calcd for $C_{23}H_{29}N_3O_5$ $[M + H]^+$, 428.23; found, 428.4.

(2*S*,4*R*)-1-((*S*)-2-(1-Cyanocyclopropane-1-carboxamido)-3,3-dimethylbutanoyl)-4-hydroxypyrrolidine-2-carboxylic Acid (46)

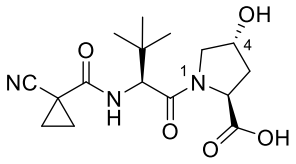

Compound **45** (2.17 g, 5.0 mmol) was dissolved in dry EtOH (50 mL) and treated with 10% Pd/C under H_2 (1 atm, balloon) for 18 h. The reaction mixture was filtered through celite and concentrated to yield a white solid. This compound was used without further purification and characterization.

4-Bromo-2,5-dichlorobenzoic Acid (47)

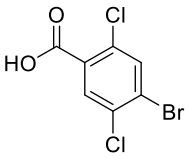

This compound was purchased from BLDpharm (Kaiserslautern, Germany).

2,5-Dichloro-4-(4-methylthiazol-5-yl)benzoic Acid (48)

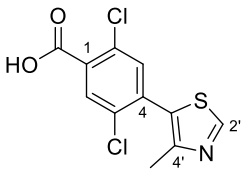

Following General Procedure B, compound **48** was obtained from 4-bromo-2,5-dichlorobenzoic acid (**47**, 1.05 g, 4.0 mmol). The crude product was purified by column chromatography (petroleum ether/EtOAc/AcOH 1:1:0.05) to obtain a white solid (0.36 mg, 34%).

mp 220-222 °C; R_f = 0.55 (petroleum ether /EtOAc/AcOH 1:1:0.05); ^{1}H NMR (500 MHz, DMSO-d_6) δ 2.27 (s, 3H, CH_3), 7.73 (s, 1H, Ar-H), 7.99 (s, 1H, Ar-H), 9.16 (s, 1H, 2′-H), 13.81 (br s, 1H, OH); ^{13}C NMR (126 MHz, DMSO-d_6) δ 15.5 (CH_3), 125.3, 130.3, 131.4, 132.1, 133.0, 134.2, 134.3 (C-1, C-2, C-3, C-4, C-5, C-5′, C-6), 151.3 (C-4′), 154.0 (C-2′), 165.1 (CO_2H). LC-MS (ESI) (90% H_2O to 100% MeCN in 10 min, then 100% MeCN to 15 min, DAD 200-600 nm), t_R = 5.14 min, 100% purity, *m/z* calcd for $C_{11}H_7Cl_2NO_2S$ $[M + H]^+$, 287.96; found, 288.0. HRMS (ESI) *m/z* calcd for $C_{11}H_7Cl_2NO_2S$ $[M + H]^+$, 287.9647; found, 287.9646.

2,5-Dichloro-*N*-methoxy-*N*-methyl-4-(4-methylthiazol-5-yl)benzamide (49)

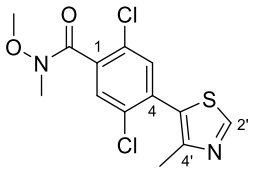

Compound **48** (0.43 g, 1.5 mmol), *N*,*O*-dimethylhydroxylamine hydrochloride (0.30 g, 3.0 mmol), EDC × HCl (0.32 g, 1.65 mmol), and Et_3N (0.23 mL, 1.65 mmol) were mixed in CH_2Cl_2 (15 mL) and stirred at room temperature for 16 h. Subsequently, the crude material was evaporated and subjected to flash column chromatography (gradient from 20% to 40% EtOAc in cyclohexane) to give the title compound as a colorless solid (0.28 mg, 57%).

mp 104-105 °C; R_f = 0.40 (petroleum ether /EtOAc 1:1 ^{1}H NMR (500 MHz, DMSO-d_6) δ 2.27 (s, 3H, CH_3), 3.31 (s, 3H, CH_3), 3.53 (s, 3H, CH_3), 7.72 (s, 1H, Ar-H), 7.83 (s, 1H, Ar-H), 9.16 (s, 1H, 2′-H); ^{13}C NMR (126 MHz, DMSO-d_6) δ 15.5 (CH_3), 31.8 (NCH_3), 61.3 (OCH_3), 125.6, 128.2, 128.6, 132.1, 132.2, 132.9, 137.1 (C-1, C-2, C-3, C-4, C-5, C-5′, C-6), 151.1 (C-4′), 153.8 (C-2′), 165.1 (CO). LC-MS (ESI) (90% H_2O to 100% MeCN in 10 min, then 100% MeCN to 15 min, DAD 200-600 nm), t_R = 5.69 min, 100% purity, *m/z* calcd for $C_{13}H_{12}Cl_2N_2O_2S$ $[M + H]^+$, 331.01; found, 331.1. HRMS (ESI) *m/z* calcd for $C_{13}H_{12}Cl_2N_2O_2S$ $[M + H]^+$, 331.0069; found, 331.0068.

2,5-Dichloro-4-(4-methylthiazol-5-yl)benzaldehyde (50)

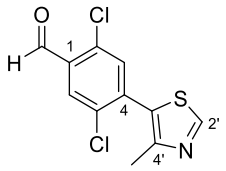

A Schlenk flask was charged with compound **49** (0.33 g, 1.0 mmol), evacuated and refilled with argon gas. The material was dissolved in try THF (15 mL) and cooled to 0 °C. $LiAlH_4$ solution (1M in THF, 0.5 mL) was added dropwise, and the mixture was stirred at this temperature for 1 h. Subsequently, it was cooled to -15 °C, and slowly quenched by the addition of 10% $KHSO_4$ solution (50 mL). The aqueous solution was extracted with Et_2O (50 mL) dried over Na_2SO_4, filtered, and concentrated *in vacuo*. The crude product was filtered through a small plug of silica gel and the product was eluted with CH_2Cl_2. Evaporation of the solid yielded **50** as a colorless solid (0.30 mg, 92%).

mp 64 °C; R_f = 0.31 (petroleum ether /EtOAc 4:1); ^{1}H NMR (500 MHz, DMSO-d_6) δ 2.29 (s, 3H, CH_3), 7.85 (d, J = 0.9 Hz, 1H, Ar-H), 8.00 (d, J = 1.0 Hz, 1H, Ar-H), 9.20 (d, J = 0.9 Hz, 1H, 2′-H), 10.28 (d, J = 1.0 Hz, 1H, CHO); ^{13}C NMR (126 MHz, DMSO-d_6) δ 15.6 (CH_3), 125.2, 130.4, 132.9, 133.1, 134.1, 134.5, 137.0 (C-1, C-2, C-3, C-4, C-5, C-5′, C-6), 151.5 (C-4′), 154.3 (C-2′), 188.4 (CHO). LC-MS (ESI) (90% H_2O to 100% MeCN in 10 min, then 100% MeCN to 15 min, DAD 200-600 nm), t_R = 6.76 min, 100% purity, *m/z* calcd for $C_{11}H_7Cl_2NOS$ $[M + H]^+$, 271.97; found, 272.0. HRMS (ESI) *m/z* calcd for $C_{11}H_7Cl_2NOS$ $[M + H]^+$, 271.9698; found, 271.9697.

3-Bromo-2-fluorophenol (51)

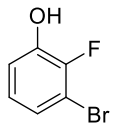

This compound was purchased from BLDpharm (Kaiserslautern, Germany).

2-Fluoro-3-(4-methylthiazol-5-yl)phenol (52)

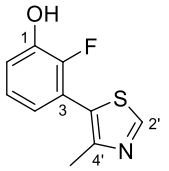

Following General Procedure B, compound **52** was obtained from 3-bromo-2-fluorophenol (**51**, 0.84 mg, 5.0 mmol). The crude product was purified by column chromatography (gradient of petroleum ether/EtOAc 4:1 to 1:1) to obtain a white solid (0.84 mg, 80%).

mp 168-172 °C; R_f = 0.48 (petroleum ether /EtOAc 1:1); ^{1}H NMR (500 MHz, DMSO-d_6) δ 2.33 (d, J = 1.2 Hz, 3H, CH_3), 6.84 (ddd, J = 7.8, 6.3, 1.9 Hz, 1H, Ar-H), 6.99 – 7.10 (m, 2H, Ar-H), 9.08 (s, 1H, 2′-H), 10.07 (br s, 1H, OH); ^{13}C NMR (126 MHz, DMSO-d_6) δ 15.7 (d, $^5J_{F,C}$ = 2.7 Hz, CH_3), 118.0 (d, $^3J_{F,C}$ = 3.2 Hz, C-6), 119.7 (d, $^2J_{F,C}$ = 12.6 Hz, C-3), 121.3, 124.1, 124.4 (d, $^3J_{F,C}$ = 4.5 Hz, C-4, C-5, C-5′), 145.6 (d, $^2J_{F,C}$ = 12.4 Hz, C-1), 148.2 (d, $^1J_{F,C}$ = 243.6 Hz, C-2), 150.0 (C-4′), 152.9 (C-2′). LC-MS (ESI) (90% H_2O to 100% MeOH in 10 min, then 100% MeOH to 20 min, DAD 220-600 nm), t_R = 4.68 min, 97% purity, *m/z* calcd for $C_{10}H_8FNOS$ $[M + H]^+$, 210.04; found, 209.9. HRMS (ESI) *m/z* calcd for $C_{10}H_8FNOS$ $[M + H]^+$, 210.0383; found, 210.0381.

3-Fluoro-2-hydroxy-4-(4-methylthiazol-5-yl)benzaldehyde (53)

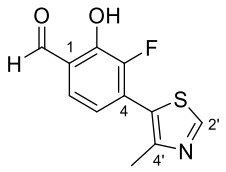

Compound **52** (0.73 g, 3.5 mmol) was dissolved in dry THF (30 mL). Et_3N (0.97 mL, 7.0 mmol) and $MgCl_2$ (0.66 g, 7.0 mmol) were added. This mixture was stirred for 10 min at rt, after which paraformaldehyde (0.32 g, 10.5 mmol) was introduced and it was heated to 60 °C for 18 h. After cooling, 10% aqueous $KHSO_4$ solution (50 mL) was added, and it was extracted with EtOAc (3 × 50 mL). The combined organic layers were washed with saturated aqueous NH_4Cl solution (50 mL) and brine (50 mL), dried over Na_2SO_4, filtered, and concentrated *in vacuo*. The crude product was purified by flash chromatography using a gradient from 20 to 40% EtOAc in petroleum ether to give **53** as a colorless solid (0.19 g. 23%).

mp 178 °C; R_f = 0.40 (petroleum ether/ EtOAc 9:1); ^{1}H NMR (500 MHz, DMSO-d_6) δ 2.39 (s, 3H, CH_3), 7.07 (dd, J = 8.2, 6.3 Hz, 1H, Ar-H), 7.56 (dd, J = 8.2, 1.3 Hz, 1H, Ar-H), 9.18 (s, 1H, 2′-H), 10.30 (s, 1H, CHO), 11.12 (s, 1H, OH); ^{13}C NMR (126 MHz, DMSO-d_6) δ 16.0 (d, $^5J_{F,C}$ = 2.9 Hz, CH_3), 121.3, 123.1 (C-5′, C-6), 123.8 (d, $^3J_{F,C}$ = 4.0 Hz, C-5), 124.6 (d, $^3J_{F,C}$ = 2.8 Hz, C-1), 125.5 (d, $^2J_{F,C}$ = 12.5 Hz, C-4), 148.6 (d, $^1J_{F,C}$ = 245.0 Hz, C-3), 148.7 (d, $^2J_{F,C}$ = 15.0 Hz, C-2), 151.2 (C-4′), 154.2 (C-2′), 190.3 (d, $^4J_{F,C}$ = 3.1 Hz, CHO). LC-MS (ESI) (90% H_2O to 100% MeCN in 10 min, then 100% MeCN to 15 min, DAD 200-600 nm), t_R = 4.08 min, 99% purity, *m/z* calcd for $C_{11}H_8FN_2OS$ $[M + H]^+$, 238.03; found, 238.0. HRMS (ESI) *m/z* calcd for $C_{11}H_8FN_2OS$ $[M + H]^+$, 238.0332; found, 238.0331.

1-(4-Bromo-2-methylphenyl)ethan-1-one (55a)

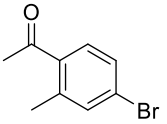

This compound was purchased from abcr GmbH (Karlsruhe, Germany).

1-(4-Bromo-3-fluorophenyl)ethan-1-one (55b)

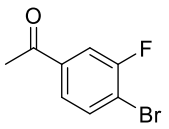

This compound was purchased from BLDpharm (Kaiserslautern, Germany).

1-(4-Bromo-5-fluoro-2-methylphenyl)ethan-1-one (55c)

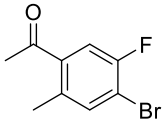

This compound was synthesized and provided by Nika Strašek, University of Ljubljana.

1-(4-Bromo-5-fluoro-2-methoxyphenyl)ethan-1-one (55d)

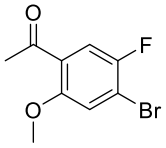

This compound was synthesized and provided by Nika Strašek, University of Ljubljana.

(*R*,*E*)-*N*-(1-(4-Bromo-2-methylphenyl)ethylidene)-2-methylpropane-2-sulfinamide (56a)

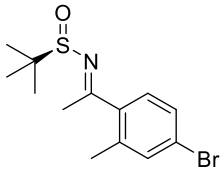

Following General Procedure D, compound **56a** was obtained from 1-(4-bromo-2-methylphenyl)ethanone (type **55**, R = 2-Me; 1.07 g, 5.0 mmol). The crude product was purified by flash column chromatography (gradient from 20 to 50% EtOAc in petroleum ether) to obtain a colourless oil (0.36 g, 23%).

R_f = 0.55 (petroleum ether/EtOAc 2:1); ^{1}H NMR (500 MHz, DMSO-d_6) δ 1.19 (s, 9H, C(CH$_3$)$_3$), 2.35 (s, 3H, CH$_3$), 2.62 (s, 3H, CH$_3$), 7.41 – 7.55 (m, 3H, Ar-H); ^{13}C NMR (126 MHz, DMSO-d_6) δ 19.8 (CH$_3$), 21.8 (C(<u>C</u>H$_3$)$_3$), 23.7 (CH$_3$), 56.1 (<u>C</u>(CH$_3$)$_3$), 122.6 (C-4), 128.7, 129.2, 133.4, 137.3 (C-1, C-3, C-5, C-6), 139.8 (C-2), 180.7 (NC). LC-MS (ESI) (90% H_2O to 100% MeCN in 10 min, then 100% MeCN to 15 min, DAD 200-600 nm), t_R = 7.20 min, 100% purity, *m/z* calcd for $C_{13}H_{18}{}^{79}BrNOS$ $[M + H]^+$, 316.04; found, 316.1.

(*R*,*E*)-*N*-(1-(4-Bromo-3-fluorophenyl)ethylidene)-2-methylpropane-2-sulfinamide (56b)

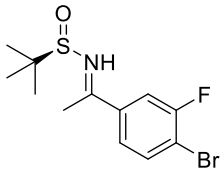

Following General Procedure D, compound **56b** was obtained from 1-(4-bromo-3-fluorophenyl)ethan-1-one (type **55**, R = 3-F; 1.08 g, 5.0 mmol). The crude product was purified by flash column chromatography (gradient from 20 to 50% EtOAc in petroleum ether) to obtain a slight yellow oil (0.52 g, 33%).

R_f = 0.57 (petroleum ether/EtOAc 2:1); ^{1}H NMR (500 MHz, DMSO-d_6) δ 1.22 (s, 9H, C(CH$_3$)$_3$), 2.71 (s, 3H, CH$_3$), 5.28 (s, 1H, NH), 7.69 (dd, *J* = 8.4, 2.1 Hz, 1H, Ar-H), 7.78 – 7.87 (m, 2H, Ar-H); ^{13}C NMR (126 MHz, DMSO-d_6) δ 22.0 (C(<u>C</u>H$_3$)$_3$), 22.2 (CH$_3$), 57.1 (<u>C</u>(CH$_3$)$_3$), 111.9

(d, $^{2}J_{F,C}$ = 21.4 Hz, C-4), 115.0 (d, $^{2}J_{F,C}$ = 23.8 Hz, C-2), 124.5 (d, $^{4}J_{F,C}$ = 3.2 Hz, C-6), 133.7 (C-5), 139.9 (d, $^{3}J_{F,C}$ = 6.3 Hz, C-1), 158.2 (d, $^{1}J_{F,C}$ = 245.4 Hz, C-3), 174.5 (NC). LC-MS (ESI) (90% H_2O to 100% MeCN in 10 min, then 100% MeCN to 15 min, DAD 200-600 nm), t_R = 7.19 min, 99% purity, *m/z* calcd for $C_{12}H_{15}{}^{79}BrFNOS$ $[M + H]^+$, 320.01; found, 320.0.

(*R*,*E*)-*N*-(1-(4-Bromo-5-fluoro-2-methylphenyl)ethylidene)-2-methylpropane-2-sulfinamide (56c)

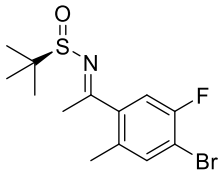

This compound was synthesized and provided by Nika Strašek, University of Ljubljana.

(*R*,*E*)-*N*-(1-(4-Bromo-5-fluoro-2-methoxyphenyl)ethylidene)-2-methylpropane-2-sulfinamide (56d)

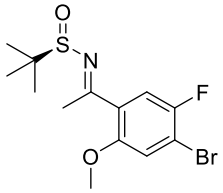

This compound was synthesized and provided by Nika Strašek, University of Ljubljana.

(*R*,*E*)-*N*-(5-Bromo-2,3-dihydro-1*H*-inden-1-ylidene)-2-methylpropane-2-sulfinamide (56e)

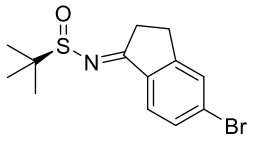

Following General Procedure D, compound **56e** was obtained from 5-bromo-1-indanone (type **55**, R = H, n = 1; 5.07 g, 24.0 mmol). The crude product was purified by flash column chromatography (gradient from 20 to 50% EtOAc in petroleum ether) to obtain a brown solid (0.52 g, 7%).

mp 96-99 °C; R_f = 0.24 (petroleum ether/EtOAc 4:1). ^{1}H NMR (500 MHz, DMSO-d_6) δ 1.22 (s, 9H, C(CH_3)$_3$), 3.00 (ddd, J = 19.3, 6.8, 4.7 Hz, 1H, CH_2), 3.08 – 3.15 (m, 2H, CH_2), 3.25 – 3.33 (m, 1H, CH_2), 7.57 (dd, J = 8.2, 1.7 Hz, 1H, Ar-H), 7.64 (d, J = 8.3 Hz, 1H, Ar-H), 7.77 (d, J = 1.7 Hz, 1H, Ar-H); ^{13}C NMR (126 MHz, DMSO-d_6) δ 22.0 (C($\underline{C}H_3$)$_3$), 28.4 (CH_2), 31.5 (CH_2), 56.7 ($\underline{C}$(CH_3)$_3$), 124.5, 127.2, 129.1, 130.4 (C-4, C-5, C-6, C-7), 137.7 (C-7a), 153.2 (C-3a), 182.5 (NC). LC-MS (ESI) (90% H_2O to 100% MeCN in 10 min, then 100% MeCN to 15 min, DAD 200-600 nm), t_R = 7.29 min, 98% purity, *m/z* calcd for $C_{13}H_{16}{}^{79}BrNOS$ $[M + H]^+$, 314.02; found, 314.0. HRMS (ESI) *m/z* calcd for $C_{13}H_{18}{}^{79}BrNOS$ $[M + H]^+$, 314.0209; found, 314.0204.

(*R*,*E*)-*N*-(5-Bromo-6-fluoro-2,3-dihydro-1*H*-inden-1-ylidene)-2-methylpropane-2-sulfinamide (56f)

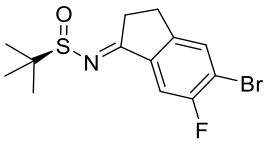

This compound was synthesized and provided by Nika Strašek, University of Ljubljana.

(*R*,*E*)-*N*-(6-Bromo-7-fluoro-3,4-dihydronaphthalen-1(2*H*)-ylidene)-2-methylpropane-2-sulfinamide (56g)

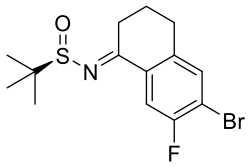

This compound was synthesized and provided by Nika Strašek, University of Ljubljana.

(*R*)-*N*-((*S*)-1-(4-Bromo-2-methylphenyl)ethyl)-2-methylpropane-2-sulfinamide (57a)

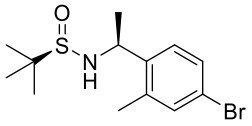

Following General Procedure E, compound **57a** was obtained from **56a** (type **56**, R = 2-Me; 0.63 g, 2.0 mmol). The crude product was purified by flash column chromatography (gradient from 20 to 50% EtOAc in petroleum ether) to obtain a colorless oil (0.20 g, 31%).

R_f = 0.15 (petroleum ether/EtOAc 1:1); ^{1}H NMR (500 MHz, DMSO-d_6) δ 1.09 (s, 9H, C(CH_3)$_3$), 1.41 (d, J = 6.7 Hz, 3H, CH_3), 2.31 (s, 3H, CH_3), 4.51 – 4.60 (m, 1H, NHC<u>H</u>), 5.30 (d, J = 5.2 Hz, 1H, NH), 7.30 – 7.39 (m, 3H, Ar-H); ^{13}C NMR (126 MHz, DMSO-d_6) δ 18.3 (CH_3), 22.6 (C(<u>C</u>H_3)$_3$), 23.4 (CH_3), 50.4 (NHCH), 54.9 (<u>C</u>(CH_3)$_3$), 119.5 (C-4), 128.6, 128.7, 132.3, 137.5 (C-2, C-3, C-5, C-6), 142.0 (C-1). LC-MS (ESI) (90% H_2O to 100% MeCN in 10 min, then 100% MeCN to 15 min, DAD 200-600 nm), t_R = 7.01 min, 100% purity, *m/z* calcd for $C_{13}H_{20}{}^{79}BrNOS$ $[M + H]^+$, 318.05; found, 318.1.

(*R*)-*N*-((*S*)-1-(4-Bromo-3-fluorophenyl)ethyl)-2-methylpropane-2-sulfinamide (57b)

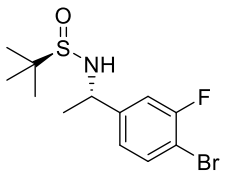

Following General Procedure E, compound **57b** was obtained from **56b** (type **56**, R = 3-F; 0.48 g, 1.5 mmol). The crude product was purified by flash column chromatography (50% EtOAc in petroleum ether) to obtain a colorless solid (0.31 g, 63%).

mp 138-139 °C; R_f = 0.20 (petroleum ether/EtOAc 1:2); ^{1}H NMR (500 MHz, DMSO-d_6) δ 1.10 (s, 9H, C(CH$_3$)$_3$), 1.44 (d, J = 6.8 Hz, 3H, CH$_3$), 4.39 – 4.47 (m, 1H, CH), 5.46 (d, J = 5.5 Hz, 1H, NH), 7.16 (dd, J = 8.4, 2.0 Hz, 1H, Ar-H), 7.33 – 7.38 (m, 1H, Ar-H), 7.65 (t, J = 7.8 Hz, 1H, Ar-H); ^{13}C NMR (126 MHz, DMSO-d_6) δ 22.5 (C(<u>C</u>H$_3$)$_3$), 24.4 (CH$_3$), 54.0 (CH), 55.0 (<u>C</u>(CH$_3$)$_3$), 105.8 (d, $^2J_{F,C}$ = 20.8 Hz, C-4), 114.8 (d, $^2J_{F,C}$ = 22.5 Hz, C-2), 124.3 (C-6), 133.1 (C-5), 147.7 (d, $^3J_{F,C}$ = 6.2 Hz, C-1), 158.0 (d, $^1J_{F,C}$ = 244.4 Hz, C-3). LC-MS (ESI) (90% H_2O to 100% MeCN in 10 min, then 100% MeCN to 15 min, DAD 200-600 nm), t_R = 6.66 min, 89% purity, *m/z* calcd for $C_{12}H_{17}{}^{79}BrFNOS$ $[M + H]^+$, 322.03; found, 322.0.

(*R*)-*N*-((*S*)-1-(4-Bromo-5-fluoro-2-methylphenyl)ethyl)-2-methylpropane-2-sulfinamide (57c)

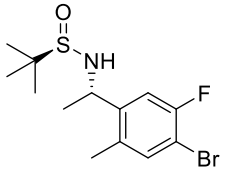

This compound was synthesized and provided by Nika Strašek, University of Ljubljana.

(*R*)-*N*-((*S*)-1-(4-Bromo-5-fluoro-2-methoxyphenyl)ethyl)-2-methylpropane-2-sulfinamide (57d)

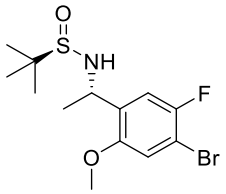

This compound was synthesized and provided by Nika Strašek, University of Ljubljana.

(*R*)-*N*-((*S*)-5-Bromo-2,3-dihydro-1*H*-inden-1-yl)-2-methylpropane-2-sulfinamide (57e)

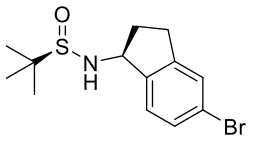

Following General Procedure E, compound **57e** was obtained from **56e** (type **56**, R = H, n = 1; 0.47 g, 1.5 mmol). The crude product was purified by flash column chromatography (gradient from 20 to 50% EtOAc in petroleum ether) to obtain a slight yellow solid (0.32 g, 68%).

mp 152-154 °C; R_f = 0.28 (petroleum ether/EtOAc 1:1); ^{1}H NMR (500 MHz, DMSO-d_6) δ 1.16 (s, 9H, C(CH$_3$)$_3$), 1.92 – 2.01 (m, 1H, CH$_2$), 2.39 – 2.47 (m, 1H, CH$_2$), 2.72 – 2.81 (m, 1H, CH$_2$), 2.91 (ddd, *J* = 16.2, 8.8, 3.2 Hz, 1H, CH$_2$), 4.61 – 4.68 (m, 1H, 1-H), 5.62 (d, *J* = 9.0 Hz, 1H, NH), 7.21 (d, *J* = 8.0 Hz, 1H), 7.38 (dd, *J* = 8.0, 1.8 Hz, 1H), 7.44 (d, *J* = 1.8 Hz, 1H, Ar-H); ^{13}C NMR (126 MHz, DMSO-d_6) δ 22.8 (C(<u>C</u>H$_3$)$_3$), 29.5 (CH$_2$), 35.2 (CH$_2$), 55.3 (<u>C</u>(CH$_3$)$_3$), 60.8 (NHCH), 120.4 (C-5), 126.3, 127.3, 129.0 (C-4, C-6, C-7), 144.1 (C-7a), 145.6 (C-3a). LC-MS (ESI) (90% H$_2$O to 100% MeCN in 10 min, then 100% MeCN to 15 min, DAD 200-600 nm), t_R = 6.74 min, 99% purity, *m/z* calcd for C$_{13}$H$_{18}$BrNOS [M + H]$^+$, 316.04; found, 316.1. HRMS (ESI) *m/z* calcd for C$_{13}$H$_{18}$BrNOS [M + H]$^+$, 316.0365; found, 316.0363.

(*R*)-*N*-((*S*)-5-Bromo-6-fluoro-2,3-dihydro-1*H*-inden-1-yl)-2-methylpropane-2-sulfinamide (57f)

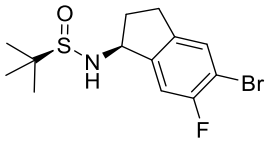

This compound was synthesized and provided by Nika Strašek, University of Ljubljana.

(*R*)-*N*-((*S*)-6-Bromo-7-fluoro-1,2,3,4-tetrahydronaphthalen-1-yl)-2-methylpropane-2-sulfinamide (57g)

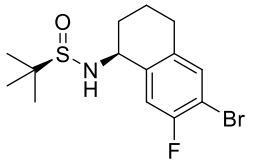

This compound was synthesized and provided by Nika Strašek, University of Ljubljana.

(*S*)-1-(4-Bromo-2-methylphenyl)ethan-1-aminium Chloride (58a)

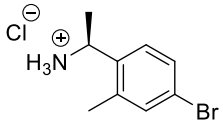

Following General Procedure F, compound **58a** was obtained from **57a** (type **57**, R = 2-Me; 0.16 g, 0.5 mmol). The product was obtained as a white solid (0.12 g, 100%).

mp > 250 °C; ^{1}H NMR (500 MHz, DMSO-d_6) δ 1.45 (d, J = 6.8 Hz, 3H, CH_3), 2.35 (s, 3H, CH_3), 4.50 (q, J = 6.8 Hz, 1H, CH), 7.45 – 7.53 (m, 3H, Ar-H), 8.44 (s, 3H, NH_3); ^{13}C NMR (126 MHz, DMSO-d_6) δ 18.4 (CH_3), 20.0 (CH_3), 45.7 (CH), 121.1 (C-4), 127.5, 129.2, 132.9, 137.1, 138.2 (C-1, C-2, C-3, C-5, C-6).

(*S*)-1-(4-Bromo-3-fluorophenyl)ethan-1-aminium Chloride (58b)

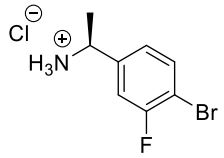

Following General Procedure F, compound **58b** was obtained from **57b** (type **57**, R = 3-F; 0.29 g, 0.9 mmol). The product was obtained as a white solid (0.23 g, 100%).

mp 248-250 °C; ^{1}H NMR (600 MHz, DMSO-d_6) δ 1.50 (d, J = 6.8 Hz, 3H, CH_3), 4.44 (q, J = 6.8 Hz, 1H, CH), 7.33 (dd, J = 8.3, 2.1 Hz, 1H, Ar-H), 7.60 (dd, J = 10.1, 2.1 Hz, 1H, Ar-H), 7.79 (t, J = 7.8 Hz, 1H, Ar-H), 8.58 (s, 3H, NH_3); 13C NMR (151 MHz, DMSO-d6) δ 20.3 (CH_3), 49.0 (CH), 107.8 (d, $^{2}J_{F,C}$ = 20.8 Hz, C-4), 115.5 (d, $^{2}J_{F,C}$ = 23.4 Hz, C-2), 124.7 (d, $^{4}J_{F,C}$ = 3.7 Hz, C-6), 133.8 (C-5), 141.6 (d, $^{3}J_{F,C}$ = 7.0 Hz, C-1), 158.1 (d, $^{1}J_{F,C}$ = 244.9 Hz, C-3).

(*S*)-1-(4-Bromo-5-fluoro-2-methylphenyl)ethan-1-aminium Chloride (58c)

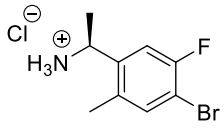

This compound was synthesized and provided by Nika Strašek, University of Ljubljana.

(*S*)-1-(4-Bromo-5-fluoro-2-methoxyphenyl)ethan-1-aminium Chloride (58d)

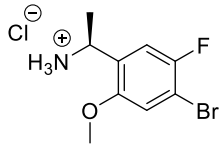

This compound was synthesized and provided by Nika Strašek, University of Ljubljana.

(*S*)-5-Bromo-2,3-dihydro-1*H*-inden-1-aminium Chloride (58e)

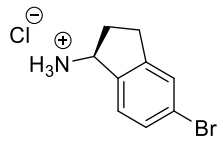

Following General Procedure F, compound **58e** was obtained from **57e** (type **57**, R = H, n = 1; 0.32 g, 1.0 mmol). The product was obtained as a white solid (0.25 g, 100%).

mp > 250 °C; ^{1}H NMR (500 MHz, DMSO-d_6) δ 1.94 – 2.08 (m, 1H, CH_2), 2.40 – 2.48 (m, 1H, CH_2), 2.83 – 2.94 (m, 1H, CH_2), 3.02 – 3.12 (m, 1H, CH_2), 4.66 (dd, *J* = 7.9, 5.5 Hz, 1H, 1-H), 7.49 (d, *J* = 7.6 Hz, 1H, Ar-H), 7.53 – 7.61 (m, 2H, Ar-H), 8.53 (s, 3H, NH_3); ^{13}C NMR (126 MHz, DMSO-d_6) δ 29.7 (CH_2), 30.3 (CH_2), 54.0 (C-1), 122.2 (C-5), 126.9, 127.8, 129.5 (C-4, C-6, C-7), 138.7 (C-7a), 146.9 (C-3a).

(*S*)-5-Bromo-6-fluoro-2,3-dihydro-1*H*-inden-1-aminium Chloride (58f)

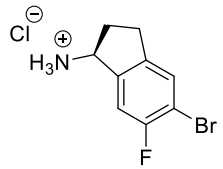

This compound was synthesized and provided by Nika Strašek, University of Ljubljana.

(*S*)-6-Bromo-7-fluoro-1,2,3,4-tetrahydronaphthalen-1-aminium Chloride (58g)

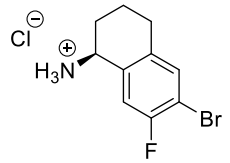

This compound was synthesized and provided by Nika Strašek, University of Ljubljana.

***tert*-Butyl (*S*)-(1-(4-Bromo-2-methylphenyl)ethyl)carbamate (59a)**

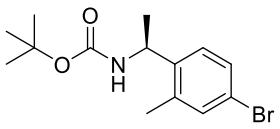

Following General Procedure G, compound **59a** was obtained from **58a** (type **58**, R = 2-Me; 0.12 g, 0.5 mmol). The product was obtained as a white solid (0.16 g, 100%).

mp 152-154 °C; R_f = 0.20 (petroleum ether/EtOAc 9:1); ^{1}H NMR (500 MHz, DMSO-d_6) δ 1.22 (d, J = 6.9 Hz, 3H, CH_3), 1.34 (s, 9H, $C(CH_3)_3$), 2.30 (s, 3H, CH_3), 4.70 – 4.78 (m, 1H, CH), 7.26 (d, J = 8.3 Hz, 1H), 7.31 – 7.39 (m, 2H), 7.45 (d, J = 7.9 Hz, 1H) (Ar-H, NH); ^{13}C NMR (126 MHz, DMSO-d_6) δ 18.1 (CH_3), 21.4 (CH_3), 28.2 ($C(\underline{C}H_3)_3$), 45.6 (CH), 77.7 ($\underline{C}(CH_3)_3$), 119.0 (C-4), 127.1, 128.8, 132.1, 136.9 (C-2, C-3, C-5, C-6), 143.4 (C-1), 154.6 (CO). LC-MS (ESI) (90% H_2O to 100% MeCN in 10 min, then 100% MeCN to 15 min, DAD 200-600 nm), t_R = 8.05 min, 100% purity, *m/z* calcd for $C_{14}H_{20}BrNO_2$ $[M + H]^+$, 314.07; found, 314.1.

***tert*-Butyl (*S*)-(1-(4-Bromo-3-fluorophenyl)ethyl)carbamate (59b)**

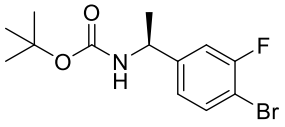

Following General Procedure G, compound **59b** was obtained from **58b** (type **58**, R = 3-F; 0.23 g, 0.9 mmol). The product was obtained as a white solid (0.28 g, 100%).

mp 124-126 °C; R_f = 0.9 (CH_2Cl_2/MeOH 9:1); ^{1}H NMR (500 MHz, DMSO-d_6) δ 1.28 (d, J = 7.0 Hz, 3H, CH_3), 1.36 (s, 9H, $C(\underline{C}H_3)_3$), 4.57 – 4.65 (m, 1H, CH), 7.10 (dd, J = 8.2, 1.9 Hz, 1H), 7.24 – 7.30 (m, 1H), 7.43 (d, J = 8.0 Hz, 1H), 7.63 (t, J = 7.8 Hz, 1H) (Ar-H, NH); ^{13}C NMR (126 MHz, DMSO-d_6) δ 22.4 (CH_3), 28.1 ($C(\underline{C}H_3)_3$), 48.9 (CH), 77.9 ($\underline{C}(CH_3)_3$), 105.4 (d, $^2J_{F,C}$ = 20.7 Hz, C-4), 114.0 (d, $^2J_{F,C}$ = 22.4 Hz, C-2), 123.5 (d, $^4J_{F,C}$ = 3.2 Hz, C-6), 133.1 (C-5), 148.2 (d, $^3J_{F,C}$ = 7.9 Hz, C-1), 154.7 (CO), 158.1 (d, $^1J_{F,C}$ = 244.4 Hz, C-3). LC-MS (ESI) (90% H_2O to 100% MeCN in 10 min, then 100% MeCN to 15 min, DAD 200-600 nm), t_R = 7.75 min, 98% purity, *m/z* calcd for $C_{13}H_{17}{}^{79}BrFNO_2$ $[M - H]^+$, 316.03; found, 316.0.

tert-Butyl (_S_)-(1-(4-Bromo-5-fluoro-2-methylphenyl)ethyl)carbamate (59c)

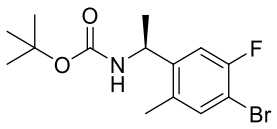

This compound was synthesized and provided by Nika Strašek, University of Ljubljana.

tert-Butyl (_S_)-(1-(4-Bromo-5-fluoro-2-methoxyphenyl)ethyl)carbamate (59d)

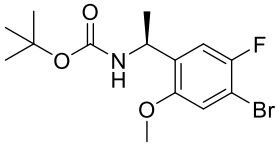

This compound was synthesized and provided by Nika Strašek, University of Ljubljana.

tert-Butyl (_S_)-(5-Bromo-2,3-dihydro-1_H_-inden-1-yl)carbamate (59e)

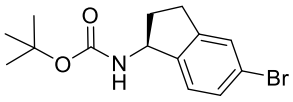

Following General Procedure G, compound **59e** was obtained from **58e** (type **58**, R = H, n = 1; 0.25 g, 1.0 mmol). The product was obtained as a white solid (0.31 g, 100%).

mp 122-124 °C; R_f = 0.33 (petroleum ether/EtOAc 9:1); ^{1}H NMR (500 MHz, DMSO-d_6) δ 1.42 (s, 9H, C(CH$_3$)$_3$), 1.76 – 1.86 (m, 1H, CH$_2$), 2.28 – 2.37 (m, 1H, CH$_2$), 2.70 – 2.79 (m, 1H, CH$_2$), 2.89 (ddd, J = 16.1, 8.7, 3.1 Hz, 1H, CH$_2$), 4.89 – 4.96 (m, 1H, 1-H), 7.12 (d, J = 8.1 Hz, 1H), 7.26 (d, J = 8.5 Hz, 1H), 7.35 (d, J = 8.0 Hz, 1H), 7.41 (d, J = 1.8 Hz, 1H) (Ar-H, NH); ^{13}C NMR (126 MHz, DMSO-d_6) δ 28.2 (C(<u>C</u>H$_3$)$_3$), 29.3 (CH$_2$), 32.5 (CH$_2$), 54.6 (C-1), 77.8 (<u>C</u>(CH$_3$)$_3$), 120.2 (C-5), 125.6, 127.3, 129.1 (C-4, C-6, C-7), 144.1 (C-7a), 145.6 (C-3a), 155.5 (CO). LC-MS (ESI) (90% H$_2$O to 100% MeCN in 10 min, then 100% MeCN to 15 min, DAD

200-600 nm), t_R = 8.09 min, 100% purity, *m/z* calcd for $C_{14}H_{18}BrNO_2$ $[M + Na]^+$, 334.04; found, 334.1. HRMS (ESI) *m/z* calcd for $C_{14}H_{18}BrNO_2$ $[M + H]^+$, 312.0594; found, 312.0589.

tert-Butyl (_S_)-(5-Bromo-6-fluoro-2,3-dihydro-1_H_-inden-1-yl)carbamate (59f)

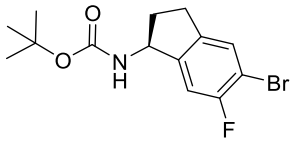

This compound was synthesized and provided by Nika Strašek, University of Ljubljana.

tert-Butyl (_S_)-(6-Bromo-7-fluoro-1,2,3,4-tetrahydronaphthalen-1-yl)carbamate (59g)

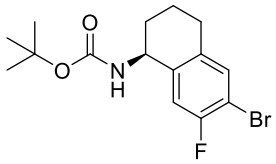

This compound was synthesized and provided by Nika Strašek, University of Ljubljana.

tert-Butyl (_S_)-(1-(2-Methyl-4-(4-methylthiazol-5-yl)phenyl)ethyl)carbamate (60a)

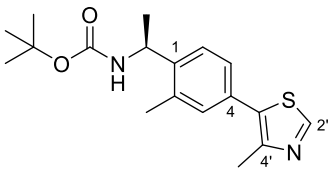

Following General Procedure B, compound **60a** was obtained from **59a** (type **59**, R = 2-Me; 0.16 g, 0.5 mmol). The crude product was purified by flash column chromatography (gradient from 20 to 50% EtOAc in petroleum ether) to obtain a colorless oil (0.04 g, 22%).

R_f = 0.18 (PE/EtOAc 4:1); ^{1}H NMR (600 MHz, DMSO-d_6) δ 1.27 (d, J = 7.0 Hz, 3H, CH_3), 1.36 (s, 9H, $C(CH_3)_3$), 2.36 (s, 3H, CH_3), 2.45 (s, 3H, CH_3), 4.79 – 4.86 (m, 1H, CH), 7.23 (d, J = 1.9 Hz, 1H), 7.30 (dd, J = 8.1, 2.0 Hz, 1H), 7.42 (d, J = 8.0 Hz, 1H), 7.47 (d, J = 8.0 Hz, 1H) (Ar-H, NH), 8.96 (s, 1H, 2′-H); ^{13}C NMR (151 MHz, DMSO-d_6) δ 16.0 (CH_3), 18.5 (CH_3), 21.7 (CH_3), 28.3 ($C(\underline{C}H_3)_3$), 45.8 (CH), 77.7 ($\underline{C}(CH_3)_3$), 125.5, 126.6, 129.4, 130.4, 131.2, 134.8 (C-2, C-3, C-4, C-5, C-5′, C-6), 143.8 (C-1), 147.6 (C-4′), 151.3 (C-2′), 154.7 (CO). LC-MS (ESI) (90% H_2O to 100% MeCN in 10 min, then 100% MeCN to 15 min, DAD 200-600 nm), t_R = 7.39 min, 98% purity, *m/z* calcd for $C_{18}H_{24}N_2O_2S$ $[M + H]^+$, 333.16; found, 333.2.

tert-Butyl (_S_)-(1-(3-Fluoro-4-(4-methylthiazol-5-yl)phenyl)ethyl)carbamate (60b)

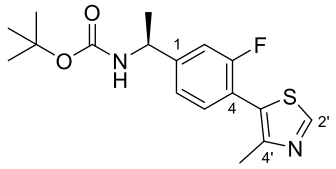

Following General Procedure B, compound **60b** was obtained from **59b** (type **59**, R = 3-F; 0.30 g, 0.9 mmol). The crude product was purified by flash column chromatography (gradient from 20 to 50% EtOAc in petroleum ether) to obtain a colorless solid (0.12 g, 38%).

mp 112 – 114 °C; R_f = 0.14 (petroleum ether/EtOAc 4:1); ^{1}H NMR (600 MHz, DMSO-d_6) δ 1.33 (s, 3H, CH_3), 1.38 (s, 9H, $C(CH_3)_3$), 2.33 (s, 3H, CH_3), 4.65 – 4.72 (m, 1H, CH), 7.23 (dd, J = 8.0, 1.6 Hz, 1H), 7.27 (d, J = 11.5 Hz, 1H), 7.42 – 7.49 (m, 2H) (Ar-H, NH), 9.09 (s, 1H, 2′-H); ^{13}C NMR (151 MHz, DMSO-d_6) δ 15.7 (CH_3), 22.6 (CH_3), 28.2 ($C(\underline{C}H_3)_3$) , 49.1 (CH), 77.9 ($\underline{C}(CH_3)_3$), 113.3 (d, $^2J_{F,C}$ = 22.8 Hz, C-2), 116.8 (d, $^2J_{F,C}$ = 15.7 Hz, C-4), 122.2 (d, $^4J_{F,C}$ = 2.2 Hz, C-6), 123.8, 131.9 (C-5, C-5′), 149.1 (C-1), 150.1 (C-4′), 153.1 (C-2′), 154.8 (CO), 158.8 (d, $^2J_{F,C}$ = 246.5 Hz, C-3). LC-MS (ESI) (90% H_2O to 100% MeCN in 10 min, then 100% MeCN to 15 min, DAD 200-600 nm), t_R = 7.11 min, 96% purity, *m/z* calcd for $C_{17}H_{21}FN_2O_2S$ $[M - H]^+$, 337.14; found, 337.2.

tert-Butyl (_S_)-(1-(5-Fluoro-2-methyl-4-(4-methylthiazol-5-yl)phenyl)ethyl)carbamate (60c)

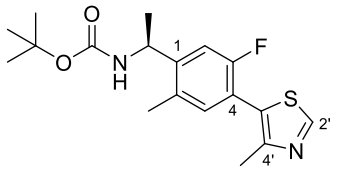

This compound was synthesized and provided by Nika Strašek, University of Ljubljana.

tert-Butyl (_S_)-(1-(5-Fluoro-2-methoxy-4-(4-methylthiazol-5-yl)phenyl)ethyl)carbamate (60d)

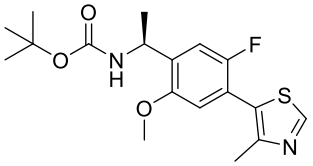

This compound was synthesized and provided by Nika Strašek, University of Ljubljana.

tert-Butyl (_S_)-(5-(4-Methylthiazol-5-yl)-2,3-dihydro-1_H_-inden-1-yl)carbamate (60e)

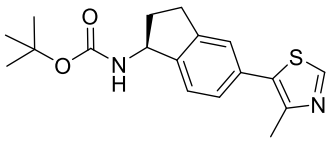

Following General Procedure B, compound **60e** was obtained from **59e** (type **59**, R = H, n = 1; 0.47 g, 1.0 mmol). The crude product was purified by flash column chromatography (gradient from 20 to 50% EtOAc in petroleum ether) to obtain a pale yellow solid (0.32 g, 68%).

mp 114 °C; R_f = 0.60 (petroleum ether/EtOAc 1:1); ^{1}H NMR (500 MHz, DMSO-d_6) δ 1.44 (s, 9H, C(CH_3)$_3$), 1.79 – 1.90 (m, 1H, CH_2), 2.33 – 2.41 (m, 1H, CH_2), 2.44 (s, 3H, CH_3), 2.75 – 2.85 (m, 1H, CH_2), 2.90 – 2.98 (m, 1H, CH_2), 4.98 – 5.05 (m, 1H, 1-H), 7.21 – 7.35 (m, 4H,

Ar-H, NH), 8.97 (s, 1H, 2′-H); ^{13}C NMR (126 MHz, DMSO-d_6) δ 15.9 (CH_3), 28.2 (C($\underline{C}H_3)_3$), 29.5 (CH_2), 32.6 (CH_2), 54.9 (C-1), 77.8 ($\underline{C}(CH_3)_3$), 124.1 (C-5′), 125.0, 127.3, 130.4, 131.5 (C-4, C-5, C-6, C-7), 143.6 (C-7a), 144.6 (C-3a), 147.6 (C-4′), 151.3 (C-2′), 155.6 (CO). LC-MS (ESI) (90% H_2O to 100% MeCN in 10 min, then 100% MeCN to 15 min, DAD 200-600 nm), t_R = 7.55 min, 100% purity, *m/z* calcd for $C_{18}H_{22}N_2O_2S$ $[M + H]^+$, 331.15; found, 331.2. HRMS (ESI) *m/z* calcd for $C_{18}H_{22}N_2O_2S$ $[M + H]^+$, 331.1475; found, 331.1470.

tert-Butyl (*S*)-(6-Fluoro-5-(4-methylthiazol-5-yl)-2,3-dihydro-1*H*-inden-1-yl)carbamate (60f)

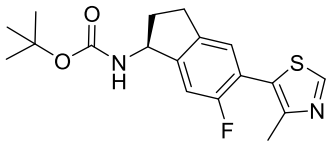

This compound was synthesized and provided by Nika Strašek, University of Ljubljana.

tert-Butyl (*S*)-(7-Fluoro-6-(4-methylthiazol-5-yl)-1,2,3,4-tetrahydronaphthalen-1-yl)carbamate (60g)

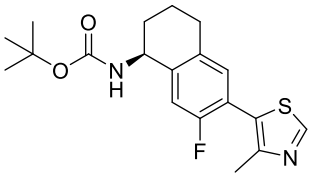

This compound was synthesized and provided by Nika Strašek, University of Ljubljana.

Benzyl (2*S*,4*R*)-1-((*S*)-2-(1-Fluorocyclopropane-1-carboxamido)-3,3-dimethylbutanoyl)-4-hydroxypyrrolidine-2-carboxylate (61)

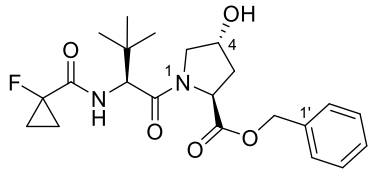

Following General Procedure C, compound **61** was obtained using Boc-protected amine **44** (102 mg, 0.3 mmol) and 1-fluoro-1-cyclopropanecarboxylic acid (101 mg, 0.3 mmol). The residue was purified by flash column chromatography using a gradient from 0 to 10% MeOH in CH_2Cl_2 to afford **61** as a white solid (90 mg, 51%).

mp 118-120 °C; R_f = 0.42 (CH_2Cl_2/MeOH 9:1); ^{1}H NMR (600 MHz, DMSO-d_6) δ 0.92 (s, 9H, C(CH_3)$_3$), 1.17 – 1.25 (m, 2H, CH_2CF), 1.30 – 1.41 (m, 2H, CH_2CF), 1.90 – 1.97 (m, 1H, 3-H), 2.13 – 2.19 (m, 1H, 3-H), 3.59 – 3.64 (m, 1H, 5-H), 3.67 (dd, J = 10.8, 3.9 Hz, 1H, 5-H), 4.32 – 4.36 (m, 1H), 4.46 (dd, J = 9.2, 7.8 Hz, 1H), 4.59 (d, J = 9.2 Hz, 1H) (2-H, 4-H, NHC<u>H</u>), 5.13 (dd, J = 12.3, 12.1, 2H, Ar-CH_2), 5.23 (d, J = 3.9 Hz, 1H, OH), 7.26 (dd, J = 9.3, 2.9 Hz, 1H, CONH), 7.31 – 7.39 (m, 5H, Ar-H); ^{13}C NMR (151 MHz, DMSO-d_6) δ 12.7 (d, $^2J_{F,C}$ = 10.3 Hz, <u>C</u>H_2CF), 12.9 (d, $^2J_{F,C}$ = 10.2 Hz, <u>C</u>H_2CF), 26.0 (C(<u>C</u>H_3)$_3$), 35.8 (<u>C</u>(CH_3)$_3$), 37.2 (C-3), 56.3, 56.4, 57.9, 66.0, 68.8 (C-2, C-4, C-5, NHCH, Ar-CH_2), 78.0 (d, $^1J_{F,C}$ = 232.7 Hz, CF), 127.9 (C-2′, C-6′), 128.0 (C-4′), 128.4 (C-3′, C-5′), 135.8 (C-1′), 168.1 (d, $^2J_{F,C}$ = 20.9 Hz), 169.3, 171.5 (CO). LC-MS (ESI) (90% H_2O to 100% MeCN in 10 min, then 100% MeCN to 15 min, DAD 200-600 nm), t_R = 6.39 min, 99% purity, *m/z* calcd for $C_{22}H_{29}FN_2O_5$ $[M + H]^+$, 421.21; found, 421.3.

(2*S*,4*R*)-1-((*S*)-2-(1-Fluorocyclopropane-1-carboxamido)-3,3-dimethylbutanoyl)-4-hydroxypyrrolidine-2-carboxylic Acid (62)

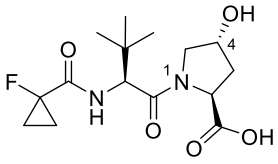

Compound **62** (2.10 g, 5 mmol) was dissolved in dry EtOH (50 mL) and treated with 10% Pd/C under H_2 (1 atm, balloon) for 18 h. The reaction mixture was filtered through celite and was concentrated to yield a white solid. This compound was used in the next step without further purification and characterization.

3,5-Difluoro-4-hydroxybenzaldehyde (63)

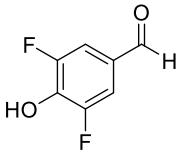

This compound was purchased from abcr GmbH (Karlsruhe, Germany).

(*Z*)-2,6-Difluoro-4-((2-methyl-5-oxooxazol-4(5*H*)-ylidene)methyl)phenyl acetate (64)[226]

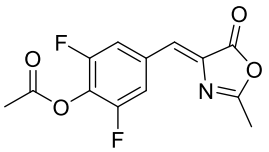

3,5-Difluoro-4-hydroxybenzaldehyde (**63**, 900 mg, 5.70 mmol), *N*-acetylglycine (667 mg, 5.70 mmol), anhydrous sodium acetate (467 mg, 5.70 mmol), and acetic anhydride (2.1 ml) were stirred at 110 °C for 2 h. After allowing the reaction to cool to rt, cold ethanol (20 ml) was added and the reaction was left overnight at 4 °C. The resulting crystalline solid was then

washed with cold ethanol (20 mL), hot water (20 mL), hexanes (20 mL) and dried to afford **64** as a bright yellow solid (1.12 g, 70%).

mp 160-162 °C; R_f = 0.33 (petroleum ether/EtOAc 9:1); ^{1}H NMR (600 MHz, DMSO-d_6) δ 2.42 (s, 3H, CH_3), 2.43 (s, 3H, CH_3), 7.23 (s, 1H, CH), 8.08 (d, J = 9.1 Hz, 2H, Ar-H); ^{13}C NMR (151 MHz, DMSO-d_6) δ 15.5 (CH_3), 19.7 ($\underline{C}H_3CO$), 115.21 (dd, $^2J_{F,C}$ = 19.7 Hz, $^4J_{F,C}$ = 4.1 Hz, C-3, C-5), 125.8 (CH), 127.79 (t, $^2J_{F,C}$ = 16.6 Hz, C-1), 132.31 (t, $^3J_{F,C}$ = 9.7 Hz, C-4), 134.7 (N$\underline{C}$CO), 154.22 (dd, $^1J_{F,C}$ = 248.4 Hz, $^1J_{F,C}$ = 4.9 Hz, C-2, C-6), 166.8, 167.3 (CO), 168.5 (CO). LC-MS (ESI) (90% H_2O to 100% MeCN in 10 min, then 100% MeCN to 15 min, DAD 200-600 nm), t_R = 6.89 min, 98% purity, *m/z* calcd for Chemical Formula: $C_{13}H_9F_2NO_4$ $[M + H]^+$, 282.22; found, 282.0.

(*Z*)-5-(3,5-Difluoro-4-hydroxybenzylidene)-2-methyl-3-(prop-2-yn-1-yl)-3,5-dihydro-4*H*-imidazol-4-one (65)

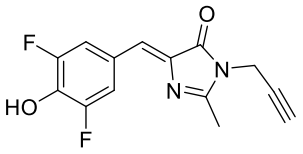

Compound **64** (500 mg, 1.78 mmol) was refluxed with 10 ml of ethanol, propargylamine (0.38 mL, 5.87 mmol), and potassium carbonate (350 mg, 2.50 mmol) for 3 h. After allowing the reaction to cool to rt, the resulting orange precipitate containing the product was filtered and washed briefly with 20 mL cold ethanol. The precipitate was then redissolved in a 1:1 mixture of ethyl acetate and 500 mM sodium acetate (pH 3.0). The organic layer was separated, dried over Na_2SO_4, filtered, and concentrated *in vacuo*. The crude product was purified by flash column chromatography using a gradient from 0 to 20% in CH_2Cl_2 to obtain **65** as a yellow solid (49 mg, 10%).

mp 200-202 °C (lit.[295] 204-207 °C); R_f = 0.48 (CH_2Cl_2/ MeOH EtOAc 9:1); ^{1}H NMR (600 MHz, DMSO-d_6) δ 2.44 (s, 3H, CH_3), 3.37 (t, J = 2.5 Hz, 1H, C≡CH), 4.45 (d, J = 2.5 Hz, 2H, CH_2N), 6.98 (s, 1H, CH), 7.97 (dd, J = 8.4, 1.6 Hz, 2H, Ar-H), 10.97 (br s, 1H, OH); ^{13}C NMR (151 MHz, DMSO-d_6) δ 15.4 (CH_3), 29.0 (CH_2N), 74.7 (C≡$\underline{C}$H), 78.2 ($\underline{C}$≡CH), 115.33 (dd, $^2J_{F,C}$ = 16.8 Hz, $^4J_{F,C}$ = 5.5 Hz, C-2, C-6), 124.1 (CH), 124.35 (t, $^3J_{F,C}$ = 9.3 Hz, C-1), 136.02 (t,

$^{2}J_{F,C}$ = 16.5 Hz, C-4), 137.4 (N<u>C</u>CO), 151.81 (dd, $^{1}J_{F,C}$ = 241.3 Hz, $^{3}J_{F,C}$ = 7.5 Hz, C-3, C-5), 162.6 (NCN), 168.4 (CO). LC-MS (ESI) (90% H_2O to 100% MeCN in 10 min, then 100% MeCN to 15 min, DAD 200-600 nm), t_R = 3.17 min, 100% purity, *m/z* calcd for $C_{14}H_{10}F_2N_2O_2$ $[M + H]^+$, 277.08; found, 277.1.

Alternative: Compound **69** (0.20 g, 1.5 mmol), 3,5-difluoro-4-hydroxybenzaldehyde (**63**, 0.24 g, 1.5 mmol), a catalytic amount of piperidine (30 µL, 0.3 mmol) were dissolved in 10 mL toluene. The reaction mixture was stirred for 16 h at rt, after which 50 mL CH_2Cl_2 was added. The organic phase was washed with 50 mL H_2O and 50 mL brine, dried over Na_2SO_4, filtered, and concentrated *in vacuo*. The crude product was purified by flash column chromatography using a gradient from 0 to 20% in CH_2Cl_2 to obtain **65** a yellow solid (275 mg, 66%). The material was identical with that obtained before (see above).

Propargylamine (66)

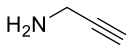

This compound was purchased from TCI Deutschland (Eschborn, Germany).

***N*-(Prop-2-yn-1-yl)acetamide (67)**

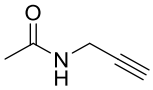

This compound was synthesized similar to a previously reported procedure.[296] Propargylamine (**66**, 2.2 mL, 35.0 mmol) and triethylamine (7.3 mL, 52.5 mmol) were dissolved in dry CH_2Cl_2 (50 mL) and were cooled to 0 °C. Acetyl chloride (2.7 mL, 38.5 mmol) was added dropwise and the solution was then left to warm to rt and stirred overnight. Subsequently, the mixture was diluted with H_2O (50 mL), and extracted with CH_2Cl_2 (3 × 50 mL). The organic extracts were combined, dried over Na_2SO_4, filtered, and concentrated *in vacuo*. The residue was

purified by column chromatography (gradient from 50 to 100% EtOAc in petroleum ether) to obtain **67** as white solid (2.29 g, 67%).

mp. 80-82 °C (lit.[297] 83-85 °C); R_f = 0.14 (petroleum ether/EtOAc 1:1); ^{1}H NMR (600 MHz, DMSO-d_6) δ 1.81 (s, 3H, CH_3), 3.07 (t, J = 2.5 Hz, 1H, C≡CH), 3.82 (dd, J = 5.5, 2.6 Hz, 2H, CH_2), 8.24 (s, 1H, NH); ^{13}C NMR (151 MHz, DMSO-d_6) δ 22.3 (CH_3), 27.7 (CH_2), 72.8 (C≡CH), 81. (C≡CH), 168.9 (CO); IR (KBr): $\tilde{\nu}$ (cm^{-1}) = 541, 608, 640, 714, 777, 1030, 1252, 1300, 1382, 1398, 1420, 1476, 1639, 2932, 2976, 3449.

_N_-Acetyl-2-azido-_N_-(prop-2-yn-1-yl)acetamide (68)

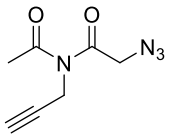

This compound was synthesized similar to a previously reported procedure.[298] 2-Chloroacetyl chloride (1.84 mL, 23.1 mol) was added dropwise to the solution of **67** (2.0 g, 21.0 mmol) and Et_3N (4.0 mL, 28.7 mmol) in 20 mL CH_2Cl_2. The solution was stirred for 2 h at rt, then diluted with H_2O (50 mL) and extracted with CH_2Cl_2 (3 × 30 mL). The organic layers were combined and washed with H_2O (3 × 30 mL) and brine (30 mL), dried over Na_2SO_4 and evaporated *in vacuo*. The residue was dissolved in 20 mL DMF and sodium azide (2.73 g, 42 mmol) was added to the resulting solution in one portion. The reaction mixture was stirred at rt for 16 h, then poured into ice water and extracted with EtOAc (3 × 50 mL). The combined layers were washed with H_2O (3 × 30 mL) and brine (30 mL), dried over Na_2SO_4 and concentrated under reduced pressure. The residue was purified by column chromatography (gradient gradient from 20 to 50% EtOAc in petroleum ether) to obtain **68** as yellow oil (0.45 g, 12%).

R_f = 0.90 (petroleum ether/EtOAc 4:1); ^{1}H NMR (500 MHz, DMSO-d_6) δ 2.41 (s, 3H, CH_3), 3.32 (t, J = 2.4 Hz, 1H, C≡CH), 4.47 (s, 2H, CH_2N_3), 4.52 (d, J = 2.5 Hz, 2H, CH_2N); ^{13}C NMR (126 MHz, DMSO-d_6) δ 24.9 (CH_3), 33.5 (CH_2N), 54.3 (CH_2N_3), 74.5 (C≡CH), 79.1 (C≡CH), 170.6 (CO), 172.4 (CO); IR (KBr): $\tilde{\nu}$ (cm-1) = 429, 551, 607, 647, 696, 782, 822, 925, 975, 1040, 1085, 1122, 1191, 1247, 1402, 1442, 1525, 1707, 2108 (s) [ν(N=N=N)], 2201, 2885, 2931, 2961, 3288, 3425.

2-Methyl-3-(prop-2-yn-1-yl)-3,5-dihydro-4*H*-imidazol-4-one (69)

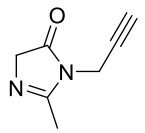

This compound was synthesized similar to a previously reported procedure.[298] Triphenylphosphine (1.01 g, 3.8 mmol) was added to a solution of compound (**68**, 0.63 g, 3.5 mmol) in toluene (20 mL). The reaction mixture was stirred at rt for 16 h, and evaporated to give a residue, which was subjected to column chromatography (gradient from 50 to 100% EtOAc in petroleum ether) to afford the title compound as colorless oil (0.16 g, 33%).

R_f = 0.38 (EtOAc); ^{1}H NMR (600 MHz, DMSO-d_6) δ 2.21 – 2.23 (m, 3H, CH_3), 3.32 (t, J = 2.5 Hz, 1H, C≡CH), 4.05 (q, J = 2.2 Hz, 2H, CH_2CO), 4.30 (d, J = 2.6 Hz, 2H, CH_2N); ^{13}C NMR (151 MHz, DMSO-d_6) δ 15.4 (CH_3), 28.6 (CH_2N), 57.4 (CH_2CO), 74.4 (C≡CH), 78.5 (C≡CH), 161.2 (CH_3C), 179.8 (CO).

2-(2-Chloroethoxy)ethan-1-ol (70a)

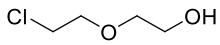

This compound was purchased from Sigma Aldrich (Schnelldorf, Germany).

2-(2-(2-Chloroethoxy)ethoxy)ethan-1-ol (70b)

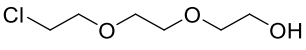

This compound was purchased from TCI Deutschland (Eschborn, Germany).

Tetraethylene Glycol (71a)

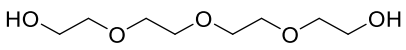

This compound was purchased from TCI Deutschland (Eschborn, Germany).

Pentaethylene Glycol (71b)

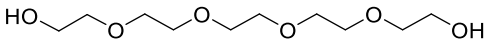

This compound was purchased from TCI Deutschland (Eschborn, Germany).

2-(2-(2-(2-Hydroxyethoxy)ethoxy)ethoxy)ethyl 4-Methylbenzenesulfonate (72)

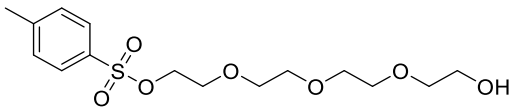

To a solution of tetraethylene glycol (**71a**, 98.8 g, 200.0 mmol) in dry CH_2Cl_2 (120 mL), Et_3N (21.1 mL, 150.0 mmol) was added and was cooled to 0 °C. Subsequently, *p*-toluenesulfonyl chloride (19.1 g, 100.0 mmol) was added dropwise at 0 °C, followed by stirring of the mixture at rt for 18 h. The mixture was quenched with H_2O (50 mL), and the separated organic phase was washed with H_2O (3 × 50 mL), dried over Na_2SO_4, filtered, and concentrated *in vacuo*. The crude product was purified by column chromatography (CH_2Cl_2/MeOH 9:1) to obtain **72** as a colorless oil (13.60 g, 39%).

R_f = 0.44 (CH_2Cl_2/MeOH 9:1); ^{1}H NMR (500 MHz, DMSO-d_6) δ 2.42 (s, 3H, CH_3), 3.39 – 3.42 (m, 2H, CH_2), 3.45 (s, 4H, CH_2), 3.46 – 3.51 (m, 6H, CH_2), 3.56 – 3.59 (m, 2H, CH_2), 4.08 – 4.14 (m, 2H, CH_2), 4.53 (t, J = 5.4 Hz, 1H, OH), 7.46 – 7.50 (m, 2H, Ar-H), 7.76 – 7.80 (m, 2H, Ar-H); ^{13}C NMR (126 MHz, DMSO-d_6) δ 21.0 (CH_3), 60.2 ($HOCH_2$), 67.8 (CH_2), 69.6 (CH_2), 69.7 (CH_2), 69.7 (CH_2), 69.8 (CH_2), 69.9 (CH_2), 72.3 (CH_2), 127.6 (C-Ar), 130.1 (C-Ar), 132.4 (C-4), 144.8 (C-1). LC-MS (ESI) (90% H_2O to 100% MeCN in 10 min, then 100%

MeCN to 15 min, DAD 200-600 nm), t_R = 4.81 min, 99% purity, *m/z* calcd for $C_{15}H_{24}O_7S$ [M + H]$^+$, 349.13; found, 349.2.

14-Hydroxy-3,6,9,12-tetraoxatetradecyl 4-Methylbenzenesulfonate (73)

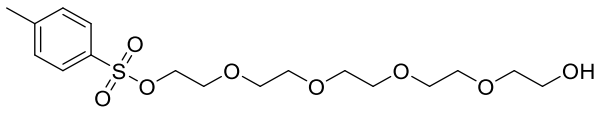

To a solution of pentaethylene glycol (**71b**, 9.5 g, 40.0 mmol) in dry CH_2Cl_2 (30 mL), Et_3N (4.2 mL, 30.0 mmol) was added and was cooled to 0 °C. Subsequently, *p*-toluenesulfonyl chloride (3.8 g, 20.0 mmol) was added dropwise at 0 °C, followed by stirring of the mixture at rt for 18 h. The mixture was quenched with H_2O (50 mL), and the separated organic phase was washed with H_2O (3 × 50 mL), dried over Na_2SO_4, filtered, and concentrated *in vacuo*. The crude product was purified by column chromatography (CH_2Cl_2/MeOH 9:1) to obtain **73** a colorless oil (3.00 g, 38%).

R_f = 0.50 (CH_2Cl_2/MeOH 9:1); ^{1}H NMR (600 MHz, DMSO-d_6) δ 2.42 (s, 3H, CH_3), 3.40 – 3.42 (m, 2H, CH_2), 3.45 (s, 4H, CH_2), 3.47 – 3.50 (m, 6H, CH_2), 3.50 (s, 5H, CH_2), 3.55 – 3.60 (m, 2H, CH_2), 4.07 – 4.14 (m, 2H, OH, CH_2), 7.48 (d, *J* = 8.0 Hz, 2H, Ar-H), 7.76 – 7.80 (m, 2H, Ar-H); ^{13}C NMR (151 MHz, DMSO-d_6) δ 21.1 (CH_3), 60.2 ($HOCH_2$), 67.8 (CH_2), 69.6 (CH_2), 69.7 (CH_2), 69.7 (CH_2) 69.7 (CH_2), 69.8 (CH_2), 69.9 (CH_2), 72.3 (CH_2), 127.6 (C-Ar), 130.1 (C-Ar), 132.4 (C-4), 144.8 (C-1); one CH_2 signals is missing due to overlapping signals. LC-MS (ESI) (90% H_2O to 100% MeCN in 10 min, then 100% MeCN to 15 min, DAD 200-600 nm), t_R = 4.95 min, 100% purity, *m/z* calcd for $C_{17}H_{28}O_8S$ [M + H]$^+$, 393.16; found, 393.2.

2-(2-Azidoethoxy)ethan-1-ol (74)

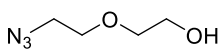

This compound was synthesized and provided by Tim Keuler, University of Bonn.

2-(2-(2-Azidoethoxy)ethoxy)ethan-1-ol (75)

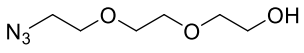

This compound was synthesized and provided by Tim Keuler, University of Bonn.

2-(2-(2-(2-Azidoethoxy)ethoxy)ethoxy)ethan-1-ol (76)

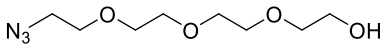

The monotosylated tetraethylene glycol **72** (12.54 g, 36.0 mmol) was dissolved in dry DMF (50 mL), and sodium azide (4.68 g, 72.0 mmol) was added. The reaction mixture was stirred at 80 °C for 18 h. After cooling to rt, it was poured into H_2O (50 mL) and then partitioned between H_2O and EtOAc (3 × 50 mL). The combined organic layers were washed with H_2O (50 mL), dried over Na_2SO_4, filtered, and concentrated *in vacuo*. The crude product was purified by column chromatography (CH_2Cl_2/MeOH 19:1) to obtain **76** as a yellow oil (7.21 g, 91%).

R_f = 0.34 (CH_2Cl_2/MeOH 19:1); ^{1}H NMR (500 MHz, DMSO-d_6) δ 3.40 (dt, J = 13.3, 5.1 Hz, 4H, CH_2), 3.47 – 3.50 (m, 2H, CH_2), 3.50 – 3.57 (m, 8H, CH_2), 3.59 – 3.62 (m, 2H, CH_2), 4.52 (t, J = 5.5 Hz, 1H, OH); ^{13}C NMR (126 MHz, DMSO-d_6) δ 50.0 (CH_2N_3), 60.2 ($HOCH_2$), 69.2 (CH_2), 69.7 (CH_2), 69.7 (CH_2), 69.8 (CH_2), 69.8 (CH_2), 72.3 (CH_2). LC-MS (ESI) (90% H_2O to 100% MeCN in 10 min, then 100% MeCN to 15 min, DAD 200-600 nm), t_R = 1.72 min, *m/z* calcd for $C_8H_{17}N_3O_4$ $[M + H]^+$, 220.13; found, 220.1.

14-Azido-3,6,9,12-tetraoxatetradecan-1-ol (77)

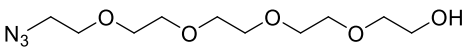

The monotosylated tetraethylene glycol **73** (2.74 g, 7.0 mmol) was dissolved in dry DMF (20 mL), and sodium azide (0.91 g, 14.0 mmol) was added. The reaction mixture was stirred at

80 °C for 18 h. After cooling to rt, it was poured into H_2O (20 mL) and then partitioned between H_2O and EtOAc (3 × 20 mL). The combined organic layers were washed with H_2O (20 mL), dried over Na_2SO_4, filtered, and concentrated *in vacuo*. The crude product was purified by column chromatography (CH_2Cl_2/MeOH 19:1) to obtain **77** as a yellow oil (0.84 g, 46%).

R_f = 0.25 (CH_2Cl_2/MeOH 19:1); ^{1}H NMR (500 MHz, DMSO-d_6) δ 3.40 (dt, J = 12.3, 5.1 Hz, 4H, CH_2), 3.48 (t, J = 5.3 Hz, 2H, CH_2), 3.50 – 3.58 (m, 12H, CH_2), 3.59 – 3.62 (m, 2H, CH_2), 4.52 (t, J = 5.5 Hz, 1H, OH); ^{13}C NMR (126 MHz, DMSO-d_6) δ 50.0 (CH_2N_3), 60.2 ($HOCH_2$), 69.2 (CH_2), 69.7 (CH_2), 69.7 (CH_2), 69.7 (CH_2), 69.8 (CH_2), 69.8 (CH_2), 72.3 (CH_2); one CH_2 signals is missing due to overlapping signals. LC-MS (ESI) (90% H_2O to 100% MeCN in 10 min, then 100% MeCN to 15 min, DAD 200-600 nm), t_R = 2.67 min, *m/z* calcd for $C_{10}H_{21}N_3O_5$ $[M + H]^+$, 264.16; found, 264.1.

tert-Butyl 2-(2-(2-Azidoethoxy)ethoxy)acetate (78)

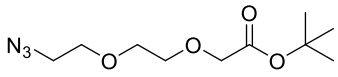

This compound was synthesized and provided by Tim Keuler, University of Bonn.

tert-Butyl 2-(2-(2-(2-Azidoethoxy)ethoxy)ethoxy)acetate (79)

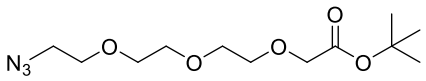

This compound was synthesized and provided by Tim Keuler, University of Bonn.

tert-Butyl 14-Azido-3,6,9,12-tetraoxatetradecanoate (80)

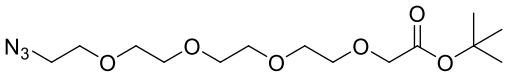

This compound was synthesized similar to a previously reported procedure.[299] To a solution of **76** (6.58 g, 30.0 mmol) in toluene (100 mL) was added tetrabutylammonium hydrogen sulfate (5.09 g, 15.0 mmol) and *tert*-butyl bromoacetate (17.56 g, 90.0 mmol). The yellow clear mixture was cooled to 0 °C, and 9.5 M NaOH (85 mL, 90.0 mmol) was added. The solution was vigorously stirred at rt for 18 h. After the addition of H_2O (100 mL), it was extracted with Et_2O (3 × 50 mL). The combined organic layers were washed with brine (50 mL), dried over Na_2SO_4, filtered, and concentrated *in vacuo*. The crude product was purified by column chromatography (CH_2Cl_2/MeOH 29:1) to obtain **80** as a yellow oil (2.42 g, 24%).

R_f = 0.30 (CH_2Cl_2/MeOH 29:1); ^{1}H NMR (600 MHz, DMSO-d_6) δ 1.42 (s, 9H, C(CH_3)$_3$), 3.39 (dd, J = 5.6, 4.4 Hz, 2H, CH_2), 3.51 – 3.55 (m, 8H, CH_2), 3.55 – 3.58 (m, 4H, CH_2), 3.59 – 3.61 (m, 2H, CH_2), 3.98 (s, 2H, CH_2CO_2); ^{13}C NMR (151 MHz, DMSO-d_6) δ 27.7 (C(<u>C</u>H_3)$_3$), 50.0 (CH_2N_3), 68.1 (CH_2), 69.2 (CH_2), 69.7 (CH_2), 69.7 (CH_2), 69.7 (CH_2), 69.8 (CH_2), 69.8 (CH_2), 69.8 (CH_2), 80.6 (<u>C</u>(CH_3)$_3$), 169.3 (CO). LC-MS (ESI) (90% H_2O to 100% MeCN in 10 min, then 100% MeCN to 15 min, DAD 200-600 nm), t_R = 5.91 min, *m/z* calcd for $C_{14}H_{27}N_3O_6$ [M + NH_4]$^+$, 351.22; found, 351.3.

tert-Butyl 17-Azido-3,6,9,12,15-pentaoxaheptadecanoate (81)

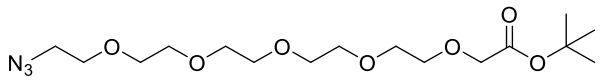

This compound was synthesized similar to a previously reported procedure.[299] To a solution of **77** (0.79 g, 3.0 mmol) in toluene (60 mL) was added tetrabutylammonium hydrogen sulfate (0.51 g, 1.5 mmol) and *tert*-butyl bromoacetate (1.76 g, 9.0 mmol). The yellow clear mixture was cooled to 0 °C, and 9.5 M NaOH (8.5 mL, 9.0 mmol) was added. The solution was vigorously stirred at rt for 18 h. After the addition of H_2O (60 mL), it was extracted with Et_2O (3 × 50 mL). The combined organic layers were washed with brine (50 mL), dried over Na_2SO_4, filtered, and concentrated *in vacuo*. The crude product was purified by column chromatography (CH_2Cl_2/MeOH 29:1) to obtain **81** as a yellow oil (0.44 g, 39%).

R_f = 0.24 (CH_2Cl_2/MeOH 29:1); ^{1}H NMR (600 MHz, DMSO-d_6) δ 1.42 (s, 9H, C(CH_3)$_3$), 3.39 (dd, J = 5.6, 4.4 Hz, 2H, CH_2), 3.51 – 3.55 (m, 12H, CH_2), 3.55 – 3.58 (m, 4H, CH_2), 3.59 –

3.61 (m, 2H, CH_2), 3.98 (s, 2H, CH_2CO_2); ^{13}C NMR (151 MHz, DMSO-d_6) δ 27.7 (C($\underline{C}H_3)_3$), 50.0 (CH_2N_3), 67.7 (CH_2), 68.1 (CH_2), 69.2 (CH_2), 69.7 (CH_2), 69.7 (CH_2), 69.8 (CH_2), 69.8 (CH_2), 69.8 (CH_2), 69.8 (CH_2), 80.6 ($\underline{C}(CH_3)_3$), 169.3 (CO); one CH_2 signal is missing due to overlapping signals. LC-MS (ESI) (90% H_2O to 100% MeCN in 10 min, then 100% MeCN to 15 min, DAD 200-600 nm), t_R = 5.93 min, *m/z* calcd for $C_{16}H_{31}N_3O_7$ $[M + NH_4]^+$, 395.25; found, 395.3.

(*S*)-1-(4-Bromophenyl)ethan-1-amine (82)

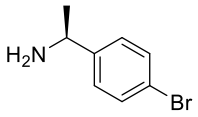

This compound was purchased from BLDpharm (Kaiserslautern, Germany).

***tert*-Butyl (S)-(1-(4-Bromophenyl)ethyl)carbamate (83)**

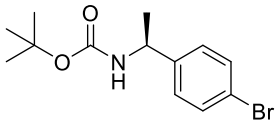

This compound was synthesized similar to a previously reported procedure.[43] (*S*)-1-(4-Bromophenyl)ethan-1-amine (**82**, 5.00 g, 25.0 mmol) and $NaHCO_3$ (1.58 g, 18.8 mmol) were dissolved in H_2O (12.5 mL) and EtOAc (12.5 mL) and the mixture was cooled to 0 °C. Boc_2O (6.55 g, 30.0 mmol) was dissolved in EtOAc (5.0 mL) and was added dropwise. After stirring for 2 h at 0 °C, the precipitate was collected, resuspended in H_2O/hexane (1/1) (25 mL), stirred for further 30 min and collected again. The residue was washed with hexane (3 × 15 mL) and dried under high vacuum to obtain **83** as a white solid (6.58 g, 88%).

mp 145-148 °C; R_f = 0.40 (petroleum ether/EtOAc 9:1); ^{1}H NMR (500 MHz, DMSO-d_6) δ 1.28 (d, *J* = 7.1 Hz, 3H, CHC$\underline{H}_3$), 1.35 (s, 9H, C($CH_3)_3$), 4.52 – 4.61 (m, 1H, CH), 7.25 (d, *J* = 8.2 Hz, 2H, Ar-H), 7.35 – 7.40 (m, 1H, NH), 7.45 – 7.52 (m, 2H, Ar-H); ^{13}C NMR (126 MHz, DMSO) δ 22.5 (CH_3), 28.2 (C($\underline{C}H_3)_3$), 49.1 (CH), 77.7 ($\underline{C}(CH_3)_3$), 119.4 (C-4), 128.0, 131.0

(C-2, C-3, C-5, C-6), 144.9 (C-1), 154.7 (CO). LC-MS (ESI) (90% H_2O to 100% MeCN in 10 min, then 100% MeCN to 15 min, DAD 200-600 nm), t_R = 7.62 min, 100% purity, *m/z* calcd for $C_{13}H_{18}{}^{79}BrNO_2$ $[M - H]^-$, 298.04; found, 297.9.

tert-Butyl (*S*)-(1-(4-(4-Methylthiazol-5-yl)phenyl)ethyl)carbamate (84)

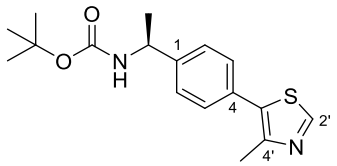

Following General Procedure B, compound **84** was obtained from *tert*-butyl (*S*)-(1-(4-bromophenyl)ethyl)carbamate (**83**, 6.00 g, 20.0 mmol). The crude product was purified by column chromatography (gradient from 20 to 50% EtOAc in petroleum ether) to yield **84** as a white solid (5.35 g, 84%).

mp 130-132 °C; R_f = 0.15 (petroleum ether/EtOAc 4:1); ^{1}H NMR (500 MHz, DMSO-d_6) δ 1.33 (d, J = 7.1 Hz, 3H, CHC$\underline{H}_3$), 1.37 (s, 9H, C(CH_3)$_3$), 2.45 (s, 3H, CH_3), 4.61 – 4.70 (m, 1H, CH), 7.36 – 7.41 (m, 3H), 7.41 – 7.45 (m, 2H) (Ar-H, NH), 8.97 (s, 1H, 2″-H); ^{13}C NMR (126 MHz, DMSO) δ 15.9 (CH_3), 22.7 (CH$\underline{C}H_3$), 28.2 (C($\underline{C}H_3$)$_3$), 49.2 (CH), 77.7 ($\underline{C}$(CH_3)$_3$), 126.3, 128.7 (C-2, C-3, C-5, C-6), 129.6, 131.1, 145.3 (C-1, C-4, C-5′), 147.7 (C-4′), 151.3 (C-2′), 154.8 (CO). LC-MS (ESI) (90% H_2O to 100% MeCN in 10 min, then 100% MeCN to 15 min, DAD 200-600 nm), t_R = 6.91 min, 99% purity, *m/z* calcd for $C_{17}H_{22}N_2O_2S$ $[M + H]^+$, 319.15; found, 319.2.

(2*S*,4*R*)-1-((*S*)-2-((*tert*-Butoxycarbonyl)amino)-3,3-dimethylbutanoyl)-4-hydroxypyrrolidine-2-carboxylic acid (85)

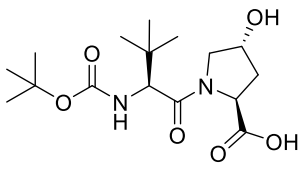

Compound **44** (3.37 g, 10.0 mmol) was dissolved in dry EtOH (50 mL) and treated with 10% Pd/C under H_2 (1 atm, balloon) for 18 h. The reaction mixture was filtered through celite and concentrated to yield a white solid. This compound was used without further purification and characterization.

***tert*-Butyl ((*S*)-1-((2*S*,4*R*)-4-Hydroxy-2-(((*S*)-1-(4-(4-methylthiazol-5-yl)phenyl)ethyl)carbamoyl)pyrrolidine-1-yl)-3,3-dimethyl-1-oxobutan-2-yl)carbamate (86)**

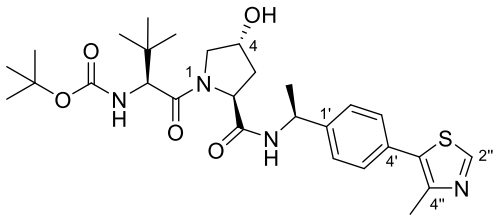

Following General Procedure C, compound **86** was obtained using Boc-protected amine **84** (1.75 mg, 5.5 mmol) and acid **44** (1.32 mg, 5.5 mmol). The residue was purified by column chromatography (CH_2Cl_2/MeOH 19:1) to afford **86** as a white solid (1.83 mg, 61%).

mp 200-202 °C; R_f = 0.25 (CH_2Cl_2/MeOH 19:1); ^{1}H NMR (600 MHz, DMSO-d_6) δ 0.93 (s, 9H, C(CH_3)$_3$), 1.35 – 1.41 (m, 12H, CHC$\underline{H}_3$, OC(CH_3)$_3$), 1.75 – 1.82 (m, 1H, 3-H), 1.99 – 2.06 (m, 1H, 3-H), 2.45 (s, 3H, CH_3), 3.53 – 3.64 (m, 2H, 5-H), 4.14 (d, *J* = 9.1 Hz, 1H), 4.28 (s, 1H), 4.45 (t, *J* = 8.0 Hz, 1H) (2-H, 4-H, NHC$\underline{H}$), 4.86 – 4.93 (m, 1H, C$\underline{H}$CH$_3$), 5.10 (s, 1H, OH), 6.37 (d, *J* = 9.3 Hz, 1H, CONH), 7.37 (d, *J* = 8.2 Hz, 2H, Ar-H), 7.42 – 7.44 (m, 2H, Ar-H,), 8.37 (d, *J* = 7.7 Hz, 1H, CONH), 8.98 (s, 1H, 2′′-H); ^{13}C NMR (151 MHz, DMSO) δ 15.9 (CH_3), 22.4 (CH$\underline{C}$H$_3$), 26.3 (C($\underline{C}$H$_3$)$_3$), 28.2 (OC($\underline{C}$H$_3$)$_3$), 35.3 ($\underline{C}$(CH$_3$)$_3$), 37.7 (C-3), 38.2 (NHCH), 47.7 ($\underline{C}$HCH$_3$), 56.2, 58.5 (C-2, C-5), 68.8 (C-4), 78.1 (O$\underline{C}$(CH$_3$)$_3$), 126.3, 128.8 (C-2, C-3, C-5, C-6), 129.6, 131.1, 144.7 (C-1′, C-4′, C-5′′), 147.7 (C-4′′), 151.4 (C-2′′), 155.3 (CO), 169.7 (CO), 170.6 (CO). LC-MS (ESI) (90% H_2O to 100% MeCN in 10 min, then 100% MeCN to 15 min, DAD 220-600 nm), t_R = 6.36 min, 98% purity, *m/z* calcd for $C_{28}H_{40}N_4O_5S$ $[M + H]^+$, 545.28; found 545.3.

(2*S*,4*R*)-1-((*S*)-2-(2-(2-(2-Azidoethoxy)ethoxy)acetamido)-3,3-dimethylbutanoyl)-4-hydroxy-*N*-((S)-1-(4-(4-methylthiazol-5-yl)phenyl)ethyl)pyrrolidine-2-carboxamide (87)

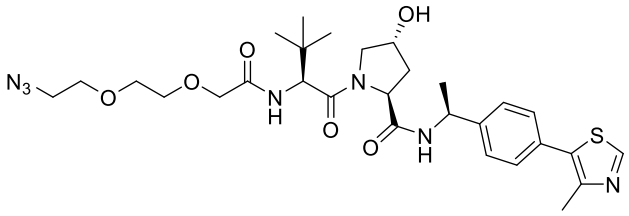

This compound was synthesized and provided by Tim Keuler, University of Bonn.

(2*S*,4*R*)-1-((*S*)-14-Azido-2-(*tert*-butyl)-4-oxo-6,9,12-trioxa-3-azatetradecanoyl)-4-hydroxy-*N*-((*S*)-1-(4-(4-methylthiazol-5-yl)phenyl)ethyl)pyrrolidine-2-carboxamide (88)

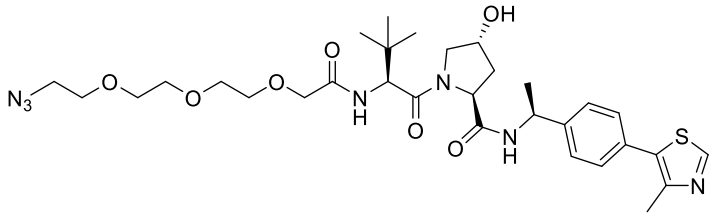

This compound was synthesized and provided by Tim Keuler, University of Bonn.

(2*S*,4*R*)-1-((*S*)-17-Azido-2-(*tert*-butyl)-4-oxo-6,9,12,15-tetraoxa-3-azaheptadecanoyl)-4-hydroxy-*N*-((*S*)-1-(4-(4-methylthiazol-5-yl)phenyl)ethyl)pyrrolidine-2-carboxamide (89)

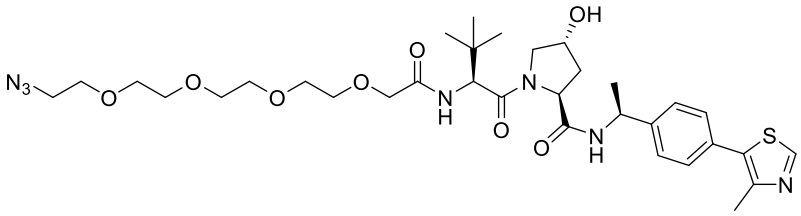

The Boc-protected VHL ligand (**86**, 0.54 g, 1.0 mmol) and Boc-protected linker (**80**, 0.33 g, 1.0 mmol) were each dissolved in anhydrous CH_2Cl_2 (5 mL), and TFA (5 mL) was each added. The mixtures were stirred at rt for 2 h, and then concentrated under high vacuum. Both

deprotected compounds were dissolved in anhydrous DMF (5 mL) and DIPEA (0.7 mL, 4.0 mmol) was added, followed by the addition of HATU (0.42 g, 1.1 mmol) after 5 min. The mixture was stirred at rt for 18 h, after which H_2O (25 mL) was added, and extracted with EtOAc (3 × 50 mL/mmol). The combined organic phases were washed with brine (50 mL), dried over Na_2SO_4, filtered, and concentrated *in vacuo*. The residue was purified by flash column chromatography using a gradient from 0 to 10% MeOH in CH_2Cl_2 to afford **89** as a slightly yellow resin (493 mg, 70%).

R_f = 0.40 (CH_2Cl_2/MeOH 9:1); ^{1}H NMR (600 MHz, DMSO-d_6) δ 0.94 (s, 9H, C(CH_3)$_3$), 1.38 (d, J = 7.0 Hz, 3H, CHC<u>H</u>$_3$), 1.75 – 1.81 (m, 1H, 3-H), 2.02 – 2.07 (m, 1H, 3-H), 2.45 (s, 3H, CH_3), 3.37 – 3.41 (m, 2H, 5-H), 3.52 – 3.63 (m, 16H, CH_2), 3.96 (s, 2H, CH_2), 4.26 – 4.31 (m, 1H), 4.45 (t, J = 8.1 Hz, 1H), 4.55 (d, J = 9.5 Hz, 1H) (2-H, 4-H, NHC<u>H</u>), 4.88 – 4.94 (m, 1H, C<u>H</u>CH$_3$), 5.11 (d, J = 3.5 Hz, 1H, OH), 7.34 – 7.39 (m, 3H), 7.41 – 7.46 (m, 2H) (Ar-H, CONH), 8.41 (d, J = 7.7 Hz, 1H, CONH), 8.98 (s, 1H, 2″-H); ^{13}C NMR (151 MHz, DMSO) δ 15.9 (CH_3), 22.4 (CH<u>C</u>H$_3$), 26.2 (C(<u>C</u>H$_3$)$_3$), 35.7 (<u>C</u>(CH$_3$)$_3$), 37.7 (C-3), 47.7 (<u>C</u>HCH$_3$), 50.0 (CH_2N_3), 55.7, 56.5, 58.5 (C-2, C-5, NHCH), 68.7 (C-4), 69.2, 69.6, 69.6, 69.7, 69.8, 69.8, 70.4 (CH_2), 126.3, 128.8 (C-2, C-3, C-5, C-6), 129.7, 131.1, 144.7 (C-1′, C-4′, C-5″), 147.7 (C-4″), 151.4 (C-2″), 168.5 (CO), 169.0 (CO), 170.4 (CO); one CH_2 signal is missing due to overlapping signals. LC-MS (ESI) (90% H_2O to 100% MeCN in 10 min, then 100% MeCN to 15 min, DAD 200-600 nm), t_R = 5.97 min, 99% purity, *m/z* calcd for $C_{33}H_{49}N_7O_8S$ $[M + H]^+$, 704.34; found, 704.5.

(2*S*,4*R*)-1-((*S*)-20-Azido-2-(*tert*-butyl)-4-oxo-6,9,12,15,18-pentaoxa-3-azaicosanoyl)-4-hydroxy-*N*-((*S*)-1-(4-(4-methylthiazol-5-yl)phenyl)ethyl)pyrrolidine-2-carboxamide (90)

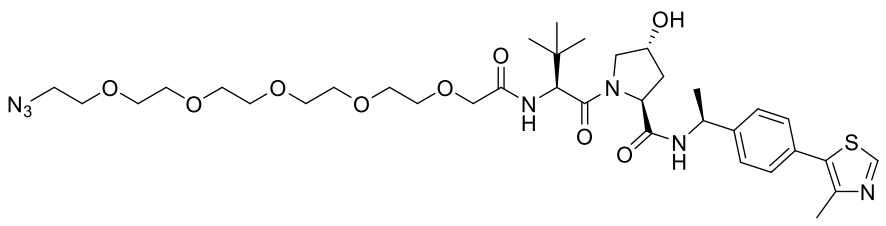

The Boc-protected VHL ligand (**86**, 0.54 g, 1.0 mmol) and Boc-protected linker (**81**, 0.38 g, 1.0 mmol) were each dissolved in anhydrous CH_2Cl_2 (5 mL), and TFA (5 mL) was each added. The mixtures were stirred at rt for 2 h, and then concentrated under high vacuum. Both

deprotected compounds were dissolved in anhydrous DMF (5 mL) and DIPEA (0.7 mL, 4.0 mmol) was added, followed by the addition of HATU (0.42 g, 1.1 mmol) after 5 min. The mixture was stirred at rt for 18 h, after which H_2O (25 mL) was added, and extracted with EtOAc (3 × 50 mL/mmol). The combined organic phases were washed with brine (50 mL), dried over Na_2SO_4, filtered, and concentrated *in vacuo*. The residue was purified by flash column chromatography using a gradient from 0 to 10% MeOH in CH_2Cl_2 to afford **90** as a slightly yellow resin (479 mg, 64%).

R_f = 0.40 (CH_2Cl_2/MeOH 9:1); ^{1}H NMR (600 MHz, DMSO-d_6) δ 0.94 (d, J = 4.7 Hz, 9H, $C(CH_3)_3$), 1.38 (d, J = 7.0 Hz, 3H, $CHC\underline{H}_3$), 1.71 – 1.82 (m, 1H, 3-H), 2.01 – 2.08 (m, 1H, 3-H), 2.45 (s, 3H, CH_3), 3.37 – 3.41 (m, 2H, 5-H), 3.53 (s, 4H, CH_2), 3.53 – 3.56 (m, 8H, CH_2), 3.56 – 3.63 (m, 8H, CH_2), 3.96 (s, 2H, CH_2), 4.27 – 4.30 (m, 1H), 4.45 (t, J = 8.2 Hz, 1H), 4.55 (d, J = 9.5 Hz, 1H) (2-H, 4-H, NHC$\underline{H}$), 4.88 – 4.93 (m, 1H, C$\underline{H}CH_3$), 7.34 – 7.39 (m, 3H), 7.42 – 7.46 (m, 2H) (Ar-H, CONH), 8.41 (d, J = 7.7 Hz, 1H, CONH), 8.98 (s, 1H, 2″-H); ^{13}C NMR (151 MHz, DMSO) δ 15.9 (CH_3), 22.4 (CH$\underline{C}H_3$), 26.2 ($C(\underline{C}H_3)_3$), 35.7 ($\underline{C}(CH_3)_3$), 37.7 (C-3), 47.7 ($\underline{C}HCH_3$), 50.0 (CH_2N_3), 55.7, 56.5, 58.5 (C-2, C-5, NHCH), 68.7 (C-4), 69.2, 69.6, 69.6, 69.7, 69.8, 69.8, 69.8, 69.8, 70.4 (CH_2), 126.3, 128.8 (C-2, C-3, C-5, C-6), 129.7, 131.1, 144.7 (C-1′, C-4′, C-5″), 147.7 (C-4″), 151.4 (C-2″), 168.5 (CO), 169.0 (CO), 170.4 (CO); one OH signal is not visible and one CH_2 signal is missing due to overlapping signals. LC-MS (ESI) (90% H_2O to 100% MeCN in 10 min, then 100% MeCN to 15 min, DAD 200-600 nm), t_R = 5.99 min, 99% purity, *m/z* calcd for $C_{35}H_{53}N_7O_9S$ $[M + H]^+$, 748.37; found, 748.6.

4-((2-(2-(2-Azidoethoxy)ethoxy)ethyl)amino)-2-(2,6-dioxopiperidin-3-yl)isoindoline-1,3-dione (91)

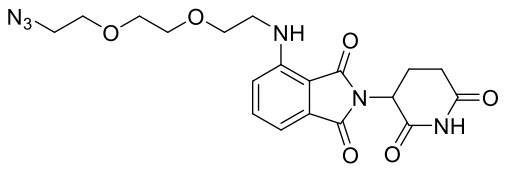

This compound was synthesized and provided by Tim Keuler, University of Bonn.

4-((2-(2-(2-(2-Azidoethoxy)ethoxy)ethoxy)ethyl)amino)-2-(2,6-dioxopiperidin-3-yl)isoindoline-1,3-dione (92)

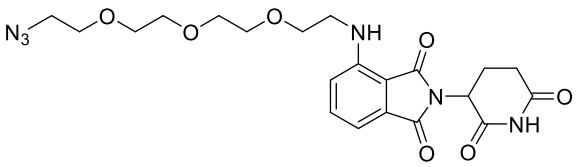

This compound was synthesized and provided by Tim Keuler, University of Bonn.

4-((14-Azido-3,6,9,12-tetraoxatetradecyl)amino)-2-(2,6-dioxopiperidin-3-yl)isoindoline-1,3-dione (93)

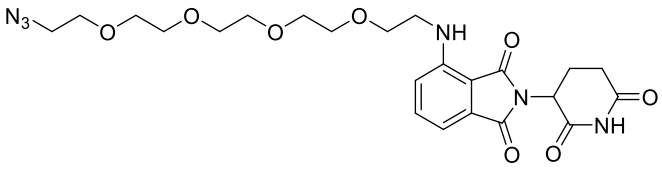

This compound was synthesized and provided by Tim Keuler, University of Bonn.

4-((17-Azido-3,6,9,12,15-pentaoxaheptadecyl)amino)-2-(2,6-dioxopiperidin-3-yl)isoindoline-1,3-dione (94)

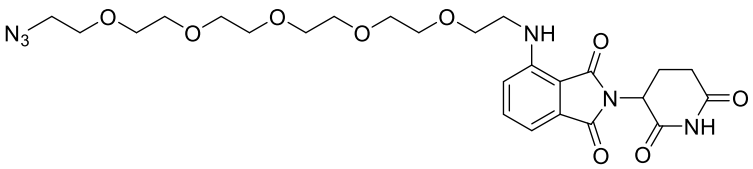

This compound was synthesized and provided by Tim Keuler, University of Bonn.

(2*S*,4*R*)-1-((*S*)-2-(2-(2-(4-((4-((*Z*)-3,5-Difluoro-4-hydroxybenzylidene)-2-methyl-5-oxo-4,5-dihydro-1*H*-imidazol-1-yl)methyl)-1*H*-1,2,3-triazol-1-yl)ethoxy)ethoxy)acetamido)-3,3-dimethylbutanoyl)-4-hydroxy-*N*-((*S*)-1-(4-(4-methylthiazol-5-yl)phenyl)ethyl)pyrrolidine-2-carboxamide (95)

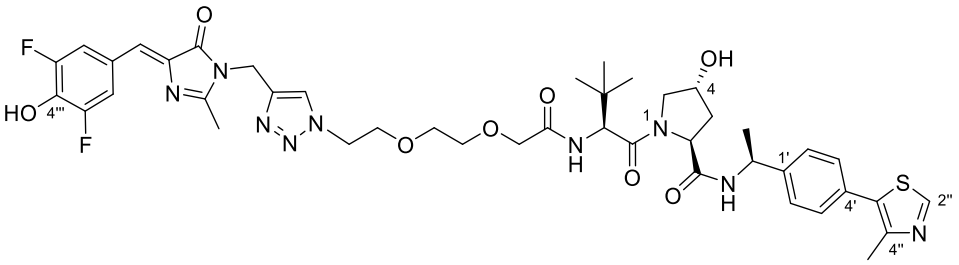

Following General Procedure H, compound **95** was obtained from **87** (98 mg, 0.16 mmol). The crude product was purified by flash column chromatography using a gradient from 0 to 20% MeOH in CH_2Cl_2 to obtain **95** as an orange solid (105 mg, 74%).

mp 118-120 °C; R_f = 0.55 (CH_2Cl_2/MeOH 9:1); ^{1}H NMR (600 MHz, DMSO-d_6) δ 0.93 (s, 9H, C(CH_3)$_3$), 1.32 (d, J = 7.0 Hz, 3H, CHC<u>H</u>$_3$), 1.74 – 1.81 (m, 1H, 3-H), 2.02 – 2.08 (m, 1H, 3-H), 2.42 (s, 3H, CH_3), 2.45 (s, 3H, CH_3), 3.51 – 3.62 (m, 7H, 5-H, OCH_2), 3.80 – 3.85 (m, 2H, OCH_2), 3.91 – 3.95 (m, 1H, OCH_2), 4.29 (s, 1H), 4.42 – 4.47 (m, 1H), 4.50 – 4.57 (m, 3H) (2-H, 4-H, NHC<u>H</u>, NC<u>H</u>$_2$$CH_2$), 4.84 – 4.92 (m, 2H, NCH_2, C<u>H</u>CH_3), 5.12 (d, J = 3.6 Hz, 1H, OH), 6.93 (d, J = 3.5 Hz, 1H, CH), 7.32 – 7.40 (m, 3H), 7.40 – 7.44 (m, 2H) (Ar-H, NH), 7.96 (d, J = 8.8 Hz, 1H, 2‴-H, 6‴-H), 8.09 (s, 1H, NCH), 8.39 (dd, J = 10.8, 6.6 Hz, 1H, NH), 8.98 (s, 1H, 2″-H), 10.93 (br s, 1H, OH); ^{13}C NMR (151 MHz, DMSO) δ 15.7 (CH_3), 15.9 (CH_3), 22.3 (CH<u>C</u>H_3), 26.2 (C(<u>C</u>H_3)$_3$), 35.1 (CON<u>C</u>H_2), 35.8 (<u>C</u>(CH_3)$_3$), 37.7 (C-3), 47.7 (<u>C</u>HCH_3), 49.3 (N<u>C</u>$H_2$$CH_2$), 55.7, 56.5, 58.6 (C-2, C-5, NHCH), 68.8 (C-4), 69.3, 69.6, 70.3 (OCH_2), 115.2 (dd, $^2J_{F,C}$ = 17.1 Hz, $^4J_{F,C}$ = 4.8 Hz, C-2‴, C-6‴), 123.6 (CH), 124.6 (C-1‴), 126.3, 128.8, 129.7, 131.1 (C-Ar), 135.8 (C-4‴), 137.9 (N<u>C</u>CO), 142.2 (NCH), 144.6 (C-Ar), 147.7 (C-4″), 151.4 (C-2″), 151.8 (dd, $^1J_{F,C}$ = 241.6 Hz, $^1J_{F,C}$ = 7.3 Hz, C-3‴, C-5‴), 163.6, 168.5, 169.1, 169.1, 170.4 (NCN, CO); one CH_2 signal is missing due to overlapping signals. LC-MS (ESI) (90% H_2O to 100% MeCN in 10 min, then 100% MeCN to 15 min, DAD 200-600 nm), t_R =5.20 min, 98% purity, *m/z* calcd for $C_{43}H_{51}F_2N_9O_8S$ $[M + H]^+$, 892.36; found, 892.6. HRMS (ESI) *m/z* calcd for $C_{43}H_{51}F_2N_9O_8S$ $[M + H]^+$, 892.3622; found, 892.3613.

(2*S*,4*R*)-1-((*S*)-2-(*tert*-Butyl)-14-(4-((4-((*Z*)-3,5-difluoro-4-hydroxybenzylidene)-2-methyl-5-oxo-4,5-dihydro-1*H*-imidazol-1-yl)methyl)-1*H*-1,2,3-triazol-1-yl)-4-oxo-6,9,12-trioxa-3-azatetradecanoyl)-4-hydroxy-*N*-((*S*)-1-(4-(4-methylthiazol-5-yl)phenyl)ethyl)pyrrolidine-2-carboxamide (96)

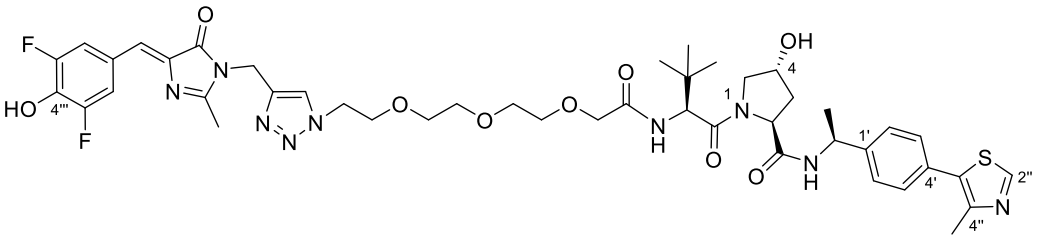

Following General Procedure H, compound **96** was obtained from **88** (105 mg, 0.16 mmol). The crude product was purified by flash column chromatography using a gradient from 0 to 20% MeOH in CH_2Cl_2 to obtain **96** as a yellow solid (87 mg, 58%).

mp 98-100 °C; R_f = 0.55 (CH_2Cl_2/MeOH 9:1); ^{1}H NMR (600 MHz, DMSO-d_6) δ 0.93 (s, 9H, C(CH_3)$_3$), 1.34 (d, J = 7.0 Hz, 3H, CHC$\underline{H}_3$), 1.73 – 1.80 (m, 1H, 3-H), 2.01 – 2.09 (m, 1H, 3-H), 2.43 (s, 3H, CH_3), 2.45 (s, 3H, CH_3), 3.45 – 3.55 (m, 6H, 5-H, OCH_2), 3.56 – 3.62 (m, 4H, OCH_2), 3.81 (t, J = 5.3 Hz, 2H, OCH_2), 3.95 (s, 2H, OCH_2), 4.28 (s, 1H), 4.44 (t, J = 8.3 Hz, 1H), 4.51 (t, J = 5.2 Hz, 2H), 4.54 (d, J = 9.5 Hz, 1H) (2-H, 4-H, NHC$\underline{H}$, NC$\underline{H}_2$$CH_2$), 4.84 – 4.92 (m, 3H, CONCH_2, C$\underline{H}$$CH_3$), 5.11 (d, J = 4.1 Hz, 1H, OH), 6.94 (s, 1H, CH), 7.32 – 7.39 (m, 3H), 7.40 – 7.46 (m, 2H) (Ar-H, NH), 7.97 (d, J = 8.2 Hz, 2H, 2‴-H, 6‴-H), 8.05 (s, 1H, NCH), 8.39 (d, J = 7.7 Hz, 1H, NH), 8.98 (s, 1H, 2″-H), 10.93 (br s, 1H, OH); ^{13}C NMR (151 MHz, DMSO) δ 15.6 (CH_3), 15.9 (CH_3), 22.4 (CH$\underline{C}$$H_3$), 26.2 (C($\underline{C}$$H_3$)$_3$), 35.1 (CON$\underline{C}$$H_2$), 35.7 ($\underline{C}$(C$H_3$)$_3$), 37.7 (C-3), 47.7 ($\underline{C}HCH_3$), 49.4 (N$\underline{C}$$H_2$$CH_2$), 55.7, 56.5, 58.5 (C-2, C-5, NHCH), 68.6 (C-4), 68.7, 69.5, 69.5, 69.6, 69.7, 70.4 (OCH_2), 115.2 (dd, $^2J_{F,C}$ = 19.8 Hz, $^4J_{F,C}$ = 3.3 Hz, C-2‴, C-6‴), 123.5 (CH), 124.5 (C-1‴), 126.3, 128.8, 129.7, 131.1 (C-Ar), 135.9 (C-4‴), 137.9 (N$\underline{C}$CO), 142.2 (NCH), 144.7 (C-Ar), 147.8 (C-4″), 151.4 (C-2″), 151.7 (d, $^1J_{F,C}$ = 237.4 Hz, C-3‴, C-5‴), 163.5, 168.5, 169.0, 169.0, 170.4 (NCN, CO). LC-MS (ESI) (90% H_2O to 100% MeCN in 10 min, then 100% MeCN to 15 min, DAD 200-600 nm), t_R = 5.24 min, 99% purity, *m/z* calcd for $C_{45}H_{55}F_2N_9O_9S$ $[M + H]^+$, 936.39; found, 936.6. HRMS (ESI) *m/z* calcd for $C_{45}H_{55}F_2N_9O_9S$ $[M + H]^+$, 936.3884; found, 936.3886.

(2*S*,4*R*)-1-((*S*)-2-(*tert*-Butyl)-17-(4-((4-((*Z*)-3,5-difluoro-4-hydroxybenzylidene)-2-methyl-5-oxo-4,5-dihydro-1*H*-imidazol-1-yl)methyl)-1*H*-1,2,3-triazol-1-yl)-4-oxo-6,9,12,15-tetraoxa-3-azaheptadecanoyl)-4-hydroxy-*N*-((*S*)-1-(4-(4-methylthiazol-5-yl)phenyl)ethyl)pyrrolidine-2-carboxamide (97)

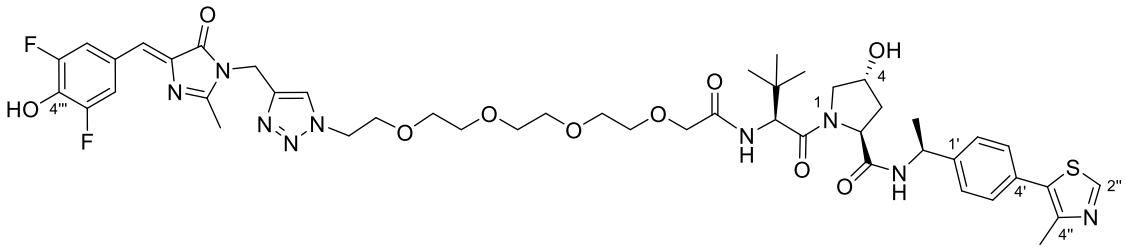

Following General Procedure H, compound **97** was obtained from **89** (112 mg, 0.16 mmol). The crude product was purified by flash column chromatography using a gradient from 0 to 20% MeOH in CH_2Cl_2 to obtain **97** as a yellow solid (128 mg, 82%).

mp 94-97 °C; R_f = 0.54 (CH_2Cl_2/MeOH 9:1); ^{1}H NMR (600 MHz, DMSO-d_6) δ 0.93 (s, 9H, C(CH_3)$_3$), 1.36 (d, J = 7.0 Hz, 3H, CHC$\underline{H}_3$), 1.73 – 1.82 (m, 1H, 3-H), 2.00 – 2.09 (m, 1H, 3-H), 2.42 (s, 3H, CH_3), 2.45 (s, 3H, CH_3), 3.45 – 3.53 (m, 8H, 5-H, OCH_2), 3.53 – 3.58 (m, 3H, OCH_2), 3.58 – 3.62 (m, 3H, OCH_2), 3.80 (t, J = 5.2 Hz, 2H, OCH_2), 3.95 (s, 2H, OCH_2), 4.28 (s, 1H), 4.44 (t, J = 8.2 Hz, 1H), 4.50 (t, J = 5.2 Hz, 2H), 4.54 (d, J = 9.5 Hz, 1H) (2-H, 4-H, NHC$\underline{H}$, NC$\underline{H}_2$$CH_2$), 4.86 (s, 2H, CONC$H_2$), 4.87 – 4.93 (m, 1H, C$\underline{H}$$CH_3$), 5.11 (d, J = 3.5 Hz, 1H, OH), 6.93 (s, 1H, CH), 7.32 – 7.39 (m, 3H), 7.41 – 7.46 (m, 2H) (Ar-H, NH), 7.97 (dd, J = 8.2, 1.8 Hz, 2H, 2‴-H, 6‴-H), 8.05 (s, 1H, NCH), 8.40 (d, J = 7.7 Hz, 1H, NH), 8.97 (s, 1H, 2″-H), 10.93 (br s, 1H, OH); ^{13}C NMR (151 MHz, DMSO) δ 15.6 (CH_3), 15.9 (CH_3), 22.4 (CH$\underline{C}H_3$), 26.2 (C($\underline{C}H_3$)$_3$), 35.1 (CON$\underline{C}H_2$), 35.7 ($\underline{C}$(CH_3)$_3$), 37.7 (C-3), 47.7 ($\underline{C}$HCH_3), 49.4 (N$\underline{C}H_2CH_2$), 55.7, 56.5, 58.5 (C-2, C-5, NHCH), 68.6 (C-4), 68.7, 69.5, 69.6, 69.6, 69.6, 69.7, 69.8, 70.4 (OCH_2), 115.2 (dd, $^2J_{F,C}$ = 16.8 Hz, $^4J_{F,C}$ = 5.4 Hz, C-2‴, C-6‴), 123.5 (CH), 124.5 (t, $^3J_{F,C}$ = 8.6 Hz, C-1‴), 126.3, 128.8, 129.7, 131.1 (C-Ar), 135.8 (t, $^2J_{F,C}$ = 17.3 Hz, C-4‴), 137.9 (N$\underline{C}$CO), 142.2 (NCH), 144.7 (C-Ar), 147.7 (C-4″), 151.4 (C-2″), 151.8 (dd, $^1J_{F,C}$ = 241.4 Hz, $^3J_{F,C}$ = 7.4 Hz, C-3‴, C-5‴), 163.5, 168.5, 169.0, 169.0, 170.4 (NCN, CO). LC-MS (ESI) (90% H_2O to 100% MeCN in 10 min, then 100% MeCN to 15 min, DAD 200-600 nm), t_R = 5.37 min, 99% purity, *m/z* calcd for $C_{47}H_{59}F_2N_9O_{10}S$ [M + H]$^+$, 980.41; found, 980.5. HRMS (ESI) *m/z* calcd for $C_{47}H_{59}F_2N_9O_{10}S$ [M + H]$^+$, 980.4146; found, 980.4155.

(2*S*,4*R*)-1-((*S*)-2-(*tert*-Butyl)-20-(4-((4-((*Z*)-3,5-difluoro-4-hydroxybenzylidene)-2-methyl-5-oxo-4,5-dihydro-1*H*-imidazol-1-yl)methyl)-1*H*-1,2,3-triazol-1-yl)-4-oxo-6,9,12,15,18-pentaoxa-3-azaicosanoyl)-4-hydroxy-*N*-((*S*)-1-(4-(4-methylthiazol-5-yl)phenyl)ethyl)pyrrolidine-2-carboxamide (98)

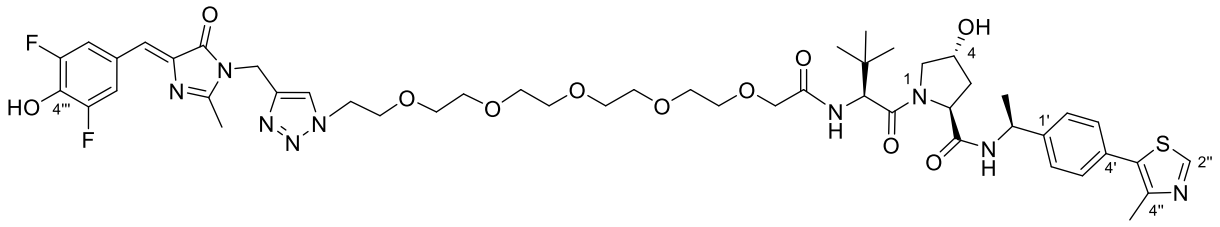

Following General Procedure H, compound **98** was obtained from **90** (120 mg, 0.16 mmol). The crude product was purified by flash column chromatography using a gradient from 0 to 20% MeOH in CH_2Cl_2 to obtain **98** as a yellow solid (140 mg, 85%).

mp 101-102 °C; R_f = 0.54 (CH_2Cl_2/MeOH 9:1); ^{1}H NMR (600 MHz, DMSO-d_6) δ 0.93 (s, 9H, C(CH_3)$_3$), 1.37 (d, J = 7.0 Hz, 3H, CHC$\underline{H}_3$), 1.75 – 1.80 (m, 1H, 3-H), 2.01 – 2.07 (m, 1H, 3-H), 2.42 (s, 3H, CH_3), 2.45 (s, 3H, CH_3), 3.44 – 3.48 (m, 7H, 5-H, OCH_2), 3.49 – 3.54 (m, 5H, OCH_2), 3.54 – 3.58 (m, 3H, OCH_2), 3.58 – 3.63 (m, 3H, OCH_2), 3.80 (t, J = 5.2 Hz, 2H, OCH_2), 3.95 (s, 2H, OCH_2), 4.28 (s, 1H), 4.44 (t, J = 8.2 Hz, 1H), 4.49 (t, J = 5.2 Hz, 2H), 4.54 (d, J = 9.5 Hz, 1H) (2-H, 4-H, NHC$\underline{H}$, NC$\underline{H}_2$CH$_2$), 4.86 (s, 2H, CONCH_2), 4.87 – 4.93 (m, 1H, C$\underline{H}$CH$_3$), 5.11 (d, J = 3.6 Hz, 1H, OH), 6.93 (s, 1H, CH), 7.33 – 7.39 (m, 3H), 7.41 – 7.46 (m, 2H) (Ar-H, NH), 7.97 (dd, J = 8.4, 1.6 Hz, 2H, 2‴-H, 6‴-H), 8.05 (s, 1H, NCH), 8.40 (d, J = 7.7 Hz, 1H, NH), 8.97 (s, 1H, 2″-H), 10.93 (br s, 1H, OH); ^{13}C NMR (151 MHz, DMSO) δ 15.6 (CH_3), 15.9 (CH_3), 22.4 (CH$\underline{C}$H$_3$), 26.2 (C($\underline{C}$H$_3$)$_3$), 35.1 (CON$\underline{C}$H$_2$), 35.7 ($\underline{C}$(CH$_3$)$_3$), 37.7 (C-3), 47.7 ($\underline{C}$HCH$_3$), 49.4 (N$\underline{C}$H$_2$CH$_2$), 55.7, 56.5, 58.5 (C-2, C-5, NHCH), 69.5 (C-4), 69.6, 69.6, 69.7, 69.7, 69.7, 69.8, 70.4 (OCH_2), 115.2 (dd, $^2J_{F,C}$ = 16.5 Hz, $^4J_{F,C}$ = 4.8 Hz, C-2‴, C-6‴), 123.5 (CH), 124.5 (C-1‴), 126.3, 128.8, 129.7, 131.1 (C-Ar), 135.8 (C-4‴), 137.8 (N$\underline{C}$CO), 142.2 (NCH), 144.7 (C-Ar), 147.7 (C-4″), 151.41 (C-2″), 151.8 (dd, $^1J_{F,C}$ = 241.3 Hz, $^3J_{F,C}$ = 7.5 Hz, C-3‴, C-5‴), 163.5, 168.5, 169.0, 169.0, 170.4 (NCN, CO); three CH_2 signals are missing due to overlapping signals. LC-MS (ESI) (90% H_2O to 100% MeCN in 10 min, then 100% MeCN to 15 min, DAD 200-600 nm), t_R = 5.39 min, 99% purity, *m/z* calcd for $C_{49}H_{63}F_2N_9O_{11}S$ $[M + H]^+$, 1024.44; found, 1024.4. HRMS (ESI) *m/z* calcd for $C_{49}H_{63}F_2N_9O_{11}S$ $[M + H]^+$, 1024.4409; found, 1024.4404.

(*Z*)-4-((2-(2-(2-(4-((4-(3,5-Difluoro-4-hydroxybenzylidene)-2-methyl-5-oxo-4,5-dihydro-1*H*-imidazol-1-yl)methyl)-1*H*-1,2,3-triazol-1-yl)ethoxy)ethoxy)ethyl)amino)-2-(2,6-dioxopiperidin-3-yl)isoindoline-1,3-dione (99)

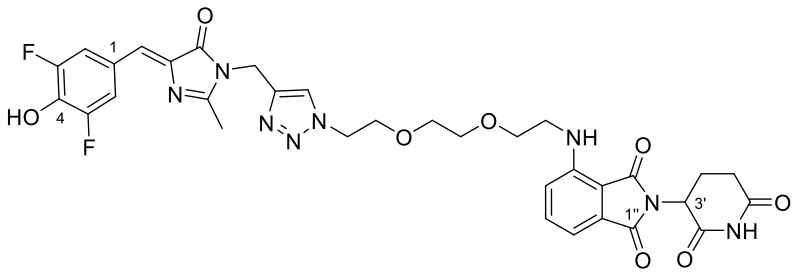

Following General Procedure H, compound **99** was obtained from **91** (69 mg, 0.16 mmol). The crude product was purified by flash column chromatography using a gradient from 0 to 20% MeOH in CH_2Cl_2 to obtain **99** as a yellow solid (36 mg, 32%).

mp 115-117 °C; R_f = 0.65 (CH_2Cl_2/MeOH 9:1); ^{1}H NMR (600 MHz, DMSO-d_6) δ 1.99 – 2.05 (m, 1H, CH_2), 2.41 (s, 3H, CH_3), 2.53 – 2.62 (m, 2H, CH_2), 2.82 – 2.91 (m, 1H, CH_2), 3.37 – 3.45 (m, 2H), 3.51 (s, 4H), 3.56 (t, J = 5.4 Hz, 2H), 3.80 (t, J = 5.2 Hz, 2H) (OCH_2, $NHCH_2$), 4.48 (t, J = 5.2 Hz, 2H, NCH_2CH_2), 4.84 (s, 2H, $CONCH_2$), 5.04 (dd, J = 12.9, 5.5 Hz, 1H, 3′-H), 6.56 (t, J = 5.8 Hz, 1H, $NHCH_2$), 6.90 (s, 1H, CH), 7.02 (d, J = 7.0 Hz, 1H, Ar-H), 7.09 (d, J = 8.5 Hz, 1H, Ar-H), 7.55 (dd, J = 8.5, 7.1 Hz, 1H, Ar-H), 7.91 – 7.94 (m, 2H, 2-H, 6-H), 8.03 (s, 1H, NCH), 10.92 (br s, 1H, OH), 11.06 (s, 1H, NH); ^{13}C NMR (151 MHz, DMSO) δ 15.6 (CH_3), 22.1 (C-4′), 30.9 (C-5′), 35.1 ($CONCH_2$), 41.6 ($NHCH_2$), 48.5 (C-3′), 49.4 (NCH_2CH_2), 68.6, 68.8, 69.5, 69.6 (OCH_2), 109.2, 110.6 (C-3a″, C-7″), 115.1 – 115.3 (m, C-2, C-6), 117.3 (C-5″), 123.5 (CH), 124.5 (t, $^3J_{F,C}$ = 9.7 Hz, C-1), 132.0 (C-7a″), 135.9 (t, $^2J_{F,C}$ = 17.6 Hz, C-4) 136.1 (C-6″), 137.8 (NCCO), 142.2 (NCH), 146.3 (C-4″), 151.8 (dd, $^1J_{F,C}$ = 241.4 Hz, $^3J_{F,C}$ = 7.4 Hz, C-3, C-5), 163.5, 167.2, 168.9, 169.0, 170.0, 172.7 (NCN, CO). LC-MS (ESI) (90% H_2O to 100% MeCN in 10 min, then 100% MeCN to 15 min, DAD 200-600 nm), t_R = 4.54 min, 99% purity, *m/z* calcd for $C_{33}H_{32}F_2N_8O_8$ $[M + H]^+$, 707.24; found, 707.4. HRMS (ESI) *m/z* calcd for $C_{33}H_{32}F_2N_8O_8$ $[M + H]^+$, 707.2384; found, 707.2381.

(*Z*)-4-((2-(2-(2-(2-(4-((4-(3,5-Difluoro-4-hydroxybenzylidene)-2-methyl-5-oxo-4,5-dihydro-1*H*-imidazol-1-yl)methyl)-1*H*-1,2,3-triazol-1-yl)ethoxy)ethoxy)ethoxy)ethyl)amino)-2-(2,6-dioxopiperidin-3-yl)isoindoline-1,3-dione (100)

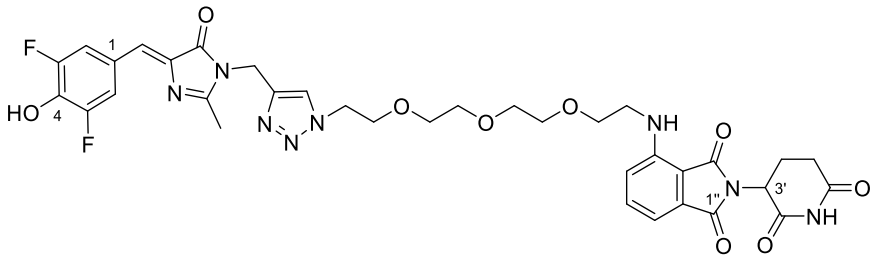

Following General Procedure H, compound **100** was obtained from **92** (76 mg, 0.16 mmol). The crude product was purified by flash column chromatography using a gradient from 0 to 20% MeOH in CH_2Cl_2 to obtain **100** as a yellow solid (63 mg, 53%).

mp 92-94 °C; R_f = 0.65 (CH_2Cl_2/MeOH 9:1); ^{1}H NMR (600 MHz, DMSO-d_6) δ 1.99 – 2.05 (m, 1H, CH_2), 2.41 (s, 3H, CH_3), 2.56 – 2.62 (m, 1H, CH_2), 2.83 – 2.91 (m, 2H, CH_2), 3.41 – 3.50 (m, 8H), 3.52 (dd, J = 5.9, 3.4 Hz, 2H), 3.60 (t, J = 5.4 Hz, 2H), 3.77 (t, J = 5.3 Hz, 2H) (OCH_2, $NHCH_2$), 4.47 (t, J = 5.2 Hz, 2H, NCH_2CH_2), 4.85 (s, 2H, $CONCH_2$), 5.04 (dd, J = 12.9, 5.4 Hz, 1H, 3′-H), 6.57 (t, J = 5.9 Hz, 1H, $NHCH_2$), 6.92 (s, 1H, CH), 7.02 (d, J = 7.0 Hz, 1H, Ar-H), 7.11 (d, J = 8.6 Hz, 1H, Ar-H), 7.56 (dd, J = 8.5, 7.1 Hz, 1H, Ar-H), 7.92 – 7.97 (m, 2H, 2-H, 6-H), 8.03 (s, 1H, NCH), 10.93 (br s, 1H, OH), 11.07 (s, 1H, NH); ^{13}C NMR (151 MHz, DMSO) δ 15.6 (CH_3), 22.1 (C-4′), 31.0 (C-5′), 35.1 ($CONCH_2$), 41.7 ($NHCH_2$), 48.5 (C-3′), 49.4 (NCH_2CH_2), 68.5, 68.8, 69.5, 69.7, 69.7, 69.7 (OCH_2), 109.2, 110.6 (C-3a″, C-7″), 115.2 (dd, $^2J_{F,C}$ = 16.1 Hz, $^4J_{F,C}$ = 4.8 Hz, C-2, C-6), 117.4 (C-5″), 123.5 (CH), 124.4 (t, $^3J_{F,C}$ = 8.0 Hz, C-1), 132.0 (C-7a″), 135.9 (t, $^2J_{F,C}$ = 16.1 Hz, C-4) 136.2 (C-6″), 137.8 ($NCCO$), 142.2 (NCH), 146.4 (C-4″), 151.8 (dd, $^1J_{F,C}$ = 241.3 Hz, $^3J_{F,C}$ = 7.4 Hz, C-3, C-5), 163.5, 167.2, 168.9, 169.0, 170.0, 172.7 (NCN, CO). LC-MS (ESI) (90% H_2O to 100% MeCN in 10 min, then 100% MeCN to 15 min, DAD 200-600 nm), t_R = 5.70 min, 100% purity, *m/z* calcd for $C_{35}H_{36}F_2N_8O_9$ $[M + H]^+$, 751.26; found, 751.5. HRMS (ESI) *m/z* calcd for $C_{35}H_{36}F_2N_8O_9$ $[M + H]^+$, 751,2646; found, 751.2652.

(*Z*)-4-((14-(4-((4-(3,5-Difluoro-4-hydroxybenzylidene)-2-methyl-5-oxo-4,5-dihydro-1*H*-imidazol-1-yl)methyl)-1*H*-1,2,3-triazol-1-yl)-3,6,9,12-tetraoxatetradecyl)amino)-2-(2,6-dioxopiperidin-3-yl)isoindoline-1,3-dione (101)

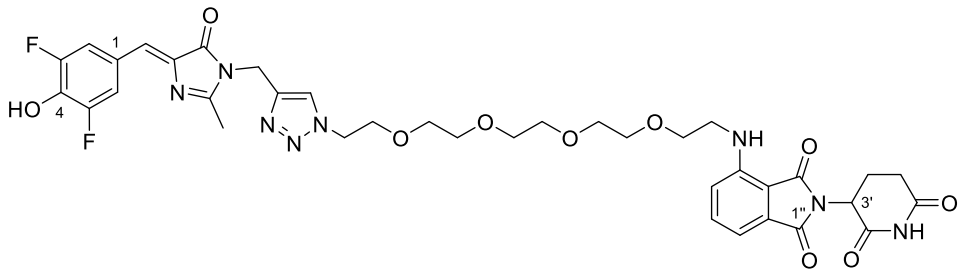

Following General Procedure H, compound **101** was obtained from **93** (83 mg, 0.16 mmol). The crude product was purified by flash column chromatography using a gradient from 0 to 20% MeOH in CH_2Cl_2 to obtain **101** as a yellow solid (59 mg, 46%).

mp 86-89 °C; R_f = 0.63 (CH_2Cl_2/MeOH 9:1); ^{1}H NMR (600 MHz, DMSO-d_6) δ 1.99 – 2.05 (m, 1H, CH_2), 2.41 (s, 3H, CH_3), 2.52 – 2.62 (m, 2H, CH_2), 2.84 – 2.91 (m, 1H, CH_2), 3.42 – 3.49 (m, 10H), 3.49 – 3.55 (m, 4H), 3.60 (t, J = 5.5 Hz, 2H), 3.78 (t, J = 5.2 Hz, 2H) (OCH_2, $NHC\underline{H}_2$), 4.48 (t, J = 5.2 Hz, 2H, $NC\underline{H}_2CH_2$), 4.85 (s, 2H, $CONCH_2$), 5.04 (dd, J = 12.8, 5.4 Hz, 1H, 3′-H), 6.58 (t, J = 5.9 Hz, 1H, $N\underline{H}CH_2$), 6.92 (s, 1H, CH), 7.03 (d, J = 7.0 Hz, 1H, Ar-H), 7.12 (d, J = 8.6 Hz, 1H, Ar-H), 7.56 (dd, J = 8.5, 7.1 Hz, 1H, Ar-H), 7.91 – 7.98 (m, 2H, 2-H, 6-H), 8.04 (s, 1H, NCH), 10.93 (br s, 1H, OH), 11.07 (s, 1H, NH); ^{13}C NMR (151 MHz, DMSO) δ 15.6 (CH_3), 22.1 (C-4′), 31.0 (C-5′), 35.1 ($CON\underline{C}H_2$), 41.7 ($NHCH_2$), 48.5 (C-3′), 49.4 ($N\underline{C}H_2CH_2$), 68.5, 68.8, 69.5, 69.6, 69.7, 69.7, 69.8 (OCH_2), 109.2, 110.6 (C-3a″, C-7″), 115.2 (dd, $^2J_{F,C}$ = 16.1 Hz, $^4J_{F,C}$ = 5.8 Hz, C-2, C-6), 117.4 (C-5″), 123.5 (CH), 124.5 (t, $^3J_{F,C}$ = 9.2 Hz, C-1), 132.1 (C-7a″), 135.9 (t, $^2J_{F,C}$ = 19.4 Hz, C-4), 136.2 (C-6″), 137.8 ($N\underline{C}CO$), 142.2 (NCH), 146.4 (C-4″), 151.8 (dd, $^1J_{F,C}$ = 241.4 Hz, $^3J_{F,C}$ = 7.5 Hz, C-3, C-5), 163.5, 167.2, 168.9, 169.0, 170.0, 172.7 (NCN, CO); one CH_2 signal is missing due to overlapping signals. LC-MS (ESI) (90% H_2O to 100% MeCN in 10 min, then 100% MeCN to 15 min, DAD 200-600 nm), t_R = 4.94 min, 98% purity, *m/z* calcd for $C_{37}H_{40}F_2N_8O_{10}$ $[M + H]^+$, 795.29; found, 795.4. HRMS (ESI) *m/z* calcd for $C_{37}H_{40}F_2N_8O_{10}$ $[M + H]^+$, 795.2908; found, 795.2918.

(*Z*)-4-((17-(4-((4-(3,5-Difluoro-4-hydroxybenzylidene)-2-methyl-5-oxo-4,5-dihydro-1*H*-imidazol-1-yl)methyl)-1*H*-1,2,3-triazol-1-yl)-3,6,9,12,15-pentaoxaheptadecyl)amino)-2-(2,6-dioxopiperidin-3-yl)isoindoline-1,3-dione (102)

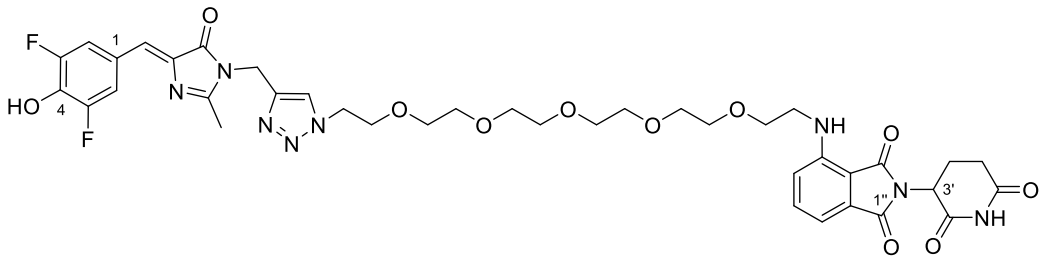

Following General Procedure H, compound **101** was obtained from **94** (90 mg, 0.16 mmol). The crude product was purified by flash column chromatography using a gradient from 0 to 20% MeOH in CH_2Cl_2 to obtain **102** as a yellow solid (80 mg, 60%).

mp 88-90 °C; R_f = 0.63 (CH_2Cl_2/MeOH 9:1); ^{1}H NMR (600 MHz, DMSO-d_6) δ 1.99 – 2.05 (m, 1H, CH_2), 2.42 (s, 3H, CH_3), 2.51 – 2.63 (m, 2H, CH_2), 2.84 – 2.91 (m, 1H, CH_2), 3.42 – 3.50 (m, 14H), 3.50 – 3.56 (m, 4H), 3.61 (t, J = 5.4 Hz, 2H), 3.78 (t, J = 5.2 Hz, 2H) (OCH_2, $NHCH_2$), 4.48 (t, J = 5.2 Hz, 2H, NCH_2CH_2), 4.86 (s, 2H, $CONCH_2$), 5.05 (dd, J = 12.9, 5.4 Hz, 1H, 3′-H), 6.58 (t, J = 5.8 Hz, 1H, $NHCH_2$), 6.92 (s, 1H, CH), 7.03 (d, J = 7.0 Hz, 1H, Ar-H), 7.13 (d, J = 8.6 Hz, 1H, Ar-H), 7.57 (dd, J = 8.5, 7.1 Hz, 1H, Ar-H), 7.96 (dd, J = 8.2, 1.7 Hz, 2H, 2-H, 6-H), 8.04 (s, 1H, NCH), 10.93 (br s, 1H, OH), 11.07 (s, 1H, NH); ^{13}C NMR (151 MHz, DMSO) δ 15.6 (CH_3), 22.1 (C-4′), 31.0 (C-5′), 35.1 ($CONCH_2$), 41.7 ($NHCH_2$), 48.5 (C-3′), 49.4 (NCH_2CH_2), 68.5, 68.9, 69.5, 69.6, 69.7, 69.7, 69.7, 69.8 (OCH_2), 109.2, 110.6 (C-3a″, C-7″), 115.2 (dd, $^2J_{F,C}$ = 17.7 Hz, $^4J_{F,C}$ = 5.0 Hz, C-2, C-6), 117.4 (C-5″), 123.5 (CH), 124.5 (t, $^3J_{F,C}$ = 8.2 Hz, C-1), 132.1 (C-7a″), 135.8 (t, $^2J_{F,C}$ = 17.1 Hz, C-4), 136.2 (C-6″), 137.8 ($NCCO$), 142.2 (NCH), 146.4 (C-4″), 151.8 (dd, $^1J_{F,C}$ = 241.2 Hz, $^3J_{F,C}$ = 7.5 Hz, C-3, C-5), 163.5, 167.2, 168.9, 169.0, 170.0, 172.7 (NCN, CO); two CH_2 signals are missing due to overlapping signals. LC-MS (ESI) (90% H_2O to 100% MeCN in 10 min, then 100% MeCN to 15 min, DAD 200-600 nm), t_R = 5.00 min, 98% purity, *m/z* calcd for $C_{39}H_{44}F_2N_8O_{11}$ $[M + H]^+$, 839.32; found, 839.4. HRMS (ESI) *m/z* calcd for $C_{39}H_{44}F_2N_8O_{11}$ $[M + H]^+$, 839.3170; found, 839.3170.

10 References

(1) Berndsen, C. E.; Wolberger, C. New Insights into Ubiquitin E3 Ligase Mechanism. *Nat. Struct. Mol. Biol.* **2014**, *21*, 301–307.

(2) Ivan, M.; Kondo, K.; Yang, H.; Kim, W.; Valiando, J.; Ohh, M.; Salic, A.; Asara, J. M.; Lane, W. S.; Kaelin, W. G. HIFalpha Targeted for VHL-Mediated Destruction by Proline Hydroxylation: Implications for O2 Sensing. *Science* **2001**, *292*, 464–468.

(3) Jaakkola, P.; Mole, D. R.; Tian, Y. M.; Wilson, M. I.; Gielbert, J.; Gaskell, S. J.; von Kriegsheim, A.; Hebestreit, H. F.; Mukherji, M.; Schofield, C. J.; Maxwell, P. H.; Pugh, C. W.; Ratcliffe, P. J. Targeting of HIF-Alpha to the von Hippel-Lindau Ubiquitylation Complex by O2-Regulated Prolyl Hydroxylation. *Science* **2001**, *292*, 468–472.

(4) Samanta, D.; Semenza, G. L. Maintenance of Redox Homeostasis by Hypoxia-Inducible Factors. *Redox Biol.* **2017**, *13*, 331–335.

(5) Diehl, C. J.; Ciulli, A. Discovery of Small Molecule Ligands for the von Hippel-Lindau (VHL) E3 Ligase and Their Use as Inhibitors and PROTAC Degraders. *Chem. Soc. Rev.* **2022**, *51*, 8216–8257.

(6) Kaelin, W. G. Von Hippel-Lindau Disease: Insights into Oxygen Sensing, Protein Degradation, and Cancer. *J. Clin. Invest.* **2022**, *132*, e162480.

(7) Nguyen, H. C.; Wang, W.; Xiong, Y. Cullin-RING E3 Ubiquitin Ligases: Bridges to Destruction. *Subcell. Biochem.* **2017**, *83*, 323–347.

(8) Shang, F.; Taylor, A. Ubiquitin-Proteasome Pathway and Cellular Responses to Oxidative Stress. *Free Radic. Biol. Med.* **2011**, *51*, 5–16.

(9) Komander, D.; Rape, M. The Ubiquitin Code. *Annu. Rev. Biochem.* **2012**, *81*, 203–229.

(10) Li, K.; Crews, C. M. PROTACs: Past, Present and Future. *Chem. Soc. Rev.* **2022**, *51*, 5214–5236.

(11) Kleiger, G.; Mayor, T. Perilous Journey: A Tour of the Ubiquitin–Proteasome System. *Trends Cell Biol.* **2014**, *24*, 352–359.

(12) Bulatov, E.; Ciulli, A. Targeting Cullin-RING E3 Ubiquitin Ligases for Drug Discovery: Structure, Assembly and Small-Molecule Modulation. *Biochem. J.* **2015**, *467*, 365–386.

(13) Bedford, L.; Lowe, J.; Dick, L. R.; Mayer, R. J.; Brownell, J. E. Ubiquitin-like Protein Conjugation and the Ubiquitin-Proteasome System as Drug Targets. *Nat. Rev. Drug Discov.* **2011**, *10*, 29–46.

(14) Min, J.-H.; Yang, H.; Ivan, M.; Gertler, F.; Kaelin, W. G.; Pavletich, N. P. Structure of an HIF-1alpha -PVHL Complex: Hydroxyproline Recognition in Signaling. *Science* **2002**, *296*, 1886–1889.

(15) Willam, C.; Masson, N.; Tian, Y.-M.; Mahmood, S. A.; Wilson, M. I.; Bicknell, R.; Eckardt, K.-U.; Maxwell, P. H.; Ratcliffe, P. J.; Pugh, C. W. Peptide Blockade of HIFα Degradation Modulates Cellular Metabolism and Angiogenesis. *Proc. Natl. Acad. Sci.* **2002**, *99*, 10423–10428.

(16) Eltzschig, H. K.; Bratton, D. L.; Colgan, S. P. Targeting Hypoxia Signalling for the Treatment of Ischaemic and Inflammatory Diseases. *Nat. Rev. Drug Discov.* **2014**, *13*, 852–869.

(17) Maurer, E.; Gütschow, M.; Stirnberg, M. Matriptase-2 (TMPRSS6) Is Directly up-Regulated by Hypoxia Inducible Factor-1: Identification of a Hypoxia-Responsive Element in the TMPRSS6 Promoter Region. *Biol. Chem.* **2012**, *393*, 535–540.

(18) Strowitzki, M. J.; Cummins, E. P.; Taylor, C. T. Protein Hydroxylation by Hypoxia-Inducible Factor (HIF) Hydroxylases: Unique or Ubiquitous? *Cells* **2019**, *8*, 384.

(19) Latif, F.; Tory, K.; Gnarra, J.; Yao, M.; Duh, F.-M.; Orcutt, M. L.; Stackhouse, T.; Kuzmin, I.; Modi, W.; Geil, L.; Schmidt, L.; Zhou, F.; Li, H.; Wei, M. H.; Chen, F.; Glenn, G.; Choyke, P.; Walther, M. M.; Weng, Y.; Duan, D.-S. R.; Dean, M.; Glavač, D.; Richards, F. M.; Crossey, P. A.; Ferguson-Smith, M. A.; Le Paslier, D.; Chumakov, llya; Cohen, D.; Chinault, A. C.; Maher, E. R.; Linehan, W. M.; Zbar, B.; Lerman, M. I. Identification of the von Hippel-Lindau Disease Tumor Suppressor Gene. *Science* **1993**, *260*, 1317–1320.

(20) Gossage, L.; Eisen, T.; Maher, E. R. VHL, the Story of a Tumour Suppressor Gene. *Nat. Rev. Cancer* **2015**, *15*, 55–64.

(21) Kaelin, W. G. Von Hippel-Lindau Disease. *Annu. Rev. Pathol. Mech. Dis.* **2007**, *2*, 145–173.

(22) Collins, E. T. Intra-Ocular Growths. Two Cases, Brother and Sister, with Peculiar Vascular New-Growth Probably Primarily Retinal, Affecting Both Eyes. *Trans. Ophthalmol. Soc UK* **1894**, No. 14, 141–149.

(23) von Hippel, E. Über Eine sehr seltene Erkrankung der Netzhaut. *Graefes Arch. Ophthalmol.* **1904**, *59*, 83–106.

(24) Lindau, A. Zur Frage der Angiomatosis Retinae und ihrer Hirnkomplikationen. *Acta Ophthalmol.* **1927**, *4*, 193–226.

(25) Maher, E. R.; Neumann, H. P.; Richard, S. Von Hippel–Lindau Disease: A Clinical and Scientific Review. *Eur. J. Hum. Genet.* **2011**, *19*, 617–623.

(26) Iliopoulos, O.; Ohh, M.; Kaelin, W. G. $pVHL_{19}$ Is a Biologically Active Product of the von Hippel–Lindau Gene Arising from Internal Translation Initiation. *Proc. Natl. Acad. Sci.* **1998**, *95*, 11661–11666.

(27) Iliopoulos, O.; Kibel, A.; Gray, S.; Kaelin, W. G. Tumour Suppression by the Human von Hippel-Lindau Gene Product. *Nat. Med.* **1995**, *1*, 822–826.

(28) Schoenfeld, A.; Davidowitz, E. J.; Burk, R. D. A Second Major Native von Hippel-Lindau Gene Product, Initiated from an Internal Translation Start Site, Functions as a Tumor Suppressor. *Proc. Natl. Acad. Sci. U. S. A.* **1998**, *95*, 8817–8822.

(29) Maxwell, P. H.; Wiesener, M. S.; Chang, G.-W.; Clifford, S. C.; Vaux, E. C.; Cockman, M. E.; Wykoff, C. C.; Pugh, C. W.; Maher, E. R.; Ratcliffe, P. J. The Tumour Suppressor Protein VHL Targets Hypoxia-Inducible Factors for Oxygen-Dependent Proteolysis. *Nature* **1999**, *399*, 271–275.

(30) Chowdhury, R.; Candela-Lena, J. I.; Chan, M. C.; Greenald, D. J.; Yeoh, K. K.; Tian, Y.-M.; McDonough, M. A.; Tumber, A.; Rose, N. R.; Conejo-Garcia, A.; Demetriades, M.; Mathavan, S.; Kawamura, A.; Lee, M. K.; van Eeden, F.; Pugh, C. W.; Ratcliffe, P. J.; Schofield, C. J. Selective Small Molecule Probes for the Hypoxia Inducible Factor (HIF) Prolyl Hydroxylases. *ACS Chem. Biol.* **2013**, *8*, 1488–1496.

(31) McDonough, M. A.; McNeill, L. A.; Tilliet, M.; Papamicaël, C. A.; Chen, Q.-Y.; Banerji, B.; Hewitson, K. S.; Schofield, C. J. Selective Inhibition of Factor Inhibiting Hypoxia-Inducible Factor. *J. Am. Chem. Soc.* **2005**, *127*, 7680–7681.

(32) Rentsch, A.; Landsberg, D.; Brodmann, T.; Bülow, L.; Girbig, A.-K.; Kalesse, M. Synthesis and Pharmacology of Proteasome Inhibitors. *Angew. Chem. Int. Ed. Engl.* **2013**, *52*, 5450–5488.

(33) Frost, J.; Galdeano, C.; Soares, P.; Gadd, M. S.; Grzes, K. M.; Ellis, L.; Epemolu, O.; Shimamura, S.; Bantscheff, M.; Grandi, P.; Read, K. D.; Cantrell, D. A.; Rocha, S.; Ciulli, A. Potent and Selective Chemical Probe of Hypoxic Signalling Downstream of HIF-α Hydroxylation via VHL Inhibition. *Nat. Commun.* **2016**, *7*, 13312.

(34) Buckley, D. L.; Van Molle, I.; Gareiss, P. C.; Tae, H. S.; Michel, J.; Noblin, D. J.; Jorgensen, W. L.; Ciulli, A.; Crews, C. M. Targeting the von Hippel-Lindau E3 Ubiquitin Ligase Using Small Molecules to Disrupt the VHL/HIF-1α Interaction. *J. Am. Chem. Soc.* **2012**, *134*, 4465–4468.

(35) Buckley, D. L.; Gustafson, J. L.; Van Molle, I.; Roth, A. G.; Tae, H. S.; Gareiss, P. C.; Jorgensen, W. L.; Ciulli, A.; Crews, C. M. Small-Molecule Inhibitors of the Interaction between the E3 Ligase VHL and HIF1α. *Angew. Chem. Int. Ed Engl.* **2012**, *51*, 11463–11467.

(36) Van Molle, I.; Thomann, A.; Buckley, D. L.; So, E. C.; Lang, S.; Crews, C. M.; Ciulli, A. Dissecting Fragment-Based Lead Discovery at the von Hippel-Lindau Protein:Hypoxia Inducible Factor 1α Protein-Protein Interface. *Chem. Biol.* **2012**, *19*, 1300–1312.

(37) Dias, D. M.; Van Molle, I.; Baud, M. G. J.; Galdeano, C.; Geraldes, C. F. G. C.; Ciulli, A. Is NMR Fragment Screening Fine-Tuned to Assess Druggability of Protein-Protein Interactions? *ACS Med. Chem. Lett.* **2014**, *5*, 23–28.

(38) Galdeano, C.; Gadd, M. S.; Soares, P.; Scaffidi, S.; Van Molle, I.; Birced, I.; Hewitt, S.; Dias, D. M.; Ciulli, A. Structure-Guided Design and Optimization of Small Molecules Targeting the Protein-Protein Interaction between the von Hippel-Lindau (VHL) E3 Ubiquitin Ligase and the Hypoxia Inducible Factor (HIF) Alpha Subunit with in Vitro Nanomolar Affinities. *J. Med. Chem.* **2014**, *57*, 8657–8663.

(39) Soares, P.; Gadd, M. S.; Frost, J.; Galdeano, C.; Ellis, L.; Epemolu, O.; Rocha, S.; Read, K. D.; Ciulli, A. Group-Based Optimization of Potent and Cell-Active Inhibitors of the von Hippel-Lindau (VHL) E3 Ubiquitin Ligase: Structure-Activity Relationships Leading to the Chemical Probe (2*S*,4*R*)-1-((*S*)-2-(1-Cyanocyclopropanecarboxamido)-3,3-dimethylbutanoyl)-4-hydroxy-*N*-(4-(4-methylthiazol-5-yl)benzyl)pyrrolidine-2-carboxamide (VH298). *J. Med. Chem.* **2018**, *61*, 599–618.

(40) Soares, P.; Lucas, X.; Ciulli, A. Thioamide Substitution to Probe the Hydroxyproline Recognition of VHL Ligands. *Bioorg. Med. Chem.* **2018**, *26*, 2992–2995.

(41) Testa, A.; Lucas, X.; Castro, G. V.; Chan, K.-H.; Wright, J. E.; Runcie, A. C.; Gadd, M. S.; Harrison, W. T. A.; Ko, E.-J.; Fletcher, D.; Ciulli, A. 3-Fluoro-4-Hydroxyprolines: Synthesis, Conformational Analysis, and Stereoselective Recognition by the VHL E3 Ubiquitin Ligase for Targeted Protein Degradation. *J. Am. Chem. Soc.* **2018**, *140*, 9299–9313.

(42) de Castro, G. V.; Ciulli, A. Spy vs. Spy: Selecting the Best Reporter for 19F NMR Competition Experiments. *Chem. Commun. Camb. Engl.* **2019**, *55*, 1482–1485.

(43) Raina, K.; Lu, J.; Qian, Y.; Altieri, M.; Gordon, D.; Rossi, A. M. K.; Wang, J.; Chen, X.; Dong, H.; Siu, K.; Winkler, J. D.; Crew, A. P.; Crews, C. M.; Coleman, K. G. PROTAC-Induced BET Protein Degradation as a Therapy for Castration-Resistant Prostate Cancer. *Proc. Natl. Acad. Sci. U. S. A.* **2016**, *113*, 7124–7129.

(44) Han, X.; Wang, C.; Qin, C.; Xiang, W.; Fernandez-Salas, E.; Yang, C.-Y.; Wang, M.; Zhao, L.; Xu, T.; Chinnaswamy, K.; Delproposto, J.; Stuckey, J.; Wang, S. Discovery of

ARD-69 as a Highly Potent Proteolysis Targeting Chimera (PROTAC) Degrader of Androgen Receptor (AR) for the Treatment of Prostate Cancer. *J. Med. Chem.* **2019**, *62*, 941–964.

(45) Hu, J.; Hu, B.; Wang, M.; Xu, F.; Miao, B.; Yang, C.-Y.; Wang, M.; Liu, Z.; Hayes, D. F.; Chinnaswamy, K.; Delproposto, J.; Stuckey, J.; Wang, S. Discovery of ERD-308 as a Highly Potent Proteolysis Targeting Chimera (PROTAC) Degrader of Estrogen Receptor (ER). *J. Med. Chem.* **2019**, *62*, 1420–1442.

(46) Nalawansha, D. A.; Crews, C. M. PROTACs: An Emerging Therapeutic Modality in Precision Medicine. *Cell Chem. Biol.* **2020**, *27*, 998–1014.

(47) Verma, R.; Mohl, D.; Deshaies, R. J. Harnessing the Power of Proteolysis for Targeted Protein Inactivation. *Mol. Cell* **2020**, *77*, 446–460.

(48) Tran, N. L.; Leconte, G. A.; Ferguson, F. M. Targeted Protein Degradation: Design Considerations for PROTAC Development. *Curr. Protoc.* **2022**, *2*, e611.

(49) Krieger, J.; Sorrell, F. J.; Wegener, A. A.; Leuthner, B.; Machrouhi-Porcher, F.; Hecht, M.; Leibrock, E. M.; Müller, J. E.; Eisert, J.; Hartung, I. V.; Schlesiger, S. Systematic Potency and Property Assessment of VHL Ligands and Implications on PROTAC Design. *ChemMedChem* **2023**, *18*, e2022006.

(50) Hopkins, A. L.; Groom, C. R. The Druggable Genome. *Nat. Rev. Drug Discov.* **2002**, *1*, 727–730.

(51) Lai, A. C.; Crews, C. M. Induced Protein Degradation: An Emerging Drug Discovery Paradigm. *Nat. Rev. Drug Discov.* **2017**, *16*, 101–114.

(52) Deshaies, R. J. Prime Time for PROTACs. *Nat. Chem. Biol.* **2015**, *11*, 634–635.

(53) Pettersson, M.; Crews, C. M. PROteolysis TArgeting Chimeras (PROTACs) - Past, Present and Future. *Drug Discov. Today Technol.* **2019**, *31*, 15–27.

(54) Salami, J.; Crews, C. M. Waste Disposal—An Attractive Strategy for Cancer Therapy. *Science* **2017**, *355*, 1163–1167.

(55) Paiva, S.-L.; Crews, C. M. Targeted Protein Degradation: Elements of PROTAC Design. *Curr. Opin. Chem. Biol.* **2019**, *50*, 111–119.

(56) Bond, M. J.; Crews, C. M. Proteolysis Targeting Chimeras (PROTACs) Come of Age: Entering the Third Decade of Targeted Protein Degradation. *RSC Chem. Biol.* **2021**, *2*, 725–742.

(57) Kostic, M.; Jones, L. H. Critical Assessment of Targeted Protein Degradation as a Research Tool and Pharmacological Modality. *Trends Pharmacol. Sci.* **2020**, *41*, 305–317.

(58) Sakamoto, K. M.; Kim, K. B.; Kumagai, A.; Mercurio, F.; Crews, C. M.; Deshaies, R. J. Protacs: Chimeric Molecules That Target Proteins to the Skp1-Cullin-F Box Complex for Ubiquitination and Degradation. *Proc. Natl. Acad. Sci. U. S. A.* **2001**, *98*, 8554–8559.

(59) Sakamoto, K. M.; Kim, K. B.; Verma, R.; Ransick, A.; Stein, B.; Crews, C. M.; Deshaies, R. J. Development of Protacs to Target Cancer-Promoting Proteins for Ubiquitination and Degradation. *Mol. Cell. Proteomics* **2003**, *2*, 1350–1358.

(60) Schneekloth, J. S.; Fonseca, F. N.; Koldobskiy, M.; Mandal, A.; Deshaies, R.; Sakamoto, K.; Crews, C. M. Chemical Genetic Control of Protein Levels: Selective in Vivo Targeted Degradation. *J. Am. Chem. Soc.* **2004**, *126*, 3748–3754.

(61) Schneekloth, A. R.; Pucheault, M.; Tae, H. S.; Crews, C. M. Targeted Intracellular Protein Degradation Induced by a Small Molecule: En Route to Chemical Proteomics. *Bioorg. Med. Chem. Lett.* **2008**, *18*, 5904–5908.

(62) Itoh, Y.; Ishikawa, M.; Naito, M.; Hashimoto, Y. Protein Knockdown Using Methyl Bestatin−Ligand Hybrid Molecules: Design and Synthesis of Inducers of Ubiquitination-Mediated Degradation of Cellular Retinoic Acid-Binding Proteins. *J. Am. Chem. Soc.* **2010**, *132*, 5820–5826.

(63) Ito, T.; Ando, H.; Suzuki, T.; Ogura, T.; Hotta, K.; Imamura, Y.; Yamaguchi, Y.; Handa, H. Identification of a Primary Target of Thalidomide Teratogenicity. *Science* **2010**, *327*, 1345–1350.

(64) Lopez-Girona, A.; Mendy, D.; Ito, T.; Miller, K.; Gandhi, A. K.; Kang, J.; Karasawa, S.; Carmel, G.; Jackson, P.; Abbasian, M.; Mahmoudi, A.; Cathers, B.; Rychak, E.; Gaidarova, S.; Chen, R.; Schafer, P. H.; Handa, H.; Daniel, T. O.; Evans, J. F.; Chopra, R. Cereblon Is a Direct Protein Target for Immunomodulatory and Antiproliferative Activities of Lenalidomide and Pomalidomide. *Leukemia* **2012**, *26*, 2326–2335.

(65) Fischer, E. S.; Böhm, K.; Lydeard, J. R.; Yang, H.; Stadler, M. B.; Cavadini, S.; Nagel, J.; Serluca, F.; Acker, V.; Lingaraju, G. M.; Tichkule, R. B.; Schebesta, M.; Forrester, W. C.; Schirle, M.; Hassiepen, U.; Ottl, J.; Hild, M.; Beckwith, R. E. J.; Harper, J. W.; Jenkins, J. L.; Thomä, N. H. Structure of the DDB1–CRBN E3 Ubiquitin Ligase in Complex with Thalidomide. *Nature* **2014**, *512*, 49–53.

(66) Lu, J.; Qian, Y.; Altieri, M.; Dong, H.; Wang, J.; Raina, K.; Hines, J.; Winkler, J. D.; Crew, A. P.; Coleman, K.; Crews, C. M. Hijacking the E3 Ubiquitin Ligase Cereblon to Efficiently Target BRD4. *Chem. Biol.* **2015**, *22*, 755–763.

(67) Winter, G. E.; Buckley, D. L.; Paulk, J.; Roberts, J. M.; Souza, A.; Dhe-Paganon, S.; Bradner, J. E. Phthalimide Conjugation as a Strategy for in Vivo Target Protein Degradation. *Science* **2015**, *348*, 1376–1381.

(68) Buckley, D. L.; Raina, K.; Darricarrere, N.; Hines, J.; Gustafson, J. L.; Smith, I. E.; Miah, A. H.; Harling, J. D.; Crews, C. M. HaloPROTACS: Use of Small Molecule PROTACs to Induce Degradation of HaloTag Fusion Proteins. *ACS Chem. Biol.* **2015**, *10*, 1831–1837.

(69) Ohana, R. F.; Encell, L. P.; Zhao, K.; Simpson, D.; Slater, M. R.; Urh, M.; Wood, K. V. HaloTag7: A Genetically Engineered Tag That Enhances Bacterial Expression of Soluble Proteins and Improves Protein Purification. *Protein Expr. Purif.* **2009**, *68*, 110–120.

(70) Bondeson, D. P.; Mares, A.; Smith, I. E. D.; Ko, E.; Campos, S.; Miah, A. H.; Mulholland, K. E.; Routly, N.; Buckley, D. L.; Gustafson, J. L.; Zinn, N.; Grandi, P.; Shimamura, S.; Bergamini, G.; Faelth-Savitski, M.; Bantscheff, M.; Cox, C.; Gordon, D. A.; Willard, R. R.; Flanagan, J. J.; Casillas, L. N.; Votta, B. J.; den Besten, W.; Famm, K.; Kruidenier, L.; Carter, P. S.; Harling, J. D.; Churcher, I.; Crews, C. M. Catalytic in Vivo Protein Knockdown by Small-Molecule PROTACs. *Nat. Chem. Biol.* **2015**, *11*, 611–617.

(71) Zengerle, M.; Chan, K.-H.; Ciulli, A. Selective Small Molecule Induced Degradation of the BET Bromodomain Protein BRD4. *ACS Chem. Biol.* **2015**, *10*, 1770–1777.

(72) Mullard, A. Targeted Protein Degraders Crowd into the Clinic. *Nat. Rev. Drug Discov.* **2021**, *20*, 247–250.

(73) Békés, M.; Langley, D. R.; Crews, C. M. PROTAC Targeted Protein Degraders: The Past Is Prologue. *Nat. Rev. Drug Discov.* **2022**, *21*, 181–200.

(74) Cecchini, C.; Pannilunghi, S.; Tardy, S.; Scapozza, L. From Conception to Development: Investigating PROTACs Features for Improved Cell Permeability and Successful Protein Degradation. *Front. Chem.* **2021**, *9*, 672267.

(75) Roy, M. J.; Winkler, S.; Hughes, S. J.; Whitworth, C.; Galant, M.; Farnaby, W.; Rumpel, K.; Ciulli, A. SPR-Measured Dissociation Kinetics of PROTAC Ternary Complexes Influence Target Degradation Rate. *ACS Chem. Biol.* **2019**, *14*, 361–368.

(76) Gadd, M. S.; Testa, A.; Lucas, X.; Chan, K.-H.; Chen, W.; Lamont, D. J.; Zengerle, M.; Ciulli, A. Structural Basis of PROTAC Cooperative Recognition for Selective Protein Degradation. *Nat. Chem. Biol.* **2017**, *13*, 514–521.

(77) Liu, X.; Zhang, X.; Lv, D.; Yuan, Y.; Zheng, G.; Zhou, D. Assays and Technologies for Developing Proteolysis Targeting Chimera Degraders. *Future Med. Chem.* **2020**, *12*, 1155–1179.

(78) Lu, C.; Wang, Z.-X. Quantitative Analysis of Ligand Induced Heterodimerization of Two Distinct Receptors. *Anal. Chem.* **2017**, *89*, 6926–6930.

(79) Douglass, E. F.; Miller, C. J.; Sparer, G.; Shapiro, H.; Spiegel, D. A. A Comprehensive Mathematical Model for Three-Body Binding Equilibria. *J. Am. Chem. Soc.* **2013**, *135*, 6092–6099.

(80) Roy, R. D.; Rosenmund, C.; Stefan, M. I. Cooperative Binding Mitigates the High-Dose Hook Effect. *BMC Syst. Biol.* **2017**, *11*, 74.

(81) Stoltenburg, R.; Reinemann, C.; Strehlitz, B. SELEX—A (r)Evolutionary Method to Generate High-Affinity Nucleic Acid Ligands. *Biomol. Eng.* **2007**, *24*, 381–403.

(82) Ni, S.; Zhuo, Z.; Pan, Y.; Yu, Y.; Li, F.; Liu, J.; Wang, L.; Wu, X.; Li, D.; Wan, Y.; Zhang, L.; Yang, Z.; Zhang, B.-T.; Lu, A.; Zhang, G. Recent Progress in Aptamer Discoveries and Modifications for Therapeutic Applications. *ACS Appl. Mater. Interfaces* **2021**, *13*, 9500–9519.

(83) Tuerk, C.; Gold, L. Systematic Evolution of Ligands by Exponential Enrichment: RNA Ligands to Bacteriophage T4 DNA Polymerase. *Science* **1990**, *249*, 505–510.

(84) Ellington, A. D.; Szostak, J. W. In Vitro Selection of RNA Molecules That Bind Specific Ligands. *Nature* **1990**, *346*, 818–822.

(85) Otte, D.-M.; Choukeife, M.; Patwari, T.; Mayer, G. Nucleic Acid Aptamers: From Basic Research to Clinical Applications. In *Handbook of Chemical Biology of Nucleic Acids*; Sugimoto, N., Ed.; Springer Nature Singapore: Singapore, 2022; pp 1–25.

(86) Darmostuk, M.; Rimpelova, S.; Gbelcova, H.; Ruml, T. Current Approaches in SELEX: An Update to Aptamer Selection Technology. *Biotechnol. Adv.* **2015**, *33*, 1141–1161.

(87) Bunka, D. H. J.; Stockley, P. G. Aptamers Come of Age – at Last. *Nat. Rev. Microbiol.* **2006**, *4*, 588–596.

(88) Zhou, J.; Rossi, J. Aptamers as Targeted Therapeutics: Current Potential and Challenges. *Nat. Rev. Drug Discov.* **2017**, *16*, 181–202.

(89) Zhou, J.; Swiderski, P.; Li, H.; Zhang, J.; Neff, C. P.; Akkina, R.; Rossi, J. J. Selection, Characterization and Application of New RNA HIV Gp 120 Aptamers for Facile Delivery of Dicer Substrate SiRNAs into HIV Infected Cells. *Nucleic Acids Res.* **2009**, *37*, 3094–3109.

(90) Ng, E. W. M.; Shima, D. T.; Calias, P.; Cunningham, E. T.; Guyer, D. R.; Adamis, A. P. Pegaptanib, a Targeted Anti-VEGF Aptamer for Ocular Vascular Disease. *Nat. Rev. Drug Discov.* **2006**, *5*, 123–132.

(91) Zhu, G.; Niu, G.; Chen, X. Aptamer–Drug Conjugates. *Bioconjug. Chem.* **2015**, *26*, 2186–2197.

(92) Kuwahara, M.; Sugimoto, N. Molecular Evolution of Functional Nucleic Acids with Chemical Modifications. *Molecules* **2010**, *15*, 5423–5444.

(93) Gupta, S.; Drolet, D. W.; Wolk, S. K.; Waugh, S. M.; Rohloff, J. C.; Carter, J. D.; Mayfield, W. S.; Otis, M. R.; Fowler, C. R.; Suzuki, T.; Hirota, M.; Ishikawa, Y.; Schneider, D. J.; Janjic, N. Pharmacokinetic Properties of DNA Aptamers with Base Modifications. *Nucleic Acid Ther.* **2017**, *27*, 345–353.

(94) Zhu, G.; Chen, X. Aptamer-Based Targeted Therapy. *Adv. Drug Deliv. Rev.* **2018**, *134*, 65–78.

(95) Martínez-Roque, M. A.; Franco-Urquijo, P. A.; García-Velásquez, V. M.; Choukeife, M.; Mayer, G.; Molina-Ramírez, S. R.; Figueroa-Miranda, G.; Mayer, D.; Alvarez-Salas, L. M. DNA Aptamer Selection for SARS-CoV-2 Spike Glycoprotein Detection. *Anal. Biochem.* **2022**, *645*, 114633.

(96) Schmitz, A.; Weber, A.; Bayin, M.; Breuers, S.; Fieberg, V.; Famulok, M.; Mayer, G. A SARS-CoV-2 Spike Binding DNA Aptamer That Inhibits Pseudovirus Infection by an RBD-Independent Mechanism. *Angew. Chem. Int. Ed.* **2021**, *60*, 10279–10285.

(97) Amini, R.; Zhang, Z.; Li, J.; Gu, J.; Brennan, J. D.; Li, Y. Aptamers for SARS-CoV-2: Isolation, Characterization, and Diagnostic and Therapeutic Developments. *Anal. Sens.* **2022**, *2*, e20220001.

(98) Tipton, K.; Boyce, S. History of the Enzyme Nomenclature System. *Bioinforma. Oxf. Engl.* **2000**, *16*, 34–40.

(99) Puente, X. S.; Sánchez, L. M.; Overall, C. M.; López-Otín, C. Human and Mouse Proteases: A Comparative Genomic Approach. *Nat. Rev. Genet.* **2003**, *4*, 544–558.

(100) Turk, B. Targeting Proteases: Successes, Failures and Future Prospects. *Nat. Rev. Drug Discov.* **2006**, *5*, 785–799.

(101) Rawlings, N. D.; Barrett, A. J.; Bateman, A. MEROPS: The Database of Proteolytic Enzymes, Their Substrates and Inhibitors. *Nucleic Acids Res.* **2012**, *40*, D343–D350.

(102) Hedstrom, L. Serine Protease Mechanism and Specificity. *Chem. Rev.* **2002**, *102*, 4501–4524.

(103) Schechter, I.; Berger, A. On the Size of the Active Site in Proteases. I. Papain. *Biochem. Biophys. Res. Commun.* **1967**, *27*, 157–162.

(104) Blow, D. M. The Tortuous Story of Asp…His…Ser: Structural Analysis of α-Chymotrypsin. *Trends Biochem. Sci.* **1997**, *22*, 405–408.

(105) Kraut, J. Serine Proteases: Structure and Mechanism of Catalysis. *Annu. Rev. Biochem.* **1977**, *46*, 331–358.

(106) Di Cera, E. Serine Proteases. *IUBMB Life* **2009**, *61*, 510–515.

(107) Erez, E.; Fass, D.; Bibi, E. How Intramembrane Proteases Bury Hydrolytic Reactions in the Membrane. *Nature* **2009**, *459*, 371–378.

(108) López-Otín, C.; Bond, J. S. Proteases: Multifunctional Enzymes in Life and Disease. *J. Biol. Chem.* **2008**, *283*, 30433–30437.

(109) Wendelboe, A. M.; Raskob, G. E. Global Burden of Thrombosis: Epidemiologic Aspects. *Circ. Res.* **2016**, *118*, 1340–1347.

(110) Mackman, N.; Bergmeier, W.; Stouffer, G. A.; Weitz, J. I. Therapeutic Strategies for Thrombosis: New Targets and Approaches. *Nat. Rev. Drug Discov.* **2020**, *19*, 333–352.

(111) Alkarithi, G.; Duval, C.; Shi, Y.; Macrae, F. L.; Ariëns, R. A. S. Thrombus Structural Composition in Cardiovascular Disease. *Arterioscler. Thromb. Vasc. Biol.* **2021**, *41*, 2370–2383.

(112) Lundblad, R.; Bradshaw, R.; Gabriel, D.; Ortel, T.; Lawson, J.; Mann, K. A Review of the Therapeutic Uses of Thrombin. *Thromb. Haemost.* **2004**, *91*, 851–860.

(113) Davie, E. W.; Kulman, J. D. An Overview of the Structure and Function of Thrombin. *Semin. Thromb. Hemost.* **2006**, *32*, 3–15.

(114) Wojtukiewicz, M. Z.; Hempel, D.; Sierko, E.; Tucker, S. C.; Honn, K. V. Thrombin—Unique Coagulation System Protein with Multifaceted Impacts on Cancer and Metastasis. *Cancer Metastasis Rev.* **2016**, *35*, 213–233.

(115) Bendas, G.; Borsig, L. Cancer Cell Adhesion and Metastasis: Selectins, Integrins, and the Inhibitory Potential of Heparins. *Int. J. Cell Biol.* **2012**, *2012*, 1–10.

(116) Di Nisio, M.; Middeldorp, S.; Büller, H. R. Direct Thrombin Inhibitors. *N. Engl. J. Med.* **2005**, *353*, 1028–1040.

(117) Keisu, M.; Andersson, T. B. Drug-Induced Liver Injury in Humans: The Case of Ximelagatran. In *Adverse Drug Reactions*; Uetrecht, J., Ed.; Handbook of Experimental Pharmacology; Springer Berlin Heidelberg: Berlin, Heidelberg, 2010; Vol. 196, pp 407–418.

(118) van Ryn, J.; Goss, A.; Hauel, N.; Wienen, W.; Priepke, H.; Nar, H.; Clemens, A. The Discovery of Dabigatran Etexilate. *Front. Pharmacol.* **2013**, *4*.

(119) Nelson, T. D.; LeBlond, C. R.; Frantz, D. E.; Matty, L.; Mitten, J. V.; Weaver, D. G.; Moore, J. C.; Kim, J. M.; Boyd, R.; Kim, P.-Y.; Gbewonyo, K.; Brower, M.; Sturr, M.; McLaughlin, K.; McMasters, D. R.; Kress, M. H.; McNamara, J. M.; Dolling, U. H. Stereoselective Synthesis of a Potent Thrombin Inhibitor by a Novel P2−P3 Lactone Ring Opening. *J. Org. Chem.* **2004**, *69*, 3620–3627.

(120) Morrissette, M. M.; Stauffer, K. J.; Williams, P. D.; Lyle, T. A.; Vacca, J. P.; Krueger, J. A.; Lewis, S. D.; Lucas, B. J.; Wong, B. K.; White, R. B.; Miller-Stein, C.; Lyle, E. A.; Wallace, A. A.; Leonard, Y. M.; Welsh, D. C.; Lynch, J. J.; McMasters, D. R. Low Molecular Weight Thrombin Inhibitors with Excellent Potency, Metabolic Stability, and Oral Bioavailability. *Bioorg. Med. Chem. Lett.* **2004**, *14*, 4161–4164.

(121) Chobanian, H. R.; Pio, B.; Guo, Y.; Shen, H.; Huffman, M. A.; Madeira, M.; Salituro, G.; Terebetski, J. L.; Ormes, J.; Jochnowitz, N.; Hoos, L.; Zhou, Y.; Lewis, D.; Hawes, B.; Mitnaul, L.; O'Neill, K.; Ellsworth, K.; Wang, L.; Biftu, T.; Duffy, J. L. Improved Stability of Proline-Derived Direct Thrombin Inhibitors through Hydroxyl to Heterocycle Replacement. *ACS Med. Chem. Lett.* **2015**, *6*, 553–557.

(122) Kettner, C.; Shaw, E. D-Phe-Pro-ArgCH_2C1-A Selective Affinity Label for Thrombin. *Thromb. Res.* **1979**, *14*, 969–973.

(123) Das, J.; Kimball, S. D. Thrombin Active Site Inhibitors. *Bioorg. Med. Chem.* **1995**, *3*, 999–1007.

(124) Furie, B.; Furie, B. C. The Molecular Basis of Blood Coagulation. *Cell* **1988**, *53*, 505–518.

(125) Davie, E. W.; Fujikawa, K.; Kisiel, W. The Coagulation Cascade: Initiation, Maintenance, and Regulation. *Biochemistry* **1991**, *30*, 10363–10370.

(126) Macfarlane, R. G. An Enzyme Cascade in the Blood Clotting Mechanism, and Its Function as a Biochemical Amplifier. *Nature* **1964**, *202*, 498–499.

(127) Mann, K. G. Thrombin Formation. *Chest* **2003**, *124*, 4S-10S.

(128) Patel, N. R.; Patel, D. V.; Murumkar, P. R.; Yadav, M. R. Contemporary Developments in the Discovery of Selective Factor Xa Inhibitors: A Review. *Eur. J. Med. Chem.* **2016**, *121*, 671–698.

(129) Mackman, N. Triggers, Targets and Treatments for Thrombosis. *Nature* **2008**, *451*, 914–918.

(130) Ansell, J. Factor Xa or Thrombin: Is Factor Xa a Better Target? *J. Thromb. Haemost.* **2007**, *5*, 60–64.

(131) Perzborn, E.; Roehrig, S.; Straub, A.; Kubitza, D.; Misselwitz, F. The Discovery and Development of Rivaroxaban, an Oral, Direct Factor Xa Inhibitor. *Nat. Rev. Drug Discov.* **2011**, *10*, 61–75.

(132) Lassen, M. R.; Davidson, B. L.; Gallus, A.; Pineo, G.; Ansell, J.; Deitchman, D. The Efficacy and Safety of Apixaban, an Oral, Direct Factor Xa Inhibitor, as Thromboprophylaxis in Patients Following Total Knee Replacement. *J. Thromb. Haemost.* **2007**, *5*, 2368–2375.

(133) Parasrampuria, D. A.; Marbury, T.; Matsushima, N.; Chen, S.; Wickremasingha, P. K.; He, L.; Dishy, V.; Brown, K. S. Pharmacokinetics, Safety, and Tolerability of Edoxaban in End-Stage Renal Disease Subjects Undergoing Haemodialysis. *Thromb. Haemost.* **2015**, *113*, 719–727.

(134) Eriksson, B. I.; Quinlan, D. J.; Eikelboom, J. W. Novel Oral Factor Xa and Thrombin Inhibitors in the Management of Thromboembolism. *Annu. Rev. Med.* **2011**, *62*, 41–57.

(135) Velasco, G.; Cal, S.; Quesada, V.; Sánchez, L. M.; López-Otín, C. Matriptase-2, a Membrane-Bound Mosaic Serine Proteinase Predominantly Expressed in Human Liver and Showing Degrading Activity against Extracellular Matrix Proteins. *J. Biol. Chem.* **2002**, *277*, 37637–37646.

(136) Velasco, G.; Cal, S.; Quesada, V.; Sánchez, L. M.; López-Otín, C. Withdrawal: Matriptase-2, a Membrane-Bound Mosaic Serine Proteinase Predominantly Expressed in Human Liver and Showing Degrading Activity against Extracellular Matrix Proteins. *J. Biol. Chem.* **2019**, *294*, 1430.

(137) Ramsay, A., J. The Type II Transmembrane Serine Protease Matriptase-2 - Identification, Structural Features, Enzymology, Expression Pattern and Potential Roles. *Front. Biosci.* **2008**, *13*, 569.

(138) Hooper, J. D.; Clements, J. A.; Quigley, J. P.; Antalis, T. M. Type II Transmembrane Serine Proteases. *J. Biol. Chem.* **2001**, *276*, 857–860.

(139) Szabo, R.; Wu, Q.; Dickson, R.; Netzel-Arnett, S.; Antalis, T.; Bugge, T. Type II Transmembrane Serine Proteases. *Thromb. Haemost.* **2003**, *90*, 185–193.

(140) Bugge, T. H.; Antalis, T. M.; Wu, Q. Type II Transmembrane Serine Proteases. *J. Biol. Chem.* **2009**, *284*, 23177–23181.

(141) Stirnberg, M.; Gütschow, M. Matriptase-2, a Regulatory Protease of Iron Homeostasis: Possible Substrates, Cleavage Sites and Inhibitors. *Curr. Pharm. Des.* **2013**, *19*, 1052–1061.

(142) Du, X.; She, E.; Gelbart, T.; Truksa, J.; Lee, P.; Xia, Y.; Khovananth, K.; Mudd, S.; Mann, N.; Moresco, E. M. Y.; Beutler, E.; Beutler, B. The Serine Protease TMPRSS6 Is Required to Sense Iron Deficiency. *Science* **2008**, *320*, 1088–1092.

(143) Finberg, K. E.; Heeney, M. M.; Campagna, D. R.; Aydinok, Y.; Pearson, H. A.; Hartman, K. R.; Mayo, M. M.; Samuel, S. M.; Strouse, J. J.; Markianos, K.; Andrews, N. C.; Fleming, M. D. Mutations in TMPRSS6 Cause Iron-Refractory Iron Deficiency Anemia (IRIDA). *Nat. Genet.* **2008**, *40*, 569–571.

(144) Folgueras, A. R.; de Lara, F. M.; Pendás, A. M.; Garabaya, C.; Rodríguez, F.; Astudillo, A.; Bernal, T.; Cabanillas, R.; López-Otín, C.; Velasco, G. Membrane-Bound Serine Protease Matriptase-2 (Tmprss6) Is an Essential Regulator of Iron Homeostasis. *Blood* **2008**, *112*, 2539–2545.

(145) Nemeth, E.; Tuttle, M. S.; Powelson, J.; Vaughn, M. B.; Donovan, A.; Ward, D. M.; Ganz, T.; Kaplan, J. Hepcidin Regulates Cellular Iron Efflux by Binding to Ferroportin and Inducing Its Internalization. *Science* **2004**, *306*, 2090–2093.

(146) Ramsay, A. J.; Hooper, J. D.; Folgueras, A. R.; Velasco, G.; Lopez-Otin, C. Matriptase-2 (TMPRSS6): A Proteolytic Regulator of Iron Homeostasis. *Haematologica* **2009**, *94*, 840–849.

(147) Nemeth, E. Targeting the Hepcidin-Ferroportin Axis in the Diagnosis and Treatment of Anemias. *Adv. Hematol.* **2010**, *2010*, 1–9.

(148) Ganz, T.; Nemeth, E. Hepcidin and Iron Homeostasis. *Biochim. Biophys. Acta* **2012**, *1823*, 1434–1443.

(149) Silvestri, L.; Pagani, A.; Nai, A.; De Domenico, I.; Kaplan, J.; Camaschella, C. The Serine Protease Matriptase-2 (TMPRSS6) Inhibits Hepcidin Activation by Cleaving Membrane Hemojuvelin. *Cell Metab.* **2008**, *8*, 502–511.

(150) Hentze, M. W.; Muckenthaler, M. U.; Galy, B.; Camaschella, C. Two to Tango: Regulation of Mammalian Iron Metabolism. *Cell* **2010**, *142*, 24–38.

(151) Finberg, K. E.; Whittlesey, R. L.; Fleming, M. D.; Andrews, N. C. Down-Regulation of Bmp/Smad Signaling by Tmprss6 Is Required for Maintenance of Systemic Iron Homeostasis. *Blood* **2010**, *115*, 3817–3826.

(152) Krijt, J.; Frýdlová, J.; Kukačková, L.; Fujikura, Y.; Přikryl, P.; Vokurka, M.; Nečas, E. Effect of Iron Overload and Iron Deficiency on Liver Hemojuvelin Protein. *PLOS ONE* **2012**, *7*, e37391.

(153) De Falco, L.; Sanchez, M.; Silvestri, L.; Kannengiesser, C.; Muckenthaler, M. U.; Iolascon, A.; Gouya, L.; Camaschella, C.; Beaumont, C. Iron Refractory Iron Deficiency Anemia. *Haematologica* **2013**, *98*, 845–853.

(154) Béliveau, F.; Désilets, A.; Leduc, R. Probing the Substrate Specificities of Matriptase, Matriptase-2, Hepsin and DESC1 with Internally Quenched Fluorescent Peptides. *FEBS J.* **2009**, *276*, 2213–2226.

(155) Wysocka, M.; Gruba, N.; Miecznikowska, A.; Popow-Stellmaszyk, J.; Gütschow, M.; Stirnberg, M.; Furtmann, N.; Bajorath, J.; Lesner, A.; Rolka, K. Substrate Specificity of Human Matriptase-2. *Biochimie* **2014**, *97*, 121–127.

(156) Sisay, M. T.; Steinmetzer, T.; Stirnberg, M.; Maurer, E.; Hammami, M.; Bajorath, J.; Gütschow, M. Identification of the First Low-Molecular-Weight Inhibitors of Matriptase-2. *J. Med. Chem.* **2010**, *53*, 5523–5535.

(157) Hammami, M.; Rühmann, E.; Maurer, E.; Heine, A.; Gütschow, M.; Klebe, G.; Steinmetzer, T. New 3-Amidinophenylalanine-Derived Inhibitors of Matriptase. *MedChemComm* **2012**, *3*, 807.

(158) Dosa, S.; Stirnberg, M.; Lülsdorff, V.; Häußler, D.; Maurer, E.; Gütschow, M. Active Site Mapping of Trypsin, Thrombin and Matriptase-2 by Sulfamoyl Benzamidines. *Bioorg. Med. Chem.* **2012**, *20*, 6489–6505.

(159) Duchêne, D.; Colombo, E.; Désilets, A.; Boudreault, P.-L.; Leduc, R.; Marsault, E.; Najmanovich, R. Analysis of Subpocket Selectivity and Identification of Potent Selective Inhibitors for Matriptase and Matriptase-2. *J. Med. Chem.* **2014**, *57*, 10198–10204.

(160) St-Georges, C.; Désilets, A.; Béliveau, F.; Ghinet, M.; Dion, S. P.; Colombo, É.; Boudreault, P.-L.; Najmanovich, R. J.; Leduc, R.; Marsault, É. Modulating the Selectivity of Matriptase-2 Inhibitors with Unnatural Amino Acids. *Eur. J. Med. Chem.* **2017**, *129*, 110–123.

(161) Janoff, A.; Scherer, J. Mediators of Inflammation in Leukocyte Lysosomes. IX. Elastinolytic Activity in Granules of Human Polymorphonuclear Leukocytes. *J. Exp. Med.* **1968**, *128*, 1137–1155.

(162) Johnson, U.; Ohlsson, K.; Olsson, I. Effects of Granulocyte Neutral Proteases on Complement Components. *Scand. J. Immunol.* **1976**, *5*, 421–426.

(163) McDonald, J. A.; Kelley, D. G. Degradation of Fibronectin by Human Leukocyte Elastase. Release of Biologically Active Fragments. *J. Biol. Chem.* **1980**, *255*, 8848–8858.

(164) Pipoly, D. J.; Crouch, E. C. Degradation of Native Type IV Procollagen by Human Neutrophil Elastase. Implications for Leukocyte-Mediated Degradation of Basement Membranes. *Biochemistry* **1987**, *26*, 5748–5754.

(165) Korkmaz, B.; Moreau, T.; Gauthier, F. Neutrophil Elastase, Proteinase 3 and Cathepsin G: Physicochemical Properties, Activity and Physiopathological Functions. *Biochimie* **2008**, *90*, 227–242.

(166) Hampton, M. B.; Kettle, A. J.; Winterbourn, C. C. Inside the Neutrophil Phagosome: Oxidants, Myeloperoxidase, and Bacterial Killing. *Blood* **1998**, *92*, 3007–3017.

(167) Belaaouaj, A. Neutrophil Elastase-Mediated Killing of Bacteria: Lessons from Targeted Mutagenesis. *Microbes Infect.* **2002**, *4*, 1259–1264.

(168) Brinkmann, V.; Reichard, U.; Goosmann, C.; Fauler, B.; Uhlemann, Y.; Weiss, D. S.; Weinrauch, Y.; Zychlinsky, A. Neutrophil Extracellular Traps Kill Bacteria. *Science* **2004**, *303*, 1532–1535.

(169) Pham, C. T. N. Neutrophil Serine Proteases: Specific Regulators of Inflammation. *Nat. Rev. Immunol.* **2006**, *6*, 541–550.

(170) Henriksen, P.; Sallenave, J. Human Neutrophil Elastase: Mediator and Therapeutic Target in Atherosclerosis. *Int. J. Biochem. Cell Biol.* **2008**, *40*, 1095–1100.

(171) Korkmaz, B.; Horwitz, M. S.; Jenne, D. E.; Gauthier, F. Neutrophil Elastase, Proteinase 3, and Cathepsin G as Therapeutic Targets in Human Diseases. *Pharmacol. Rev.* **2010**, *62*, 726–759.

(172) Khandpur, R.; Carmona-Rivera, C.; Vivekanandan-Giri, A.; Gizinski, A.; Yalavarthi, S.; Knight, J. S.; Friday, S.; Li, S.; Patel, R. M.; Subramanian, V.; Thompson, P.; Chen, P.; Fox, D. A.; Pennathur, S.; Kaplan, M. J. NETs Are a Source of Citrullinated Autoantigens and Stimulate Inflammatory Responses in Rheumatoid Arthritis. *Sci. Transl. Med.* **2013**, *5*, 178ra40.

(173) Siedle, B.; Hrenn, A.; Merfort, I. Natural Compounds as Inhibitors of Human Neutrophil Elastase. *Planta Med.* **2007**, *73*, 401–420.

(174) von Nussbaum, F.; Li, V. M.-J. Neutrophil Elastase Inhibitors for the Treatment of (Cardio)Pulmonary Diseases: Into Clinical Testing with Pre-Adaptive Pharmacophores. *Bioorg. Med. Chem. Lett.* **2015**, *25*, 4370–4381.

(175) Crocetti, L.; Quinn, M.; Schepetkin, I.; Giovannoni, M. A Patenting Perspective on Human Neutrophil Elastase (HNE) Inhibitors (2014-2018) and Their Therapeutic Applications. *Expert Opin. Ther. Pat.* **2019**, *29*, 555–578.

(176) Kawabata, K.; Suzuki, M.; Sugitani, M.; Imaki, K.; Toda, M.; Miyamoto, T. ONO-5046, a Novel Inhibitor of Human Neutrophil Elastase. *Biochem. Biophys. Res. Commun.* **1991**, *177*, 814–820.

(177) Thorpe, M.; Fu, Z.; Chahal, G.; Akula, S.; Kervinen, J.; de Garavilla, L.; Hellman, L. Extended Cleavage Specificity of Human Neutrophil Cathepsin G: A Low Activity

Protease with Dual Chymase and Tryptase-Type Specificities. *PLOS ONE* **2018**, *13*, e0195077.

(178) Belaaouaj, A.; McCarthy, R.; Baumann, M.; Gao, Z.; Ley, T. J.; Abraham, S. N.; Shapiro, S. D. Mice Lacking Neutrophil Elastase Reveal Impaired Host Defense against Gram Negative Bacterial Sepsis. *Nat. Med.* **1998**, *4*, 615–618.

(179) Reeves, E. P.; Lu, H.; Jacobs, H. L.; Messina, C. G. M.; Bolsover, S.; Gabella, G.; Potma, E. O.; Warley, A.; Roes, J.; Segal, A. W. Killing Activity of Neutrophils Is Mediated through Activation of Proteases by K^+ Flux. *Nature* **2002**, *416*, 291–297.

(180) Verma, R.; Mohl, D.; Deshaies, R. J. Harnessing the Power of Proteolysis for Targeted Protein Inactivation. *Mol. Cell* **2020**, *77*, 446–460.

(181) Burslem, G. M.; Crews, C. M. Proteolysis-Targeting Chimeras as Therapeutics and Tools for Biological Discovery. *Cell* **2020**, *181*, 102–114.

(182) Schiedel, M.; Herp, D.; Hammelmann, S.; Swyter, S.; Lehotzky, A.; Robaa, D.; Oláh, J.; Ovádi, J.; Sippl, W.; Jung, M. Chemically Induced Degradation of Sirtuin 2 (Sirt2) by a Proteolysis Targeting Chimera (PROTAC) Based on Sirtuin Rearranging Ligands (SirReals). *J. Med. Chem.* **2018**, *61*, 482–491.

(183) Steinebach, C.; Kehm, H.; Lindner, S.; Vu, L. P.; Köpff, S.; López Mármol, Á.; Weiler, C.; Wagner, K. G.; Reichenzeller, M.; Krönke, J.; Gütschow, M. PROTAC-Mediated Crosstalk between E3 Ligases. *Chem. Commun.* **2019**, *55*, 1821–1824.

(184) Testa, A.; Hughes, S. J.; Lucas, X.; Wright, J. E.; Ciulli, A. Structure-Based Design of a Macrocyclic PROTAC. *Angew. Chem. Int. Ed.* **2020**, *59*, 1727–1734.

(185) Steinebach, C.; Ng, Y. L. D.; Sosič, I.; Lee, C.-S.; Chen, S.; Lindner, S.; Vu, L. P.; Bricelj, A.; Haschemi, R.; Monschke, M.; Steinwarz, E.; Wagner, K. G.; Bendas, G.; Luo, J.; Gütschow, M.; Krönke, J. Systematic Exploration of Different E3 Ubiquitin Ligases: An Approach towards Potent and Selective CDK6 Degraders. *Chem. Sci.* **2020**, *11*, 3474–3486.

(186) Khan, S.; Zhang, X.; Lv, D.; Zhang, Q.; He, Y.; Zhang, P.; Liu, X.; Thummuri, D.; Yuan, Y.; Wiegand, J. S.; Pei, J.; Zhang, W.; Sharma, A.; McCurdy, C. R.; Kuruvilla, V. M.; Baran, N.; Ferrando, A. A.; Kim, Y.-M.; Rogojina, A.; Houghton, P. J.; Huang, G.; Hromas, R.; Konopleva, M.; Zheng, G.; Zhou, D. A Selective BCL-XL PROTAC Degrader Achieves Safe and Potent Antitumor Activity. *Nat. Med.* **2019**, *25*, 1938–1947.

(187) Farnaby, W.; Koegl, M.; Roy, M. J.; Whitworth, C.; Diers, E.; Trainor, N.; Zollman, D.; Steurer, S.; Karolyi-Oezguer, J.; Riedmueller, C.; Gmaschitz, T.; Wachter, J.; Dank, C.; Galant, M.; Sharps, B.; Rumpel, K.; Traxler, E.; Gerstberger, T.; Schnitzer, R.; Petermann, O.; Greb, P.; Weinstabl, H.; Bader, G.; Zoephel, A.; Weiss-Puxbaum, A.; Ehrenhöfer-Wölfer, K.; Wöhrle, S.; Boehmelt, G.; Rinnenthal, J.; Arnhof, H.; Wiechens, N.; Wu, M.-Y.; Owen-Hughes, T.; Ettmayer, P.; Pearson, M.; McConnell, D. B.; Ciulli, A. BAF Complex Vulnerabilities in Cancer Demonstrated via Structure-Based PROTAC Design. *Nat. Chem. Biol.* **2019**, *15*, 672–680.

(188) Lucas, X.; Van Molle, I.; Ciulli, A. Surface Probing by Fragment-Based Screening and Computational Methods Identifies Ligandable Pockets on the von Hippel-Lindau (VHL) E3 Ubiquitin Ligase. *J. Med. Chem.* **2018**, *61*, 7387–7393.

(189) Steinebach, C.; Voell, S. A.; Vu, L. P.; Bricelj, A.; Sosič, I.; Schnakenburg, G.; Gütschow, M. A Facile Synthesis of Ligands for the von Hippel–Lindau E3 Ligase. *Synthesis* **2020**, *52*, 2521–2527.

(190) Bricelj, A.; Steinebach, C.; Kuchta, R.; Gütschow, M.; Sosič, I. E3 Ligase Ligands in Successful PROTACs: An Overview of Syntheses and Linker Attachment Points. *Front. Chem.* **2021**, *9*, 707317.

(191) Maniaci, C.; Hughes, S. J.; Testa, A.; Chen, W.; Lamont, D. J.; Rocha, S.; Alessi, D. R.; Romeo, R.; Ciulli, A. Homo-PROTACs: Bivalent Small-Molecule Dimerizers of the VHL E3 Ubiquitin Ligase to Induce Self-Degradation. *Nat. Commun.* **2017**, *8*, 830.

(192) Zoppi, V.; Hughes, S. J.; Maniaci, C.; Testa, A.; Gmaschitz, T.; Wieshofer, C.; Koegl, M.; Riching, K. M.; Daniels, D. L.; Spallarossa, A.; Ciulli, A. Iterative Design and Optimization of Initially Inactive Proteolysis Targeting Chimeras (PROTACs) Identify VZ185 as a Potent, Fast, and Selective von Hippel-Lindau (VHL) Based Dual Degrader Probe of BRD9 and BRD7. *J. Med. Chem.* **2019**, *62*, 699–726.

(193) Smith, B. E.; Wang, S. L.; Jaime-Figueroa, S.; Harbin, A.; Wang, J.; Hamman, B. D.; Crews, C. M. Differential PROTAC Substrate Specificity Dictated by Orientation of Recruited E3 Ligase. *Nat. Commun.* **2019**, *10*, 131.

(194) Osby, J. O.; Heinzman, S. W.; Ganem, Bruce. Studies on the Mechanism of Transition-Metal-Assisted Sodium Borohydride and Lithium Aluminum Hydride Reductions. *J. Am. Chem. Soc.* **1986**, *108*, 67–72.

(195) Johnson, C. N.; Adelinet, C.; Berdini, V.; Beke, L.; Bonnet, P.; Brehmer, D.; Calo, F.; Coyle, J. E.; Day, P. J.; Frederickson, M.; Freyne, E. J. E.; Gilissen, R. A. H. J.; Hamlett, C. C. F.; Howard, S.; Meerpoel, L.; Mevellec, L.; McMenamin, R.; Pasquier, E.; Patel, S.; Rees, D. C.; Linders, J. T. M. Structure-Based Design of Type II Inhibitors Applied to Maternal Embryonic Leucine Zipper Kinase. *ACS Med. Chem. Lett.* **2015**, *6*, 31–36.

(196) Kaburagi, Y.; Kishi, Y. Operationally Simple and Efficient Workup Procedure for TBAF-Mediated Desilylation: Application to Halichondrin Synthesis. *Org. Lett.* **2007**, *9*, 723–726.

(197) Wynberg, H. The Reimer-Tiemann Reaction. *Chem. Rev.* **1960**, *60*, 169–184.

(198) Hofsløkken, N. U.; Skattebøl, L.; Johansson, F.; Bertilsson, S. K.; Andersson, P. G.; Møller, J.; Senning, A.; Yao, X.-K.; Wang, H.-G.; Tuchagues, J.-P.; Ögren, M. Convenient Method for the Ortho-Formylation of Phenols. *Acta Chem. Scand.* **1999**, *53*, 258–262.

(199) Hansen, T. V.; Skattebøl, L. *Ortho* -Formylation of Phenols; Preparation of 3-Bromosalicylaldehyde: (3-Bromo-2-Hydroxybenzaldehyde). In *Organic Syntheses*; John Wiley & Sons, Inc., Ed.; John Wiley & Sons, Inc.: Hoboken, NJ, USA, 2005; pp 64–68.

(200) McGaughey, G. B.; Gagné, M.; Rappé, A. K. Pi-Stacking Interactions. Alive and Well in Proteins. *J. Biol. Chem.* **1998**, *273*, 15458–15463.

(201) Chipot, C.; Jaffe, R.; Maigret, B.; Pearlman, D. A.; Kollman, P. A. Benzene Dimer: A Good Model for Π−π Interactions in Proteins? A Comparison between the Benzene and the Toluene Dimers in the Gas Phase and in an Aqueous Solution. *J. Am. Chem. Soc.* **1996**, *118*, 11217–11224.

(202) Keuler, T.; König, B.; Bückreiß, N.; Kraft, F. B.; König, P.; Schäker-Hübner, L.; Steinebach, C.; Bendas, G.; Gütschow, M.; Hansen, F. K. Development of the First Non-Hydroxamate Selective HDAC6 Degraders. *Chem. Commun.* **2022**, *58*, 11087–11090.

(203) Murgai, A.; Sosič, I.; Gobec, M.; Lemnitzer, P.; Proj, M.; Wittenburg, S.; Voget, R.; Gütschow, M.; Krönke, J.; Steinebach, C. Targeting the Deubiquitinase USP7 for Degradation with PROTACs. *Chem. Commun.* **2022**, *58*, 8858–8861.

(204) Cubillos-Rojas, M.; Loren, G.; Hakim, Y. Z.; Verdaguer, X.; Riera, A.; Nebreda, A. R. Synthesis and Biological Activity of a VHL-Based PROTAC Specific for P38α. *Cancers* **2023**, *15*, 611.

(205) Ellman, J. A.; Owens, T. D.; Tang, T. P. *N-Tert* -Butanesulfinyl Imines: Versatile Intermediates for the Asymmetric Synthesis of Amines. *Acc. Chem. Res.* **2002**, *35*, 984–995.

(206) Colyer, J. T.; Andersen, N. G.; Tedrow, J. S.; Soukup, T. S.; Faul, M. M. Reversal of Diastereofacial Selectivity in Hydride Reductions of N-Tert-Butanesulfinyl Imines. *J. Org. Chem.* **2006**, *71*, 6859–6862.

(207) Tanuwidjaja, J.; Peltier, H. M.; Ellman, J. A. One-Pot Asymmetric Synthesis of Either Diastereomer of *tert*-Butanesulfinyl-Protected Amines from Ketones. *J. Org. Chem.* **2007**, *72*, 626–629.

(208) Sosič, I.; Bricelj, A.; Steinebach, C. E3 Ligase Ligand Chemistries: From Building Blocks to Protein Degraders. *Chem. Soc. Rev.* **2022**, *51*, 3487–3534.

(209) Banik, S. M.; Pedram, K.; Wisnovsky, S.; Ahn, G.; Riley, N. M.; Bertozzi, C. R. Lysosome-Targeting Chimaeras for Degradation of Extracellular Proteins. *Nature* **2020**, *584*, 291–297.

(210) Ahn, G.; Banik, S. M.; Miller, C. L.; Riley, N. M.; Cochran, J. R.; Bertozzi, C. R. LYTACs That Engage the Asialoglycoprotein Receptor for Targeted Protein Degradation. *Nat. Chem. Biol.* **2021**, *17*, 937–946.

(211) Zhou, Y.; Teng, P.; Montgomery, N. T.; Li, X.; Tang, W. Development of Triantennary N-Acetylgalactosamine Conjugates as Degraders for Extracellular Proteins. *ACS Cent. Sci.* **2021**, *7*, 499–506.

(212) Cotton, A. D.; Nguyen, D. P.; Gramespacher, J. A.; Seiple, I. B.; Wells, J. A. Development of Antibody-Based PROTACs for the Degradation of the Cell-Surface Immune Checkpoint Protein PD-L1. *J. Am. Chem. Soc.* **2021**, *143*, 593–598.

(213) Di Giorgio, A.; Duca, M. New Chemical Modalities Enabling Specific RNA Targeting and Degradation: Application to SARS-CoV-2 RNA. *ACS Cent. Sci.* **2020**, *6*, 1647–1650.

(214) Haniff, H. S.; Tong, Y.; Liu, X.; Chen, J. L.; Suresh, B. M.; Andrews, R. J.; Peterson, J. M.; O'Leary, C. A.; Benhamou, R. I.; Moss, W. N.; Disney, M. D. Targeting the SARS-CoV-2 RNA Genome with Small Molecule Binders and Ribonuclease Targeting Chimera (RIBOTAC) Degraders. *ACS Cent. Sci.* **2020**, *6*, 1713–1721.

(215) Zhang, P.; Liu, X.; Abegg, D.; Tanaka, T.; Tong, Y.; Benhamou, R. I.; Baisden, J.; Crynen, G.; Meyer, S. M.; Cameron, M. D.; Chatterjee, A. K.; Adibekian, A.; Childs-Disney, J. L.; Disney, M. D. Reprogramming of Protein-Targeted Small-Molecule Medicines to RNA by Ribonuclease Recruitment. *J. Am. Chem. Soc.* **2021**, *143*, 13044–13055.

(216) Costales, M. G.; Matsumoto, Y.; Velagapudi, S. P.; Disney, M. D. Small Molecule Targeted Recruitment of a Nuclease to RNA. *J. Am. Chem. Soc.* **2018**, *140*, 6741–6744.

(217) Ji, C. H.; Kim, H. Y.; Lee, M. J.; Heo, A. J.; Park, D. Y.; Lim, S.; Shin, S.; Ganipisetti, S.; Yang, W. S.; Jung, C. A.; Kim, K. Y.; Jeong, E. H.; Park, S. H.; Bin Kim, S.; Lee, S. J.; Na, J. E.; Kang, J. I.; Chi, H. M.; Kim, H. T.; Kim, Y. K.; Kim, B. Y.; Kwon, Y. T. The AUTOTAC Chemical Biology Platform for Targeted Protein Degradation via the Autophagy-Lysosome System. *Nat. Commun.* **2022**, *13*, 904.

(218) Keefe, A. D.; Pai, S.; Ellington, A. Aptamers as Therapeutics. *Nat. Rev. Drug Discov.* **2010**, *9*, 537–550.

(219) Kulkarni, J. A.; Witzigmann, D.; Thomson, S. B.; Chen, S.; Leavitt, B. R.; Cullis, P. R.; van der Meel, R. The Current Landscape of Nucleic Acid Therapeutics. *Nat. Nanotechnol.* **2021**, *16*, 630–643.

(220) Wang, W.; He, S.; Dong, G.; Sheng, C. Nucleic-Acid-Based Targeted Degradation in Drug Discovery. *J. Med. Chem.* **2022**, *65*, 10217–10232.

(221) Ghidini, A.; Cléry, A.; Halloy, F.; Allain, F. H. T.; Hall, J. RNA-PROTACs: Degraders of RNA-Binding Proteins. *Angew. Chem. Int. Ed.* **2021**, *60*, 3163–3169.

(222) Samarasinghe, K. T. G.; Jaime-Figueroa, S.; Burgess, M.; Nalawansha, D. A.; Dai, K.; Hu, Z.; Bebenek, A.; Holley, S. A.; Crews, C. M. Targeted Degradation of Transcription Factors by TRAFTACs: TRAnscription Factor TArgeting Chimeras. *Cell Chem. Biol.* **2021**, *28*, 648-661.e5.

(223) Liu, J.; Chen, H.; Kaniskan, H. Ü.; Xie, L.; Chen, X.; Jin, J.; Wei, W. TF-PROTACs Enable Targeted Degradation of Transcription Factors. *J. Am. Chem. Soc.* **2021**, *143*, 8902–8910.

(224) He, S.; Gao, F.; Ma, J.; Ma, H.; Dong, G.; Sheng, C. Aptamer-PROTAC Conjugates (APCs) for Tumor-Specific Targeting in Breast Cancer. *Angew. Chem. Int. Ed. Engl.* **2021**, *60*, 23299–23305.

(225) Zhang, L.; Li, L.; Wang, X.; Liu, H.; Zhang, Y.; Xie, T.; Zhang, H.; Li, X.; Peng, T.; Sun, X.; Dai, J.; Liu, J.; Wu, W.; Ye, M.; Tan, W. Development of a Novel PROTAC Using the Nucleic Acid Aptamer as a Targeting Ligand for Tumor Selective Degradation of Nucleolin. *Mol. Ther. Nucleic Acids* **2022**, *30*, 66–79.

(226) Paige, J. S.; Wu, K. Y.; Jaffrey, S. R. RNA Mimics of Green Fluorescent Protein. *Science* **2011**, *333*, 642–646.

(227) Paige, J. S.; Nguyen-Duc, T.; Song, W.; Jaffrey, S. R. Fluorescence Imaging of Cellular Metabolites with RNA. *Science* **2012**, *335*, 1194.

(228) Song, W.; Strack, R. L.; Svensen, N.; Jaffrey, S. R. Plug-and-Play Fluorophores Extend the Spectral Properties of Spinach. *J. Am. Chem. Soc.* **2014**, *136*, 1198–1201.

(229) Strack, R. L.; Jaffrey, S. R. Live-Cell Imaging of Mammalian RNAs with Spinach2. In *Methods in Enzymology*; Elsevier, 2015; Vol. 550, pp 129–146.

(230) Autour, A.; Westhof, E.; Ryckelynck, M. ISpinach: A Fluorogenic RNA Aptamer Optimized for in Vitro Applications. *Nucleic Acids Res.* **2016**, *44*, 2491–2500.

(231) Warner, K. D.; Chen, M. C.; Song, W.; Strack, R. L.; Thorn, A.; Jaffrey, S. R.; Ferré-D'Amaré, A. R. Structural Basis for Activity of Highly Efficient RNA Mimics of Green Fluorescent Protein. *Nat. Struct. Mol. Biol.* **2014**, *21*, 658–663.

(232) Okuda, M.; Fourmy, D.; Yoshizawa, S. Use of Baby Spinach and Broccoli for Imaging of Structured Cellular RNAs. *Nucleic Acids Res.* **2017**, *45*, 1404–1415.

(233) Soni, R.; Sharma, D.; Krishna, A. M.; Sathiri, J.; Sharma, A. A Highly Efficient Baby Spinach-Based Minimal Modified Sensor (BSMS) for Nucleic Acid Analysis. *Org. Biomol. Chem.* **2019**, *17*, 7222–7227.

(234) Dao, N. T.; Haselsberger, R.; Khuc, M. T.; Phan, A. T.; Voityuk, A. A.; Michel-Beyerle, M.-E. Photophysics of DFHBI Bound to RNA Aptamer Baby Spinach. *Sci. Rep.* **2021**, *11*, 7356.

(235) Filonov, G. S.; Moon, J. D.; Svensen, N.; Jaffrey, S. R. Broccoli: Rapid Selection of an RNA Mimic of Green Fluorescent Protein by Fluorescence-Based Selection and Directed Evolution. *J. Am. Chem. Soc.* **2014**, *136*, 16299–16308.

(236) You, M.; Litke, J. L.; Jaffrey, S. R. Imaging Metabolite Dynamics in Living Cells Using a Spinach-Based Riboswitch. *Proc. Natl. Acad. Sci.* **2015**, *112*.

(237) Guet, D.; Burns, L. T.; Maji, S.; Boulanger, J.; Hersen, P.; Wente, S. R.; Salamero, J.; Dargemont, C. Combining Spinach-Tagged RNA and Gene Localization to Image Gene Expression in Live Yeast. *Nat. Commun.* **2015**, *6*, 8882.

(238) Fernandez-Millan, P.; Autour, A.; Ennifar, E.; Westhof, E.; Ryckelynck, M. Crystal Structure and Fluorescence Properties of the ISpinach Aptamer in Complex with DFHBI. *RNA* **2017**, *23*, 1788–1795.

(239) Hein, C. D.; Liu, X.-M.; Wang, D. Click Chemistry, A Powerful Tool for Pharmaceutical Sciences. *Pharm. Res.* **2008**, *25*, 2216–2230.

(240) Thirumurugan, P.; Matosiuk, D.; Jozwiak, K. Click Chemistry for Drug Development and Diverse Chemical–Biology Applications. *Chem. Rev.* **2013**, *113*, 4905–4979.

(241) Breugst, M.; Reissig, H. The Huisgen Reaction: Milestones of the 1,3-Dipolar Cycloaddition. *Angew. Chem. Int. Ed.* **2020**, *59*, 12293–12307.

(242) Meldal, M.; Tornøe, C. W. Cu-Catalyzed Azide−Alkyne Cycloaddition. *Chem. Rev.* **2008**, *108*, 2952–3015.

(243) Wurz, R. P.; Dellamaggiore, K.; Dou, H.; Javier, N.; Lo, M.-C.; McCarter, J. D.; Mohl, D.; Sastri, C.; Lipford, J. R.; Cee, V. J. A "Click Chemistry Platform" for the Rapid Synthesis of Bispecific Molecules for Inducing Protein Degradation. *J. Med. Chem.* **2018**, *61*, 453–461.

(244) Fleming, I.; Williams, D. Infrared and Raman Spectra. In *Spectroscopic Methods in Organic Chemistry*; Springer International Publishing: Cham, 2019; pp 85–121.

(245) Smelcerovic, A.; Dzodic, P.; Pavlovic, V.; Cherneva, E.; Yancheva, D. Cyclodidepsipeptides with a Promising Scaffold in Medicinal Chemistry. *Amino Acids* **2014**, *46*, 825–840.

(246) Pavlovic, V.; Djordjevic, A.; Cherneva, E.; Yancheva, D.; Smelcerovic, A. Stimulatory Effect on Rat Thymocytes Proliferation and Antimicrobial Activity of Two 6-(Propan-2-Yl)-4-Methyl-Morpholine-2,5-Diones. *Food Chem. Toxicol. Int. J. Publ. Br. Ind. Biol. Res. Assoc.* **2012**, *50*, 761–766.

(247) Yancheva, D.; Daskalova, L.; Cherneva, E.; Mikhova, B.; Djordjevic, A.; Smelcerovic, Z.; Smelcerovic, A. Synthesis, Structure and Antimicrobial Activity of 6-(Propan-2-Yl)-3-Methyl-Morpholine-2,5-Dione. *J. Mol. Struct.* **2012**, *1016*, 147–154.

(248) An, R.; Ahmed, M.; Li, H.; Wang, Y.; Zhang, A.; Bi, Y.; Yu, Z. Isolation, Purification and Identification of Biological Compounds from Beauveria Sp. and Their Evaluation as Insecticidal Effectiveness against Bemisia Tabaci. *Sci. Rep.* **2021**, *11*, 12020.

(249) Smelcerovic, A.; Rangelov, M.; Smelcerovic, Z.; Veljkovic, A.; Cherneva, E.; Yancheva, D.; Nikolic, G. M.; Petronijevic, Z.; Kocic, G. Two 6-(Propan-2-Yl)-4-Methyl-Morpholine-2,5-Diones as New Non-Purine Xanthine Oxidase Inhibitors and Anti-Inflammatory Agents. *Food Chem. Toxicol.* **2013**, *55*, 493–497.

(250) Vu, L. P.; Gütschow, M. Diketomorpholines: Synthetic Accessibility and Utilization. *ACS Omega* **2022**, *7*, 48–54.

(251) Maryanoff, B. E.; Greco, M. N.; Zhang, H.-C.; Andrade-Gordon, P.; Kauffman, J. A.; Nicolaou, K. C.; Liu, A.; Brungs, P. H. Macrocyclic Peptide Inhibitors of Serine Proteases. Convergent Total Synthesis of Cyclotheonamides A and B via a Late-Stage Primary Amine Intermediate. Study of Thrombin Inhibition under Diverse Conditions. *J. Am. Chem. Soc.* **1995**, *117*, 1225–1239.

(252) Cingolani, G. M.; Di Stefano, A.; Mosciatti, B.; Napolitani, F.; Giorgioni, G.; Ricciutelli, M.; Claudi, F. Synthesis of L-(+)-3-(3-Hydroxy-4-Pivaloyloxybenzyl)-2,5-

Diketomorpholine as Potential Prodrug of L-Dopa. *Bioorg. Med. Chem. Lett.* **2000**, *10*, 1385–1388.

(253) Hughes, A. B.; Sleebs, M. M. Total Synthesis of Bassiatin and Its Stereoisomers: Novel Divergent Behavior of Substrates in Mitsunobu Cyclizations. *J. Org. Chem.* **2005**, *70*, 3079–3088.

(254) Khalil, Z. G.; Huang, X.; Raju, R.; Piggott, A. M.; Capon, R. J. Shornephine A: Structure, Chemical Stability, and P-Glycoprotein Inhibitory Properties of a Rare Diketomorpholine from an Australian Marine-Derived Aspergillus Sp. *J. Org. Chem.* **2014**, *79*, 8700–8705.

(255) Aparicio-Cuevas, M. A.; Rivero-Cruz, I.; Sánchez-Castellanos, M.; Menéndez, D.; Raja, H. A.; Joseph-Nathan, P.; González, M. D. C.; Figueroa, M. Dioxomorpholines and Derivatives from a Marine-Facultative Aspergillus Species. *J. Nat. Prod.* **2017**, *80*, 2311–2318.

(256) Wang, M.-Z.; Si, T.-X.; Ku, C.-F.; Zhang, H.-J.; Li, Z.-M.; Chan, A. S. C. Synthesis of Javanicunines A and B, 9-Deoxy-PF1233s A and B, and Absolute Configuration Establishment of Javanicunine B. *J. Org. Chem.* **2019**, *84*, 831–839.

(257) Shi, C.-X.; Guo, Y.-T.; Wu, Y.-H.; Li, Z.-Y.; Wang, Y.-Z.; Du, F.-S.; Li, Z.-C. Synthesis and Controlled Organobase-Catalyzed Ring-Opening Polymerization of Morpholine-2,5-Dione Derivatives and Monomer Recovery by Acid-Catalyzed Degradation of the Polymers. *Macromolecules* **2019**, *52*, 4260–4269.

(258) Koch, C.-J.; Šimonyiová, S.; Pabel, J.; Kärtner, A.; Polborn, K.; Wanner, K. T. Asymmetric Synthesis with 6-Tert-Butyl-5-Methoxy-6-Methyl-3,6-Dihydro-2H-1,4-Oxazin-2-One as a New Chiral Glycine Equivalent: Preparation of Enantiomerically Pure α-Tertiary and α-Quaternary α-Amino Acids. *Eur. J. Org. Chem.* **2003**, *2003*, 1244–1263.

(259) Pedras, M. S. C.; Chumala, P. B.; Quail, J. W. Chemical Mediators: The Remarkable Structure and Host-Selectivity of Depsilairdin, a Sesquiterpenic Depsipeptide Containing a New Amino Acid. *Org. Lett.* **2004**, *6*, 4615–4617.

(260) Grab, T.; Bräse, S. Efficient Synthesis of Lactate-Containing Depsipeptides by the Mitsunobu Reaction of Lactates. *Adv. Synth. Catal.* **2005**, *347*, 1765–1768.

(261) Fujita, S.; Nishikawa, K.; Iwata, T.; Tomiyama, T.; Ikenaga, H.; Matsumoto, K.; Shindo, M. Asymmetric Total Synthesis of (−)-Stemonamine and Its Stereochemical Stability. *Chem. Eur. J.* **2018**, *24*, 1539–1543.

(262) Scott, B. O.; Siegmund, A. C.; Marlowe, C. K.; Pei, Y.; Spear, K. L. Solid Phase Organic Synthesis (SPOS): A Novel Route to Diketopiperazines and Diketomorpholines. *Mol. Divers.* **1996**, *1*, 125–134.

(263) Szardenings, A. K.; Burkoth, T. S.; Lu, H. H.; Tien, D. W.; Campbell, D. A. A Simple Procedure for the Solid Phase Synthesis of Diketopiperazine and Diketomorpholine Derivatives. *Tetrahedron* **1997**, *53*, 6573–6593.

(264) Tian, W.; Chen, Q.; Yu, C.; Shen, J. Amino-Terminated Poly(Ethylene Glycol) as the Initiator for the Ring-Opening Polymerization of 3-Methylmorpholine-2,5-Dione. *Eur. Polym. J.* **2003**, *39*, 1935–1938.

(265) Feng, Y.; Lu, J.; Behl, M.; Lendlein, A. Progress in Depsipeptide-Based Biomaterials. *Macromol. Biosci.* **2010**, *10*, 1008–1021.

(266) Peng, X.; Behl, M.; Zhang, P.; Mazurek-Budzyńska, M.; Razzaq, M. Y.; Lendlein, A. Hexyl-Modified Morpholine-2,5-Dione-Based Oligodepsipeptides with Relatively Low Glass Transition Temperature. *Polymer* **2016**, *105*, 318–326.

(267) Peng, X.; Behl, M.; Zhang, P.; Mazurek-Budzyńska, M.; Feng, Y.; Lendlein, A. Synthesis of Well-Defined Dihydroxy Telechelics by (Co)Polymerization of Morpholine-2,5-Diones Catalyzed by Sn(IV) Alkoxide. *Macromol. Biosci.* **2018**, *18*, 1800257.

(268) Smelcerovic, A.; Yancheva, D.; Cherneva, E.; Petronijevic, Z.; Lamshoeft, M.; Herebian, D. Identification and Synthesis of Three Cyclodidepsipeptides as Potential Precursors of Enniatin B in Fusarium Sporotrichioides. *J. Mol. Struct.* **2011**, *985*, 397–402.

(269) Trost, B. M.; Bai, W.-J.; Hohn, C.; Bai, Y.; Cregg, J. J. Palladium-Catalyzed Asymmetric Allylic Alkylation of 3-Substituted 1 H-Indoles and Tryptophan Derivatives with Vinylcyclopropanes. *J. Am. Chem. Soc.* **2018**, *140*, 6710–6717.

(270) Nakayama, Y.; Odagaki, Y.; Fujita, S.; Matsuoka, S.; Hamanaka, N.; Nakai, H.; Toda, M. Clarification of Mechanism of Human Sputum Elastase Inhibition by a New Inhibitor, ONO-5046, Using Electrospray Ionization Mass Spectrometry. *Bioorg. Med. Chem. Lett.* **2002**, *12*, 2349–2353.

(271) Al Subeh, Z. Y.; Raja, H. A.; Burdette, J. E.; Falkinham, J. O.; Hemby, S. E.; Oberlies, N. H. Three Diketomorpholines from a Penicillium Sp. (Strain G1071). *Phytochemistry* **2021**, *189*, 112830.

(272) Jiang, C.-X.; Yu, B.; Miao, Y.-M.; Ren, H.; Xu, Q.; Zhao, C.; Tian, L.-L.; Yu, Z.-Q.; Zhou, P.-P.; Wang, X.; Fang, J.; Zhang, J.; Zhang, J. Z.; Wu, Q.-X. Indole Alkaloids from a Soil-Derived *Clonostachys Rosea*. *J. Nat. Prod.* **2021**, *84*, 2468–2474.

(273) Leung, D.; Abbenante, G.; Fairlie, D. P. Protease Inhibitors: Current Status and Future Prospects. *J. Med. Chem.* **2000**, *43*, 305–341.

(274) Powers, J. C.; Asgian, J. L.; Ekici, O. D.; James, K. E. Irreversible Inhibitors of Serine, Cysteine, and Threonine Proteases. *Chem. Rev.* **2002**, *102*, 4639–4750.

(275) Bachovchin, D. A.; Cravatt, B. F. The Pharmacological Landscape and Therapeutic Potential of Serine Hydrolases. *Nat. Rev. Drug Discov.* **2012**, *11*, 52–68.

(276) Luan, B.; Huynh, T.; Cheng, X.; Lan, G.; Wang, H.-R. Targeting Proteases for Treating COVID-19. *J. Proteome Res.* **2020**, *19*, 4316–4326.

(277) Vu, L. P.; Zyulina, M.; Hingst, A.; Schnakenburg, G.; Gütschow, M. Combinatorial Assembly, Traceless Generation and *In Situ* Evaluation of Inhibitors for Therapeutically Relevant Serine Proteases. *Bioorg. Chem.* **2022**, *121*, 105676.

(278) Wiley, M. R.; Chirgadze, N. Y.; Clawson, D. K.; Craft, T. J.; Gifford-Moore, D. S.; Jones, N. D.; Olkowski, J. L.; Weir, L. C.; Smith, G. F. D-Phe-Pro-p-Amidinobenzylamine: A Potent and Highly Selective Thrombin Inhibitor. *Bioorg. Med. Chem. Lett.* **1996**, *6*, 2387–2392.

(279) Tucker, T. J.; Lumma, W. C.; Mulichak, A. M.; Chen, Z.; Naylor-Olsen, A. M.; Lewis, S. D.; Lucas, R.; Freidinger, R. M.; Kuo, L. C. Design of Highly Potent Noncovalent Thrombin Inhibitors That Utilize a Novel Lipophilic Binding Pocket in the Thrombin Active Site. *J. Med. Chem.* **1997**, *40*, 830–832.

(280) Steinmetzer, T.; Sturzebecher, J.; Schuster, O.; Sturzebecher, U.; Schweinitz, A.; Sturzebecher, A. New Substrate Analogue Inhibitors of Factor Xa Containing 4-Amidinobenzylamide as P1 Residue: Part 1. *Med. Chem.* **2006**, *2*, 349–361.

(281) Steinmetzer, T.; Baum, B.; Biela, A.; Klebe, G.; Nowak, G.; Bucha, E. Beyond Heparinization: Design of Highly Potent Thrombin Inhibitors Suitable for Surface Coupling. *ChemMedChem* **2012**, *7*, 1965–1973.

(282) Meyer, D.; Sielaff, F.; Hammami, M.; Böttcher-Friebertshäuser, E.; Garten, W.; Steinmetzer, T. Identification of the First Synthetic Inhibitors of the Type II

Transmembrane Serine Protease TMPRSS2 Suitable for Inhibition of Influenza Virus Activation. *Biochem. J.* **2013**, *452*, 331–343.

(283) Phoo, W. W.; Zhang, Z.; Wirawan, M.; Chew, E. J. C.; Chew, A. B. L.; Kouretova, J.; Steinmetzer, T.; Luo, D. Structures of Zika Virus NS2B-NS3 Protease in Complex with Peptidomimetic Inhibitors. *Antiviral Res.* **2018**, *160*, 17–24.

(284) Stewart, D. E.; Sarkar, A.; Wampler, J. E. Occurrence and Role of Cis Peptide Bonds in Protein Structures. *J. Mol. Biol.* **1990**, *214*, 253–260.

(285) Breidenbach, J.; Lemke, C.; Pillaiyar, T.; Schäkel, L.; Al Hamwi, G.; Diett, M.; Gedschold, R.; Geiger, N.; Lopez, V.; Mirza, S.; Namasivayam, V.; Schiedel, A. C.; Sylvester, K.; Thimm, D.; Vielmuth, C.; Vu, L. P.; Zyulina, M.; Bodem, J.; Gütschow, M.; Müller, C. E. Targeting the Main Protease of SARS-CoV-2: From the Establishment of High Throughput Screening to the Design of Tailored Inhibitors. *Angew. Chem. Int. Ed.* **2021**, *60*, 10423–10429.

(286) Owen, D. R.; Allerton, C. M. N.; Anderson, A. S.; Aschenbrenner, L.; Avery, M.; Berritt, S.; Boras, B.; Cardin, R. D.; Carlo, A.; Coffman, K. J.; Dantonio, A.; Di, L.; Eng, H.; Ferre, R.; Gajiwala, K. S.; Gibson, S. A.; Greasley, S. E.; Hurst, B. L.; Kadar, E. P.; Kalgutkar, A. S.; Lee, J. C.; Lee, J.; Liu, W.; Mason, S. W.; Noell, S.; Novak, J. J.; Obach, R. S.; Ogilvie, K.; Patel, N. C.; Pettersson, M.; Rai, D. K.; Reese, M. R.; Sammons, M. F.; Sathish, J. G.; Singh, R. S. P.; Steppan, C. M.; Stewart, A. E.; Tuttle, J. B.; Updyke, L.; Verhoest, P. R.; Wei, L.; Yang, Q.; Zhu, Y. An Oral SARS-CoV-2 M^{pro} Inhibitor Clinical Candidate for the Treatment of COVID-19. *Science* **2021**, *374*, 1586–1593.

(287) Cantrill, C.; Chaturvedi, P.; Rynn, C.; Petrig Schaffland, J.; Walter, I.; Wittwer, M. B. Fundamental Aspects of DMPK Optimization of Targeted Protein Degraders. *Drug Discov. Today* **2020**, *25*, 969–982.

(288) Lipinski, C. A.; Lombardo, F.; Dominy, B. W.; Feeney, P. J. Experimental and Computational Approaches to Estimate Solubility and Permeability in Drug Discovery and Development Settings. *Adv. Drug Deliv. Rev.* **2001**, *46*, 3–26.

(289) DeGoey, D. A.; Chen, H.-J.; Cox, P. B.; Wendt, M. D. Beyond the Rule of 5: Lessons Learned from AbbVie's Drugs and Compound Collection: Miniperspective. *J. Med. Chem.* **2018**, *61*, 2636–2651.

(290) Zorba, A.; Nguyen, C.; Xu, Y.; Starr, J.; Borzilleri, K.; Smith, J.; Zhu, H.; Farley, K. A.; Ding, W.; Schiemer, J.; Feng, X.; Chang, J. S.; Uccello, D. P.; Young, J. A.; Garcia-Irrizary, C. N.; Czabaniuk, L.; Schuff, B.; Oliver, R.; Montgomery, J.; Hayward, M. M.; Coe, J.; Chen, J.; Niosi, M.; Luthra, S.; Shah, J. C.; El-Kattan, A.; Qiu, X.; West, G. M.; Noe, M. C.; Shanmugasundaram, V.; Gilbert, A. M.; Brown, M. F.; Calabrese, M. F. Delineating the Role of Cooperativity in the Design of Potent PROTACs for BTK. *Proc. Natl. Acad. Sci.* **2018**, *115*, E7285–E7292.

(291) Bemis, T. A.; La Clair, J. J.; Burkart, M. D. Unraveling the Role of Linker Design in Proteolysis Targeting Chimeras: Miniperspective. *J. Med. Chem.* **2021**, *64*, 8042–8052.

(292) Chen, X.; Zhang, D.; Su, N.; Bao, B.; Xie, X.; Zuo, F.; Yang, L.; Wang, H.; Jiang, L.; Lin, Q.; Fang, M.; Li, N.; Hua, X.; Chen, Z.; Bao, C.; Xu, J.; Du, W.; Zhang, L.; Zhao, Y.; Zhu, L.; Loscalzo, J.; Yang, Y. Visualizing RNA Dynamics in Live Cells with Bright and Stable Fluorescent RNAs. *Nat. Biotechnol.* **2019**, *37*, 1287–1293.

(293) Huang, K.; Chen, X.; Li, C.; Song, Q.; Li, H.; Zhu, L.; Yang, Y.; Ren, A. Structure-Based Investigation of Fluorogenic Pepper Aptamer. *Nat. Chem. Biol.* **2021**, *17*, 1289–1295.

(294) Rees, H. C.; Gogacz, W.; Li, N.-S.; Koirala, D.; Piccirilli, J. A. Structural Basis for Fluorescence Activation by Pepper RNA. *ACS Chem. Biol.* **2022**, *17*, 1866–1875.

(295) Riedl, J.; Ménová, P.; Pohl, R.; Orság, P.; Fojta, M.; Hocek, M. GFP-like Fluorophores as DNA Labels for Studying DNA–Protein Interactions. *J. Org. Chem.* **2012**, *77*, 8287–8293.

(296) Migliorini, F.; Dei, F.; Calamante, M.; Maramai, S.; Petricci, E. Micellar Catalysis for Sustainable Hydroformylation. *ChemCatChem* **2021**, *13*, 2794–2806.

(297) Jackson, W.; Perlmutter, P.; Smallridge, A. The Stereochemistry of Organometallic Compounds. XXXII. Hydrocyanation of Derivatives of Amino Alkynes. *Aust. J. Chem.* **1988**, *41*, 1201.

(298) Wu, L.; Burgess, K. Syntheses of Highly Fluorescent GFP-Chromophore Analogues. *J. Am. Chem. Soc.* **2008**, *130*, 4089–4096.

(299) Blanc, A.; Todorovic, M.; Perrin, D. M. Solid-Phase Synthesis of a Novel Phalloidin Analog with on-Bead and off-Bead Actin-Binding Activity. *Chem. Commun.* **2019**, *55*, 385–388.

Appendix

This section contains the full-length papers of the chapters 3, 6, and 7, including the supporting information, and the NMR spectra of compounds reported in the chapters 4 and 5. Please note that the copyright of the papers belongs to the publishers of the respective journals, as indicated by the copyright statements denoted before each paper.

Appendix I. Publication I: A Facile Synthesis of Ligands for the von Hippel-Lindau E3 Ligase

The following pages include the article "A Facile Synthesis of Ligands for the von Hippel–Lindau E3 Ligase" as it was published in Synthesis by Georg Thieme Verlag KG and an adapted version of the supporting information.

Steinebach, C.; Voell, S. A.; Vu, L. P.; Bricelj, A.; Sosič, I.; Schnakenburg, G.; Gütschow, M. A Facile Synthesis of Ligands for the von Hippel–Lindau E3 Ligase. *Synthesis* **2020**, *52*, 2521-2527. doi: 10.1055/s-0040-1707400

Synthesis C. Steinebach et al. PSP

A Facile Synthesis of Ligands for the von Hippel–Lindau E3 Ligase

Christian Steinebach[a]
Sabine Anna Voell[a]
Lan Phuong Vu[a]
Aleša Bricelj[b]
Izidor Sosič[b]
Gregor Schnakenburg[c]
Michael Gütschow*[a]

[a] Pharmaceutical Institute, University of Bonn, An der Immenburg 4, 53121 Bonn, Germany
guetschow@uni-bonn.de
[b] Faculty of Pharmacy, University of Ljubljana, Aškerčeva cesta 7, 1000 Ljubljana, Slovenia
[c] Institute of Inorganic Chemistry, University of Bonn, Gerhard-Domagk-Str. 1, 53121 Bonn, Germany

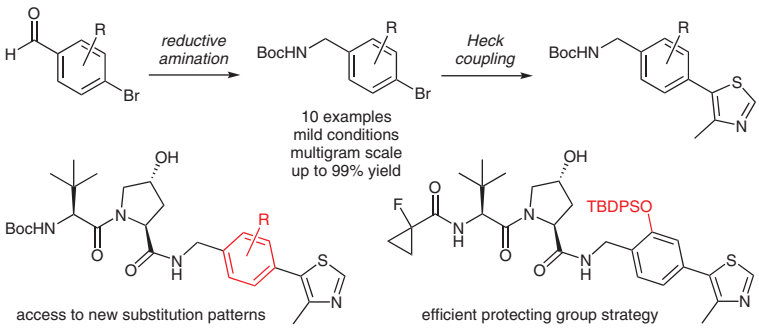

Received: 05.03.2020
Accepted after revision: 06.05.2020
Published online: 27.05.2020
DOI: 10.1055/s-0040-1707400; Art ID: ss-2020-t0128-psp

Abstract The proteolysis-targeting chimeras (PROTACs) have become an integral part of different stages of drug discovery. This growing field, therefore, benefits from advancements in all segments of the design of these compounds. Herein, an efficient and optimized synthetic protocol to various von Hippel-Lindau (VHL) ligands is presented, which enables easy access to multigram quantities of these essential PROTAC building blocks. Moreover, the elaborated synthesis represents a straightforward approach to further explore the chemical space of VHL ligands.

Key words PROTACs, protein degradation, von Hippel–Lindau, VHL, E3 ligase, reductive amination, protecting group

Introduction

Proteolysis-targeting chimeras (PROTACs) have received much attention in drug discovery processes in recent years. These bifunctional molecules consist of a target binding unit, a linker, and an E3 ligase binding moiety. The chemically-mediated orchestration of these tripartite binding events ultimately leads to ubiquitination and proteasomal degradation of target proteins by using the cell's ubiquitin-proteasome system.

E3 ubiquitin ligases such as Cereblon (CRBN) and von Hippel–Lindau (VHL) play a central role in this new technique.[1] In addition to the tremendous success in academic PROTAC research,[2] this novel paradigm is also finding its way into clinical and industrial applications.[3] As shown by the example of CRBN, the development of efficient protocols for the synthesis of ligase ligands is of particular importance for further PROTAC advancements.[4] This work aims at the development of a robust and practical method for multigram synthesis of VHL ligands, which is also potentially relevant for industrial applications. Since structural diversity is an essential aspect in the development of new VHL ligands,[5] the development of novel synthetic routes can provide access to advanced chemical entities.

Two access points have been successfully established for the connection of linkers to a VHL ligand.[6] On the one hand, in several prototypical PROTACs, the amino group of ligand VH032 (**1**, Figure 1) was used, and an amide moiety was generated between the linker and the ligand. On the other hand, the central phenolic group in **2** was utilized for linker attachment via an ether bridge. Compound **2** represents an exemplary member of this chemotype of VHL ligands. Affinity to VHL is maintained when the cyano group of **2** is replaced by fluorine or when a 3-methyl-2-(1-oxoisoindolin-2-yl)butanoyl residue is attached to the hydroxyproline (Hyp) nitrogen.[5b,6b]

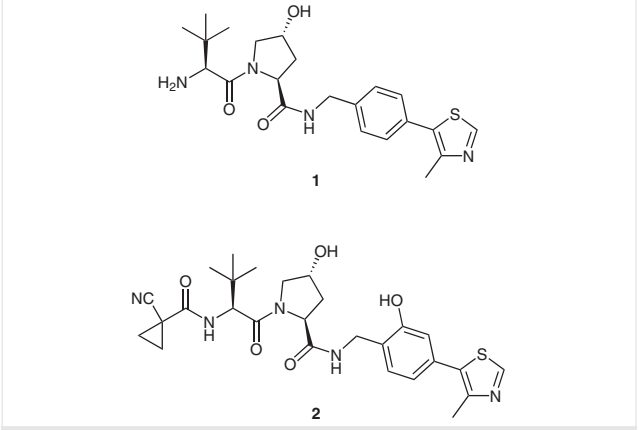

Figure 1 Selected building blocks for VHL-based PROTACs

Whereas the initially published synthetic route towards VHL ligand **1** started from 4-bromobenzonitrile,[7] recent studies made use of commercially available 4-bromobenzylamine.[5g]

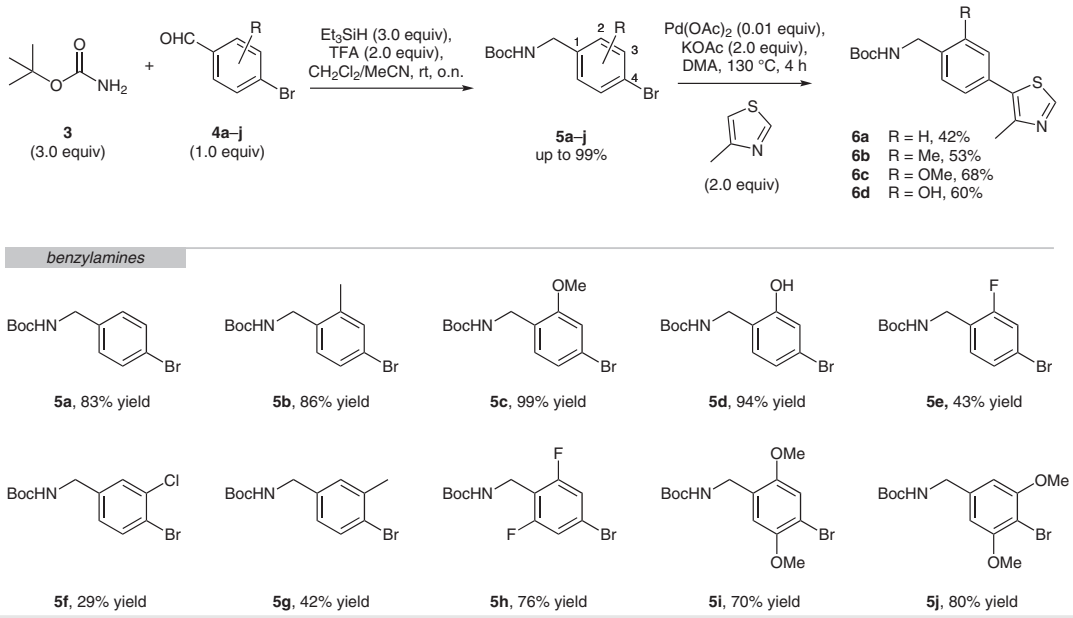

Scheme 1 Synthesis of Boc-protected 4-bromobenzylamines and their use as building blocks for new VHL ligand

In this study, we sought for an easy access to multigram quantities of such benzylamine building blocks useful for the synthesis of established and novel ligands for the E3 ligase VHL, which is a crucial player in the PROTAC field.

As the key step of the newly envisaged strategy, *tert*-butyl carbamate (**3**) was reacted with readily available 4-bromobenzaldehydes **4a–j**. The corresponding reductive amination reactions utilized **3** as the nitrogen and triethylsilane as the hydrogen source.[8] These reactions proceeded under very mild conditions and allowed us to establish a scalable synthetic protocol for the assembly of protected intermediates **5a–j** with attractive substitution patterns (Scheme 1). These include 2-substituted derivatives **5b–e**, 3-substituted derivatives **5f** and **5g**, and highly functionalized arenes such as **5h–j**. The Boc-amino group was compatible with the subsequent Heck coupling, as exemplified by the further conversions to give the biaryl building blocks **6**. Our method proceeded with fair to excellent yields in both steps. The facile access to VHL building blocks **6a–c** allowed us to assemble known and to contrive advanced VHL ligands of

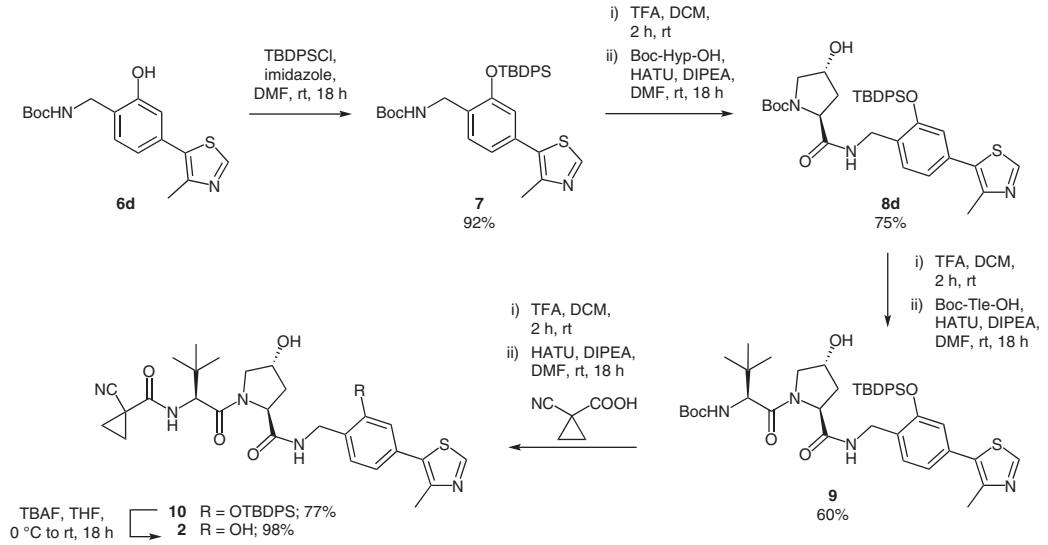

Scheme 2 New protecting group strategy for the synthesis of phenolic VHL ligands

chemotype **1**. The Boc-amino groups were deprotected quantitatively and employed in the peptide syntheses of VHL ligands (see Supporting Information).

Scope and Limitations

Derivative **6d**, containing a hydroxyl group in position 2, represents an important precursor for the synthesis of phenolic VHL ligands of chemotype **2**. Compound **6d** was synthesized in high yield starting from 4-bromosalicylic aldehyde (**4d**). In the subsequent three amide couplings, we paid attention to a reported side reaction, which occurs as an undesired acylation of the phenolic moiety.[6a,9,10] To circumvent such diacylated side products, we introduced a protecting group, which is stable under a variety of conditions and yet labile for deprotection. Accordingly, **6d** was converted with *tert*-butyldiphenylsilyl chloride (TBDPSCl) into the silyl ether **7** (Scheme 2). After conducting two HATU-promoted amide coupling reactions, the orthogonally protected intermediate **9** was obtained. This compound can be employed in the design of PROTACs using multiple exit vectors.[2f] By introducing the 1-cyanocyclopropyl capping group, the TBDPS-protected precursor **10** was obtained. The silyl protecting group is known to be readily cleavable with fluorine reagents, such as tetrabutylammonium fluoride (TBAF),[11] which we applied with THF as a solvent to obtain the desired VHL ligand **2**. Although including two more steps, this new route is an improvement since it avoids multiple side reactions, and good to excellent yields were achieved throughout the synthesis.

Besides **10**, the protected analogue **11** bearing a fluorine substituent in place of the cyano group was prepared accordingly (Figure 2), which represents a further important precursor for the assembly of VHL-based PROTACs.[6b] Moreover, the isoindolinyl derivative **12** and its non-VHL-binding stereoisomer **13** (Figure 2), which were previously used as precursors for HaloPROTACs,[12] that is, small molecules to induce the degradation of HaloTag fusion proteins, were prepared using this optimized route.

The key entry steps towards VHL ligands are the reductive amination and Heck coupling. They can be reproducibly performed on multigram scales. The synthetic route commenced with 4-halobenzaldehydes, which are commercially available or easily accessible.[14] This allows for the incorporation of further building blocks, to ultimately generate new VHL ligands such as **15** and **16** (Figure 2) and establish novel insights into structure-activity relationships concerning structural diversity at the phenyl part of VHL ligands.

Further investigations are needed to overcome one limitation of the reported process, that is, the lacking opportunity to introduce a substituent at the benzylic methylene position. Such modifications are attractive in the light of the reported increased affinity to VHL.[15]

In summary, we have developed a highly efficient protocol for the robust synthesis of multigram quantities of VHL ligands. Several precursors for valuable VHL ligands were successfully prepared through a synthetic route comprising clear advantages over previously reported procedures. In addition to the ease of synthesis and purification, the synthetic strategy can easily be accommodated for a broad scope of new tailored VHL ligands.

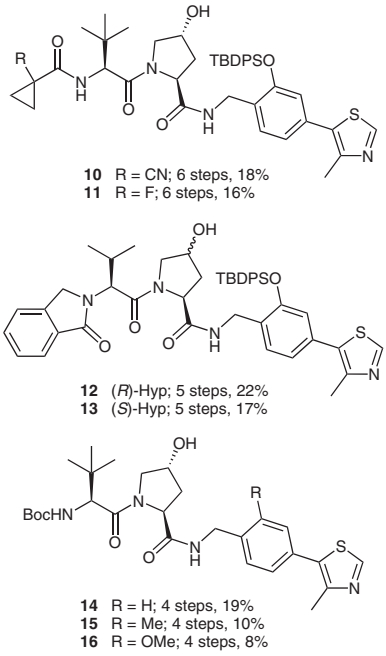

Figure 2 Synthesized VHL ligands via the new reaction sequences

The structures of the newly synthesized compounds were in accordance with analytical data (see Supporting Information). Finally, to unambiguously confirm one of our syntheses, we subjected **14** (Figure 2) to an X-ray diffraction analysis (Figure 3). As expected, *tert*-leucine and hydroxyproline are connected via a *trans* peptide bond as indicated by the omega torsion angle of 179.8°. The planes of the phenyl and methylthiazole part are twisted with respect to each other by 29°.

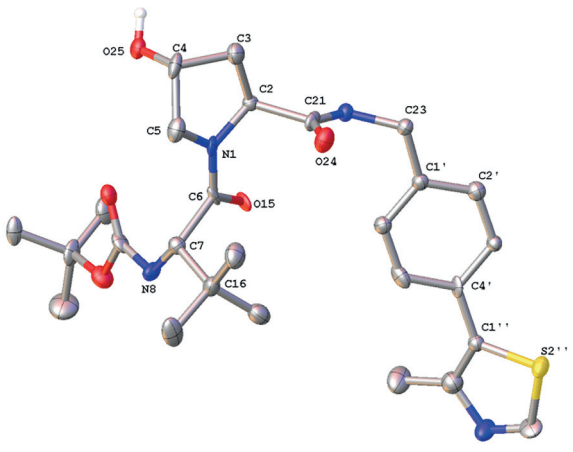

Figure 3 Molecular plot of the Boc-protected VHL ligand **14** showing the 2*S*,4*R*-stereochemistry of hydroxyproline[13]

Preparative column chromatography was performed using Merck silica gel 60 (63–200 mesh) or using an automated flash chromatography system CombiFlash Rf 200. Petroleum ether (PE) used was a mixture of alkanes boiling between 40–60 °C. Melting points were determined on a Büchi 510 oil bath apparatus or on a Reichelt hot-stage apparatus and are uncorrected. ^{1}H NMR and ^{13}C NMR spectra were recorded on a Bruker Avance 400 MHz NMR spectrometer, Bruker Avance 500 MHz NMR spectrometer or on a Bruker Avance III 600 MHz NMR spectrometer, respectively. NMR spectra were processed and analyzed in MestReNova. Chemical shifts are given in parts per million (ppm), coupling constants *J* are given in hertz (Hz), and standard abbreviations are used to indicate spin multiplicities. All multiplets related with $J_{C,F}$ couplings in ^{13}C NMR spectra are centered. In case of overlapping extraneous solvent peaks, multiplet analyses in ^{1}H NMR spectra were performed using qGSD (quantitative Global Spectral Deconvolution). In the case of rotamers, only the peaks for the major rotamer are given, resonance assignments were made based on one- and two-dimensional NMR techniques, which include ^{1}H, ^{13}C, DEPT, HSQC, and HMBC experiments. HRMS was recorded on a micrOTOF-Q mass spectrometer (Bruker) with ESI-source coupled with an HPLC Dionex UltiMate 3000 (Thermo Scientific). The purity and identity of the compounds were determined by HPLC-UV obtained on an LC-MS instrument (Applied Biosystems API 2000 LC/MS/MS, HPLC Agilent 1100) or separately on an LC instrument (Acquity UPLC) and mass spectrometer (Thermo Scientific Q Exactive Plus). The purity of all the final compounds was confirmed to be ≥95% purity by LC.

Reductive Amination with Hydrosilanes; General Procedure I

tert-Butyl carbamate (**3**; 17.57 g, 150 mmol) and the corresponding benzaldehyde **4** (50 mmol) were dissolved in CH_2Cl_2 (100 mL) and MeCN (300 mL). Et_3SiH (17.44 g, 23.96 mL, 150 mmol) was slowly added followed by the dropwise addition of trifluoroacetic acid (11.40 g, 7.65 mL, 100 mmol). After stirring for 18 h at rt, the mixture was carefully quenched by the addition of sat. aq $NaHCO_3$ (100 mL) and the aqueous layer was extracted with CH_2Cl_2 (3 × 100 mL). The combined organic phases were washed with brine (100 mL), dried (Na_2SO_4), filtered, and concentrated in vacuo.

Heck Coupling; General Procedure II

The corresponding bromoaryl compound **5** (25 mmol), $Pd(OAc)_2$ (56 mg, 0.25 mmol), and anhyd K_2CO_3 (4.91 g, 50 mmol) were dissolved in *N*,*N*-dimethylacetamide (25 mL). 4-Methylthiazole (4.96 g, 4.55 mL, 50 mmol) was added, and the solution was heated to 130 °C under an argon atmosphere for 4 h. Subsequently, the mixture was cooled to rt, diluted with H_2O (100 mL), and extracted with CH_2Cl_2 (3 × 100 mL). The combined organic layers were washed with brine (100 mL), dried (Na_2SO_4), filtered, and concentrated in vacuo.

TBDPS-Protection; General Procedure III

The corresponding phenol **6d** (15 mmol) was dissolved in anhyd DMF (30 mL), and imidazole (2.04 g, 30 mmol) was added. Subsequently, *tert*-butyldiphenylsilyl chloride (4.33 g, 4.10 mL, 15.75 mmol) was added dropwise. The mixture was allowed to stir at rt for 18 h, after which it was quenched by the addition of EtOH (1 mL). H_2O (150 mL) was added, and the mixture was extracted with CH_2Cl_2 (2 × 150 mL). The combined organic layers were washed with brine (150 mL), dried (Na_2SO_4), filtered, and concentrated in vacuo.

Boc Deprotection and HATU Coupling;[2e] General Procedure IV

The corresponding Boc-protected amine (1 equiv) was dissolved in anhyd CH_2Cl_2 (5 mL/mmol), and TFA (5 mL/mmol) was added. The mixture was stirred at rt for 2 h. After removal of the volatiles, the oily residue was further dried under high vacuum. The crude deprotected amine was dissolved in anhyd DMF (5 mL/mmol), and the appropriate acid (1 equiv) was added. While stirring the solution, DIPEA (4 equiv) was added, followed by the addition of HATU (1.1 equiv) after 5 min. The mixture was stirred at rt for 1 h, after which H_2O (50 mL/mmol) was added, and extracted with EtOAc (3 × 25 mL/mmol). The combined organic phases were washed with brine (50 mL/mmol), dried (Na_2SO_4), filtered, and concentrated in vacuo.

(2*S*,4*R*)-4-Hydroxy-*N*-{[2-hydroxy-4-(4-methylthiazol-5-yl)phenyl]methyl}-1-{(2*S*)-2-[(1-isocyanocyclopropanecarbonyl)amino]-3,3-dimethylbutanoyl}pyrrolidine-2-carboxamide (2)

[CAS Reg. No. 2244684-43-1]

Silyl ether **10** (0.78 g, 1.0 mmol) was dissolved in anhyd THF (10 mL) and cooled to 0 °C. TBAF (1 M in THF, 3 mL) was added and the mixture was stirred for 18 h at rt. It was quenched by the addition of sat. aq NH_4Cl (100 mL) and extracted with CH_2Cl_2 (3 × 50 mL). The combined organic layers were washed with aq 1 N HCl and brine (each 100 mL), dried (Na_2SO_4), filtered, and concentrated in vacuo. The crude product was purified by column chromatography (CH_2Cl_2/MeOH 19:1) to obtain a colorless solid; yield: 0.53 g (98%); mp 128–130 °C (lit. mp: no report found); R_f = 0.38 (CH_2Cl_2/MeOH 9:1).

^{1}H NMR (600 MHz, DMSO-d_6): δ = 0.94 [s, 9 H, C(CH_3)$_3$], 1.45–1.52 (m, 2 H), 1.57–1.65 (m, 2 H, 2‴-H), 1.87–1.93 (m, 1 H), 2.03–2.09 (m, 1 H, 3-H), 2.43 (s, 3 H, CH_3), 3.55 (d, *J* = 10.8 Hz, 1 H), 3.60–3.65 (m, 1 H, 5-H), 4.15–4.27 (m, 2 H), 4.31–4.37 (m, 1 H), 4.47–4.53 (m, 2 H, 2-H, 4-H, NHC*H*, NHC*H*$_2$), 5.13 (d, *J* = 3.6 Hz, 1 H, OH), 6.82 (d, *J* = 7.8 Hz, 1 H), 6.87–6.93 (m, 1 H), 7.28–7.36 (m, 2 H, ArH, CONH), 8.49 (t, *J* = 6.0 Hz, 1 H, CONH), 8.94 (s, 1 H, 2″-H), 9.78 (s, 1 H, ArO*H*).

^{13}C NMR (151 MHz, DMSO-d_6): δ = 13.90 (C-1‴), 16.22 (CH_3), 16.77, 16.95 (C-2‴), 26.25 [C(*C*H$_3$)$_3$], 36.39 [*C*(CH$_3$)$_3$], 37.48 (C-3), 38.02 (NHCH$_2$), 56.78, 57.52, 58.93 (C-2, C-5, NHCH), 69.05 (C-4), 115.19 (C-3′), 119.49 (C-5′), 120.28 (CN), 125.39 (C-1′), 128.71 (C-6′), 130.83, 131.47 (C-4′, C-5″), 147.63 (C-4″), 151.40 (C-2″), 154.97 (C-2′), 164.59, 168.87, 172.07 (C=O).

LC-MS (ESI): *m*/*z* [M + H]$^+$ calcd for $C_{27}H_{33}N_5O_5S$: 540.22; found: 540.3.

HRMS (ESI): *m*/*z* [M + H]$^+$ calcd for $C_{27}H_{33}N_5O_5S$: 540.2236; found: 540.2264.

tert-Butyl *N*-[(4-Bromophenyl)methyl]carbamate (5a)

[CAS Reg. No. 68819-84-1]

This compound was prepared using General Procedure I and 4-bromobenzaldehyde (**4a**; 9.25 g). The crude product was purified by column chromatography (PE/EtOAc 10:1) to obtain a colorless solid; yield: 11.88 g (83%); mp 86–88 °C (Lit.[16] mp 86–88 °C); R_f = 0.39 (PE/EtOAc 10:1).

^{1}H NMR (600 MHz, DMSO-d_6): δ = 1.37 [s, 9 H, C(CH_3)$_3$], 4.07 (d, *J* = 6.2 Hz, 2 H, CH_2), 7.13–7.22 (m, 2 H, ArH), 7.39 (t, *J* = 6.3 Hz, 1 H, NH), 7.45–7.54 (m, 2 H, ArH).

^{13}C NMR (151 MHz, DMSO-d_6): δ = 28.39 [C(*C*H$_3$)$_3$)], 42.96 (NHCH$_2$), 78.08 [*C*(CH$_3$)$_3$], 119.79 (C-4), 129.34, 131.25 (C-2, C-3), 139.85 (C-1), 155.95 (C=O).

LC-MS (ESI) (90% H_2O to 100% MeOH in 10 min, then 100% MeOH to 20 min, DAD 200–400 nm): t_R = 11.34 min, 99% purity; *m*/*z* [M + H]$^+$ calcd for $C_{12}H_{16}{}^{81}BrNO_2$: 286.04; found. 285.9.

HRMS (ESI): *m*/*z* [M + H]$^+$ calcd for $C_{12}H_{16}{}^{81}BrNO_2$: 286.0437; found: 286.0430.

tert-Butyl *N*-{[4-(4-Methylthiazol-5-yl)phenyl]methyl}carbamate (6a)

[CAS Reg. No. 2308507-34-6]

This compound was prepared using General Procedure II and compound **5a** (7.15 g). The crude product was purified by column chromatography (gradient of PE/EtOAc 10:1 to 2:1) to obtain a colorless solid; yield: 3.20 g (42%); mp 112–114 °C (lit. mp: no report found); R_f = 0.50 (PE/EtOAc 1:1).

^{1}H NMR (500 MHz, DMSO-d_6): δ = 1.39 [s, 9 H, C(CH$_3$)$_3$], 2.44 (s, 3 H, CH$_3$), 4.16 (d, *J* = 6.3 Hz, 2 H, CH$_2$), 7.29–7.35 (m, 2 H, ArH), 7.40 (t, *J* = 6.2 Hz, 1 H, NH), 7.41–7.46 (m, 2 H, ArH), 8.96 (s, 1 H, 2′-H).

^{13}C NMR (126 MHz, DMSO-d_6): δ = 16.08 (CH$_3$), 28.39 [C(*C*H$_3$)$_3$], 43.20 (CH$_2$), 78.00 [*C*(CH$_3$)$_3$], 127.58, 128.97 (C-2, C-3), 129.96, 131.24 (C-1, C-5′), 140.24 (C-4), 147.94 (C-4′), 151.54 (C-2′), 155.96 (C=O).

LC-MS (ESI) (90% H_2O to 100% MeOH in 10 min, then 100% MeOH to 20 min, DAD 220–400 nm): t_R = 10.85 min, 96% purity; *m*/*z* [M + H]$^+$ calcd for $C_{16}H_{20}N_2O_2S$: 305.13; found: 304.9.

HRMS (ESI): *m*/*z* [M + H]$^+$ calcd for $C_{16}H_{20}N_2O_2S$: 305.1318; found: 305.1311.

tert-Butyl *N*-[(4-Bromo-2-hydroxyphenyl)methyl]carbamate (5d)

[CAS Reg. No. 1402664-46-3]

This compound was prepared using General Procedure I and 4-bromo-2-hydroxybenzaldehyde (**4d**; 10.05 g). The crude product was purified by column chromatography (gradient of PE/EtOAc 8:1 to 6:1) to obtain a colorless solid; yield: 14.20 g (94%); mp 110–112 °C (lit. mp: no report found); R_f = 0.28 (PE/EtOAc 8:1).

^{1}H NMR (600 MHz, DMSO-d_6): δ = 1.38 [s, 9 H, C(CH$_3$)$_3$], 4.01 (d, *J* = 6.1 Hz, 2 H, CH$_2$), 6.91–6.96 (m, 2 H), 7.00 (d, *J* = 8.3 Hz, 1 H, 3-H, 5-H, 6-H), 7.16 (t, *J* = 6.1 Hz, 1 H, NH), 9.94 (br s, 1 H, OH).

^{13}C NMR (151 MHz, DMSO-d_6): δ = 28.40 [C(*C*H$_3$)$_3$], 38.25 (CH$_2$), 78.03 [*C*(CH$_3$)$_3$], 117.48, 119.61, 121.64, 125.87, 129.39 (C-1, C-3, C-4, C-5, C-6), 155.84, 156.06 (C-2, C=O).

LC-MS (ESI): (90% H_2O to 100% MeOH in 10 min, then 100% MeOH to 20 min, DAD 220–400 nm): t_R = 11.01 min, 99% purity; *m*/*z* [M + H]$^+$ calcd for $C_{12}H_{16}{}^{81}BrNO_3$: 304.04; found: 303.9.

HRMS (ESI): *m*/*z* [M + H]$^+$ calcd for $C_{12}H_{16}{}^{79}BrNO_3$: 302.0386; found: 302.0366.

tert-Butyl *N*-{[2-Hydroxy-4-(4-methylthiazol-5-yl)phenyl]methyl}carbamate (6d)

[CAS Reg. No. 2086300-37-8]

This compound was prepared using General Procedure II and compound **5d** (7.55 g). The crude product was purified by column chromatography (gradient of PE/EtOAc 2:1 to 1:1) to obtain a colorless solid; yield: 4.81 g (60%); mp 142–144 °C (lit. mp: no report found); R_f = 0.36 (PE/EtOAc 1:1).

^{1}H NMR (600 MHz, DMSO-d_6): δ = 1.39 [s, 9 H, C(CH$_3$)$_3$], 2.44 (s, 3 H, CH$_3$), 4.10 (d, *J* = 6.1 Hz, 2 H, CH$_2$), 6.93–6.87 (m, 2 H), 7.24–7.12 (m, 2 H, ArH, NH), 8.94 (s, 1 H, 2″-H), 9.72 (s, 1 H, OH).

^{13}C NMR (151 MHz, DMSO-d_6): δ = 16.07 (CH$_3$), 28.24 [C(*C*H$_3$)$_3$], 38.26 (CH$_2$), 77.81 [*C*(CH$_3$)$_3$], 115.03 (C-3′), 119.42 (C-5″), 125.98, 127.96, 130.59, 131.25 (ArC), 147.46 (C-4″), 151.16 (C-2″), 154.66 (C-2′), 155.94 (C=O).

LC-MS (ESI): (90% H_2O to 100% MeOH in 10 min, then 100% MeOH to 20 min, DAD 200–400 nm): t_R = 10.68 min, 98% purity; *m*/*z* [M + H]$^+$ calcd for $C_{16}H_{20}N_2O_3S$: 321.12; found: 320.9.

HRMS (ESI): *m*/*z* [M + H]$^+$ calcd for $C_{16}H_{20}N_2O_3S$: 321.1228; found: 321.1285.

tert-Butyl *N*-({2-[*tert*-Butyl(diphenyl)silyl]oxy-4-(4-methylthiazol-5-yl)phenyl}methyl)carbamate (7)

This compound was prepared using General Procedure III and compound **6d** (4.81 g). The crude product was purified by column chromatography (gradient of PE/EtOAc 4:1 to 2:1) to obtain a colorless solid; yield: 7.71 g (92%); mp 110–112 °C; R_f = 0.28 (PE/EtOAc 8:1).

^{1}H NMR (600 MHz, DMSO-d_6): δ = 1.06 [s, 9 H, SiC(CH$_3$)$_3$], 1.44 [s, 9 H, OC(CH$_3$)$_3$], 1.82 (s, 3 H, CH$_3$), 4.41 (d, *J* = 6.2 Hz, 2 H, CH$_2$), 6.38 (s, 1 H, NH), 6.98 (dd, *J* = 1.9, 8.0 Hz, 1 H), 7.26 (d, *J* = 7.9 Hz, 1 H), 7.35 (t, *J* = 6.0 Hz, 1 H), 7.52–7.41 (m, 6 H), 7.73–7.68 (m, 4 H, ArH, SiArH), 8.79 (s, 1 H, 2″-H).

^{13}C NMR (151 MHz, DMSO-d_6): δ = 15.34 (CH$_3$), 18.94 [SiC(CH$_3$)$_3$], 26.21 [SiC(*C*H$_3$)$_3$)], 28.27 [OC(*C*H$_3$)$_3$)], 38.70 (CH$_2$), 77.92 [OC(CH$_3$)$_3$], 117.97 (C-3′), 121.66 (C-5″), 128.00, 128.19, 129.43, 130.12, 130.37, 130.52, 131.44, 134.95 (ArC), 147.36 (C-4″), 151.39 (C-2″), 152.20 (C-2′), 155.87 (C=O).

LC-MS (ESI) (90% H_2O to 100% MeOH in 10 min, then 100% MeOH to 20 min, DAD 200-400 nm): t_R = 13.28 min, 99% purity; *m*/*z* [M + H]$^+$ calcd for $C_{32}H_{38}N_2O_3SSi$: 559.24; found: 559.1.

HRMS (ESI): *m*/*z* [M + H]$^+$ calcd for $C_{32}H_{38}N_2O_3SSi$: 559.2456; found: 559.2435.

tert-Butyl (2*S*,4*R*)-2-({2-[*tert*-Butyl(diphenyl)silyl]oxy-4-(4-methylthiazol-5-yl)phenyl}methylcarbamoyl)-4-hydroxypyrrolidine-1-carboxylate (8d)

This compound was prepared using General Procedure IV, compound **7** (5.59 g, 10 mmol), and Boc-Hyp-OH (2.31 g, 10 mmol). The crude product was purified by column chromatography (gradient of PE/EtOAc 1:1 to EtOAc) to obtain a colorless solid; yield: 5.06 g (75%); mp 98–100 °C; R_f = 0.46 (EtOAc).

^{1}H NMR (600 MHz, DMSO-d_6): δ (major rotamer) = 1.06 [s, 9 H, SiC(CH$_3$)$_3$], 1.35 [s, 9 H, OC(CH$_3$)$_3$], 1.84 (s, 3 H, CH$_3$), 1.99–1.90 (m, 1 H), 2.16–2.07 (m, 1 H, 3-H), 3.34 (m, 1 H), 3.51–3.40 (m, 1 H, 2-H, 4-H), 4.25–4.34 (m, 2 H, CH$_2$), 4.41 (dd, *J* = 5.4, 16.0 Hz, 1 H, 5-H), 4.65 (dd, *J* = 6.2, 16.0 Hz, 1 H, 5-H), 5.00–5.05 (m, 1 H, OH), 6.39 (dd, *J* = 1.7, 8.9 Hz, 1 H), 6.96 (d, *J* = 7.8 Hz, 1 H), 7.27 (d, *J* = 7.9 Hz, 1 H), 7.52–7.42 (m, 6 H), 7.71 (t, *J* = 6.4 Hz, 4 H, ArH, SiArH), 8.45–8.38 (m, 1 H, CONH), 8.80 (s, 1 H, 2″-H).

^{13}C NMR (151 MHz, DMSO-d_6): δ = 15.32 (CH$_3$), 18.96 [SiC(CH$_3$)$_3$], 26.20 [SiC(*C*H$_3$)$_3$], 27.95 [OC(*C*H$_3$)$_3$], 37.30 (C-3), 38.66 (NHCH$_2$), 54.83, 58.97 (C-2, C-5), 67.88 (C-4), 78.59 [OC(CH$_3$)$_3$], 118.10 (C-3′), 121.54 (C-5″), 128.19, 128.80, 130.38, 130.46, 131.42, 134.93 (ArC), 147.41 (C-4″), 151.44 (C-2″), 152.37 (C-2′), 153.57 (COO), 172.84 (CONH).

LC-MS (ESI) (90% H_2O to 100% MeOH in 10 min, then 100% MeOH to 20 min, DAD 200–400 nm): t_R = 12.58 min, 99% purity; *m*/*z* [M + H]$^+$ calcd for $C_{37}H_{45}N_3O_5SSi$: 672.29; found: 672.4.

HRMS (ESI): *m*/*z* [M + H]$^+$ calcd for $C_{37}H_{45}N_3O_5SSi$: 672.2922; found: 672.2948.

***tert*-Butyl *N*-{(1*S*)-1-[(2*S*,4*R*)-2-({2-[*tert*-butyl(diphenyl)silyl]oxy-4-(4-methylthiazol-5-yl)phenyl}methylcarbamoyl)-4-hydroxypyrrolidine-1-carbonyl]-2,2-dimethylpropyl}carbamate (9)**

This compound was prepared using General Procedure IV, compound **8d** (1.34 g, 2.0 mmol), and Boc-Tle-OH (0.46 g, 2.0 mmol). The crude product was purified by flash chromatography on silica gel (0% to 5% MeOH in CH_2Cl_2) to yield the title compound as a colorless solid; yield: 0.94 g (60%); mp 108–110 °C; R_f = 0.43 (CH_2Cl_2/MeOH 9:1).

^{1}H NMR (600 MHz, DMSO-d_6): δ = 0.94 [s, 9 H, C(CH_3)$_3$], 1.06 [s, 9 H, SiC(CH_3)$_3$], 1.39 [s, 9 H, OC(CH_3)$_3$], 1.84 (s, 3 H, CH_3), 1.94–2.01 (m, 1 H), 2.05–2.12 (m, 1 H, 3-H), 3.59–3.72 (m, 2 H, 5-H), 4.13–4.20 (m, 1 H), 4.36–4.46 (m, 2 H), 4.50–4.59 (m, 2 H, 2-H, 4-H, NHC*H*, NHCH_2), 5.15 (d, *J* = 2.5 Hz, 1 H, OH), 6.37 (d, *J* = 1.3 Hz, 1 H), 6.88 (dd, *J* = 1.7, 7.9 Hz, 1 H), 7.43–7.52 (m, 8 H), 7.69–7.73 (m, 4 H, ArH, CONH), 8.54 (t, *J* = 6.3 Hz, 1 H, CONH), 8.80 (s, 1 H, 2″-H).

^{13}C NMR (151 MHz, DMSO-d_6): δ = 15.35 (CH_3), 18.96 [SiC(CH_3)$_3$], 26.25 [SiC(CH_3)$_3$, CHC(CH_3)$_3$], 28.18 [OC(CH_3)$_3$], 35.36 [CHC(CH_3)$_3$], 37.60 (C-3), 38.22 (NHCH_2), 56.36, 58.42, 58.83 (C-2, C-5, NHCH), 69.92 (C-4), 78.08 [OC(CH_3)$_3$], 117.76 (C-3′), 121.43 (C-5″), 128.21, 128.77, 130.01, 130.39, 131.44, 134.94 (C-Ar), 147.30 (C-4″), 151.38 (C-2″), 152.18 (C-2′), 155.35, 169.93, 172.17 (C=O).

LC-MS (ESI) (90% H_2O to 100% MeOH in 10 min, then 100% MeOH to 20 min, DAD 200–350 nm): t_R = 12.82 min, 95% purity; *m*/*z* [M + H]$^+$calcd for $C_{43}H_{57}N_4O_6SSi$: 785.38; found: 785.5.

HRMS (ESI): *m*/*z* [M + H]$^+$ calcd for $C_{43}H_{57}N_4O_6SSi$: 785.3763; found: 785.3739.

(2*S*,4*R*)-*N*-({2-[*tert*-Butyl(diphenyl)silyl]oxy-4-(4-methylthiazol-5-yl)phenyl}methyl)-1-{(2*S*)-2-[(1-cyanocyclopropanecarbonyl)-amino]-3,3-dimethylbutanoyl}-4-hydroxypyrrolidine-2-carboxamide (10)

This compound was prepared using General Procedure IV, compound **9** (0.79 g, 1.0 mmol), and 1-cyano-1-cyclopropanecarboxylic acid (0.11 g, 1.0 mmol). The crude product was purified by flash chromatography on silica gel (0% to 5% MeOH in CH_2Cl_2) to afford the title compound as a slight yellow solid; yield: 0.60 g (77%); mp 112–114 °C; R_f = 0.37 (CH_2Cl_2/MeOH 9:1).

^{1}H NMR (600 MHz, DMSO-d_6): δ = 0.97 [s, 9 H, C(CH_3)$_3$], 1.07 [s, 9 H, SiC(CH_3)$_3$], 1.45–1.56 (m, 2 H), 1.58–1.66 (m, 2 H, 2‴-H), 1.84 (s, 3 H, CH_3), 1.94–2.00 (m, 1 H), 2.09–2.15 (m, 1 H, 3-H), 3.59 (d, *J* = 11.0 Hz, 1 H), 3.64–3.68 (m, 1 H, 5-H), 4.27–4.40 (m, 1 H), 4.42–4.61 (m, 4 H, 2-H, 4-H, NHC*H*, NHCH_2), 5.17 (d, *J* = 3.7 Hz, 1 H, OH), 6.38 (d, *J* = 1.7 Hz, 1 H), 6.90 (dd, *J* = 1.7, 7.9 Hz, 1 H), 7.37–7.53 (m, 8 H), 7.69–7.73 (m, 4 H, ArH, CONH), 8.59 (t, *J* = 5.9 Hz, 1 H, CONH), 8.80 (s, 1 H, 2″-H).

^{13}C NMR (151 MHz, DMSO-d_6): δ = 13.72 (C-1‴), 15.33 (CH_3), 16.58, 16.77 (C-2‴), 18.96 [C(CH_3)$_3$], 26.05 [C(CH_3)$_3$], 26.24 [C(CH_3)$_3$], 36.21 [*C*(CH_3)$_3$], 37.60 (C-3), 37.90 (NHCH_2), 56.65, 57.36, 58.87 (C-2, C-5, NHCH), 69.89 (C-4), 117.86 (C-3′), 120.10 (CN), 121.43 (C-5″), 128.22, 128.65, 130.12, 130.38, 130.52, 131.39, 134.94 (C-Ar, C-1′, C-4′, C-5′, C-6′), 147.33 (C-4″), 151.40 (C-2″), 152.24 (C-2′), 164.42, 168.75, 171.87 (C=O).

LC-MS (ESI) (90% H_2O to 100% MeOH in 10 min, then 100% MeOH to 20 min, DAD 200–330 nm): t_R = 12.51 min, 100% purity; *m*/*z* [M + H]$^+$calcd for $C_{43}H_{52}N_5O_5SSi$: 779.05; found: 778.7.

HRMS (ESI): *m*/*z* [M + H]$^+$ calcd for $C_{43}H_{52}N_5O_5SSi$: 778.3453; found: 778.3431.

Funding Information

I.S. acknowledges funding by the Javna Agencija za Raziskovalno Dejavnost RS [Slovenian Research Agency (ARRS)] through research core funding No. P1-0208.

Acknowledgment

G. S. thanks Prof. A. C. Filippou for support. The authors thank Hannes Buthmann, Deborah Schlipphack, Nicole Schmitt, and Eva Wiemann for synthetic support.

Supporting Information

Supporting information for this article is available online at https://doi.org/10.1055/s-0040-1707400.

References

(1) (a) Churcher, I. *J. Med. Chem.* **2018**, *61*, 444. (b) An, S.; Fu, L. *EBioMedicine* **2018**, *36*, 553. (c) Maniaci, C.; Ciulli, A. *Curr. Opin. Chem. Biol.* **2019**, *52*, 145. (d) Burslem, G. M.; Crews, C. M. *Cell* **2020**, *181*, 102. (e) Verma, R.; Mohl, D.; Deshaies, R. J. *Mol. Cell* **2020**, *77*, 446.

(2) (a) Zengerle, M.; Chan, K.-H.; Ciulli, A. *ACS Chem. Biol.* **2015**, *10*, 1770. (b) Lai, A. C.; Toure, M.; Hellerschmied, D.; Salami, J.; Jaime-Figueroa, S.; Ko, E.; Hines, J.; Crews, C. M. *Angew. Chem. Int. Ed.* **2016**, *55*, 807. (c) Gadd, M. S.; Testa, A.; Lucas, X.; Chan, K.-H.; Chen, W.; Lamont, D. J.; Zengerle, M.; Ciulli, A. *Nat. Chem. Biol.* **2017**, *13*, 514. (d) Schiedel, M.; Herp, D.; Hammelmann, S.; Swyter, S.; Lehotzky, A.; Robaa, D.; Oláh, J.; Ovádi, J.; Sippl, W.; Jung, M. *J. Med. Chem.* **2018**, *61*, 482. (e) Steinebach, C.; Kehm, H.; Lindner, S.; Vu, L. P.; Köpff, S.; López Mármol, Á.; Weiler, C.; Wagner, K. G.; Reichenzeller, M.; Krönke, J.; Gütschow, M. *Chem. Commun.* **2019**, *55*, 1821. (f) Testa, A.; Hughes, S. J.; Lucas, X.; Wright, J. E.; Ciulli, A. *Angew. Chem. Int. Ed.* **2020**, *59*, 1727. (g) Steinebach, C.; Ng, Y. L. D.; Sosič, I.; Lee, C.-S.; Chen, S.; Lindner, S.; Vu, L. P.; Bricelj, A.; Haschemi, R.; Monschke, M.; Steinwarz, E.; Wagner, K. G.; Bendas, G.; Luo, J.; Gütschow, M.; Krönke, J. *Chem. Sci.* **2020**, *11*, 3474.

(3) (a) Khan, S.; Zhang, X.; Lv, D.; Zhang, Q.; He, Y.; Zhang, P.; Liu, X.; Thummuri, D.; Yuan, Y.; Wiegand, J. S.; Pei, J.; Zhang, W.; Sharma, A.; McCurdy, C. R.; Kuruvilla, V. M.; Baran, N.; Ferrando, A. A.; Kim, Y.; Rogojina, A.; Houghton, P. J.; Huang, G.; Hromas, R.; Konopleva, M.; Zheng, G.; Zhou, D. *Nat. Med.* **2019**, *25*, 1938. (b) Farnaby, W.; Koegl, M.; Roy, M. J.; Whitworth, C.; Diers, E.; Trainor, N.; Zollman, D.; Steurer, S.; Karolyi-Oezguer, J.; Riedmueller, C.; Gmaschitz, T.; Wachter, J.; Dank, C.; Galant, M.; Sharps, B.; Rumpel, K.; Traxler, E.; Gerstberger, T.; Schnitzer, R.; Petermann, O.; Greb, P.; Weinstabl, H.; Bader, G.; Zoephel, A.; Weiss-Puxbaum, A.; Ehrenhöfer-Wölfer, K.; Wöhrle, S.; Boehmelt, G.; Rinnenthal, J.; Arnhof, H.; Wiechens, N.; Wu, M.-Y.; Owen-Hughes, T.; Ettmayer, P.; Pearson, M.; McConnell, D. B.; Ciulli, A. *Nat. Chem. Biol.* **2019**, *15*, 672.

(4) (a) Lohbeck, J.; Miller, A. K. *Bioorg. Med. Chem. Lett.* **2016**, *26*, 5260. (b) Papatzimas, J.; Gorobets, E.; Brownsey, D.; Maity, R.; Bahlis, N.; Derksen, D. *Synlett* **2017**, *28*, 2881. (c) Wurz, R. P.; Dellamaggiore, K.; Dou, H.; Javier, N.; Lo, M.-C.; McCarter, J. D.; Mohl, D.; Sastri, C.; Lipford, J. R.; Cee, V. J. *J. Med. Chem.* **2018**, *61*, 453. (d) Qiu, X.; Sun, N.; Kong, Y.; Li, Y.; Yang, X.; Jiang, B. *Org. Lett.* **2019**, *21*, 3838. (e) Steinebach, C.; Sosič, I.; Lindner, S.;

Bricelj, A.; Kohl, F.; Ng, Y. L. D.; Monschke, M.; Wagner, K. G.; Krönke, J.; Gütschow, M. *Med. Chem. Commun.* **2019**, *10*, 1037.

(5) (a) Frost, J.; Galdeano, C.; Soares, P.; Gadd, M. S.; Grzes, K. M.; Ellis, L.; Epemolu, O.; Shimamura, S.; Bantscheff, M.; Grandi, P.; Read, K. D.; Cantrell, D. A.; Rocha, S.; Ciulli, A. *Nat. Commun.* **2016**, *7*, 13312. (b) Soares, P.; Gadd, M. S.; Frost, J.; Galdeano, C.; Ellis, L.; Epemolu, O.; Rocha, S.; Read, K. D.; Ciulli, A. *J. Med. Chem.* **2018**, *61*, 599. (c) Testa, A.; Lucas, X.; Castro, G. V.; Chan, K.-H.; Wright, J. E.; Runcie, A. C.; Gadd, M. S.; Harrison, W. T. A.; Ko, E.-J.; Fletcher, D.; Ciulli, A. *J. Am. Chem. Soc.* **2018**, *140*, 9299. (d) Soares, P.; Lucas, X.; Ciulli, A. *Bioorg. Med. Chem.* **2018**, *26*, 2992. (e) Lucas, X.; Van Molle, I.; Ciulli, A. *J. Med. Chem.* **2018**, *61*, 7387. (f) de Castro, G. V.; Ciulli, A. *Chem. Commun.* **2019**, *55*, 1482. (g) Han, X.; Wang, C.; Qin, C.; Xiang, W.; Fernandez-Salas, E.; Yang, C.-Y.; Wang, M.; Zhao, L.; Xu, T.; Chinnaswamy, K.; Delproposto, J.; Stuckey, J.; Wang, S. *J. Med. Chem.* **2019**, *62*, 941.

(6) (a) Maniaci, C.; Hughes, S. J.; Testa, A.; Chen, W.; Lamont, D. J.; Rocha, S.; Alessi, D. R.; Romeo, R.; Ciulli, A. *Nat. Commun.* **2017**, *8*, 830. (b) Zoppi, V.; Hughes, S. J.; Maniaci, C.; Testa, A.; Gmaschitz, T.; Wieshofer, C.; Koegl, M.; Riching, K. M.; Daniels, D. L.; Spallarossa, A.; Ciulli, A. *J. Med. Chem.* **2019**, *62*, 699. (c) Smith, B. E.; Wang, S. L.; Jaime-Figueroa, S.; Harbin, A.; Wang, J.; Hamman, B. D.; Crews, C. M. *Nat. Commun.* **2019**, *10*, 131.

(7) Galdeano, C.; Gadd, M. S.; Soares, P.; Scaffidi, S.; Van Molle, I.; Birced, I.; Hewitt, S.; Dias, D. M.; Ciulli, A. *J. Med. Chem.* **2014**, *57*, 8657.

(8) Johnson, C. N.; Adelinet, C.; Berdini, V.; Beke, L.; Bonnet, P.; Brehmer, D.; Calo, F.; Coyle, J. E.; Day, P. J.; Frederickson, M.; Freyne, E. J. E.; Gilissen, R. A. H. J.; Hamlett, C. C. F.; Howard, S.; Meerpoel, L.; Mevellec, L.; McMenamin, R.; Pasquier, E.; Patel, S.; Rees, D. C.; Linders, J. T. M. *ACS Med. Chem. Lett.* **2015**, *6*, 31.

(9) Buckley, D. L.; Raina, K.; Darricarrere, N.; Hines, J.; Gustafson, J. L.; Smith, I. E.; Miah, A. H.; Harling, J. D.; Crews, C. M. *ACS Chem. Biol.* **2015**, *10*, 1831.

(10) For the characterization of the *O*-acyl side product occurring during the coupling of phenol **6d** with Boc-Hyp-OH, see Supporting Information.

(11) Kaburagi, Y.; Kishi, Y. *Org. Lett.* **2007**, *9*, 723.

(12) (a) Buckley, D. L.; Van Molle, I.; Gareiss, P. C.; Tae, H. S.; Michel, J.; Noblin, D. J.; Jorgensen, W. L.; Ciulli, A.; Crews, C. M. *J. Am. Chem. Soc.* **2012**, *134*, 4465. (b) Tovell, H.; Testa, A.; Maniaci, C.; Zhou, H.; Prescott, A. R.; Macartney, T.; Ciulli, A.; Alessi, D. R. *ACS Chem. Biol.* **2019**, *14*, 882.

(13) The X-ray crystallographic data collection for compounds **14** was performed on a Bruker X8-Kappa ApexII diffractometer at 100(2) K. The diffractometer was equipped with a low-temperature device (Kryoflex I, Bruker AXS) and used Mo-K_α radiation (λ = 0.71073 Å). Intensities were measured by fine-slicing ϕ- and ω-scans and corrected for background, polarization, and Lorentz effects. Semiempirical absorption corrections were applied for all data sets by using Bruker's SADABS program. The structures were solved by direct methods and refined anisotropically by the least-squares procedure implemented in the ShelX-2014/7 program system. Hydrogen atoms were included isotopically using the riding model on the bound carbon atoms. CCDC 1986177 contains the supplementary crystallographic data for this paper. The data can be obtained free of charge from The Cambridge Crystallographic Data Centre via www.ccdc.cam.ac.uk/getstructures.

(14) For the feasible synthesis of aldehyde **4d** from 3-bromophenol or 4-bromosalicylic acid, see Supporting Information.

(15) (a) Raina, K.; Lu, J.; Qian, Y.; Altieri, M.; Gordon, D.; Rossi, A. M. K.; Wang, J.; Chen, X.; Dong, H.; Siu, K.; Winkler, J. D.; Crew, A. P.; Crews, C. M.; Coleman, K. G. *Proc. Natl. Acad. Sci. U. S. A.* **2016**, *113*, 7124. (b) Hu, J.; Hu, B.; Wang, M.; Xu, F.; Miao, B.; Yang, C.-Y.; Wang, M.; Liu, Z.; Hayes, D. F.; Chinnaswamy, K.; Delproposto, J.; Stuckey, J.; Wang, S. *J. Med. Chem.* **2019**, *62*, 1420. (c) Wei, J.; Hu, J.; Wang, L.; Xie, L.; Jin, M. S.; Chen, X.; Liu, J.; Jin, J. *J. Med. Chem.* **2019**, *62*, 10897.

(16) Yamazaki, Y.; Kohno, K.; Yasui, H.; Kiso, Y.; Akamatsu, M.; Nicholson, B.; Deyanat-Yazdi, G.; Neuteboom, S.; Potts, B.; Lloyd, G. K.; Hayashi, Y. *ChemBioChem* **2008**, *9*, 3074.

Appendix I. Publication I: A Facile Synthesis of Ligands for the von Hippel-Lindau E3 Ligase

selected parts of the

Supporting Information

A Facile Synthesis of Ligands for the von Hippel–Lindau E3 Ligase

***Synthesis* 2020**

Only selected compounds are shown which were synthesized or resynthesized by the author of the thesis during the course of the doctoral studies.

For the full supporting information please refer to the following link:

https://doi.org/10.1055/s-0040-1707400

A facile synthesis of ligands for the von Hippel-Lindau E3 ligase

Christian Steinebach,[a] Sabine Anna Voell,[a] Lan Phuong Vu,[a] Aleša Bricelj,[b]
Izidor Sosič,[b] Gregor Schnakenburg,[c] and Michael Gütschow*[a]

[a] Pharmaceutical Institute, University of Bonn, An der Immenburg 4, 53121 Bonn, Germany
E-mail: guetschow@uni-bonn.de
[b] Faculty of Pharmacy, University of Ljubljana, Aškerčeva cesta 7, 1000 Ljubljana, Slovenia
[c] Institute of Inorganic Chemistry, University of Bonn, Gerhard-Domagk-Str. 1, 53121 Bonn, Germany

Supplementary Notes

Availability of 4-bromobenzaldehydes:

A large set of substituted 4-bromobenzaldehydes is commercially available. Some examples used in this study are depicted in Figure S1. However, as exemplified for compound **4d**, this class of compounds is easily accessible from different precursor molecules.

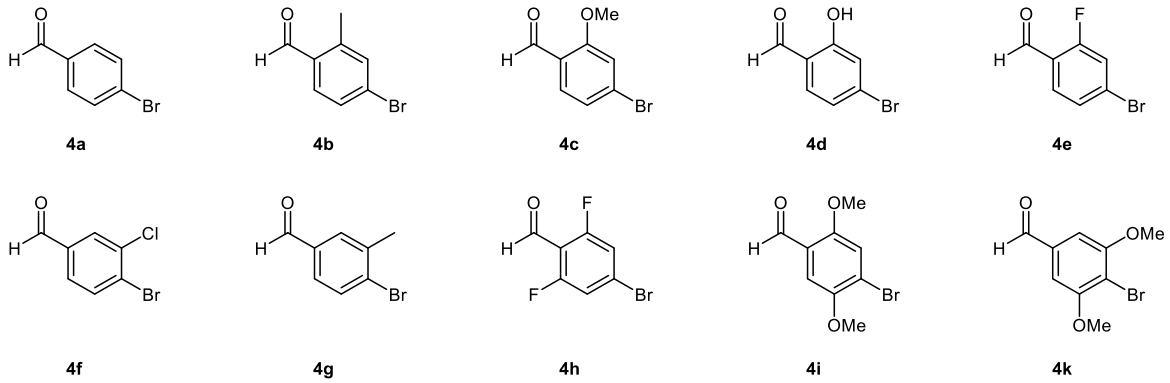

Figure S1: Commercially available 4-bromobenzaldehydes used in this study.

4-Bromo-2-hydroxy-benzaldehyde (4d)

CAS: 22532-62-3

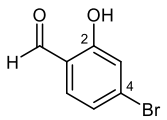

Method A: ortho-formylation

This compound was synthesized as reported previously.[1] In brief, to a solution of 3-bromophenol (10 mmol, 1.73 g) in anhydrous THF (20 mL) was added Et_3N (20 mmol, 2.02 g, 2.78 mL) and anhydrous $MgCl_2$ (20 mmol, 1.90 g). After stirring for 10 min, paraformaldehyde (30 mmol, 0.90 g) was added and the mixture was stirred at reflux for 6 h. The mixture was cooled to rt, 10% aqueous $KHSO_4$ was added, and the product was extracted with EtOAc (2 × 50 mL). The combined organic extracts were washed with saturated NH_4Cl solution and brine (50 mL each), dried (Na_2SO_4), filtered, and concentrated under reduced pressure. The crude product was purified by column chromatography (petroleum ether/EtOAc 19:1) to give the title compound as a colorless solid. Yield (0.64 g, 32%); mp 70 – 72 °C, lit. mp 50 – 51.5 °C[1]; R_f = 0.30 (petroleum ether/EtOAc 10:1).

^{1}H NMR (600 MHz, DMSO-d_6) δ 7.13 (dd, J = 1.9, 8.3 Hz, 1H), 7.19 (d, J = 1.8 Hz, 1H), 7.56 (d, J = 8.4 Hz, 1H, Ar-H), 10.22 (s, 1H), 11.10 (s, 1H, OH, CHO).

^{13}C NMR (151 MHz, DMSO-d_6) δ 120.15 (C-3), 121.99 (C-1), 122.86 (C-5), 129.67 (C-4), 130.55 (C-6), 161.38 (C-2), 190.35 (CO).

LC-MS (ESI) (90% H_2O to 100% MeOH in 10 min, then 100% MeOH to 20 min, DAD 220-450 nm), t_R = 10.03 min, 95% purity, m/z $[M + H]^+$ calcd for $C_7H_5{}^{79}BrO_2$, 199.95; found, 199.8.

Supplementary Schemes

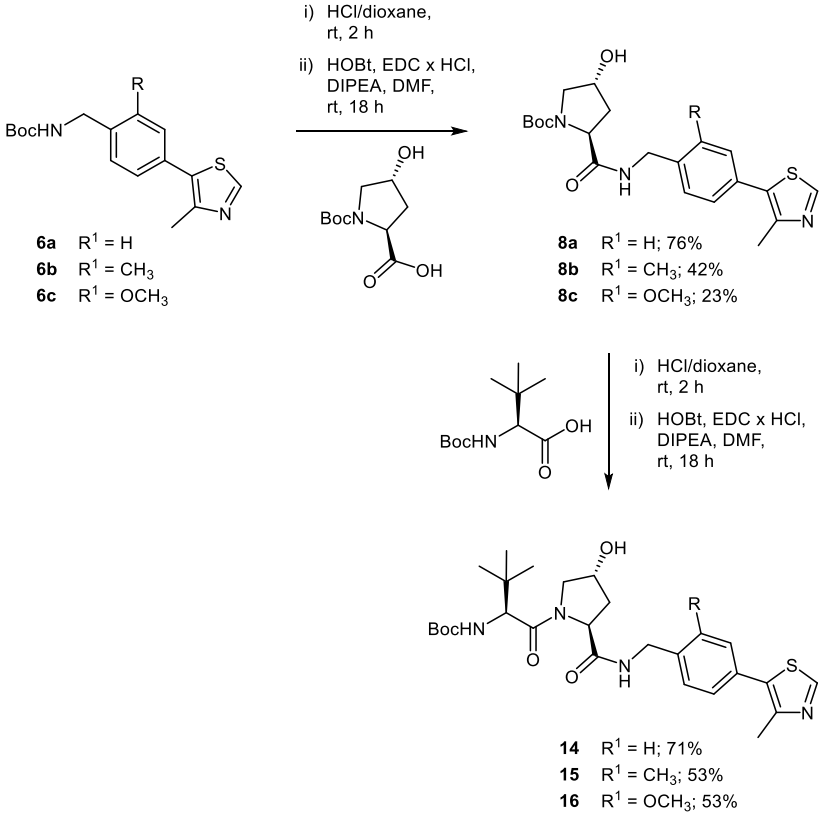

Scheme S1: Synthesis of protected VHL ligands of chemotype 1 including derivatives with new substitution patterns.

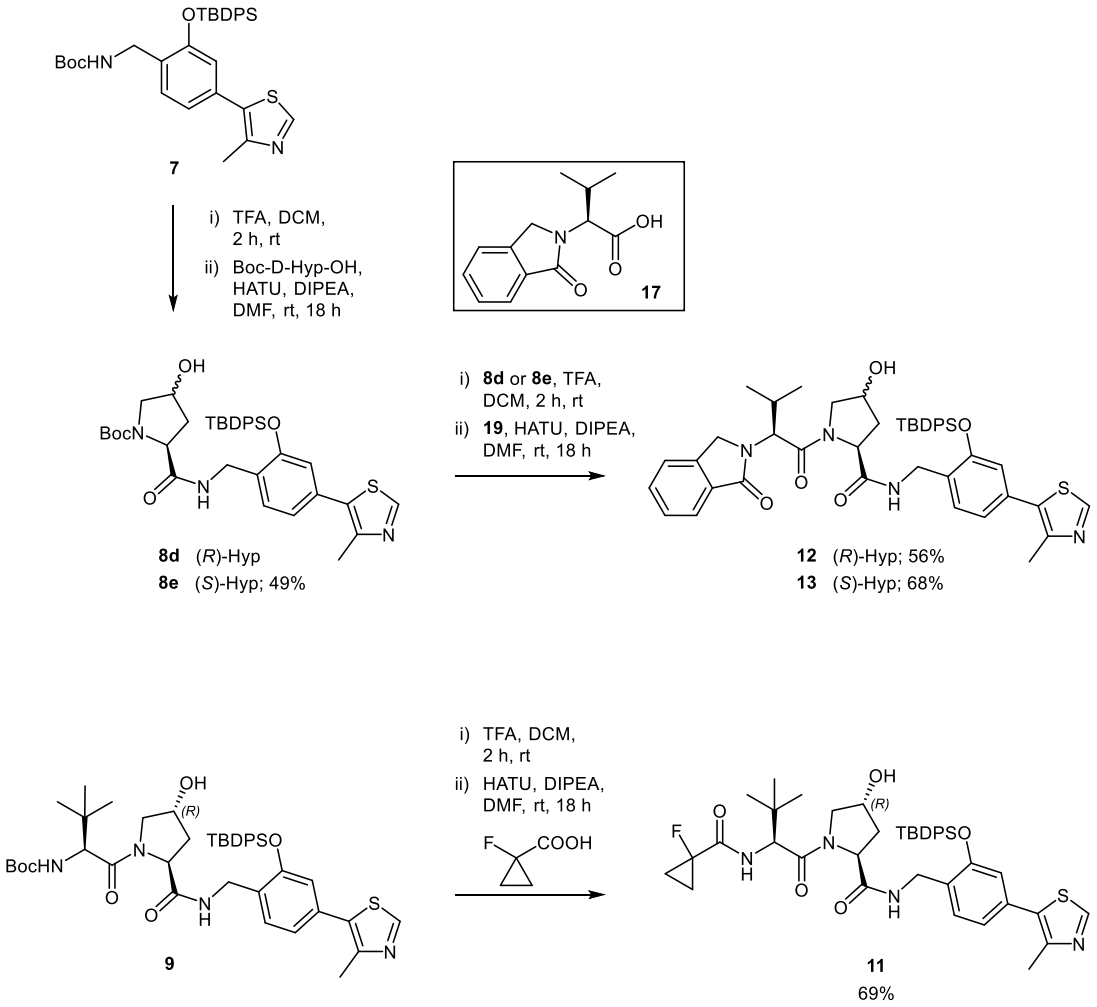

Scheme S2: Protected VHL ligands of chemotype **2**, synthesized following the newly developed protecting group strategy.

Extended Experimental Section

tert-Butyl *N*-[(4-bromo-2-methyl-phenyl)methyl]carbamate (5b)

CAS: 1352896-24-2

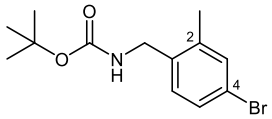

By using the General Procedure **I**, this compound was prepared on a 5 mmol scale from **4b** (1.00 g). The crude product was purified by column chromatography (petroleum ether/EtOAc 9:1) to obtain a colorless solid. Yield (1.28 g, 86%); mp 80 – 82 °C; R_f = 0.30 (petroleum ether/EtOAc 9:1).

^{1}H NMR (600 MHz, DMSO-d_6) δ 1.39 (s, 9H, C(CH_3)$_3$), 2.25 (s, 3H, CH_3), 4.06 (d, J = 6.0 Hz, 2H, CH_2), 7.12 (d, J = 8.0 Hz, 1H, Ar-H), 7.30 (t, J = 5.6 Hz, 1H, NH), 7.33 – 7.36 (m, 2H, Ar-H).

^{13}C NMR (151 MHz, DMSO-d_6) δ 18.15 (CH_3), 28.18 (C($\underline{C}H_3$)$_3$), 40.80 (CH_2), 77.80 ($\underline{C}$(CH_3)$_3$), 119.42 (C-4), 128.37, 129.07 (C-5, C-6), 132.10 (C-3), 137.27, 138.15 (C-1, C-2), 155.62 (CO).

LC-MS (ESI) (90% H_2O to 100% MeOH in 10 min, then 100% MeOH to 20 min, DAD 220-400 nm), t_R = 11.63 min, 97% purity, *m/z* [M + H]$^+$ calcd for $C_{13}H_{18}{}^{79}BrNO_2$, 300.06; found, 300.0.

***tert*-Butyl *N*-[(4-bromo-2-methoxy-phenyl)methyl]carbamate (5c)**

CAS: 1402664-44-1

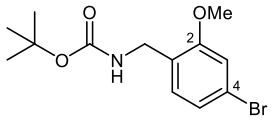

By using the General Procedure **I**, this compound was prepared on a 5 mmol scale from **4c** (1.08 g). The crude product was purified by column chromatography (petroleum ether/EtOAc 9:1) to obtain a colorless solid. Yield (1.57 g, 99%); mp 68 – 70 °C; R_f = 0.30 (petroleum ether/EtOAc 9:1).

^{1}H NMR (600 MHz, DMSO-d_6) δ 1.39 (s, 9H, $C(CH_3)_3$), 3.81 (s, 2H, CH_3), 4.04 (d, J = 6.0 Hz, 2H, CH_2), 7.07 (d, J = 8.0 Hz, 1H), 7.10 – 7.15 (m, 2H, Ar-H), 7.19 (t, J = 5.7 Hz, 1H, NH).

^{13}C NMR (151 MHz, DMSO-d_6) δ 28.21 ($C(\underline{C}H_3)_3$), 38.00 (CH_2), 55.78 (OCH_3), 77.81 ($\underline{C}(CH_3)_3$), 113.60 (C-3), 120.13 (C-4), 122.85 (C-1), 127.14, 128.64 (C-5, C-6), 155.72 (CO), 157.25 (C-2).

LC-MS (ESI) (90% H_2O to 100% MeOH in 10 min, then 100% MeOH to 20 min, DAD 220-400 nm), t_R = 11.48 min, 100% purity, *m/z* $[M + H]^+$ calcd for $C_{13}H_{18}{}^{79}BrNO_3$, 316.05; found, 315.9.

***tert*-Butyl *N*-[(4-bromo-2-fluoro-phenyl)methyl]carbamate (5e)**

CAS: 864262-97-5

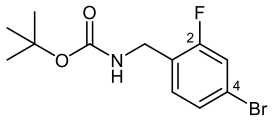

By using the General Procedure **I**, this compound was prepared on a 1 mmol scale from **4e** (0.20 g). The crude product was purified by column chromatography (petroleum ether/EtOAc 10:1) to obtain a colorless solid. Yield (130 mg, 43%); mp 78 – 80 °C; R_f = 0.30 (petroleum ether/EtOAc 6:1).

^{1}H NMR (500 MHz, DMSO-d_6) δ 1.37 (s, 9H, CH_3), 4.11 (d, J = 6.0 Hz, 2H, CH_2), 7.24 (t, J = 8.2 Hz, 1H, NH), 7.34 – 7.42 (m, 2H), 7.47 (dd, J = 2.0, 9.7 Hz, 1H, Ar-H).

^{13}C NMR (126 MHz, DMSO-d_6) δ 28.32 (C($\underline{C}H_3)_3$), 36.99 (CH_2), 78.21 ($\underline{C}(CH_3)_3$), 118.50 (d, $^2J_{CF}$ = 24.9 Hz, C-3), 120.03 (d, $^3J_{CF}$ = 9.6 Hz, C-4), 126.53 (d, $^2J_{CF}$ = 14.8 Hz, C-1), 127.56 (d, $^4J_{CF}$ = 3.5 Hz, C-5), 130.91 (d, $^3J_{CF}$ = 5.3 Hz, C-6), 155.79 (CO), 159.87 (d, $^1J_{CF}$ = 249.3 Hz, C-2).

LC-MS (ESI) (90% H_2O to 100% MeOH in 10 min, then 100% MeOH to 20 min, DAD 220-400 nm), t_R = 11.43 min, 98% purity, *m/z* $[M + H]^+$ calcd for $C_{12}H_{15}{}^{81}BrFNO_2$, 306.03; found, 306.0.

tert-Butyl *N*-[(4-bromo-3-chloro-phenyl)methyl]carbamate (5f)

CAS: 864266-05-7

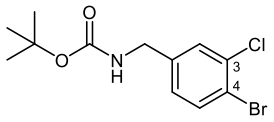

By using the General Procedure **I**, this compound was prepared on a 1 mmol scale from **4f** (0.22 g). The crude product was purified by column chromatography (petroleum ether/EtOAc 10:1) to obtain a colorless solid. Yield (93 mg, 29%); mp 98 – 100 °C; R_f = 0.49 (petroleum ether/EtOAc 6:1).

^{1}H NMR (500 MHz, DMSO-d_6) δ 1.38 (s, 9H, CH_3), 4.08 (d, J = 6.1 Hz, 2H, CH_2), 7.13 (dd, J = 2.1, 8.4 Hz, 1H, Ar-H), 7.42 (t, J = 7.2 Hz, 1H, NH), 7.45 (d, J = 2.1 Hz, 1H), 7.70 (d, J = 8.2 Hz, 1H, Ar-H).

^{13}C NMR (126 MHz, DMSO-d_6) δ 28.32 (C($\underline{C}H_3)_3$), 42.55 (CH_2), 78.23 ($\underline{C}(CH_3)_3$), 119.40 (C-4), 127.61, 128.96 (C-3, C-6), 132.95, 133.80 (C-2, C-5), 142.25 (C-1), 155.89 (CO).

LC-MS (ESI) (90% H_2O to 100% MeOH in 10 min, then 100% MeOH to 20 min, DAD 220-400 nm), t_R = 11.66 min, 97% purity, *m/z* $[M + H]^+$ calcd for $C_{12}H_{15}{}^{81}BrClNO_2$, 322.00; found, 321.9.

***tert*-Butyl *N*-[(4-bromo-3-methyl-phenyl)methyl]carbamate (5g)**

CAS: 1220039-91-7

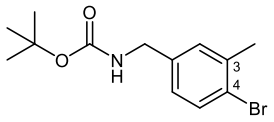

By using the General Procedure **I**, this compound was prepared on a 1 mmol scale from **4g** (0.20 g). The crude product was purified by column chromatography (petroleum ether/EtOAc 10:1) to obtain a colorless solid. Yield (126 mg, 42%); mp 88 – 90 °C; R_f = 0.30 (petroleum ether/EtOAc 6:1).

^{1}H NMR (500 MHz, DMSO-d_6) δ 1.38 (s, 9H, C(CH_3)$_3$), 2.31 (s, 3H, CH_3), 4.04 (d, J = 6.2 Hz, 2H, CH_2), 6.98 (dd, J = 2.2, 8.2 Hz, 1H), 7.19 (d, J = 2.5 Hz, 1H, Ar-H), 7.34 (t, J = 6.5 Hz, 1H, NH), 7.49 (d, J = 8.2 Hz, 1H, Ar-H).

^{13}C NMR (126 MHz, DMSO-d_6) δ 22.52 (CH_3), 28.36 (C($\underline{C}H_3$)$_3$), 42.91 (CH_2), 78.00 ($\underline{C}$(CH_3)$_3$), 122.17 (C-4), 126.59 (C-6), 129.86 (C-2), 132.01 (C-5), 136.96 (C-1), 140.03 (C-3), 155.88 (CO).

LC-MS (ESI) (90% H_2O to 100% MeOH in 10 min, then 100% MeOH to 20 min, DAD 220-400 nm), t_R = 11.65 min, 99% purity, *m/z* [M + H]$^+$ calcd for $C_{13}H_{18}{}^{81}BrNO_2$, 302.05; found, 301.9.

***tert*-Butyl *N*-[(4-bromo-2,6-difluoro-phenyl)methyl]carbamate (5h)**

CAS: 1402673-66-8

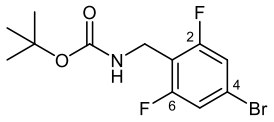

By using the General Procedure **I**, this compound was prepared on a 5 mmol scale from **4h** (1.10 g). The crude product was purified by column chromatography (petroleum ether/EtOAc 9:1) to obtain a colorless solid. Yield (1.23 g, 76%); mp 142 – 145 °C; R_f = 0.16 (petroleum ether/EtOAc 9:1).

^{1}H NMR (600 MHz, DMSO-d_6) δ 1.36 (s, 9H, CH_3), 6.31 (supressed t, J = 7.2 Hz, 1H, NH), 7.23 – 7.75 (m, 2H, Ar-H); the signal for CH_2 was not visuable.

^{13}C NMR (151 MHz, DMSO-d_6) δ 28.07 (C($\underline{C}H_3)_3$), 52.61 (CH_2), 78.59 ($\underline{C}(CH_3)_3$), 115.53 (C-3, C-5), 116.26 (C-1), 121.00 (C-4), 153.94 (CO), 160.02 (d, $^1J_{CF}$ = 252.0 Hz), 160.08 (d, $^1J_{CF}$ = 252.9 Hz, C-2, C-6).

LC-MS (ESI) (90% H_2O to 100% MeOH in 10 min, then 100% MeOH to 20 min, DAD 210-400 nm), t_R = 11.72 min, 96% purity, *m/z* $[M + H]^+$ calcd for $C_{12}H_{14}{}^{79}BrF_2NO_2$, 322.02; found, 322.0.

***tert*-Butyl *N*-[(4-bromo-2,5-dimethoxy-phenyl)methyl]carbamate (5i)**

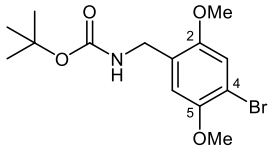

By using the General Procedure **I**, this compound was prepared on a 1 mmol scale from **4i** (245 mg). The crude product was purified by column chromatography (petroleum ether/EtOAc 10:1) to obtain a colorless solid. Yield (242 mg, 70%); mp 74 – 76 °C; R_f = 0.31 (petroleum ether/EtOAc 6:1).

^{1}H NMR (500 MHz, DMSO-d_6) δ1.39 (s, 9H, CH_3), 3.74 (br s, 6H, OCH_3), 4.05 (d, J = 6.0 Hz, 2H, CH_2), 6.92 (s, 1H), 7.15 (s, 1H, Ar-H), 7.20 (t, J = 6.2 Hz, 1H, NH).

^{13}C NMR (126 MHz, DMSO-d_6) δ 28.35 (C($\underline{C}H_3)_3$), 38.38 (CH_2), 56.34, 56.68 (OCH_3), 78.05 ($\underline{C}(CH_3)_3$), 108.59 (C-4), 112.42, 115.70 (C-3, C-6), 128.45 (C-1), 149.50, 150.93 (C-2, C-5), 155.93 (CO).

LC-MS (ESI) (90% H_2O to 100% MeOH in 10 min, then 100% MeOH to 20 min, DAD 220-400 nm), t_R = 11.27 min, 99% purity, *m/z* $[M + H]^+$ calcd for $C_{14}H_{20}{}^{79}BrNO_4$, 346.06; found, 346.1.

***tert*-Butyl *N*-[(4-bromo-3,5-dimethoxy-phenyl)methyl]carbamate (5k)**

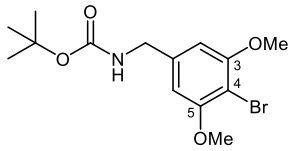

By using the General Procedure **I**, this compound was prepared on a 1 mmol scale from **4k** (245 mg). The crude product was purified by column chromatography (petroleum ether/EtOAc 10:1) to obtain a colorless solid. Yield (277 mg, 80%); mp 98 – 100 °C; R_f = 0.16 (petroleum ether/EtOAc 6:1).

^{1}H NMR (500 MHz, DMSO-d_6) δ 1.39 (s, 9H, CH_3), 3.79 (br s, 6H, OCH_3), 4.10 (d, J = 6.1 Hz, 2H, CH_2), 6.62 (s, 2H, Ar-H), 7.37 (t, J = 6.8 Hz, 1H).

^{13}C NMR (126 MHz, DMSO-d_6) δ 28.34 (C($\underline{C}H_3)_3$), 43.68 (CH_2), 56.34 (OCH_3), 78.09 ($\underline{C}(CH_3)_3$), 97.76 (C-4), 103.77 (C-2, C-6), 141.62 (C-1), 155.97 (CO), 156.47 (C-3, C-5).

LC-MS (ESI) (90% H_2O to 100% MeOH in 10 min, then 100% MeOH to 20 min, DAD 220-400 nm), t_R = 10.84 min, 98% purity, *m/z* $[M + H]^+$ calcd for $C_{14}H_{20}{}^{79}BrNO_4$, 346.06; found, 346.1.

***tert*-Butyl *N*-[[2-methyl-4-(4-methylthiazol-5-yl)phenyl]methyl]carbamate (6b)**

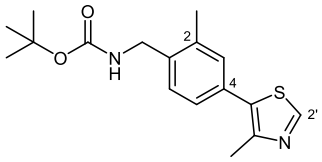

By using the General Procedure **II,** this compound was prepared on a 2 mmol scale from compound **5b** (0.60 g). The crude product was purified by column chromatography (gradient of petroleum ether/EtOAc 10:1 to 2:1) to obtain a colorless oil. Yield (0.34 g, 53%); R_f = 0.50 (petroleum ether/EtOAc 1:1).

^{1}H NMR (600 MHz, DMSO-d_6) δ 1.40 (s, 9H, C(CH_3)$_3$), 2.31 (s, 3H, CH_3), 2.45 (s, 3H, CH_3), 4.14 (d, J = 5.9 Hz, 2H, CH_2), 7.25 – 7.30 (m, 3H, Ar-H), 7.34 (t, J = 5.8 Hz, 1H, NH), 8.97 (s, 1H, 2''-H).

^{13}C NMR (151 MHz, DMSO-d_6) δ 15.95 (CH_3), 18.46 (CH_3), 28.23 (C($\underline{C}H_3$)$_3$), 41.05 (CH_2), 77.80 ($\underline{C}$(CH_3)$_3$), 126.25 (C-5''), 127.44, 129.73, 130.29, 131.13 (C-3, C-4, C-5, C-6), 136.02 (C-2), 137.76 (C-1), 147.66 (C-4''), 151.30 (C-2''), 155.71 (CO).

LC-MS (ESI) (90% H_2O to 100% MeOH in 10 min, then 100% MeOH to 20 min, DAD 220-400 nm), t_R = 11.21 min, 92% purity, *m/z* $[M + H]^+$ calcd for $C_{17}H_{22}N_2O_2S$, 319.14; found, 318.9.

***tert*-Butyl *N*-[[2-methyl-4-(4-methylthiazol-5-yl)phenyl]methyl]carbamate (6c)**

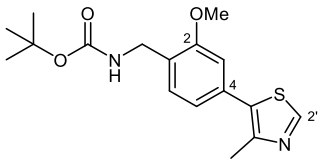

By using the General Procedure **II,** this compound was prepared on a 2 mmol scale from compound **5c** (0.63 g). The crude product was purified by column chromatography (gradient of petroleum ether/EtOAc 10:1 to 2:1) to obtain a colorless oil. Yield (0.45 g, 68%); R_f = 0.50 (petroleum ether/EtOAc 1:1).

^{1}H NMR (600 MHz, DMSO-d_6) δ 1.40 (s, 9H, C(CH_3)$_3$), 2.47 (s, 3H, CH_3), 3.84 (s, 3H, OCH_3), 4.13 (d, *J* = 6.0 Hz, 2H, CH_2), 7.01 (d, J = 1.4 Hz, 1H), 7.04 (d, J = 7.7 Hz, 1H), 7.19 – 7.24 (m, 2H, Ar-H, NH), 8.98 (s, 1H, 2''-H).

^{13}C NMR (151 MHz, DMSO-d_6) δ 16.00 (CH_3), 28.24 (C($\underline{C}H_3$)$_3$), 38.15 (CH_2), 55.49 (OCH_3), 77.79 ($\underline{C}$(CH_3)$_3$), 111.00 (C-3), 120.90 (C-5''), 127.40, 127.58, 131.01, 131.25 (C-1, C-4, C-5, C-6), 147.91 (C-4''), 151.41 (C-2''), 155.79 (CO), 156.48 (C-2').

LC-MS (ESI) (90% H_2O to 100% MeOH in 10 min, then 100% MeOH to 20 min, DAD 220-400 nm), t_R = 11.12 min, 90% purity, *m/z* $[M + H]^+$ calcd for $C_{17}H_{22}N_2O_3S$, 335.14; found, 334.9.

General Procedure V: Boc-deprotection and EDC coupling

The Boc-protected amine (16.5 mmol) was dissolved in dry CH_2Cl_2 (30 mL), followed by the addition of 4M HCl in dioxane (16 mL). The reaction mixture was stirred at rt for 2 h. The solvent was removed under reduced pressure and coevaporated with Et_2O (3 × 20 mL). The residue was further dried in high vacuum.

To a solution of the corresponding carboxylic acid (15 mmol) in dry CH_2Cl_2 (50 mL) EDC × HCl (19.5 mmol, 3.74 g), HOBt hydrate (19.5 mmol, 2.99 g) and DIPEA (45 mmol, 5.82 g, 7.84 mL) were added under argon atmosphere. A solution of the deprotected amine (16.5 mmol) in dry CH_2Cl_2 (10 mL) was added dropwise at 0 °C, followed by stirring of the mixture at rt for 24 h. Subsequently, the solution was diluted with CH_2Cl_2 (200 mL), washed with saturated $NaHCO_3$ solution, 0.5M HCl and brine (each 200 mL), dried over Na_2SO_4, filtered, and concentrated *in vacuo*.

***tert*-Butyl (2*S*,4*R*)-4-hydroxy-2-[[2-methyl-4-(4-methylthiazol-5-yl)phenyl]methyl-carbamoyl]pyrrolidine-1-carboxylate (8b)**

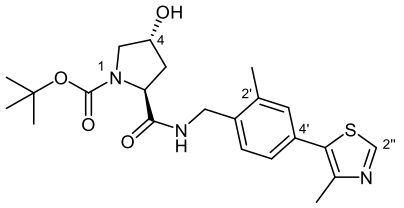

By using the General Procedure **V,** this compound was prepared on a 1.42 mmol scale from compound **6b** (0.45 g) and Boc-Hyp-OH (0.30 g). The crude product was purified by column chromatography (EtOAc) to give a colorless solid. Yield (0.26 g, 42%); mp 190 – 192 °C; R_f = 0.14 (EtOAc).

^{1}H NMR (600 MHz, DMSO-d_6) δ 1.27 and 1.41 (each s, 9H, the major and minor rotamer, C(CH_3)$_3$), 1.83 – 1.91 (m, 1H, 3-H), 2.01 – 2.12 (m, 1H, 3-H), 2.30 and 2.34 (each s, 3H, the major and minor rotamer, CH_3), 2.44 (s, 3H, CH_3), 3.37 – 3.49 (m, 1H), 4.14 – 4.29 (m, 3H), 4.29 – 4.38 (m, 1H), 4.97 and 4.98 (d, J = 3.3 Hz, 1H, major and minor rotamer, OH), 7.20 – 7.39 (m, 3H, 3'-H, 5'-H, 6'-H), 8.28 – 8.36 (m, 1H, NH), 8.97 (s, 1H, 2''-H).

^{13}C NMR (126 MHz, DMSO-d_6, the major rotamer) δ 15.88 (CH_3), 18.60 (CH_3), 27.87 (C($\underline{C}H_3$)$_3$), 38.61 (C-3), 54.73, 58.80 (C-2, C-5), 67.79 (C-4), 78.42 ($\underline{C}$(CH_3)$_3$), 126.12, 128.53, 129.99, 130.36, 131.07 (C-5'', C-Ar), 136.45 (C-2'), 137.05 (C-1'), 147.67 (C-4''), 151.33 (C-2''), 153.52 (NCO), 172.35 (CONH); the signal for NH$\underline{C}H_2$ is not visible (overlapping solvent peak).

LC-MS (ESI) (90% H_2O to 100% MeOH in 10 min, then 100% MeOH to 20 min, DAD 220-400 nm), t_R = 10.46 min, 98% purity, *m/z* $[M + H]^+$ calcd for $C_{22}H_{29}N_3O_4S$, 432.19; found, 432.0.

***tert*-Butyl (2*S*,4*R*)-4-hydroxy-2-[[2-methyl-4-(4-methylthiazol-5-yl)phenyl]methyl-carbamoyl]pyrrolidine-1-carboxylate (8c)**

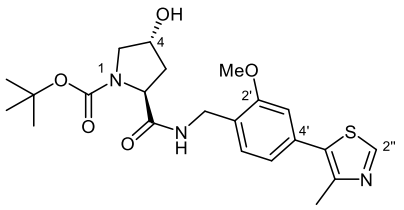

By using the General Procedure **V,** this compound was prepared on a 1.35 mmol scale from compound **6c** (0.45 g) and Boc-Hyp-OH (0.28 g). The crude product was purified by column chromatography (EtOAc) to give a colorless solid. Yield (0.14 g, 23%); mp 86 – 88 °C; R_f = 0.32 (CH_2Cl_2/MeOH 9:1).

^{1}H NMR (500 MHz, DMSO-d_6) δ 1.28 and 1.41 (each s, 9H, the major and minor rotamer, C(CH_3)$_3$), 1.84 – 1.92 (m, 1H, 3-H), 2.02 – 2.12 (m, 1H, 3-H), 2.46 (s, 3H, CH_3), 3.38 – 3.47 (m, 1H), 3.85 (s, 3H, OCH_3), 4.15 – 4.36 (m, 4H), 4.97 and 4.98 (d, *J* = 3.4 Hz, 1H, major and minor rotamer, OH), 6.99 – 7.04 (m, 2H), 7.25 (d, *J* = 7.7 Hz, 1H, 3'-H, 5'-H, 6'-H), 8.27 (t, *J* = 5.9 Hz, 1H, NH), 8.98 (s, 1H, 2''-H).

^{13}C NMR (126 MHz, DMSO-d_6) δ 15.90 (CH_3), 27.87 (C($\underline{C}H_3$)$_3$), 36.88 (C-3), 54.37, 55.51, 58.82 (OCH_3, C-2, C-5), 67.81 (C-4), 78.43 ($\underline{C}(CH_3)_3$), 111.15 (C-3'), 120.73 (C-5''), 127.70, 128.36, 131.26 (C-3', C-5', C-6'), 147.91 (C-4''), 151.43 (C-2''), 153.51 (NCO), 156.71 (C-2'), 172.58 (CONH); signal for NH$\underline{C}H_2$ is not visible (overlapping solvent peak).

LC-MS (ESI) (90% H_2O to 100% MeOH in 10 min, then 100% MeOH to 20 min, DAD 220-400 nm), t_R = 10.29 min, 96% purity, *m/z* $[M + H]^+$ calcd for $C_{22}H_{29}N_3O_5S$, 448.19; found, 448.0.

***tert*-Butyl (2*S*,4*S*)-2-[[2-[*tert*-butyl(diphenyl)silyl]oxy-4-(4-methylthiazol-5-yl)phenyl] methylcarbamoyl]-4-hydroxy-pyrrolidine-1-carboxylate (8e)**

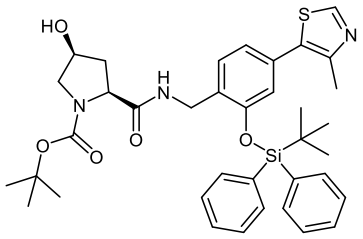

This compound was prepared using the General Procedure **IV**, compound **7** (2.0 mmol, 1.12 g), and Boc-D-Hyp-OH (2.0 mmol, 0.46 g). The crude product was purified by column chromatography (gradient of petroleum ether/EtOAc 1:1 to EtOAc) to obtain a colorless solid. Yield (0.66 g, 49%); mp 86 – 88 °C; R_f = 0.45 (EtOAc).

^{1}H NMR (600 MHz, DMSO-d_6) δ 1.06 (s, 9H, SiC(CH_3)$_3$), 1.35 (s, 9H, OC(CH_3)$_3$, 1.84 (s, 3H, CH_3), 1.89 – 1.97 (m, 1H), 2.06 – 2.16 (m, 1H, 3-H), 3.36 – 3.52 (m, 2H, 2-H, 4-H), 4.28 (dt, *J* = 7.9, 15.9 Hz, 2H, CH_2), 4.37 – 4.49 (m, 1H, 5-H), 4.54 – 4.68 (m, 2H, 5-H), 5.01 (s, 1H, OH), 6.38 (d, *J* = 7.5 Hz, 1H), 6.96 (d, *J* = 7.5 Hz, 1H), 7.27 (d, *J* = 7.9 Hz, 1H), 7.43-7.51 (m, 6H), 7.71 (t, *J* = 7.5 Hz, 4H, Ar-H), 8.38 – 8.43 (m, 1H, NH), 8.80 (s, 1H, 2”-H).

^{13}C NMR (151 MHz, DMSO-d_6) δ 15.32 (CH_3), 18.96 (SiC(CH_3)$_3$), 26.21 (SiC(CH_3)$_3$), 27.95 (OC(CH_3)$_3$), 37.30 (C-3), 38.66 ($NHCH_2$), 54.83, 58.97 (C-2, C-5), 67.88 (C-4), 78.59 (OC(CH_3)$_3$), 118.10 (C-3’), 121.54 (C-5’’), 128.19, 128.81, 130.39, 130.46, 131.42, 134.93 (C-Ar), 147.41 (C-4”), 151.46 (C-2”), 152.37 (C-2’), 153.57 (COO), 172.83 (CONH).

LC-MS (ESI) (90% H_2O to 100% MeOH in 10 min, then 100% MeOH to 20 min, DAD 220-400 nm), t_R = 12.38 min, 95% purity, *m/z* $[M + H]^+$ calcd for $C_{37}H_{45}N_3O_5SSi$, 672.29; found, 672.4.

HRMS (ESI) *m/z* $[M + H]^+$ calcd for $C_{37}H_{45}N_3O_5SSi$, 672.2922; found, 672.2905.

(2*S*,4*R*)-*N*-[[2-[*tert*-Butyl(diphenyl)silyl]oxy-4-(4-methylthiazol-5-yl)phenyl]methyl]-4-hydroxy-1-[(2*S*)-3-methyl-2-(1-oxoisoindolin-2-yl)butanoyl]pyrrolidine-2-carboxamide (12)

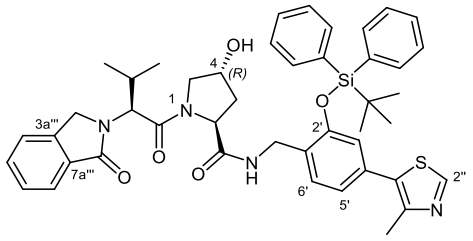

By using the General Procedure **IV**, this compound was prepared from **8d** (7 mmol, 5.59 g) and acid **17** (7 mmol, 1.63 g). The crude product was purified by column chromatography (CH_2Cl_2/MeOH 29:1) to obtain a colorless solid. Yield (3.09 g, 56%); mp 126 – 128 °C; R_f = 0.24 (CH_2Cl_2/MeOH 19:1).

^{1}H NMR (600 MHz, DMSO-d_6, the major rotamer) δ 0.75 (d, *J* = 6.5 Hz, 3H, CH(C$\underline{H}_3$)$_2$), 1.00 (d, *J* = 6.5 Hz, 3H, CH(C$\underline{H}_3$)$_2$), 1.07 (s, 9H, SiC(C$\underline{H}_3$)$_3$), 1.84 (s, 3H, CH_3), 1.95 – 2.02 (m, 1H), 2.05 – 2.11 (m, 1H, 3-H), 2.31 – 2.39 (m, 1H, C$\underline{H}$(CH$_3$)$_2$), 3.70 – 3.74 (m, 1H), 3.81 (dd, *J* = 4.4, 10.7 Hz, 1H, 5-H), 4.38 – 4.34 (m, 1H), 4.52 – 4.44 (m, 3H, 4-H, NHC$\underline{H}_2$, C$\underline{H}$CH(CH$_3$)$_2$), 4.59 – 4.54 (m, 2H, 3a'''-H), 4.74 (d, *J* = 10.8 Hz, 1H, 2-H), 5.10 (d, *J* = 4.1 Hz, 1H, OH), 6.39 (d, *J* = 1.7 Hz, 1H), 6.96 (dd, *J* = 1.7, 7.9 Hz, 1H), 7.39 (d, *J* = 7.9 Hz, 1H), 7.54 – 7.42 (m, 7H), 7.75 – 7.59 (m, 7H, Ar-H, SiAr-H), 8.48 (t, *J* = 5.8 Hz, 1H, CONH), 8.80 (s, 1H, 2''-H).

^{13}C NMR (151 MHz, DMSO-d_6, the major rotamer) δ 15.35 (CH_3), 18.60 (C($\underline{C}$H$_3$)$_2$), 18.91 (Si$\underline{C}$(CH$_3$)$_3$), 18.97 (C($\underline{C}$H$_3$)$_2$), 26.25 (SiC($\underline{C}$H$_3$)$_3$), 28.36 ($\underline{C}$(CH$_3$)$_2$), 37.38 (NHCH$_2$), 38.22 (C-3), 46.81 (C-3a'''), 55.41 (C-5), 57.80 ($\underline{C}$HCH(CH$_2$)$_3$), 58.76 (C-2), 68.62 (C-4), 117.92 (C-3'), 121.57 (C-5''), 123.00, 123.60, 127.88, 128.21, 128.23, 128.51, 128.72, 130.20, 130.40, 130.53, 131.36, 131.42, 131.56, 134.95, 134.96 (Ar-C), 142.19 (C-7a'''), 147.37 (C-4''), 151.42 (C-2''), 152.29 (C-2'), 167.49, 168.15, 171.68 (CO).

LC-MS (ESI) (90% H_2O to 100% MeOH in 10 min, then 100% MeOH to 20 min, DAD 200-400 nm), t_R = 12.75 min, 99% purity, *m/z* [M + H]$^+$ calcd for $C_{45}H_{50}N_4O_5SSi$, 787.33; found, 787.6.

HRMS (ESI) m/z [M + H]$^+$ calcd for $C_{45}H_{50}N_4O_5SSi$, 787.3344; found, 787.3319.

(2*S*,4*S*)-*N*-[[2-[*tert*-Butyl(diphenyl)silyl]oxy-4-(4-methylthiazol-5-yl)phenyl]methyl]-4-hydroxy-1-[(2*S*)-3-methyl-2-(1-oxoisoindolin-2-yl)butanoyl]pyrrolidine-2-carboxamide (13)

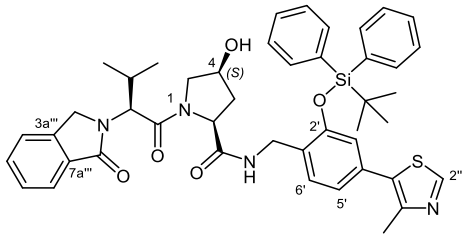

By using the General Procedure **IV**, this compound was prepared from **8e** (0.75 mmol, 0.50 g) and acid **17** (0.75 mmol, 175 mg). The crude product was purified by column chromatography (CH_2Cl_2/MeOH 29:1) to obtain a colorless solid. Yield (0.40 g, 68%); mp 84 – 86 °C; R_f = 0.37 (CH_2Cl_2/MeOH 9:1).

^{1}H NMR (600 MHz, DMSO-d_6) δ 0.72 (d, J = 6.8 Hz, 3H), 0.99 (d, J = 6.4 Hz, 3H, CH(C$\underline{H}_3$)$_2$), 1.03 (s, 9H, SiCH(C$\underline{H}_3$)$_2$), 1.81 (s, 3H, CH_3), 1.82 – 1.88 (m, 1H), 2.05 – 2.12 (m, 1H, 3-H), 2.33 – 2.42 (m, 1H, C$\underline{H}$(CH$_3$)$_2$), 3.32 – 3.37 (m, 1H), 3.55 – 3.61 (m, 1H, 5-H), 4.25 – 4.31 (m, 1H), 4.32 – 4.38 (m, 1H), 4.39 – 4.57 (m, 4H), 4.67 (d, J = 10.5 Hz, 1H, 2-H, 4-H, NCH, NHC$\underline{H}_2$, NCH$_2$), 5.12 (d, J = 3.4 Hz, 1H, OH), 6.36 (d, J = 1.8 Hz, 1H), 6.91 (dd, J = 1.7, 8.0 Hz, 1H), 7.32 (d, J = 7.9 Hz, 1H), 7.41 – 7.50 (m, 9H), 7.75 – 7.66 (m, 6H, Ar-H), 8.51 (t, J = 5.9 Hz, 1H, CONH), 8.80 (s, 1H, 2''-H).

^{13}C NMR (151 MHz, DMSO-d_6) δ 15.34 (CH_3), 18.25 (CH(C$\underline{H}_3$)$_2$), 18.94 (SiC$\underline{H}$(CH$_3$)$_2$), 19.84 (CH(C$\underline{H}_3$)$_2$), 26.22 (CH(C$\underline{H}_3$)$_3$), 27.47 (C$\underline{H}$(CH$_3$)$_2$), 37.36 (C-3), 38.22 (NHCH$_2$), 46.36 (C-2'''), 55.30 (C-5), 57.77 (C-2), 58.55 (NCH), 68.73 (C-4), 117.91 (C-3'), 121.57 (C-5''), 123.11, 123.41 (C-4''', C-7'''), 127.84 (C-6'''), 128.20, 128.43, 128.60, 130.20, 130.38, 130.50, 131.20, 131.40, 131.54, 134.92 (C-Ar, C-1', C-4', C-5', C-6' ,C-6''', C-7a'''), 142.10 (C-3a'''), 147.37 (C-4''), 151.43 (C-2''), 152.25 (C-2'), 167.32, 167.56, 172.00 (CO).

LC-MS (ESI) (90% H_2O to 100% MeOH in 10 min, then 100% MeOH to 20 min, DAD 200-330 nm), t_R = 12.59 min, 95% purity, m/z [M + H]$^+$ calcd for $C_{45}H_{50}N_4O_5SSi$, 787.33; found, 787.6.

HRMS (ESI) m/z [M + H]$^+$ calcd for $C_{45}H_{50}N_4O_5SSi$, 787.3344; found, 787.3325.

***tert*-Butyl *N*-[(1*S*)-1-[(2*S*,4*R*)-4-hydroxy-2-[[2-methyl-4-(4-methylthiazol-5-yl)phenyl] methylcarbamoyl]pyrrolidine-1-carbonyl]-2,2-dimethyl-propyl]carbamate (15)**

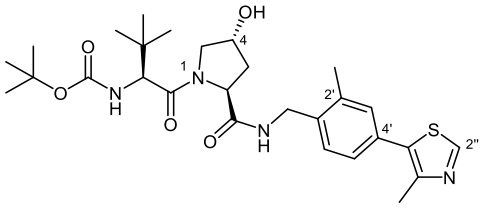

By using the General Procedure **V,** this compound was prepared on a 0.55 mmol scale from compound **8b** (0.24 g) and Boc-Tle-OH (0.12 g). The crude product was purified by column chromatography (EtOAc) to give a white solid. Yield (0.16 g, 53%); mp 94 – 96 °C; R_f = 0.42 (CH_2Cl_2/MeOH 9:1).

^{1}H NMR (500 MHz, DMSO-d_6) δ 0.92 (s, 9H, C(CH_3)$_3$), 1.38 (s, 9H, OC(CH_3)$_3$), 1.88 – 1.94 (m, 1H 3-H), 2.00 – 2.07 (m, 1H, 3-H), 2.29 (s, 3H, CH_3), 2.44 (s, 3H, CH_3), 3.57 – 3.69 (m, 2H), 4.11 – 4.22 (m, 2H), 4.35 (dd, *J* = 5.9, 15.7 Hz, 2H), 4.47 (t, *J* = 7.9 Hz, 1H, 2-H, 4-H, 5-H, NHC<u>H</u>, CHC<u>H</u>$_2$), 5.11 (d, *J* = 2.1 Hz, 1H, OH), 6.39 (d, *J* = 7.7 Hz, 1H, BocNH), 7.21 (d, *J* = 7.8 Hz, 1H), 7.26 (s, 1H), 7.44 (d, *J* = 7.9 Hz, 1H, 3'-H, 5'-H, 6'-H), 8.41 (t, *J* = 5.2 Hz, 1H, CONH), 8.96 (s, 1H, 2''-H).

^{13}C NMR (126 MHz, DMSO-d_6) δ 15.89 (CH_3), 18.44 (CH_3), 26.22 (C(<u>C</u>H$_3$)$_3$), 28.13 (OC(<u>C</u>H$_3$)$_3$), 35.31 (<u>C</u>(CH$_3$)$_3$), 37.87 (C-3), 56.28, 58.34, 58.63 (C-2, C-5, NHCH), 68.86 (C-4), 78.03 (O<u>C</u>(CH$_3$)$_3$), 126.05 , 127.88 , 129.72 , 130.15 , 131.16 (C-3', C-4', C-5', C-6', C-5''), 136.25 (C-2') , 136.98 (C-1'), 147.59 (C-4''), 151.26 (C-2''), 155.28 (NCO), 169.76, 171.64 (CO); the signal for NH<u>C</u>H$_2$ is not visible (overlapping solvent peak).

LC-MS (ESI) (90% H_2O to 100% MeOH in 10 min, then 100% MeOH to 20 min, DAD 220-400 nm), t_R = 11.40 min, 98% purity, *m/z* $[M + H]^+$ calcd for $C_{28}H_{40}N_4O_5S$, 545.28; found, 545.3.

HRMS (ESI) *m/z* $[M + H]^+$ calcd for $C_{28}H_{40}N_4O_5S$, 545.2753; found, 545.2771.

***tert*-Butyl *N*-[(1*S*)-1-[(2*S*,4*R*)-4-hydroxy-2-[[2-methoxy-4-(4-methylthiazol-5-yl)phenyl] methylcarbamoyl]pyrrolidine-1-carbonyl]-2,2-dimethyl-propyl]carbamate (16)**

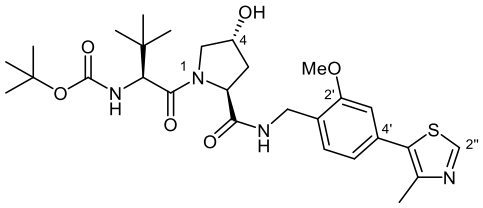

By using the General Procedure **V,** this compound was prepared on a 0.25 mmol scale from compound **8c** (0.11 g) and Boc-Tle-OH (0.05 g). The crude product was purified by column chromatography (EtOAc) to give a white solid. Yield (0.07 g, 53%); mp 78 – 80 °C; R_f = 0.44 (CH_2Cl_2/MeOH 9:1).

^{1}H NMR (500 MHz, DMSO-d_6) δ 0.92 (s, 9H, C(CH_3)$_3$), 1.39 (s, 9H, OC(CH_3)$_3$), 1.89 – 1.95 (m, 1H, 3-H), 2.00 – 2.08 (m, 1H, 3-H), 2.46 (s, 3H, CH_3), 3.60 (d, *J* = 10.9 Hz, 1H), 3.65 (dd, *J* = 4.1, 10.5 Hz, 1H), 3.85 (s, 3H, OCH_3), 4.17 (dd, *J* = 4.4, 16.4 Hz, 2H), 4.28 (dd, *J* = 6.3, 16.4, Hz, 1H), 4.36 (s, 1H), 4.49 (t, *J* = 8.0 Hz, 1H, 2-H, 4-H, 5-H, NHC<u>H</u>, CHC<u>H</u>$_2$), 5.11 (d, *J* = 3.1 Hz, 1H, OH), 6.41 (d, *J* = 9.3 Hz, 1H, BocNH) 6.94 (dd, *J* = 1.4, 7.7 Hz, 1H), 7.01 (d, *J* = 1.4 Hz, 1H), 7.44 (d, *J* = 7.8 Hz, 1H, 3'-H, 5'-H, 6'-H), 8.40 (t, *J* = 5.8 Hz, 1H, CONH), 8.98 (s, 1H, 2''-H).

^{13}C NMR (126 MHz, DMSO-d_6) δ 15.94 (CH_3) , 26.21 (C(<u>C</u>H$_3$)$_3$), 28.15 (OC(<u>C</u>H$_3$)$_3$), 35.32 (<u>C</u>(CH$_3$)$_3$), 37.11 (NH<u>C</u>H$_2$), 37.80 (C-3), 55.48, 56.27, 58.35, 58.68 (OCH_3, C-2, C-5, NHCH), 68.87 (C-4), 78.05 (O<u>C</u>(CH$_3$)$_3$), 110.80 (C-3'), 120.73 (C-5''), 126.86, 127.90, 130.87, 131.29 (C-1', C-4', C-5', C-6'), 147.81 (C-4''), 151.36(C-2'') , 155.30 (NCO), 156.48 (C-2') , 169.84 , 171.92 (CO).

LC-MS (ESI) (90% H_2O to 100% MeOH in 10 min, then 100% MeOH to 20 min, DAD 220-400 nm), t_R = 11.24 min, 98% purity, *m/z* [M + H]$^+$ calcd for $C_{28}H_{40}N_4O_6S$, 561.27; found, 561.1.

HRMS (ESI) *m/z* [M + H]$^+$ calcd for $C_{28}H_{40}N_4O_6S$, 561.2702; found, 561.2752.

Author Contributions

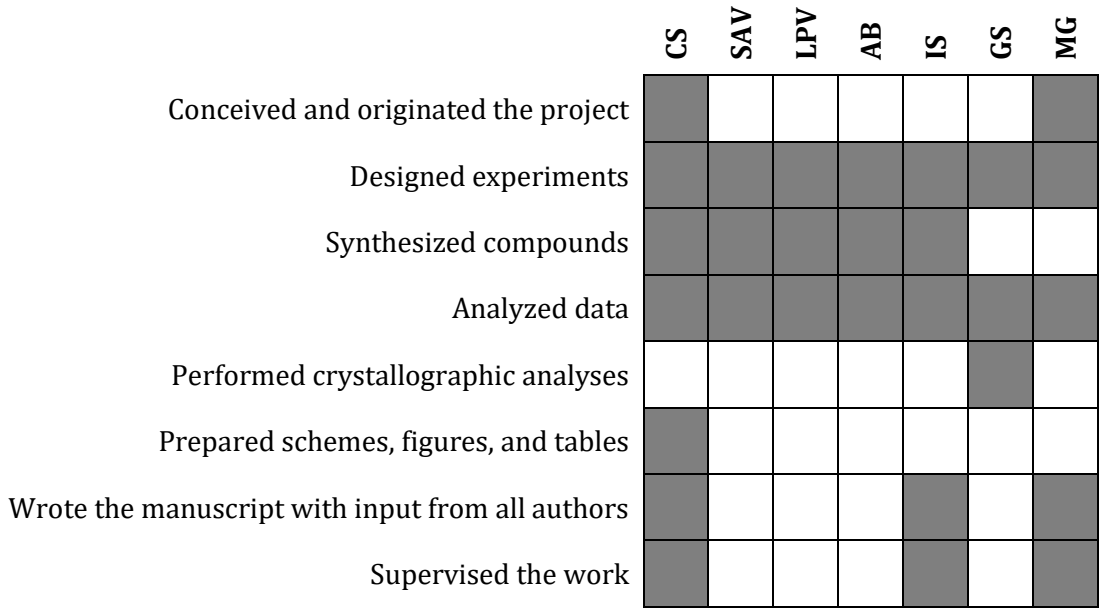

References

(1) Pergomet, J. L.; Kaufman, T. S.; Bracca, A. B. J. *Helv. Chim. Acta* **2016**, *99*, 398.

(2) *Category 4, Compounds with Two Carbon Heteroatom Bonds: Aldehydes*; Brückner, Ed.; 1st ed.; Georg Thieme Verlag: Stuttgart, **2007**.

(2) Buckley, D. L.; Raina, K.; Darricarrere, N.; Hines, J.; Gustafson, J. L.; Smith, I. E.; Miah, A. H.; Harling, J. D.; Crews, C. M. *ACS Chem. Biol.* **2015**, *10*, 1831.

(3) Allin, S. M.; Hodkinson, C. C.; Taj, N. *Synlett* **1996**, *1996*, 781.

(4) Steinebach, C.; Kehm, H.; Lindner, S.; Vu, L. P.; Köpff, S.; López Mármol, Á.; Weiler, C.; Wagner, K. G.; Reichenzeller, M.; Krönke, J.; Gütschow, M. *Chem. Commun.* **2019**, *55*, 1821.

(5) (a) Spek, A. L. *J. Appl. Cryst.* **2003**, *36*, 7; (b) Spek, A. L. *Acta Cryst.* **2009**, *D65*, 148.

Appendix II. Publication II: Diketomorpholines: Synthetic Accessibility and Utilization

The following pages include the mini-review article "Diketomorpholines: Synthetic Accessibility and Utilization" as it was published in ACS Omega by ACS Publications. According to the ACS copyright and license, the reuse of this article for a thesis or dissertation is allowed, as long as the thesis or dissertation is not published commercially and no creations of adaptations or other derivative works are made.

The article is reprinted with permission from:

Vu, L. P.; Gütschow, M. Diketomorpholines: Synthetic Accessibility and Utilization. *ACS Omega* **2022**, *7*, 48–54. doi.org/10.1021/acsomega.1c05964

ACS OMEGA

http://pubs.acs.org/journal/acsodf

Mini-Review

Diketomorpholines: Synthetic Accessibility and Utilization

Lan Phuong Vu and Michael Gütschow*

Cite This: *ACS Omega* 2022, 7, 48−54

Read Online

ACCESS | Metrics & More | Article Recommendations

ABSTRACT: Diketomorpholines (DKMs; morpholine-2,5-diones) possess a six-membered ring with a lactone and lactam moiety and belong to the family of cyclodepsipeptides. In this review, the synthetic accessibility of DKMs is summarized and their utilization, in particular, for ring-opening polymerization reactions, is highlighted. The occurrence of the DKM scaffold in natural products encompasses small monocyclic compounds but also complex, polycyclic representatives with a fused DKM ring.

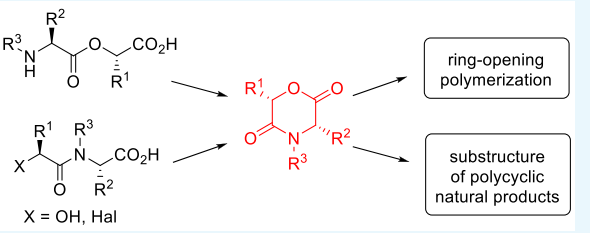

1. INTRODUCTION

Diketomorpholines (DKMs; morpholine-2,5-diones) constitute derivatives of the heterocyclic structure **1** (Figure 1).

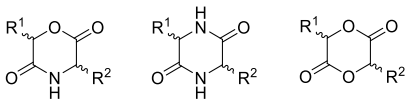

Figure 1. General structures of diketomorpholines (**1**), diketopiperazines (**2**), and substituted glycolides (**3**).

DKMs bear one lactam and one lactone moiety, which occur each two-fold in highly abundant diketopiperazines **2** and glycolides **3**, respectively (Figure 1). With the lactam and lactone group in the same six-membered ring, DKMs can be regarded as the simplest members of the large family of cyclodepsipeptides and are also referred to as cyclodepsidipeptides.[1] In this review, a comprehensive overview on the synthetic access to DKMs is given, and some remarkable applications and the occurrence of the DKM scaffold in natural products are described.

2. SOLUTION-PHASE SYNTHESES

In the following, recent and representative examples showing the synthetic access to DKMs will be summarized (Schemes 1 and 2). In both schemes, only one possible configuration for the two chiral carbons is shown. However, not only the depicted (3*S*,6*S*)-configured products have been prepared by the different outlined methods, but also diastereomers with other defined configurations, racemic products, as well as achiral compounds **1** and **10**, in which R^1 and R^2 are hydrogens. Further protocols employed for DKM synthesis are summarized elsewhere.[1]

DKMs are available through cyclative lactonizations (Scheme 1). For the ring-closure reactions, precursors **4**−**9** have been utilized, all of which already contain a central amide bond. In the resulting product structures **1** and **10**, it appears as an unsubstituted or substituted lactam moiety, respectively. The formation of the lactone bond from free acids **4** or **5** was accomplished either by proton-catalyzed condensations or in the presence of coupling reagents or under Mitsunobu conditions. Acid- or base-promoted conversions of the esters **6** or **7** produced products **1** and **10** in the course of interesterifications. Furthermore, halogen-substituted educts **8** or **9** were employed for lactone generation under basic conditions. In some cases, ester progenitor compounds were saponified to the corresponding acids **8** or **9** prior to the cyclocondensation.

As a second opportunity, educts **11** and **12** with a preformed central ester group have been subjected to lactamization, leading to cyclized products **1** and **10** (Scheme 2). The conversions include the successful application of the Mukaiyama reagent. Typically, the terminal amino group was deprotected before the cyclization occurred.

Macrocyclic analogues of DKMs have been prepared from lactams bearing an *ε*-hydroxyacyl residue at the cyclic nitrogen atom. Attack of the terminal oxygen at the ring carbonyl led to side-chain insertion to bicyclic cyclols, and the subsequent ring expansion gave monocyclic products which represent macrocyclic counterparts of DKMs **1**.[14]

Recently, in a study on macrocyclo-oligomerizations, it was observed that the tetradepsipeptide **13** underwent an intramolecular attack of the carboxylate at the central ester, leading to an anhydride isomer **14**, followed by fragmentation due to

Received: October 25, 2021
Accepted: December 7, 2021
Published: December 22, 2021

Scheme 1. Synthetic Entries to DKMs from Hydroxyacyl or Haloacyl Derivatives[a]

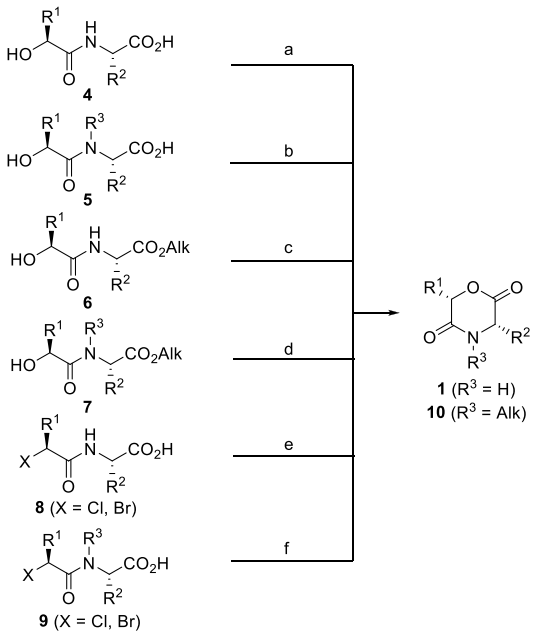

[a]Reagents and conditions: (a) DMAP, BOP reagent, CH_2Cl_2,[2] or $MeSO_3H$, $CHCl_3$, Δ;[3] (b) DEAD, THF;[2] (c) Amberlyst 15, toluene, Δ,[2] or *p*-TsOH, toluene, Δ;[4,5] (d) *p*-TsOH, toluene, Δ,[4] or DBU, MS 4 Å, toluene;[6] (e) $NaHCO_3$, DMF, Δ,[7,8] or TEA, DMF, Δ,[2,9] or DIPEA, $CHCl_3$, Δ,[10] or (1) NaOH, EtOH, H_2O, (2) H_2SO_4;[2] (f) DIPEA, DMSO,[11] or (1) K_2CO_3, H_2O, (2) HCl,[12] or (1) NaOH, EtOH, H_2O, (2) HCl.[2]

Scheme 2. Synthetic Entries to DKMs from Aminoacyl Derivatives[a]

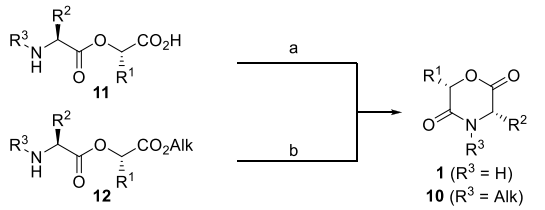

[a]Reagents and conditions: (a) 2-chloro-1-methylpyridinium iodide, DIPEA, CH_2Cl_2,[13] or 2-chloro-1-methylpyridinium iodide, TEA, CH_2Cl_2;[13] (b) piperidine, DMF,[13] DMAP, pyridine, Δ.[13]

the nucleophilic attack of the alcoholic group and generation of the protected compound **15** and DKM **16** (Scheme 3).[15]

Scheme 4 shows ester-based prodrugs (**17**) of glucagon-like peptide 1 (GLP) in its biologically active form GLP(7−36) and fused to peptide CEX, a nine-amino-acid C-terminal extension.[16] The N-terminal phenylalanine was replaced with phenyllactic acid, and the prodrugs dissociate under physiological conditions through formation of DKMs **1** and liberate the active peptide **18**.

3. SOLID-PHASE SYNTHESES

DKMs are accessible through various polymer-supported methods.[17] Cyclization of resin-bound bromides **19** (Scheme 5) was induced by treatment with TFA, initially leading to cleavage from the Wang resin, followed by ring closure to DKMs (R^1 = H or alkyl, R^2 = alkyl).[18] A resin which consisted

Scheme 3. Proposed Mechanism for the Self-Cleavage of a Tetradepsipeptide

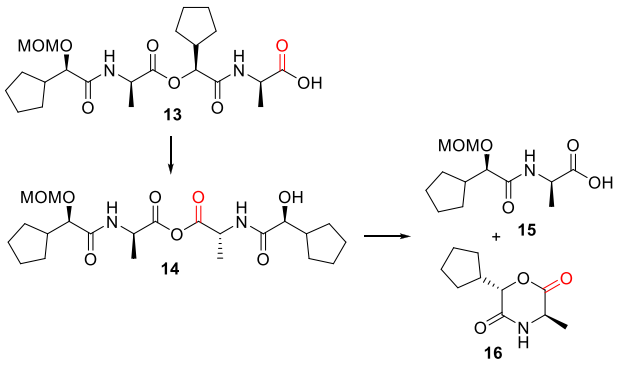

Scheme 4. Hydroxy-Mediated Ester Cleavage of GLP Prodrugs (pH 7.4, 37 °C)

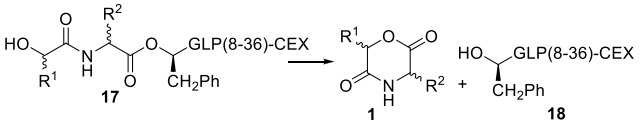

Scheme 5. General Entries to DKMs via Solid-Phase Synthesis[a]

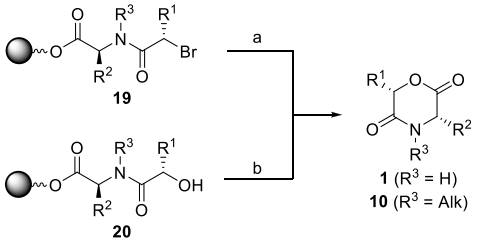

[a]Reagents and conditions: (a) TFA (Wang resin);[18] (b) TEA, CH_2Cl_2 (TentaGel resin).[18] Racemic mixtures were applied,[18] and only single (*S*,*S*)-configured stereoisomers are depicted here.

of polyethylene glycol attached to cross-linked polystyrene through an ether linkage was employed for DKM synthesis.[18] Here, the resin-bound structure **20** (R^1 = alkyl, R^2 = alkyl) was assembled by Ugi reaction, and the NR^3 portion of the products corresponded to the structure of amino acid amides with R^3 = CH(alkyl)CONH(cyclohexyl).

DKM precursors were coupled to the polymer matrix via a photolabile 5-bromo-7-nitroindoline moiety (**21**), and alanine, leucine, and phenylalanine-based DKMs **22** were produced in the course of an intramolecular photoinduced cyclorelease (Scheme 6).[19]

Scheme 6. Photoinduced Cleavage of DKMs from the Resin

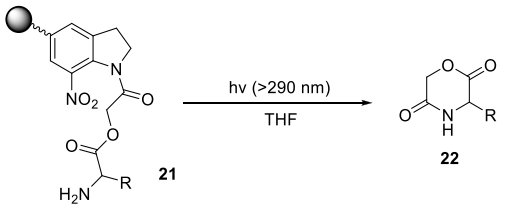

https://doi.org/10.1021/acsomega.1c05964
ACS Omega 2022, 7, 48−54

The resin-bound structure **23** was produced by loading *tert*-butyl serine, deprotection, alkylation with bromoketones, and acylation (Scheme 7).[11] TFA-mediated liberation from the

Scheme 7. Formation of Bi- and Monocylic DKMs

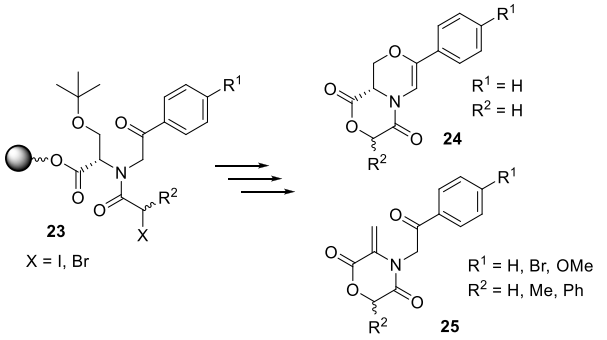

solid support triggered a cyclization to the 3,4-dihydro-2*H*-1,4-oxazine scaffold, followed by based-catalyzed lactonization to the fused second ring. At prolonged reaction time, eliminative cleavage occurred and monocyclic DKMs **25** were formed, for example, from **24**. An analogous protocol could be used for the solid-phase-supported generation of tricyclic DKMs **29** (Scheme 8).[20]

Scheme 8. Formation of Tricylic DKMs[a]

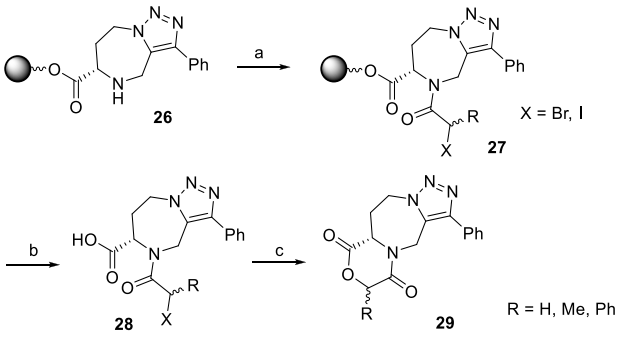

[a]Reagents and conditions: (a) halocarboxylic acid, DIC, CH_2Cl_2; (b) TFA, CH_2Cl_2; (c) DIPEA, DMSO.

An N-terminal degradation of peptoid oligomers through sequential cleavage of N-substituted glycine units was accomplished on a solid phase.[21] The protocol relied on the treatment of resin-bound bromoacetylated peptoids **31** with silver perchlorate, leading to an intramolecular lactonization, releasing the terminal residue as part of an N-substituted DKM **34**, and resulting in the truncated peptoid **33** (Scheme 9).

4. CHEMICAL REACTIVITY AND UTILIZATION IN RING-OPENING POLYMERIZATIONS

The chemical reactivity of DKMs has mainly been explored to perform ring-opening polymerization reactions (see below). In a model transformation, N-substituted, racemic DKMs **35** were treated with ethanolic ammonia to undergo ring opening to diamides 36 (Scheme 10). The second step leading to intermediates **37** occurred slower and involved the intramolecular participation of the primary carboxamide moiety. The imides **37** were susceptible to subsequent conversions with nucleophiles.[22] The regioselective course of the ring

Scheme 9. Iterative Peptoid Sequencing through DKM Liberation[a]

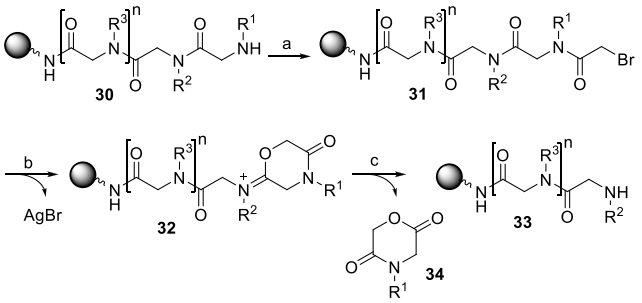

[a]Reagents and conditions: (a) $BrCH_2CO_2H$, DIC, DMF; (b) $AgClO_4$, THF, (c) H_2O.

Scheme 10. Ammonolysis of DKMs to Diamides and Acyl Transfer to Imides[a]

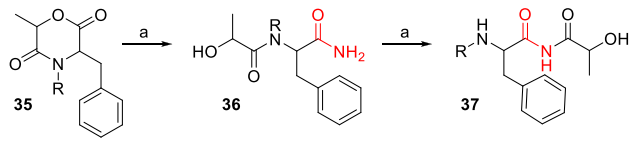

[a]Reagents and conditions: (a) 5 M NH_3/EtOH, room temperature.

opening of **35** reflected the expected higher electrophilic reactivity of the lactone group compared to that of the lactam group in DKMs. The cleavage of a defined DKM with a functionalized benzylamine was utilized for the preparation of a thrombin inhibitor.[22]

Overall, the synthetic potential of DKMs to generate defined low-molecular weight compounds with tailored properties has not yet been fully exploited. In contrast, DKMs have been frequently utilized as monomers for polymerization reactions.

Polydepsipeptides are alternating copolymers of an α-amino and an α-hydroxy acid. They are valued for their nontoxic properties and their degradability and are suitable for numerous applications, such as tissue engineering and drug delivery. Compared to polypeptides, polydepsipeptides do not necessarily require enzymes for their degradation because of the hydrolytic susceptibility of the ester groups. The presence of the carboxamide portions in polydepsipeptides allows for strong intramolecular hydrogen bond interactions, in contrast to polyesters. These hydrogen bonds influence their mechanical and thermal properties, which can be fine-tuned by variations of the amino acid moieties. In particular, telechelic oligodepsipeptides, capable of entering into further polymerization or other reactions through their reactive terminal groups, serve as valuable building blocks for biomedical applications.[3,23]

Polydepsipeptides (**38**) are generally accessibly by employing DKMs (**1**) in ring-opening polymerization reactions (Scheme 11). Several attempts have been made to control copolymer compositions, molecular weights, crystallinity, and degradability by using different polymerization conditions.[10,23]

As a catalyst, stannous octoate (tin(II) 2-ethylhexanoate, $Sn(Oct)_2$) has frequently been used. Following the "coordination−insertion" mechanism, a tin alkoxide is formed from $Sn(Oct)_2$ and a hydroxyl group of the initiator molecule, the carbonyl oxygen coordinates the metal center, followed by the nucleophilic attack of the alkoxide ligand and subsequent

https://doi.org/10.1021/acsomega.1c05964
ACS Omega 2022, 7, 48−54

Scheme 11. Ring-Opening Polymerization to Produce Polydepsipeptides from DKMs[a]

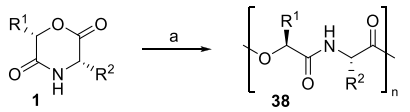

[a]Reagents and conditions: (a) $Sn(Oct)_2$, $CHCl_3$,[10] or BnOH, TBD or DBU, THF or $CHCl_3$.[7,8]

lactone bond cleavage, thus generating an analogous, active species.[23] 1,5,7-Triazabicyclo[4.4.0]dec-5-ene (TBD) was a particularly active catalyst for the generation of polymers **38** (R^1 = H, R^2 = H or alkyl) from corresponding DKMs **1** using benzyl alcohol as an initiator.[7] Several bases, such as 1,8-diazabicyclo[5.4.0]undec-7-ene (DBU), were investigated in polymerizations of methionine-derived DKMs **1** (R^1 = H or alkyl, R^2 = $CH_2CH_2SCH_3$).[8] The resulting poly(ester amides) **38** were applicable for postpolymerization modifications via "methionine click" chemistry.[8,24]

DKMs could be copolymerized with substituted glycolides (**3**, Figure 1) or lactones such as ε-caprolactone to achieve copolymers with tailored properties.[10,23] A detailed description has been provided elsewhere.[23] Instead of $Sn(Oct)_2$ as the catalyst and ethylene glycol as the initiator,[23] a single Sn(IV) organotin compound could perform both tasks. 2,2-Dibutyl-1,3,2-dioxastannolane, prepared from dibutyltin oxide and ethylene glycol, was employed in the ring-opening polymerization to prepare **39** (Scheme 12).[3] The softness of the metal

Scheme 12. Generation of Block Polymers by Ring-Opening Polymerization Reactions of DKMs[a]

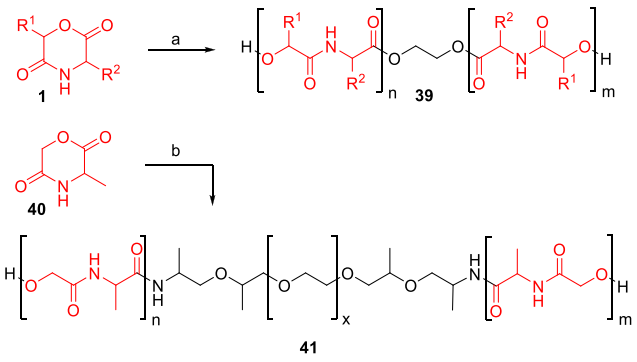

[a]Reagents and conditions: (a) $Sn(Oct)_2$, ethylene glycol, 140 °C;[23] or (1) dibutyltin oxide, ethylene glycol, (2) bulk, 140 °C;[3] (b) Jeffamines ED-600, ED-900, or ED-2001, THF, 140 °C.[23]

catalyst influenced the outcome of the polymerization, and $Fe(OAc)_2$ performed best among non-$Sn(Oct)_2$ catalysts in ring-opening polymerizations with different DKMs and 1,8-octanediol as an initiator.[9] Block copolymers **41** were synthesized by means of ring-opening polymerization with 3-methylmorpholine-2,5-dione (**40**) and an amino-terminated polyethylene glycol (PEG) as an initiator.[23]

DKMs are expected to be involved in the chemical evolution from amino acids to peptides. Model prebiotic molecules were generated from monomers by wet−dry cycling experiments and DKMs such as **61** identified in the obtained mixtures, in addition to depsipeptides, polyesters, peptides, and yet unreacted hydroxy and amino acids (Scheme 13).[25]

Scheme 13. DKM 61 as an Intermediate in a Proposed Pathway to Trimeric Prebiotic Compounds

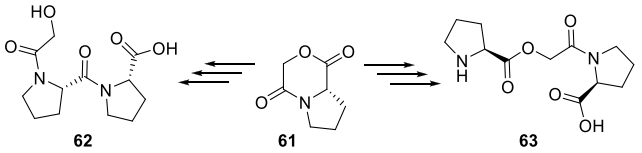

5. NATURAL PRODUCTS

Monocyclic DKMs have been reported as natural products. Examples are shown in Figure 2. Enniatins are mixtures of

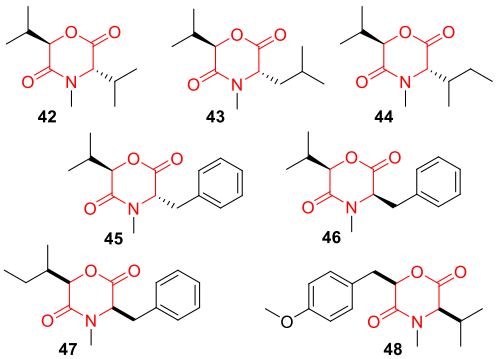

Figure 2. Monocyclic DKMs from natural sources.

cyclic hexadepsipeptides found in *Fusarium* fungi. Enniatin B forms an 18-membered ring composed of each three alternating *N*-methyl-(*S*)-valine and (*R*)-2-hydroxy-3-methyl-butanoic acid building blocks. The DKM congeners **42**−**44**, supposed side products of the nonribosomal enniatin B biosynthesis, were isolated from *Fusarium sporotrichioides* (Figure 2).[12] DKM **42**, which contained the two enniatin B building blocks, was present in prevailing amounts in the broth and mycelium of *Fusarium sporotrichioides*, whereas the production of **43** and **44** was presumably due to low substrate specificity of the enniatin synthetase for (*S*)-amino acids.[12] Compound **42** exhibited inhibitory properties against xanthine oxidase and anti-inflammatory activity in human peripheral blood mononuclear cells.[26] Aliphatic DKM derivatives such as **42** and **43** have been evaluated with respect to their antimicrobial, antioxidant, immunomodulatory, and antiproliferative activities.[1,26]

Bassiatin (**45**) was isolated from the cultured broth of the entomopathogenic sac fungus *Beauveria bassiana*, in addition to depsipeptides of a higher oligomerization state such as the cyclic hexadepsipeptide beauvericin.[27] Bassiatin possessed insecticidal activities against *Bemisia tabaci*, a whitefly and important agricultural pest, in contact and feeding assays. Bassiatin inhibited the ADP-induced platelet aggregation.[27] A diastereomer (**46**) from the sac fungus *Isaria japonica* induced apoptotic cell death in human leukemia cells in the micromolar range.[27] DKM **47** was identified as a constituent of the traditional Chinese medicine *Bombyx batryticatus*, the dried dead larva of silkworms after infection by *Beauveria bassiana*.[27] DKM **48** was isolated from the sea hare *Bursatella leachii*.[27] Other DKMs bearing *N*-benzyl substituents have been synthesized and investigated as inhibitors of glucosidases, as summarized elsewhere.[1]

https://doi.org/10.1021/acsomega.1c05964
ACS Omega 2022, 7, 48−54

The greater propensity of proline and *N*-methyl-substituted amino acids to adopt a *cis* conformation and the consequent preferred DKM cyclization might account for the more frequent appearance of bicyclic DKMs such as **61** (Scheme 13)[25] and *N*-methyl-substituted DKMs such as **42**−**48** (Figure 2).

DKMs are substructures of naturally occurring polycyclic indole alkaloids. Respective natural products mainly contain a diketopiperazine ring fused to the terminal five-membered ring of the pyrrolidinoindoline system.[5] However, there are also natural products in which a DKM unit replaced the diketopiperazine core. Such tetracyclic compounds (**49**−**58**) are depicted in Figure 3. Mollenines A (**49**) and B (**50**) were

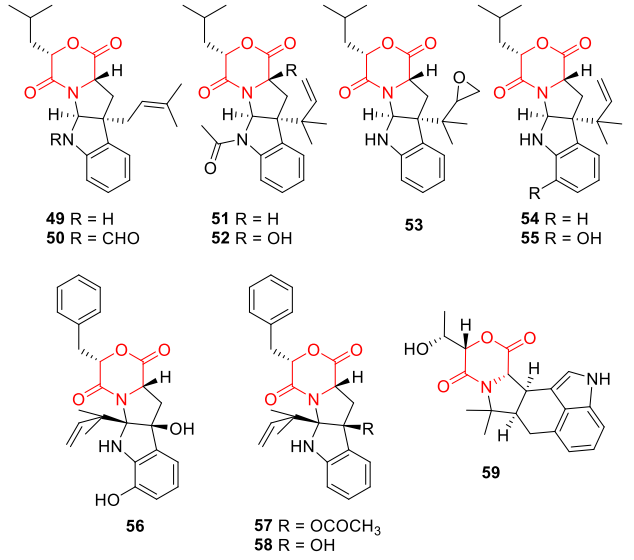

Figure 3. Polycyclic natural products with a fused DKM ring.

isolated from the sclerotioid ascostromata of *Eupenicillium molle*.[28] The total synthesis of **49** was realized either by the preparation of a prenylated pyrrolidinoindoline ester from tryptophan and the final connection with leucic acid[6] or by a one-pot reaction of the DKM composed of tryptophan and leucic acid with a vinyl cyclopropane reagent.[28] Mollenine A possessed cytotoxic and antibacterial activity against *Bacillus subtilis*.[28] Javanicunines A (**51**) and B (**52**) are isoprenylated DKM alkaloids isolated from the extract of *Eupenicillium javanicum*.[28] The key step of the synthetic access to these DKMs was the linkage of the prenylated pyrrolidinoindoline ester with leucic acid followed by lactonization.[5] Recently, similar DKM natural products, such as deacetyl-javanicunine A (**54**), javanicunine C (**53**), and javanicunine D (**55**), were identified from a *Penicillium* species.[28]

The DKM alkaloids PF1233 B, also referred to as shornephine A (**56**) and 9-deoxy-PF1233 A (**57**) and B (**58**), were identified from marine-sediment-derived *Aspergillus* species.[4] Methanolysis of **56** occurred at the lactone moiety and led to the opening of the DKM cycle.[4] The total synthesis of **57** and **58** was accomplished via an epoxidation of the intermediate DKM containing a tryptophan and leucic acid moiety. Subsequent intramolecular epoxide opening led to the tetracyclic scaffold.[5] PF1233 B (**56**) was reported as a noncytotoxic inhibitor of P-glycoprotein transporters, key mediators of drug efflux in multi-drug-resistant human cancer cells.[4] Clonorosin A (**59**) with the DKM ring fused to a tetracyclic isoindolo[4,5,6-*cd*]indole system was isolated from the soil-derived fungus *Clonostachys rosea*. It showed activity against *Fusarium oxysporum*, an ascomycete fungus which is pathogenic to plants.[29]

Further DKM alkaloids such as acu-dioxomorpholines from the fungus *Aspergillus aculeatus* were identified using a fungal artificial chromosome and metabolomic scoring platform. Due to this technology, the DKM biosynthetic pathway was elucidated, and nonribosomal peptide synthetase gene clusters responsible for the production of DKM alkaloids were characterized.[30]

6. CONCLUSIONS

Despite the striking simplicity of the diketomorpholine structure, this chemotype has received less general attention than expected. This review highlights the various synthetic routes to DKMs and their chemical reactivity, in particular, in the application of ring-opening reactions leading to tailored polymers. Furthermore, compounds bearing the DKM scaffold are represented among natural products, particularly fungal metabolites. Naturally occurring DKMs comprise small, monocyclic compounds but also complex alkaloids with a fused DKM substructure. Obviously, the class of DKMs still has not been fully explored and gives space for further research and application. Hence, this review might encourage scientists to increasingly take account of several aspects of diketomorpholine synthetic and natural product chemistry for their own research.

AUTHOR INFORMATION

Corresponding Author

Michael Gütschow − *Pharmaceutical Institute, Pharmaceutical & Medicinal Chemistry, University of Bonn, 53121 Bonn, Germany*; orcid.org/0000-0002-9376-7897; Email: guetschow@uni-bonn.de

Author

Lan Phuong Vu − *Pharmaceutical Institute, Pharmaceutical & Medicinal Chemistry, University of Bonn, 53121 Bonn, Germany*

Complete contact information is available at: https://pubs.acs.org/10.1021/acsomega.1c05964

Notes

The authors declare no competing financial interest.

Biographies

Lan Phuong Vu received her B.Sc. and M.Sc. degrees in Chemistry from the University of Bonn in 2016 and 2018, respectively. Currently, she is pursuing a Ph.D. in the Gütschow group in the Department of Pharmaceutical & Medicinal Chemistry at the University of Bonn. Her research interest is focused on the development VHL-based PROTACs.

Michael Gütschow studied Biochemistry at the University of Leipzig, Germany, and received his Ph.D. in Pharmaceutical Chemistry. He was a Scientific Assistant at the Department of Biosciences at the University of Leipzig and a Postdoctoral researcher at the Georgia Institute of Technology, Atlanta, Georgia, USA. In 1998, he received his Habilitation at the University of Leipzig in the field of Pharmaceutical Chemistry. Since 2001, he is Professor for Pharmaceutical Chemistry at the University of Bonn. His research interests include (i) design of inhibitors and activity-based probes for cysteine and serine proteases, (ii) synthesis of bioactive heterocycles,

https://doi.org/10.1021/acsomega.1c05964
ACS Omega 2022, 7, 48−54

(iii) peptidic and peptidomimetic drugs, (iv) development of PROTACs, and (v) biochemistry of enzyme-drug interactions. He published more than 280 publications to the scientific topics mentioned.

REFERENCES

(1) Smelcerovic, A.; Dzodic, P.; Pavlovic, V.; Cherneva, E.; Yancheva, D. Cyclodidepsipeptides with a promising scaffold in medicinal chemistry. *Amino Acids* **2014**, *46*, 825−840.

(2) (a) Maryanoff, B. E.; Greco, M. N.; Zhang, H. C.; Andrade-Gordon, P.; Kauffman, J. A.; Nicolaou, K. C.; Liu, A.; Brungs, P. H. Macrocyclic peptide inhibitors of serine proteases. Convergent total synthesis of cyclotheonamides A and B via a late-stage primary amine intermediate. Study of thrombin inhibition under diverse conditions. *J. Am. Chem. Soc.* **1995**, *117*, 1225−1239. (b) Hughes, A. B.; Sleebs, M. M. Total synthesis of bassiatin and its stereoisomers: novel divergent behavior of substrates in Mitsunobu cyclizations. *J. Org. Chem.* **2005**, *70*, 3079−3088. (c) Shi, C. X.; Guo, Y. T.; Wu, Y. H.; Li, Z. Y.; Wang, Y. Z.; Du, F. S.; Li, Z. C. Synthesis and controlled organobase-catalyzed ring-opening polymerization of morpholine-2,5-dione derivatives and monomer recovery by acid-catalyzed degradation of the polymers. *Macromolecules* **2019**, *52*, 4260−4269. (d) Cingolani, G. M.; Di Stefano, A.; Mosciatti, B.; Napolitani, F.; Giorgioni, G.; Ricciutelli, M.; Claudi, F. Synthesis of L-(+)-3-(3-hydroxy-4-pivaloyloxybenzyl)-2,5-diketomorpholine as potential pro-drug of L-dopa. *Bioorg. Med. Chem. Lett.* **2000**, *10*, 1385−1388. (e) Yancheva, D.; Daskalova, L.; Cherneva, E.; Mikhova, B.; Djordjevic, A.; Smelcerovic, Z.; Smelcerovic, A. Synthesis, structure and antimicrobial activity of 6-(propan-2-yl)-3-methyl-morpholine-2,5-dione. *J. Mol. Struct.* **2012**, *1016*, 147−154. (f) Porzi, G.; Sandri, G. Enantioselective synthesis of (*R*)-and (*S*)-α-aminoacids using (6*S*)- and (6*R*)-6-methyl-morpholine-2,5-dione derivatives. *Tetrahedron: Asymmetry* **1996**, *7*, 189−196.

(3) Peng, X.; Behl, M.; Zhang, P.; Mazurek-Budzyńska, M.; Feng, Y.; Lendlein, A. Synthesis of well-defined dihydroxy telechelics by (Co) polymerization of morpholine-2,5-diones catalyzed by Sn(IV) alkoxide. *Macromol. Biosci.* **2018**, *18*, 1800257.

(4) (a) Khalil, Z. G.; Huang, X. C.; Raju, R.; Piggott, A. M.; Capon, R. J. Shornephine A: structure, chemical stability, and P-glycoprotein inhibitory properties of a rare diketomorpholine from an Australian marine-derived *Aspergillus* sp. *J. Org. Chem.* **2014**, *79*, 8700−8705. (b) Aparicio-Cuevas, M. A.; Rivero-Cruz, I.; Sánchez-Castellanos, M.; Menéndez, D.; Raja, H. A.; Joseph-Nathan, P.; del Carmen González, M.; Figueroa, M. Dioxomorpholines and derivatives from a marine-facultative *Aspergillus* species. *J. Nat. Prod.* **2017**, *80*, 2311−2318.

(5) Wang, M. Z.; Si, T. X.; Ku, C. F.; Zhang, H. J.; Li, Z. M.; Chan, A. S. Synthesis of javanicunines A and B, 9-deoxy-PF1233s A and B, and absolute configuration establishment of javanicunine B. *J. Org. Chem.* **2019**, *84*, 831−839.

(6) Shiomi, S.; Wada, K.; Umeda, Y.; Kato, H.; Tsukamoto, S.; Ishikawa, H. Total syntheses and stereochemical reassignments of mollenines A and B. *Bioorg. Med. Chem. Lett.* **2018**, *28*, 2766−2769.

(7) Dirauf, M.; Bandelli, D.; Weber, C.; Görls, H.; Gottschaldt, M.; Schubert, U. S. TBD-catalyzed ring-opening polymerization of alkyl-substituted morpholine-2,5-dione derivatives. *Macromol. Rapid Commun.* **2018**, *39*, 1800433.

(8) Lian, J.; Li, M.; Wang, S.; Tao, Y.; Wang, X. Organocatalytic polymerization of morpholine-2,5-diones toward methionine-containing poly(ester amide)s: preparation and facile functionalization. *Macromolecules* **2020**, *53*, 10830−10836.

(9) Naolou, T.; Lendlein, A.; Neffe, A. T. Influence of metal softness on the metal-organic catalyzed polymerization of morpholine-2,5-diones to oligodepsipeptides. *Eur. Polym. J.* **2016**, *85*, 139−149.

(10) Barrera, D. A.; Zylstra, E.; Lansbury, P. T.; Langer, R. Copolymerization and degradation of poly(lactic acid-co-lysine). *Macromolecules* **1995**, *28*, 425−432.

(11) Králová, P.; Benická, S.; Soural, M. Polymer-assisted synthesis of single and fused diketomorpholines. *ACS Comb. Sci.* **2019**, *21*, 154−157.

(12) Smelcerovic, A.; Yancheva, D.; Cherneva, E.; Petronijevic, Z.; Lamshoeft, M.; Herebian, D. Identification and synthesis of three cyclodidepsipeptides as potential precursors of enniatin B in Fusarium sporotrichioides. *J. Mol. Struct.* **2011**, *985*, 397−402.

(13) (a) Koch, C. J.; Šimonyiová, S.; Pabel, J.; Kärtner, A.; Polborn, K.; Wanner, K. T. Asymmetric Synthesis with 6-*tert*-butyl-5-methoxy-6-methyl-3,6-dihydro-2*H*-1,4-oxazin-2-one as a new chiral glycine equivalent: Preparation of enantiomerically pure α-tertiary and α-quaternary α-amino acids. *Eur. J. Org. Chem.* **2003**, *2003*, 1244−1263. (b) Pedras, M. S.; Chumala, P. B.; Quail, J. W. Chemical mediators: the remarkable structure and host-selectivity of depsilairdin, a sesquiterpenic depsipeptide containing a new amino acid. *Org. Lett.* **2004**, *6*, 4615−4617. (c) Grab, T.; Bräse, S. Efficient synthesis of lactate-containing depsipeptides by the Mitsunobu reaction of lactates. *Adv. Synth. Catal.* **2005**, *347*, 1765−1768. (d) Fujita, S.; Nishikawa, K.; Iwata, T.; Tomiyama, T.; Ikenaga, H.; Matsumoto, K.; Shindo, M. Asymmetric total synthesis of (−)-stemonamine and its stereochemical stability. *Chem. - Eur. J.* **2018**, *24*, 1539−1543.

(14) (a) Stephens, T. C.; Lawer, A.; French, T.; Unsworth, W. P. Iterative assembly of macrocyclic lactones using successive ring expansion reactions. *Chem. - Eur. J.* **2018**, *24*, 13947−13953. (b) Lawer, A.; Epton, R. G.; Stephens, T. C.; Palate, K. Y.; Lodi, M.; Marotte, E.; Lamb, K. J.; Sangha, J. K.; Lynam, J. M.; Unsworth, W. P. Evaluating the viability of successive ring-expansions based on amino acid and hydroxyacid side-chain insertion. *Chem. - Eur. J.* **2020**, *26*, 12674−12683.

(15) Smith, A. N.; Johnston, J. N. The formation of impossible rings in macrocyclooligomerizations for cyclodepsipeptide synthesis: The 18-from-12 Paradox. *J. Org. Chem.* **2021**, *86*, 7904−7919.

(16) De, A.; DiMarchi, R. D. Synthesis and characterization of ester-based prodrugs of glucagon-like peptide 1. *Biopolymers* **2010**, *94*, 448−456.

(17) Cankařová, N.; Schütznerová, E.; Krchňák, V. Traceless solid-phase organic synthesis. *Chem. Rev.* **2019**, *119*, 12089−12207.

(18) (a) Scott, B. O.; Siegmund, A. C.; Marlowe, C. K.; Pei, Y.; Spear, K. L. Solid phase organic synthesis (SPOS): A novel route to diketopiperazines and diketomorpholines. *Mol. Diversity* **1996**, *1*, 125−134. (b) Szardenings, A. K.; Burkoth, T. S.; Lu, H. H.; Tien, D. W.; Campbell, D. A. A simple procedure for the solid phase synthesis of diketopiperazine and diketomorpholine derivatives. *Tetrahedron* **1997**, *53*, 6573−6593.

(19) Nicolaou, K. C.; Safina, B. S.; Winssinger, N. A new photolabile linker for the photoactivation of carboxyl groups. *Synlett* **2001**, *2001*, 0900−0903.

(20) Králová, P.; Soural, M. Reagent-based diversity-oriented synthesis of triazolo[1,5-*a*][1,4]diazepine derivatives from polymer-supported homoazidoalanine. *J. Org. Chem.* **2021**, *86*, 7963−7974.

(21) Proulx, C.; Noë, F.; Yoo, S.; Connolly, M. D.; Zuckermann, R. N. On-resin N-terminal peptoid degradation: Toward mild sequencing conditions. *Biopolymers* **2016**, *106*, 726−736.

(22) (a) Arcelli, A.; Bongini, A.; Porzi, G.; Rinaldi, S. Ammonolysis of morpholine-2,5-diones: Participation of the primary amide group. Part 2. *J. Phys. Org. Chem.* **2012**, *25*, 132−141. (b) Nelson, T. D.; LeBlond, C. R.; Frantz, D. E.; Matty, L.; Mitten, J. V.; Weaver, D. G.; Moore, J. C.; Kim, J. M.; Boyd, R.; Kim, P. Y.; Gbewonyo, K.; Brower, M.; Sturr, M.; McLaughlin, K.; McMasters, D. R.; Kress, M. H.; McNamara, J. M.; Dolling, U. H. Stereoselective synthesis of a potent thrombin inhibitor by a novel P2-P3 lactone ring opening. *J. Org. Chem.* **2004**, *69*, 3620−3627.

(23) (a) Feng, Y.; Lu, J.; Behl, M.; Lendlein, A. Progress in depsipeptide-based biomaterials. *Macromol. Biosci.* **2010**, *10*, 1008−1021. (b) Peng, X.; Behl, M.; Zhang, P.; Mazurek-Budzyńska, M.; Razzaq, M. Y.; Lendlein, A. Hexyl-modified morpholine-2,5-dione-based oligodepsipeptides with relatively low glass transition temperature. *Polymer* **2016**, *105*, 318−326. (c) Tian, W.; Chen, Q.; Yu, C.; Shen, J. Amino-terminated poly(ethylene glycol) as the initiators for

https://doi.org/10.1021/acsomega.1c05964
ACS Omega 2022, 7, 48−54

the ring-opening polymerization of 3-methylmorpholine-2,5-dione. *Eur. Polym. J.* **2003**, *39*, 1935−1938.
(24) Kramer, J. R.; Deming, T. J. Preparation of multifunctional and multireactive polypeptides via methionine alkylation. *Biomacromolecules* **2012**, *13*, 1719−1723.
(25) Ervin, J. N.; Bouza, M.; Fernández, F. M.; Forsythe, J. G. Proline behavior in model prebiotic peptides formed by wet-dry cycling. *ACS Earth Space Chem.* **2020**, *4*, 1349−1359.
(26) (a) Smelcerovic, A.; Rangelov, M.; Smelcerovic, Z.; Veljkovic, A.; Cherneva, E.; Yancheva, D.; Nikolic, G. M.; Petronijevic, Z.; Kocic, G. Two 6-(propan-2-yl)-4-methyl-morpholine-2,5-diones as new non-purine xanthine oxidase inhibitors and anti-inflammatory agents. *Food Chem. Toxicol.* **2013**, *55*, 493−497. (b) Pavlovic, V.; Djordjevic, A.; Cherneva, E.; Yancheva, D.; Smelcerovic, A. Stimulatory effect on rat thymocytes proliferation and antimicrobial activity of two 6-(propan-2-yl)-4-methyl-morpholine-2,5-diones. *Food Chem. Toxicol.* **2012**, *50*, 761−766.
(27) (a) Xu, Y.; Orozco, R.; Wijeratne, E. M.; Gunatilaka, A. A.; Stock, S. P.; Molnár, I. Biosynthesis of the cyclooligomer depsipeptide beauvericin, a virulence factor of the entomopathogenic fungus *Beauveria bassiana*. *Chem. Biol.* **2008**, *15*, 898−907. (b) An, R.; Ahmed, M.; Li, H.; Wang, Y.; Zhang, A.; Bi, Y.; Yu, Z. Isolation, purification and identification of biological compounds from *Beauveria* sp. and their evaluation as insecticidal effectiveness against *Bemisia tabaci*. *Sci. Rep.* **2021**, *11*, 12020. (c) Oh, H.; Kim, T.; Oh, G. S.; Pae, H. O.; Hong, K. H.; Chai, K. Y.; Kwon, T. O.; Chung, H. T.; Lee, H. S. (3*R*,6*R*)-4-methyl-6-(1-methylethyl)-3-phenylmethyl-perhydro-1,4-oxazine-2,5-dione: an apoptosis-inducer from the fruiting bodies of *Isaria japonica*. *Planta Med.* **2002**, *68*, 345−348. (d) Cheng, S. M.; Huang, J.; Wang, H. Y.; Li, G. Y.; Lin, R. C.; Wang, J. H. Two new compounds from *Bombyx batryticatus*. *J. Asian Nat. Prod. Res.* **2014**, *16*, 825−829. (e) Suntornchashwej, S.; Chaichit, N.; Isobe, M.; Suwanborirux, K. Hectochlorin and morpholine derivatives from the Thai sea hare, *Bursatella leachii*. *J. Nat. Prod.* **2005**, *68*, 951−955.
(28) (a) Trost, B. M.; Bai, W. J.; Hohn, C.; Bai, Y.; Cregg, J. J. Palladium-catalyzed asymmetric allylic alkylation of 3-substituted 1*H*-indoles and tryptophan derivatives with vinylcyclopropanes. *J. Am. Chem. Soc.* **2018**, *140*, 6710−6717. (b) Nakadate, S.; Nozawa, K.; Horie, H.; Fujii, Y.; Nagai, M.; Komai, S. I.; Hosoe, T.; Kawai, K. I.; Yaguchi, T.; Fukushima, K. New Dioxomorpholine Derivatives, Javanicunine A and B, from *Eupenicillium javanicum*. *Heterocycles* **2006**, *68*, 1969−1972. (c) Al Subeh, Z. Y.; Raja, H. A.; Burdette, J. E.; Falkinham, J. O.; Hemby, S. E.; Oberlies, N. H. Three diketomorpholines from a *Penicillium* sp. (strain G1071). *Phytochemistry* **2021**, *189*, 112830.
(29) Jiang, C. X.; Yu, B.; Miao, Y. M.; Ren, H.; Xu, Q.; Zhao, C.; Tian, L. L.; Yu, Z. Q.; Zhou, P. P.; Wang, X.; Fang, J.; Zhang, J.; Zhang, J. Z.; Wu, Q. X. Indole alkaloids from a soil-derived *Clonostachys rosea*. *J. Nat. Prod.* **2021**, *84*, 2468−2474.
(30) Robey, M. T.; Ye, R.; Bok, J. W.; Clevenger, K. D.; Islam, M. N.; Chen, C.; Gupta, R.; Swyers, M.; Wu, E.; Gao, P.; Thomas, M. P.; Wu, C. C.; Keller, N. P.; Kelleher, N. L. Identification of the first diketomorpholine biosynthetic pathway using FAC-MS technology. *ACS Chem. Biol.* **2018**, *13*, 1142−1147.

https://doi.org/10.1021/acsomega.1c05964
ACS Omega 2022, 7, 48−54

Appendix III. Publication III: Combinatorial Assembly, Traceless Generation and *In Situ* Evaluation of Inhibitors for Therapeutically Relevant Serine Proteases

The following pages include the article "Combinatorial assembly, traceless generation and *in situ* evaluation of inhibitors for therapeutically relevant serine proteases" and its supplementary material as it was published in Bioorganic Chemistry by Elsevier. As guaranteed by the author rights policy of the Elsevier publishing group, the authors of this Elsevier article retain the right to include the article in a thesis or dissertation, provided it not published commercially.

The article is reprinted with permission from:

Vu, L. P.; Zyulina, M.; Hingst, A.; Schnakenburg, G.; Gütschow, M. Combinatorial Assembly, Traceless Generation and *In Situ* Evaluation of Inhibitors for Therapeutically Relevant Serine Proteases, *Bioorg. Chem.* **2022**, *121*, 1105676. doi: 10.1016/j.bioorg.2022.105676

Bioorganic Chemistry 121 (2022) 105676

Contents lists available at ScienceDirect

Bioorganic Chemistry

journal homepage: www.elsevier.com/locate/bioorg

Combinatorial assembly, traceless generation and *in situ* evaluation of inhibitors for therapeutically relevant serine proteases

Lan Phuong Vu [a], Maria Zyulina [a], Alexandra Hingst [a], Gregor Schnakenburg [b], Michael Gütschow [a,*]

[a] Pharmaceutical Institute, Pharmaceutical & Medicinal Chemistry, University of Bonn, An der Immenburg 4, D-53121 Bonn, Germany
[b] Institute of Inorganic Chemistry, University of Bonn, Gerhard-Domagk-Straße 1, D-53121 Bonn, Germany

ARTICLE INFO

This work is dedicated to Professor Dr. Kurt Eger on the occasion of his 80th birthday.

Keywords:
Combinatorial chemistry
Diketomorpholines
In situ evaluation
Serine proteases
Substrate-analogue inhibitors

ABSTRACT

A combinatorial method was devised and applied for the design and identification of substrate-analogue inhibitors of therapeutically relevant serine proteases, such as thrombin and factor Xa. We conceptualized imino acid derived diketomorpholines as generally applicable key intermediates prepared through solid-phase synthesis and prone to be cleaved with primary amines in a traceless fashion. The approach led to a compound library whose members were prepared under bioassay-compatible conditions and directly subjected to the *in situ* evaluation, allowing a fast prediction of hit compounds. Highly active inhibitors for serine proteases of the coagulation cascade have been identified. The most potent dual inhibitor, **16K**, has a binding affinity of 23.9 nM to thrombin and 32.8 nM to factor Xa.

1. Introduction

Serine proteases play crucial roles in a variety of (patho)physiological processes and are targets of approved drugs for several indications. The catalytic activity of serine proteases involves the nucleophilic attack of the active-site serine at the carbonyl group of the scissile peptide bond and makes use of an acyl transfer mechanism, finally leading to the hydrolytic cleavage of the substrate. A plethora of peptidomimetic serine protease inhibitors, either acting covalently or non-covalently, have been developed to interfere with this important class of enzymes [1–4].

The application of combinatorial chemistry science has revolutionized high-throughput screening technologies and chemical lead optimization [5–11]. In this study, we contrived a combinatorial approach that enables the immediate access to the bioactive compounds which can directly be subjected to the biochemical evaluation. The successful accomplishment would require (i) at least two reactants, each of which to introduce one point of diversity into the product (ii) a traceless one-pot reaction free from by-products and distinguished by high atom economy (iii) preferably no assay activity of the reactants (iv) an assay-compatible solvent and (v) promising product structures with respect to the biological target.

In a protease substrate, the residues R^1, R^2, R^3 of the amino acids at P1, P2, P3 position bind to the pockets S1, S2, S3. C-terminal residues interact with the primed sites of the protease. The peptide bond between the P1 and P1′ amino acid is proteolytically cleaved (Fig. 1). Whereas the product (X = CO_2H) rapidly dissociates and regenerates the active protease, a substrate-analogue inhibitor (X = H) occupies the active site. In our inhibitor design, residues R^1, R^2 and R^3 constitute three points of diversity. We expected diketomorpholines (DKMs) to be appropriate educts for a traceless *in situ* generation of bioactive compounds in the course of a ring cleavage upon treatment with primary amines to generate substrate-analogue inhibitors of serine proteases [17–22].

2. Results and discussion

A first DKM was assembled from (*S*)-leucic acid (**1**) and (*S*)-proline (Scheme 1). The α-hydroxy acid and the benzyl ester protected amino acid underwent a uronium salt-mediated coupling. Deprotection of **7** and proton-catalyzed lactonization gave DKM **12**. Of note, the lactam bond adopts a structurally forced *cis* configuration, and a pre-equilibrium between the *trans* and *cis* form (**8** and **8′**) accounts for its entropy-driven formation. When we subjected (*S*)-phenylalanine benzyl ester, instead of (*S*)-proline benzyl ester, to this route, a TFA-promoted

* Corresponding author.
E-mail address: guetschow@uni-bonn.de (M. Gütschow).

https://doi.org/10.1016/j.bioorg.2022.105676
Received 7 December 2021; Received in revised form 24 January 2022; Accepted 8 February 2022
Available online 11 February 2022

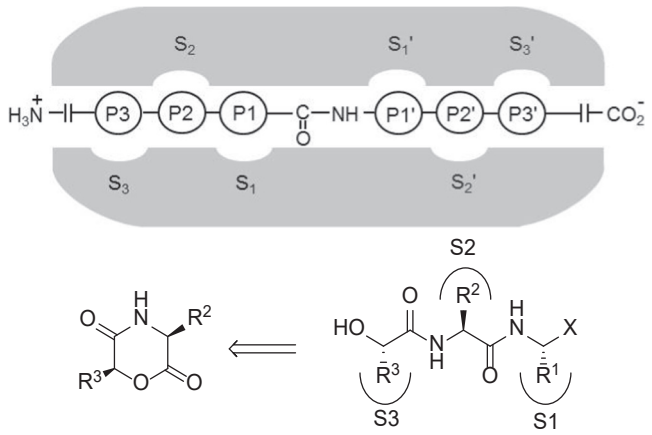

Fig. 1. Active site of a substrate-bound serine protease. The peptide sequence covering P3 to P3′ residues and the corresponding subsites comprising S3 to S3′ (top). General structure of DKMs [12–16] and a retrosynthetic approach to substrate-analogue inhibitors of serine proteases (bottom).

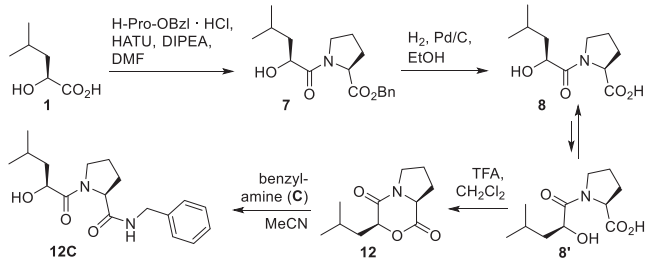

Scheme 1. Solution-phase synthesis of diketomorpholine **12** and conversion to the proline amide **12C**.

cyclization was not observed (Scheme S2, Supplementary Material). This finding with our dipeptide-type compounds reflects what is known from proteins, where only 0.05% of all non-proline peptide bonds occur in the *cis* conformation, while peptide bonds with the imino acid proline adopt the *cis* form at about 6.5% [23]. Hence, the lactonization is restricted to imino acids at the P2 position. However, proline was highly advantageous at the P2 position of several substrate-analogue inhibitors, *e.g.* against thrombin [17–20]. The greater propensity of proline to adopt a *cis* conformation and the consequent preferred DKM cyclization has also been discussed with respect to the formation of model prebiotic peptides studied in wet-dry cycling experiments [24].

Compound **12** was exemplary reacted with benzylamine (**C**) in acetonitrile at 45 °C for 24 h to generate **12C**, an aminolyzed diketomorpholine (ADKM), as a first potential inhibitor (Scheme 1). Both compounds, DKM **12** and ADKM **12C**, were subjected to X-ray crystallography (Fig. 2). As expected, the *cis* configuration of the amide bond in **12** and the *trans* configuration of the same bond in **12C** was ascertained.

In order to facilitate the reaction, reduce the number of steps and prepare a broad range of DKMs, a solid phase approach was introduced. In Scheme 2, the reaction of polymer-bound 2-chlorotrityl proline (**9**) with (*S*)-leucic acid (**1**) is exemplarily outlined. Three resins, *i.e.* **9**, polymer-bound 2-chlorotrityl homoproline (**10**) and Fmoc-protected sarcosine loaded on a Wang resin (**11**), and six hydroxyl acids (**1-6**) were applied (Schemes S3-S5). The so compiled small library of 18 DKMs (**12-29**) is shown in Fig. 3. The excess of the respective α-hydroxy acid in the solid-phase reaction allowed for complete consumption of the resin-bound nucleophile and the easy removal of a potentially formed lactide. The resulting resin-bound amide was treated with a mixture of TFA and CH_2Cl_2 in the presence of triisoproylsilane (TIPS) acting as a scavenger of carbocations (Schemes S3, S4 and S5). It was insignificant whether the successful generation of DKMs occurred through a cyclative

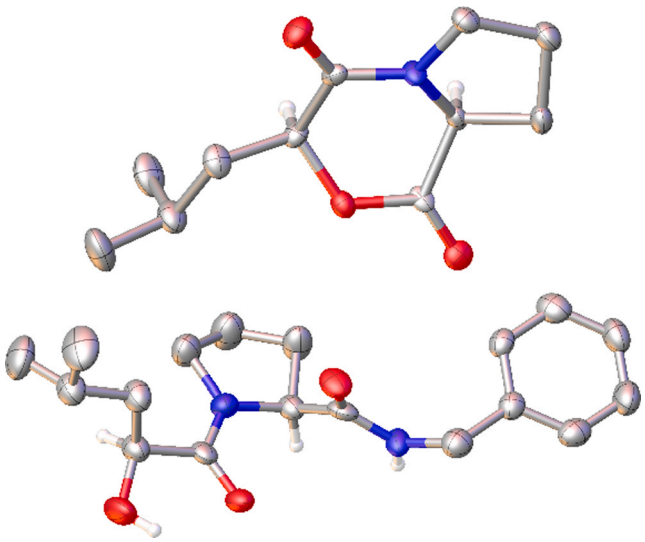

Fig. 2. Molecular structure of DKM **12** (top) and ADKM **12C** (bottom).

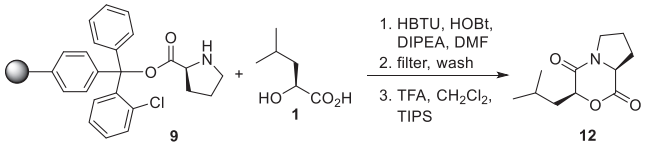

Scheme 2. Resin-based lactonization to DKM derivatives.

cleavage or in the second step of a cleavage-cyclocondensation sequence [25]. Compounds **12-29** were purified by preparative chromatography and their purity confirmed by GC–MS.

The 18 DKMs in our hands already differed with respect to the imino acid and the hydroxy acid from which each was assembled. We continued with our combinatorial approach and introduced a third point of diversity by reacting them with a tailored selection of primary amines **A-K** (Fig. 3) following the exemplary conversion of **12** to **12C** (Scheme 1) and generating a library of 198 members. These ADKMs constitute the envisaged substrate-analogue inhibitors of serine proteases with the hydroxy acid at P3 and the imino acid at P2 position, whereas the primary amine provides the residue for interaction with the S1 subsite. Accordingly, primary amines with aliphatic (**A**, **B**) aromatic (**C**, **D**) and basic residues (**E-K**) were applied to preferentially address proteases with primary substrate specificity for aliphatic, aromatic and basic amino acids at P1 position, respectively.

To generate the library, each DKM (**12-29**) was incubated with each primary amine (**A-K**) in acetonitrile at 45 °C for 24 h. In cases of **J** and **K**, the amidinium salts were converted to sufficiently soluble amidine bases with sodium hydride. In the traceless ring cleavage, both educts were used in equimolar amounts, nearly complete conversion was assumed (see Fig. S1), and purification of the samples was not required. Due to the appropriate choice of solvent, the ADKMs could instantly be subjected to enzyme kinetic assays. The following novel *in situ* evaluation was suitable for a high throughput screening without cumbersome purification procedures of each individual library member.

We performed the screening campaign with five therapeutically relevant human serine proteases, *i.e.* thrombin, factor Xa, matriptase 2, elastase and cathepsin G. After incubations to produce the respective ADKM, aliquots were added to well-plates with fluorogenic peptide substrates and buffer, the biochemical reactions were started by enzyme addition, and product formation was monitored for 30 min. Initially, we evaluated all *in situ* generated ADKMs at an apparent concentration of 50 μM. Kinetic data indicated that library members were particularly active against thrombin (Fig. 4), whereas the other four proteases were

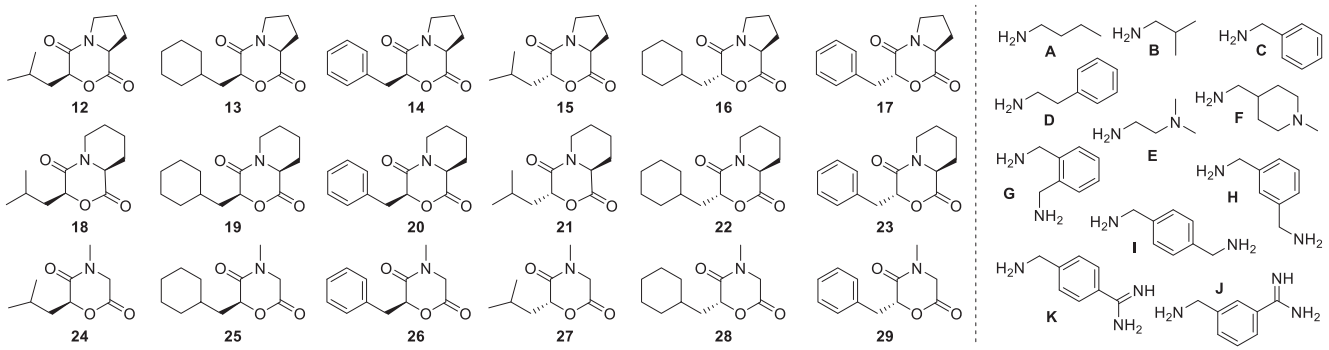

Fig. 3. DKMs **12–29** (vertically and horizontally arranged with respect to substructures) and amines **A–K** for the combinatorial approach (see also Scheme S1).

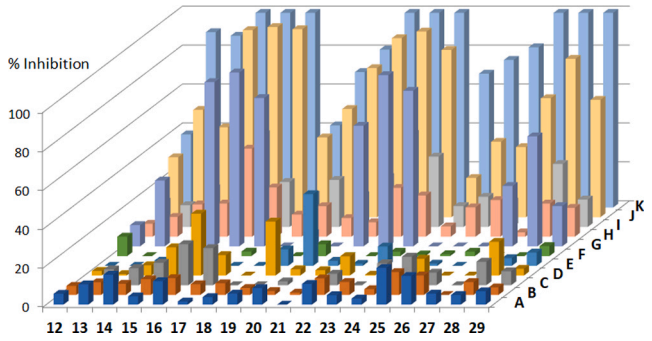

Fig. 4. Inhibition of human thrombin by ADKMs. The structure of each inhibitor is composed of the corresponding DKM **12-29** and the corresponding primary amine **A-K**. The enzyme-catalyzed formation of 7-amino-4-methylcoumarin (AMC) from the fluorogenic substrate Cbz-Gly-Gly-Arg-AMC was followed for 30 min. Mean values from duplicate measurements are shown. The apparent inhibitor concentration was 50 μM, assuming complete conversion during the prior incubation of DKM and primary amine. Neither DKMs **12-29**, nor primary amines **A-K**, each at 50 μM, inhibited thrombin.

inhibited to less extent and by fewer samples (Figs. S2-S6). For the subsequent assessment, inhibition was only considered valid when neither the respective DKM nor the primary amine affected protease activity (see Table S3). As a next step of refinement, *in situ* generated ADKMs that performed best at particular enzymes were screened at an apparent 10 μM concentration and, based on these results, concentration-dependent inhibition was determined (Table S1).

At this stage, guided by biochemical data, selected representatives were synthesized, purified, and characterized as authentic compounds. Following the established streamlined access, we obtained seven new ADKMs, besides **12C** (Scheme 1), by converting DKMs with primary amines (Scheme S6). The resulting authentic ADKMs, shown in Fig. 5, were subjected to an in-depth kinetic analysis. Inhibitory potency against the five target proteases was determined and expressed as K_i values (Fig. 5). ADKMs **12C, 12G** and **14B** were included as inactive screening compounds for reasons of comparison. The other five ADKMs were predominant hits from our combinatorial discovery.

None of the eight ADKMs inhibited leukocyte elastase or cathepsin G (Table S2), two major enzymes stored in primary granules and secreted by human neutrophils. Elastase or cathepsin G can rapidly degrade the connective tissue and are involved in inflammatory processes [26,27]. Elastase has a primary substrate specificity for aliphatic amino acids, such as valine, in P1 position. Hence, we expected inhibition by an ADKM with an *N*-isobutylamide residue and comprised **14B** (Fig. 5), whose proline amide portion is present in a reported micromolar elastase inhibitor [28]. However, authentic **14B** showed no elastase inhibition, in accordance with the screening result (Fig. S5).

Human matriptase-2, a type II transmembrane serine protease, has

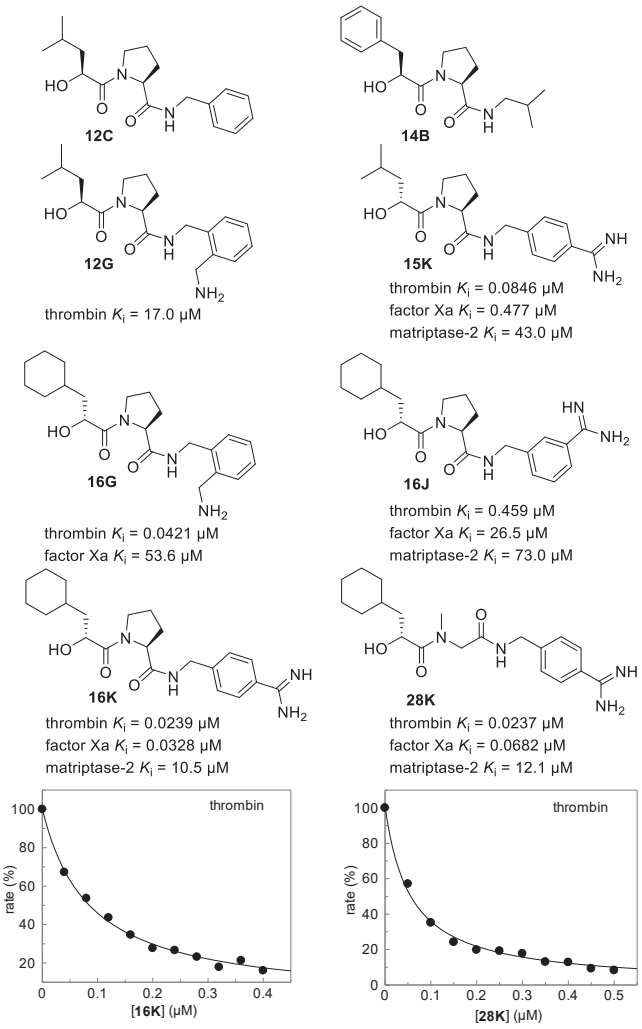

Fig. 5. Authentic ADKMs prepared and investigated as inhibitors of serine proteases. K_i values were determined from duplicate measurements. The kinetic analysis of thrombin inhibition by **16K** and **28K** is exemplarily shown (bottom).

attracted attention because of its critical role in iron homeostasis [29,30]. We did not receive a substrate-analogue inhibitor for matriptase-2 with a stronger potency than **16K** (K_i = 10.5 μM; Fig. 5). The *para*-benzamidine, a well-known arginine surrogate, accounts for inhibition, since matriptase-2 preferentially cleaves substrates after basic amino acids.

The serine proteases thrombin and factor Xa constitute key components of the blood coagulation cascade and have been proven to be

viable targets for the development of antithrombotic drugs [31]. Low-molecular weight, direct inhibitors of thrombin (argatroban, dabigatran and melagatran) and of factor Xa (rivaroxaban and apixaban) are being used in routine clinical practice. Melagatran (Fig. 6) is formed from its prodrug ximelagatran, which is used in many therapeutic settings, including deep venous thrombosis and prevention of secondary venous thromboembolism and stroke. Both trypsin-like serine proteases possess a primary substrate specificity for basic amino acid residues. Gratifyingly, we received exceptionally potent inhibitors of the two human coagulation proteases. The introduction of a basic aminomethyl moiety enabling an appropriate P1-S1 interaction resulted in thrombin inhibition (**12G** *versus* **12C**). ADKM **16G** contains the (*R*)-configured α-hydroxy-cyclohexanepropanoic acid, in place of the (*S*)-configured leucic acid present in **12G**, which resulted in a 400-fold improvement of anti-thrombin activity.

Replacement of the P1 residue in the thrombin-selective compound **16G** by the *para*-benzamidine moiety in **16K** retained anti-thrombin activity, but resulted in a similarly efficient factor Xa inhibition. An exchange of the P3 residue from cyclohexylmethyl to isobutyl (**16K** *versus* **15K**) or a shift of the amidino group to the *meta* position (**16K** *versus* **16J**) was not advantageous. Beside **16K** (thrombin $K_i = 23.9$ nM; factor Xa $K_i = 32.8$ nM), we obtained with **28K** a second, highly potent dual thrombin/factor Xa inhibitor which comprises a structurally and stereochemically reduced relative of **16K** with an incorporated sarcosine in P2 position (thrombin $K_i = 23.7$ nM; factor Xa $K_i = 68.2$ nM). The expected competitive type of inhibition was exemplarily shown for the thrombin inhibition by ADKM **16G** (Fig. S7).

The inhibitory active compounds identified by this novel approach share structural similarities with melagatran (Fig. 6) bearing a 4-amidinobenzylamide, (*S*)-azetidine-2-carboxylic acid, and (*R*)-cyclohexylalanine in P1, P2 and P3 position, respectively. Our hits also resemble the thrombin inhibitor 1 (Fig. 6) with a P3 α-hydroxy acid and a P2 proline [32,33]. The thrombin inhibitor AR-H067637 (Fig. 6) combined structural features of melagatran and thrombin inhibitor 1. A prodrug of AR-H067637 has been studied in phase II clinical trials [34,35]. Noteworthy, the three thrombin inhibitors have a (*R*)-configured P3 amino acid, in agreement with the outcome of our combinatorial search. These examples emphasize that the approach is potentially valid to (i) identify inhibitors of coagulation enzymes with outmost precision and (ii) to undergo a focused design by emanating from a known inhibitor and vary only one point of diversity.

3. Conclusions

The *in situ* evaluation of combinatorially assembled ADKMs is expected to identify candidates with affinity to other targets beyond serine proteases. For example, the primary amine to cleave the DKM might be equipped with an electrophilic warhead, *e.g.* a nitrile group [36]. Compound libraries would be accessible with members resembling PF-07321332 and having OH in place of $NHCOCF_3$. Compound PF-07321332, an inhibitor of the SARS-CoV-2 main cysteine protease, is currently being developed for the treatment of COVID-19 [37].

In conclusion, this report introduces an innovative access to drug candidates based on the preparation of diketomorpholines and the subsequent traceless one-step reaction of high atom economy and feasible under assay-compatible conditions. It is expected to serve as a valuable contribution to the combinatorial discovery and rational identification of bioactive compounds.

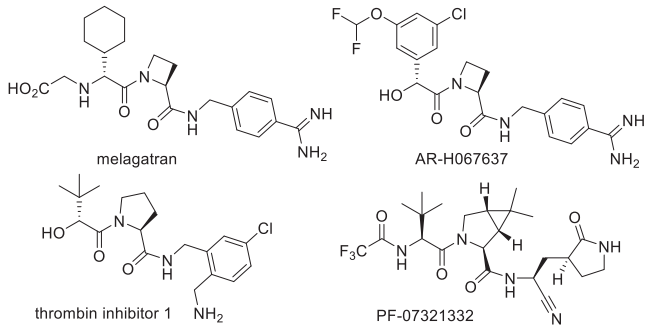

Fig. 6. Bioactive compounds with centrally arranged imino acids with structural similarity to the assembled ADKMs.

4. Experimental

4.1. Chemistry

4.1.1. Benzyl ((S)-2-hydroxy-4-methylpentanoyl)-L-prolinate (7)

To a stirring solution of (*S*)-2-hydroxy-4-methylpentanoic acid (**1**, 0.66 g, 5.0 mmol) and H-Pro-OBzl × HCl (1.21 g, 5.0 mmol) in DMF was added DIPEA (3.4 mL, 20 mmol), followed by the addition of HATU (2.09 g, 5.5 mmol) after 5 min. The mixture was stirred at room temperature overnight, after which EtOAc (100 mL) was added. The organic phase was washed with 10% $KHSO_4$ (50 mL), sat. $NaHCO_3$ (50 mL), 5% LiCl (50 mL) and brine (50 mL), dried over Na_2SO_4, filtered and concentrated *in vacuo*. The crude product was purified by column chromatography (gradient of petroleum ether/EtOAc 4:1 to 1:1) to obtain a colorless solid (0.841 g, 53% yield); $R_f = 0.30$ (petroleum ether/EtOAc 1:1); mp 78–80 °C. Compound **7** was mentioned in the literature [38] without analytical data. ^{1}H NMR (500 MHz, DMSO-d_6) δ 0.85 (d, $J = 7.0$ Hz, 3H, CH_3), 0.87 (d, $J = 6.8$ Hz, 3H, CH_3), 1.29 – 1.33 (m, 2H, $(CH_3)_2CHCH_2$), 1.69 – 1.78 (m, 1H, $(CH_3)_2CH$), 1.78 – 1.85 (m, 1H), 1.86 – 1.97 (m, 2H), 2.15 – 2.25 (m, 1H, $NCHCH_2$, NCH_2CH_2), 3.44 (dt, $J = 10.2$, 6.8 Hz, 1H, NCH_2), 3.68 (dt, $J = 10.0$, 6.7 Hz, 1H, NCH_2), 4.19 (td, $J = 7.8$, 5.0 Hz, 1H, NCH), 4.40 (dd, $J = 8.6$, 5.3 Hz, 1H, CHOH), 4.67 (d, $J = 7.5$ Hz, 1H, OH), 5.10 (d, $J = 6.8$ Hz, 2H, OCH_2Ph), 7.29 – 7.40 (m, 5H, CH_{arom}). ^{13}C NMR (126 MHz, DMSO-d_6) δ 21.5 (CH_3), 23.3 (CH_3), 23.8 (NCH_2CH_2), 24.71 ($(CH_3)_2CH$), 28.35 ($NCHCH_2$), 42.57 ($(CH_3)_2CHCH_2$), 46.11 (NCH_2), 58.67 (NCH), 65.75 (OCH_2Ph), 67.2 (CHOH), 127.7 (CH_{arom}), 127.9 (CH_{arom}), 128.3 (CH_{arom}), 135.9 (C_{arom}), 171.7 (CO), 172.5 (CO). LC-MS (ESI), $t_R = 8.55$ min, 93% purity, *m/z* calcd for $[C_{18}H_{25}NO_4 + H]^+$ 320.40; found 319.9.

4.1.2. ((S)-2-Hydroxy-4-methylpentanoyl)-L-proline (8)

A mixture of **7** (0.32 g, 1.0 mmol) and 10% Pd/C in EtOH (10 mL) was stirred under a hydrogen atmosphere at room temperature overnight. The mixture was diluted with EtOAc (20 mL), filtered through celite, and the filtrate was concentrated *in vacuo* to give the title compound as a colorless solid (0.218 g, 95% yield); mp 164–165 °C. ^{1}H NMR (600 MHz, DMSO-d_6) δ 0.92 (d, $J = 6.1$ Hz, 3H, CH_3), 0.94 (d, $J = 6.2$ Hz, 3H, CH_3), 1.54 – 1.62 (m, 1H), 1.77 – 1.89 (m, 4H), 2.00 – 2.08 (m, 1H), 2.21 – 2.27 (m, 1H, $(CH_3)_2CHCH_2$, $(CH_3)_2CH$, $NCHCH_2$, NCH_2CH_2) 3.35 – 3.45 (m, 2H, NCH_2), 4.57 (t, $J = 7.9$ Hz, 1H, NCH), 5.07 (dd, $J = 9.5$, 3.0 Hz, 1H, CHOH). The OH signals are not recognizable. ^{13}C NMR (151 MHz, DMSO-d_6) δ 21.4 (CH_3), 22.7 (CH_3), 23.1 (NCH_2CH_2), 23.9 ($(CH_3)_2CH$), 27.6 ($NCHCH_2$), 37.4 ($(CH_3)_2CHCH_2$), 44.7 (NCH_2), 57.1 (NCH), 76.4 (CHOH), 164.8 (CO), 170.0 (CO). LC-MS (ESI), $t_R = 2.60$ min, 83% purity, *m/z* calcd for $[C_{11}H_{19}NO_4 + H]^+$ 230.28; found 230.0.

4.1.3. Solution-phase synthesis of (3S,8aS)-3-isobutyltetrahydro-1H-pyrrolo[2,1-c][1,4]-oxazine-1,4(3H)-dione (12)

Compound **8** (0.16 g, 0.7 mmol) was stirred in a solution of TFA/CH_2Cl_2 (10 mL, 0.4:9.6) at room temperature for 2 h. After evaporation *in vacuo*, the crude product was purified by column chromatography (CH_2Cl_2/EtOAc 1:1) to yield the title compound as a colorless solid (0.140 g, 95% yield). The material was identical with that obtained by resin-based chemistry (see below).

4.1.4. (S)-N-Benzyl-1-((S)-2-hydroxy-4-methylpentanoyl)-pyrrolidine-2-carboxamide (12C)

Diketomorpholine **12** (1.0 mmol, 211 mg) and benzylamine (**C**, 1.0 mmol, 107 mg) were stirred in MeCN at 45 °C for 24 h. After concentration *in vacuo*, the crude product was purified by flash column chromatography (gradient of 100% CH_2Cl_2 to 10% MeOH) to yield the title compound as a colorless solid (175 mg, 55% yield); R_f = 0.24 (CH_2Cl_2/MeOH 19:1); mp 80 °C. ^{1}H NMR (500 MHz, DMSO-d_6) δ 0.88 (d, J = 2.8 Hz, 3H, CH_3), 0.90 (d, J = 2.7 Hz, 3H, CH_3), 1.31 – 1.40 (m, 2H, $(CH_3)_2CHCH_2$), 1.72 – 1.83 (m, 2H), 1.83 – 1.89 (m, 1H), 1.90 – 1.98 (m, 1H), 2.02 – 2.10 (m, 1H, $(CH_3)_2CH$, NCH_2CH_2, $NCHCH_2$), 3.45 – 3.55 (m, 1H, NCH_2), 3.60 – 3.68 (m, 1H, NCH_2), 4.19 (ddd, J = 8.9, 7.3, 4.1 Hz, 1H, NCH), 4.26 (t, J = 5.9 Hz, 2H, $NHCH_2$), 4.35 (dd, J = 8.4, 4.6 Hz, 1H, CHOH), 4.61 (d, J = 7.3 Hz, 1H, OH), 7.19 – 7.25 (m, 3H, CH_{arom}), 7.26 – 7.32 (m, 2H, CH_{arom}), 8.24 (t, J = 6.0 Hz, 1H, NH). ^{13}C NMR (126 MHz, DMSO-d_6) δ 21.5 (CH_3), 23.5 (CH_3), 23.9 (NCH_2CH_2), 24.6 ($(CH_3)_2CH$), 29.0 ($NCHCH_2$), 41.8 ($(CH_3)_2CHCH_2$), 42.5 ($CONHCH_2$), 46.4 (NCH_2), 59.7 (NCH), 67.4 (CHOH), 126.6 (CH_{arom}), 126.8 (CH_{arom}), 128.1 (C_{arom}), 139.4 (CH_{arom}), 171.6 (CO), 172.5 (CO). LC-MS (ESI), t_R = 4.92 min, 97% purity, m/z calcd for $[C_{18}H_{26}N_2O_3 + H]^+$, 319.43 found, 319.30. HRMS (ESI) m/z calcd for $[C_{18}H_{26}N_2O_3 + Na]^+$, 341.1836; found, 341.1847.

4.1.5. General Procedure a for solid phase syntheses using H-Pro-2-ClTrt and H-Pip-2-ClTrt resin

The appropriate resin, *i.e.* H-Pro-2-ClTrt (0.68 mmol/g) or H-Pip-2-ClTrt resin (0.54 mmol/g), on a 0.5 mmol scale was suspended in DMF (5 mL) and DIPEA (0.34 mL, 2.00 mmol) was added. The α-hydroxy acid (1.0 mmol), HBTU (0.38 g, 1.0 mmol) and HOBt (0.15 g, 1.0 mmol) were placed in one glass vial and DMF (5 mL) was added. The mixture was treated for 2 min in an ultrasonic bath and given to the resin 5 min after addition of DMF and DIPEA. The mixture was shaken for 2 h at 300 rpm. The resin was washed with DMF (3 × 10 mL), CH_2Cl_2 (3 × 10 mL), MeOH (3 × 10 mL) and CH_2Cl_2 (3 × 10 mL) and finally dried. The loaded resin was shaken for 1 h at 300 rpm in a mixture of trifluoroacetic acid, triisopropylsilane and CH_2Cl_2 (10 mL, 0.2:0.2:9.6). The cleavage step was repeated and the collected cleavage solutions were combined and evaporated *in vacuo*. The residue was purified by column chromatography.

4.1.6. General Procedure B for solid phase syntheses using Fmoc-Sar-Wang resin

The Fmoc-protected resin (0.58 mmol/g) on a 0.5 mmol scale was suspended in DMF (8 mL) and shaken for 5 min at 300 rpm. Piperidine (2 mL) was added and shaking was continued for 30 min. The solution was filtered off and the step was repeated. The resin was washed with DMF (3 × 10 mL), CH_2Cl_2 (3 × 10 mL), MeOH (3 × 10 mL) and CH_2Cl_2 (3 × 10 mL) and finally dried under reduced pressure. The deprotected resin was suspended in DMF (5 mL) and DIPEA (0.34 mL, 2.00 mmol) was added. The α-hydroxy acid (1.0 mmol), HBTU (0.38 g, 1.0 mmol) and HOBt (0.15 g, 1.0 mmol) were placed in one glass vial and DMF (5 mL) was added. The mixture was treated for 2 min in an ultrasonic bath and given to the resin 5 min after addition of DMF and DIPEA. The mixture was shaken for 2 h at 300 rpm. The resin was washed with DMF (3 × 10 mL), CH_2Cl_2 (3 × 10 mL), MeOH (3 × 10 mL) and CH_2Cl_2 (3 × 10 mL) and finally dried. The loaded resin was shaken for 1 h at 300 rpm in a mixture of trifluoroacetic acid, triisopropylsilane and CH_2Cl_2 (10 mL, 9.5:0.25:0:25). The cleavage step was repeated and the collected cleavage solutions were combined and evaporated *in vacuo*. The residue was purified by column chromatography.

4.1.7. Solid-phase synthesis of (3S,8aS)-3-isobutyltetrahydro-1H-pyrrolo [2,1-c][1,4]oxazine-1,4(3H)-dione (12)

By using the General Procedure A, this compound was prepared in two fritted glass reaction vessels from (*S*)-2-hydroxy-4-methylpentanoic acid (**1**, 2 mmol, 0.26 g) and H-Pro-2-ClTrt resin (1 mmol). The crude product was purified by column chromatography (CH_2Cl_2/EtOAc 1:1) to yield the title compound as a colorless solid (0.155 g, 73% yield); R_f = 0.62 (CH_2Cl_2/EtOAc 1:1); mp 156–158 °C. ^{1}H NMR (600 MHz, $CDCl_3$) δ 0.94 (d, J = 6.1 Hz, 3H, CH_3), 0.98 (d, J = 6.3 Hz, 3H, CH_3), 1.80 (t, J = 10.0 Hz, 1H, $((CH_3)_2CH)$, 1.89 – 1.99 (m, 3H, $((CH_3)_2CHCH_2$, NCH_2CH_2), 1.99 – 2.05 (m, 1H, NCH_2CH_2), 2.25 – 2.32 (m, 1H, $NCHCH_2$), 2.36 – 2.43 (m, 1H, $NCHCH_2$), 3.48 – 3.66 (m, 2H, NCH_2), 4.26 (t, J = 7.9 Hz, 1H, NCH), 4.78 (dd, J = 9.9, 2.9 Hz, 1H, COCH). ^{13}C NMR (151 MHz, $CDCl_3$) δ 21.4 (CH_3), 23.3 (CH_3), 23.4 (NCH_2CH_2), 24.2 ($(CH_3)_2CH$), 28.5 ($NCHCH_2$), 37.9 ($(CH_3)_2CHCH_2$), 45.5 (NCH_2), 57.7 (NCH), 77.6 (COCH), 165.3 (CO), 169.4 (CO). GC–MS (EI), t_R = 10.43 min, 99% purity, m/z calcd for $[C_{11}H_{17}NO_3]^{\bullet+}$ 211.26; found 211.20. HRMS (ESI) m/z calcd for $[C_{11}H_{17}NO_3 + H]^+$, 212.1281; found, 212.1282.

4.1.8. Preparation of the combinatorial ADKM library for in situ evaluation

The library of ADKMs was prepared prior to biochemical measurements. In a combinatorial approach, each DKM (**12-29**; see Fig. 3) was incubated with each primary amine (**A-K**; see Fig. 3). A volume of 25 μL of a 4 mM solution of the DKM in acetonitrile, a volume of 25 μL of a 4 mM solution of the primary amine in acetonitrile and 50 μL acetonitrile were combined in a 1.5 mL polypropylene reaction tube. Incubation of the reaction mixtures for 24 h at 45 °C and 300 rpm in a heating block (Eppendorf, Hamburg, Germany) yielded the corresponding ADKM in an apparent concentration of 1 mM.

4.2. Biology

4.2.1. Thrombin inhibition assay [39]

Assay buffer was 50 mM Tris, 150 mM NaCl, pH 8.0. The enzyme stock solution (1 U/μL) was prepared in water, kept at 0 °C and diluted 1:50 with assay buffer. A 10 mM stock solution of the fluorogenic substrate Cbz-Gly-Gly-Arg-AMC in DMSO was diluted with assay buffer to a concentration of 800 μM. Into each well, 168.8 μL assay buffer, 10 μL of an inhibitor solution in acetonitrile, 1.2 μL of DMSO and 10 μL of a substrate solution was added and thoroughly mixed. The final concentration of the substrate was 40 μM, of acetonitrile was 5%, of DMSO was 1% and of human thrombin was 1 μg/ml. The reaction was initiated by adding 10 μL of enzyme solution and followed at 25 °C for 30 min.

4.2.2. Factor Xa inhibition assay [40]

Assay buffer was 50 mM Tris, 100 mM NaCl, 10 mM $CaCl_2$, pH 8.0. The enzyme stock solution (1.47 μg/μL) was prepared in water, kept at 0 °C and diluted 1:50 with assay buffer. A 20 mM stock solution of the fluorogenic substrate Boc-Ile-Glu-Gly-Arg-AMC in DMSO was diluted with assay buffer to a concentration of 8 mM. Into each well, 182.5 μL assay buffer, 10 μL of an inhibitor solution in acetonitrile and 5 μL of a substrate solution was added and thoroughly mixed. The final concentration of the substrate was 200 μM, of acetonitrile was 5%, of DMSO was 2.5% and of human factor Xa was 3.68 ng/μL. The reaction was initiated by adding 2.5 μL of enzyme solution and followed at 25 °C for 30 min.

4.2.3. Matriptase-2 inhibition assay [39]

Assay buffer was 50 mM Tris, 150 mM NaCl, pH 8.0. As the enzyme source, recombinant human matriptase-2 from the conditioned medium of transfected HEK cells was used, kept at 0 °C and diluted with assay buffer. A 10 mM stock solution of the fluorogenic substrate Boc-Gln-Ala-Arg-AMC in DMSO was diluted with assay buffer to a concentration of 800 μM. Into each well 168.8 μL assay buffer, 10 μL of an inhibitor solution in acetonitrile, 1.2 μL of DMSO and 10 μL of a substrate solution was added and thoroughly mixed. The final concentration of the substrate was 40 μM, of acetonitrile was 5%, of DMSO was 1%. The reaction was initiated by adding 10 μL of enzyme solution and followed at 25 °C for 30 min.

4.2.4. Leukocyte elastase inhibition assay

Assay buffer was 50 mM Na_3PO_4, 500 mM NaCl, pH 7.8. The enzyme stock solution (0.1 μg/ml) was prepared in sodium acetate/acetic acid, pH 5.5 kept at 0 °C and diluted 1:100 or 1:200 with the same buffer. A 20 mM stock solution of the fluorogenic substrate MeOSuc-Ala-Ala-Pro-Val-AMC in DMSO was used. Into each well, 182 μL assay buffer, 10 μL of an inhibitor solution in acetonitrile and 2 μL of a substrate solution was added and thoroughly mixed. The final concentration of the substrate was 200 μM, of acetonitrile was 5%, of DMSO was 1% and of human elastase was 300 ng/ml or 150 ng/ml. The reaction was initiated by adding 6 μL of enzyme solution and followed at 37 °C for 30 min.

4.2.5. Cathepsin G inhibition assay

Cathepsin G inhibition assay. Assay buffer was 20 mM Tris, 150 mM NaCl, pH 8.4. The enzyme stock solution (0.1 μg/ml) was prepared in 50 mM sodium acetate, 150 mM NaCl, pH 5.5, kept at 0 °C and diluted 1:10 with the same buffer. A 50 mM stock solution of the fluorogenic substrate Suc-Ala-Ala-Pro-Phe-AMC in DMSO was diluted with assay buffer to a concentration of 20 mM. Into each well, 185.5 μL assay buffer, 10 μL of an inhibitor solution in acetonitrile, and 2 μL of a substrate solution was added and mixed thoroughly. The final assay concentration of the substrate was 200 μM, of acetonitrile was 5%, of DMSO was 1% and of human cathepsin G was 1.25 ng/ml. The reaction was initiated by adding 2.5 μL of enzyme solution and followed at 37 °C for 30 min.

Declaration of Competing Interest

The authors declare that they have no known competing financial interests or personal relationships that could have appeared to influence the work reported in this paper.

Acknowledgments

The authors acknowledge support by Carina Lemke, Dr. Martin Mangold, Dr. Jim Küppers, Lilly Hoffmann, and Marion Schneider. G.S. thanks Prof. A. C. Filippou for support.

Appendix A. Supplementary data

Supplementary data to this article can be found online at https://doi.org/10.1016/j.bioorg.2022.105676.

References

[1] D. Leung, G. Abbenante, D.P. Fairlie, Protease Inhibitors: Current Status and Future Prospects, J. Med. Chem. 43 (2000) 305–341.
[2] J.C. Powers, J.L. Asgian, Ö.D. Ekici, K.E. James, Irreversible Inhibitors of Serine, Cysteine, and Threonine Proteases, Chem. Rev. 102 (12) (2002) 4639–4750.
[3] D.A. Bachovchin, B.F. Cravatt, The Pharmacological Landscape and Therapeutic Potential of Serine Hydrolases, Nat. Rev. Drug Discov. 11 (2012) 52–68.
[4] B. Luan, T. Huynh, X. Cheng, G. Lan, H.R. Wang, Targeting Proteases for Treating COVID-19, J. Proteome Res. 19 (2020) 4316–4326.
[5] O. Ramström, J.-M. Lehn, Drug Discovery by Dynamic Combinatorial Libraries, Nat. Rev. Drug Discov. 1 (1) (2002) 26–36.
[6] N. Jung, A. Encinas, S. Bräse, Automated Synthesis of Heterocycles on Solid Supports, Curr. Opin. Drug Discov. Devel. 9 (2006) 713–728.
[7] J.P. Kennedy, L. Williams, T.M. Bridges, R.N. Daniels, D. Weaver, C.W. Lindsley, Application of Combinatorial Chemistry Science on Modern Drug Discovery, J. Comb. Chem. 10 (3) (2008) 345–354.
[8] R. Breinbauer, M. Mentel, Combinatorial Chemistry and the Synthesis of Compound Libraries, Methods Mol. Biol. 572 (2009) 73–80.
[9] T.E. Nielsen, M. Meldal, Solid-phase Synthesis of Complex and Pharmacologically Interesting Heterocycles, Curr. Opin. Drug Discov. Devel. 12 (2009) 798–810.
[10] M. Mondal, A.K. Hirsch, Dynamic Combinatorial Chemistry: A Tool to Facilitate the Identification of Inhibitors for Protein Targets, Chem. Soc. Rev. 44 (2015) 2455–2488.
[11] G. Wu, T. Zhao, D. Kang, J. Zhang, Y. Song, V. Namasivayam, J. Kongsted, C. Pannecouque, E. De Clercq, V. Poongavanam, X. Liu, P. Zhan, Overview of Recent Strategic Advances in Medicinal Chemistry, J. Med. Chem. 62 (2019) 9375–9414.
[12] T. Grab, S. Bräse, Efficient Synthesis of Lactate-Containing Depsipeptides by the Mitsunobu Reaction of Lactates, Adv. Synth. Catal. 347 (14) (2005) 1765–1768.
[13] A. Smelcerovic, P. Dzodic, V. Pavlovic, E. Cherneva, D. Yancheva, Cyclodidepsipeptides with a Promising Scaffold in Medicinal Chemistry, Amino Acids 46 (4) (2014) 825–840.
[14] P. Králová, V. Ručilová, M. Soural, Polymer-Supported Syntheses of Heterocycles Bearing Oxazine and Thiazine Scaffolds, ACS Comb. Sci. 20 (9) (2018) 529–543.
[15] P. Králová, S. Benická, M. Soural, Polymer-Assisted Synthesis of Single and Fused Diketomorpholines, ACS Comb. Sci. 21 (3) (2019) 154–157.
[16] C.-X. Shi, Y.-T. Guo, Y.-H. Wu, Z.-Y. Li, Y.-Z. Wang, F.-S. Du, Z.-C. Li, Synthesis and Controlled Organobase-Catalyzed Ring-Opening Polymerization of Morpholine-2,5-Dione Derivatives and Monomer Recovery by Acid-Catalyzed Degradation of the Polymers, Macromolecules 52 (11) (2019) 4260–4269.
[17] M.R. Wiley, M.Y. Chirgadze, D.K. Clawson, T.J. Craft, D.S. Gifford-Moore, N. D. Jones, J.L. Olkowski, L.C. Weir, G.F. Smith, D-Phe-Pro-p-Amidinobenzylamine: A Potent and Highly Selective Thrombin inhibitor, Bioorg. Med. Chem. Lett. 6 (1996) 2387–2392.
[18] T.J. Tucker, W.C. Lumma, A.M. Mulichak, Z. Chen, A.M. Naylor-Olsen, S.D. Lewis, R. Lucas, R.M. Freidinger, L.C. Kuo, Design of Highly Potent Noncovalent Thrombin Inhibitors that Utilize a Novel Lipophilic Binding Pocket in the Thrombin Active Site, J. Med. Chem. 40 (6) (1997) 830–832.
[19] M.T. Sisay, T. Steinmetzer, M. Stirnberg, E. Maurer, M. Hammami, J. Bajorath, M. Gütschow, Identification of the First Low-molecular-weight Inhibitors of Matriptase-2, J. Med. Chem. 53 (15) (2010) 5523–5535.
[20] T. Steinmetzer, B. Baum, A. Biela, G. Klebe, G. Nowak, E. Bucha, Beyond Heparinization: Design of Highly Potent Thrombin Inhibitors Suitable for Surface Coupling, ChemMedChem 7 (2012) 1965–1973.
[21] D. Meyer, F. Sielaff, M. Hammami, E. Böttcher-Friebertshäuser, W. Garten, T. Steinmetzer, Identification of the First Synthetic Inhibitors of the Type II Transmembrane Serine Protease TMPRSS2 Suitable for Inhibition of Influenza Virus Activation, Biochem. J. 452 (2013) 331–343.
[22] W.W. Phoo, Z. Zhang, M. Wirawan, E.J.C. Chew, A.B.L. Chew, J. Kouretova, T. Steinmetzer, D. Luo, Structures of Zika Virus NS2B-NS3 Protease in Complex with Peptidomimetic Inhibitors, Antiviral Res. 160 (2018) 17–24.
[23] D.E. Stewart, A. Sarkar, J.E. Wampler, Occurrence and Role of *cis* Peptide Bonds in Protein Structures, J. Mol. Biol. 214 (1) (1990) 253–260.
[24] J.N. Ervin, M. Bouza, F.M. Fernández, J.G. Forsythe, Proline Behavior in Model Prebiotic Peptides Formed by Wet−Dry Cycling, ACS Earth Space Chem. 4 (2020) 1349–1359.
[25] T.E. Nielsen, S. Le Quement, M. Meldal, Solid-phase Synthesis of Bicyclic Dipeptide Mimetics by Intramolecular Cyclization of Alcohols, Thiols, Amines, and Amides with *N*-Acyliminium Intermediates, Org. Lett. 17 (2005) 3601–3604.
[26] B. Korkmaz, M.S. Horwitz, D.E. Jenne, F. Gauthier, Neutrophil Elastase, Proteinase 3, and Cathepsin G As Therapeutic Targets in Human Diseases, Pharmacol. Rev. 62 (2010) 726–759.
[27] T. Burster, H. Macmillan, T. Hou, B.O. Boehm, E.D. Mellins, Cathepsin G: Roles in Antigen Presentation and Beyond, Mol. Immunol. 47 (2010) 658–665.
[28] C.H. Hassall, W.H. Johnson, A.J. Kennedy, N.A. Roberts, A New Class of Inhibitors of Human Leucocyte Elastase, FEBS Lett. 183 (1985) 201–205.
[29] C.Y. Wang, D. Meynard, H.Y. Lin, The Role of TMPRSS6/Matriptase-2 in Iron Regulation and Anemia, Front. Pharmacol. 5 (2014) 114.
[30] A. Gitlin-Domagalska, M. Mangold, D. Dębowski, A. Łęgowska, M. Gütschow, K. Rolka, Matriptase-2: Monitoring and Inhibiting its Proteolytic Activity, Future, Med. Chem. 10 (2018) 2745–2761.
[31] N. Mackman, W. Bergmeier, G.A. Stouffer, J.I. Weitz, Therapeutic Strategies for Thrombosis: New Targets and Approaches, Nat. Rev. Drug Discov. 19 (5) (2020) 333–352.
[32] T.D. Nelson, C.R. LeBlond, D.E. Frantz, L. Matty, J.V. Mitten, D.G. Weaver, J. C. Moore, J.M. Kim, R. Boyd, P.-Y. Kim, K. Gbewonyo, M. Brower, M. Sturr, K. McLaughlin, D.R. McMasters, M.H. Kress, J.M. McNamara, U.H. Dolling, Stereoselective Synthesis of a Potent Thrombin Inhibitor by a Novel P2–P3 Lactone Ring Opening, J. Org. Chem. 69 (11) (2004) 3620–3627.
[33] H.R. Chobanian, B. Pio, Y. Guo, H. Shen, M.A. Huffman, M. Madeira, G. Salituro, J. L. Terebetski, J. Ormes, N. Jochnowitz, L. Hoos, Y. Zhou, D. Lewis, B. Hawes, L. Mitnaul, K. O'Neill, K. Ellsworth, L. Wang, T. Biftu, J.L. Duffy, Improved Stability of Proline-Derived Direct Thrombin Inhibitors through Hydroxyl to Heterocycle Replacement, ACS Med. Chem. Lett. 6 (2015) 553–557.
[34] J. Deinum, C. Mattsson, T. Inghardt, M. Elg, Biochemical and Pharmacological Effects of the Direct Thrombin Inhibitor AR-H067637, Thromb. Haemost. 101 (2009) 1051–1059.
[35] E.M. Matsson, U.G. Eriksson, J.E. Palm, P. Artursson, M. Karlgren, L. Lazorova, M. Brännström, A. Ekdahl, K. Dunér, L. Knutson, S. Johansson, K.M. Schützer, H. Lennernäs, Combined in Vitro–in Vivo Approach to Assess the Hepatobiliary Disposition of a Novel Oral Thrombin Inhibitor, Mol. Pharmaceutics 10 (2013) 4252–4262.
[36] J. Breidenbach, C. Lemke, T. Pillaiyar, L. Schäkel, G. Al Hamwi, M. Diett, R. Gedschold, N. Geiger, V. Lopez, S. Mirza, V. Namasivayam, A.C. Schiedel, K. Sylvester, D. Thimm, C. Vielmuth, L.P. Vu, M. Zyulina, J. Bodem, M. Gütschow, C.E. Müller, Targeting the Main Protease of SARS-CoV-2: From the Establishment of High Throughput Screening to the Design of Tailored Inhibitors, Angew. Chem. Int. Ed. 60 (2021) 10423–10429.
[37] D.R. Owen, C.M. Allerton, A.S. Anderson, L. Aschenbrenner, M. Avery, S. Berritt, B. Boras, R.D. Cardin, A. Carlo, K.J. Coffman, A. Dantonio, L. Di, H. Eng, R. Ferre, K.S. Gajiwala, S.A. Gibson, S.E. Greasley, B.L. Hurst, E.P. Kadar, A.S. Kalgutkar, J. C. Lee, J. Lee, W. Liu, S.W. Mason, S. Noell, J.J. Novak, R.S. Obach, K. Ogilvie, N. C. Patel, M. Pettersson, D.K. Rai, M.R. Reese, M.F. Sammons, J.G. Sathish, R.

S. Singh, C.M. Steppan, A.E. Stewart, J.B. Tuttle, L. Updyke, P.R. Verhoest, L. Wei, Q. Yang, Y. Zhu, An Oral SARS-CoV-2 M^{pro} Inhibitor Clinical Candidate for the Treatment of COVID-19, Science 374 (2021) 1586–1593.

[38] D.S. Karanewsky, M.C. Badia, D.W. Cushman, J.M. DeForrest, T. Dejneka, M. J. Loots, M.G. Perri, E.W. Petrillo Jr, J.R. Powell, (Phosphinyloxy)acyl Amino Acid Inhibitors of Angiotensin Converting Enzyme (ACE). 1. Discovery of (*S*)-1-[6-Amino-2-[[hydroxy(4-phenylbutyl)phosphinyl]oxy]-1-oxohexyl]-L-proline a Novel Orally Active Inhibitor of ACE, J. Med. Chem. 31 (1988) 204–212.

[39] D. Häußler, M. Mangold, N. Furtmann, A. Braune, M. Blaut, J. Bajorath, M. Stirnberg, M. Gütschow, Phosphono Bisbenzguanidines as Irreversible Dipeptidomimetic Inhibitors and Activity-Based Probes of Matriptase-2, Chem. Eur. J. 22 (2016) 8525–8535.

[40] M. Hammami, E. Rühmann, E. Maurer, A. Heine, M. Gütschow, G. Klebe, T. Steinmetzer, New 3-Amidinophenylalanine Derived Inhibitors of Matriptase, Med. Chem. Commun. 3 (2012) 807–813.

Appendix III. Publication III: Combinatorial Assembly, Traceless Generation and *In Situ* Evaluation of Inhibitors for Therapeutically Relevant Serine Proteases

Supporting Information

Combinatorial Assembly, Traceless Generation and *In Situ* Evaluation of Inhibitors for Therapeutically Relevant Serine Proteases

***Bioorg. Chem*. 2022**

Combinatorial Assembly, Traceless Generation and *In Situ* Evaluation of Inhibitors for Therapeutically Relevant Serine Proteases

Lan Phuong Vu, Maria Zyulina, Alexandra Hingst, Gregor Schnakenburg and Michael Gütschow*

Table of Contents

1. Preparation of the combinatorial ADKM library for *in situ* evaluation

The procedure is part of the main body of the manuscript.

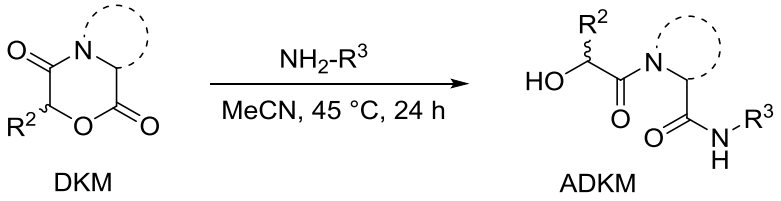

Scheme S1. Schematic view of the reactions.

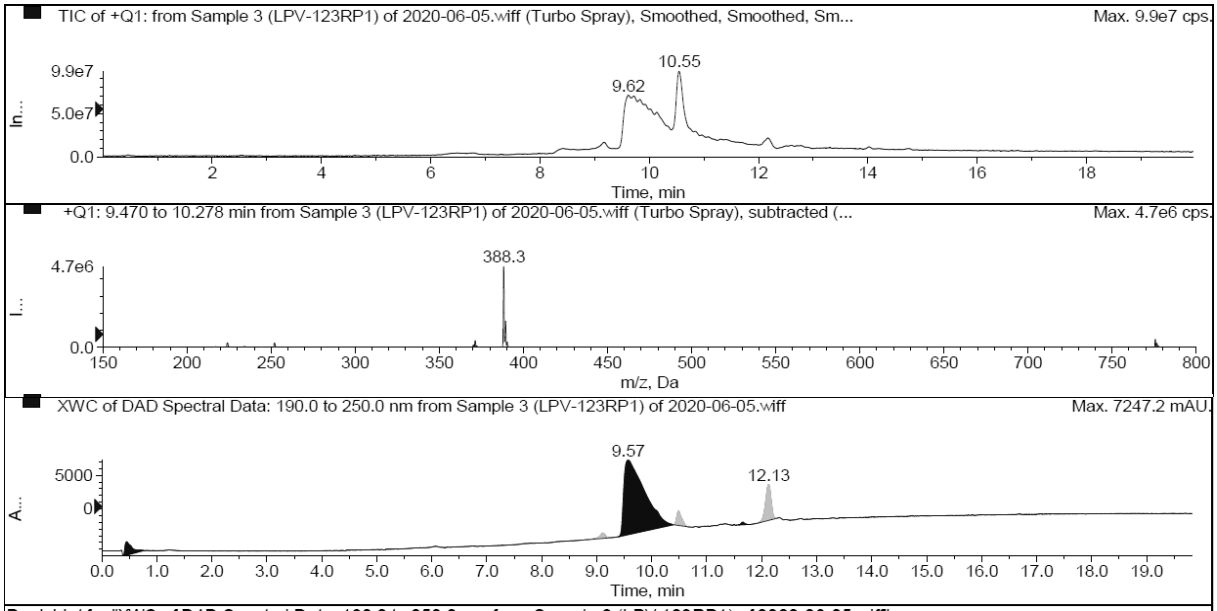

Peak List for "XWC of DAD Spectral Data: 190.0 to 250.0 nm from Sample 3 (LPV-123RP1) of 2020-06-05.wiff"

	Time (min)	Area (mAU x min)	%Area	Height (mAU)	%Height	Width (min)	Baseline Type
1	0.4516	1.7144e4	4.7739	1996.1602	9.2110	0.3867	Base to Base
2	9.1129	5348.6607	1.4894	788.0236	3.6362	0.4667	Base to Base
3	9.5709	2.8571e5	79.5589	1.1082e4	51.1377	1.0067	Base to Base
4	10.4868	1.2904e4	3.5931	2111.8361	9.7447	0.3067	Base to Base
5	11.6557	1575.5164	0.4387	380.4289	1.7554	0.2067	Base to Base
6	12.1252	3.6437e4	10.1460	5312.7581	24.5149	0.3467	Base to Base

Figure S1. LC/MS data of an exemplary crude product of the combinatorial ADKM library. DKM **16** was reacted with *o*-xylylendiamine (**G**). The crude product was subjected to LC-MS analysis, which showed the ADKM **16G** as the main component. LC-MS (ESI), t_R = 9.57 min, 84% purity, *m/z* calcd for $[C_{22}H_{33}N_3O_3+H]^+$, 388.53 found, 388.3.

2. Enzyme inhibition assays

General. Enzymatic assays of human thrombin (Sigma Aldrich, Darmstadt, Germany), human factor Xa (Enzo Life Sciences, Lörrach, Germany), human matriptase-2 (available from previous studies),[1] human leukocyte elastase (Merck, Darmstadt, Germany) and human cathepsin G (Enzo Life Sciences, Lörrach, Germany) were performed on a Fluostar Optima plate reader (BMG Labtech, Ortenberg, Germany) in clear 96-well plates with flat bottom (Sarstedt, Nümbrecht, Germany). The enzymatic reaction of the AMC substrates was monitored at an excitation wavelength of 360 nm and an emission wavelength of 460 nm. Cbz-Gly-Gly-Arg-AMC, Boc-Gln-Ala-Arg-AMC and Suc-Ala-Ala-Pro-Phe-AMC were purchased from Bachem (Bubendorf, Switzerland), MeOSuc-Ala-Ala-Pro-Val-AMC and Boc-Ile-Glu-Gly-Arg-AMC × AcOH were purchased from ABCR (Karlsruhe, Germany).

Determinations of K_m values. K_m values were determined in duplicate measurements under assay conditions noted below. Non-linear regressions were performed using the equation $v = V_{max}$ [S]/([S] + K_m), where v and V_{max} are the rate and maximum rate, respectively, [S] is the substrate concentration and K_m is the Michaelis constant. The standard errors refer to the non-linear regressions. The value for thrombin obtained with 10 different Cbz-Gly-Gly-Arg-AMC concentrations between 2.5 and 100 µM was 30.0 ± 3.5 µM. The value for factor Xa obtained with 10 different Boc-Ile-Glu-Gly-Arg-AMC concentrations between 25 and 500 µM was 144 ± 18 µM. The value for matriptase-2 obtained with 10 different Boc-Gln-Ala-Arg-AMC concentrations between 2.5 and 100 µM was 40.6 ± 4.3 µM. The value for leukocyte elastase obtained with 12 different MeOSuc-Ala-Ala-Pro-Val-AMC concentrations between 5 and 500 µM was 85.9 ± 8.8 µM. A literature K_m value for the cathepsin G substrate Suc-Ala-Ala-Pro-Phe-AMC was reported to be >100 µM.[2]

Descriptions of the inhibition assays for thrombin,[3] factor Xa, matriptase-2,[3] leukocyte elastase, and cathepsin G are part of the main body of the manuscript.

3. Inhibition of serine proteases by aminolyzed diketomorpholines

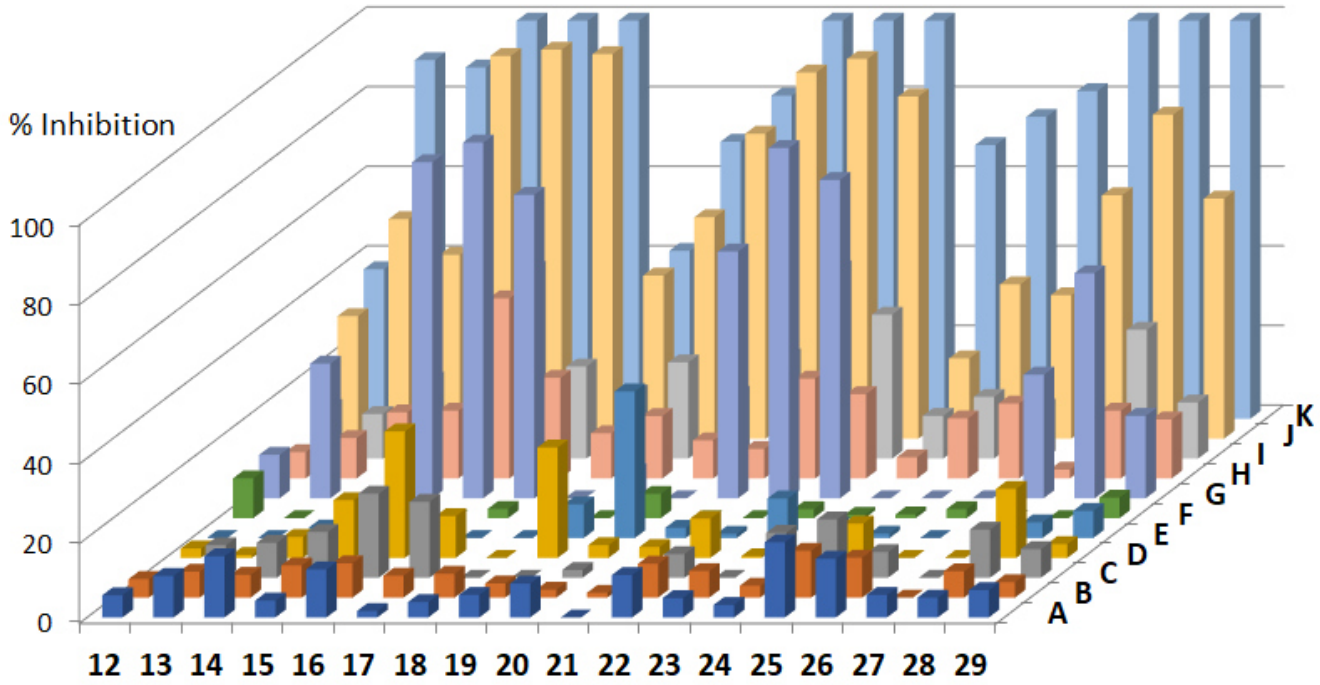

Figure S2 (*identical with Fig. 4 in the main body*). Inhibition of human thrombin by ADKMs. The structure of each inhibitor is composed of the corresponding DKM **12**-**29** and the corresponding primary amine **A**-**K**. The enzyme-catalyzed formation of 7-amino-4-methylcoumarin (AMC) from the fluorogenic substrate Cbz-Gly-Gly-Arg-AMC was followed for 30 min. Mean values from duplicate measurements are shown. The apparent inhibitor concentration was 50 µM, assuming complete conversion during the prior incubation of DKM and primary amine. Neither DKMs **12**-**19**, nor primary amines **A**-**K**, each at a concentration of 50 µM, inhibited thrombin.

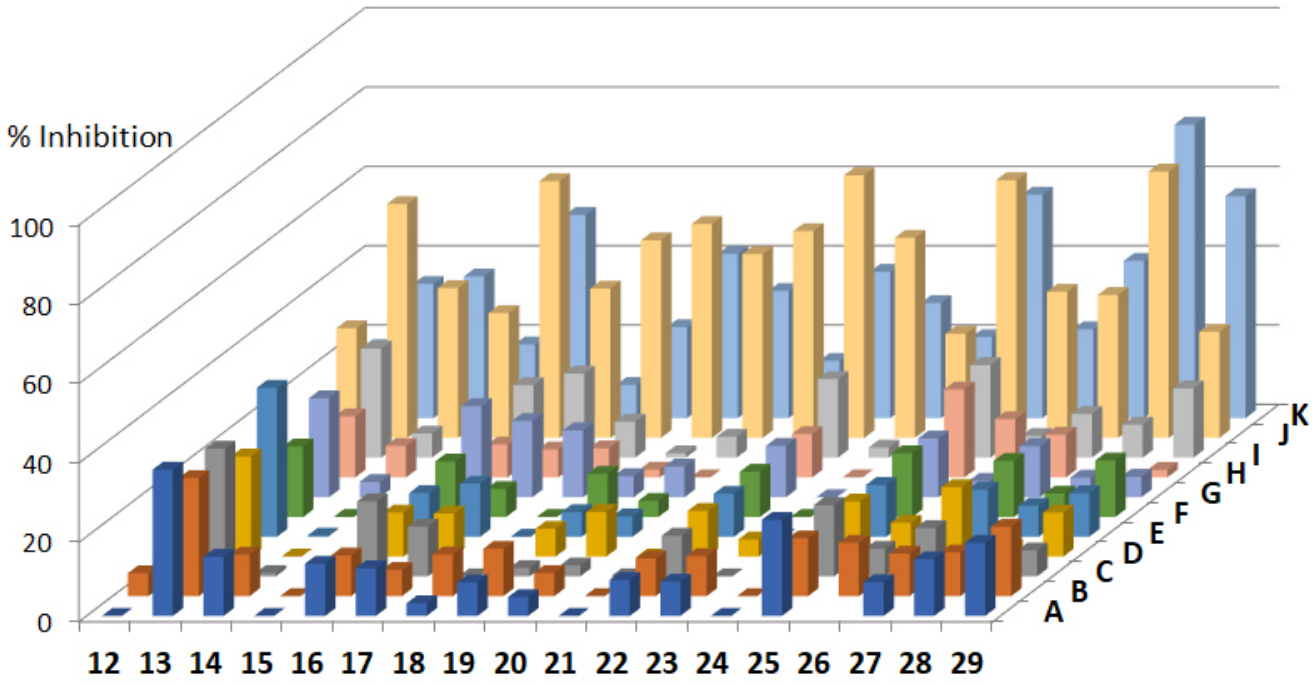

Figure S3. Inhibition of human factor Xa by ADKMs. The structure of each inhibitor is composed of the corresponding DKM **12**-**29** and the corresponding primary amine **A**-**K**. The enzyme-catalyzed formation of AMC from the fluorogenic substrate Boc-Ile-Glu-Gly-Arg-AMC was followed for 30 min. Mean values from duplicate measurements are shown. The apparent inhibitor concentration was 50 µM, assuming complete conversion during the prior incubation of DKM and primary amine. DKM **13** inhibited factor Xa (≤ 70% residual enzymatic activity at an inhibitor concentration of 50 µM) and ADKMs derived from **13** were not considered as hits for further validation. Primary amines **A**-**K** did not inhibit factor Xa.

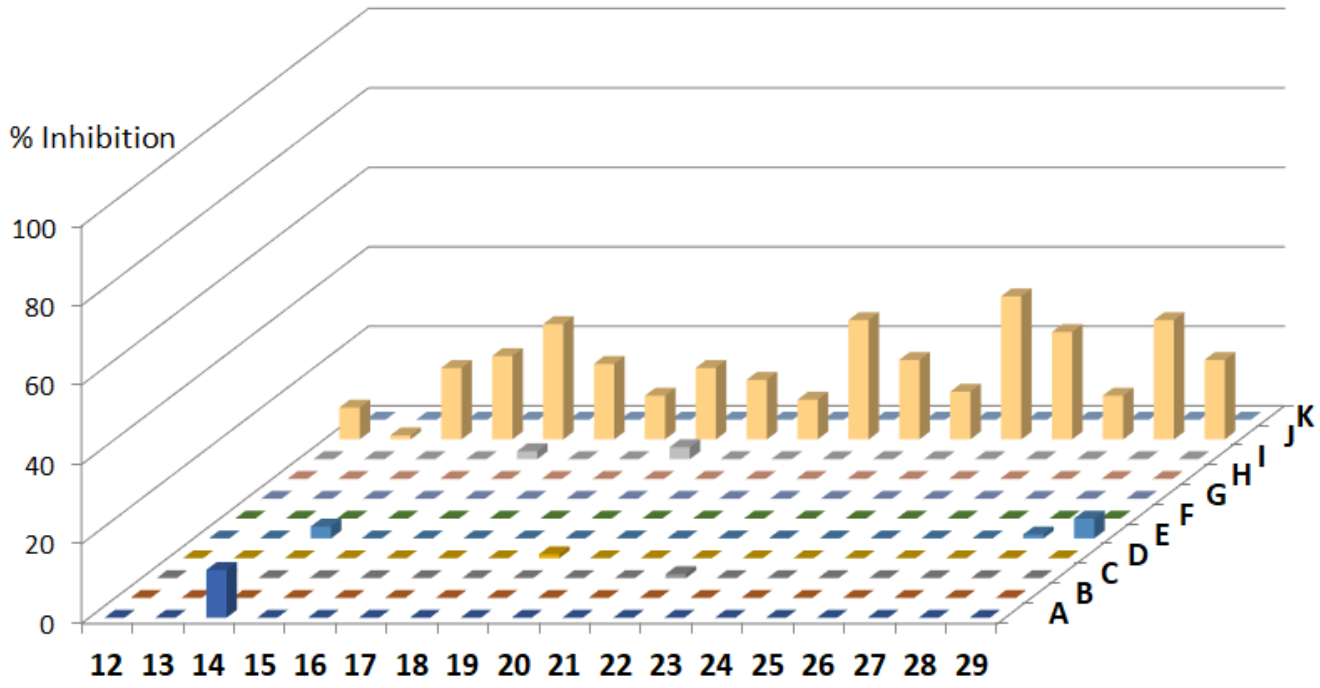

Figure S4. Inhibition of human matriptase-2 by ADKMs. The structure of each inhibitor is composed of the corresponding DKM **12**-**29** and the corresponding primary amine **A**-**K**. The enzyme-catalyzed formation of AMC from the fluorogenic substrate Boc-Gln-Ala-Arg-AMC was followed for 30 min. Mean values from duplicate measurements are shown. The apparent inhibitor concentration was 50 µM, assuming complete conversion during the prior incubation of DKM and primary amine. Neither DKMs **12**-**19**, nor primary amines **A**-**K**, each at a concentration of 50 µM, inhibited matriptase-2.

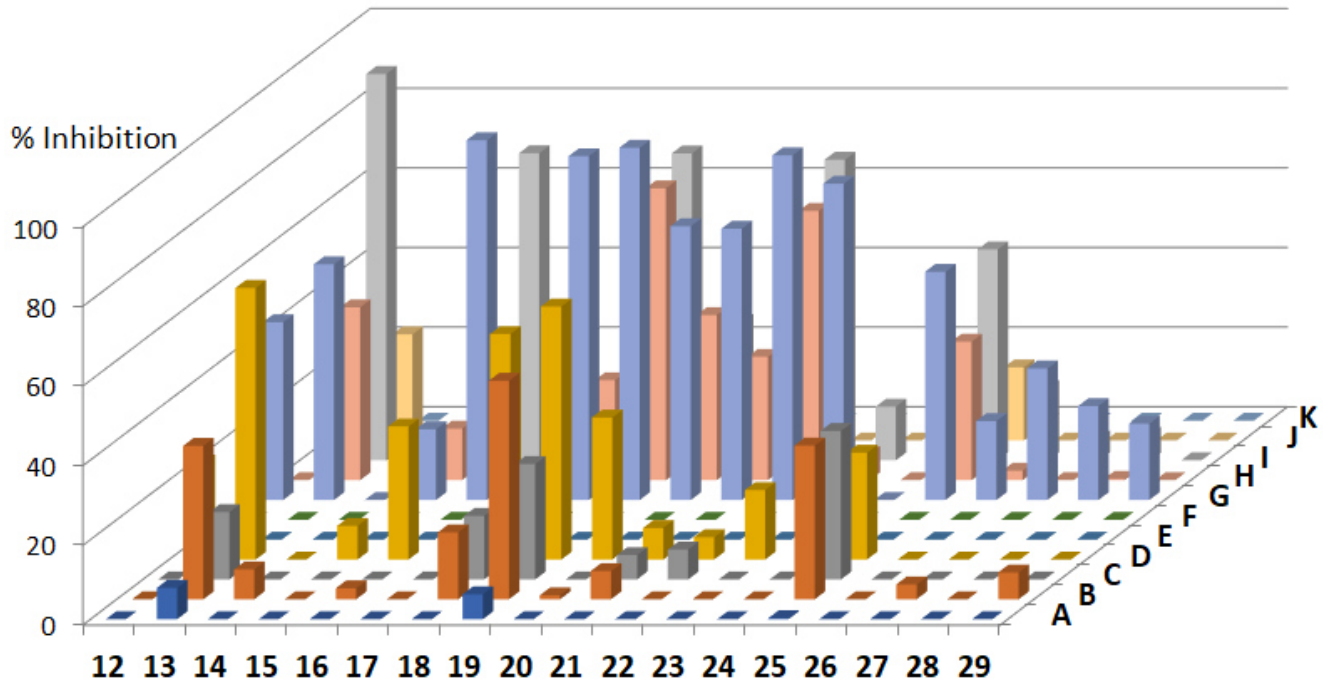

Figure S5. Inhibition of human leukocyte elastase by ADKMs. The structure of each inhibitor is composed of the corresponding DKM **12**-**29** and the corresponding primary amine **A**-**K**. The enzyme-catalyzed formation of AMC from the fluorogenic substrate MeOSuc-Ala-Ala-Pro-Val-AMC was followed for 30 min. Mean values from duplicate measurements are shown. The apparent inhibitor concentration was 50 µM, assuming complete conversion during the prior incubation of DKM and primary amine. DKMs **13**, **18**, **19**, **20**, **21**, **23**, **25**, and **27** inhibited leukocyte elastase (≤ 90% residual enzymatic activity at an inhibitor concentration of 50 µM) and ADKMs derived from these DKMs were not considered as hits for further validation. Primary amines **A**-**K** did not inhibit leukocyte elastase.

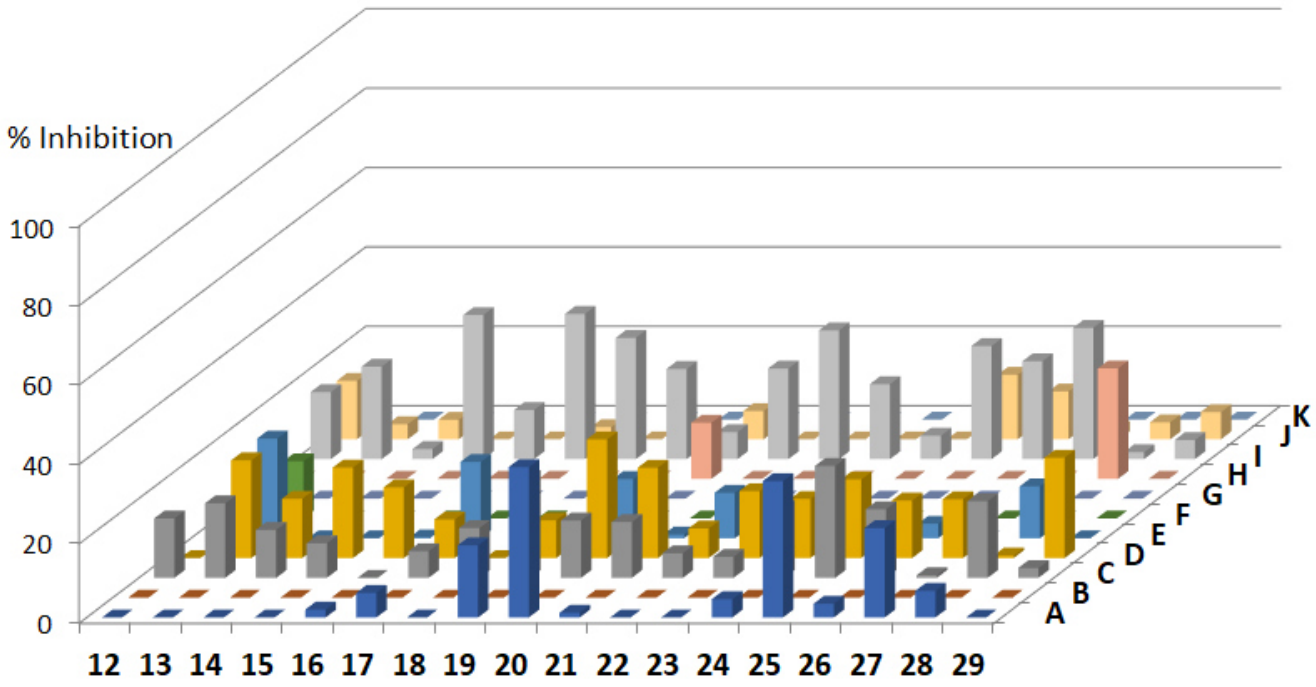

Figure S6. Inhibition of human cathepsin G by ADKMs. The structure of each inhibitor is composed of the corresponding DKM **12**-**29** and the corresponding primary amine **A**-**K**. The enzyme-catalyzed formation of AMC from the fluorogenic substrate Suc-Ala-Ala-Pro-Phe-AMC was followed for 30 min. Mean values from duplicate measurements are shown. The apparent inhibitor concentration was 50 µM, assuming complete conversion during the prior incubation of DKM and primary amine. Neither DKMs **12**-**19**, nor primary amines **A**-**K**, each at a concentration of 50 µM, inhibited cathepsin G.

Table S1. IC_{50} values for the inhibition of thrombin and factor Xa by *in situ* generated ADKMs.[a]

protease	**15J**	**15K**	**16G**	**16J**	**16K**	**22G**	**28K**	**29K**
thrombin	3.36 ± 0.49 µM	0.404 ± 0.039 µM	0.999 ± 0.119 µM	1.76 ± 0.31 µM	0.482 ± 0.046 µM	1.20 ± 0.09 µM	0.231± 0.016 µM	n.d.[b]
factor Xa	n.d.	n.d.	n.d.	n.d.	23.0 ± 4.1 µM	n.d.	17.7 ± 3.0 µM	28.9 ± 7.7 µM

[a] Enzyme-catalyzed reactions were monitored for 15 min without *in situ* generated ADKMs and in the presence of five different apparent concentrations of *in situ* generated ADKMs. Progress curves from duplicate measurements were analyzed by linear regression and slopes were used for non-linear regression with the equation $v = v_0/(1 + [I]/IC_{50})$, where v is the product formation rate, v_0 the uninhibited product formation rate, [I] the apparent inhibitor concentration, and IC_{50} the half-maximal inhibitory concentration. The standard errors (SE) refer to the non-linear regression.
[b] not determined.

Table S2. K_i values for the inhibition of serine proteases by authentic compounds.[a]

compd	thrombin	factor Xa	matriptase-2	elastase	cathepsin G
12C	n.i.[b]	n.i.	n.i.	n.i.	n.i.
12G	17.0 ± 1.8 µM	n.i.	n.i.	n.i.	n.i.
14B	n.i.	n.i.	n.i.	n.i.	n.i.
15K	0.0846 ± 0.0026 µM	0.477 ± 0.084 µM	43.0 ± 9.2 µM	n.i.	n.i.
16G	0.0421 ± 0.0217 µM	53.6 ± 4.6 µM	n.i.	n.i.	n.i.
16J	0.459 ± 0.168 µM	26.5 ± 12.4 µM	73.0 ± 11.9 µM	n.i.	n.i.
16K	0.0239 ± 0.0020 µM	0.0328 ± 0.0046 µM	10.5 ± 0.7 µM	n.i.	n.i.
28K	0.0237 ± 0.0016 µM	0.0682 ± 0.0174	12.1 ± 3.93 µM	n.i.	n.i.

[a] Enzyme-catalyzed reactions were monitored for 15 min without authentic ADKMs and in the presence of five different concentrations of authentic ADKMs. Progress curves from duplicate measurements were analyzed by linear regression and slopes were used for non-linear regression with the equation $v = v_0/(1 + [I]/IC_{50})$, where v is the product formation rate, v_0 the uninhibited product formation rate and [I] the inhibitor concentration. K_i values were calculated with the equation $K_i = IC_{50}/(1 + [S]/K_m)$, where [S] is the substrate concentration, K_m the Michaelis constant and K_i the inhibition constant. The standard errors (SE) refer to the non-linear regression.

[b] No inhibition refers to a residual enzyme activity of more than 70% in the presence of 50 µM inhibitor.

Table S3. Evaluation of the inhibition of serine proteases by building blocks.[a]

compd	K_i values (μM) or inhibition (%) @ 50 μM		
	thrombin	factor Xa	matriptase-2
12G	17.0 μM	> 70%	> 70%
12	> 70%	> 70%	> 70%
G	> 70%	> 70%	> 70%
15K	0.0846 μM	0.477 μM	43.0 μM
15	> 70%	> 70%	> 70%
K	> 70%	> 70%	> 70%
16G	0.0421μM	53.6 μM	> 70%
16	> 70%	> 70%	> 70%
G	> 70%	> 70%	> 70%
16J	0.459 μM	26.5 μM	73.0 μM
16	> 70%	> 70%	> 70%
J	> 70%	> 70%	> 70%
16K	0.0239 μM	0.0328 μM	10.5 μM
16	> 70%	> 70%	> 70%
K	> 70%	> 70%	> 70%
28K	0.0237 μM	0.0682μM	12.1 μM
28	> 70%	> 70%	> 70%
K	> 70%	> 70%	> 70%

[a] All identified hit compounds are listed. The building blocks from which they have been assembled do not inhibit the corresponding enzyme. K_i values of ADKMs **12G**, **15K**, **16G**, **16J**, **16K**, and **28K** are taken from Table S2. Inhibition data for the corresponding DKMs **12**, **15**, **16**, and **28** as well as primary amines **G**, **K**, and **J** are listed as percentage residual enzyme activity in the presence of 50 μM DKM or primary amine. The residual enzyme activity in the absence of test compounds was set 100%.

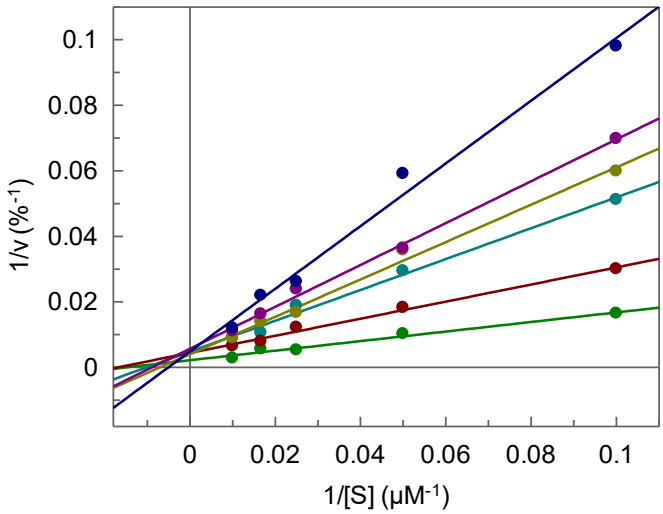

Figure S7. Determination of the inhibition type using the example of thrombin inhibition by ADKM 16G. Lineweaver-Burk plot, *i.e.* double-reciprocal diagram of steady-state rates *versus* substrate concentrations. Mean values from duplicate measurements are shown. The following concentrations of the fluorogenic substrate Cbz-Gly-Gly-Arg-AMC were used, 10 µM, 20 µM, 40 µM, 60 µM and 100 µM. The following concentrations of inhibitor **16G** were used, • 0 nM, • 50 nM, • 100 nM, • 150 nM, • 200 nM, • 250 nM. The rate in the absence of inhibitor and the presence of 20 µM substrate was set 100%. The reactions were initiated by adding the thrombin solution and were followed at 25 °C for 30 min.

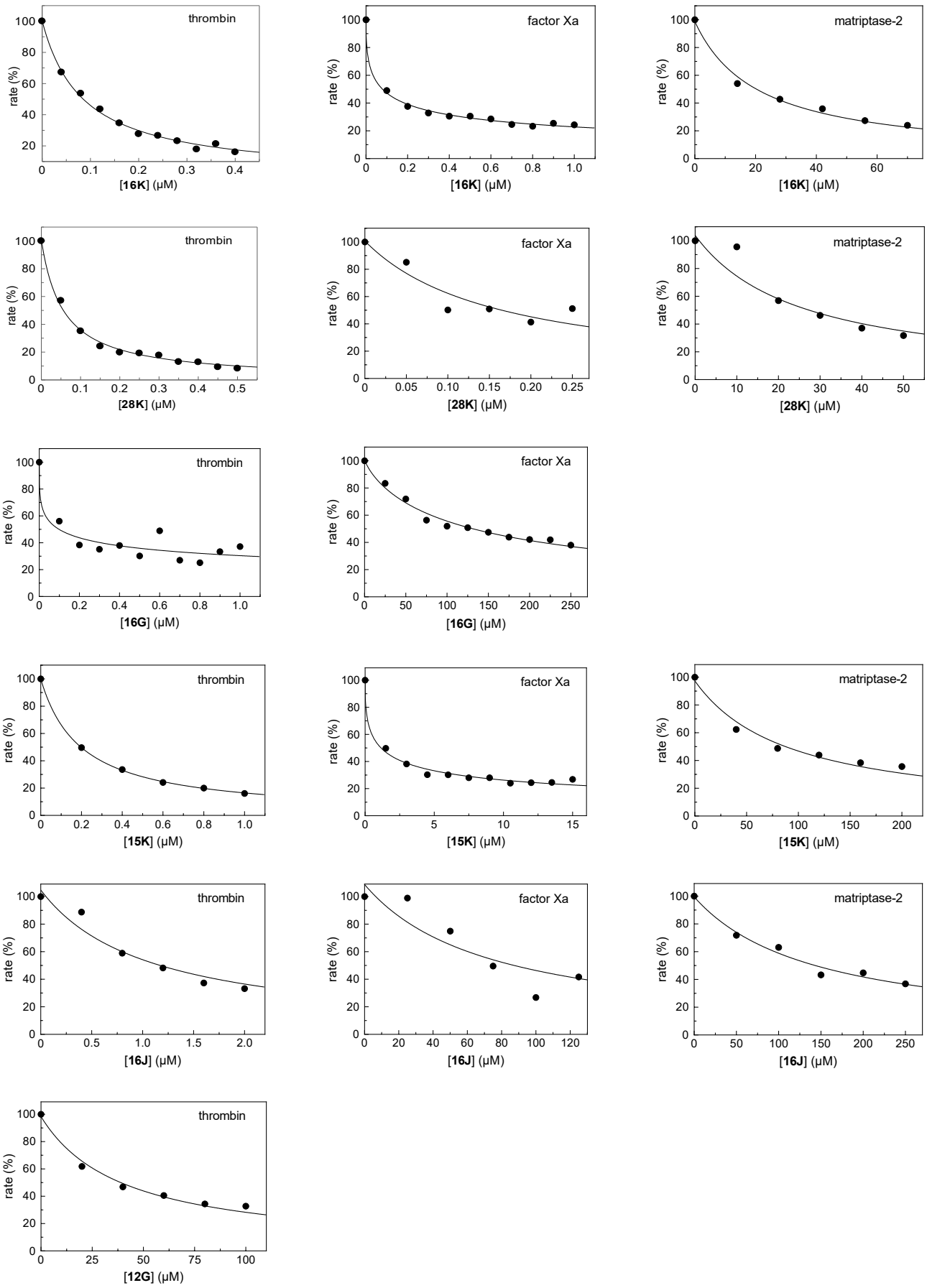

Figure S8. IC_{50} graphs. The determinations of IC_{50} values for protease inhibition by authentic ADKMs are shown. Data were from duplicate measurements. K_i values were calculated as described and are listed in Table S2.

4. General synthetic methods & instruments

Preparative column chromatography was performed on Merck silica gel (0.063-0.200 mm, 60 Å) or using an automated flash column chromatography system puriFlash XS520Plus (Interchim, Montluçon, France). Thin-layer chromatography was carried out on Merck (Darmstadt, Germany) aluminum sheets, silica gel 60 F254. Detection was performed with UV light at 254 nm. Retention factors (R_f) are indicated. Melting points were determined on a Büchi (Essen, Germany) 510 oil bath apparatus. ^{1}H NMR (500 MHz) and ^{13}C NMR (125 MHz) spectra were recorded on a Bruker (Rheinstetten, Germany) Avance DRX 500 and ^{1}H NMR (600 MHz) and ^{13}C NMR (150 MHz) spectra on a Bruker Avance III 600 NMR spectrometer. Chemical shifts δ are given in ppm referring to the signal center using the solvent peaks for reference, DMSO-d_6 2.50/39.7 ppm. In case of rotamers, only the peaks for the major rotamer are given. LC-MS analyses were carried out on an API2000 (Applied Biosystems, Darmstadt, Germany) mass spectrometer coupled to an Agilent (Santa Clara, CA, USA) 1100 LC system using an EC50/2 Nucleodur C18 Gravity 3 µm column (Macherey-Nagel, Düren, Germany). Samples (1 mg/mL) were dissolved in MeOH containing 2 mM ammonium acetate, and 8 µL of this solution was injected into the column at 25 °C. The mobile phase was a gradient of 90% H_2O to 100% MeOH containing 2 mM ammonium acetate in 10 min, then 100% MeOH containing 2 mM ammonium acetate to 20 min. Flow rate was 0.3 mL/min. For purity determination, diode array detection (DAD) was applied in the range of 220-400 nm. Positive total ion scans were observed from 150-800 m/z. GC–MS analyses were recorded on a GCMS-QP 2010 Ultra (Shimadzu, Duisburg, Germany) instrument equipped with a Zebron ZB-5MSi column (30 m × 0.25 mm × 0.25 µm) with a 5% phenylmethylpolysiloxane coating and helium as carrier gas. The mass spectrometer was operated in the scan mode from 20-600 m/z. The oven was heated from 50 °C (1 min) to 280 °C at 20 °C/min (hold 7.50 min) for a total run time of 20 min, and a constant pressure flowrate of 1.2 mL/min was maintained on the column. Samples (1 mg/mL) were dissolved in dichloromethane and 1 µL of this solution was injected into the column at 250 °C. Retention times (t_R) of all compounds are noted. High resolution mass spectrometry (HRMS) spectra were recorded on a microTOF-Q (Bruker, Köln, Germany) mass spectrometer connected to a Dionex (Thermo Scientific, Braunschweig, Germany) Ultimate 3000 LC *via* an ESI interface. Samples were dissolved in MeCN, and 1 µL of this solution was injected into the column at 25 °C. The mobile phase was MeCN containing 0.1% acetic acid. Positive or negative full scans were observed from 50-1000 m/z. Resins were purchase from Iris Biotech (Marktredwitz, Germany) and Merck (Novabiochem, Darmstadt, Germany).

5. Solution-phase synthesis of diketomorpholine 12

*The preparation of compound **7**, **8**, and **12** are part of the main body of the manuscript.*

6. Preparation of ((*S*)-2-hydroxy-4-methylpentanoyl)-L-phenylalanine (31)

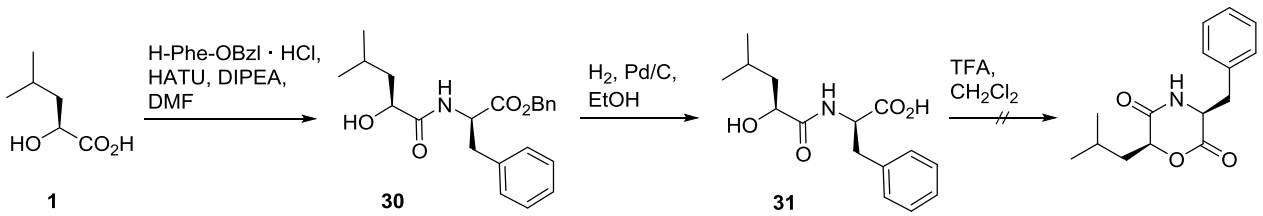

Scheme S2. Synthesis of **31** and the attempted preparation of a derived DKM.

*Benzyl ((S)-2-hydroxy-4-methylpentanoyl)-L-phenylalaninate (**30**).* To a stirring solution of *(S)*-2-hydroxy-4-methylpentanoic acid (**1**, 0.66 g, 5.0 mmol) and H-Phe-OBzl × HCl (1.46 g, 5.0 mmol) in DMF was added DIPEA (3.4 mL, 20 mmol), followed by the addition of HATU (2.09 g, 5.5 mmol) after 5 minutes. The mixture was stirred at room temperature overnight, after which EtOAc (100 mL) was added. The organic phase was washed with 10% $KHSO_4$ (50 mL), sat. $NaHCO_3$ (50 mL), 5% LiCl (50 mL) and brine (50 mL), dried over Na_2SO_4, filtered and concentrated *in vacuo*. The crude product was purified by flash column chromatography (gradient of cyclohexane/EtOAc 4:1 to 1:1) to obtain a colorless solid (1.273 g, 69% yield); R_f = 0.42 (CH_2Cl_2/MeOH 19:1); mp 106-107 °C. Compound **30** was mentioned in the literature[4] without analytical data. ^{1}H NMR (600 MHz, DMSO-d_6) δ 0.81 (d, *J* = 3.0 Hz, 3H, CH_3), 0.82 (d, *J* = 3.0 Hz, 3H, CH_3), 1.19 – 1.30 (m, 2H, $(CH_3)_2CHCH_2$), 1.60 – 1.71 (m, 1H, $(CH_3)_2CH$), 3.05 (dd, *J* = 13.8, 8.5 Hz, 1H, $CHCH_2Ph$), 3.10 (dd, *J* = 13.8, 5.7 Hz, 1H, $CHCH_2Ph$), 3.84 (ddd, *J* = 9.6, 5.9, 4.0 Hz, 1H, CHOH), 4.62 (td, *J* = 8.3, 5.7 Hz, 1H, NHCH), 5.11 (s, 2H, OCH_2Ph), 5.45 (d, *J* = 5.8 Hz, 1H, OH), 7.14 – 7.18 (m, 2H, CH_{arom}), 7.18 – 7.22 (m, 1H, CH_{arom}), 7.23 – 7.27 (m, 2H, CH_{arom}), 7.30 – 7.39 (m, 5H, CH_{arom}), 7.89 (d, *J* = 8.1 Hz, 1H, NH). ^{13}C NMR (151 MHz, DMSO-d_6) δ 21.5 (CH_3), 23.3 (CH_3), 23.7 ($(CH_3)_2CH$), 36.5 ($CHCH_2Ph$), 43.3 ($(CH_3)_2CHCH_2$), 52.7 (NHCH), 66.1 (OCH_2Ph), 69.3 (CHOH), 126.5 (CH_{arom}), 127.9 (CH_{arom}), 128.0 (CH_{arom}), 128.2 (CH_{arom}), 128.4 (CH_{arom}), 129.1 (CH_{arom}), 135.7 (C_{arom}), 136.9 (C_{arom}), 171.2 (CO), 174.3 (CO). LC-MS (ESI), t_R = 7.34 min, 95% purity, *m/z* calcd for $[C_{22}H_{27}NO_4+H]^+$ 370.47; found 370.3.

*((S)-2-Hydroxy-4-methylpentanoyl)-L-phenylalanine (**31**).* A mixture of **30** (0.37 g, 1.0 mmol) and 10% Pd/C in EtOH (10 mL) was stirred under a hydrogen atmosphere at room temperature overnight. The mixture was diluted with EtOAc (20 mL), filtered through celite, and the filtrate was concentrated *in vacuo* to give the title compound as a colorless solid (0.280 g, 100% yield); mp 120-121 °C. ^{1}H NMR (500 MHz, DMSO-d_6) δ 0.82 (d, *J* = 4.3 Hz, 3H, CH_3), 0.84 (d, *J* = 4.3 Hz, 3H, CH_3), 1.20 – 1.33 (m, 2H, $(CH_3)_2CHCH_2$), 1.63 – 1.71 (m, 1H, $(CH_3)_2CH$), 3.00 (dd, *J* = 13.8, 8.1 Hz, 1H, $CHCH_2Ph$), 3.09 (dd, *J* = 13.8, 5.1 Hz, 1H, $CHCH_2Ph$), 3.83 (dd, *J* = 9.4, 3.9 Hz, 1H, CHOH), 4.52 (td, *J* = 8.1, 5.0 Hz, 1H, NHCH), 5.49 (s, 1H, OH), 7.15 – 7.23 (m, 3H, CH_{arom}), 7.24 – 7.29 (m, 2H, CH_{arom}), 7.62 (d, *J* = 8.2 Hz, 1H, NH), 12.85 (s, 1H, OH). ^{13}C NMR (126 MHz, DMSO-d_6) δ 21.5 (CH_3), 23.3 (CH_3), 23.7 ($(CH_3)_2CH$), 36.7 ($CHCH_2Ph$), 43.4 ($(CH_3)_2CHCH_2$), 52.3 (NHCH), 69.4 (CHOH), 126.4 (CH_{arom}), 128.1 (CH_{arom}), 129.2 (CH_{arom}), 137.2 (C_{arom}), 172.7 (CO), 174.1 (CO). LC-MS (ESI), t_R = 5.47 min, 81% purity, *m/z* calcd for $[C_{15}H_{21}NO_4+H]^+$ 280.34; found 280.2.

7. Resin-based preparation of diketomorpholines

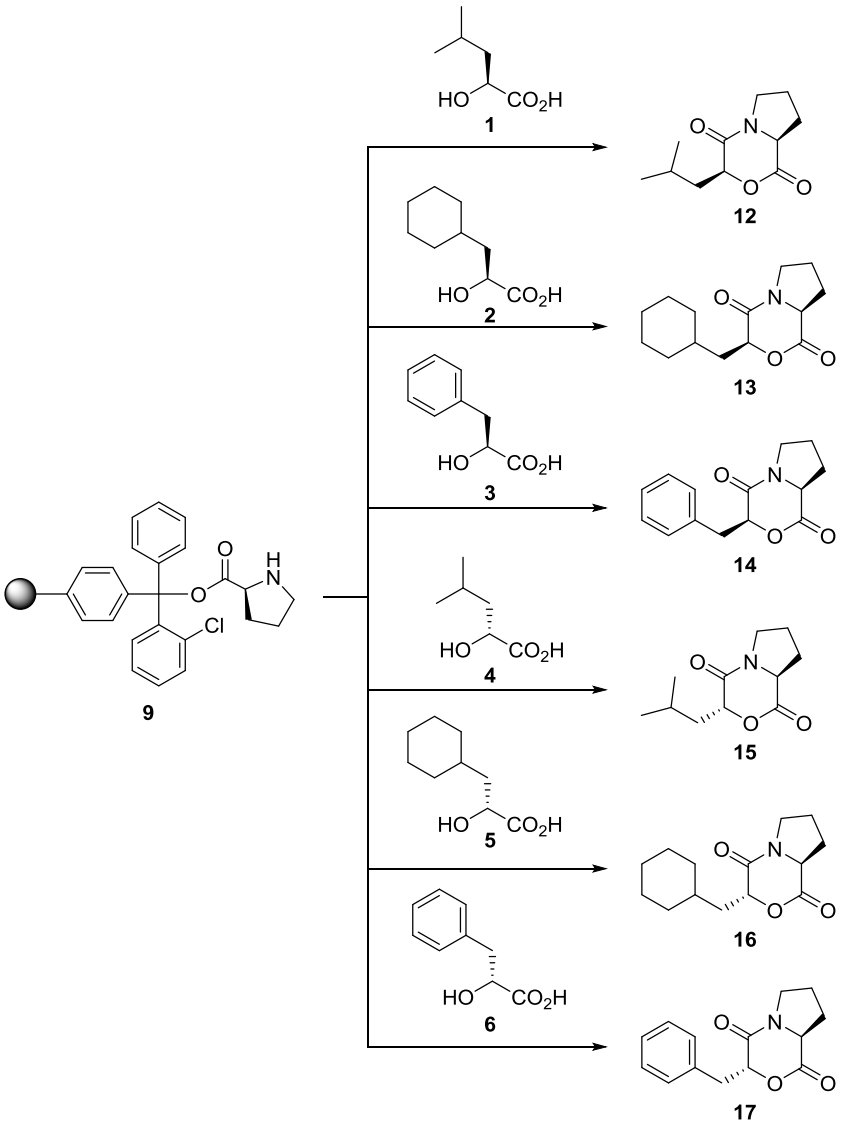

Scheme S3. Synthesis of DKMs **12**-**17** from H-Pro-2-ClTrt resin **9**.

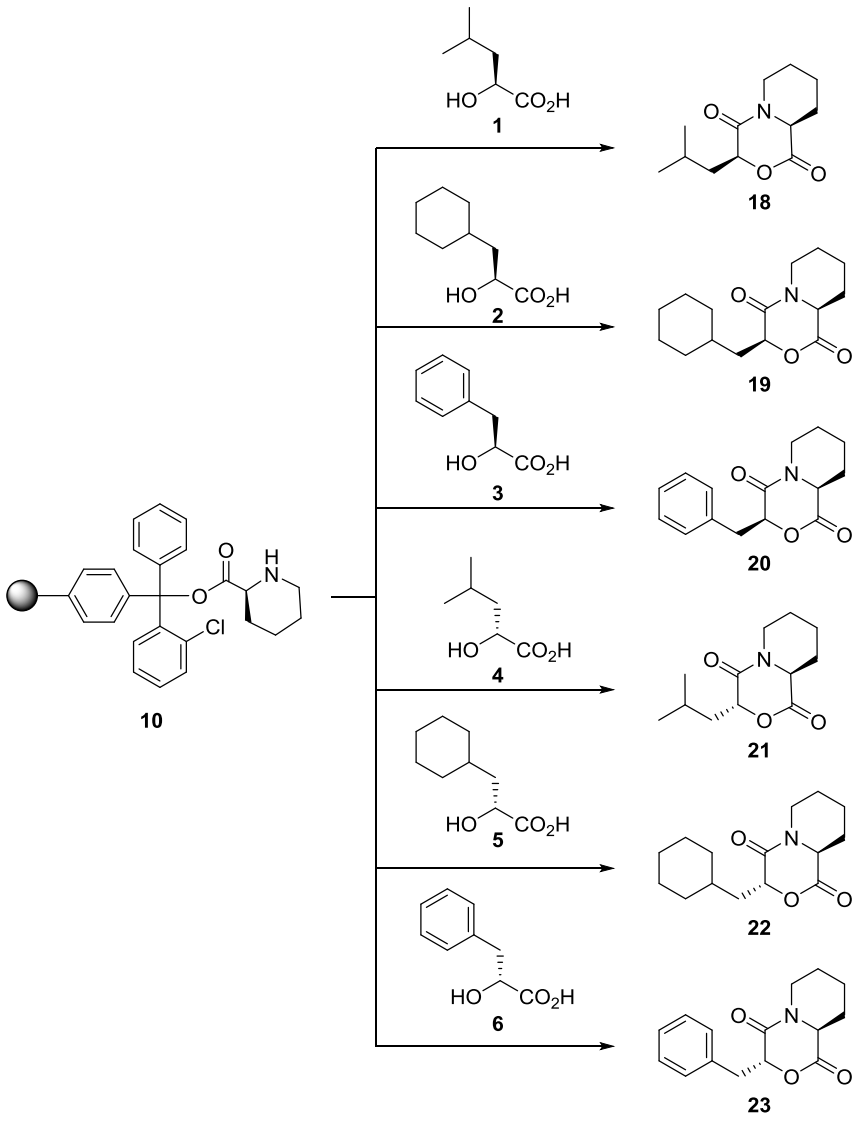

Scheme S4. Synthesis of DKMs **18**-**23** from H-Pip-2-ClTrt resin **10**.

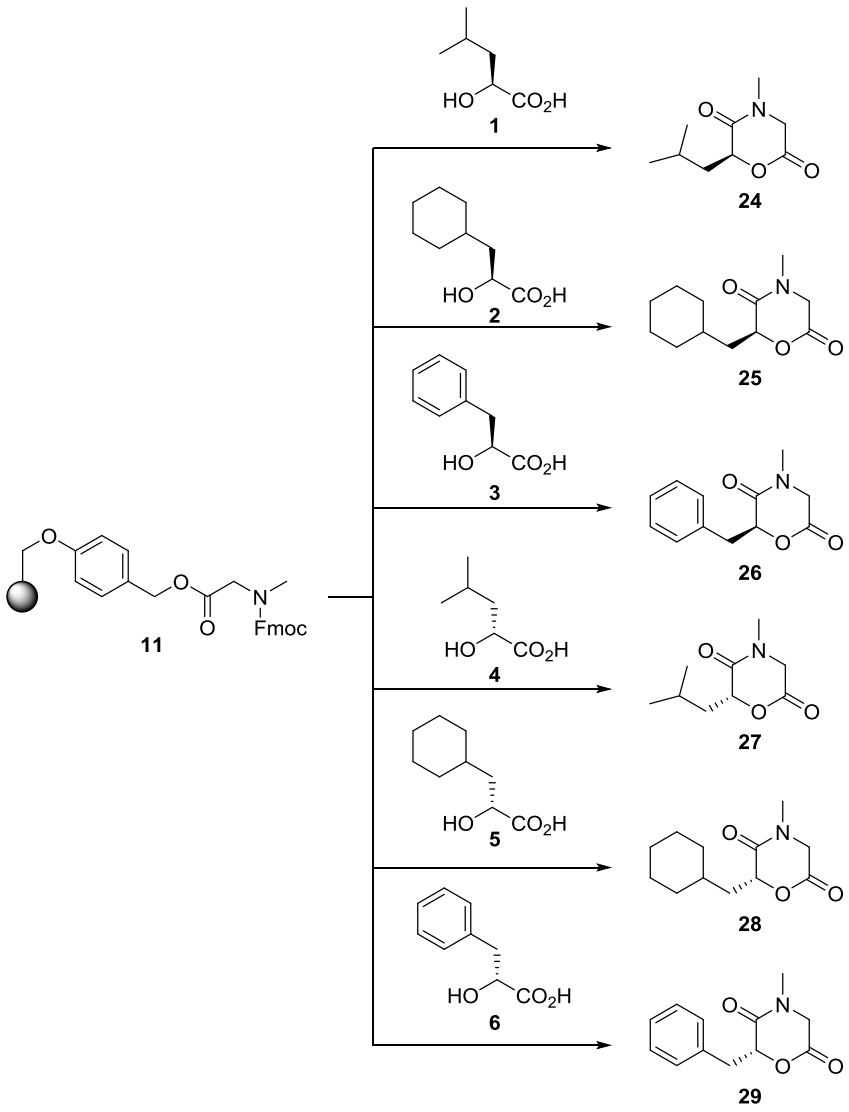

Scheme S5. Synthesis of DKMs **24**-**29** from Fmoc-Sar-Wang resin **11**.

General Procedure A for solid phase syntheses using H-Pro-2-ClTrt and H-Pip-2-ClTrt resin is part of the main body of the manuscript.

General Procedure B for solid phase syntheses using Fmoc-Sar-Wang resin is part of the main body of the manuscript.

*The synthetic procedure to (3S,8aS)-3-isobutyltetrahydro-1H-pyrrolo[2,1-c][1,4]oxazine-1,4(3H)-dione (**12**) by using the General Procedure A is part of the main body of the manuscript.*

*(3S,8aS)-3-Cyclohexylmethyl)tetrahydro-1H-pyrrolo[2,1-c][1,4]oxazine-1,4(3H)-dione (**13**).* By using the General Procedure A, this compound was prepared in two fritted glass reaction vessels from (*S*)-2-hydroxy-3-cyclohexylpropionic acid (**2**, 2 mmol, 0.34 g) and H-Pro-2-ClTrt resin (1 mmol). The crude product was purified by column chromatography (CH_2Cl_2/EtOAc 1:1) to yield the title compound as a colorless solid (0.056 g, 22% yield); R_f = 0.60 (CH_2Cl_2/EtOAc 1:1); mp 154-155 °C. ^{1}H NMR (600 MHz, DMSO-d_6) δ 0.83 – 0.92 (m, 1H), 0.93 – 1.03 (m, 1H), 1.09 – 1.27 (m, 4H), 1.42 – 1.52 (m, 1H), 1.58 – 1.72 (m, 4H), 1.78 – 1.88 (m, 4H, $NCH_2C\underline{H}_2$, $C\underline{H}(C\underline{H}_2)_5$, $COCHC\underline{H}_2$), 1.98 – 2.08 (m, 1H, $NCHC\underline{H}_2$), 2.20 – 2.27 (m, 1H, $NCHC\underline{H}_2$), 3.34 – 3.45 (m, 2H, NCH_2), 4.55 (t, *J* = 7.9 Hz, 1H, NCH), 5.11 (dd, *J* = 9.6, 3.6 Hz, 1H, COCH). ^{13}C NMR (151 MHz, DMSO-d_6) δ 22.7 ($NCH_2\underline{C}H_2$), 25.5, 25.8, 25.9 ($CH(\underline{C}H_2)_5$), 27.6, 31.6, 33.2, 33.3 ($\underline{C}H(\underline{C}H_2)_5$), $NCH\underline{C}H_2$), 36.0 ($COCH\underline{C}H_2$), 44.7 (NCH_2), 57.1 (NCH), 75.9 (COCH), 164.9 (CO), 170.0 (CO). GC-MS (EI), t_R = 12.64 min, 100% purity, *m/z* calcd for $[C_{14}H_{21}NO_3]^{\bullet+}$, 251.33 found, 251.30. HRMS (ESI) *m/z* calcd for $[C_{14}H_{21}NO_3+H]^+$, 252.1594; found, 252.1596.

*(3S,8aS)-3-Benzyltetrahydro-1H-pyrrolo[2,1-c][1,4]oxazine-1,4(3H)-dione (**14**).* By using the General Procedure A, this compound was prepared in two fritted glass reaction vessels from (*S*)-2-hydroxy-3-phenylpropionic acid (**3**, 2 mmol, 0.33 g) and H-Pro-2-ClTrt resin (1 mmol). The crude product was purified by column chromatography (CH_2Cl_2/EtOAc 1:1) to yield the title compound as a colorless solid (0.19 g, 77% yield); R_f = 0.58 (CH_2Cl_2/EtOAc 1:1); mp 126-128 °C. ^{1}H NMR (600 MHz, DMSO-d_6) δ 1.78 – 1.91 (m, 2H), 1.97 – 2.06 (m, 1H), 2.18 – 2.27 (m, 1H, $NCHC\underline{H}_2$, $NCH_2C\underline{H}_2$), 2.93 (dd, *J* = 15.0, 9.3 Hz, 1H), 3.37 (dd, *J* = 15.0, 3.6 Hz, 1H, $CHC\underline{H}_2Ph$), 3.40 – 3.49 (m, 2H, NCH_2), 4.54 (t, *J* = 8.0 Hz, 1H, NCH), 5.33 (dd, *J* = 9.3, 3.6 Hz, 1H, COCH), 7.21 – 7.25 (m, 1H, CH_{arom}), 7.29 – 7.34 (m, 4H, CH_{arom}). ^{13}C NMR (151 MHz, DMSO-d6) δ 22.7 ($NCH_2\underline{C}H_2$), 27.6 ($NCH\underline{C}H_2$), 34.7 ($CH\underline{C}H_2Ph$), 44.7 (NCH_2), 57.1 (NCH), 78.5 (COCH), 126.4 (CH_{arom}), 128.2 (CH_{arom}), 129.4 (CH_{arom}), 137.0 (C_{arom}), 164.2 (CO), 169.7 (CO). GC-MS (EI), t_R = 12.61 min, 99% purity, *m/z* calcd for $[C_{14}H_{15}NO_3]^{\bullet+}$, 245.29; found, 245.20. HRMS (ESI) *m/z* calcd for $[C_{14}H_{15}NO_3+Na]^+$, 268.0944; found, 268.0947.

*(3R,8aS)-3-Isobutyltetrahydro-1H-pyrrolo[2,1-c][1,4]oxazine-1,4(3H)-dione (**15**).* By using the General Procedure A, this compound was prepared in two fritted glass reaction vessels from (*R*)-2-hydroxy-4-methylpentanoic acid (**4**, 2 mmol, 0.26 g) and H-Pro-2-ClTrt resin (1 mmol). The crude product was purified by column chromatography (CH_2Cl_2/EtOAc 1:1) to yield the title compound as a colorless solid (0.17 g, 82% yield); R_f = 0.56 (CH_2Cl_2/EtOAc 1:1); mp 164-166 °C. ^{1}H NMR (500 MHz, DMSO-d_6) δ 0.93 (d, *J* = 6.6 Hz, 3H, CH_3), 0.95 (d, *J* = 6.7 Hz, 3H, CH_3), 1.59 (ddd, *J* = 13.9, 8.0, 5.0 Hz, 1H, $(CH_3)_2C\underline{H}$), 1.70 – 1.78 (m, 1H), 1.78 – 1.92 (m, 3H, $(CH_3)_2CHC\underline{H}_2$, $NCH_2C\underline{H}_2$), 1.92 – 2.02 (m, 1H, $NCHC\underline{H}_2$), 2.26 (dtd, *J* = 13.4, 6.7, 2.4 Hz, 1H, $NCHC\underline{H}_2$), 3.35 – 3.41 (m, 1H, NCH_2), 3.43 – 3.50 (m, 1H, NCH_2), 4.55 (dd, *J* = 9.4, 7.0 Hz, 1H, NCH), 4.70 (dd, *J* = 10.2, 5.0 Hz, 1H, COCH). ^{13}C NMR (126 MHz, DMSO-d_6) δ 21.6, 22.0, 22.6 ($(\underline{C}H_3)_2CH$, $NCH_2\underline{C}H_2$), 24.3 ($(CH_3)_2\underline{C}H$), 28.9 ($NCH\underline{C}H_2$), 39.9 ($(CH_3)_2CH\underline{C}H_2$), 45.1 ($NCH_2$), 55.9 (NCH), 79.6 (COCH), 164.4 (CO), 168.6 (CO). GC-MS (EI), t_R = 10.27 min, 97% purity, *m/z* calcd for $[C_{11}H_{17}NO_3]^{\bullet+}$, 211.12; found, 211.00. HRMS (ESI) *m/z* calcd for $[C_{11}H_{17}NO_3+H]^+$, 212.1281; found, 212.1279.

*(3R,8aS)-3-(Cyclohexylmethyl)tetrahydro-1H-pyrrolo[2,1-c][1,4]oxazine-1,4(3H)-dione (**16**).* By using the General Procedure A, this compound was prepared in two fritted glass reaction vessels from (*R*)-2-hydroxy-3-

cyclohexylpropionic acid (**5**, 2 mmol, 0.34 g) and H-Pro-2-ClTrt resin (1 mmol). The crude product was purified by column chromatography (CH_2Cl_2/EtOAc 1:1) to yield the title compound as a colorless solid (0.196 g, 78% yield); R_f = 0.65 (CH_2Cl_2/EtOAc 1:1); mp 104-106 °C. ^{1}H NMR (500 MHz, DMSO-d_6) δ 0.85 – 1.02 (m, 2H), 1.07 – 1.26 (m, 3H), 1.39 – 1.50 (m, 1H), 1.56 – 1.71 (m, 4H), 1.71 – 1.93 (m, 5H, $NCH_2C\underline{H}_2$, $C\underline{H}(C\underline{H}_2)_5$, $COCHC\underline{H}_2$), 1.93 – 2.02 (m, 1H, $NCHC\underline{H}_2$), 2.20 – 2.30 (m, 1H, $NCHC\underline{H}_2$), 3.38 (ddd, *J* = 11.6, 8.7, 3.2 Hz, 1H, NCH_2), 3.46 (ddd, *J* = 11.4, 9.0, 7.3 Hz, 1H, NCH_2), 4.54 (dd, *J* = 9.4, 7.0 Hz, 1H, NCH), 4.73 (dd, *J* = 10.3, 5.0 Hz, 1H, COCH). ^{13}C NMR (126 MHz, DMSO-d_6) δ 21.8 ($NCH_2\underline{C}H_2$), 25.4, 25.5, 25.9 ($CH(\underline{C}H_2)_5$), 28.7, 31.5, 32.7, 33.2 ($\underline{C}H(\underline{C}H_2)_5$), $NCH\underline{C}H_2$), 38.4 ($COCH\underline{C}H_2$), 44.9 (NCH_2), 55.7 (NCH), 78.9 (COCH), 164.3 (CO), 168.4 (CO). GC-MS (EI), t_R = 12.52 min, 97% purity, *m/z* calcd for $[C_{14}H_{21}NO_3]^{\bullet+}$, 251.15; found, 251.00. HRMS (ESI) *m/z* calcd for $[C_{14}H_{21}NO_3+H]^+$, 252.1594; found, 252.1593.

*(3R,8aS)-3-Benzyltetrahydro-1H-pyrrolo[2,1-c][1,4]oxazine-1,4(3H)-dione (**17**)*. By using the General Procedure A, this compound was prepared in two fritted glass reaction vessels from (*R*)-2-hydroxy-3-phenylpropionic acid (**6**, 2 mmol, 0.33 g) and H-Pro-2-ClTrt resin (1 mmol). The crude product was purified by column chromatography (CH_2Cl_2/EtOAc 1:1) to yield the title compound as a colorless solid (0.152 g, 62% yield); R_f = 0.48 (CH_2Cl_2/EtOAc 1:1); mp 164-166 °C. ^{1}H NMR (500 MHz, DMSO-d_6) δ 1.66 – 1.78 (m, 1H), 1.84 – 1.97 (m, 2H), 2.13 – 2.21 (m, 1H, $NCHC\underline{H}_2$, $NCH_2C\underline{H}_2$), 3.12 – 3.25 (m, 2H, $CHC\underline{H}_2Ph$), 3.34 – 3.39 (m, 1H, NCH_2), 3.48 (ddd, *J* = 11.5, 8.9, 7.2 Hz, 1H, NCH_2), 3.92 (dd, *J* = 9.3, 6.8 Hz, 1H, NCH), 4.96 (dd, *J* = 8.2, 4.9 Hz, 1H, COCH), 7.21 – 7.27 (m, 2H, CH_{arom}), 7.27 – 7.30 (m, 1H, CH_{arom}), 7.30 – 7.35 (m, 2H, CH_{arom}). ^{13}C NMR (126 MHz, DMSO-d_6) δ 21.5 ($NCH_2\underline{C}H_2$), 28.7 ($NCH\underline{C}H_2$), 37.6 ($CH\underline{C}H_2Ph$), 44.8 (NCH_2), 55.7 (NCH), 81.1 (COCH), 127.0 (CH_{arom}), 128.4 (CH_{arom}), 129.5 (CH_{arom}), 135.4 (C_{arom}), 163.3 (CO), 167.9 (CO). GC-MS (EI), t_R = 12.05 min, 97% purity, *m/z* calcd for $[C_{14}H_{15}NO_3]^{\bullet+}$, 245.29; found, 245.20. HRMS (ESI) *m/z* calcd for $[C_{14}H_{15}NO_3+Na]^+$, 268.0944; found, 268.0945.

*(3S,9aS)-3-Isobutyltetrahydropyrido[2,1-c][1,4]oxazine-1,4(3H,6H)-dione (**18**).* By using the General Procedure A, this compound was prepared in two fritted glass reaction vessels from (*S*)-2-hydroxy-4-methylpentanoic acid (**1**, 2 mmol, 0.26 g) and H-Pip-2-ClTrt resin (1 mmol). The crude product was purified by column chromatography (petroleum ether /EtOAc 1:1) to yield the title compound as a colorless solid (0.043 g, 19% yield); R_f = 0.32 (petroleum ether/EtOAc 1:1); mp 106-108 °C. ^{1}H NMR (600 MHz, DMSO-d_6) δ 0.91 (d, *J* = 6.3 Hz, 3H, CH_3), 0.92 (d, *J* = 6.4 Hz, 3H, CH_3), 1.22 – 1.33 (m, 1H), 1.45 – 1.58 (m, 2H), 1.64 – 1.73 (m, 2H), 1.74 – 1.86 (m, 3H), 2.08 – 2.16 (m, 1H, $(CH_3)_2C\underline{H}$, $(CH_3)_2CHC\underline{H}_2$, $NCH_2C\underline{H}_2$, $NCH_2CH_2C\underline{H}_2$, $NCHC\underline{H}_2$), 2.57 (td, *J* = 12.9, 2.9 Hz, 1H), 4.22 (dd, *J* = 11.7, 3.5 Hz, 1H), 4.27 (ddt, *J* = 13.2, 4.2, 2.0 Hz, 1H, NCH, NCH_2), 4.89 (dd, *J* = 9.7, 3.1 Hz, 1H, COCH). ^{13}C NMR (151 MHz, DMSO-d_6) δ 21.3 (CH_3), 22.8 ($NCH_2CH_2\underline{C}H_2$), 23.0 ($CH_3$), 23.6 ($NCH_2\underline{C}H_2$), 23.8 (($CH_3)_2\underline{C}H$), 29.7 ($NCH\underline{C}H_2$), 41.3, 41.4 (($CH_3)_2CH\underline{C}H_2$, NCH_2), 55.5 (NCH), 75.9 ($CO\underline{C}H$), 165.0 (CO), 167.4 (CO). GC-MS (EI), t_R = 10.59 min, 99% purity, *m/z* calcd for $[C_{12}H_{19}NO_3]^{\bullet+}$ 225.29; found 225.20. HRMS (ESI) *m/z* calcd for $[C_{12}H_{19}NO_3+H]^+$, 226.1438; found, 226.1434.

*(3S,9aS)-3-(Cyclohexylmethyl)tetrahydropyrido[2,1-c][1,4]oxazine-1,4(3H,6H)-dione (**19**).* By using the General Procedure A, this compound was prepared in two fritted glass reaction vessels from (*S*)-2-hydroxy-3-cyclohexylpropionic acid (**2**, 2 mmol, 0.34 g) and H-Pip-2-ClTrt resin (1 mmol). The crude product was purified by column chromatography (petroleum ether /EtOAc 1:1) to yield the title compound as a colorless solid (0.022 g, 8% yield); R_f = 0.61 (petroleum ether/EtOAc 1:1); mp 116-118 °C. ^{1}H NMR (600 MHz, DMSO-d_6) δ 0.85 – 0.92 (m, 1H), 0.92 – 1.00 (m, 1H), 1.10 – 1.32 (m, 5H), 1.45 – 1.54 (m, 3H), 1.59 – 1.70 (m, 7H, $C\underline{H}(C\underline{H}_2)_5$, $COCHC\underline{H}_2$, $NCH_2C\underline{H}_2$, $NCH_2CH_2C\underline{H}_2$), 1.79 – 1.85 (m, 1H, $NCHC\underline{H}_2$), 2.07 – 2.19 (m, 1H, $NCHC\underline{H}_2$), 2.56 (td, *J* = 13.1, 3.2 Hz, 1H, NCH_2), 4.20 – 4.24 (m, 1H, NCH_2), 4.27 (ddt, *J* = 13.3, 4.2, 1.9 Hz, 1H, NCH), 4.92 (dd, *J* = 9.8, 3.5 Hz, 1H, COCH). ^{13}C NMR (151 MHz, DMSO-d_6) δ 22.8, 23.6 ($NCH_2\underline{C}H_2$, $NCH_2CH_2\underline{C}H_2$), 25.5, 25.7, 25.9 ($\underline{C}H(\underline{C}H_2)_5$), 29.7 ($NCH\underline{C}H_2$), 31.5, 33.0, 33.2 ($\underline{C}H(\underline{C}H_2)_5$), 41.4 ($NCH_2$), 55.5 (NCH), 75.3 (COCH), 165.0

(CO), 167.3 (CO); one signal ($COCH\underline{C}H_2$) is obscured by the solvent peak. GC-MS (EI), t_R = 12.80 min, 100% purity, *m/z* calcd for $[C_{15}H_{23}NO_3]^{\bullet+}$ 265.35; found 265.25. HRMS (ESI) *m/z* calcd for $[C_{15}H_{23}NO_3+H]^+$, 266.1751; found, 266.1747.

*(3S,9aS)-3-Benzyltetrahydropyrido[2,1-c][1,4]oxazine-1,4(3H,6H)-dione (**20**).* By using the General Procedure A, this compound was prepared in two fritted glass reaction vessels from (*S*)-2-hydroxy-3-phenylpropionic acid (**3**, 2 mmol, 0.33 g) and H-Pip-2-ClTrt resin (1 mmol). The crude product was purified by column chromatography (CH_2Cl_2/EtOAc 1:1) to yield the title compound as a colorless solid (0.040 g, 15% yield); R_f = 0.57 (CH_2Cl_2/EtOAc 1:1); mp 162-163 °C. ^{1}H NMR (500 MHz, DMSO-d_6) δ 0.92 – 1.04 (m, 1H), 1.23 – 1.40 (m, 2H), 1.48 – 1.55 (m, 2H), 1.63 – 1.69 (m, 1H, $NCHC\underline{H}_2$, $NCH_2C\underline{H}_2$, $NCH_2CH_2\underline{C}H_2$), 2.41 (td, *J* = 13.1, 2.6 Hz, 1H, NCH_2), 3.14 (dd, *J* = 14.2, 4.5 Hz, 1H), 3.21 (dd, *J* = 14.2, 4.6 Hz, 1H, $COCHC\underline{H}_2$), 4.01 (dd, *J* = 12.3, 3.2 Hz, 1H, NCH_2), 4.31 (ddt, *J* = 13.4, 4.3, 2.0 Hz, 1H, NCH), 5.20 (t, *J* = 4.4 Hz, 1H, COCH), 7.13 – 7.18 (m, 2H, CH_{arom}), 7.24 – 7.35 (m, 3H, CH_{arom}). ^{13}C NMR (126 MHz, DMSO-d_6) δ 22.8, 23.4, 29.1 ($NCH_2\underline{C}H_2$, $NCH_2CH_2\underline{C}H_2$, $NCH\underline{C}H_2$), 38.5 ($COCH\underline{C}H_2$), 41.0 (NCH_2), 55.5 (NCH), 77.6 (COCH), 127.0 (CH_{arom}), 128.3 (CH_{arom}), 130.3 (CH_{arom}), 134.9 (C_{arom}), 161.9 (CO), 166.0 (CO). GC-MS (EI), t_R = 12.58 min, 100% purity, *m/z* calcd for $[C_{15}H_{17}NO_3]^{\bullet+}$ 259.30; found 259.30. HRMS (ESI) *m/z* calcd for $[C_{15}H_{17}NO_3+Na]^+$, 282.1101; found, 282.1099.

*(3R,9aS)-3-Isobutyltetrahydropyrido[2,1-c][1,4]oxazine-1,4(3H,6H)-dione (**21**).* By using the General Procedure A, this compound was prepared in two fritted glass reaction vessels from (*R*)-2-hydroxy-4-methylpentanoic acid (**4**, 2 mmol, 0.26 g) and H-Pip-2-ClTrt resin (1 mmol). The crude product was purified by column chromatography (CH_2Cl_2/EtOAc 4:1) to yield the title compound as a colorless solid (0.062 g, 27% yield); R_f = 0.73 (CH_2Cl_2/EtOAc 4:1); mp 100-101 °C. ^{1}H NMR (500 MHz, DMSO-d_6) δ 0.91 (d, *J* = 1.2 Hz, 3H, CH_3), 0.92 (d, *J* = 1.3 Hz, 3H, CH_3), 1.24 – 1.36 (m, 1H), 1.48 – 1.58 (m, 1H), 1.60 – 1.67 (m, 2H), 1.71 – 1.75 (m, 2H), 1.75 – 1.81 (m, 1H), 1.81 – 1.88 (m, 1H), 2.02 – 2.09 (m, 1H, $(CH_3)_2C\underline{H}$, $(CH_3)_2CHC\underline{H}_2$, $NCH_2C\underline{H}_2$, $NCH_2CH_2C\underline{H}_2$, $NCHC\underline{H}_2$), 2.57 (td, *J* = 13.1, 3.1 Hz, 1H), 4.26 – 4.35 (m, 2H, NCH, NCH_2), 4.93 (dd, *J* = 8.2, 5.1 Hz, 1H, COCH). ^{13}C NMR (126 MHz, DMSO-d_6) δ 21.2 (CH_3), 22.9 ($NCH_2CH_2\underline{C}H_2$), 23.0 ($CH_3$), 23.6 ($NCH_2\underline{C}H_2$), 23.8 ($(CH_3)_2\underline{C}H$), 29.52 ($NCH\underline{C}H_2$), 41.0, 41.5 ($(CH_3)_2CH\underline{C}H_2$, NCH_2), 55.7 (NCH), 76.0 ($CO\underline{C}H$), 164.4 (CO), 167.0 (CO). GC-MS (EI), t_R = 10.49 min, 98% purity, *m/z* calcd for $[C_{12}H_{19}NO_3]^{\bullet+}$, 225.14; found, 225.00. HRMS (ESI) *m/z* calcd for $[C_{12}H_{19}NO_3+H]^+$, 226.1438; found, 226.1433.

*(3R,9aS)-3-(Cyclohexylmethyl)tetrahydropyrido[2,1-c][1,4]oxazine-1,4(3H,6H)-dione (**22**).* By using the General Procedure A, this compound was prepared in two fritted glass reaction vessels from (*R*)-2-hydroxy-3-cyclohexylpropionic acid (**5**, 2 mmol, 0.34 g) and H-Pip-2-ClTrt resin (1 mmol). The crude product was purified by column chromatography (CH_2Cl_2/EtOAc 2:1) to yield the title compound as a colorless solid (0.035 g, 13% yield); R_f = 0.78 (CH_2Cl_2/EtOAc 2:1); mp 104-105 °C. ^{1}H NMR (600 MHz, $CDCl_3$) δ 0.89 – 1.03 (m, 2H), 1.09 – 1.20 (m, 1H), 1.20 – 1.31 (m, 2H), 1.42 – 1.75 (m, 11H), 1.89 (ddd, *J* = 14.4, 9.1, 3.5 Hz, 1H, $C\underline{H}(C\underline{H}_2)_5$, $COCHC\underline{H}_2$, $NCH_2C\underline{H}_2$, $NCH_2CH_2C\underline{H}_2$), 1.97 – 2.05 (m, 1H), 2.32 – 2.39 (m, 1H, $NCHC\underline{H}_2$), 2.54 (td, *J* = 13.1, 3.1 Hz, 1H, NCH_2), 3.99 (dd, *J* = 11.8, 3.3 Hz, 1H, NCH_2), 4.59 (ddt, *J* = 13.4, 4.1, 2.0 Hz, 1H, NCH), 4.85 (dd, *J* = 10.1, 3.5 Hz, 1H, COCH). ^{13}C NMR (151 MHz, $CDCl_3$) δ 23.9, 24.1 ($NCH_2\underline{C}H_2$, $NCH_2CH_2\underline{C}H_2$), 26.0, 26.3, 26.5 ($CH(\underline{C}H_2)_5$)), 30.8, 32.0, 33.3, 33.9 ($\underline{C}H(\underline{C}H_2)_5$), $NCH\underline{C}H_2$), 41.2, 42.6 (NCH_2, $COCH\underline{C}H_2$), 56.6 (NCH), 76.5 (COCH), 165.4 (CO), 167.0 (CO). GC-MS (EI), t_R = 12.70 min, 100% purity, *m/z* calcd for $[C_{15}H_{23}NO_3]^{\bullet+}$, 265.17; found, 265.30. HRMS (ESI) *m/z* calcd for $[C_{15}H_{23}NO_3+Na]^+$, 288.1570; found, 288.1568.

*(3R,9aS)-3-Benzyltetrahydropyrido[2,1-c][1,4]oxazine-1,4(3H,6H)-dione (**23**).* By using the General Procedure A, this compound was prepared in two fritted glass reaction vessels from (*R*)-2-hydroxy-3-phenylpropionic acid (**6**, 2 mmol, 0.33 g) and H-Pip-2-ClTrt resin (1 mmol). The crude product was purified by column chromatography (CH_2Cl_2/EtOAc 4:1) to yield the title compound as a colorless solid (0.039 mg, 15% yield); R_f =

0.70 (CH_2Cl_2/EtOAc 4:1); mp 139-140 °C. ^{1}H NMR (500 MHz, DMSO-d_6) δ 1.20 – 1.31 (m, 1H), 1.32 – 1.43 (m, 1H), 1.48 – 1.57 (m, 1H), 1.57 – 1.63 (m, 1H), 1.74 – 1.81 (m, 1H), 1.90 – 1.96 (m, 1H, NCHC$\underline{H}_2$, $NCH_2C\underline{H}_2$, $NCH_2CH_2C\underline{H}_2$), 2.37 (td, J = 13.0, 3.1 Hz, 1H, NCH_2), 3.13 – 3.25 (m, 2H, CHC$\underline{H}_2$Ph, NCH_2), 3.38 (dd, J = 12.1, 3.3 Hz, 1H, CHC$\underline{H}_2$Ph), 4.33 (ddt, J = 13.2, 4.2, 2.0 Hz, 1H, NCH), 5.23 (dd, J = 6.1, 4.3 Hz, 1H, COCH), 7.15 – 7.19 (m, 2H, CH_{arom}), 7.26 – 7.34 (m, 3H, CH_{arom}). ^{13}C NMR (126 MHz, DMSO-d_6) δ 23.0, 23.4, 29.6 ($NCH_2\underline{C}H_2$, $NCH_2CH_2\underline{C}H_2$, $NCH\underline{C}H_2$), 38.4 (CH$\underline{C}$H$_2$Ph), 41.3 (NCH_2), 55.3 (NCH), 77.7 (COCH), 127.1 (CH_{arom}), 128.3 (CH_{arom}), 129.8 (CH_{arom}), 135.3 (C_{arom}), 163.3 (CO), 166.4 (CO). GC-MS (EI), t_R = 12.36 min, 99% purity, *m/z* calcd for $[C_{15}H_{17}NO_3]^{\bullet+}$, 259.12; found, 259.25. HRMS (ESI) *m/z* calcd for $[C_{15}H_{17}NO_3+Na]^+$, 282.1101; found, 282.1098.

*(S)-6-Isobutyl-4-methylmorpholine-2,5-dione (**24**).* By using the General Procedure B, this compound was prepared in two fritted glass reaction vessels from (*S*)-2-hydroxy-4-methylpentanoic acid (**1**, 2 mmol, 0.26 g) and Fmoc-Sar-Wang resin (1 mmol). The crude product was purified by column chromatography (CH_2Cl_2/EtOAc 1:1) to yield the title compound as a colorless solid (0.150 g, 81% yield); R_f = 0.55 (CH_2Cl_2/EtOAc 1:1); mp 86-88 °C. ^{1}H NMR (600 MHz, DMSO-d_6) δ 0.91 (d, J = 6.5 Hz, 3H, CHC$\underline{H}_3$), 0.92 (d, J = 6.5 Hz, 3H, CHC$\underline{H}_3$), 1.65 – 1.74 (m, 2H, $(CH_3)_2$CHC$\underline{H}_2$), 1.74 – 1.82 (m, 1H, $(CH_3)_2$C$\underline{H}$), 2.85 (s, 3H, NCH_3), 4.21 – 4.33 (m, 2H, NCH_2), 4.89 (dd, J = 9.1, 4.5 Hz, 1H, COCH). ^{13}C NMR (151 MHz, DMSO-d_6) δ 21.3, 22.9, 23.9 (($\underline{C}H_3)_2\underline{C}$H), 32.8 ($NCH_3$), 49.3 ($NCH_2$), 76.1 (CO$\underline{C}$H), 165.8 (CO), 166.2 (CO); one signal ($(CH_3)_2CH\underline{C}H_2$) is obscured by the solvent peak. GC-MS (EI), t_R = 8.75 min, 100% purity, *m/z* calcd for $[C_9H_{15}NO_3]^{\bullet+}$, 185.11; found, 186.20. HRMS (ESI) *m/z* calcd for $[C_9H_{15}NO_3+H]^+$, 186.1125; found, 186.1124.

*(S)-6-(Cyclohexylmethyl)-4-methylmorpholine-2,5-dione (**25**).* By using the General Procedure B, this compound was prepared in two fritted glass reaction vessels from (*S*)-2-hydroxy-3-cyclohexylpropionic acid (**2**, 2 mmol, 0.34 g) and Fmoc-Sar-Wang resin (1 mmol). The crude product was purified by column chromatography (CH_2Cl_2/EtOAc 1:1) to yield the title compound as a colorless solid (0.011 g, 5% yield); R_f = 0.52 (CH_2Cl_2/EtOAc 1:1); mp 90-92 °C. ^{1}H NMR (600 MHz, DMSO-d_6) δ 0.83 – 0.92 (m, 1H), 0.92 – 1.00 (m, 1H), 1.09 – 1.26 (m, 3H), 1.42 – 1.50 (m, 1H), 1.58 – 1.70 (m, 5H), 1.72 – 1.81 (m, 2H, C$\underline{H}$($C\underline{H}_2)_5$, $C\underline{H}_2CH(CH_2)_5$), 2.84 (s, 3H, CH_3), 4.17 – 4.36 (m, 2H, NCH_2), 4.93 (dd, J = 10.0, 3.7 Hz, 1H, COCH). ^{13}C NMR (151 MHz, DMSO-d_6) δ 25.5, 25.7, 25.9 (CH($\underline{C}H_2)_5$), 31.5 ($\underline{C}H(CH_2)_5$), 32.8 (NCH_3), 33.0, 33.1 (CH($\underline{C}H_2)_5$), 38.1 ($\underline{C}H_2CH(CH_2)_5$), 49.3 ($NCH_2$), 75.5 (CO$\underline{C}$H), 165.8 (CO), 166.2 (CO). GC-MS (EI), t_R = 11.15 min, 100% purity, *m/z* calcd for $[C_{12}H_{19}NO_3]^{\bullet+}$, 225.14; found, 225.25. HRMS (EI) *m/z* calcd for $[C_{12}H_{19}NO_3]^{\bullet+}$, 225.1365; found, 225.1359.

*(S)-6-Benzyl-4-methylmorpholine-2,5-dione (**26**).* By using the General Procedure B, this compound was prepared in two fritted glass reaction vessels from (*S*)-2-hydroxy-3-phenylpropionic acid (**3**, 2 mmol, 0.33 g) and Fmoc-Sar-Wang resin (1 mmol). The crude product was purified by column chromatography (CH_2Cl_2/EtOAc 1:1) to yield the title compound as a colorless solid (0.124 g, 56% yield); R_f = 0.48 (CH_2Cl_2/EtOAc 1:1); mp 127-128 °C. ^{1}H NMR (600 MHz, DMSO-d_6) δ 2.80 (s, 3H, CH_3), 3.10 (dd, J = 14.6, 7.5 Hz, 1H, CHC$\underline{H}_2$Ph), 3.25 (dd, J = 14.6, 4.1 Hz, 1H, CHC$\underline{H}_2$Ph), 3.65 (d, J = 18.0 Hz, 1H, NCH_2), 4.18 (d, J = 18.0 Hz, 1H, NCH_2), 5.17 (dd, J = 7.5, 4.1 Hz, 1H, COCH), 7.21 – 7.24 (m, 2H), 7.25 – 7.28 (m, 1H), 7.29 – 7.33 (m, 2H, CH_{arom}). ^{13}C NMR (151 MHz, DMSO-d_6) δ 32.6 (CH_3), 37.1 (CH$\underline{C}$H$_2$Ph), 49.0 (NCH_2), 78.0 (CO$\underline{C}$H), 126.9, 128.3, 129.6 (CH_{arom}), 135.9 (C_{arom}), 164.7 (CO), 165.4 (CO). GC-MS (EI), t_R = 10.83 min, 100% purity, *m/z* calcd for $[C_{12}H_{13}NO_3]^{\bullet+}$, 219.09; found, 219.20. HRMS (ESI) *m/z* calcd for $[C_{12}H_{13}NO_3+Na]^+$, 242.0788; found, 242.0785.

*(R)-6-Isobutyl-4-methylmorpholine-2,5-dione (**27**).* By using the General Procedure B, this compound was prepared in two fritted glass reaction vessels from (*R*)-2-hydroxy-4-methylpentanoic acid (**4**, 2 mmol, 0.26 g) and Fmoc-Sar-Wang resin (1 mmol). The crude product was purified by column chromatography (CH_2Cl_2/EtOAc 1:1) to yield the title compound as a colorless solid (0.167 g, 90% yield); R_f = 0.54 (CH_2Cl_2/EtOAc 1:1); mp 142-

144 °C. ^{1}H NMR (600 MHz, DMSO-d_6) δ 0.91 (d, J = 6.5 Hz, 3H, CH_3), 0.92 (d, J = 6.5 Hz, 3H, CH_3), 1.65 – 1.74 (m, 2H, $(CH_3)_2CHC\underline{H}_2$), 1.74 – 1.82 (m, 1H, $(CH_3)_2C\underline{H}$), 2.85 (s, 3H, NCH_3), 4.21 – 4.33 (m, 2H, NCH_2), 4.89 (dd, J = 9.1, 4.5 Hz, 1H, COCH). ^{13}C NMR (151 MHz, DMSO-d_6) δ 21.3, 22.9, 23.9 ($(\underline{C}H_3)_2\underline{C}H$), 32.8 ($NCH_3$), 49.0 ($NCH_2$), 76.1 ($CO\underline{C}H$), 165.8 (CO), 166.2 (CO); one signal ($(CH_3)_2CH\underline{C}H_2$) is obscured by the solvent peak. GC-MS (EI), t_R = 8.76 min, 100% purity, *m/z* calcd for $[C_9H_{15}NO_3]^{\bullet+}$, 185.11; found, 186.20. HRMS (ESI) *m/z* calcd for $[C_9H_{15}NO_3+H]^+$, 186.1125; found, 186.1126.

*(R)-6-(Cyclohexylmethyl)-4-methylmorpholine-2,5-dione (**28**).* By using the General Procedure B, this compound was prepared in two fritted glass reaction vessels from (*R*)-2-hydroxy-3-cyclohexylpropionic acid (**5**, 2 mmol, 0.34 g) and Fmoc-Sar-Wang resin (1 mmol). The crude product was purified by column chromatography (CH_2Cl_2/EtOAc 1:1) to yield the title compound as a yellow oil (0.057 g, 25% yield); R_f = 0.62 (CH_2Cl_2/EtOAc 1:1). ^{1}H NMR (600 MHz, DMSO-d_6) δ 0.83 – 0.91 (m, 1H), 0.91 – 1.00 (m, 1H), 1.09 – 1.25 (m, 3H), 1.40 – 1.52 (m, 1H), 1.59 – 1.69 (m, 5H), 1.72 – 1.83 (m, 2H, $C\underline{H}(C\underline{H}_2)_5$, $C\underline{H}_2CH(CH_2)_5$), 2.84 (s, 3H, CH_3), 4.19 – 4.35 (m, 2H, NCH_2), 4.93 (dd, J = 9.9, 3.9 Hz, 1H, COCH). ^{13}C NMR (151 MHz, DMSO-d_6) δ 25.5, 25.7, 25.9 ($CH(\underline{C}H_2)_5$), 31.5 ($\underline{C}H(CH_2)_5$), 32.8 (NCH_3), 33.0, 33.1 ($CH(\underline{C}H_2)_5$), 38.1 ($\underline{C}H_2CH(CH_2)_5$), 49.3 ($NCH_2$), 75.5 ($CO\underline{C}H$), 165.8 (CO), 166.2 (CO). GC-MS (EI), t_R = 11.17 min, 100% purity, *m/z* calcd for $[C_{12}H_{19}NO_3]^{\bullet+}$, 225.14; found, 225.20. HRMS (ESI) *m/z* calcd for $[C_{12}H_{19}NO_3+H]^+$, 226.1438; found, 226.1435.

*(R)-6-Benzyl-4-methylmorpholine-2,5-dione (**29**).* By using the General Procedure B, this compound was prepared in two fritted glass reaction vessels from (*R*)-2-hydroxy-3-phenylpropionic acid (**6**, 2 mmol, 0.33 g) and Fmoc-Sar-Wang resin (1 mmol). The crude product was purified by column chromatography (CH_2Cl_2/EtOAc 1:1) to yield the title compound as a colorless solid (0.146 g, 67% yield); R_f = 0.48 (CH_2Cl_2/EtOAc 1:1); mp 119-120 °C. ^{1}H NMR (600 MHz, DMSO-d_6) δ 2.80 (s, 3H, CH_3), 3.10 (dd, J = 14.6, 7.5 Hz, 1H, $CHC\underline{H}_2Ph$), 3.25 (dd, J = 14.6, 4.1 Hz, 1H, $CHC\underline{H}_2Ph$), 3.65 (d, J = 18.0 Hz, 1H, NCH_2), 4.18 (d, J = 18.0 Hz, 1H, NCH_2), 5.17 (dd, J = 7.5, 4.1 Hz, 1H, COCH), 7.21 – 7.24 (m, 2H), 7.25 – 7.29 (m, 1H), 7.29 – 7.34 (m, 2H, CH_{arom}). ^{13}C NMR (151 MHz, DMSO-d_6) δ 32.6 (CH_3), 37.1 ($CH\underline{C}H_2Ph$), 49.0 (NCH_2), 78.0 ($CO\underline{C}H$), 126.9, 128.3, 129.6 (CH_{arom}), 135.9 (C_{arom}), 164.7 (CO), 165.4 (CO). GC-MS (EI), t_R = 10.84 min, 100% purity, *m/z* calcd for $[C_{12}H_{13}NO_3]^{\bullet+}$, 219.09; found, 219.15. HRMS (ESI) *m/z* calcd for $[C_{12}H_{13}NO_3+Na]^+$, 242.0788 found, 242.0796.

8. Preparation of aminolyzed diketomorpholines

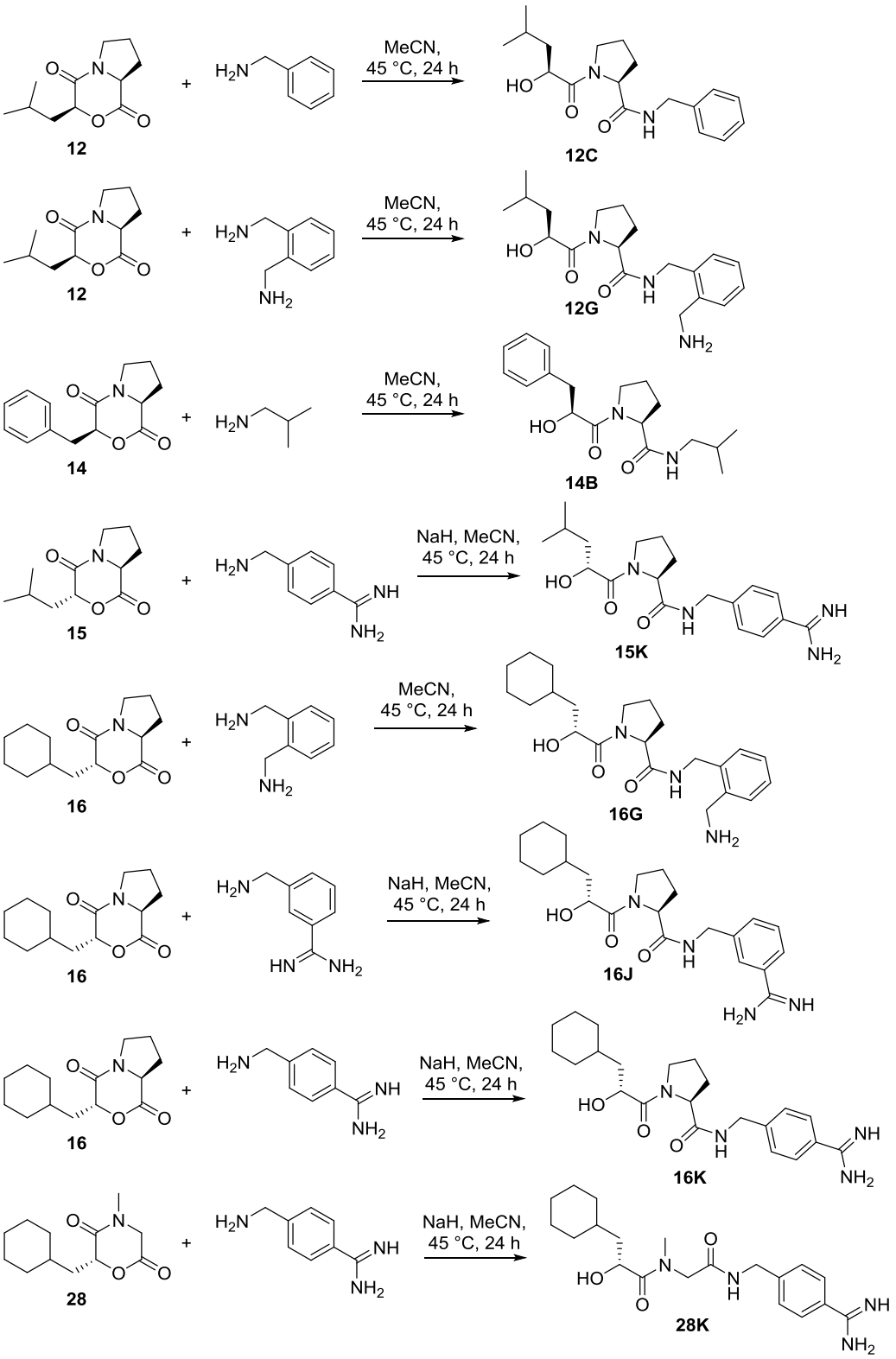

Scheme S6. Synthesis of ADKMs **12C**, **12G**, **14B**, **15K**, **16G**, **16J**, **16K**, and **28K**.

*The synthetic procedure to (S)-N-benzyl-1-((S)-2-hydroxy-4-methylpentanoyl)pyrrolidine-2-carboxamide (**12C**) is part of the main body of the manuscript.*

*(S)-N-(2-(Aminomethyl)benzyl)-1-((S)-2-hydroxy-4-methylpentanoyl)pyrrolidine-2-carboxamide (**12G**).* Diketomorpholine **12** (0.5 mmol, 106 mg) and *o*-xylylendiamine (**G**, 0.5 mmol, 68 mg) were stirred in MeCN at 45°C for 24 h. After concentration *in vacuo*, the crude product was purified by column chromatography (CH_2Cl_2/7N NH_3 in MeOH 29:1) to yield the title compound as a yellow solid (10 mg, 6% yield); R_f = 0.34 (CH_2Cl_2/7N NH_3 in MeOH 9:1); mp 104-106 °C. ^{1}H NMR (600 MHz, DMSO-d_6) δ 0.89 (d, J = 3.9 Hz, 3H, CH_3), 0.90 (d, J = 3.7 Hz, 3H, CH_3), 1.31 – 1.40 (m, 2H, $((CH_3)_2CHC\underline{H}_2)$), 1.72 – 1.81 (m, 2H), 1.82 – 1.88 (m, 1H), 1.89 – 1.99 (m, 1H), 2.02 – 2.10 (m, 1H, $(CH_3)_2C\underline{H}$, $NCH_2C\underline{H}_2$, $NCHC\underline{H}_2$), 3.44 – 3.52 (m, 1H NCH_2), 3.61 – 3.68 (m, 1H, NCH_2), 3.75 (s, 1H, $NH_2C\underline{H}_2$), 4.16 – 4.21 (m, 1H), 4.28 (dd, J = 15.3, 5.6 Hz, 1H), 4.31 – 4.38 (m, 2H, $NHC\underline{H}_2$, C<u>H</u>OH, NCH), 4.61 (s, 1H, OH), 7.11 – 7.26 (m, 3H, CH_{arom}), 7.34 – 7.39 (m, 1H, CH_{arom}), 8.26 (t, J = 5.8 Hz, 1H, NH). The NH_2 signal is not recognizable. ^{13}C NMR (151 MHz, DMSO-d_6) δ 21.5 (CH_3), 23.5 (CH_3), 23.9 ($NCH_2\underline{C}H_2$), 24.6 ($(CH_3)_2\underline{C}H$), 29.0 ($NCH\underline{C}H_2$), 40.1, 42.5, 42.6 ($(CH_3)_2CH\underline{C}H_2$, $NH\underline{C}H_2$, $NH_2\underline{C}H_2$), 46.38 (NCH_2), 59.7 (NCH), 67.4 (CHOH), 126.4 (CH_{arom}), 126.7 (CH_{arom}), 127.5 (CH_{arom}), 127.8 (CH_{arom}), 136.5 (C_{arom}), 140.5 (C_{arom}), 171.4 (CO), 172.5 (CO). LC-MS (ESI), t_R = 5.88 min, 99% purity, *m/z* calcd for $[C_{19}H_{29}N_3O_3+H]^+$, 348.47 found, 348.0. HRMS (ESI) *m/z* calcd for $[C_{19}H_{29}N_3O_3+Na]^+$, 370.2105; found, 370.2101.

*(S)-1-((S)-2-Hydroxy-3-phenylpropanoyl)-N-isobutylpyrrolidine-2-carboxamide (**14B**).* Diketomorpholine **14** (0.5 mmol, 122 mg) and isobutylamine (**B**, 0.5 mmol, 36 mg) were stirred in MeCN at 45°C for 24 h. After concentration *in vacuo*, the crude product was purified by flash column chromatography (gradient of 100% CH_2Cl_2 to 10% MeOH) to yield the title compound as a colorless oil (76 mg, 48% yield); R_f = 0.42 (CH_2Cl_2/MeOH 19:1). ^{1}H NMR (500 MHz, DMSO-d_6) δ 0.83 (d, J = 6.7 Hz, 6H, $CH(C\underline{H}_3)_2$), 1.62 – 1.74 (m, 1H), 1.74 – 1.87 (m, 2H), 1.87 – 1.96 (m, 1H) , 1.97 – 2.07 (m, 1H, $(CH_3)_2C\underline{H}$, $NCH_2C\underline{H}_2$, $NCHC\underline{H}_2$), 2.62 – 2.71 (m, 1H), 2.78 – 2.86 (m, 1H), 2.87 – 2.98 (m, 2H, $C\underline{H}_2Ph$, $NHC\underline{H}_2$), 3.46 – 3.56 (m, 1H, NCH_2), 3.61 – 3.68 (m, 1H, NCH_2), 4.30 – 4.36 (m, 1H, NCH), 4.92 (d, J = 7.8 Hz, 1H, C<u>H</u>OH), 7.16 – 7.23 (m, 2H, CH_{arom}), 7.24 – 7.29 (m, 3H, CH_{arom}), 7.65 (t, J = 6.0 Hz, 1H, NH). The OH signal is not recognizable. ^{13}C NMR (126 MHz, DMSO-d_6) δ 20.0 ($CH(\underline{C}H_3)_2$), 24.5 ($NCH_2\underline{C}H_2$), 28.1 ($(CH_3)_2\underline{C}H$), 29.1 ($NCH\underline{C}H_2$), 40.7, 45.8, 46.4 ($NHCH_2$, $\underline{C}H_2Ph$, NCH_2), 59.8 (NCH), 70.3 (CHOH), 125.9 (CH_{arom}), 127.9 (CH_{arom}), 129.5 (CH_{arom}), 138.6 (C_{arom}), 171.3 (CO), 171.6 (CO). LC-MS (ESI), t_R = 4.83 min, 98% purity, *m/z* calcd for $[C_{18}H_{26}N_2O_3+H]^+$, 319.43 found, 319.2. HRMS (ESI) *m/z* calcd for $[C_{18}H_{26}N_2O_3+Na]^+$, 341.1836; found, 341.1846.

*(S)-N-(4-Carbamimidoylbenzyl)-1-((R)-2-hydroxy-4-methylpentanoyl)pyrrolidine-2-carboxamide (**15K**).* 4-(Aminomethyl)benzamidine dihydrochloride (**K**, 0.30 mmol, 66 mg) and sodium hydride (60% dispersion in mineral oil; 0.6 mmol, 24 mg) were stirred in MeCN at 0 °C for 2 h. Diketomorpholine **15** (0.36 mmol, 76 mg) was added and the mixture was then stirred at 45 °C for 24 h. After concentration *in vacuo*, the crude product was purified by flash column chromatography (CH_2Cl_2/7N NH_3 in MeOH 19:1) to yield the title compound as a colorless solid (65 mg, 60% yield); R_f = 0.09 (CH_2Cl_2/7N NH_3 in MeOH 9:1); mp 114-116 °C. ^{1}H NMR (500 MHz, DMSO-d_6) δ 0.89 (d, J = 3.2 Hz, 3H, CH_3), 0.90 (d, J = 3.2 Hz, 3H, CH_3), 1.33 – 1.41 (m, 2H, $(CH_3)_2CHC\underline{H}_2$), 1.72 – 1.82 (m, 2H), 1.84 – 1.90 (m, 1H), 1.91 – 1.99 (m, 1H), 2.05 – 2.14 (m, 1H, $(CH_3)_2C\underline{H}$, $NCH_2C\underline{H}_2$, $NCHC\underline{H}_2$), 3.47 – 3.54 (m, 1H), 3.64 – 3.71 (m, 1H), 4.20 (dd, J = 8.5, 4.5 Hz, 1H), 4.36 (s, 1H, NCH, C<u>H</u>OH, NCH_2), 7.37 – 7.52 (m, 2H, CH_{arom}), 7.69 – 7.81 (m, 2H, CH_{arom}), 8.44 (s, 1H, NH). The OH, NH, and NH_2 signals are not recognizable. ^{13}C NMR (126 MHz, DMSO-d_6) δ 21.5 (CH_3), 23.5 (CH_3), 23.9 ($NCH_2\underline{C}H_2$), 24.7 ($(CH_3)_2\underline{C}H$), 29.1 ($NCH\underline{C}H_2$), 41.5 ($(CH_3)_2CH\underline{C}H_2$), 42.5 ($CONH\underline{C}H_2$), 46.4 ($NCH_2$), 59.8 (NCH), 67.5 (CHOH), 127.0 (C_{arom}), 127.1 (CH_{arom}), 127.8 (CH_{arom}), 145.6 (C_{arom}), 164.8 (C=NH), 171.9 (CO), 172.5 (CO).

LC-MS (ESI), t_R = 3.32 min, 98% purity, *m/z* calcd for $[C_{19}H_{28}N_4O_3+H]^+$ 361.47; found 361.3. HRMS (ESI) *m/z* calcd for $[C_{19}H_{28}N_4O_3+H]^+$, 361.2234; found, 361.2232.

(S)-N-(2-(Aminomethyl)benzyl)-1-((R)-3-cyclohexyl-2-hydroxypropanoyl)pyrrolidine-2-carboxamide ***(16G)****.* Diketomorpholine **16** (0.3 mmol, 75 mg) and *o*-xylylendiamine (**G**, 0.3 mmol, 41 mg) were stirred in MeCN at 45°C for 24 h. After concentration *in vacuo*, the crude product was purified by flash column chromatography (CH_2Cl_2/7N NH_3 19:1) to yield the title compound as a slight yellow solid (56 mg, 48% yield); R_f = 0.32 (CH_2Cl_2/7N NH_3 9:1); mp 92-94 °C. ^{1}H NMR (500 MHz, DMSO-d_6) δ 0.75 – 1.01 (m, 2H), 1.06 – 1.27 (m, 4H), 1.28 – 1.40 (m, 2H), 1.54 – 1.70 (m, 5H), 1.73 – 1.96 (m, 4H, C<u>H</u>(C<u>H</u>$_2$)$_5$, COCHC<u>H</u>$_2$, NCH$_2$C<u>H</u>$_2$, NCHC<u>H</u>$_2$), 3.39 – 3.46 (m, 2H, NCH_2), 3.63 – 3.68 (m, 1H, NCH), 3.76 (s, 2H, NH_2C<u>H</u>$_2$) , 4.18 – 4.24 (m, 1H), 4.26 – 4.35 (m, 3H, NHC<u>H</u>$_2$, C<u>H</u>OH), 7.15 – 7.27 (m, 3H, CH_{arom}), 7.33 – 7.38 (m, 1H, CH_{arom}), 8.41 (t, *J* = 5.7 Hz, 1H, NH). The OH and NH_2 signals are not recognizable. ^{13}C NMR (126 MHz, DMSO-d_6) δ 24.2 (NCH$_2$<u>C</u>H$_2$), 25.6, 25.9, 26.1 (CH(<u>C</u>H$_2$)$_5$), 29.1, 31.7, 33.2, 33.7 (<u>C</u>H(<u>C</u>H$_2$)$_5$, NCH<u>C</u>H$_2$), 40.1, 41.1, 42.7 (COCH<u>C</u>H$_2$, NH<u>C</u>H$_2$, NH$_2$<u>C</u>H$_2$), 46.2 (NCH_2), 50.0 (NCH), 67.0 (CHOH), 126.4 (CH_{arom}), 126.8 (CH_{arom}), 127.7 (CH_{arom}), 127.9 (CH_{arom}), 136.6 (C_{arom}), 140.8 (C_{arom}), 171.4 (CO), 172.8 (CO). LC-MS (ESI), t_R = 9.49 min, 95% purity, *m/z* calcd for $[C_{22}H_{33}N_3O_3+H]^+$, 388.53 found, 388.3. HRMS (ESI) *m/z* calcd for $[C_{22}H_{33}N_3O_3+H]^+$, 388.2595; found, 388.2595.

(S)-N-(3-Carbamimidoylbenzyl)-1-((R)-3-cyclohexyl-2-hydroxypropanoyl)pyrrolidine-2-carboxamide ***(16J)****.* 3-(Aminomethyl)benzamidine dihydrochloride (**J**, 0.2 mmol, 44 mg) and sodium hydride (60% dispersion in mineral oil; 0.4 mmol, 16 mg) were stirred in MeCN at 0 °C for 2 h. Diketomorpholine **16** (0.24 mmol, 60 mg) was added and the mixture was then stirred at 45 °C for 24 h. After concentration *in vacuo*, the crude product was purified by flash column chromatography (gradient of 100% H_2O to 50% MeCN) to yield the title compound as a colorless solid (18 mg, 23% yield); mp 148-150 °C. ^{1}H NMR (600 MHz, DMSO-d_6) δ 0.78 – 0.86 (m, 2H), 1.08 – 1.21 (m, 5H), 1.28 – 1.34 (m, 1H), 1.54 – 1.66 (m, 5H), 1.77 – 1.88 (m, 2H), 1.93 – 1.99 (m, 1H), 2.08 – 2.14 (m, 1H, C<u>H</u>(C<u>H</u>$_2$)$_5$, COCHC<u>H</u>$_2$, NCH$_2$C<u>H</u>$_2$, NCHC<u>H</u>$_2$), 3.46 – 3.53 (m, 1H), 3.65 – 3.71 (m, 1H, NCH_2), 4.22 – 4.29 (m, 2H), 4.31 – 4.36 (m, 2H, NCH, C<u>H</u>OH, $NHCH_2$), 4.78 (s, 1H, OH), 7.51 – 7.59 (m, 2H, CH_{arom}), 7.64 – 7.67 (m, 1H, CH_{arom}), 7.71 – 7.75 (m, 1H, CH_{arom}), 8.49 (t, *J* = 6.1 Hz, 1H, NH). The NH and NH_2 signals are not recognizable. ^{13}C NMR (151 MHz, DMSO-d_6) δ 24.8 (NCH$_2$<u>C</u>H$_2$), 25.7, 25.9, 26.1 (CH(<u>C</u>H$_2$)$_5$), 29.0, 31.8, 33.0, 33.7 (<u>C</u>H(<u>C</u>H$_2$)$_5$), NCH<u>C</u>H$_2$), 41.1, 41.4 (COCH<u>C</u>H$_2$, CONH<u>C</u>H$_2$), 46.01 (NCH_2), 60.1 (NCH), 66.8 (CHOH), 125.7 (CH_{arom}), 125.7 (CH_{arom}), 128.8 (CH_{arom}), 128.9 (CH_{arom}), 131.5 (C_{arom}), 140.7 (C_{arom}), 165.8 (C=NH), 172.2 (CO), 172.9 (CO). LC-MS (ESI), t_R = 9.82 min, 97% purity, *m/z* calcd for $[C_{22}H_{32}N_4O_3+H]^+$, 401.53 found, 401.2. HRMS (ESI) *m/z* calcd for $[C_{22}H_{32}N_4O_3+Na]^+$, 423.2367; found, 423.2385.

(S)-N-(4-Carbamimidoylbenzyl)-1-((R)-3-cyclohexyl-2-hydroxypropanoyl)pyrrolidine-2-carboxamide ***(16K)****.* 4-(Aminomethyl)benzamidine dihydrochloride (**K**, 0.2 mmol, 44 mg) and sodium hydride (60% dispersion in mineral oil; 0.4 mmol, 16 mg) were stirred in MeCN at 0 °C for 2 h. Diketomorpholine **16** (0.24 mmol, 60 mg)was added and the mixture was then stirred at 45 °C for 24 h. After concentration *in vacuo*, the crude product was purified by flash column chromatography (gradient of 100% H_2O to 50% MeCN) to yield the title compound as a colorless solid (24 mg, 30% yield); mp 156-158 °C. ^{1}H NMR (500 MHz, DMSO-d_6) δ 0.78 – 1.00 (m, 2H), 1.04 – 1.27 (m, 5H), 1.29 – 1.38 (m, 1H), 1.44 – 1.53 (m, 1H), 1.58 – 1.68 (m, 4H, C<u>H</u>(C<u>H</u>$_2$)$_5$, COCHC<u>H</u>$_2$), 1.77 – 1.89 (m, 2H), 1.91 – 1.98 (m, 1H), 2.00 – 2.12 (m, 1H, NCH$_2$C<u>H</u>$_2$, NCHC<u>H</u>$_2$), 3.40 – 3.51 (m, 1H), 3.60 – 3.71 (m, 1H, NCH_2), 4.23 (dd, *J* = 9.8, 3.3 Hz, 1H), 4.28 – 4.31 (m, 2H), 4.35 (dd, *J* = 8.4, 4.6 Hz, 1H, NCH, C<u>H</u>OH, $NHCH_2$), 6.64 (br s, 2H, NH_2), 7.24 – 7.31 (m, 2H, CH_{arom}), 7.67 – 7.74 (m, 2H, CH_{arom}), 8.31 (t, *J* = 6.1 Hz, 1H, NH). The OH and NH signals are not recognizable. ^{13}C NMR (126 MHz, DMSO-d_6) δ 24.63 (NCH$_2$<u>C</u>H$_2$), 25.63, 25.91, 26.10 (CH(<u>C</u>H$_2$)$_5$), 29.03, 31.75, 33.26, 33.79 (<u>C</u>H(<u>C</u>H$_2$)$_5$), NCH<u>C</u>H$_2$), 41.11 (COCH<u>C</u>H$_2$), 41.56 (CONH<u>C</u>H$_2$), 46.38 (NCH_2), 59.74 (NCH), 66.75 (CHOH), 126.44 (CH_{arom}), 126.49 (CH_{arom}), 134.10 (C_{arom}), 141.52 (C_{arom}), 162.54 (C=NH), 171.69 (CO), 172.64 (CO). LC-MS (ESI), t_R = 8.95 min, 100% purity, *m/z* calcd

for $[C_{22}H_{32}N_4O_3+H]^+$, 401.53 found, 401.3. HRMS (ESI) *m/z* calcd for $[C_{22}H_{32}N_4O_3+H]^+$, 401.2547; found, 401.2566.

*(R)-N-(2-((4-Carbamimidoylbenzyl)amino)-2-oxoethyl)-3-cyclohexyl-2-hydroxy-N-methylpropanamide (**28K**).* 4-(Aminomethyl)benzamidine dihydrochloride (**K**, 0.2 mmol, 44 mg) and sodium hydride (60% dispersion in mineral oil; 0.4 mmol, 16 mg) were stirred in MeCN at 0 °C for 2 h. Diketomorpholine **28** (0.24 mmol, 54 mg)was added and the mixture was then stirred at 45 °C for 24 h. After concentration *in vacuo*, the crude product was purified by flash column chromatography (gradient of 100% H_2O to 50 % MeCN) to yield the title compound as a colorless solid (16 mg, 21% yield); mp 100-102 °C. ^{1}H NMR (600 MHz, DMSO-d_6) δ 0.81 – 0.98 (m, 2H), 1.05 – 1.27 (m, 4H), 1.28 – 1.36 (m, 1H), 1.36 – 1.44 (m, 1H), 1.55 – 1.69 (m, 5H, C<u>H</u>(C<u>H</u>$_2$)$_5$, COCHC<u>H</u>$_2$), 3.02 (s, 3H, CH_3), 3.98 – 4.04 (m, 1H), 4.17 – 4.23 (m, 1H), 4.29 – 4.35 (m, 2H), 4.37 – 4.42 (m, 1H, NCH_2, $NHCH_2$, C<u>H</u>OH), 6.87 (br s, 2H, NH_2), 7.26 – 7.30 (m, 2H, CH_{arom}), 7.68 – 7.73 (m, 2H, CH_{arom}), 8.38 (s, 1H, NH). The OH and NH signals are not recognizable. ^{13}C NMR (151 MHz, DMSO-d_6) δ 25.6, 26.1, 31.7, 33.3, 33.8, 34.7 (<u>C</u>H(<u>C</u>H$_2$)$_5$), 35.8 (CH_3), 41.4, 41.7, ($NHCH_2$, COCH<u>C</u>H$_2$), 50.6 (NCH_2), 65.5 (CO<u>C</u>H), 126.6 (CH_{arom}), 126.7 (CH_{arom}), 134.0 (C_{arom}), 141.5 (C_{arom}), 162.7 (C=NH), 168.1 (CO), 174.4 (CO). LC-MS (ESI), t_R = 8.66 min, 95% purity, *m/z* calcd for $[C_{20}H_{30}N_4O_3+H]^+$, 375.49 found, 375.2. HRMS (ESI) *m/z* calcd for $[C_{20}H_{30}N_4O_3+Na]^+$, 397.2210; found, 397.2219.

9. X-ray crystal structures of compounds 12 and 12C

The X-ray crystallographic data collections were performed on a Bruker D8-Venture diffractometer (Photon I detector) at 150(2) K (for **12**) and a STOE IPDS-2T diffractometer at 123(2) K (for **12C**). The diffractometers were equipped with a low-temperature device (Oxford Cryostream 800 (**12**) and Oxford Cryostream 700 (**12C**), Oxford Cryosystems) and used mirror optic monochromated Cu-Kα radiation (λ = 1.54178 Å, **12**) or graphite monochromated Mo-Kα radiation (λ = 0.71073 Å, **12C**). Intensities were measured by fine-slicing ϕ- and ω-scans and corrected for background, polarization, and Lorentz effects. Semi-empirical absorption corrections were applied for all data sets by using Bruker's SADABS program (**12**) or STOE's X-Red program (**12C**). The structures were solved by intrinsic phasing methods and refined anisotropically by the least-squares procedure implemented in the ShelX program system.[5,6] The hydrogen atoms were included isotropically using the riding model on the bound carbon atoms. CCDC 2095215 (**12**) and CCDC 2095216 (**12C**) contain the supplementary crystallographic data for this paper. The data can be obtained free of charge from The Cambridge Crystallographic Data Centre *via* www.ccdc.cam.ac.uk/getstructures.

10. References

[1] M. Mangold, M. Gütschow, M. Stirnberg, Pharmaceuticals 11 (2018), 49.

[2] P. Kasperkiewicz, M. Poreba, S.J. Snipas, S.J. Lin, D. Kirchhofer, G.S. Salvesen, M. Drag, PLoS One 10 (2015) e0132818.

[3] D. Häußler, M. Mangold, N. Furtmann, A. Braune, M. Blaut, J. Bajorath, M. Stirnberg, M. Gütschow, Chem. Eur. J. 22 (2016) 8525–8535.

[4] Y. Wang, F. Zhang, Y. Zhang, J.O. Liu, D. Ma, Bioorg. Med. Chem. Lett. 18 (2008), 4385–4387.

[5] G.M. Sheldrick, Acta Cryst. A71 (2015) 3–8.

[6] G.M. Sheldrick, Acta Cryst. C71 (2015) 3–8.

11. ^{1}H and ^{13}C NMR spectra

*^{1}H and ^{13}C NMR spectra of compound **7***

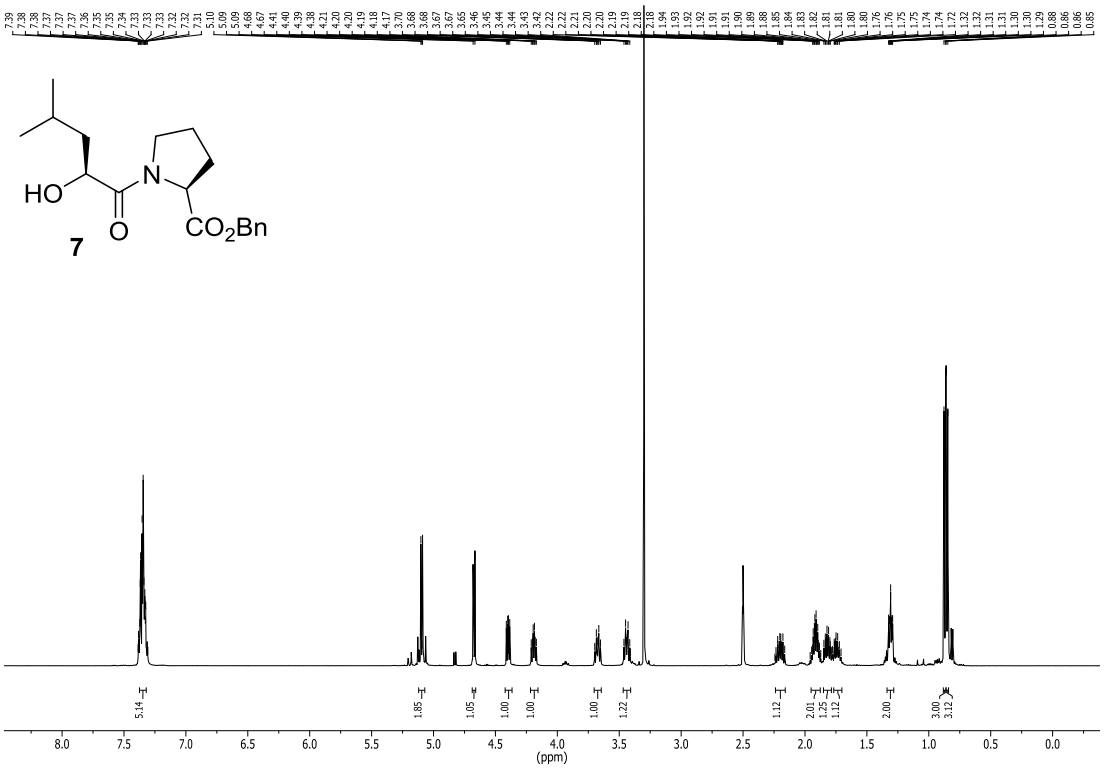

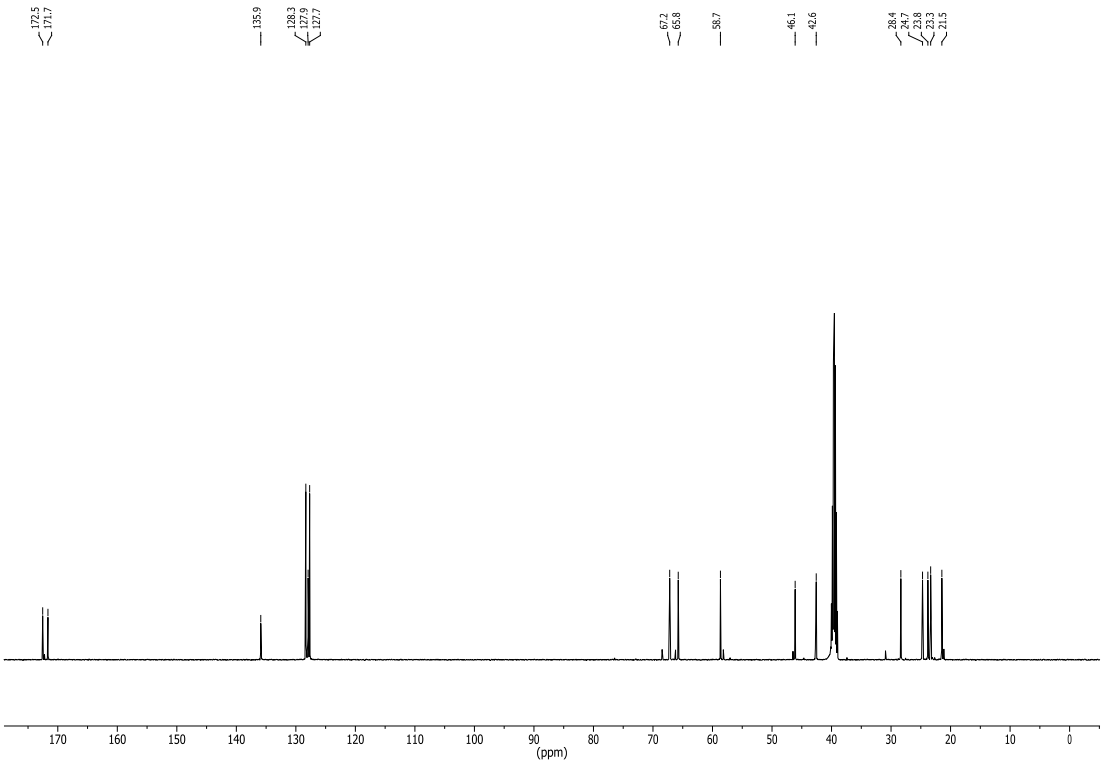

*^{1}H and ^{13}C NMR spectra of compound **8***

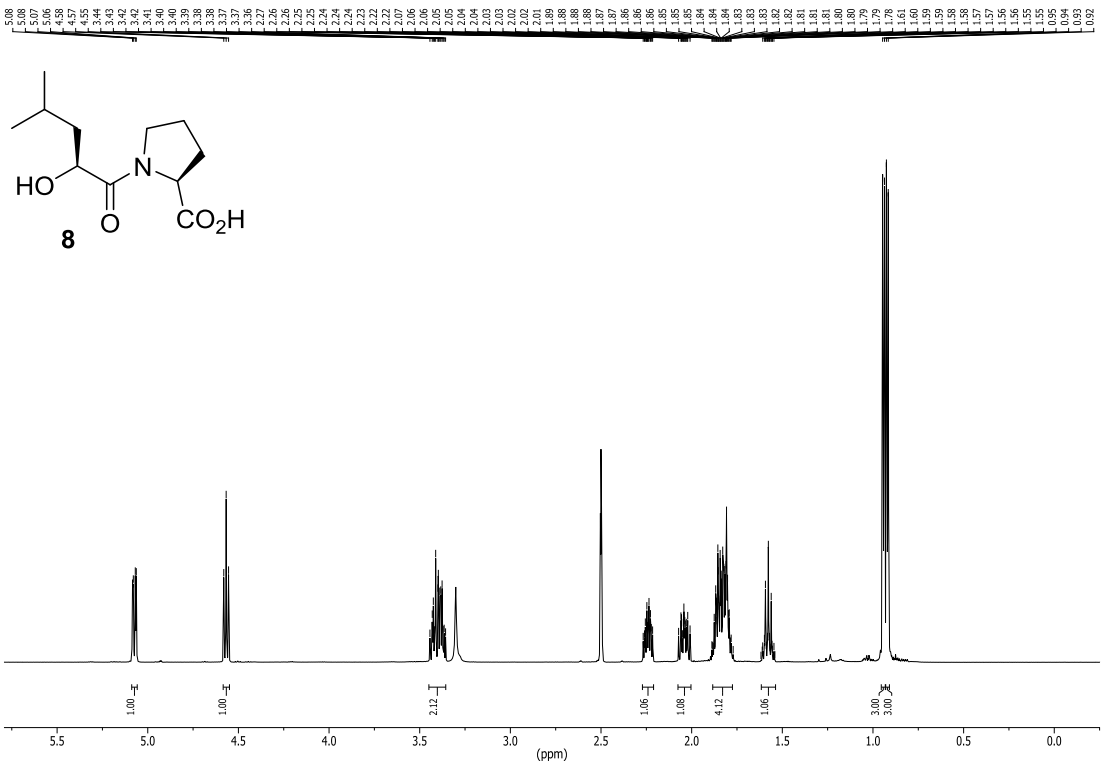

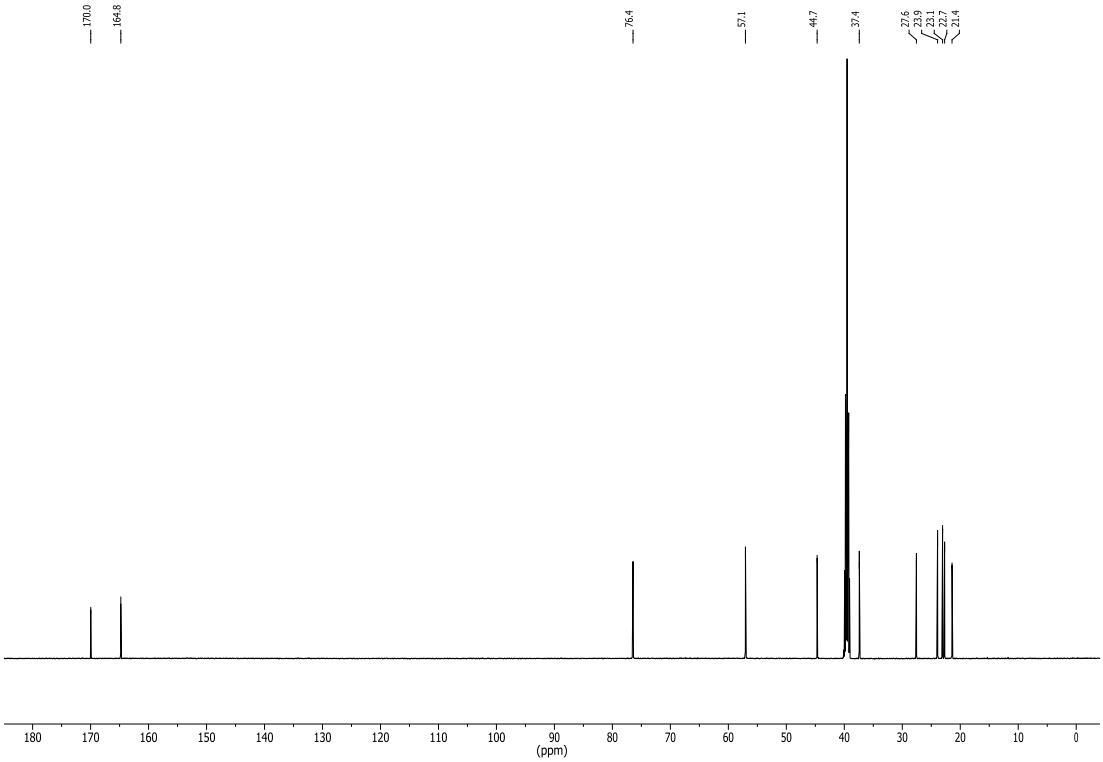

*^{1}H and ^{13}C NMR spectra of compound **12***

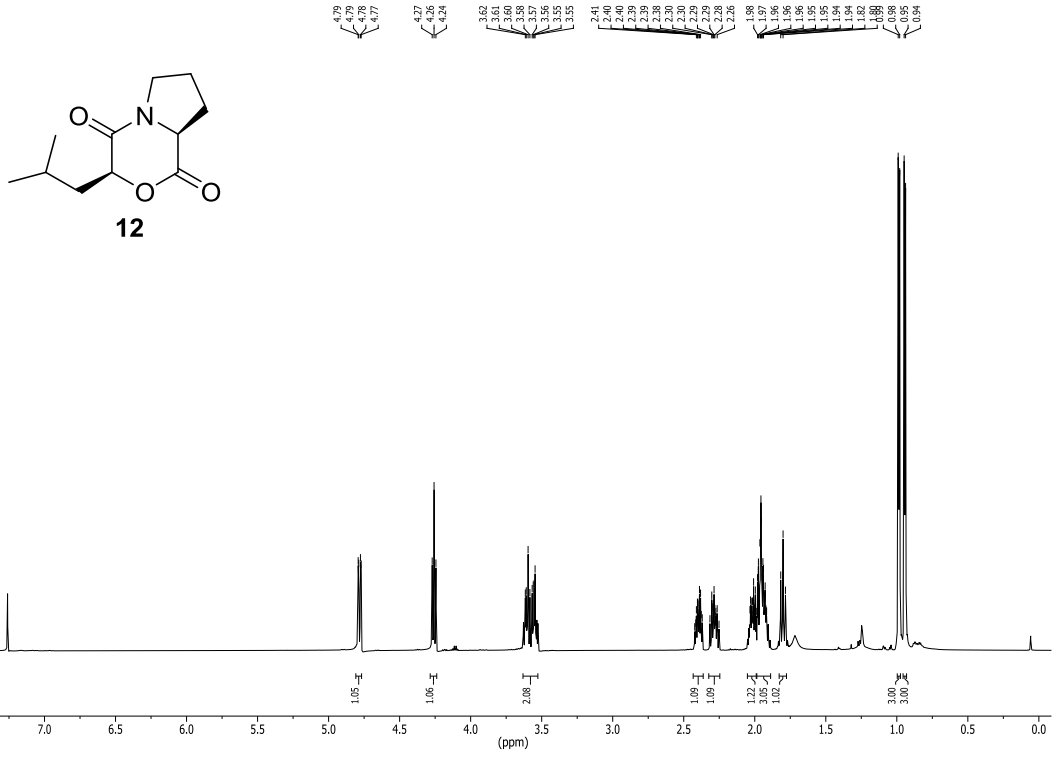

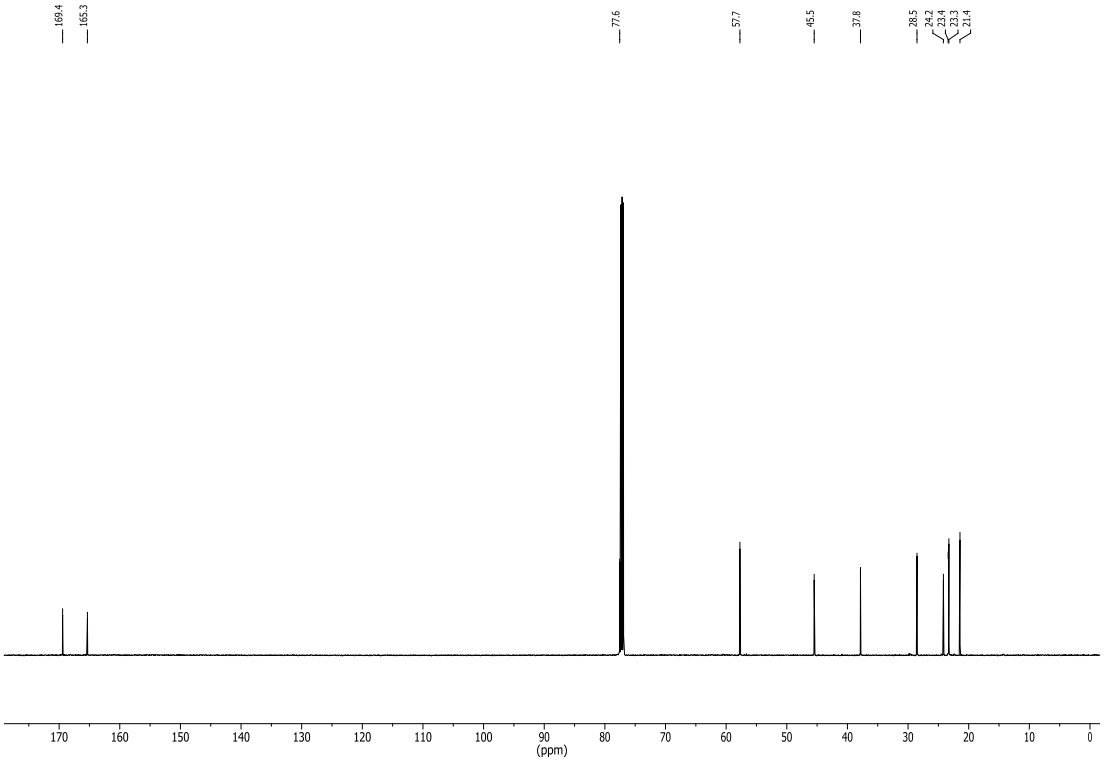

*^{1}H and ^{13}C NMR spectra of compound **13***

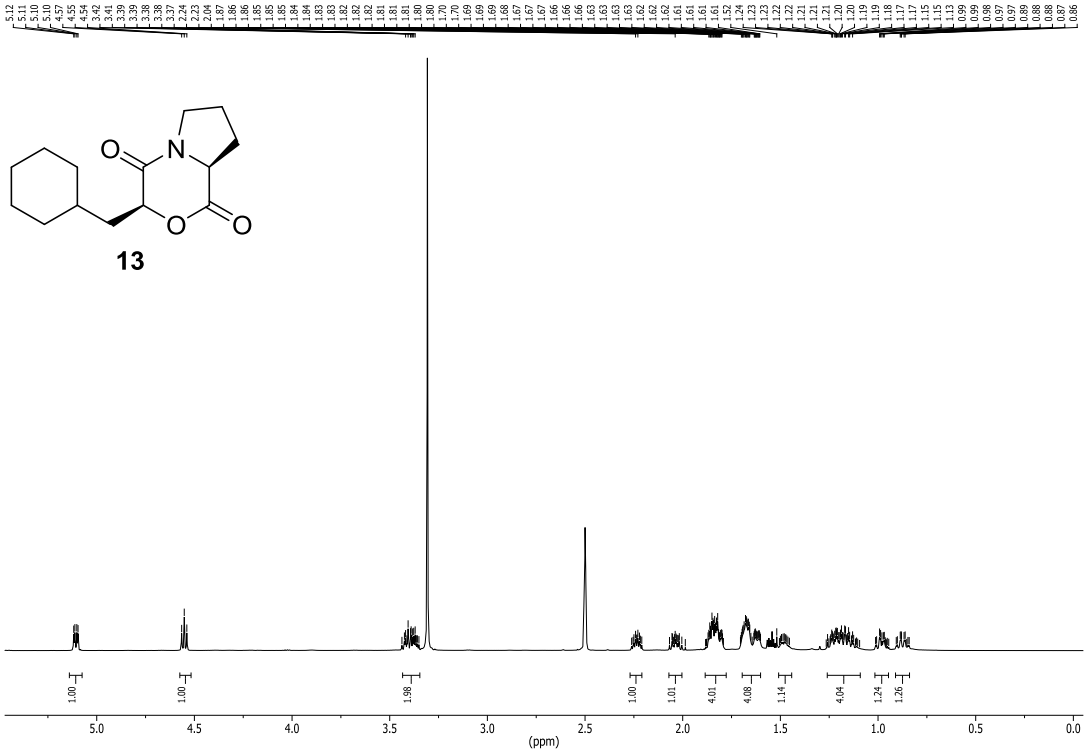

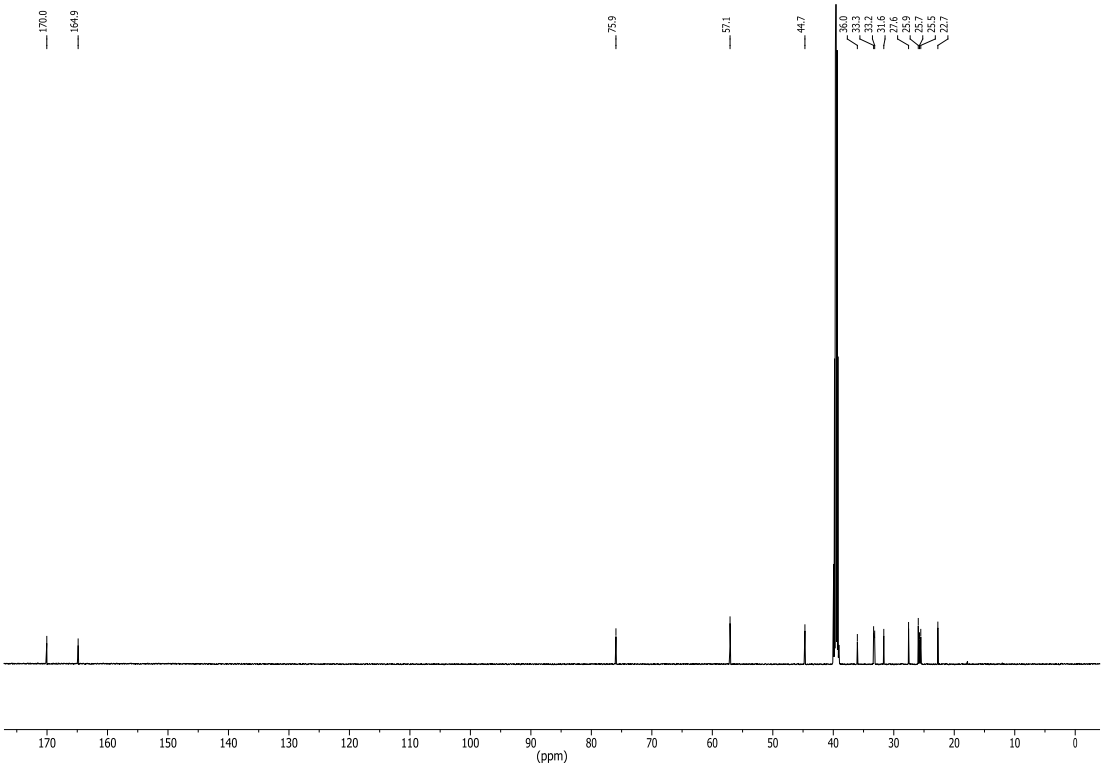

*[1]H and [13]C NMR spectra of compound **14***

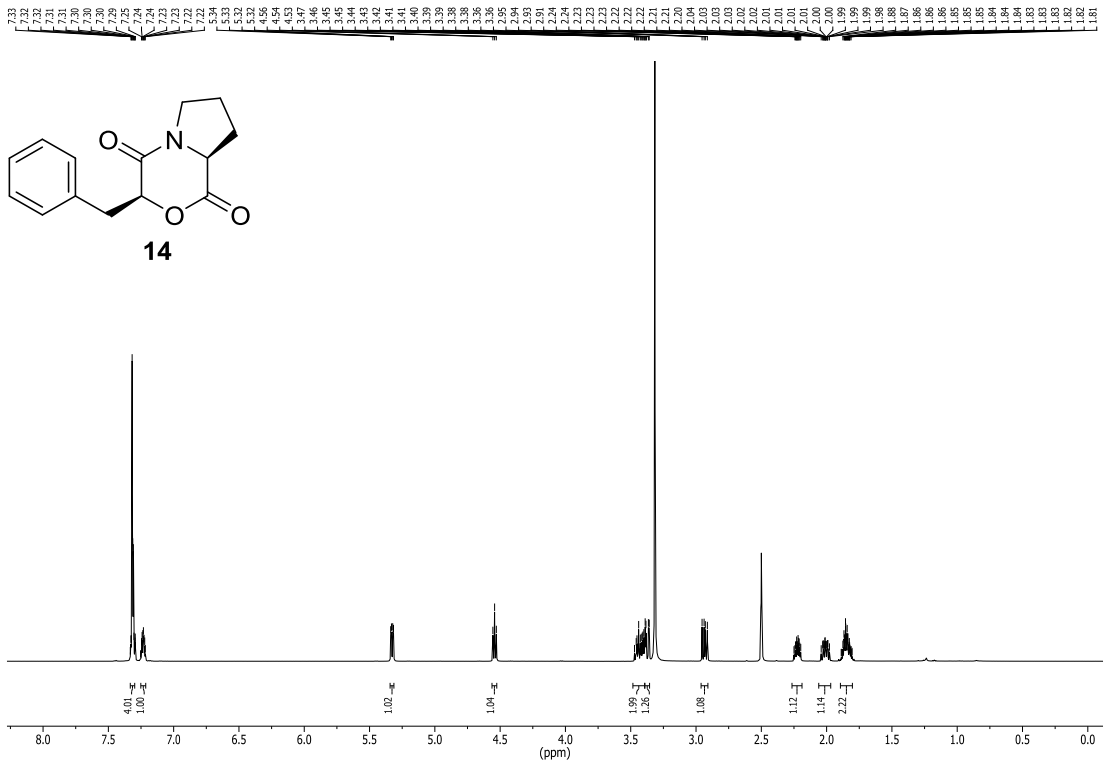

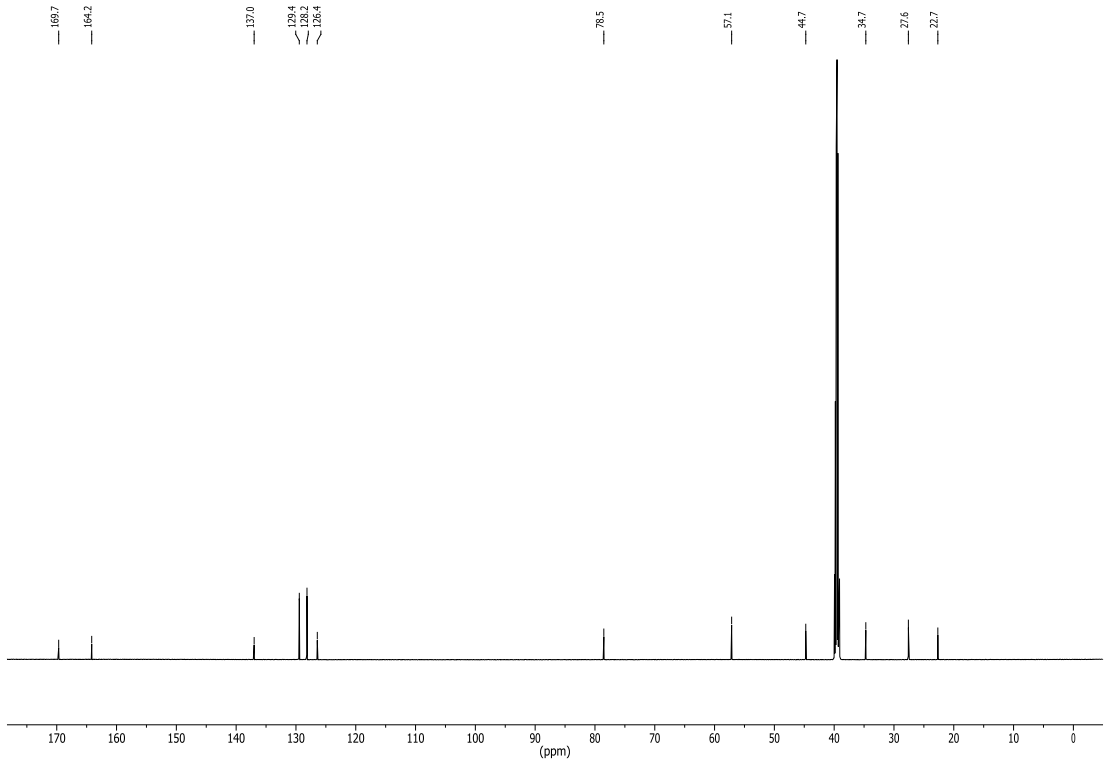

*^{1}H and ^{13}C NMR spectra of compound **15***

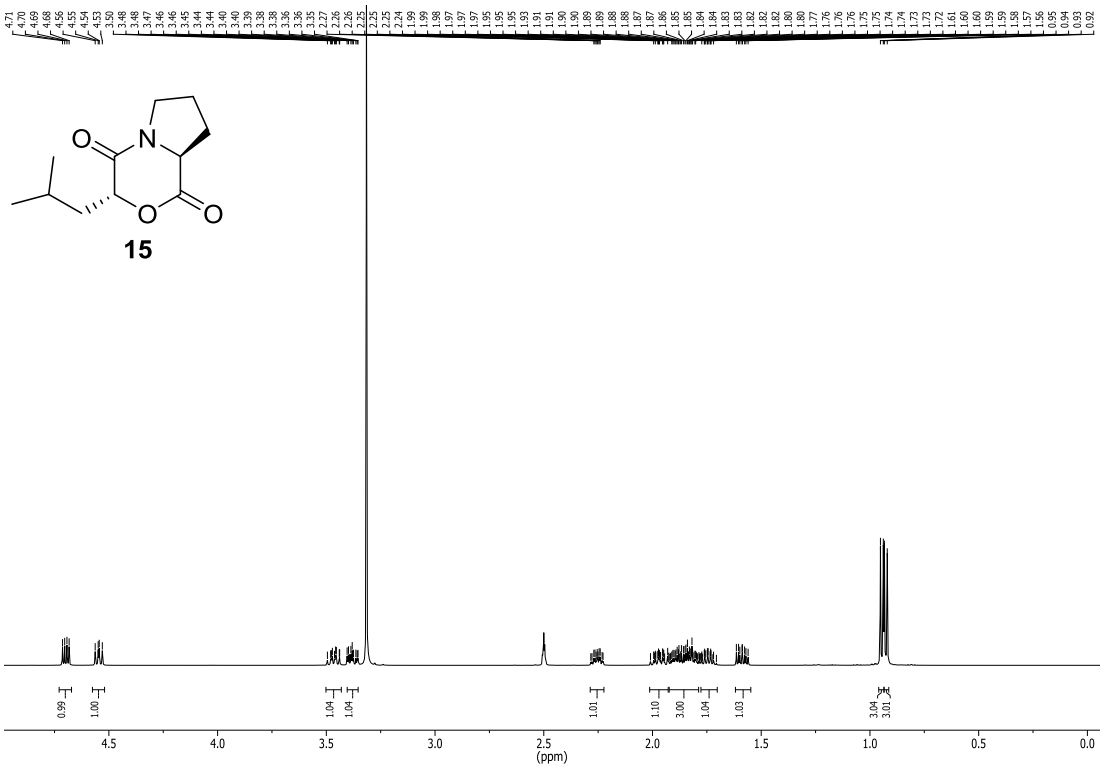

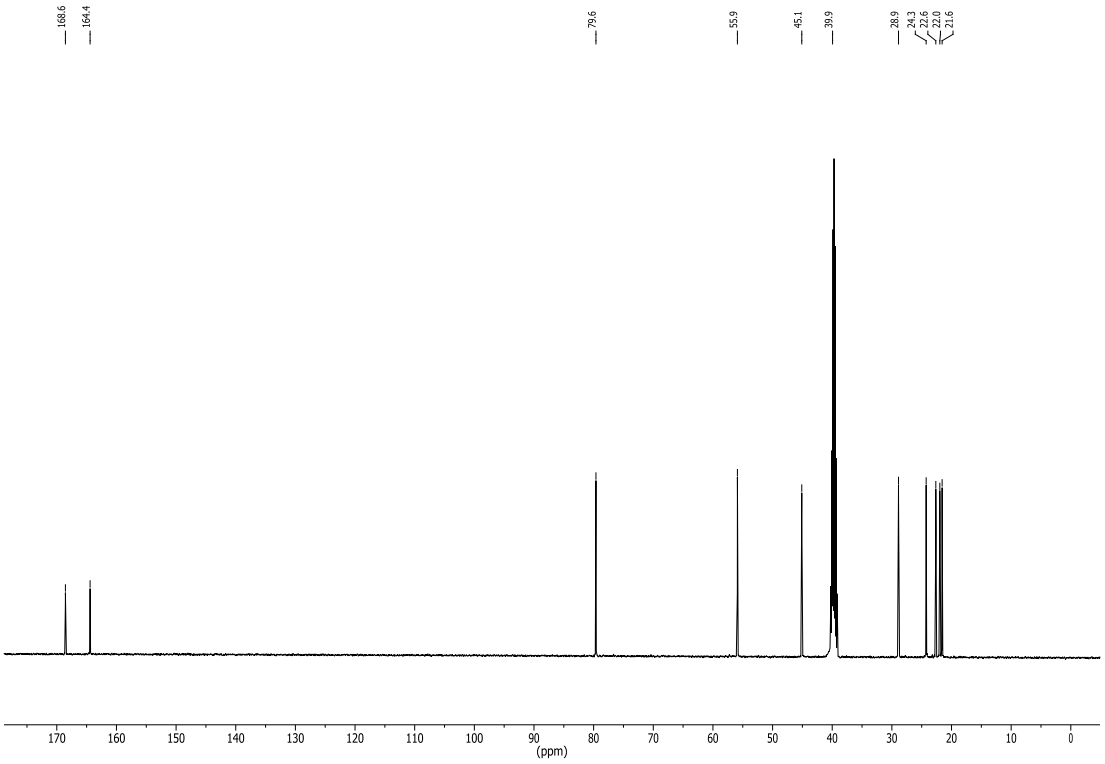

*^{1}H and ^{13}C NMR spectra of compound **16***

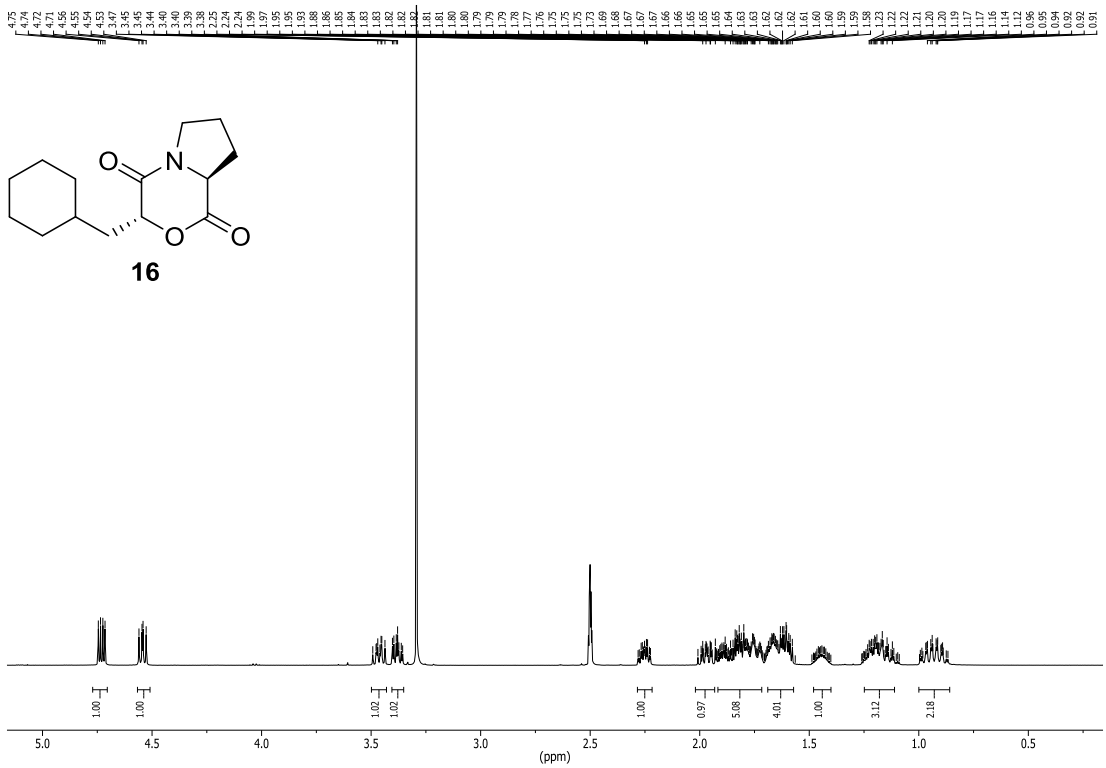

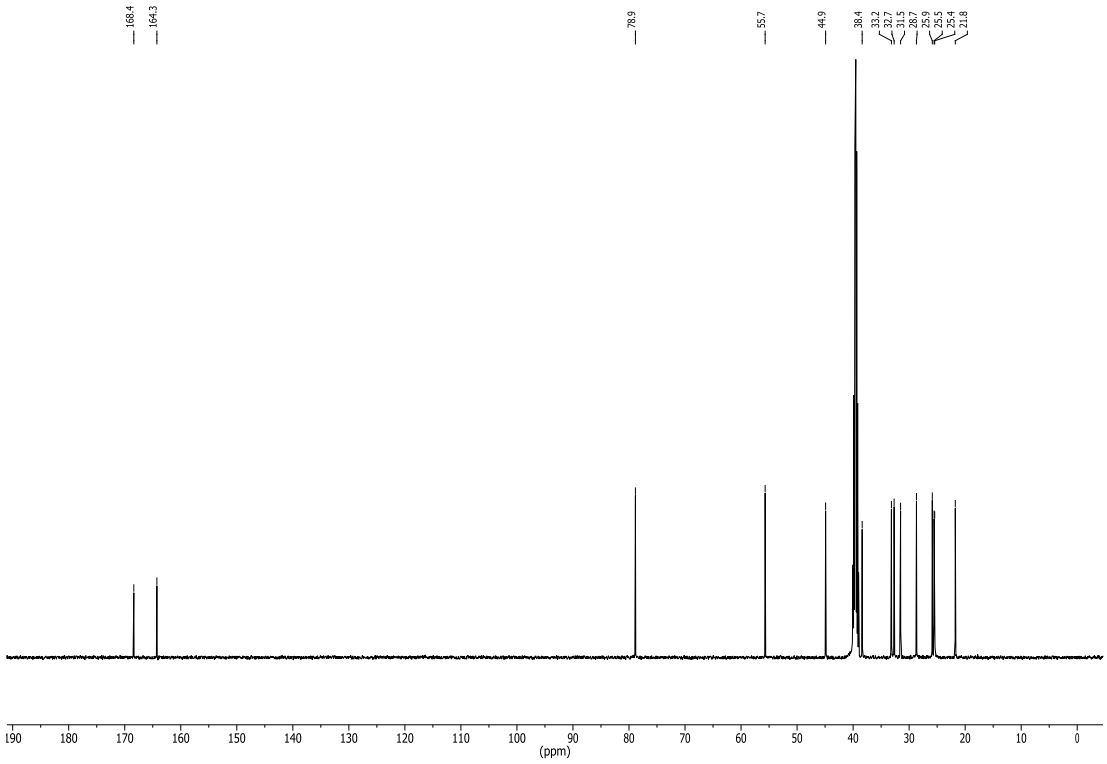

*^{1}H and ^{13}C NMR spectra of compound **17***

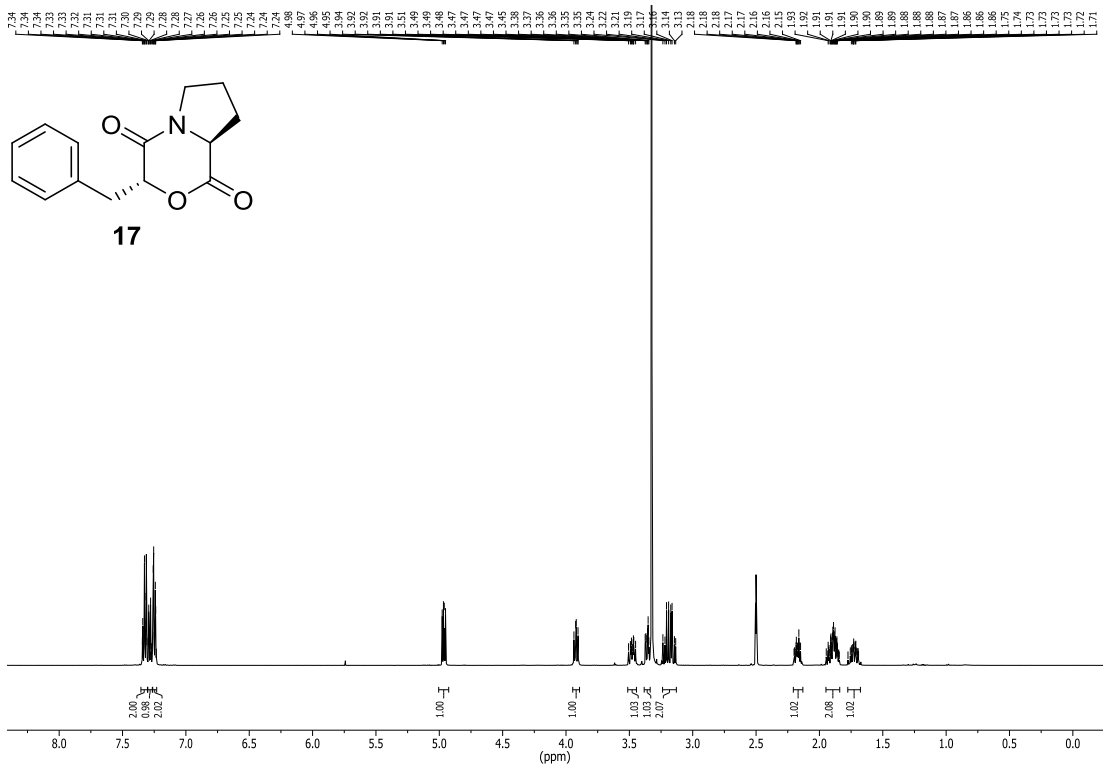

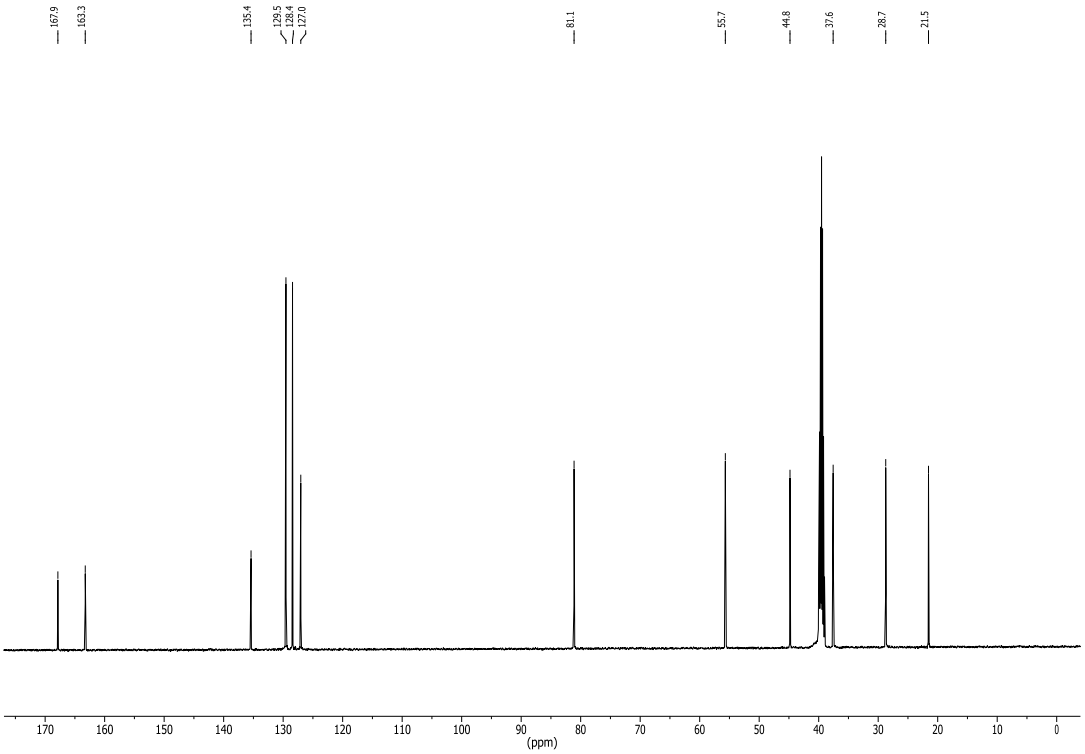

*^{1}H and ^{13}C NMR spectra of compound **18***

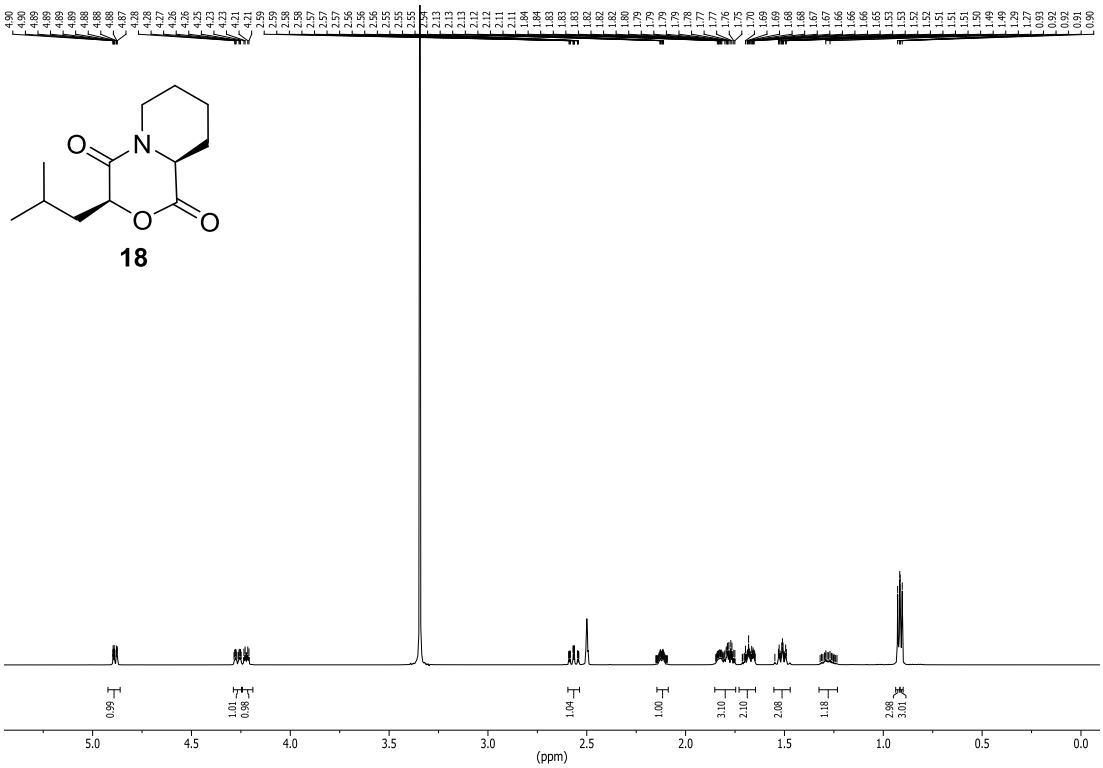

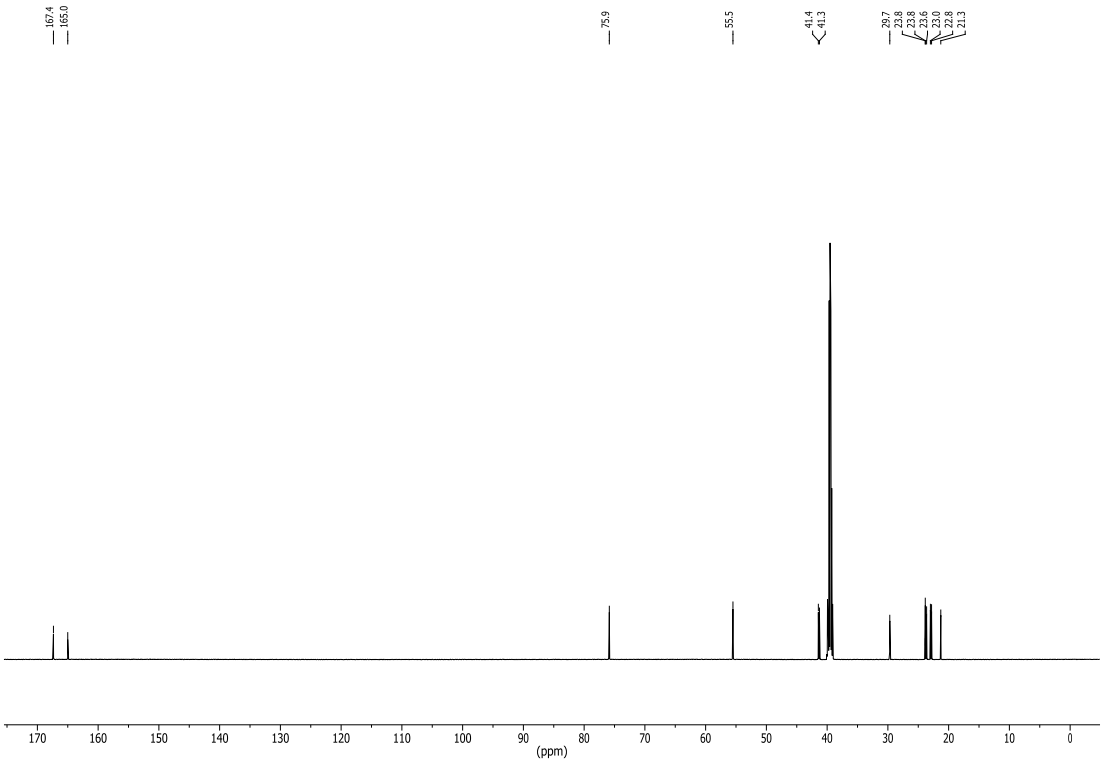

*^{1}H and ^{13}C NMR spectra of compound **19***

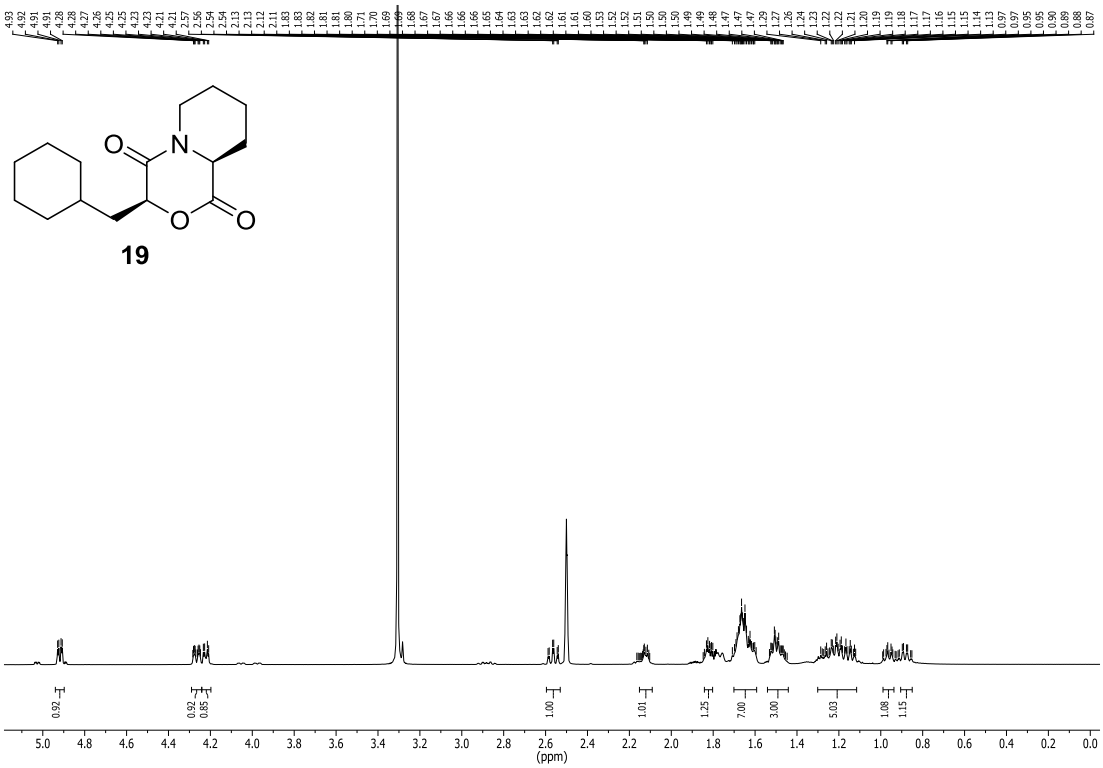

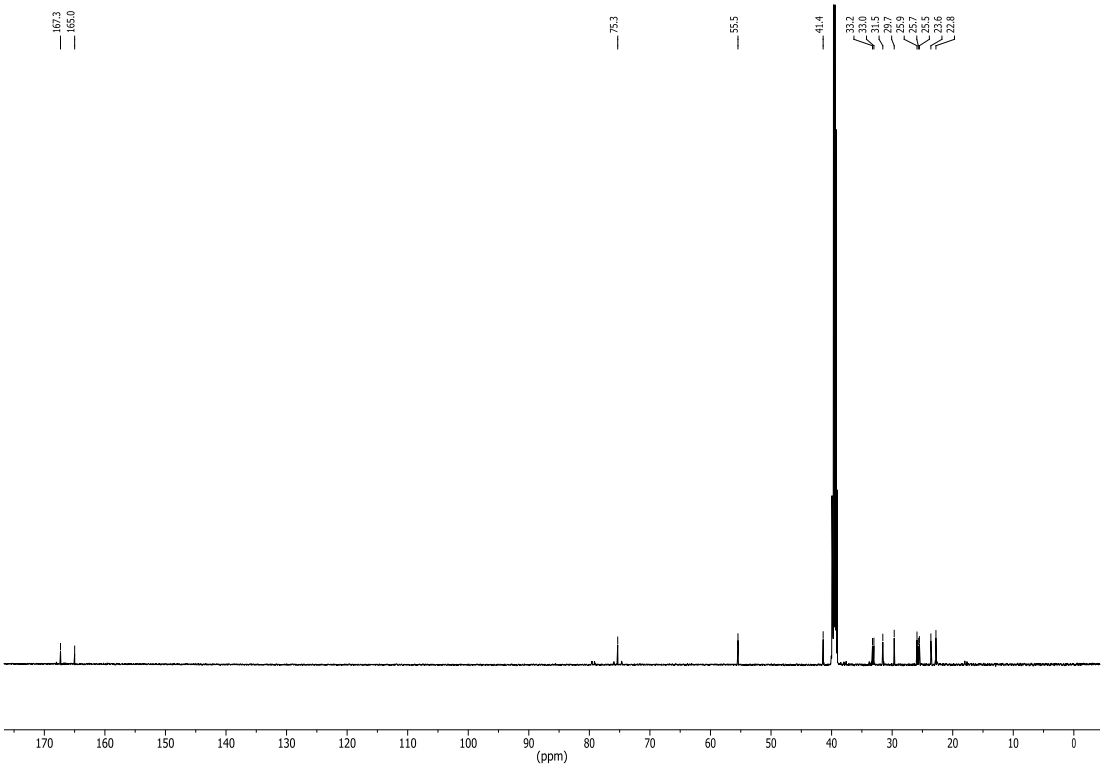

*^{1}H and ^{13}C NMR spectra of compound **20***

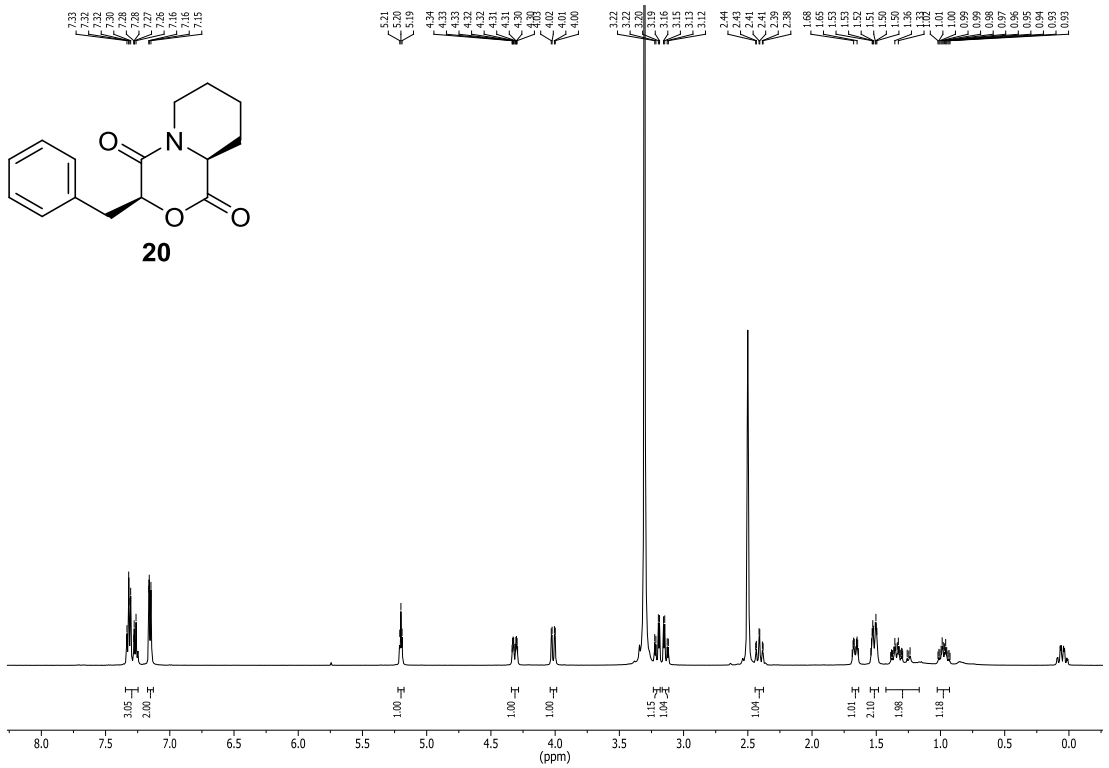

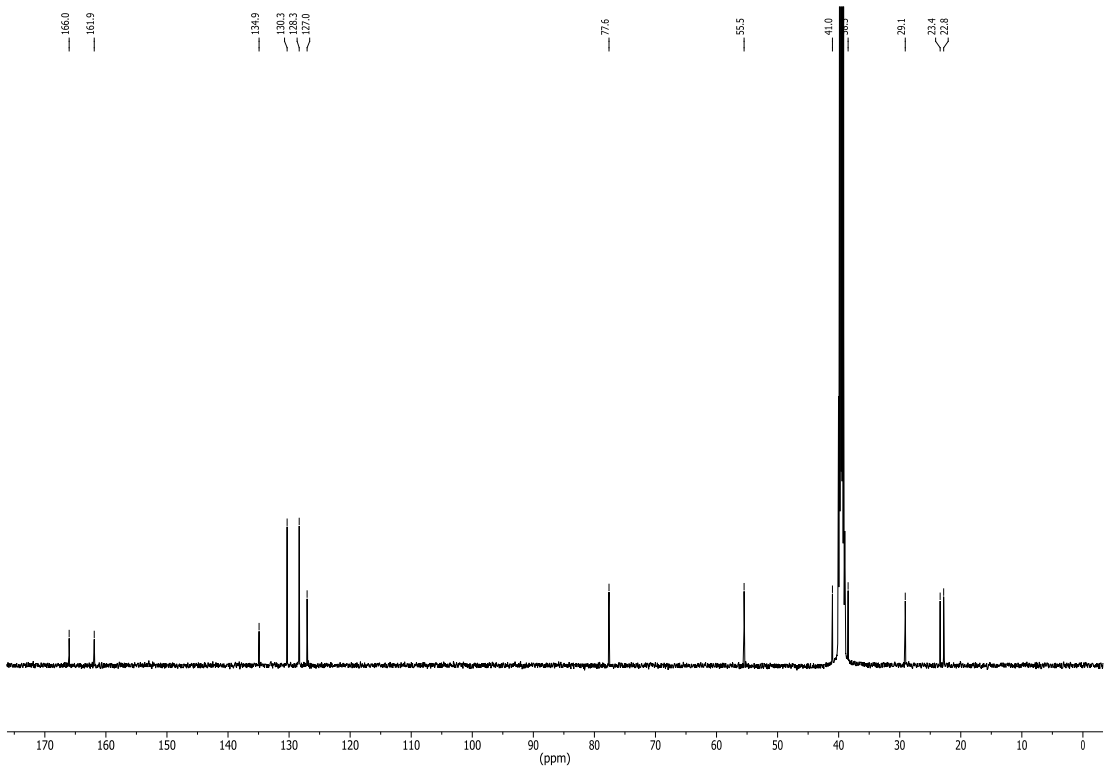

*^{1}H and ^{13}C NMR spectra of compound **21***

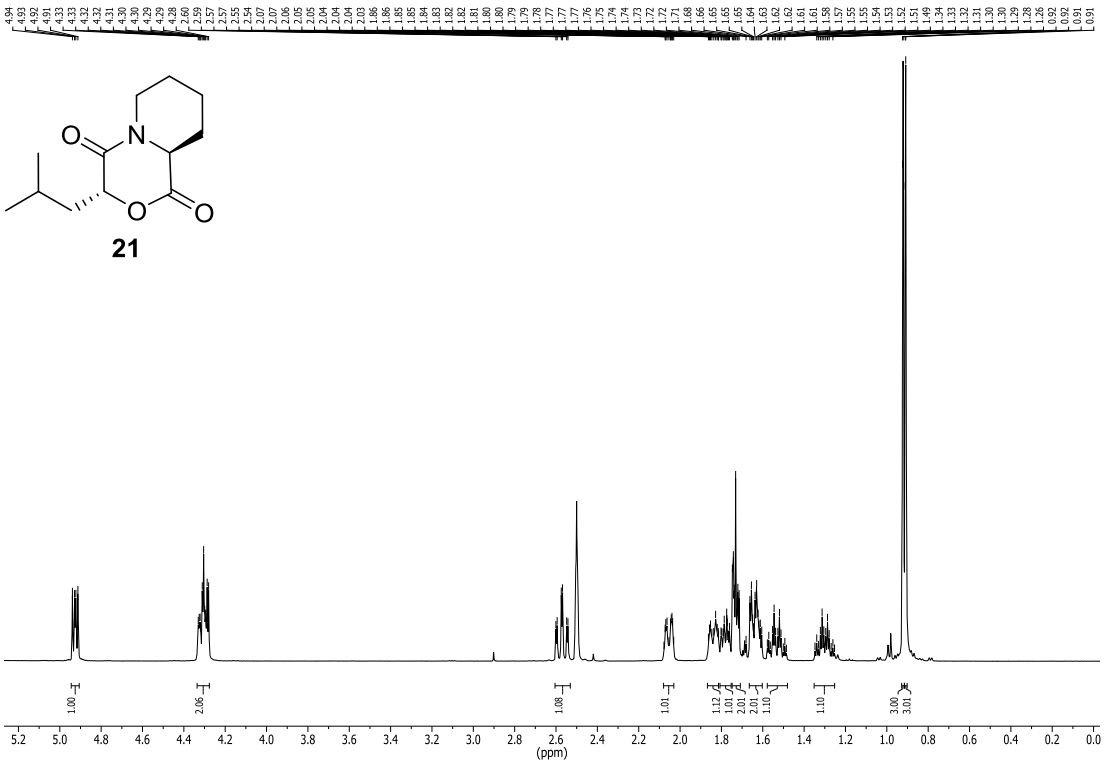

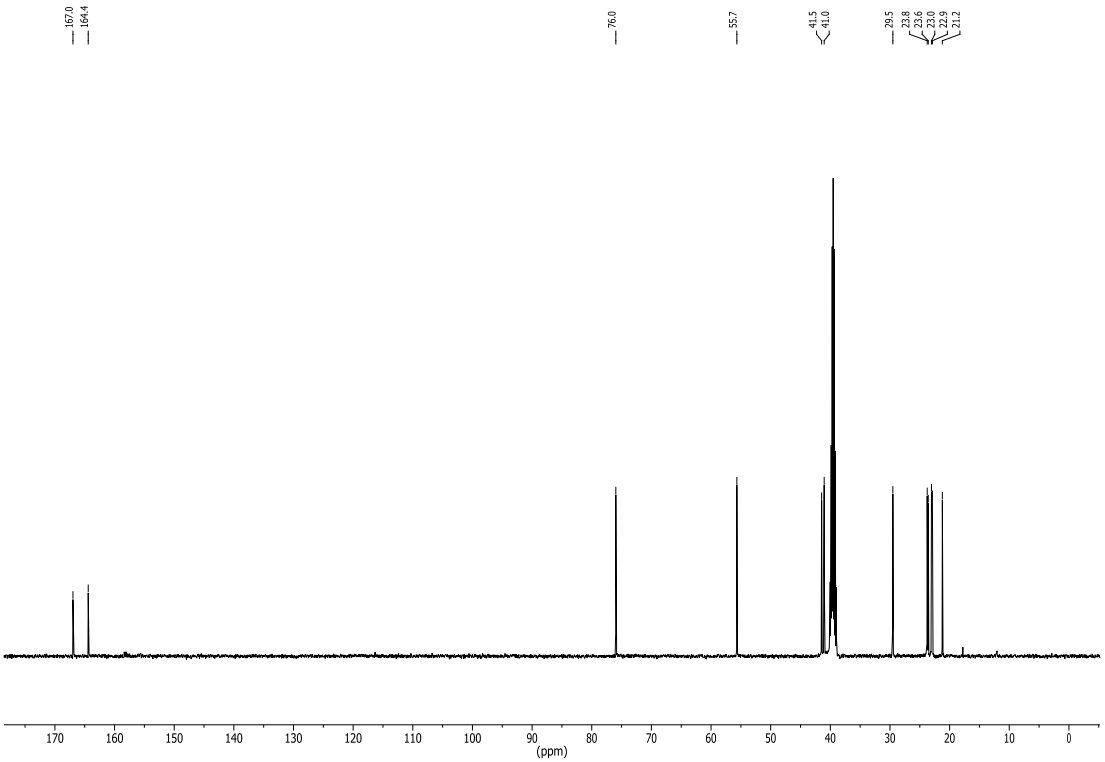

*^{1}H and ^{13}C NMR spectra of compound **22***

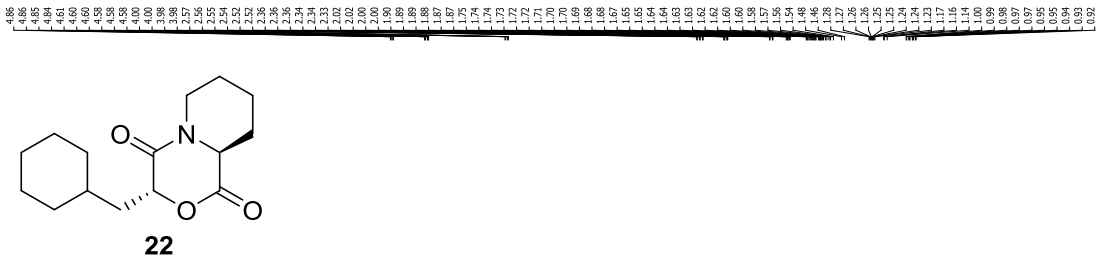

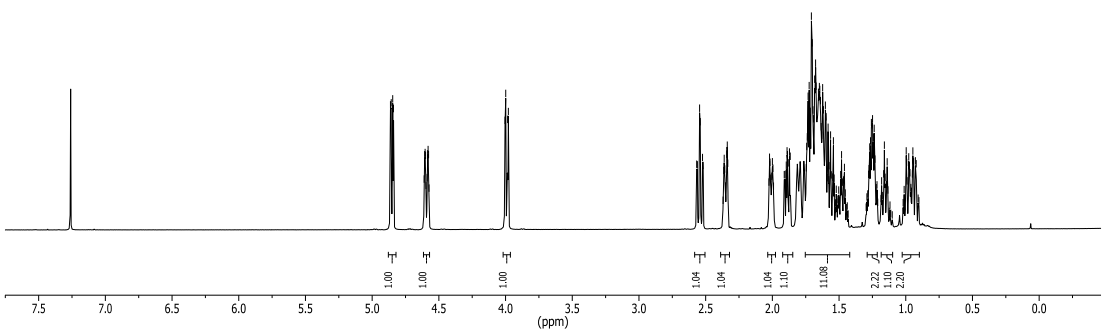

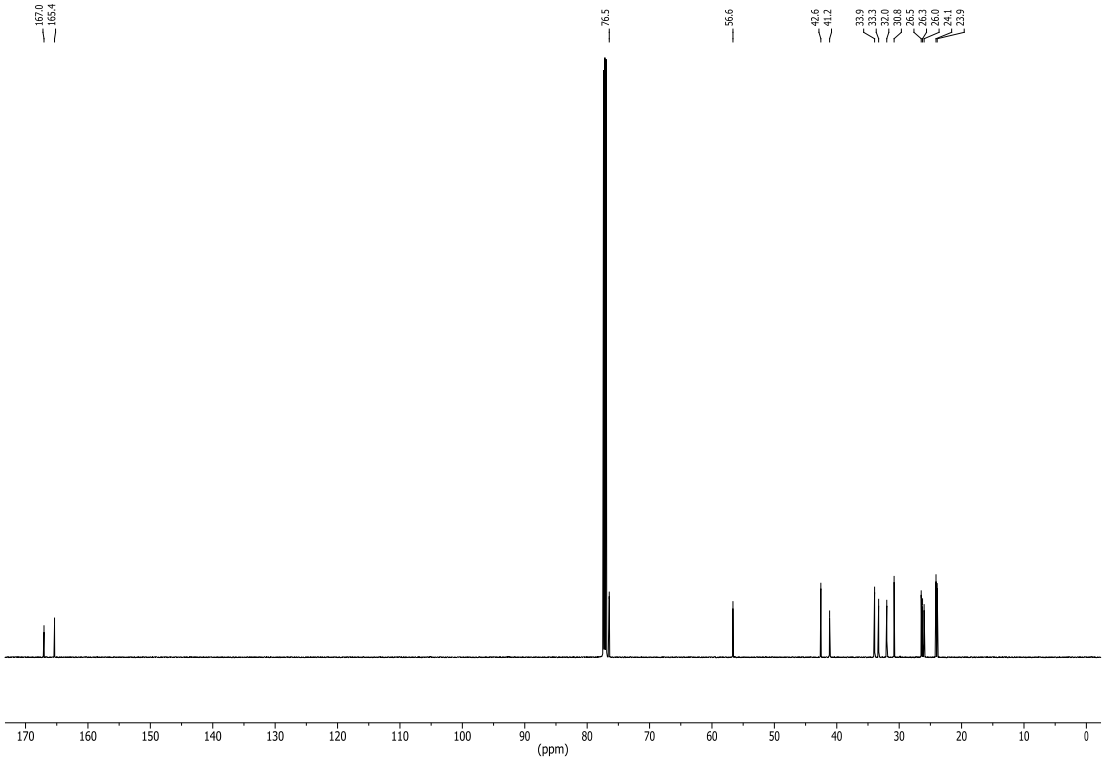

*^{1}H and ^{13}C NMR spectra of compound **23***

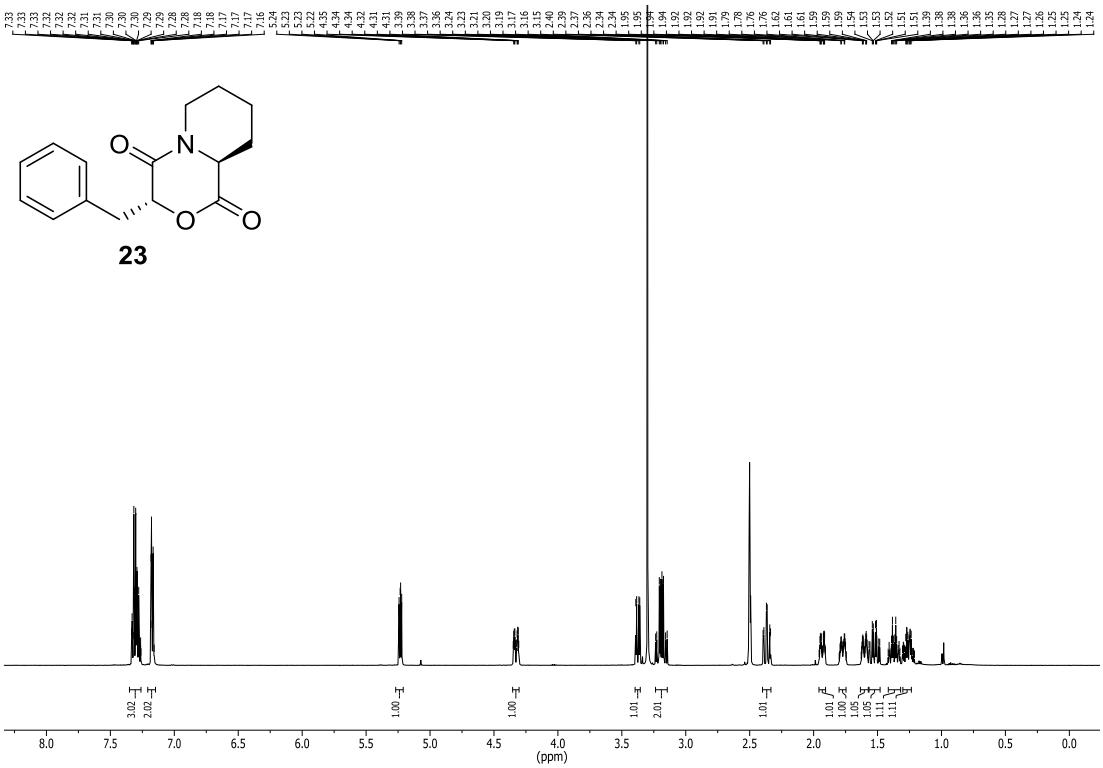

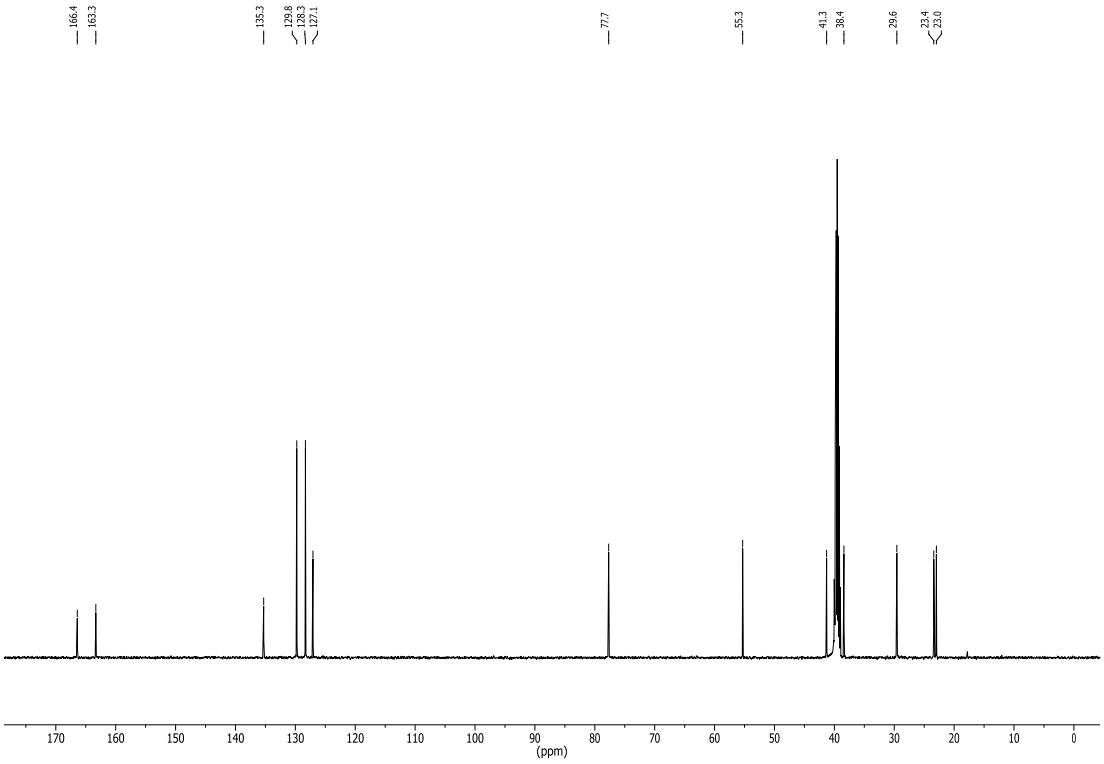

*[1]H and [13]C NMR spectra of compound **24***

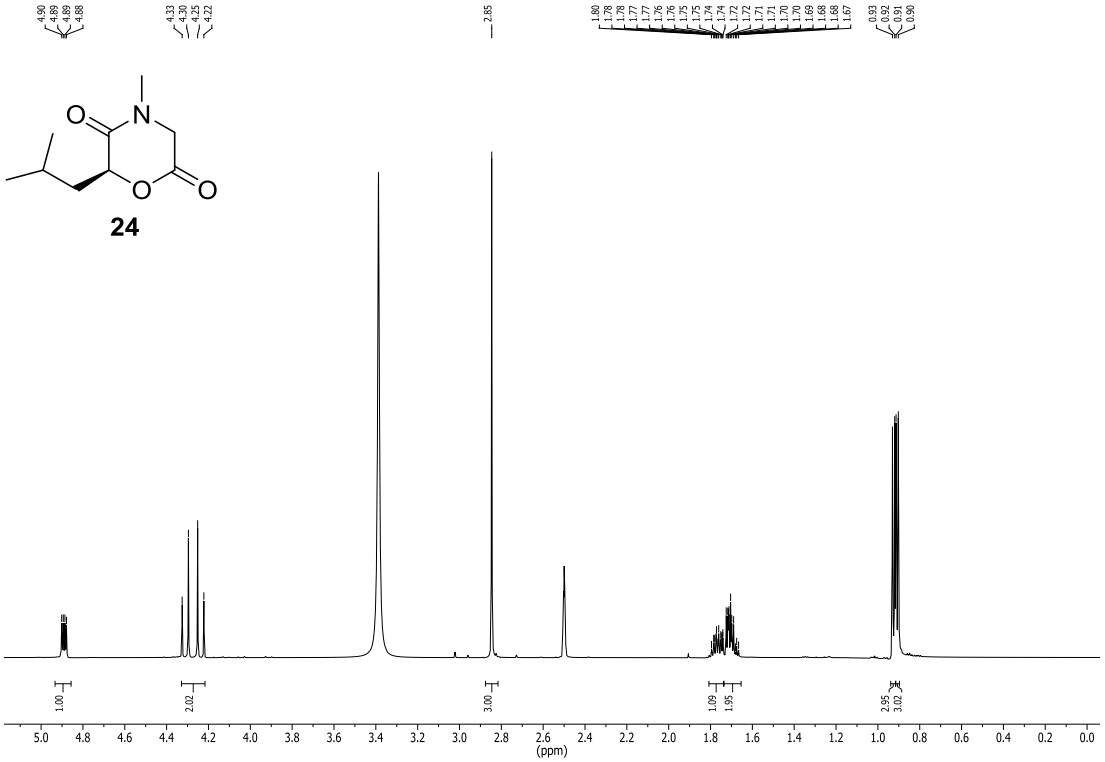

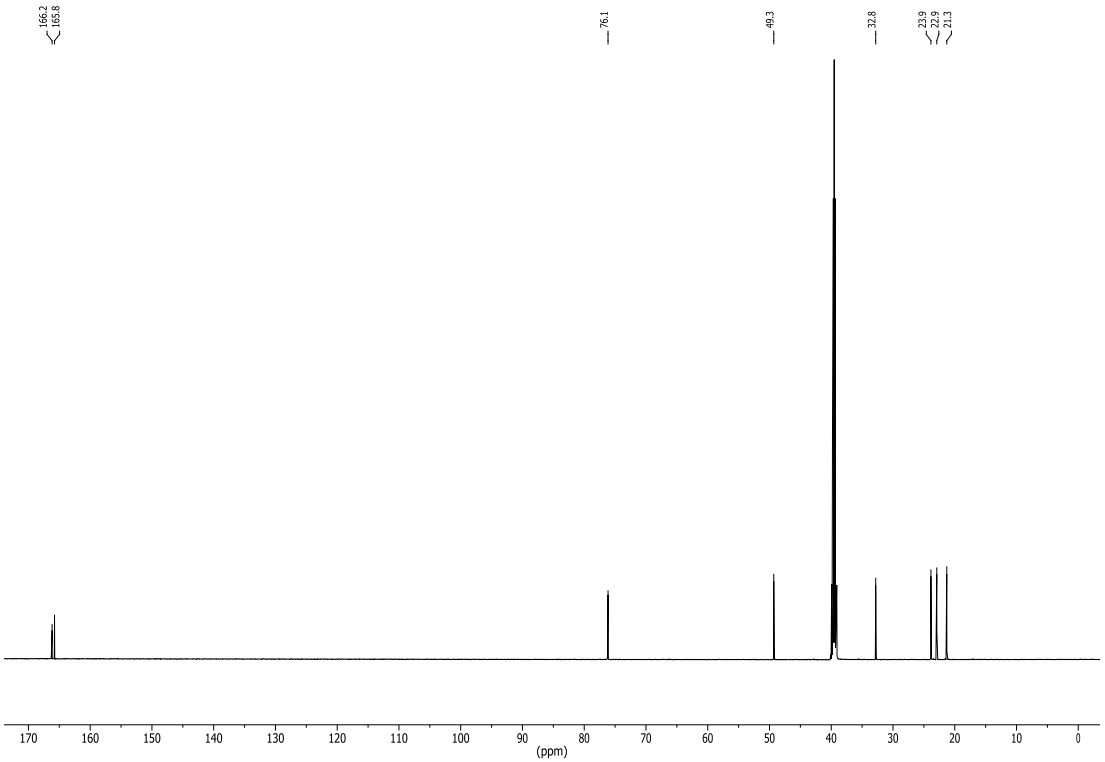

^{1}H and ^{13}C NMR spectra of compound ***25***

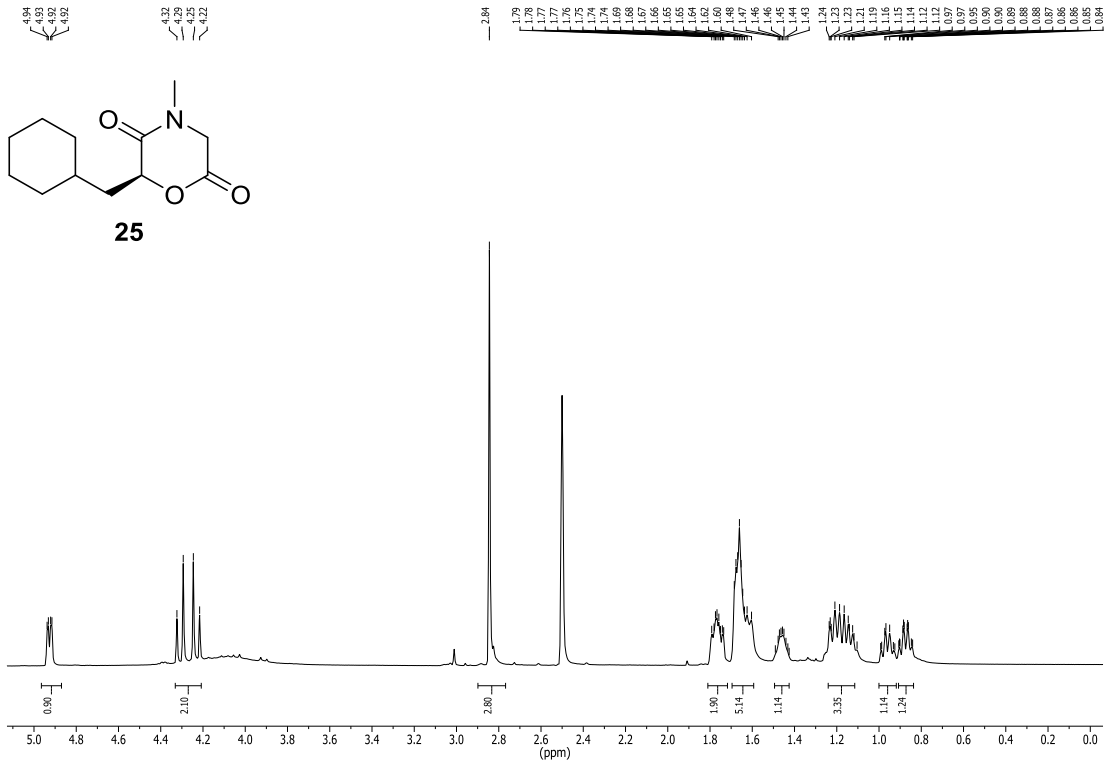

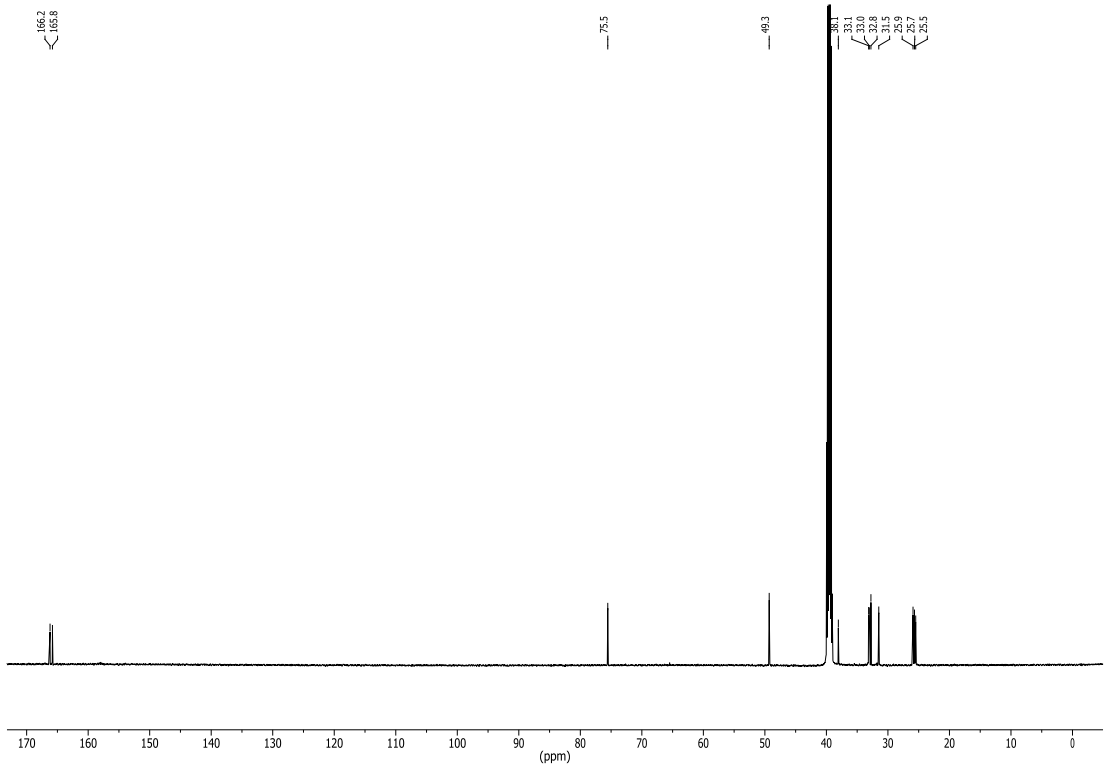

^{1}H and ^{13}C NMR spectra of compound ***26***

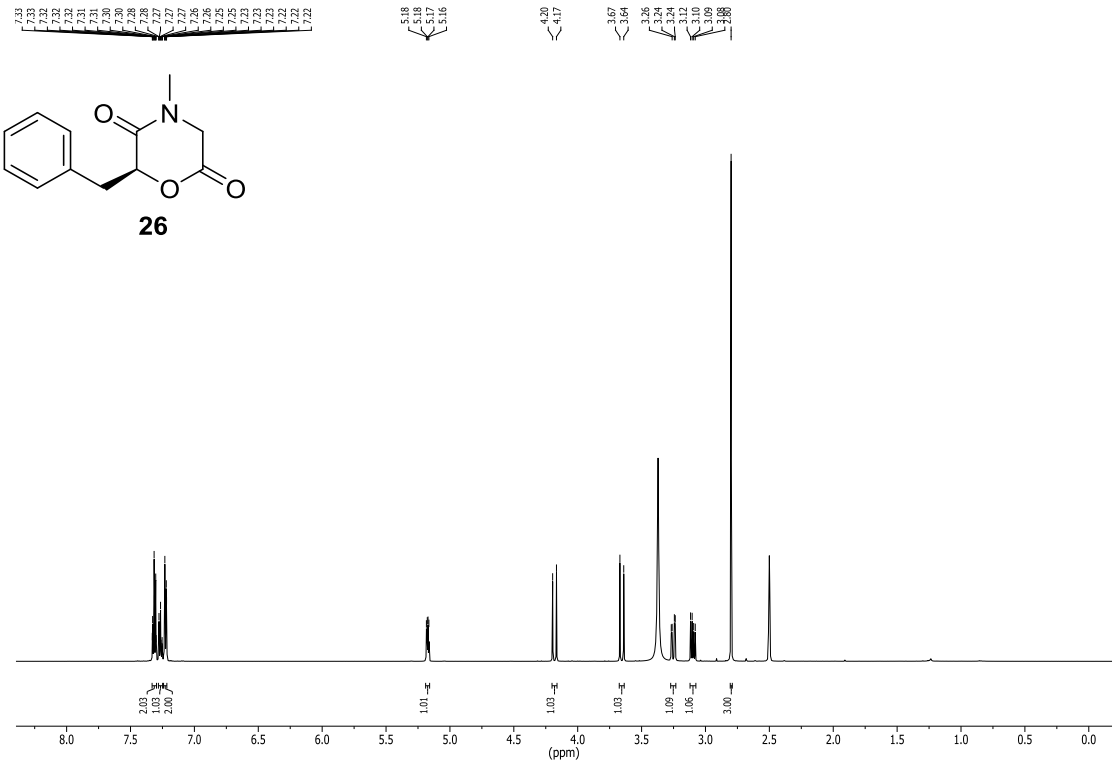

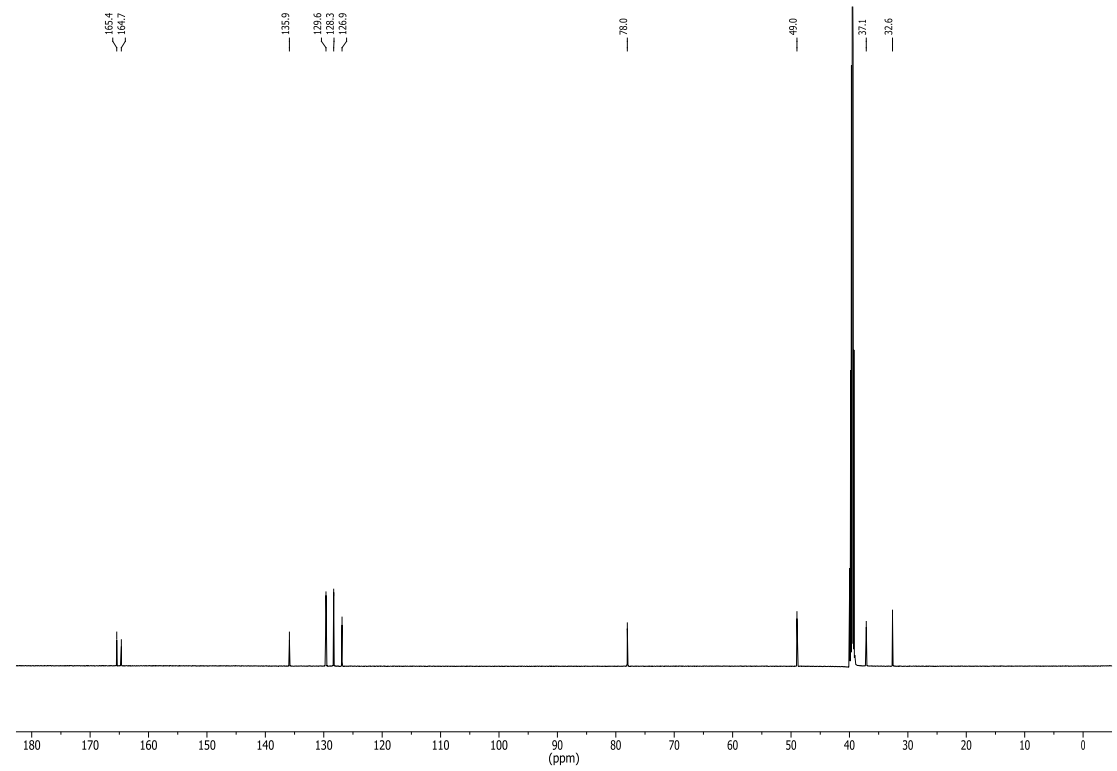

*^{1}H and ^{13}C NMR spectra of compound **27***

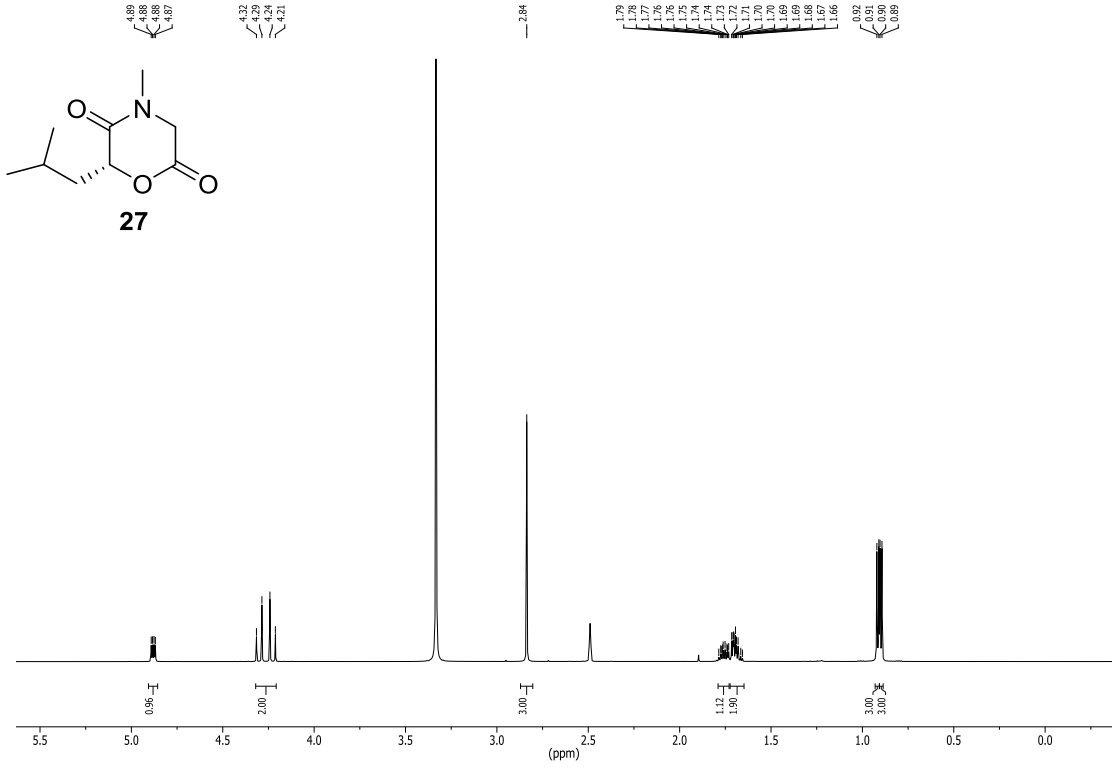

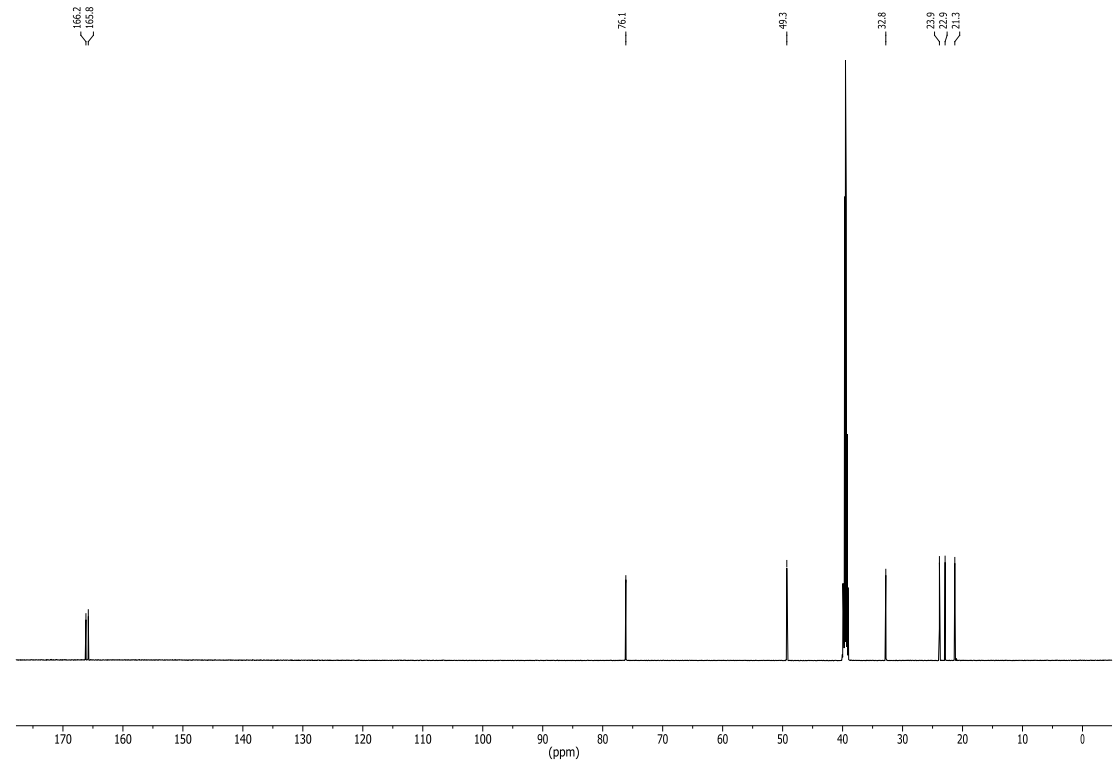

*^{1}H and ^{13}C NMR spectra of compound **28***

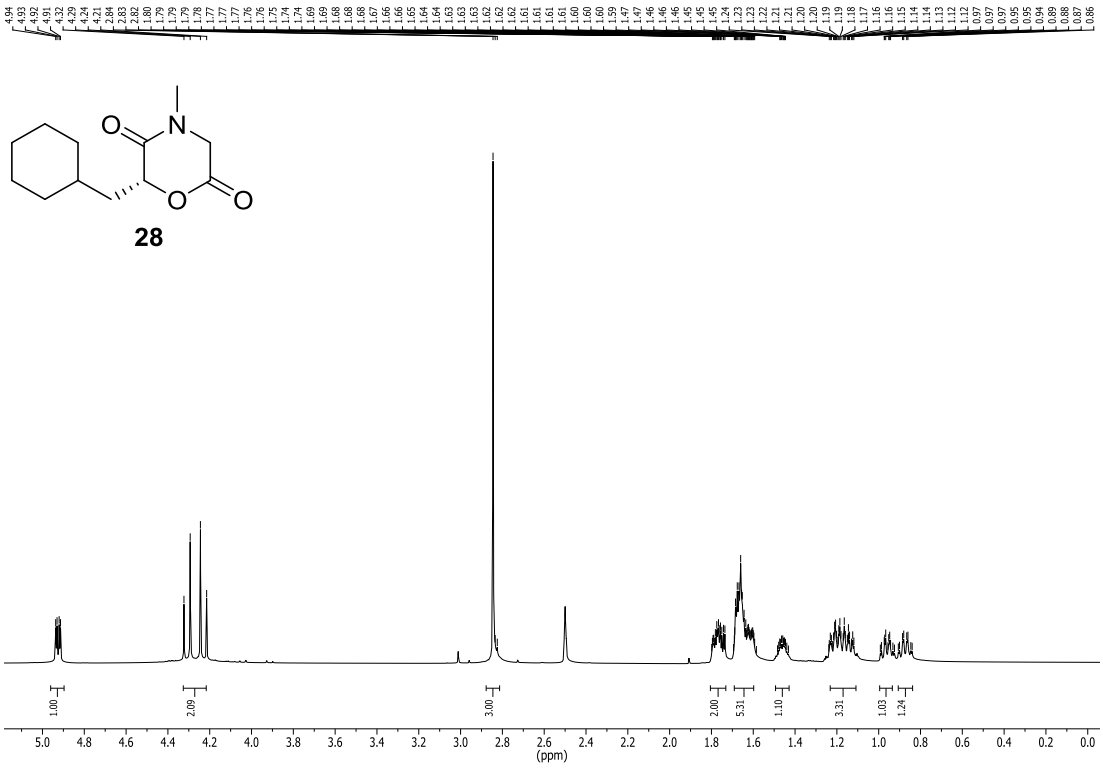

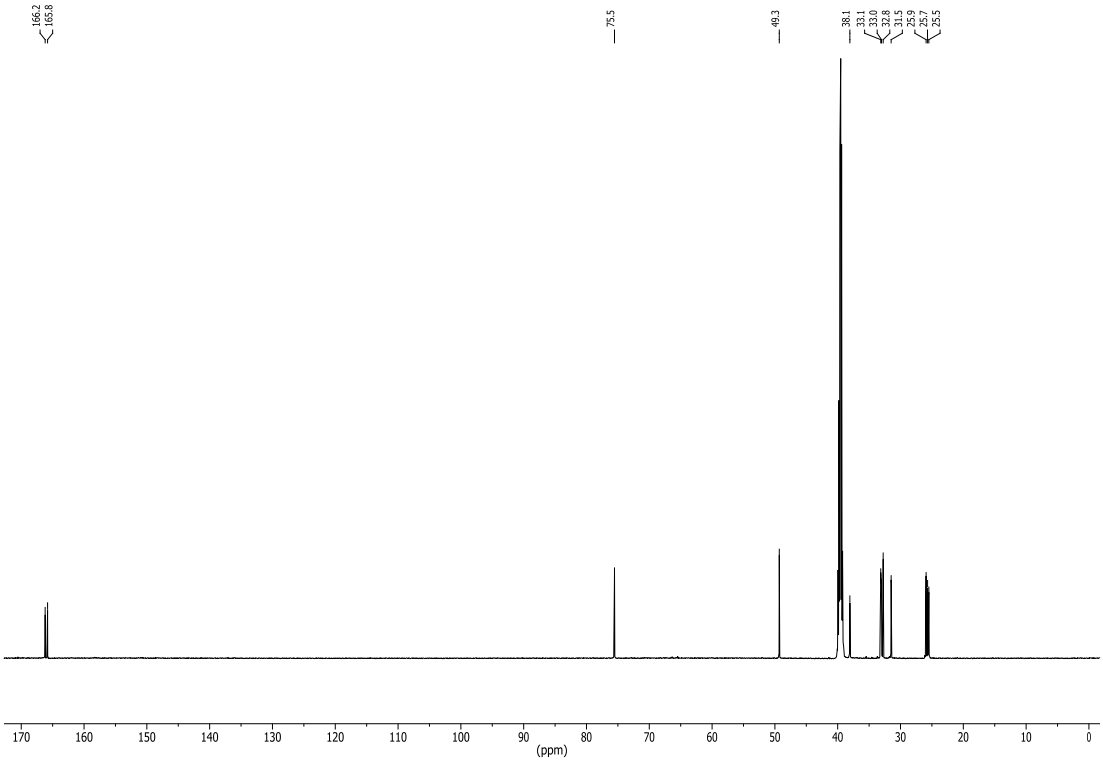

*^{1}H and ^{13}C NMR spectra of compound **29***

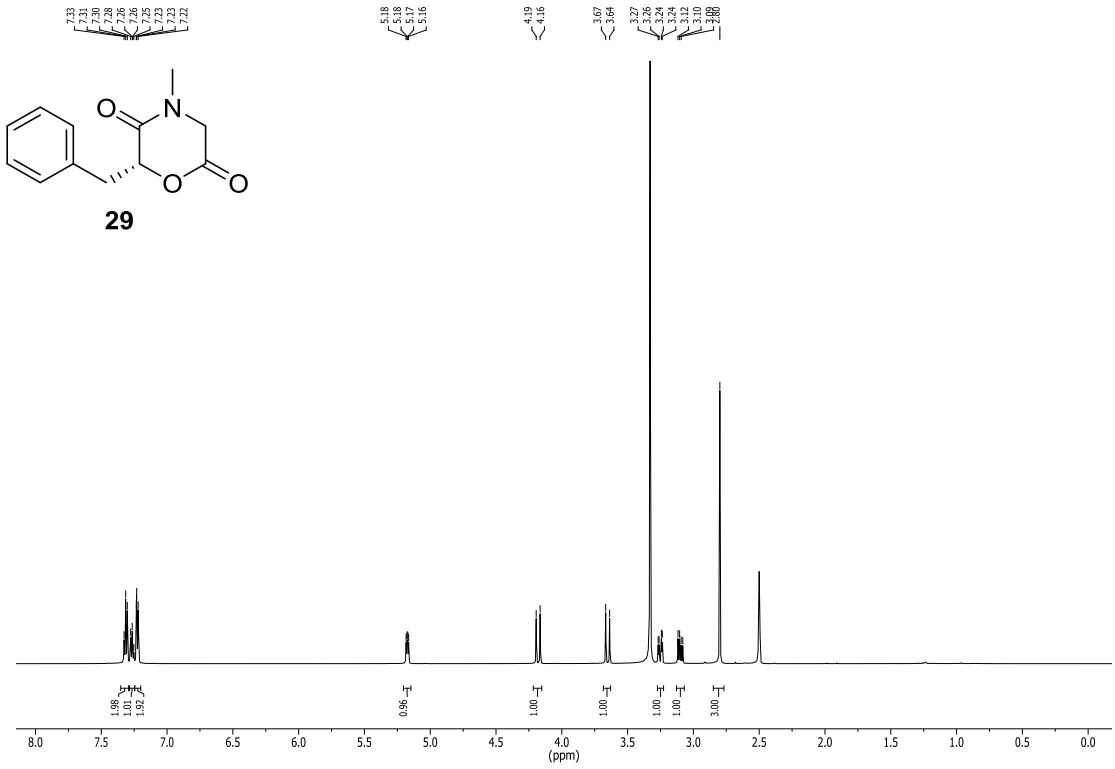

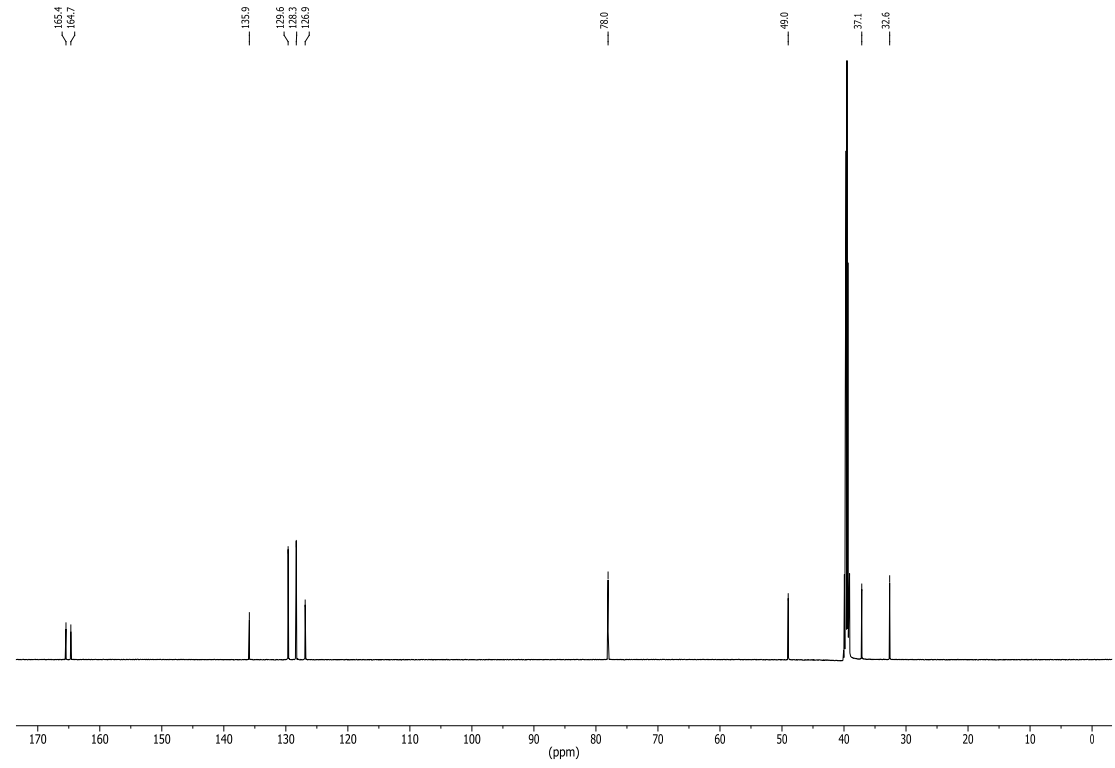

*^{1}H and ^{13}C NMR spectra of compound **30***

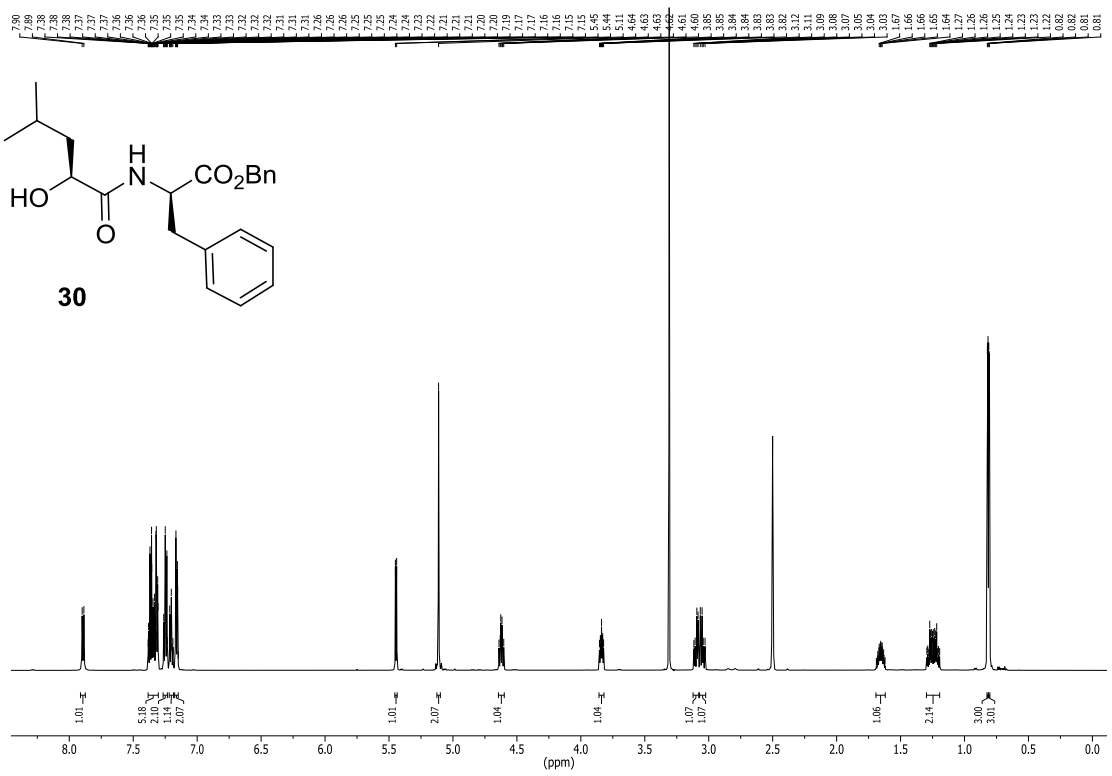

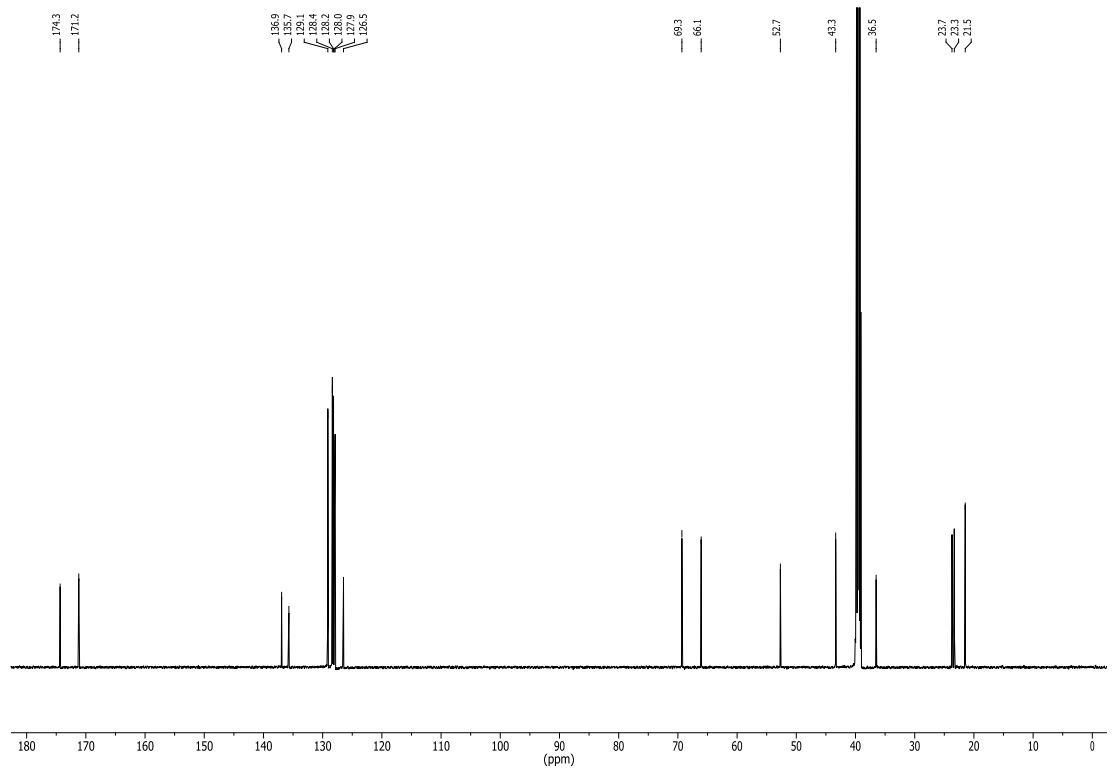

*^{1}H and ^{13}C NMR spectra of compound **31***

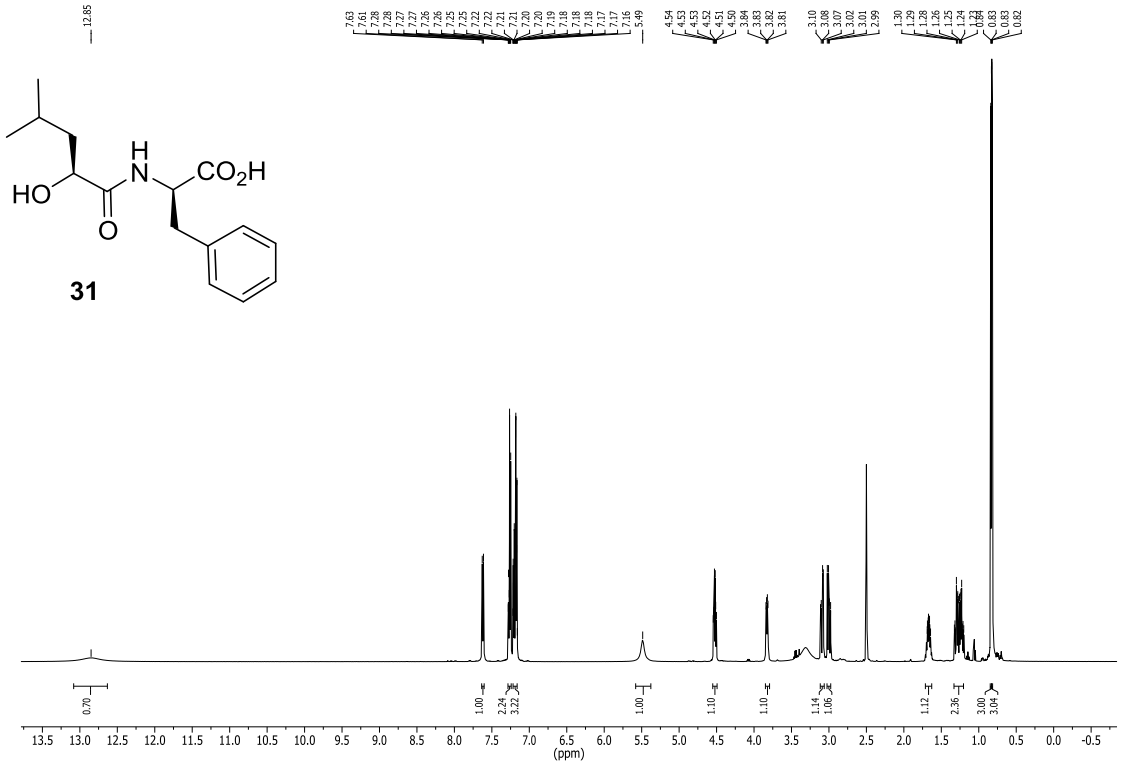

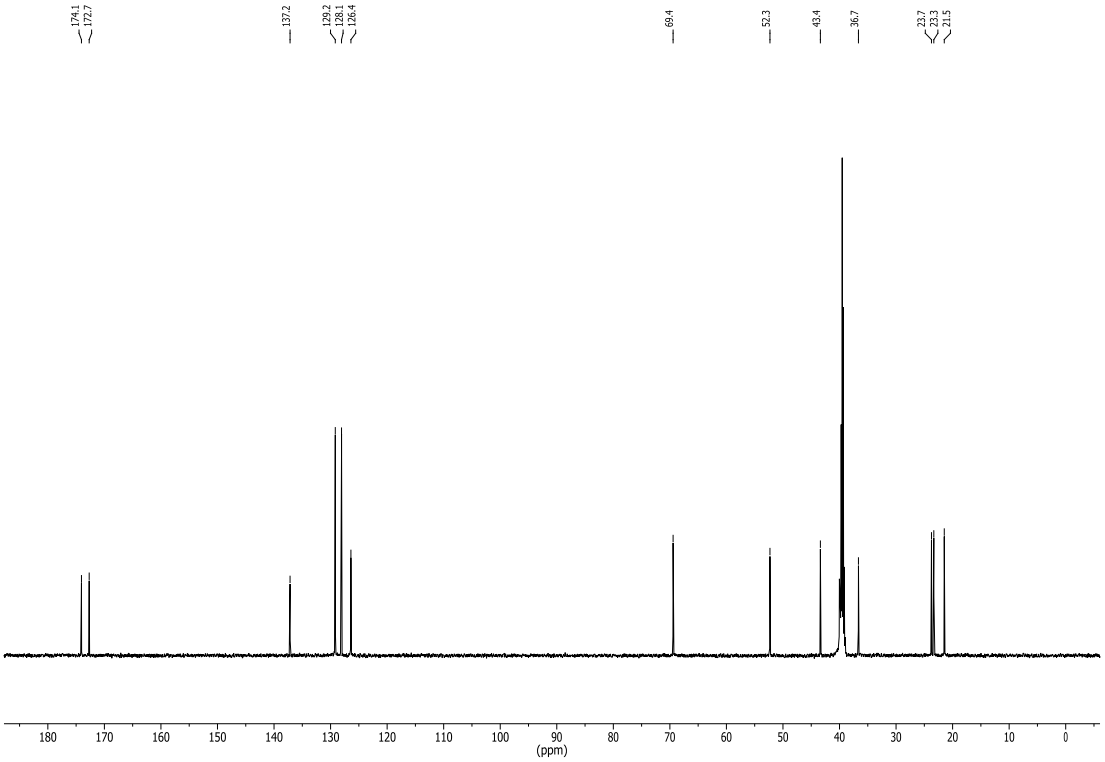

*^{1}H and ^{13}C NMR spectra of compound **12C***

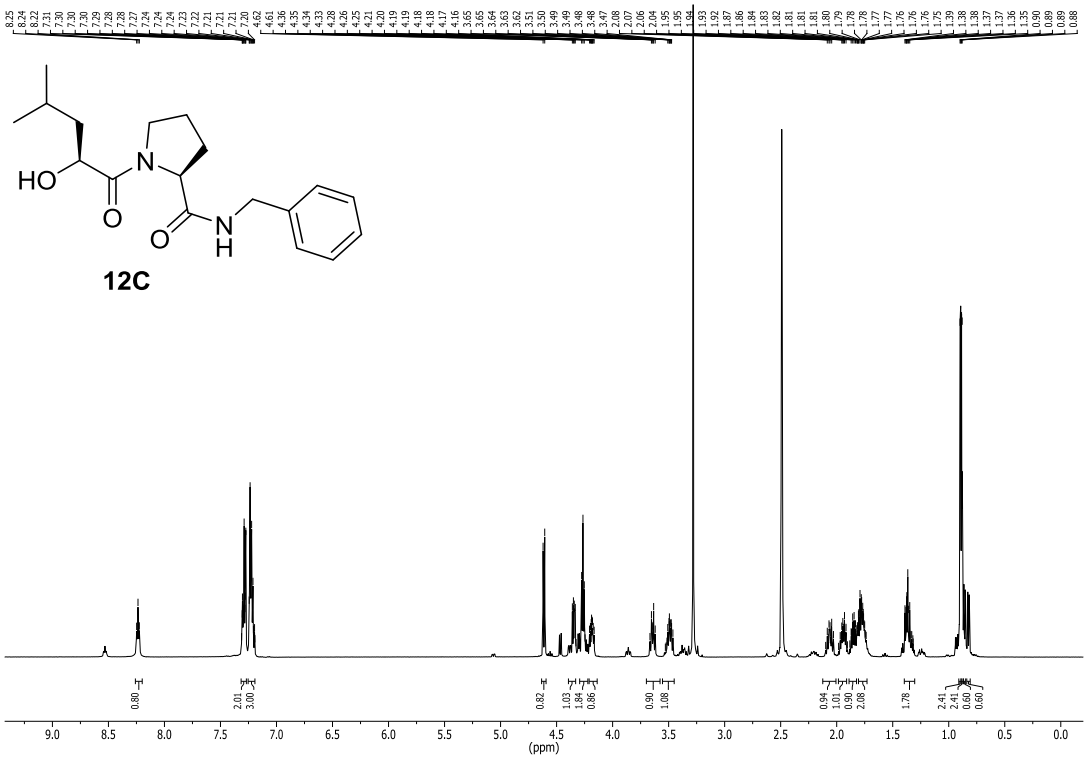

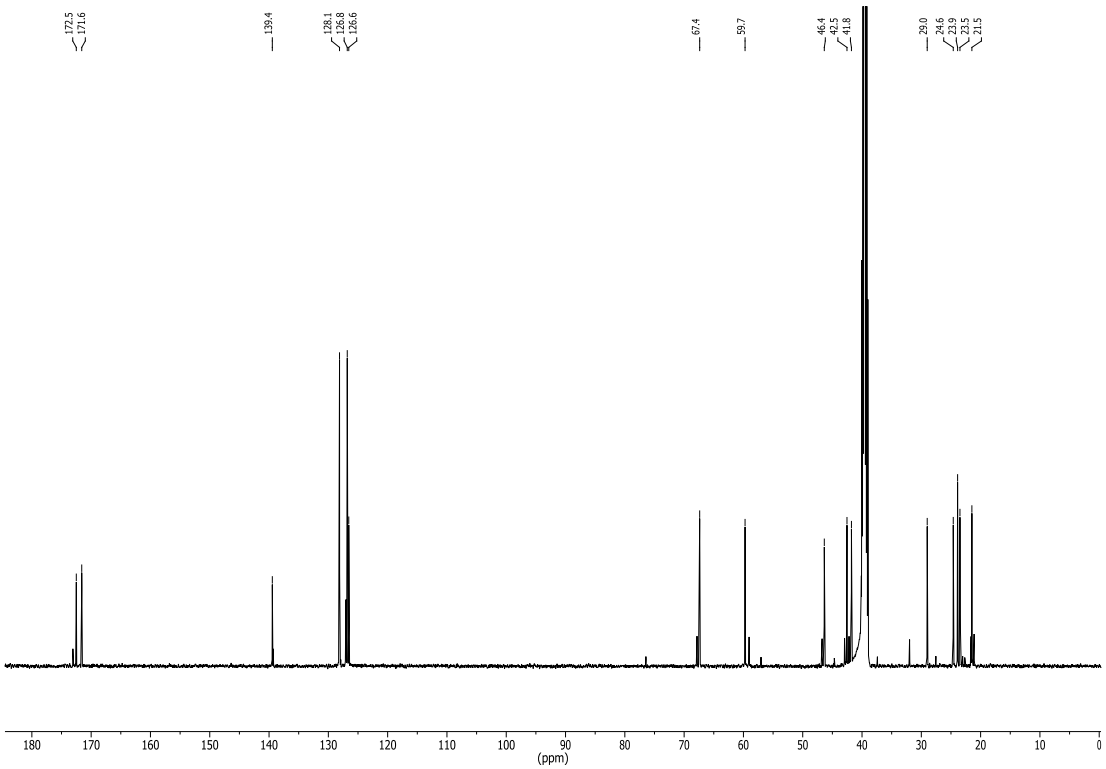

*^{1}H and ^{13}C NMR spectra of compound **12G***

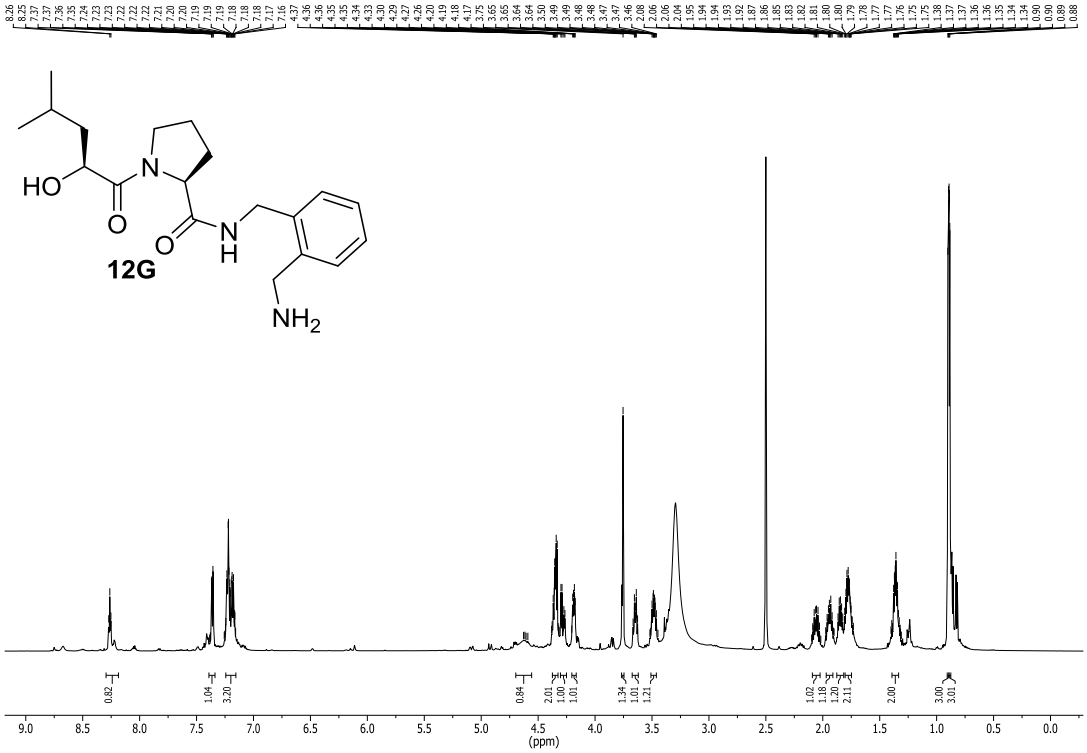

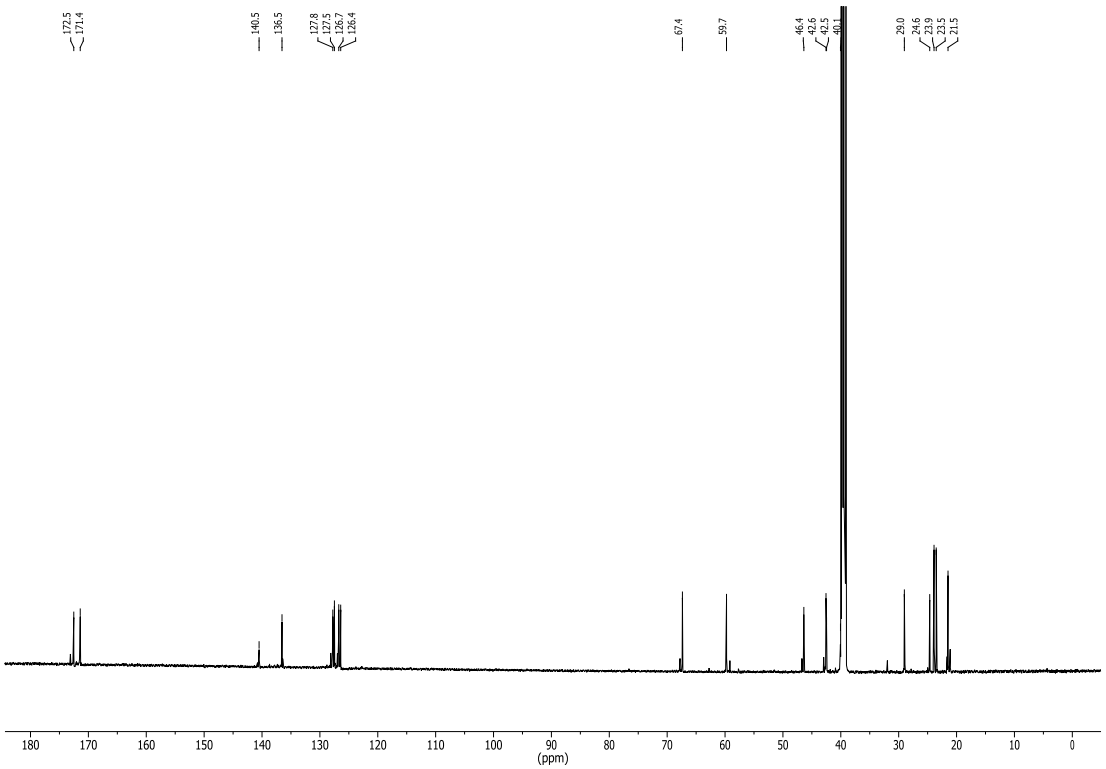

*^{1}H and ^{13}C NMR spectra of compound **14B***

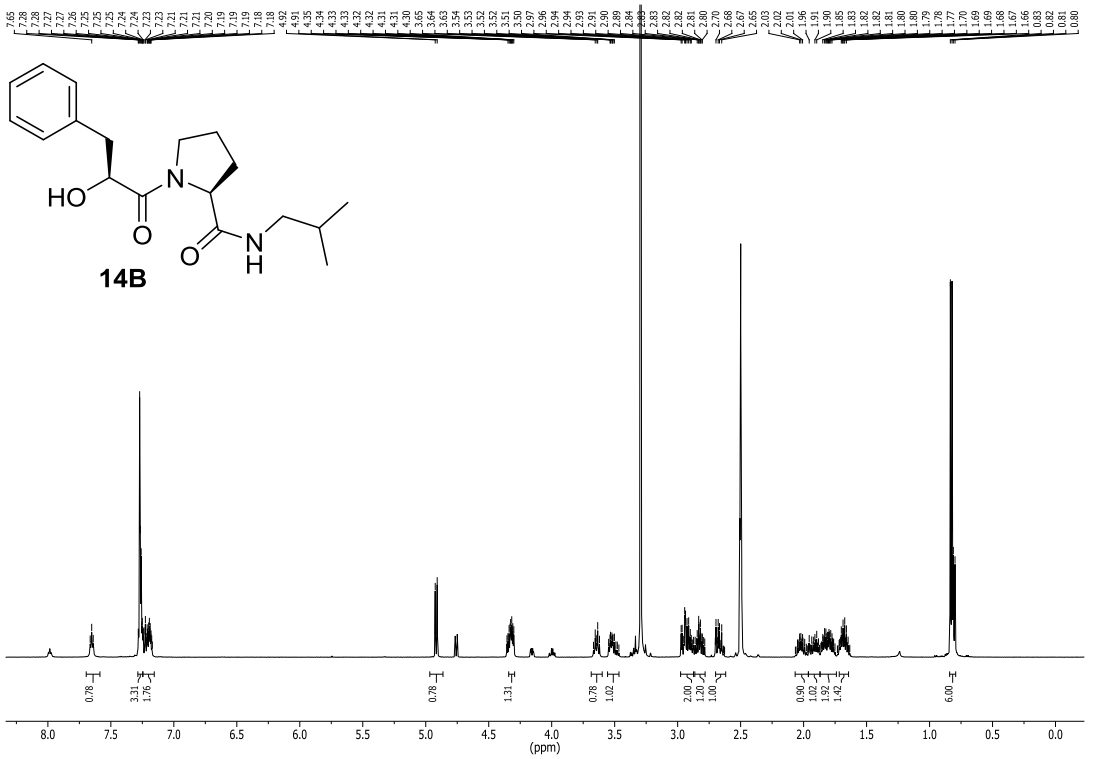

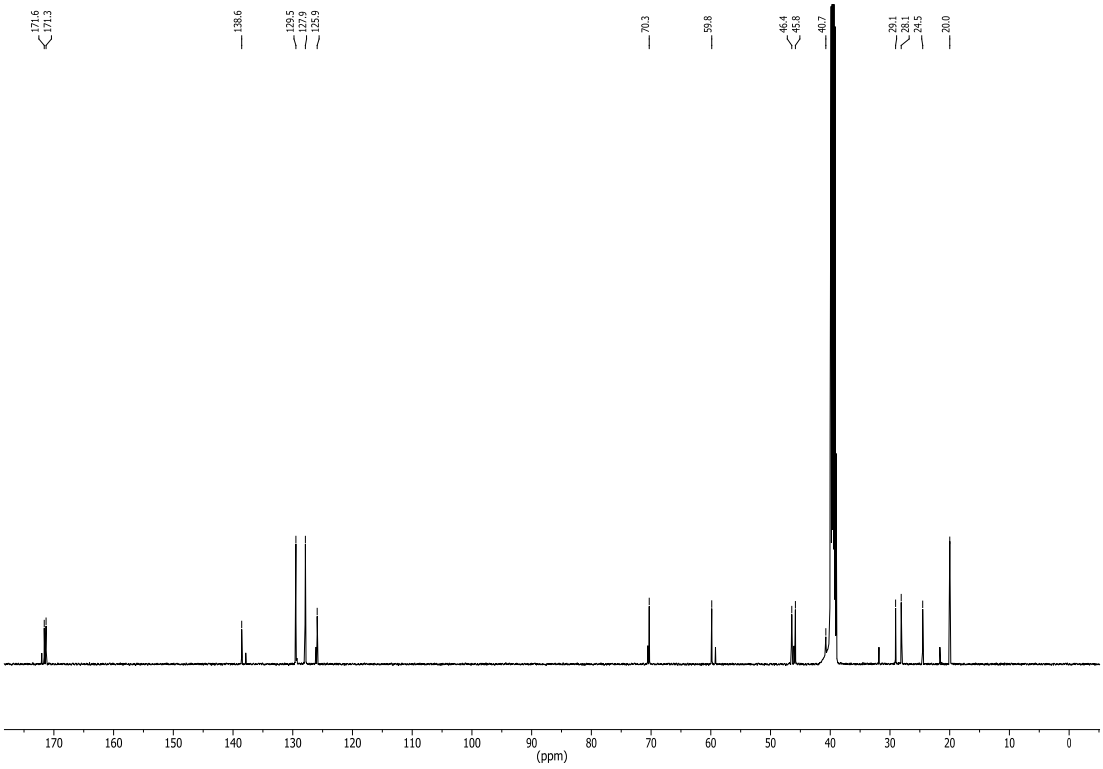

*^{1}H and ^{13}C NMR spectra of compound **15K***

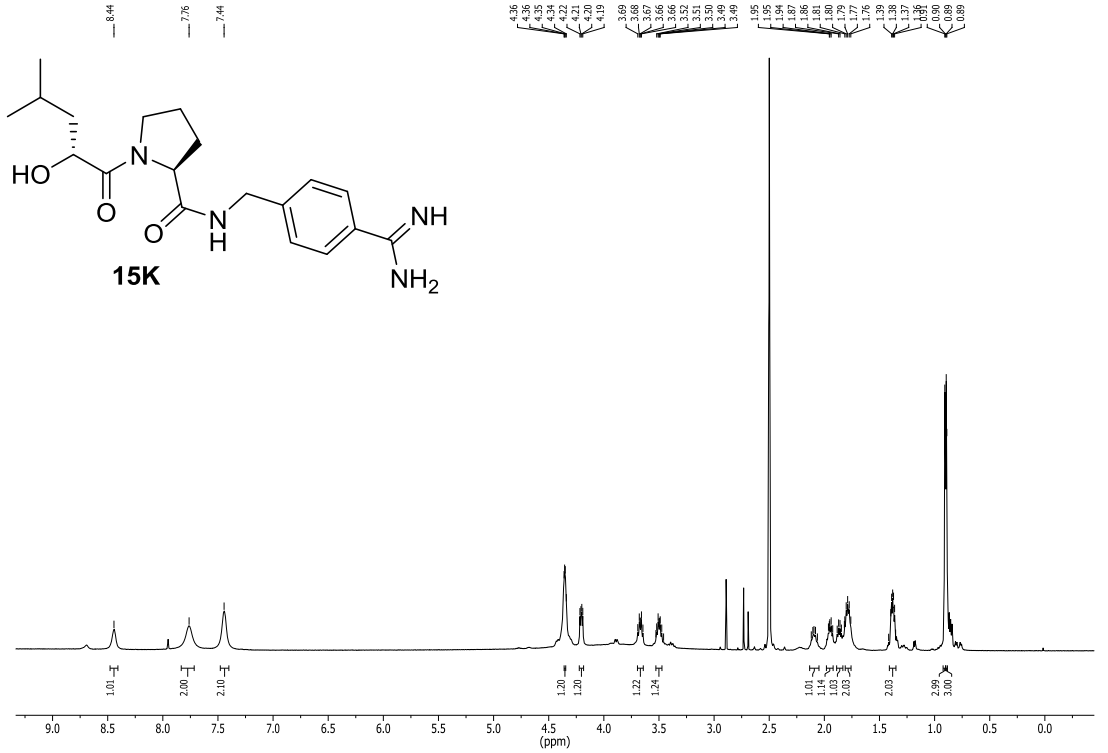

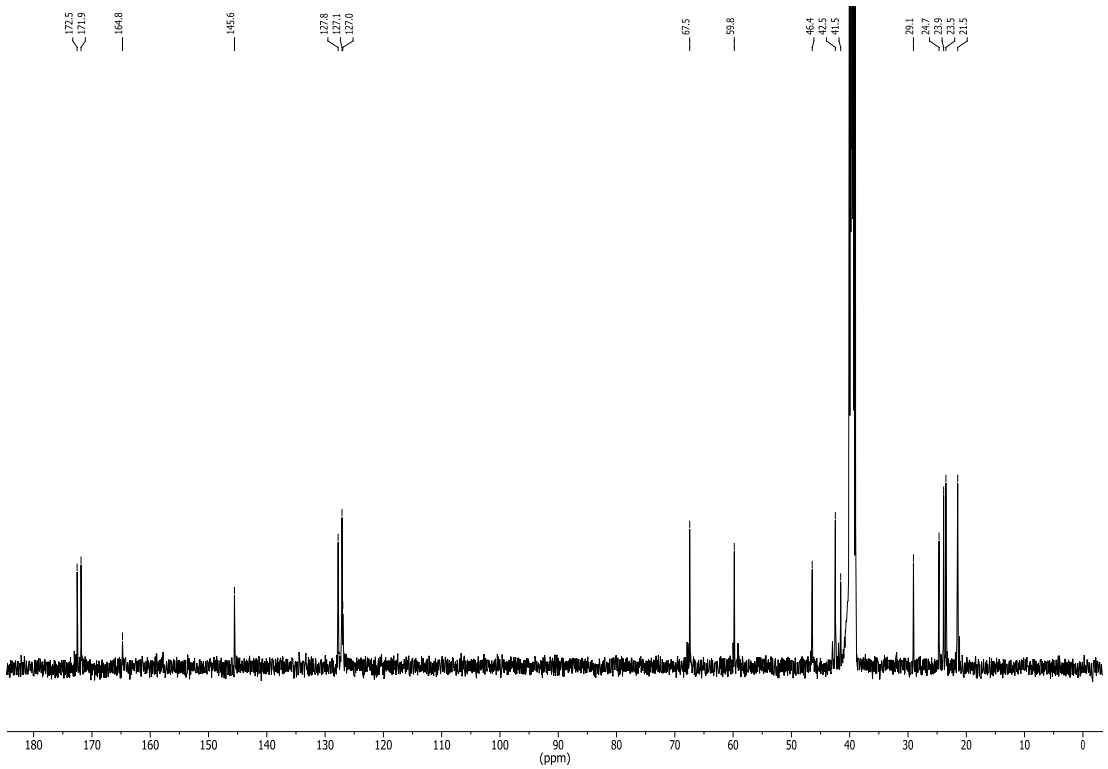

*^{1}H and ^{13}C NMR spectra of compound **16G***

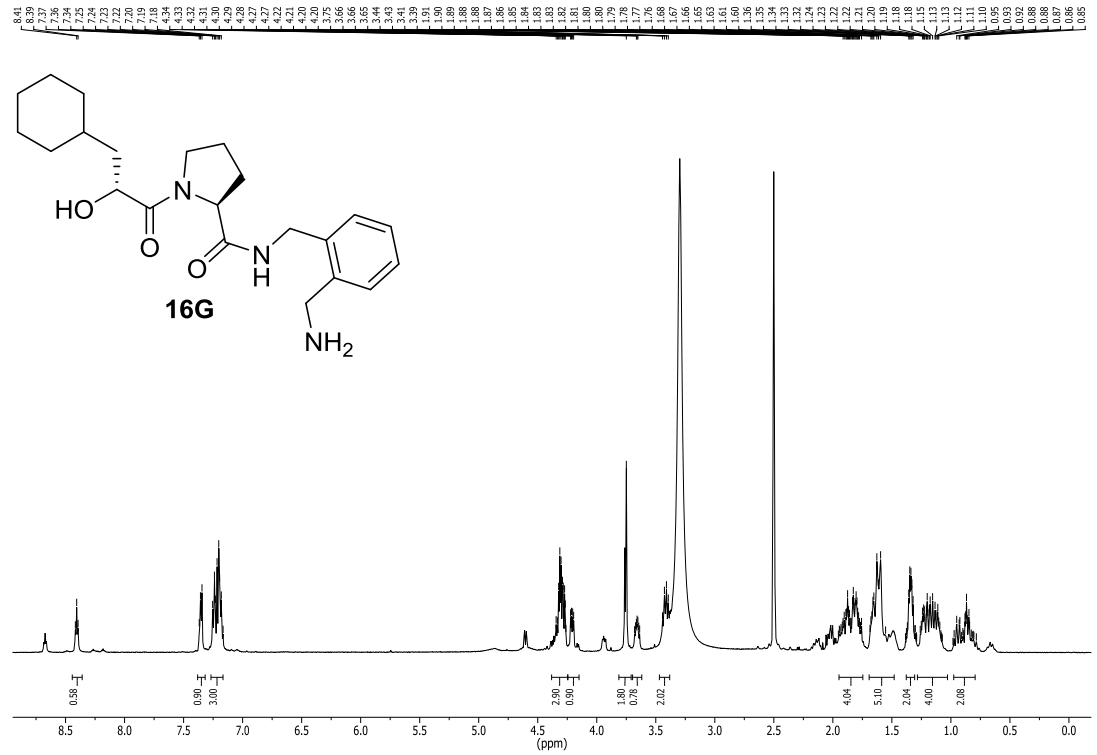

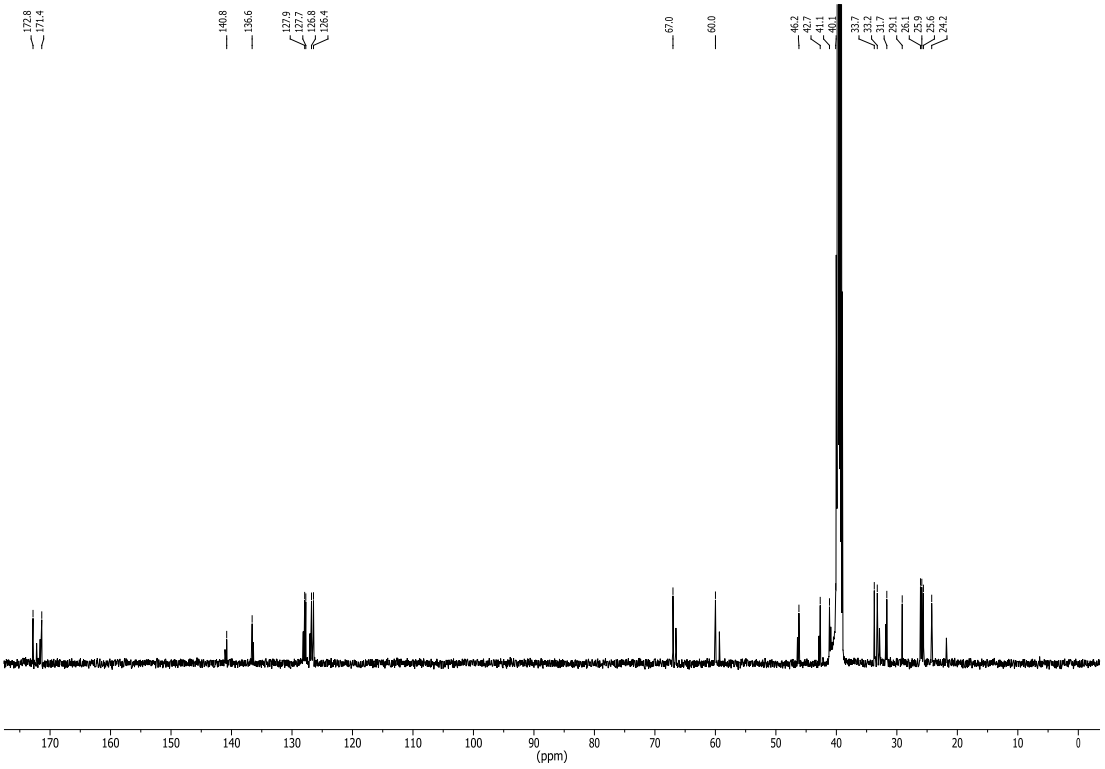

*^{1}H and ^{13}C NMR spectra of compound **16J***

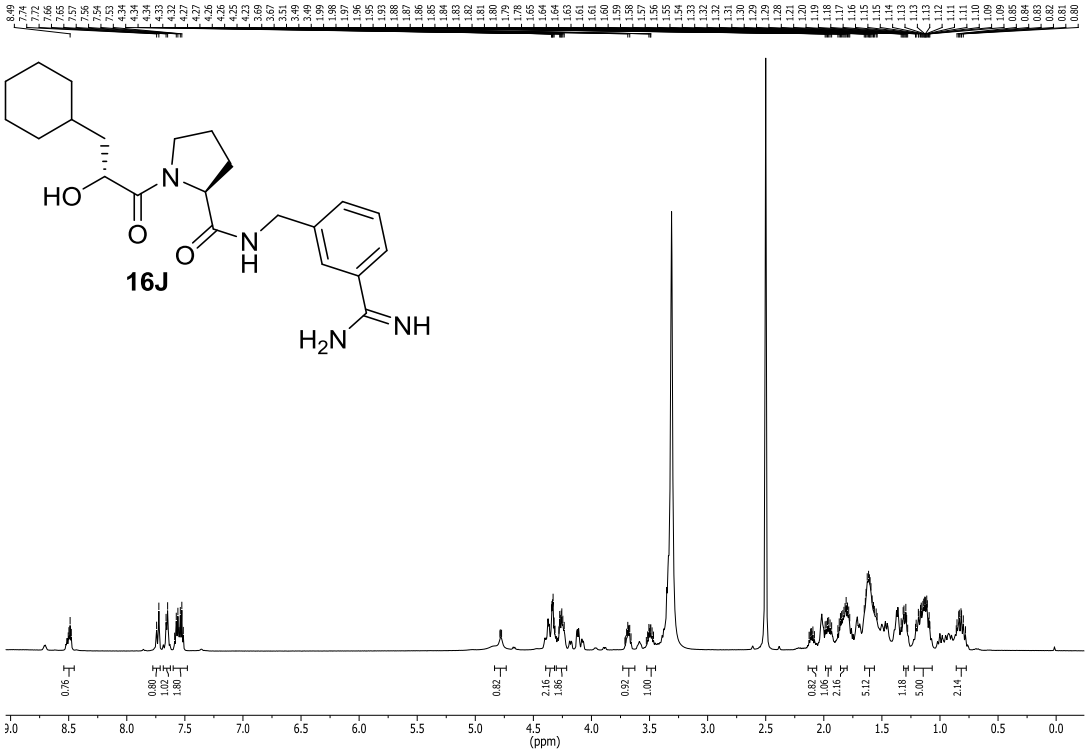

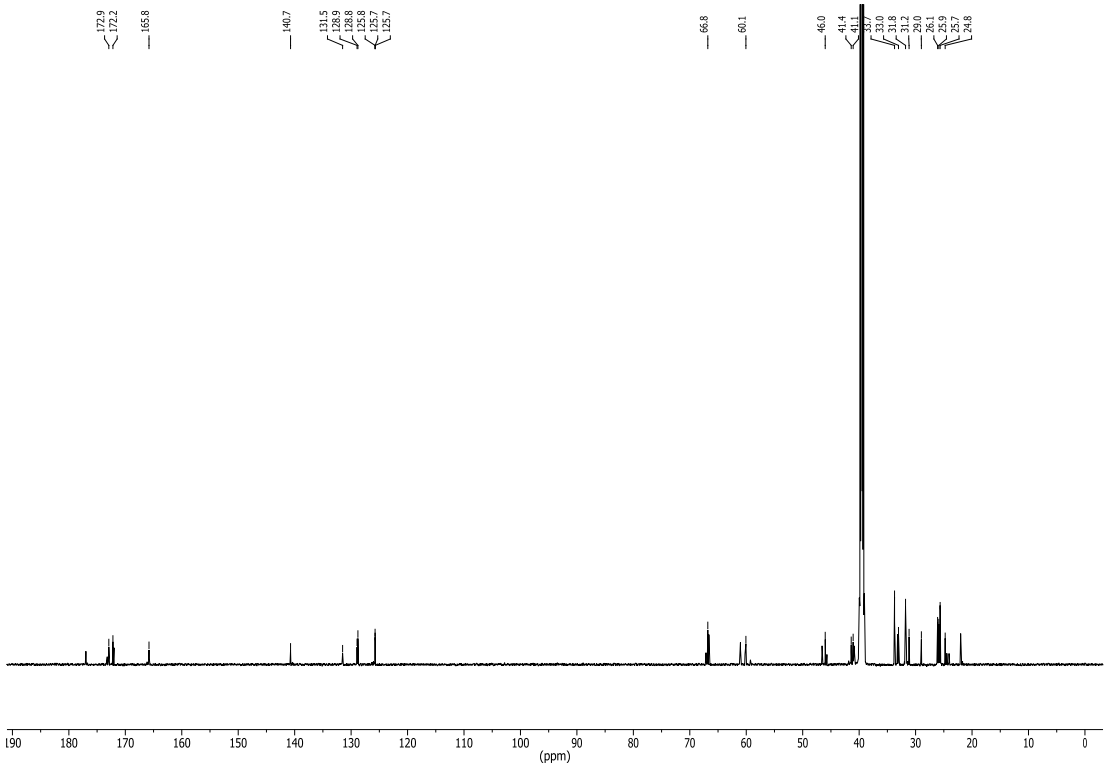

*^{1}H and ^{13}C NMR spectra of compound **16K***

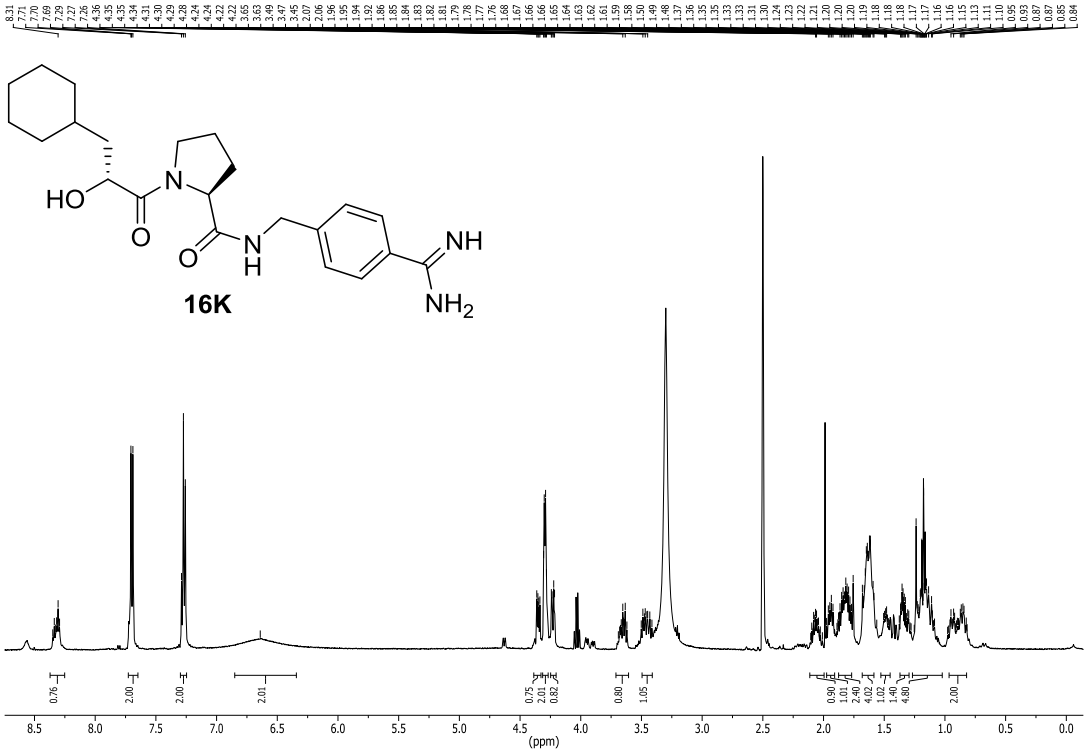

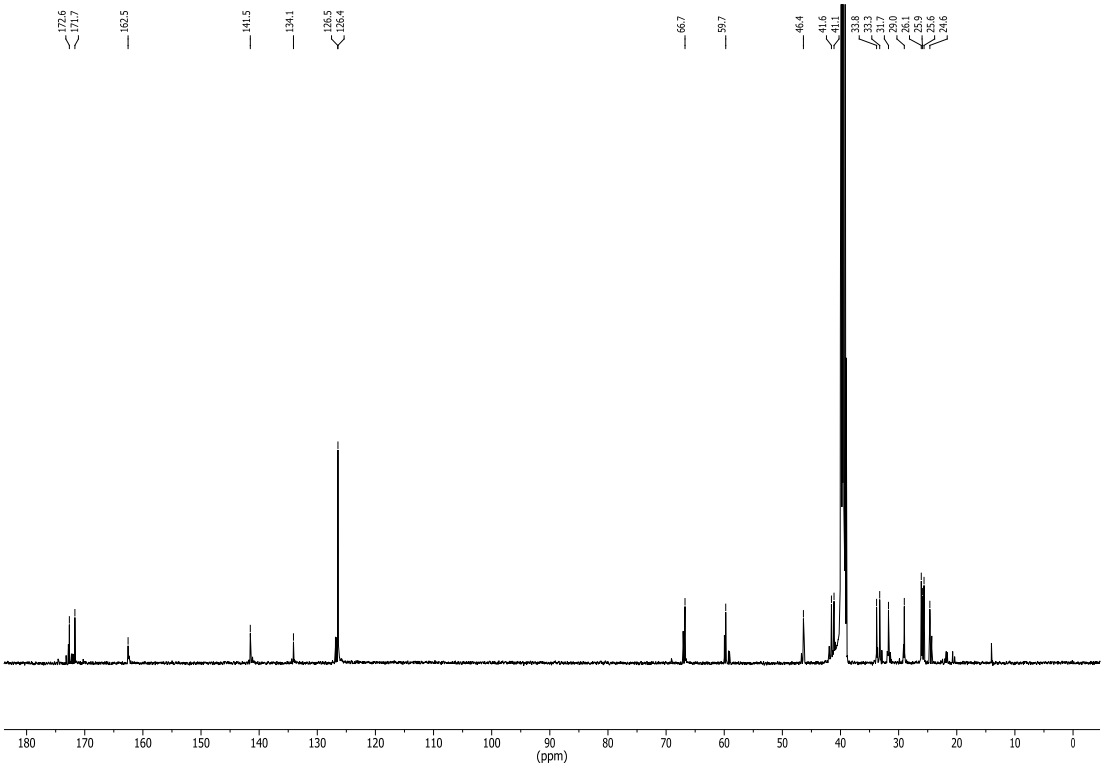

*^{1}H and ^{13}C NMR spectra of compound **28K***

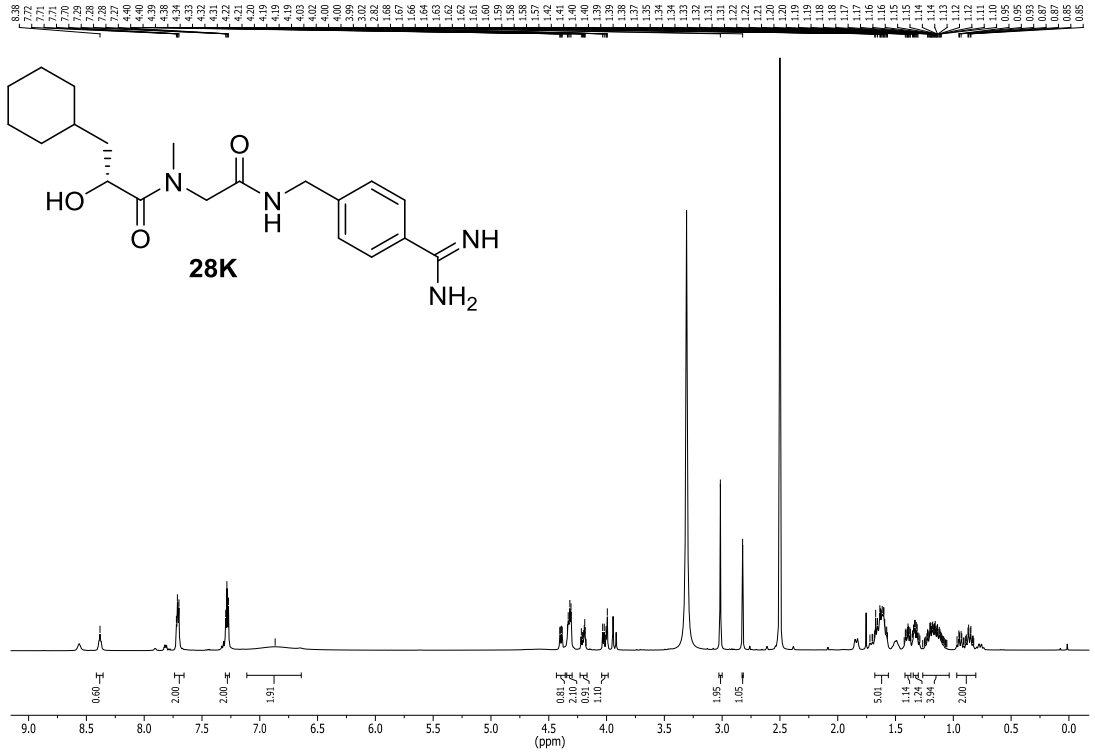

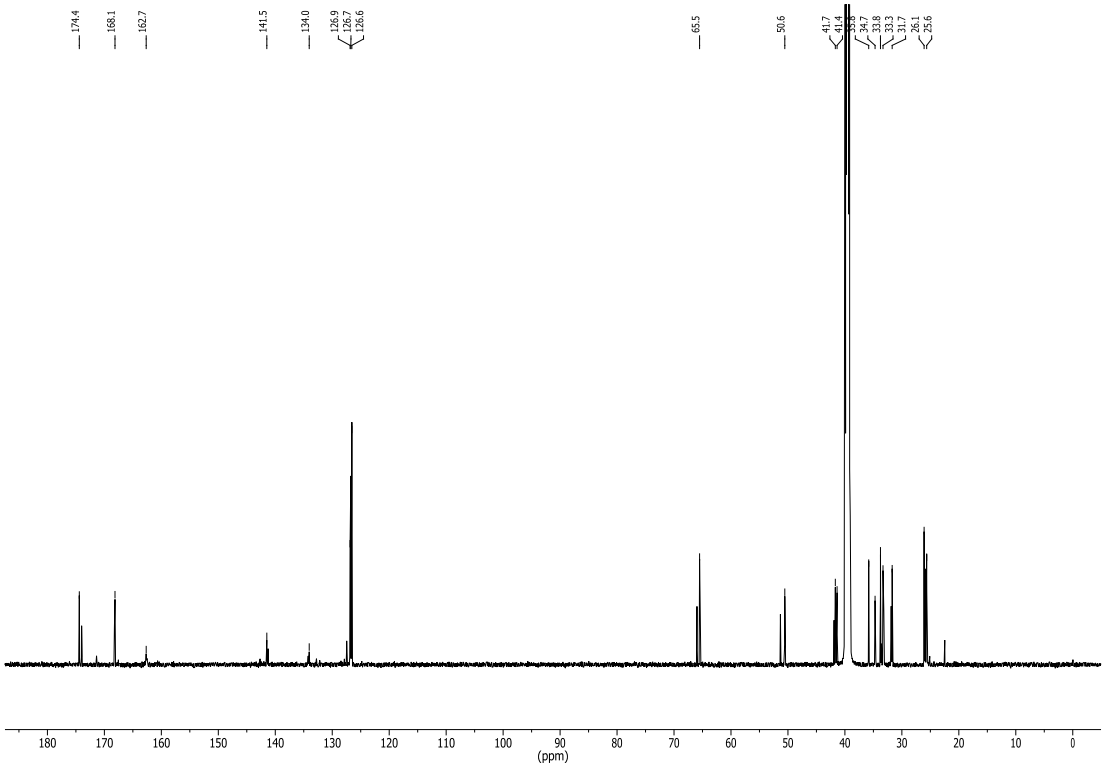

Appendix II. NMR Spectra of Compounds reported in Chapter 4

The following pages include ^{1}H and ^{13}C NMR spectra of compounds reported in chapter 4. Only spectra of final compounds are shown.

^{1}H and ^{13}C NMR spectra of compound **2**

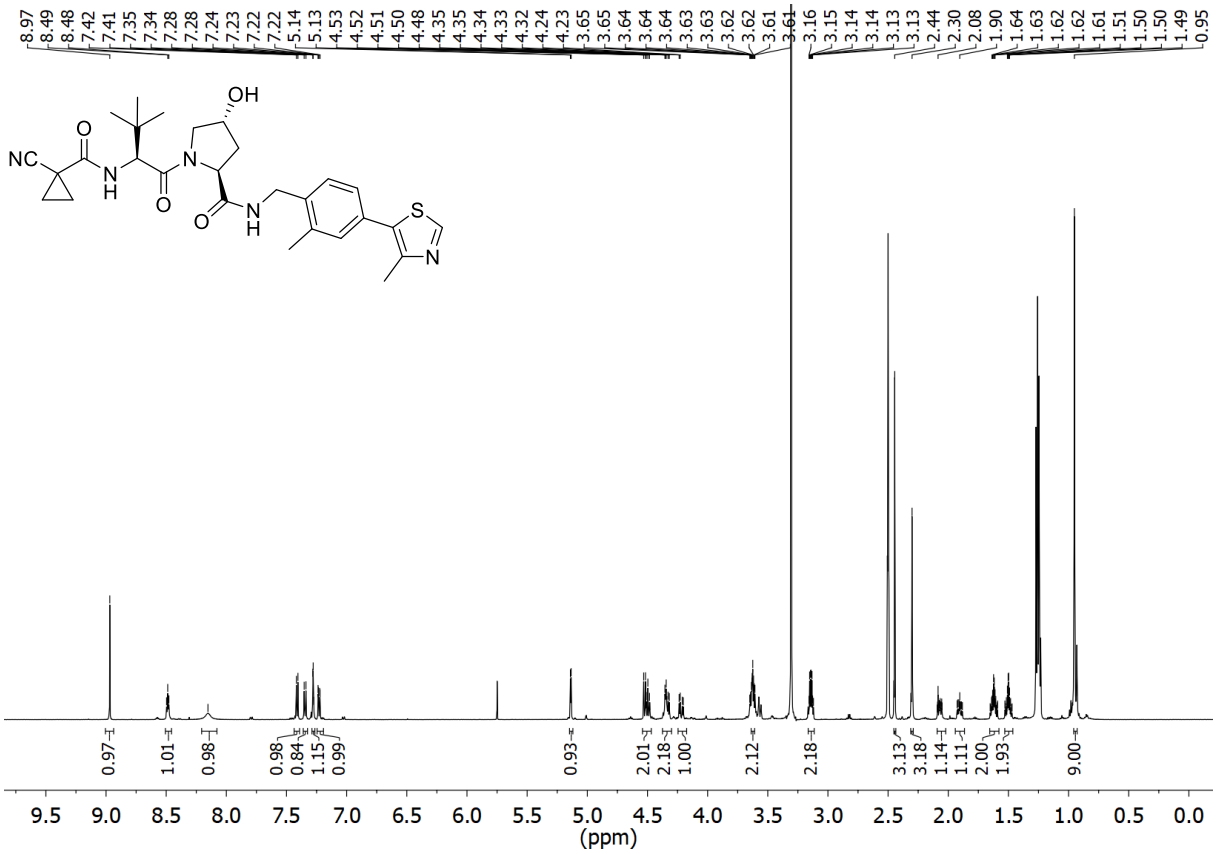

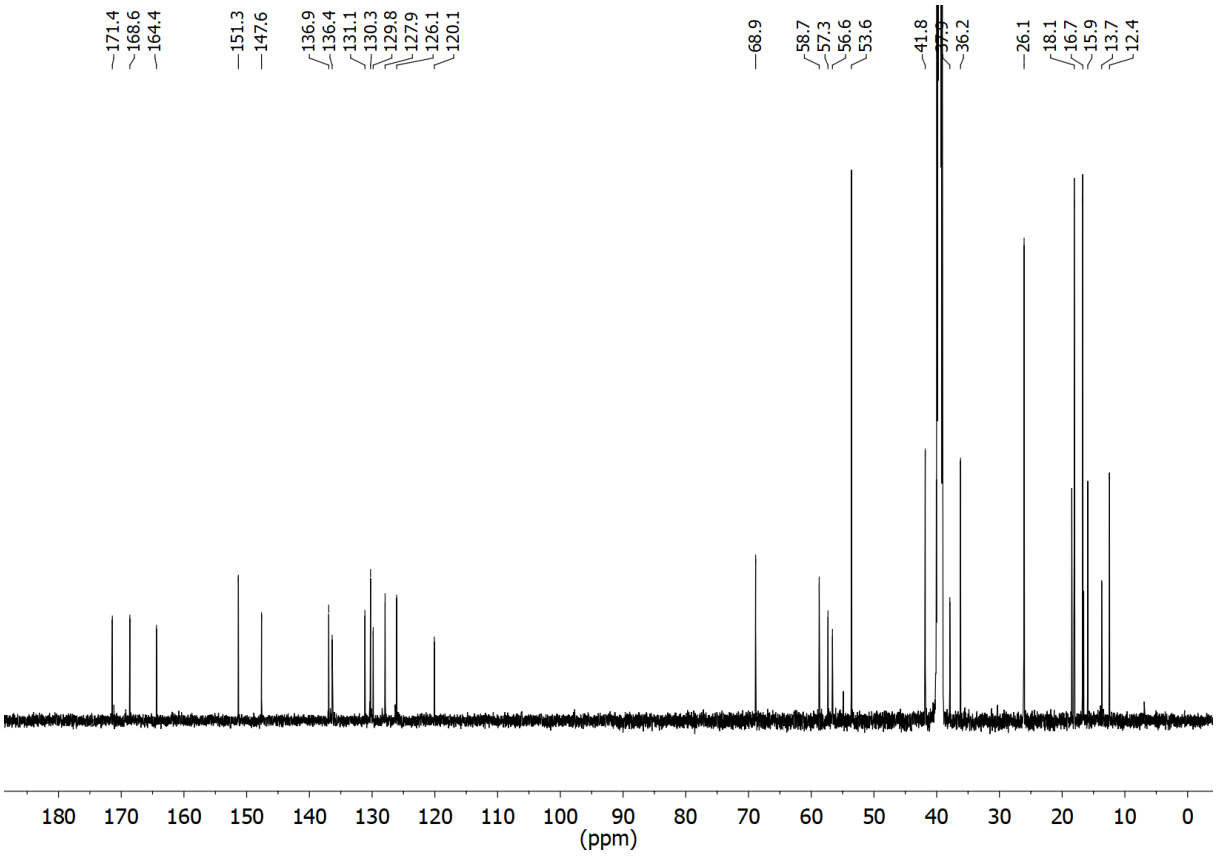

^{1}H and ^{13}C NMR spectra of compound **3**

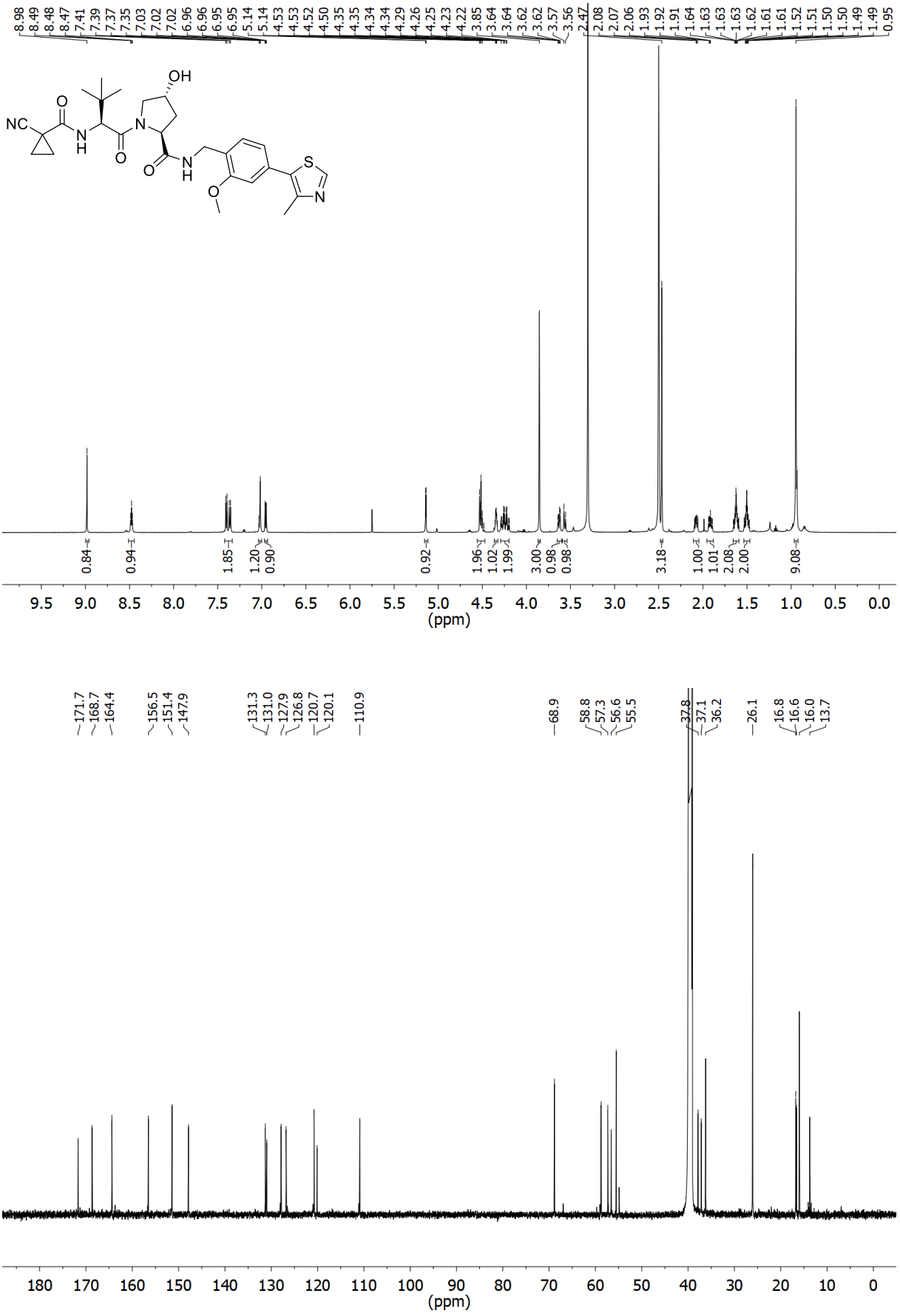

^{1}H and ^{13}C NMR spectra of compound **4**

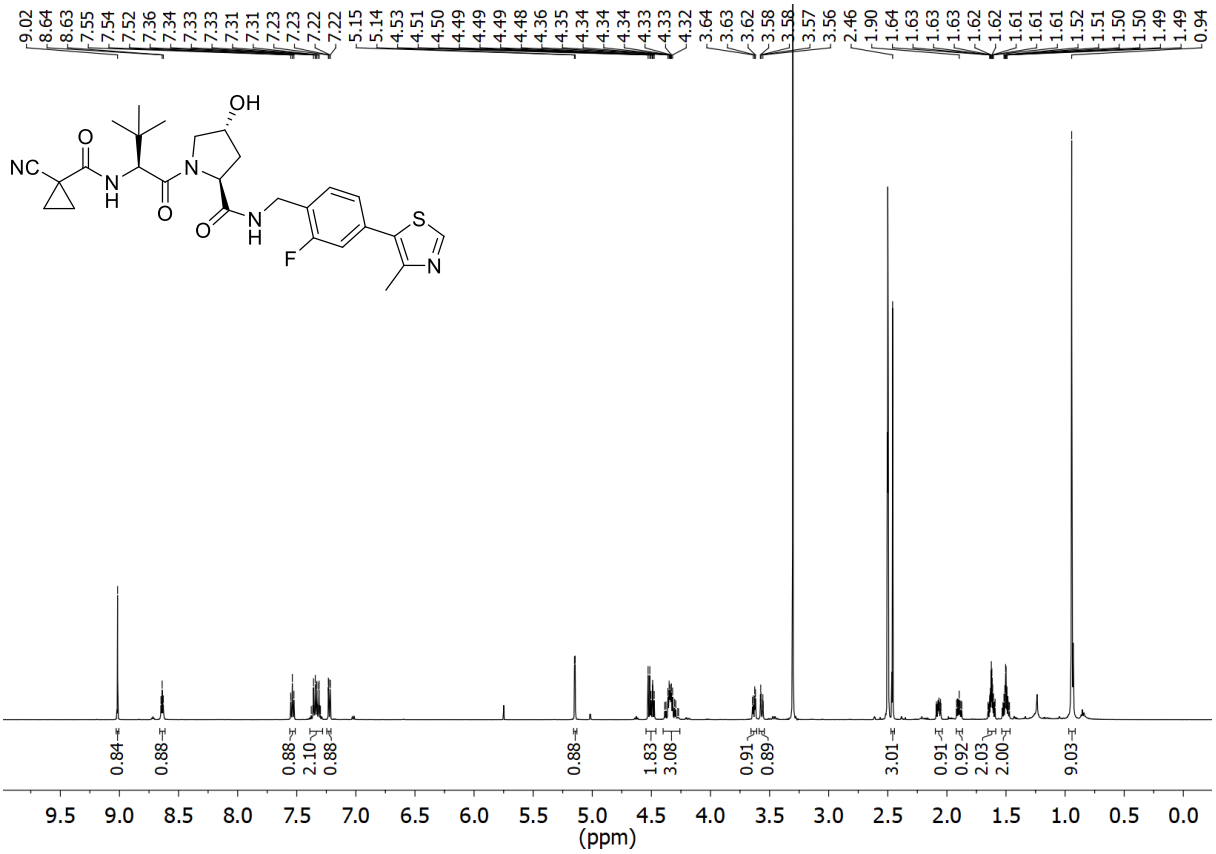

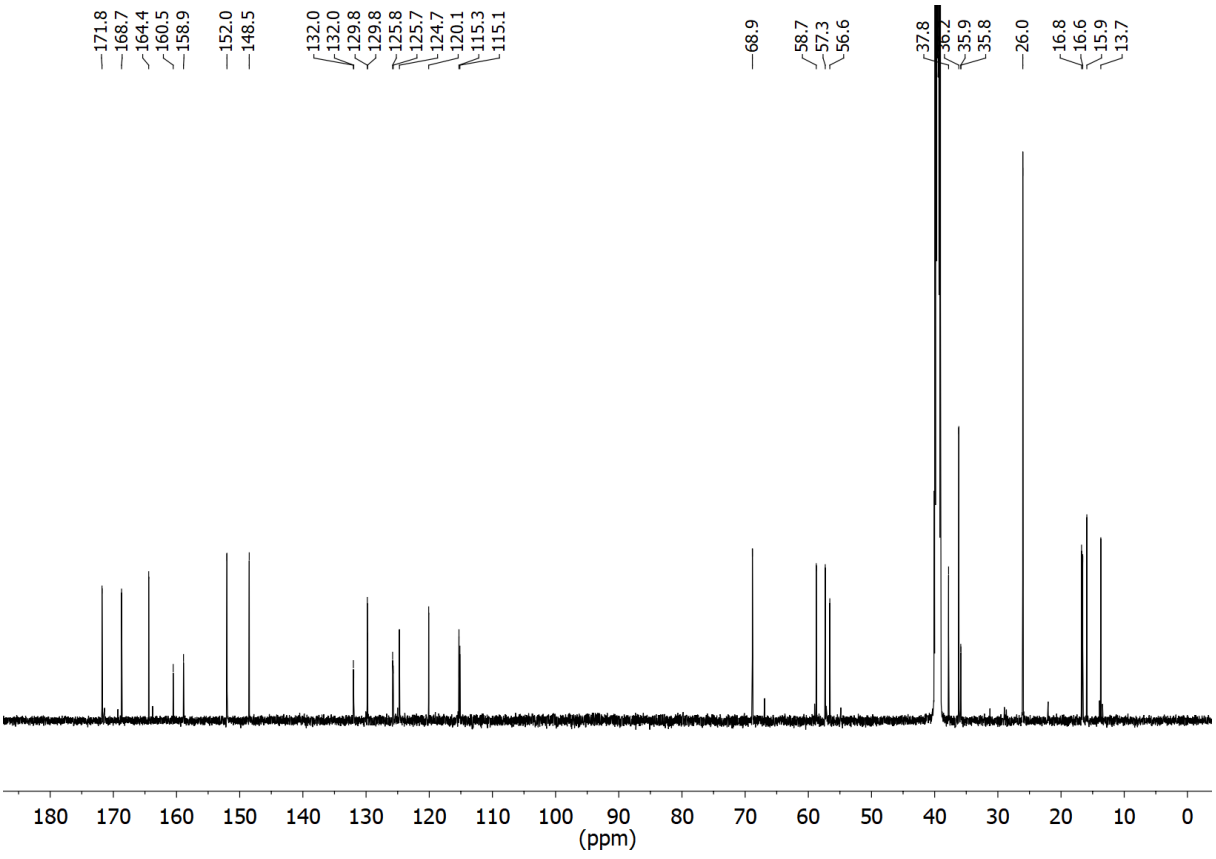

^{1}H and ^{13}C NMR spectra of compound **5**

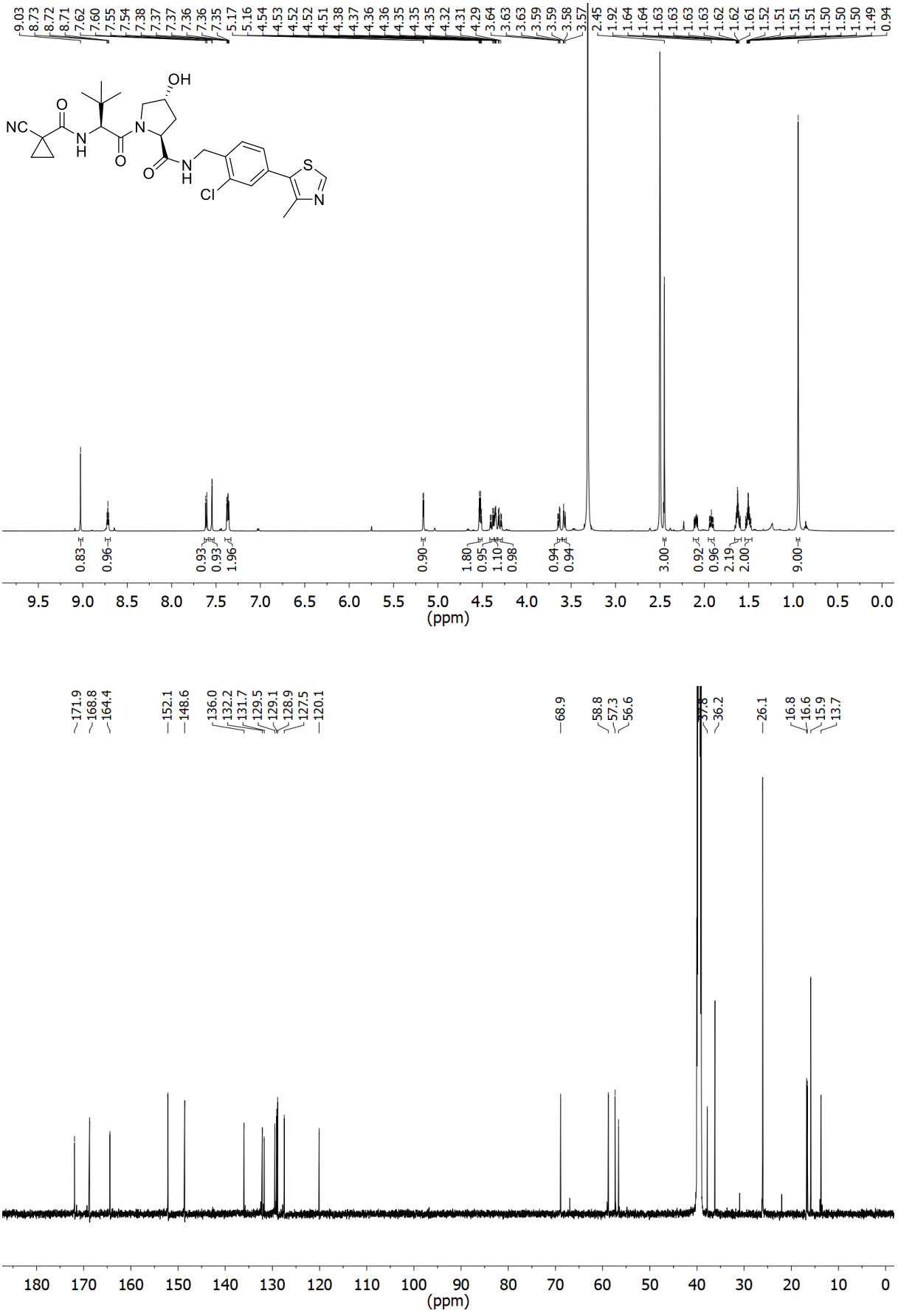

^{1}H and ^{13}C NMR spectra of compound **6**

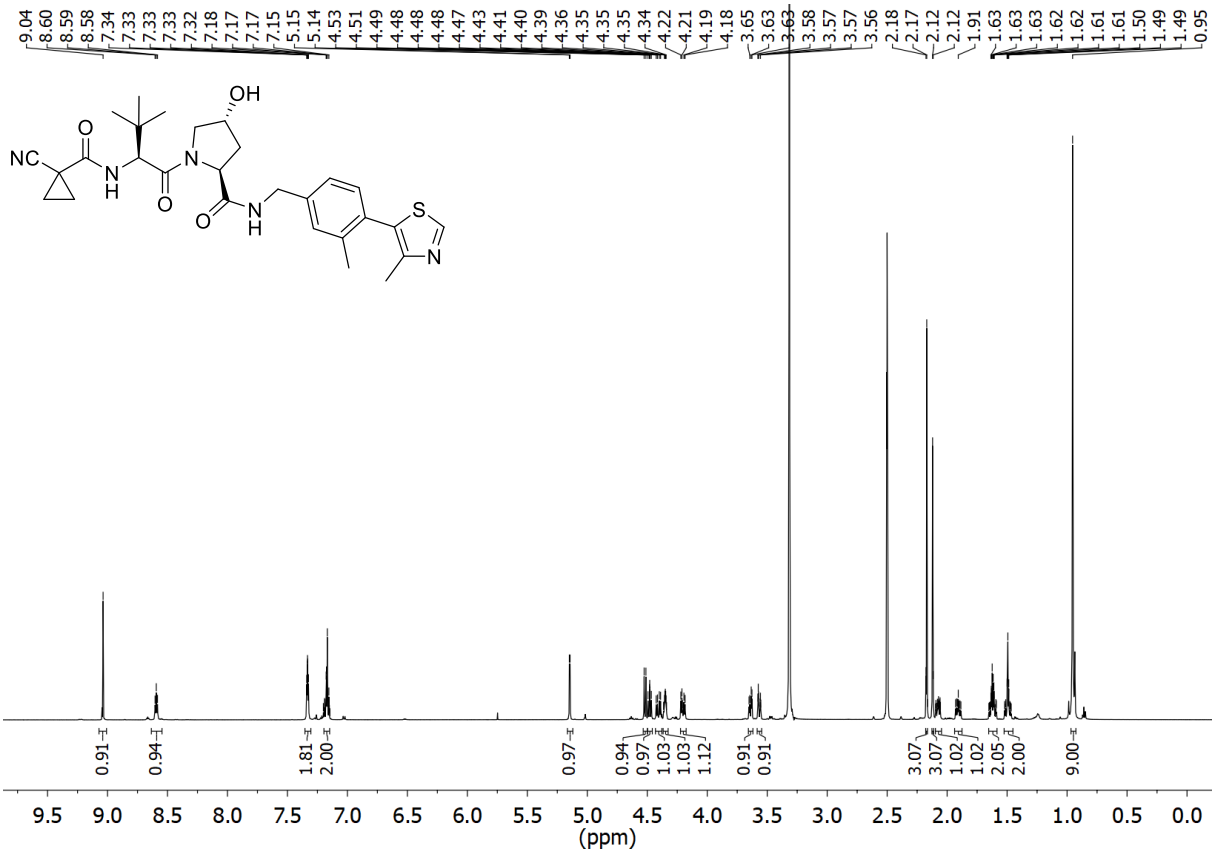

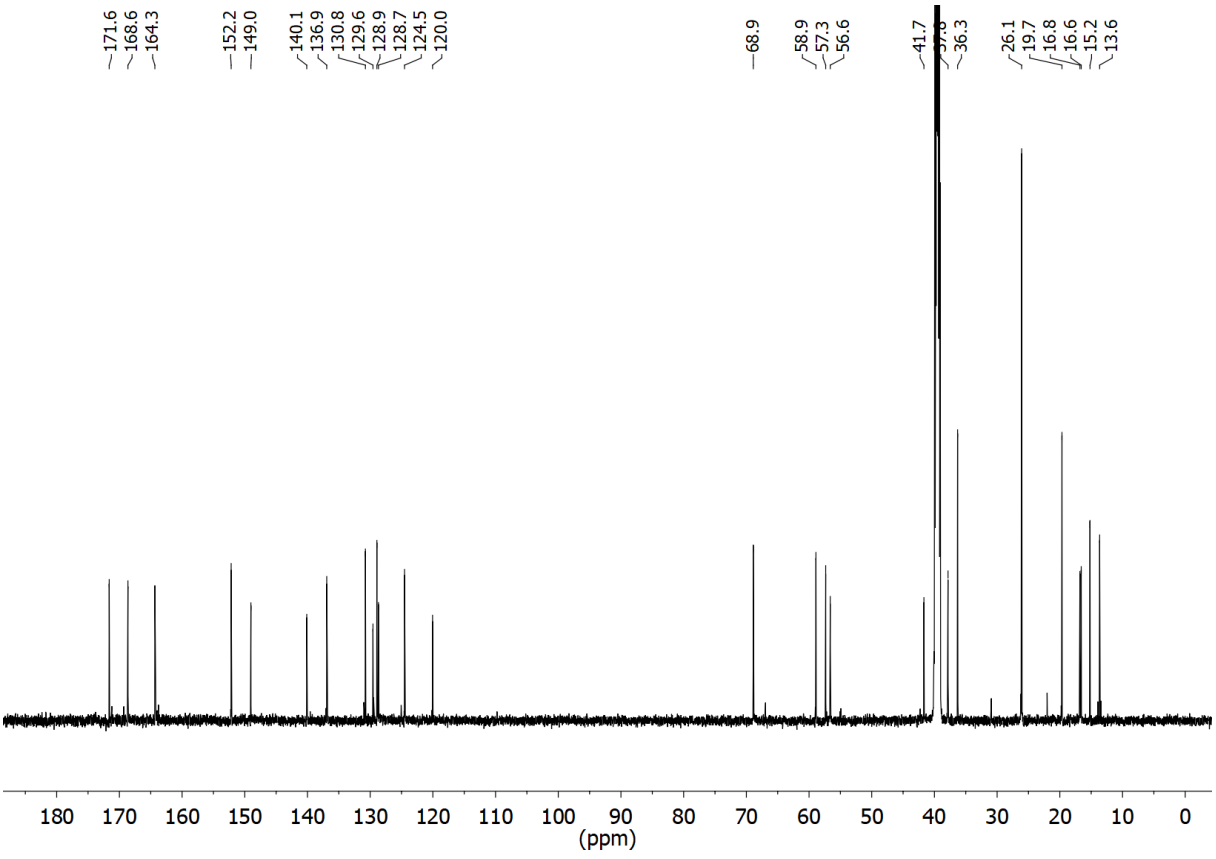

^{1}H and ^{13}C NMR spectra of compound **7**

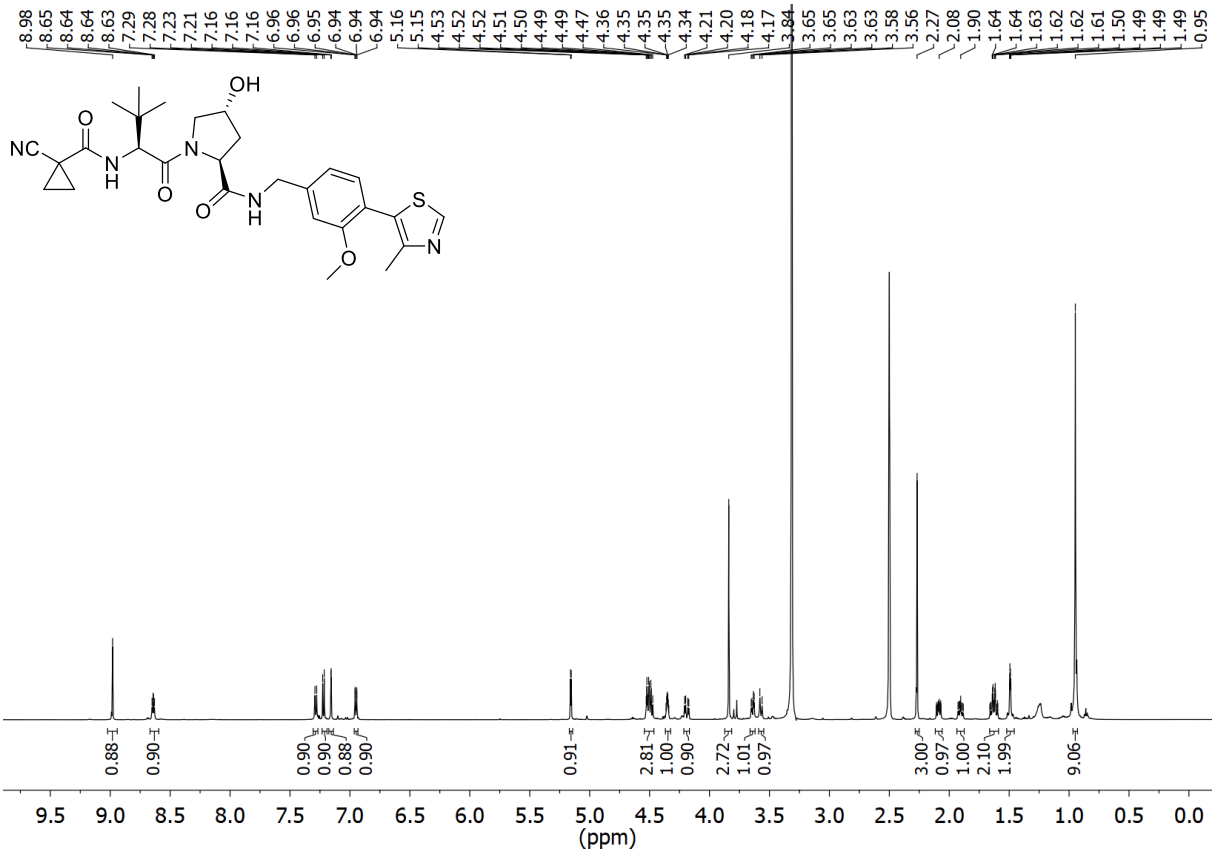

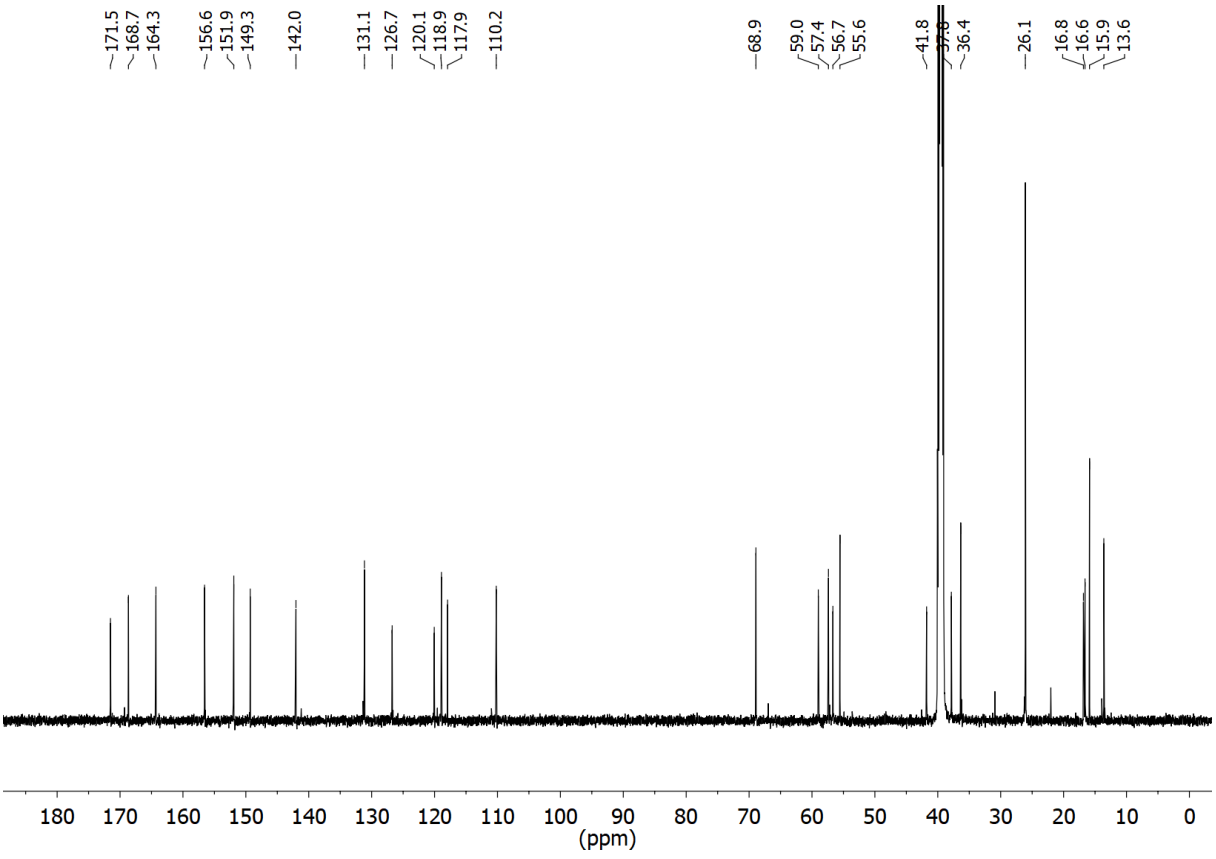

^{1}H and ^{13}C NMR spectra of compound **8**

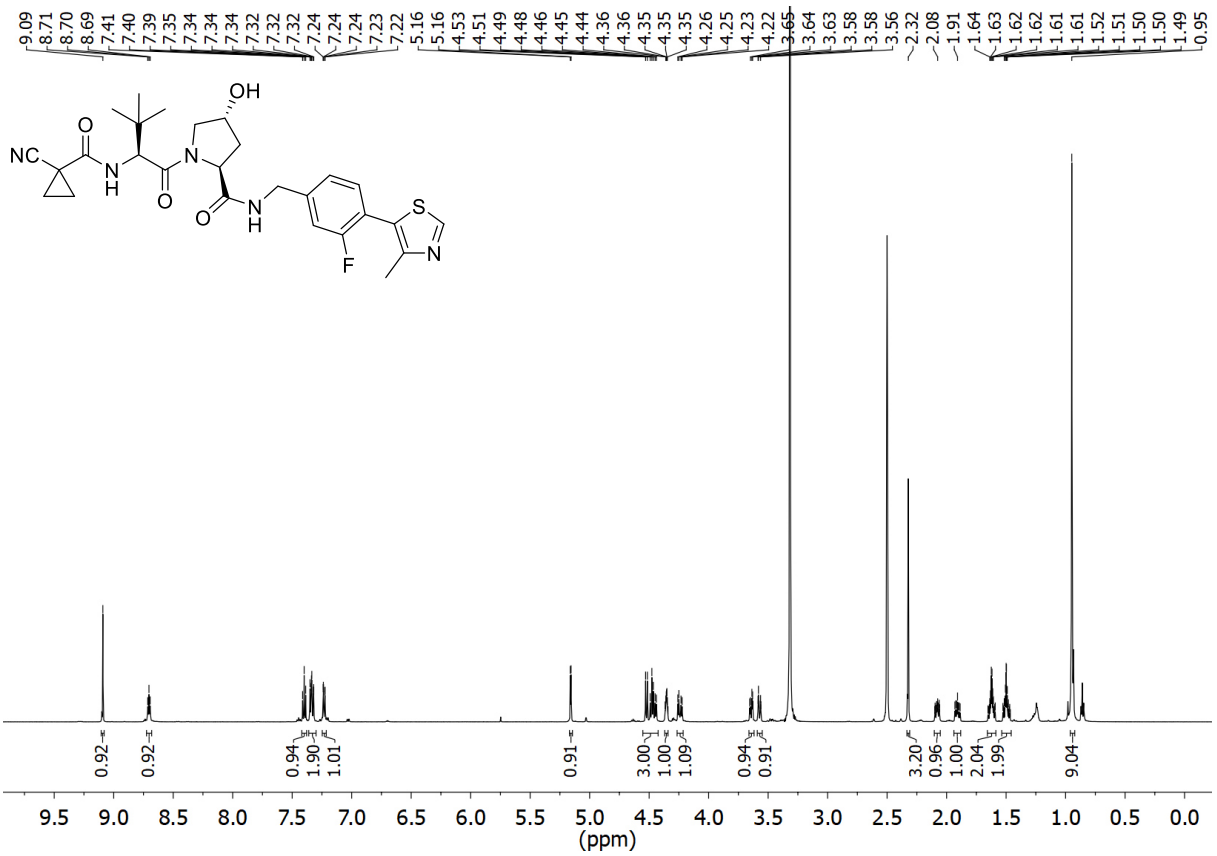

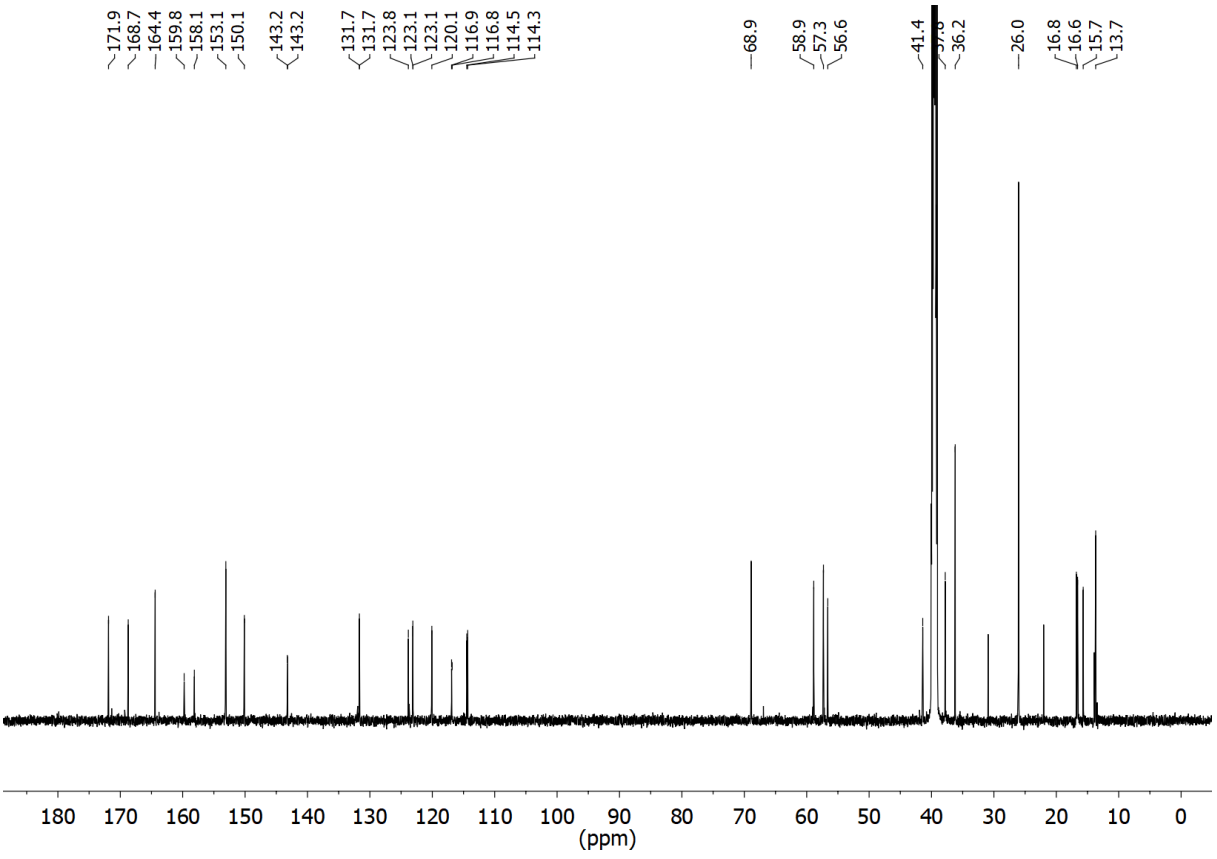

^{1}H and ^{13}C NMR spectra of compound **9**

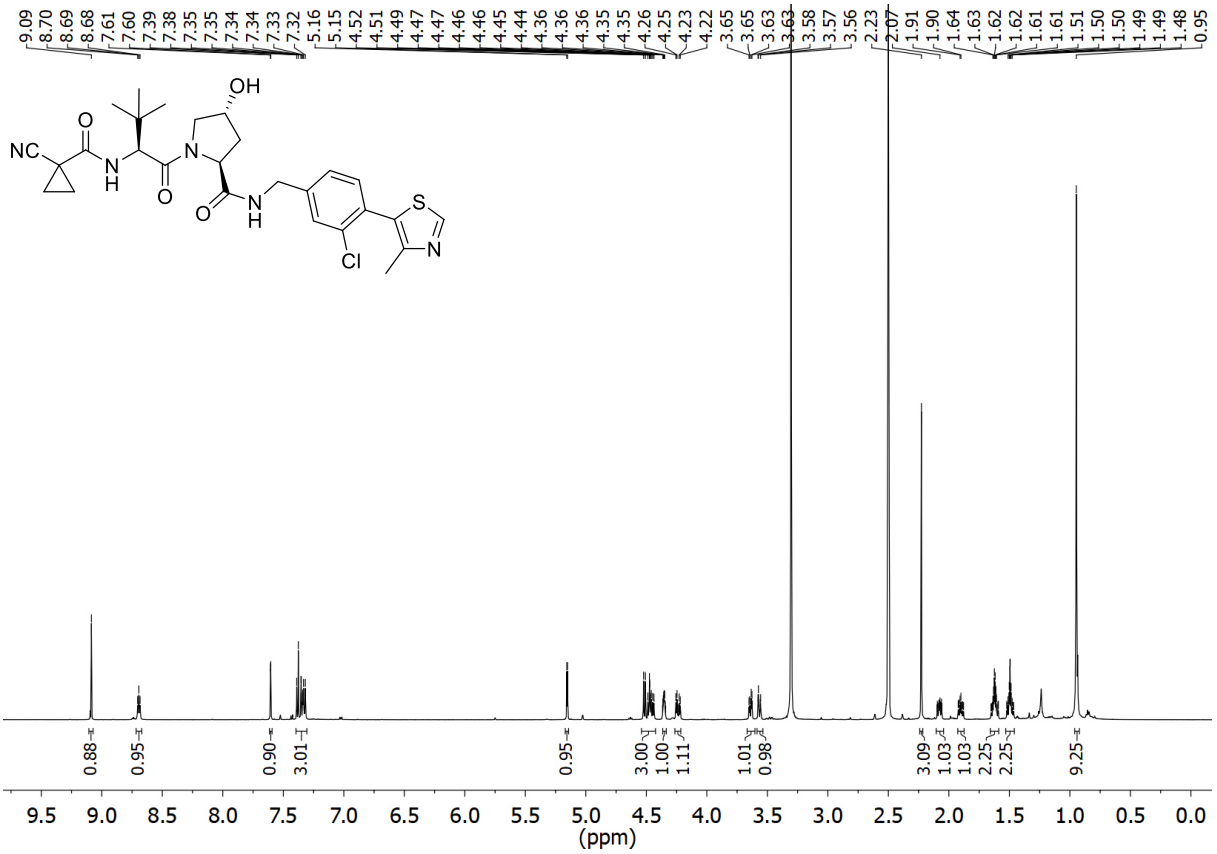

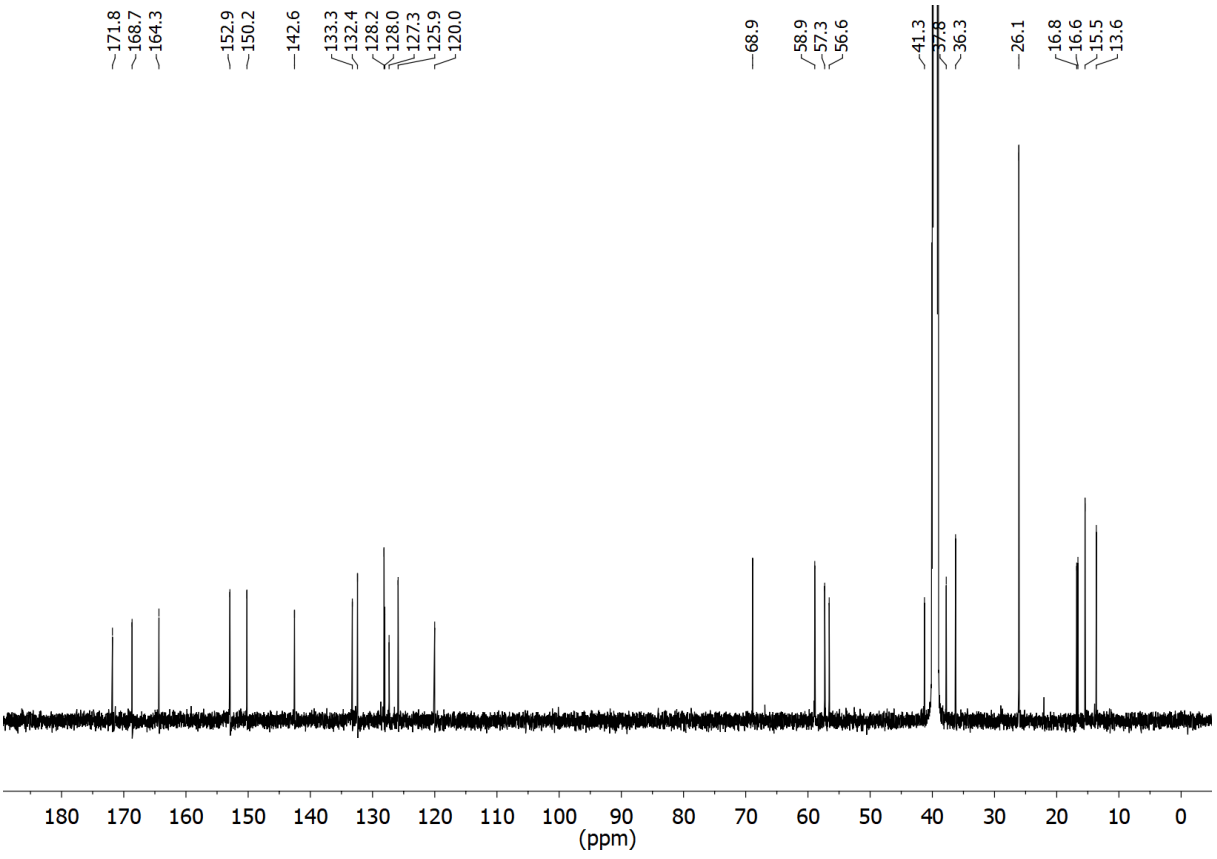

^{1}H and ^{13}C NMR spectra of compound **10**

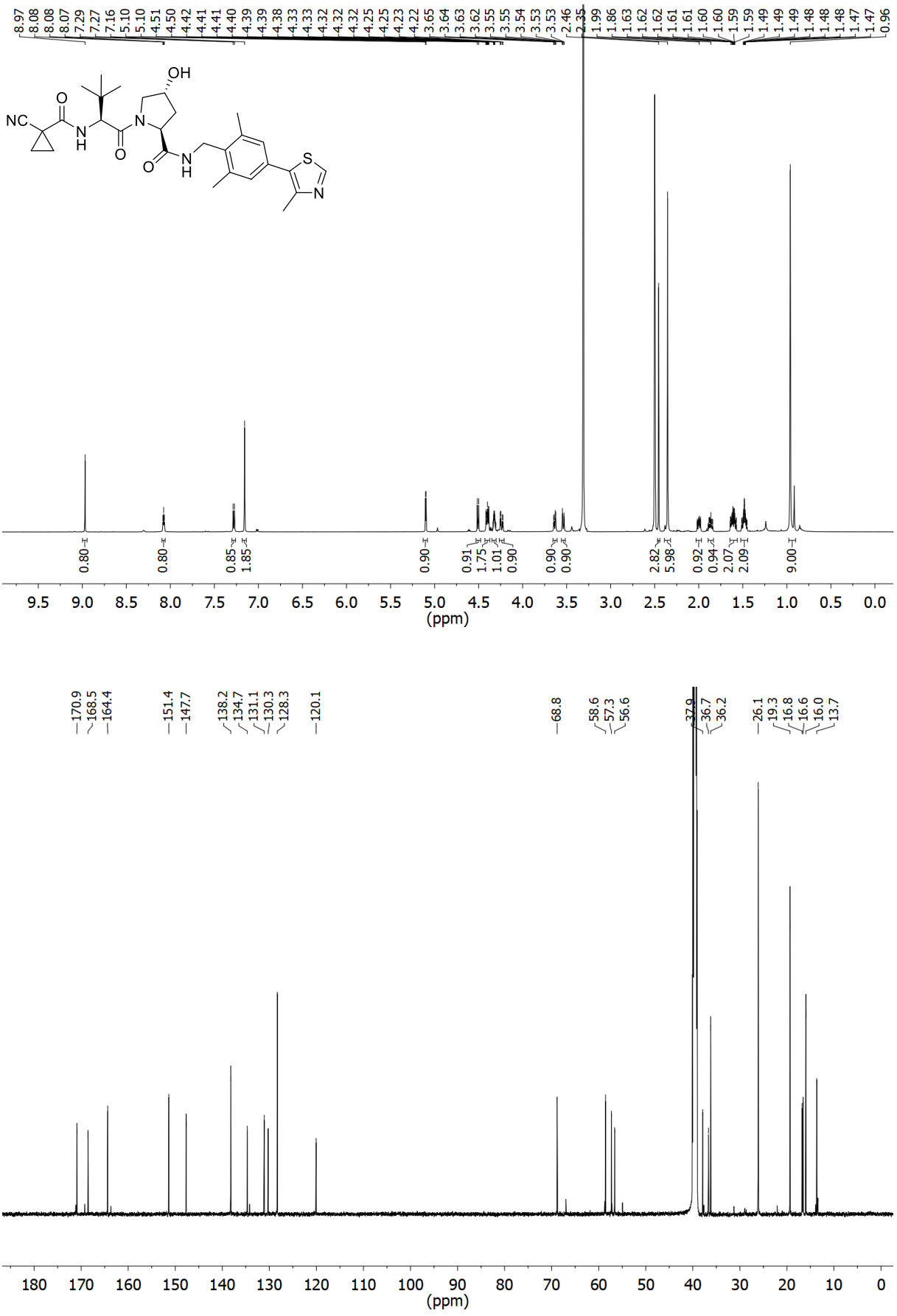

^{1}H and ^{13}C NMR spectra of compound **11**

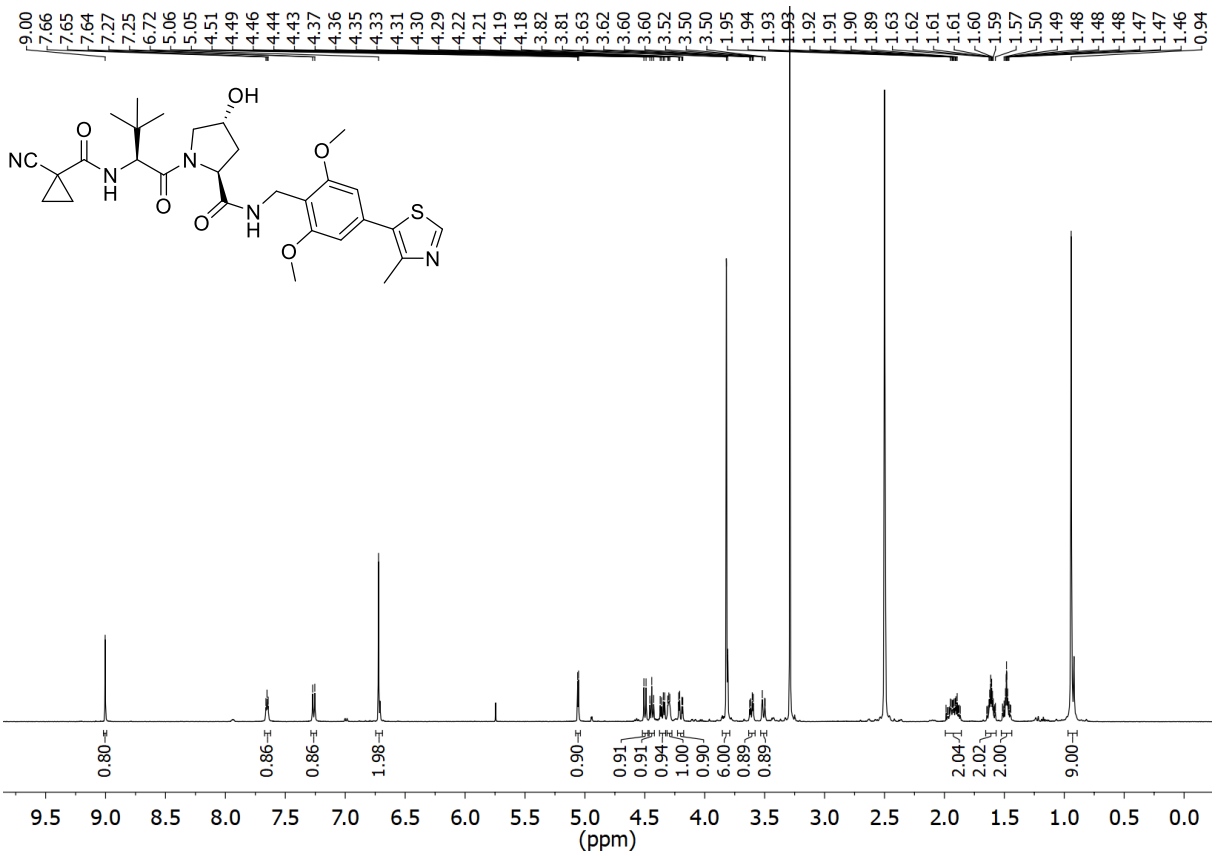

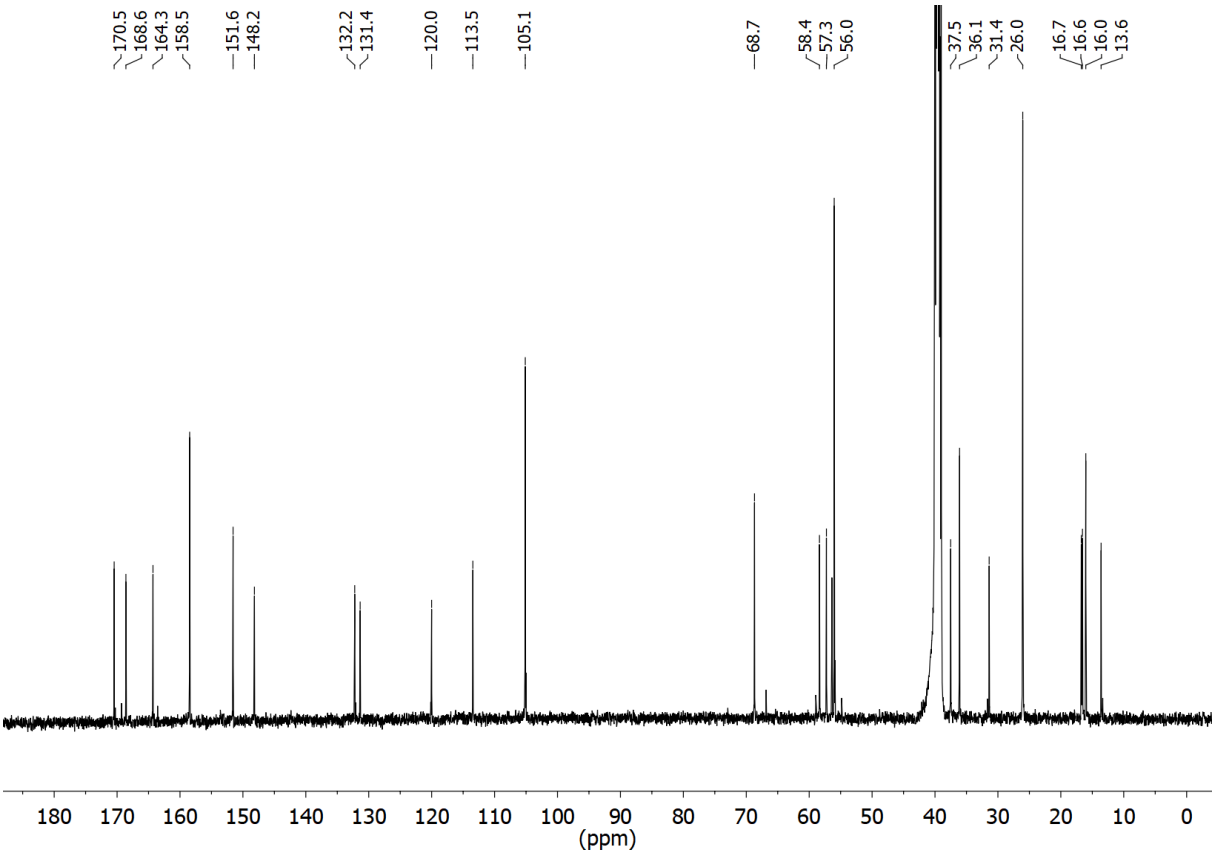

^{1}H and ^{13}C NMR spectra of compound **12**

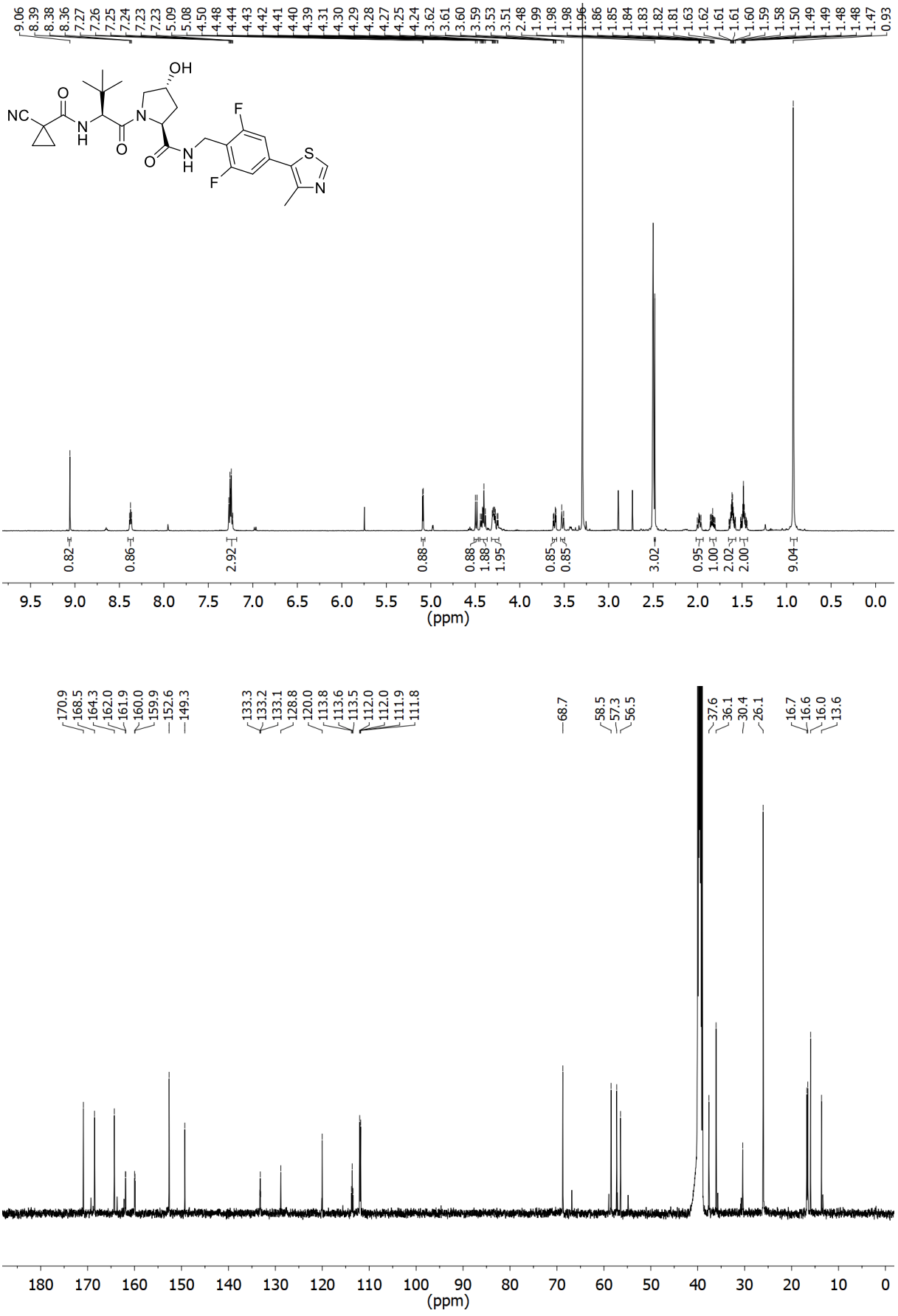

^{1}H and ^{13}C NMR spectra of compound **13**

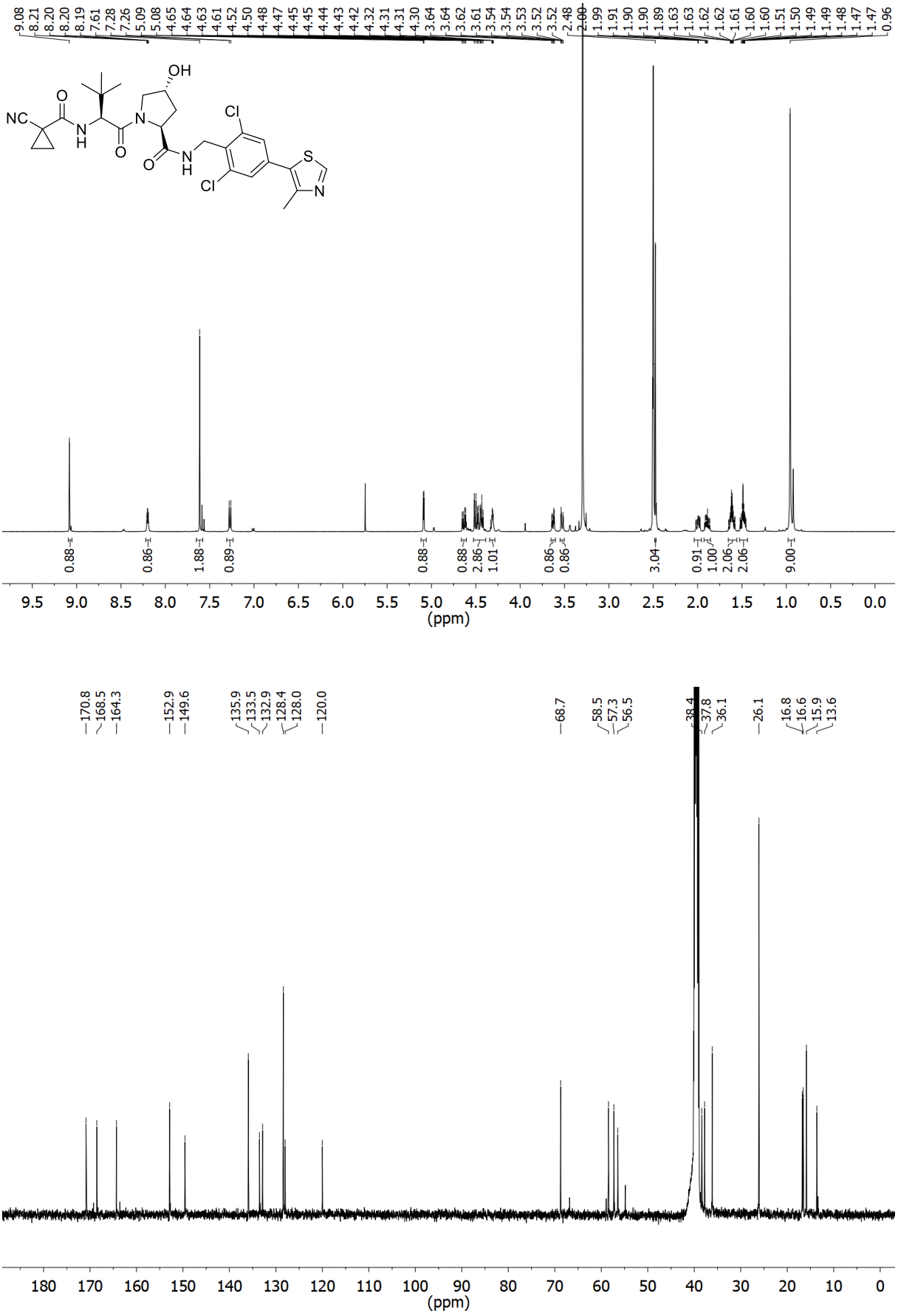

^{1}H and ^{13}C NMR spectra of compound **14**

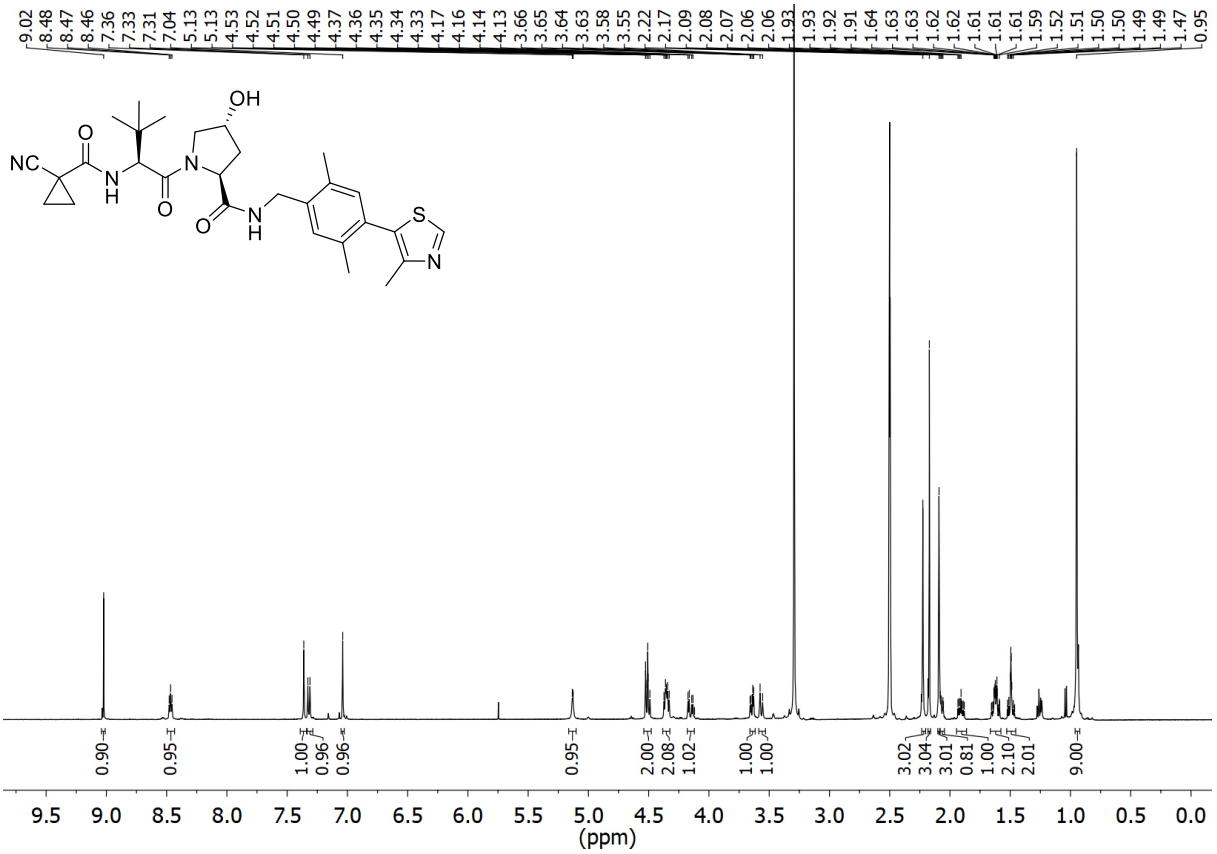

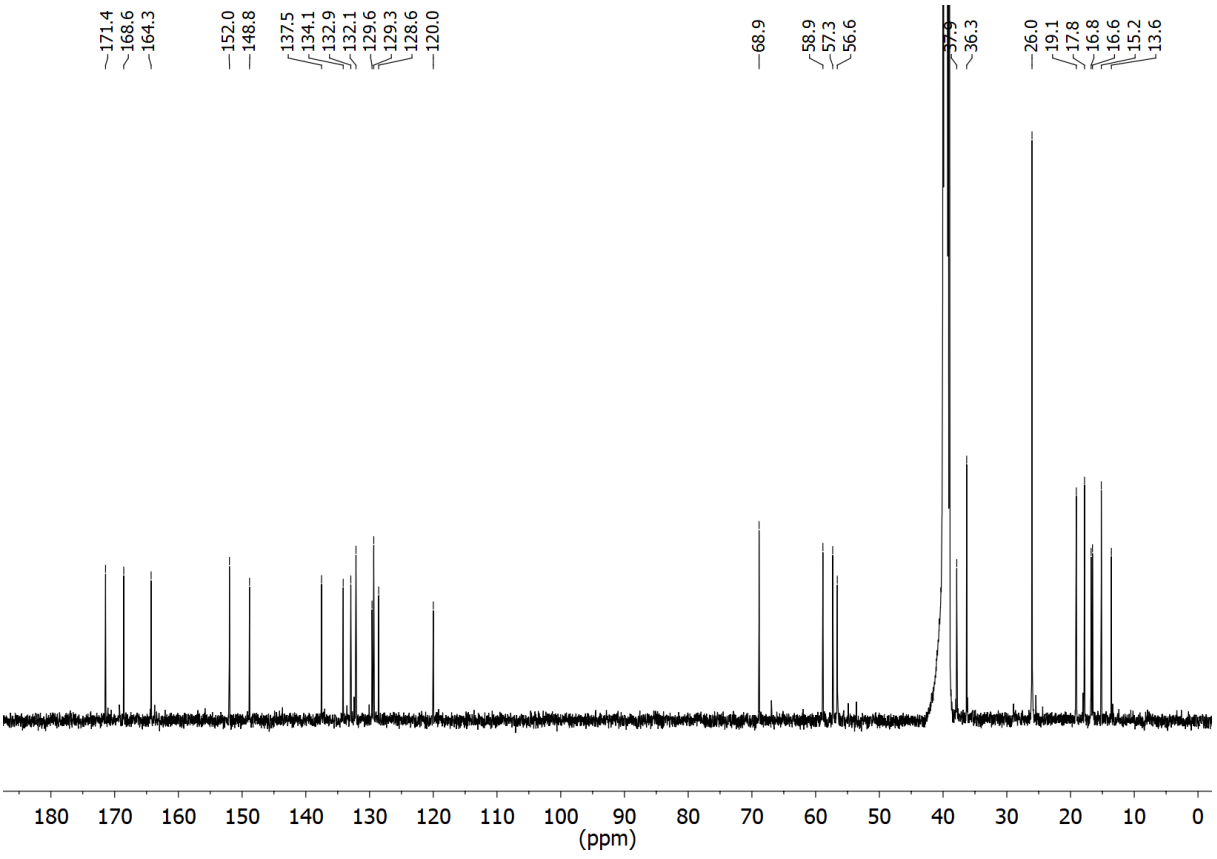

^{1}H and ^{13}C NMR spectra of compound **15**

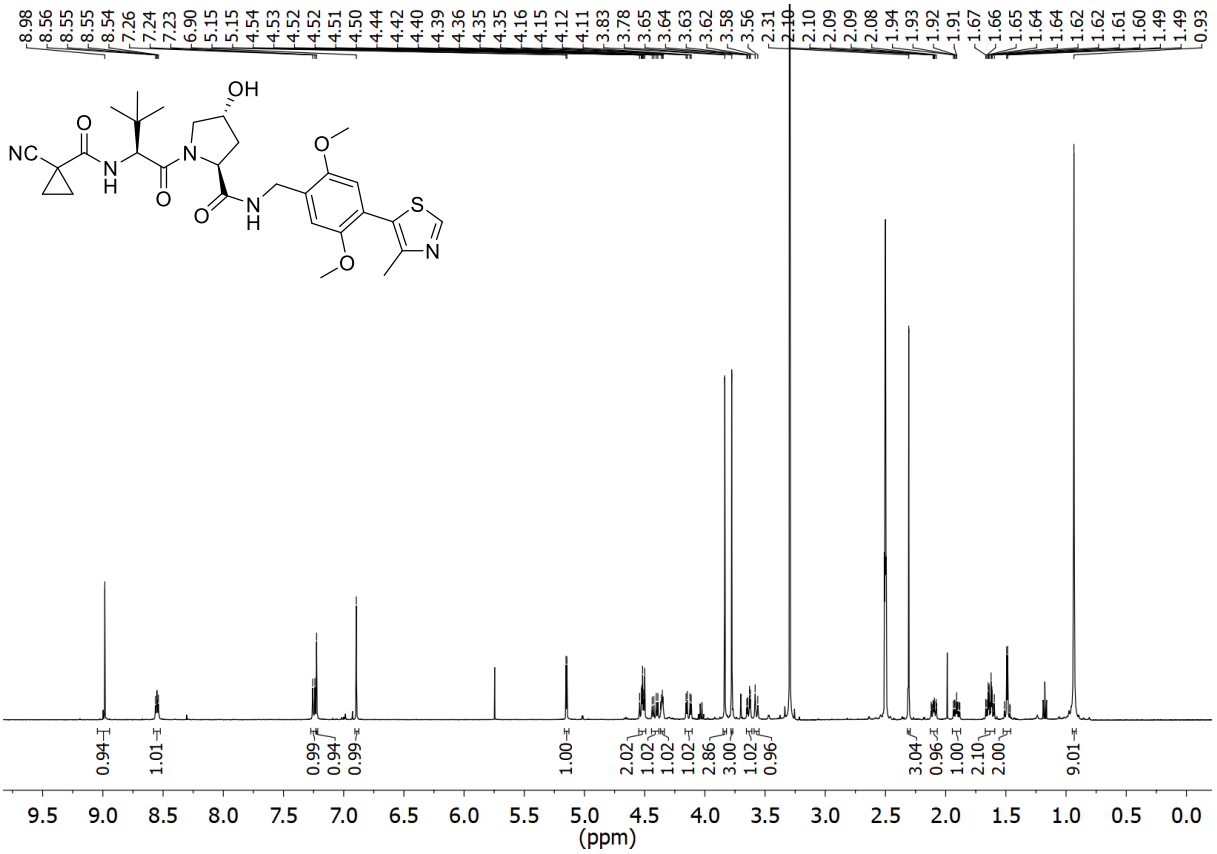

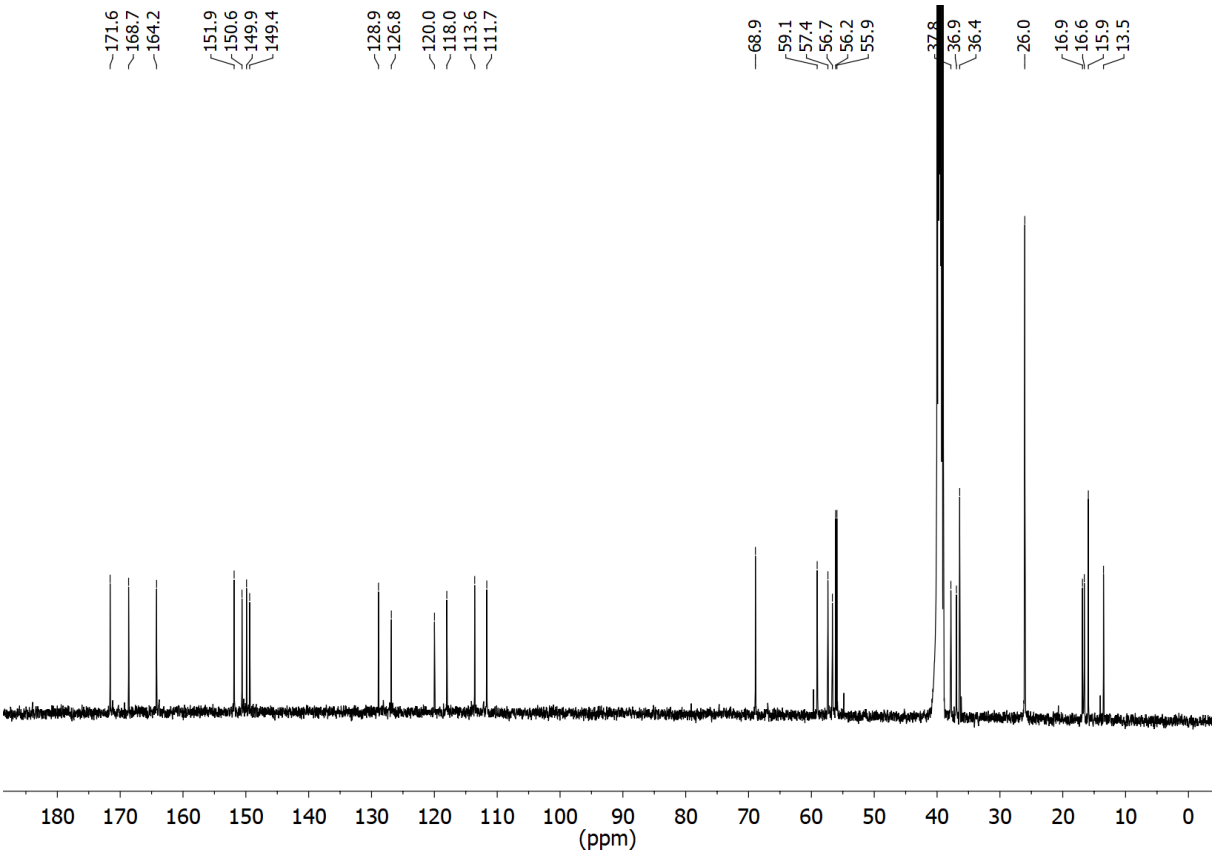

^{1}H and ^{13}C NMR spectra of compound **16**

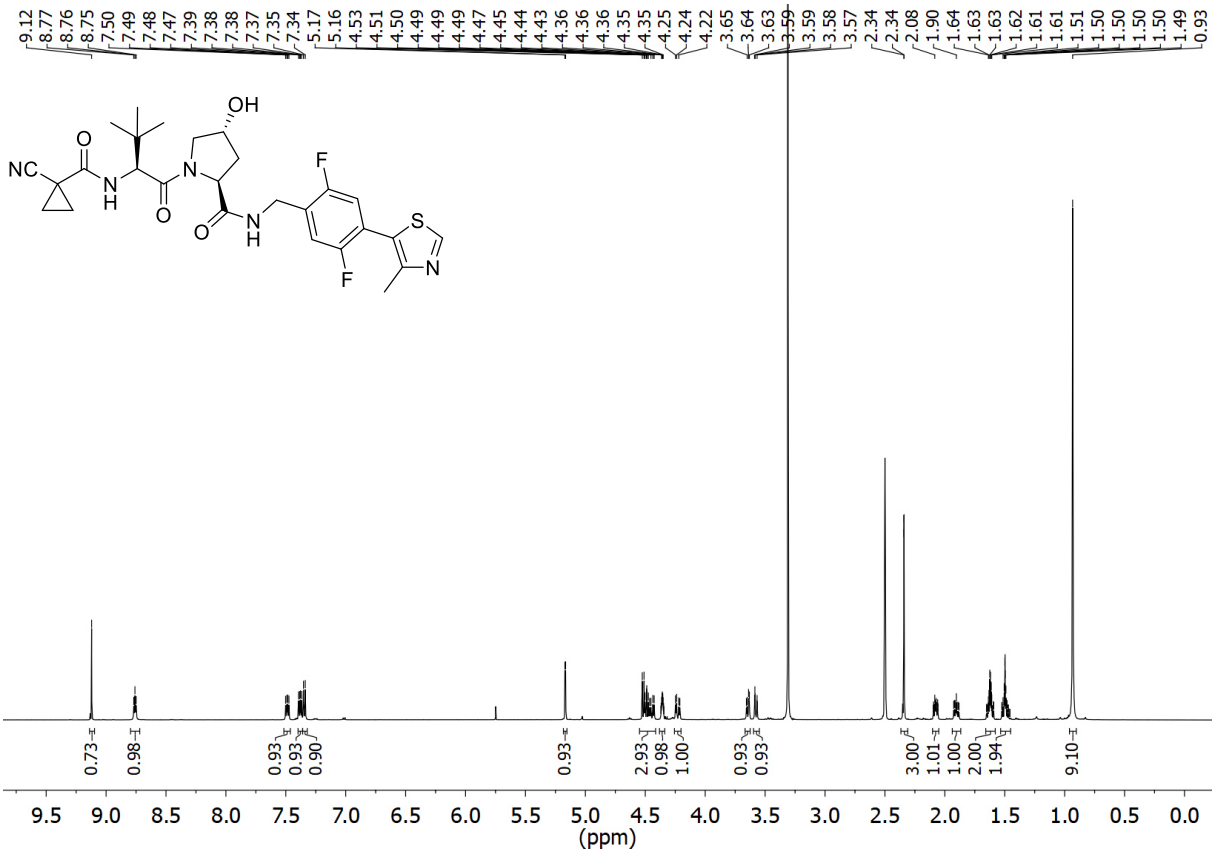

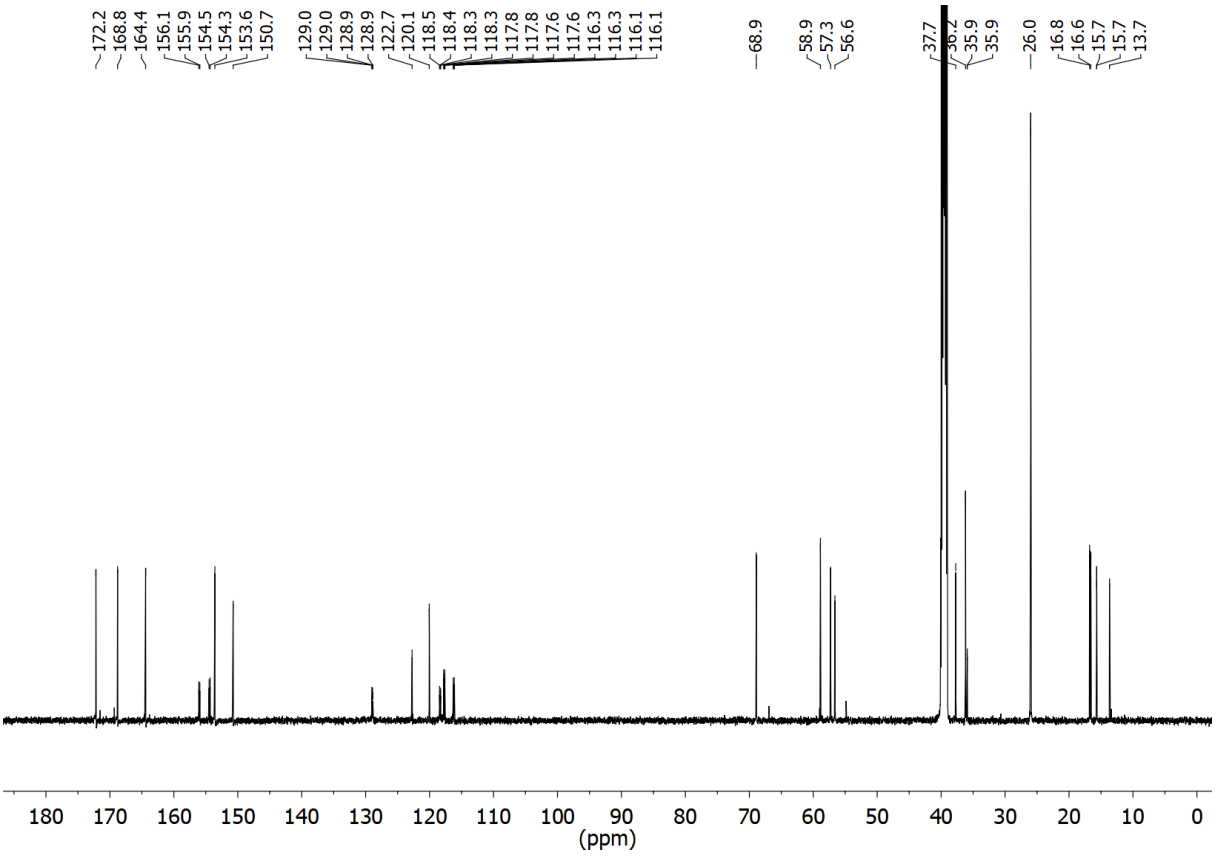

^{1}H and ^{13}C NMR spectra of compound **17**

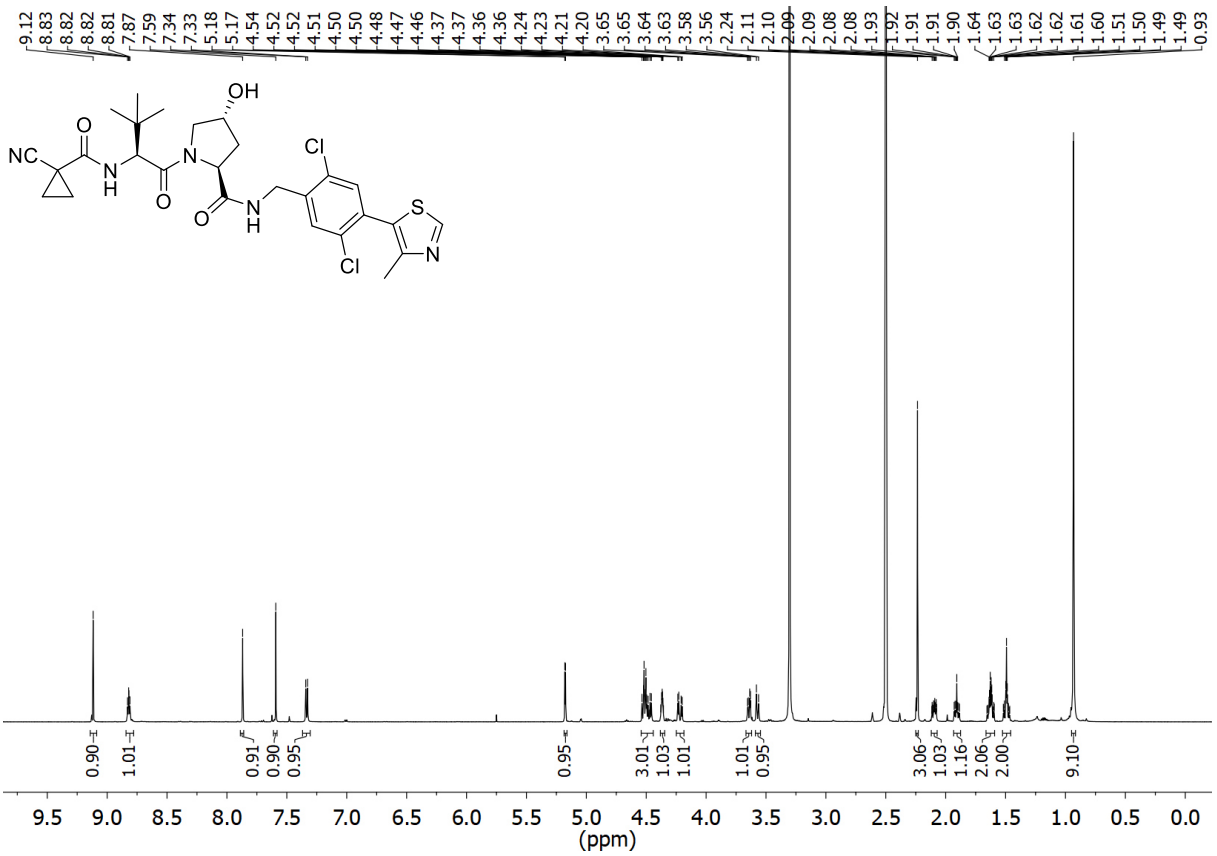

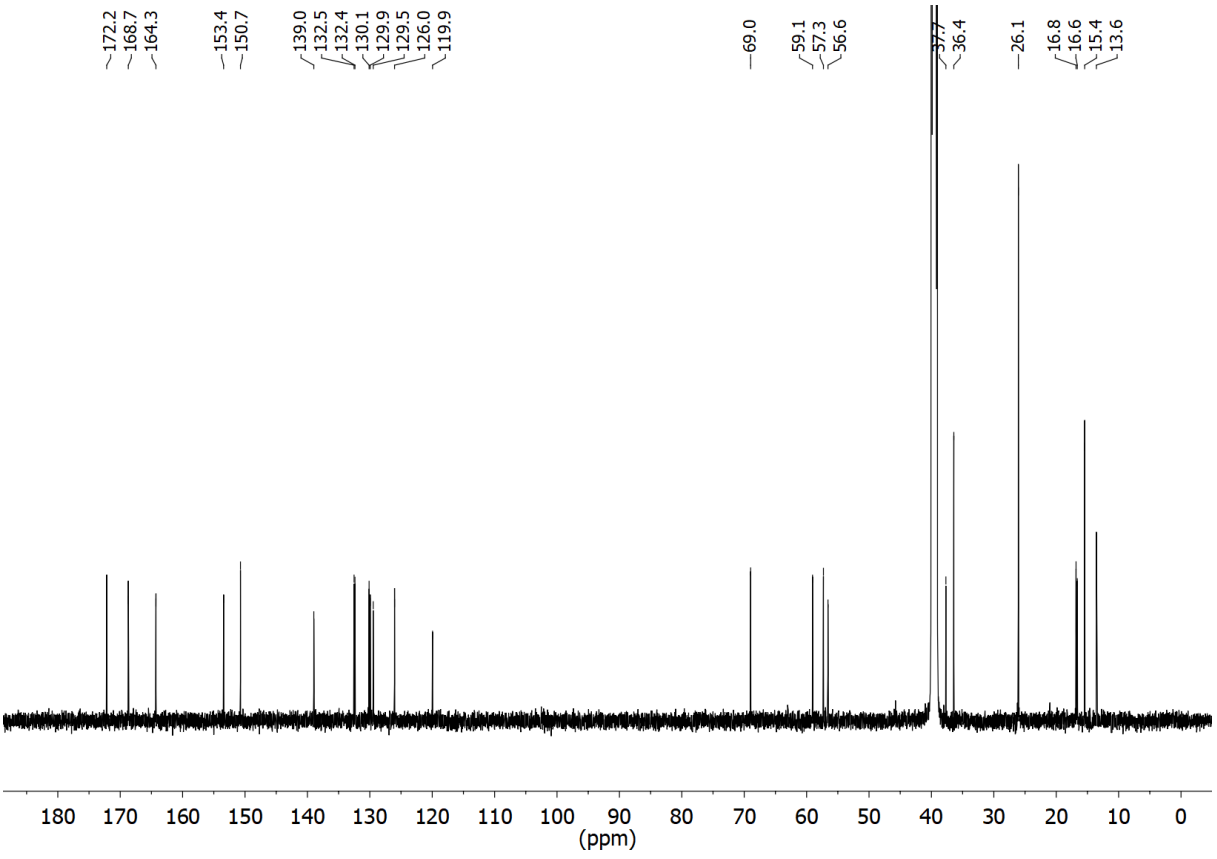

^{1}H and ^{13}C NMR spectra of compound **18**

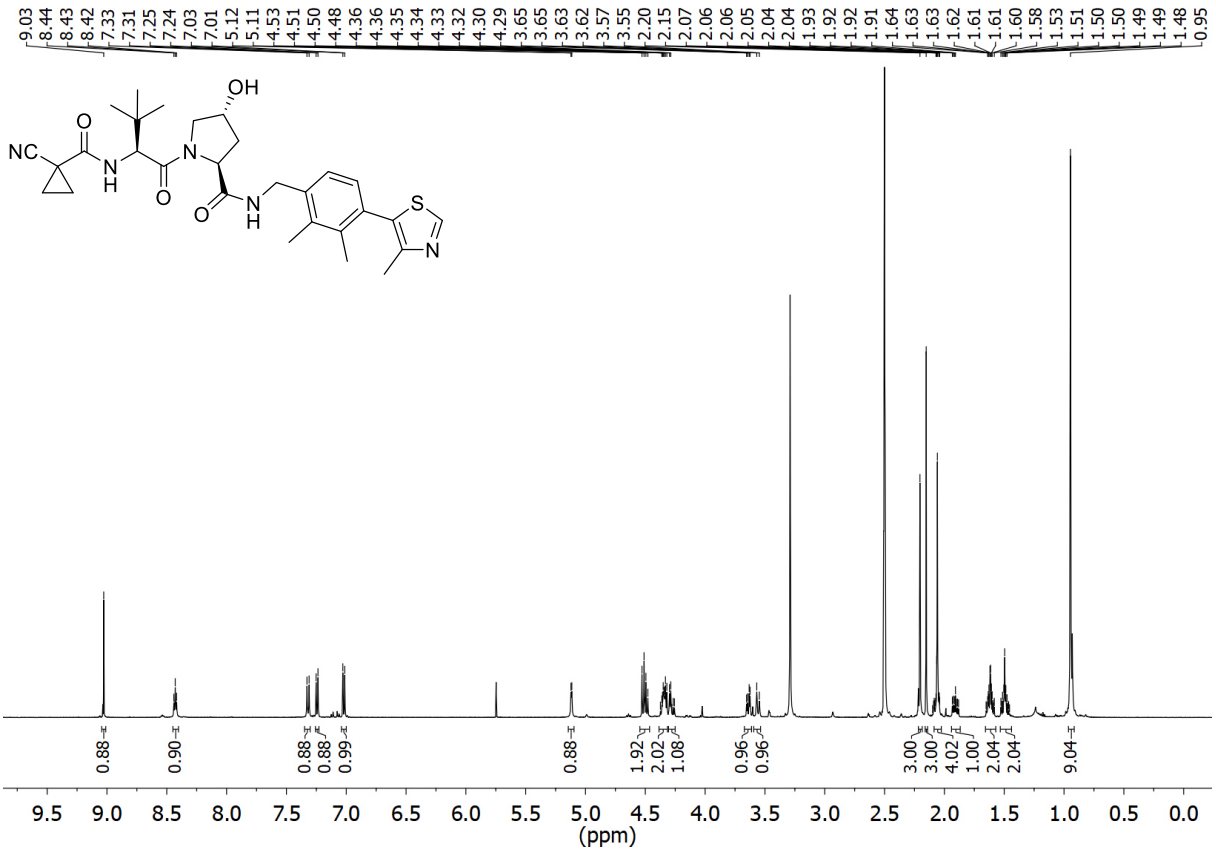

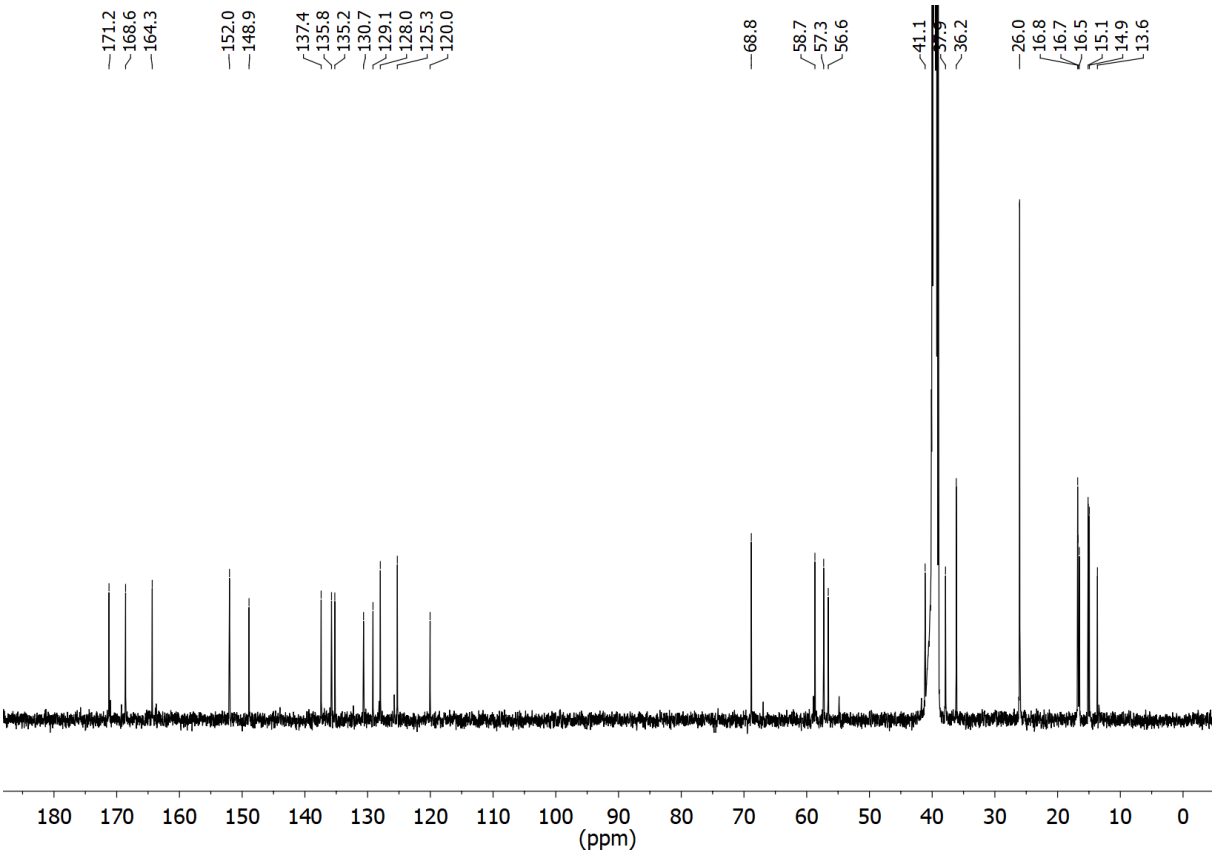

^{1}H and ^{13}C NMR spectra of compound **19**

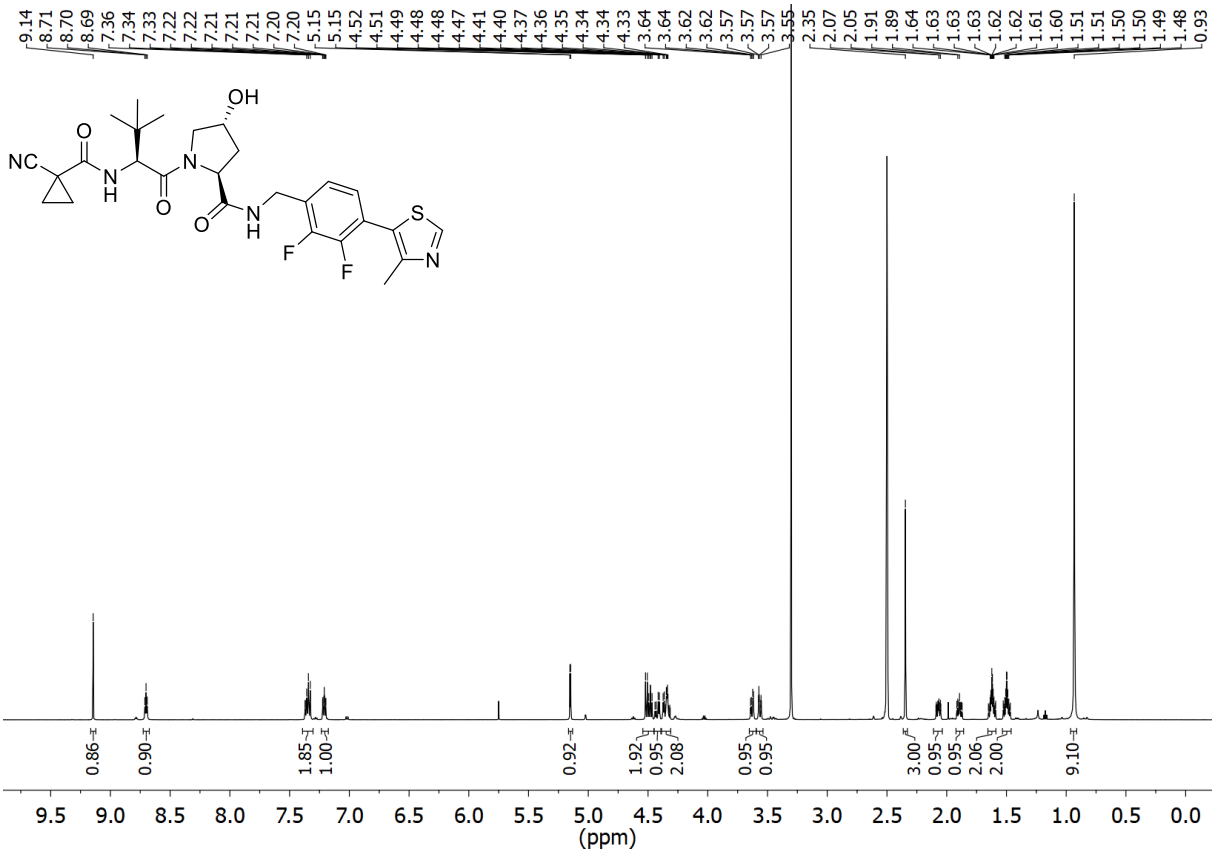

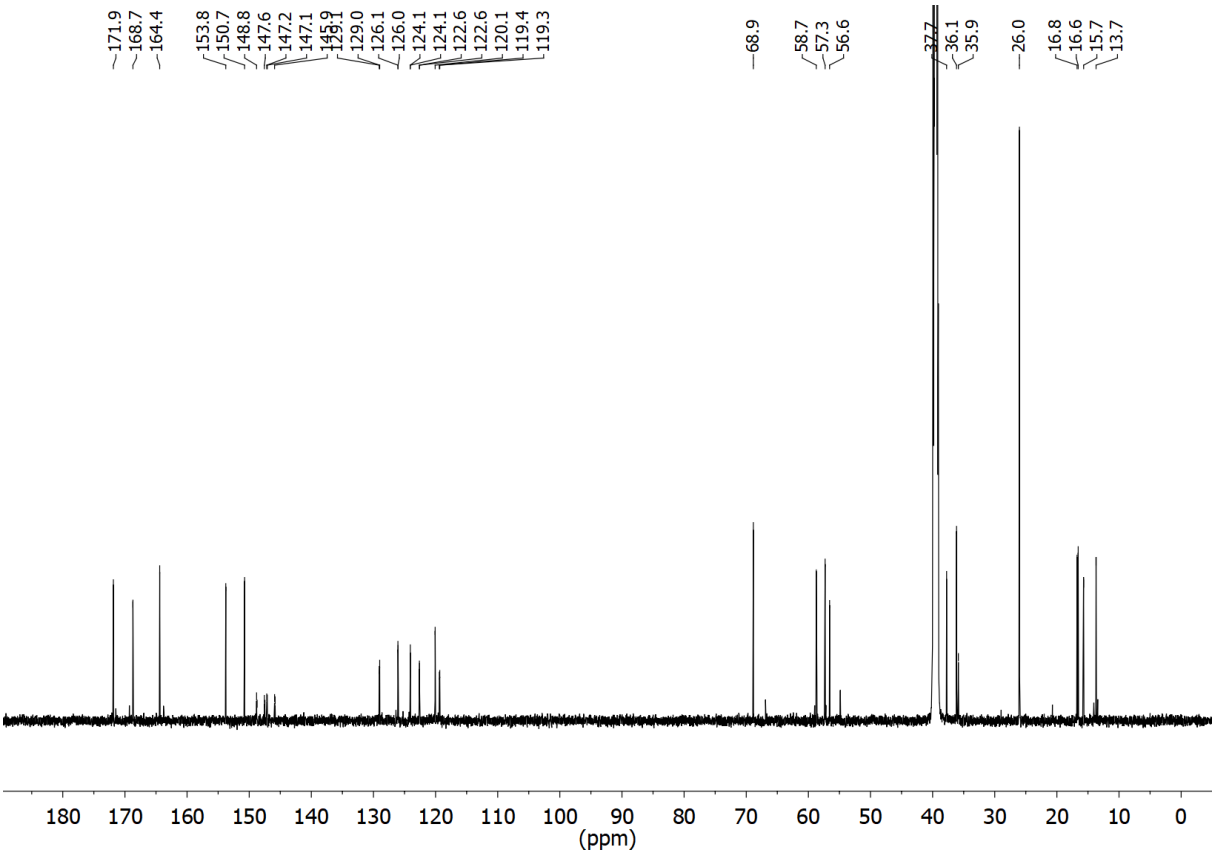

^{1}H and ^{13}C NMR spectra of compound **20**

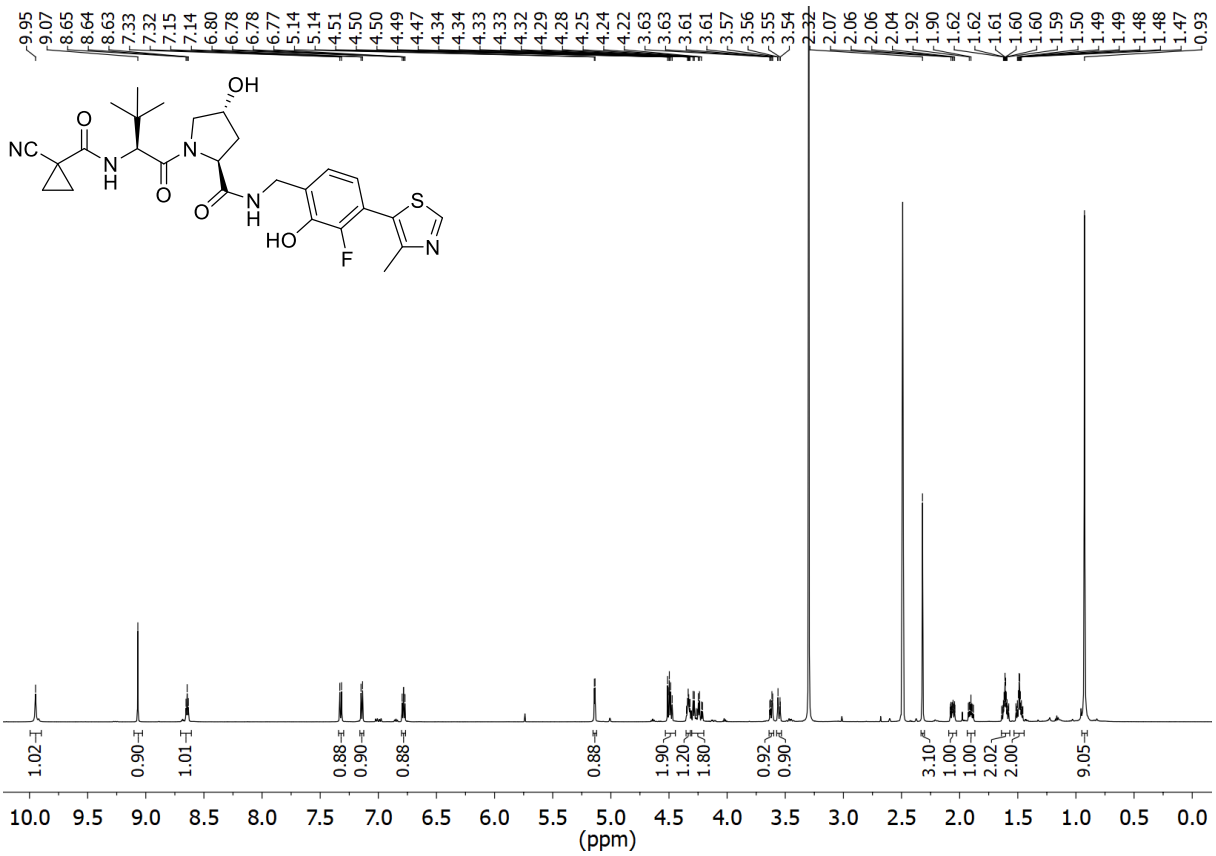

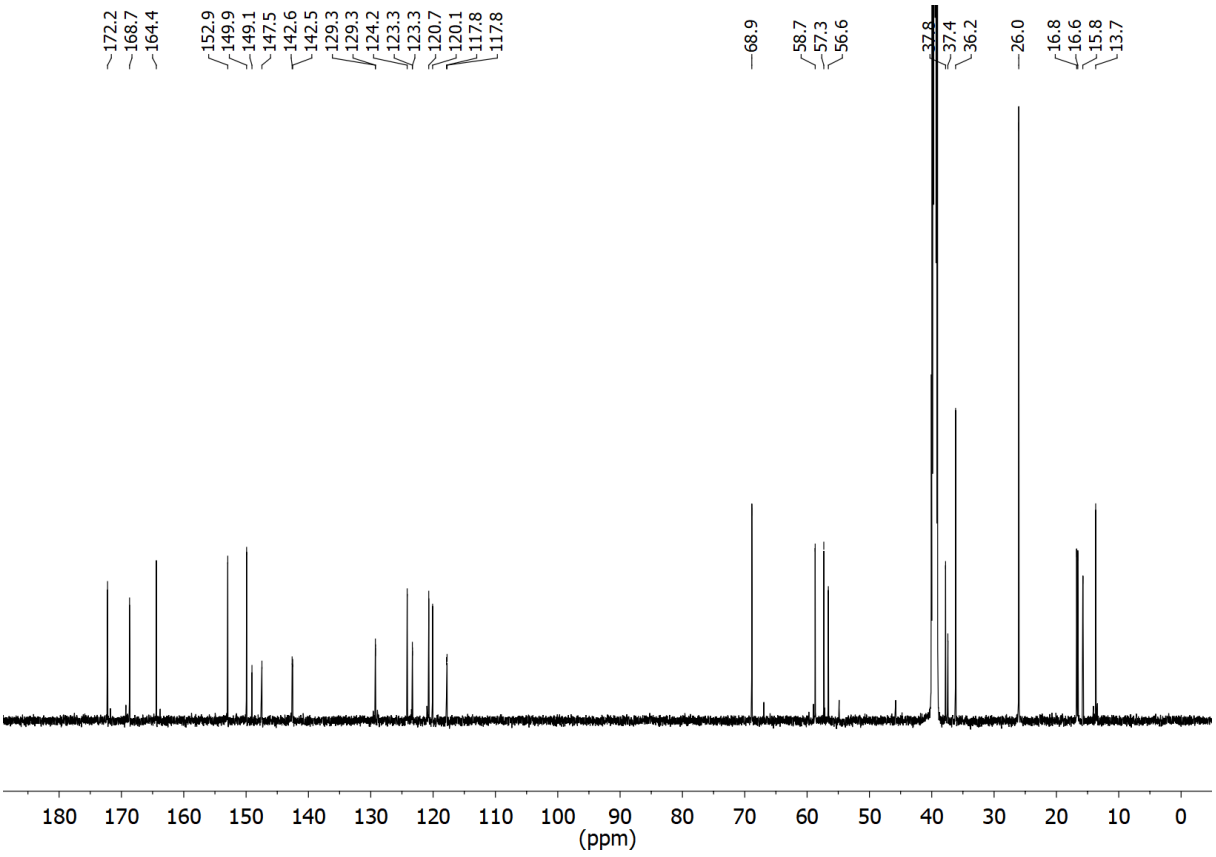

^{1}H and ^{13}C NMR spectra of compound **21**

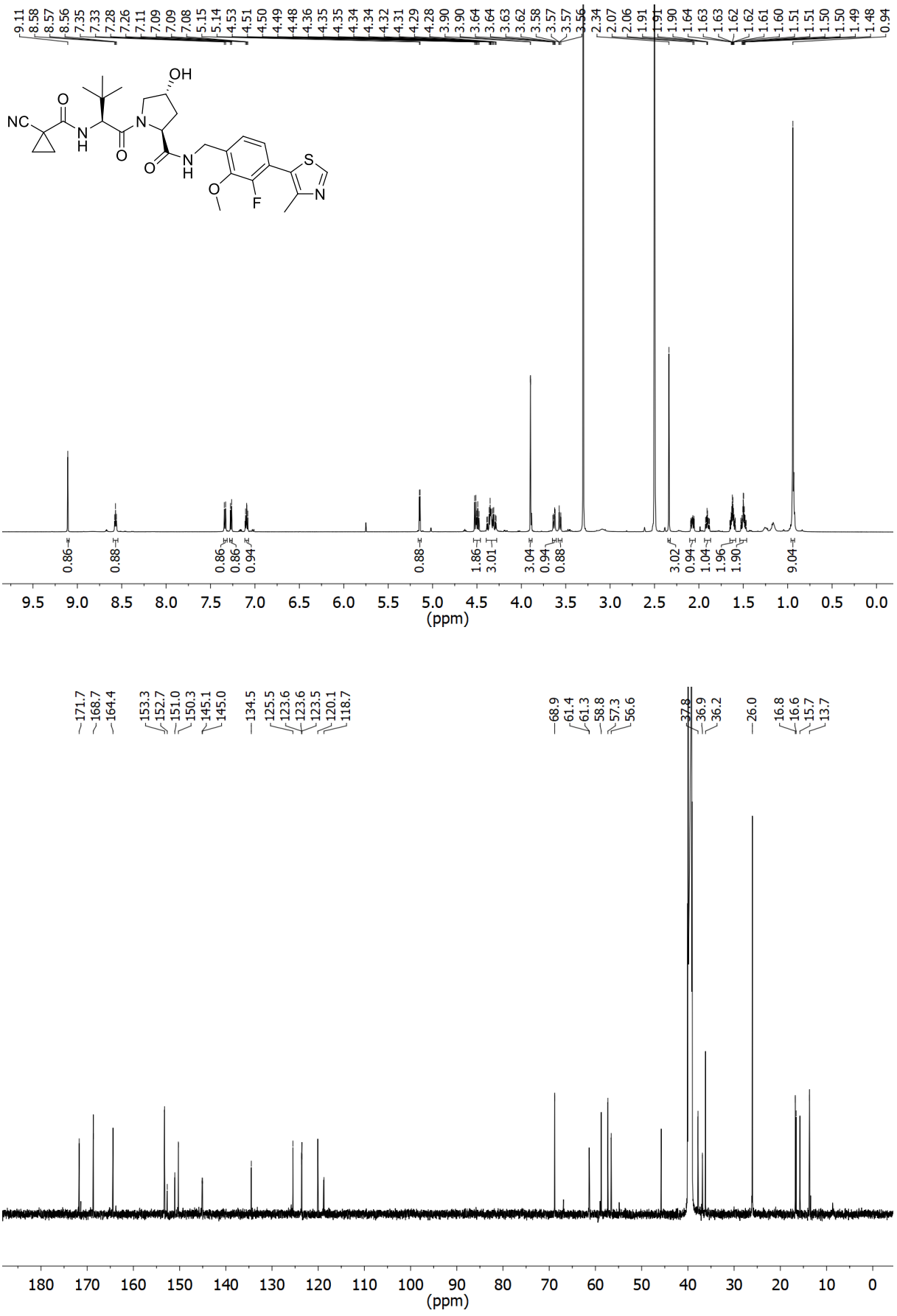

^{1}H and ^{13}C NMR spectra of compound **22**

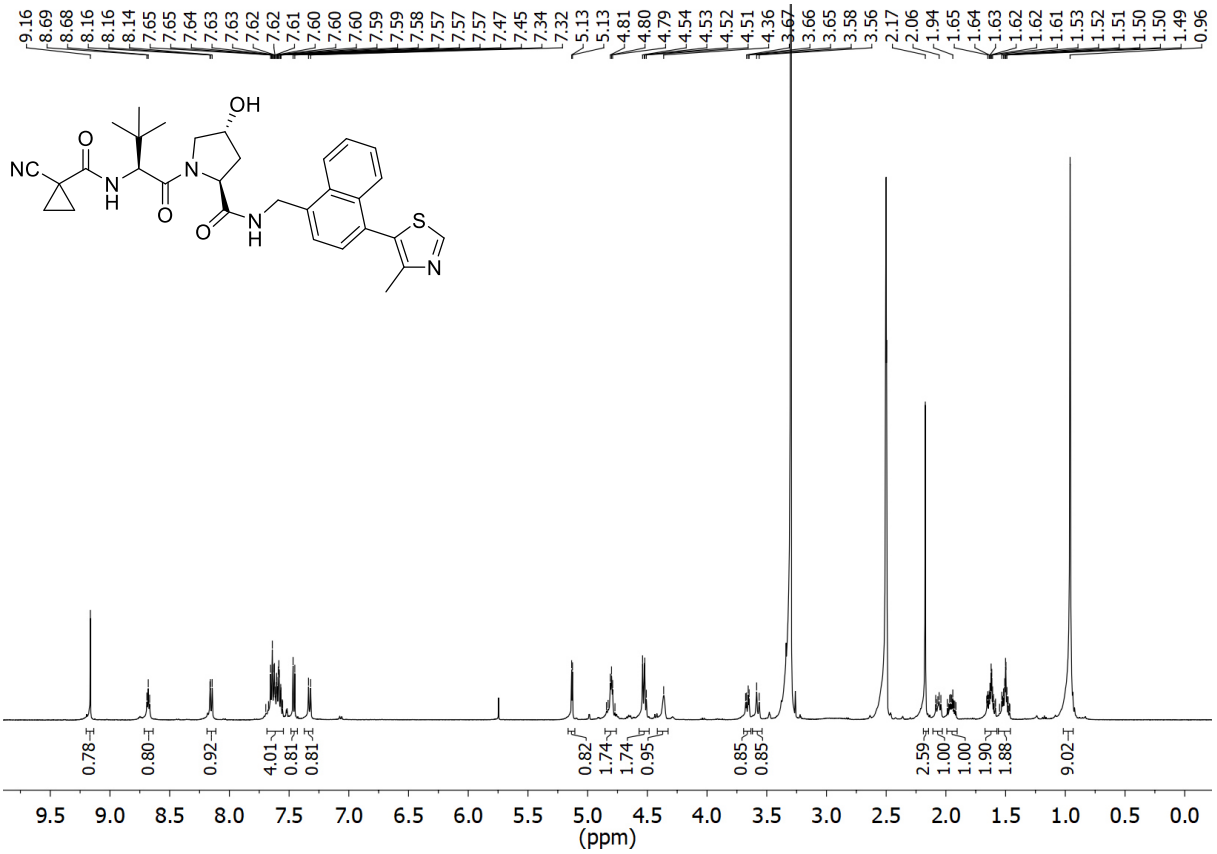

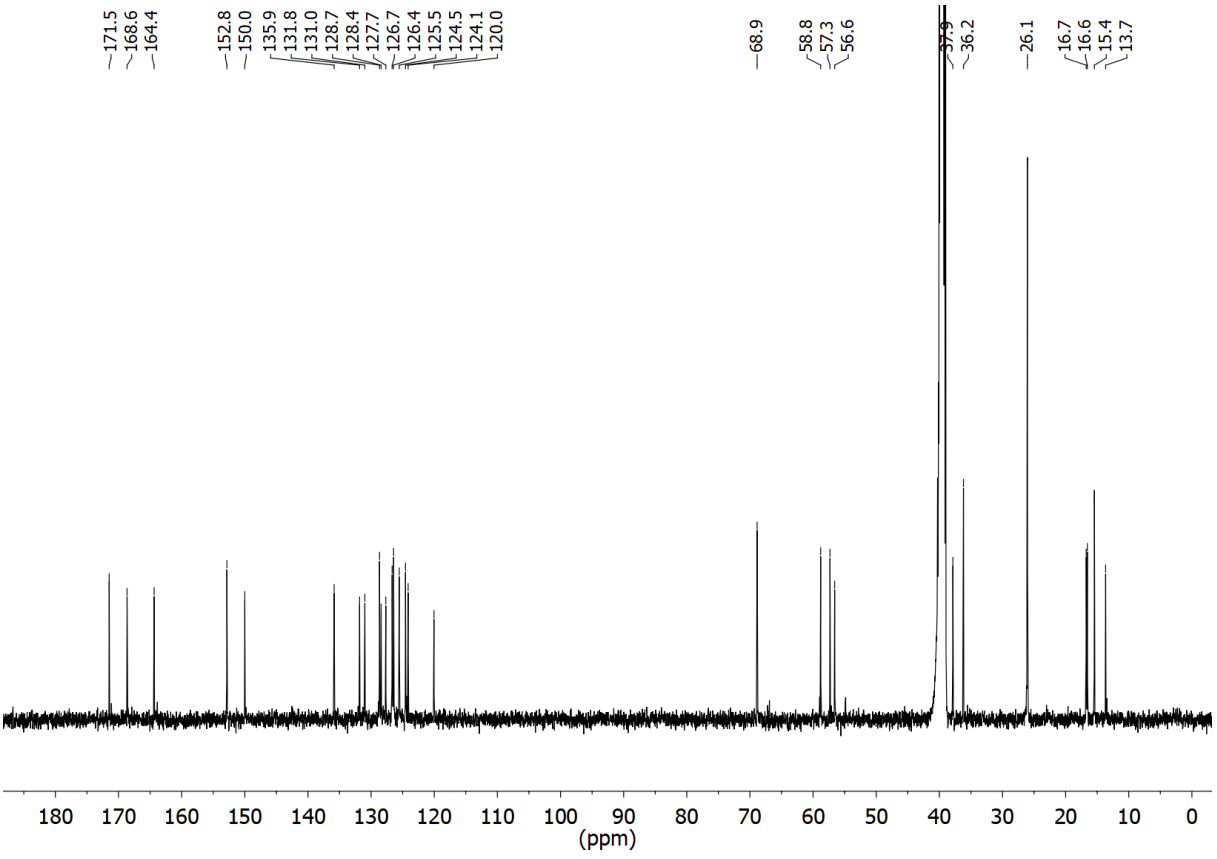

^{1}H and ^{13}C NMR spectra of compound **23**

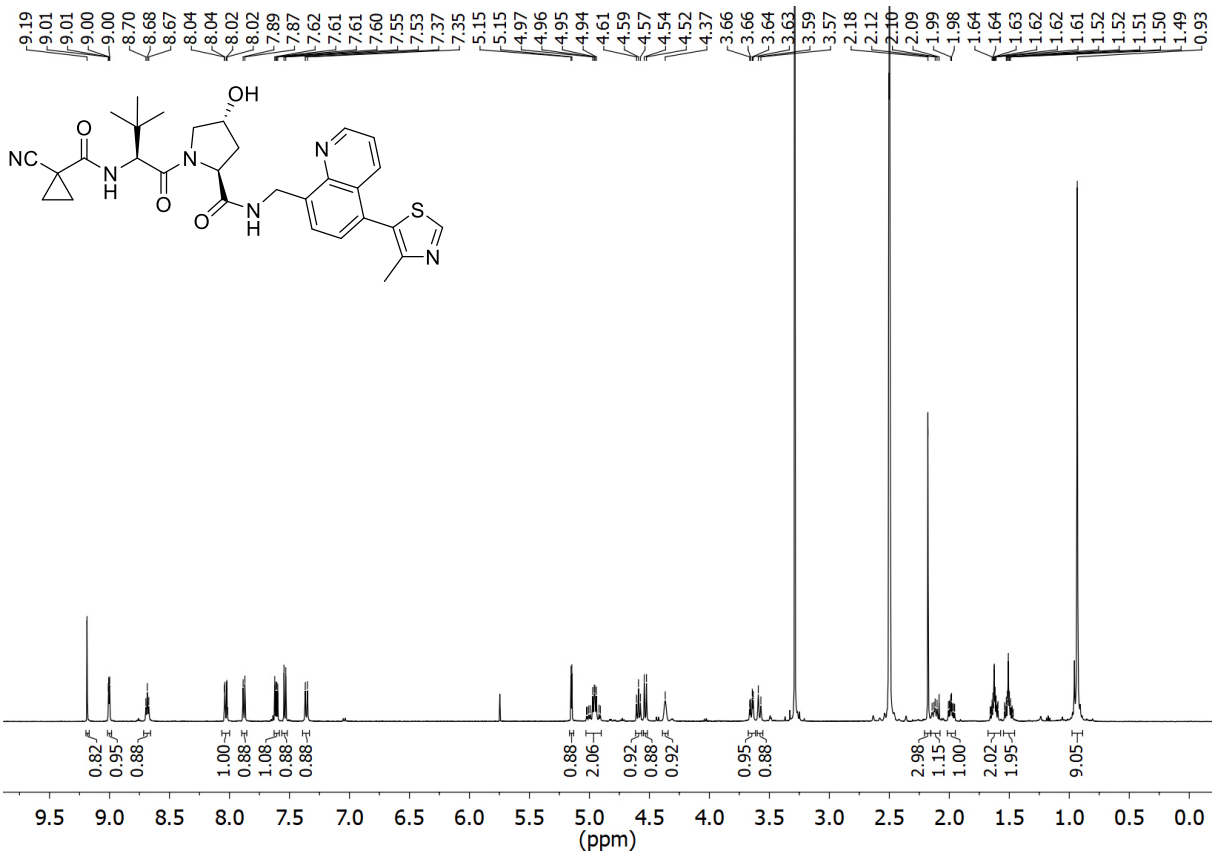

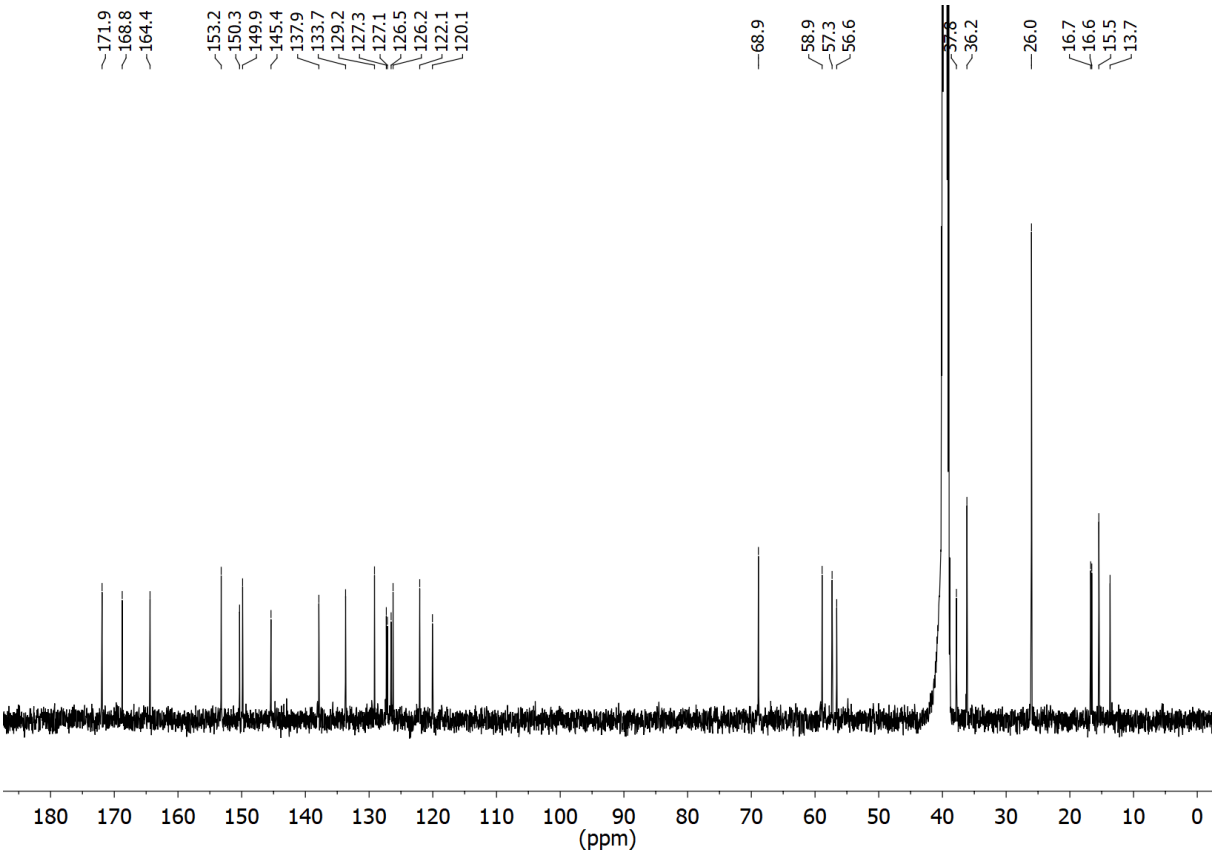

^{1}H and ^{13}C NMR spectra of compound **24**

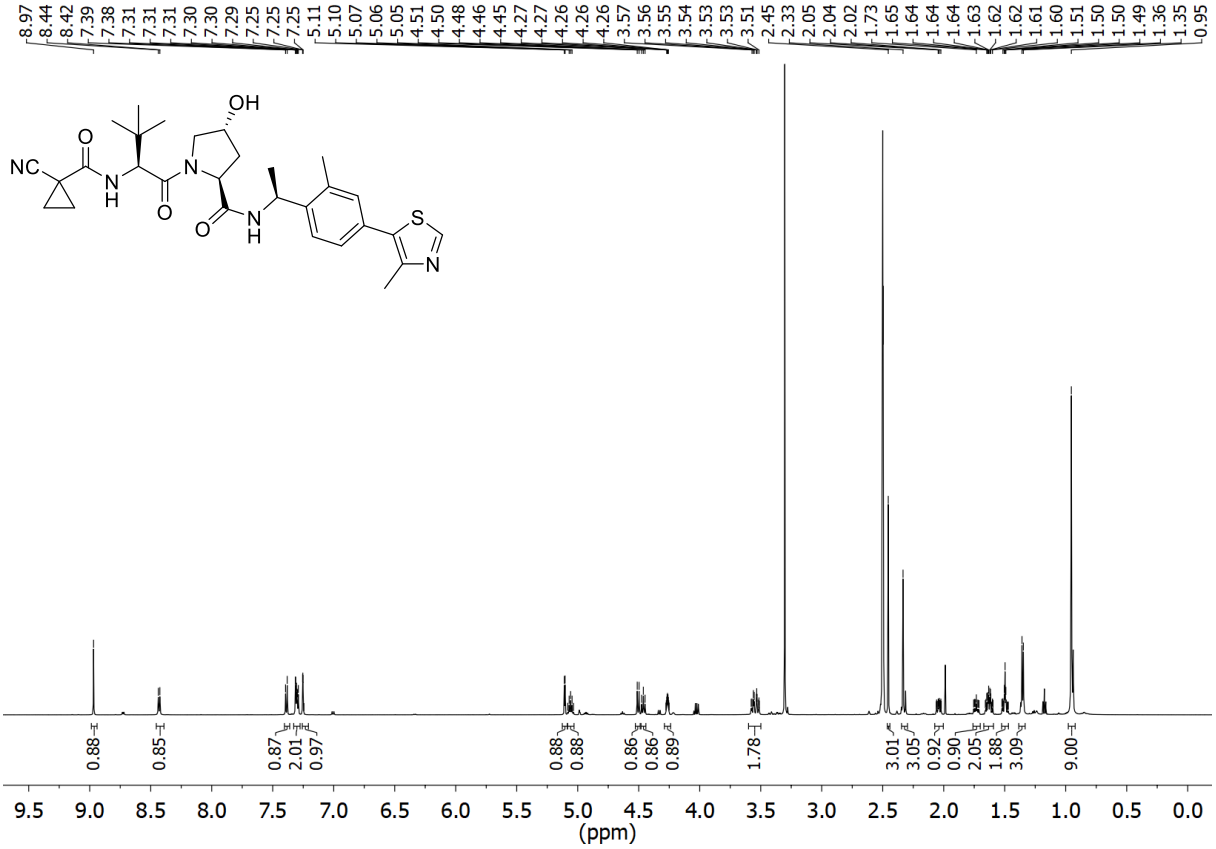

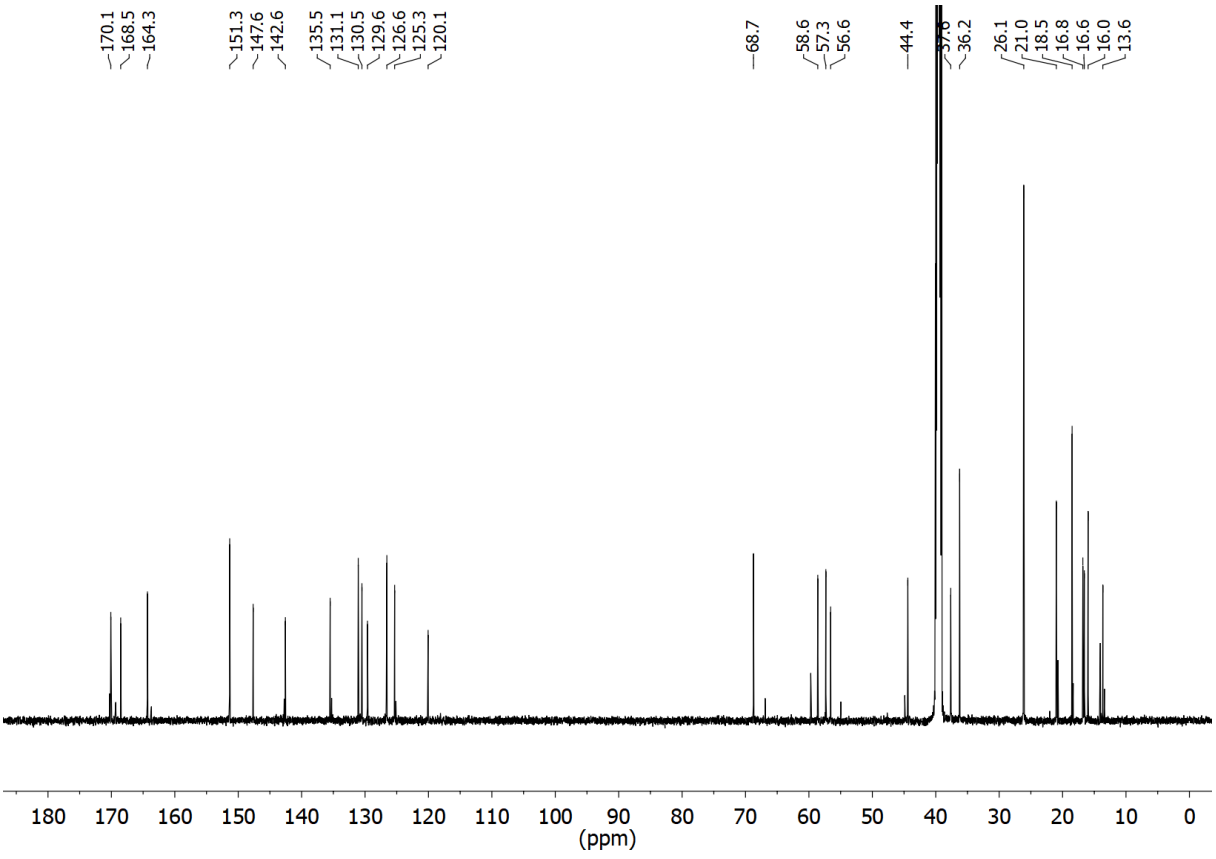

^{1}H and ^{13}C NMR spectra of compound **25**

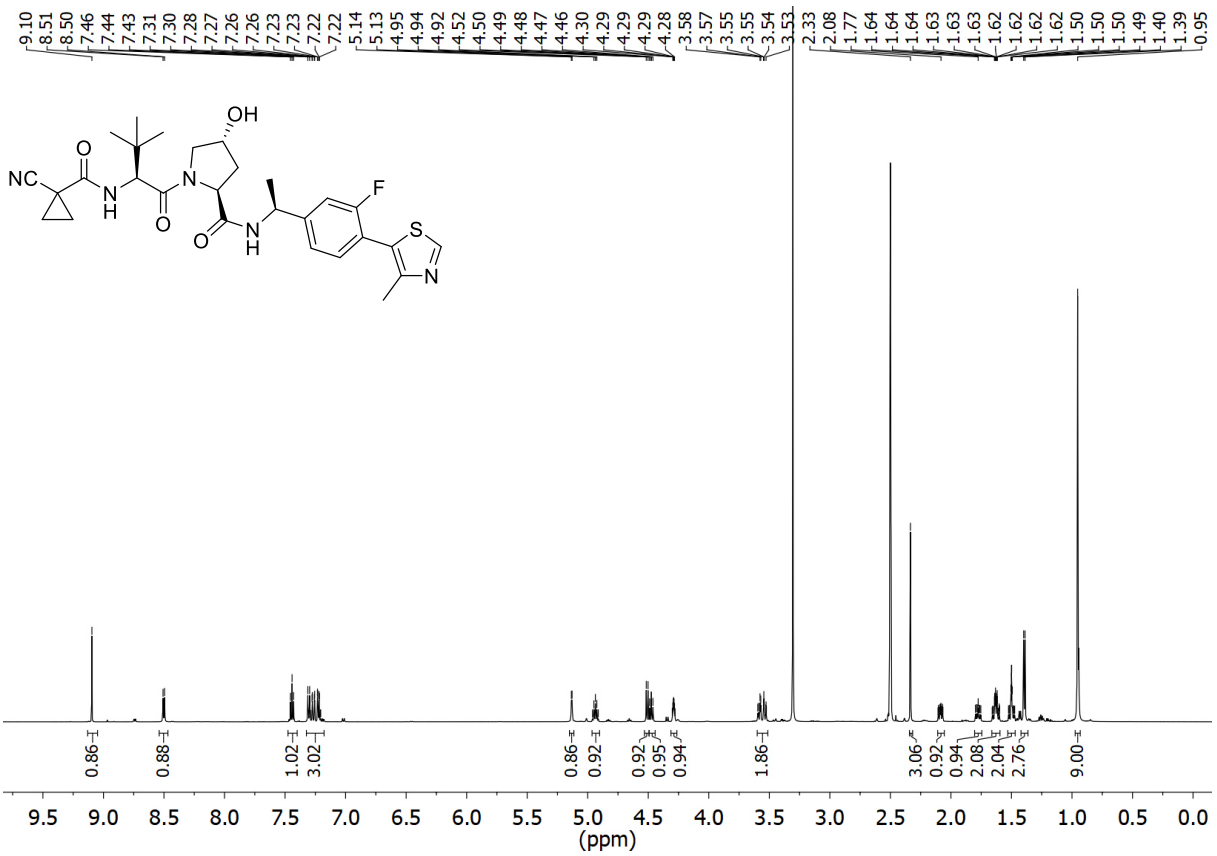

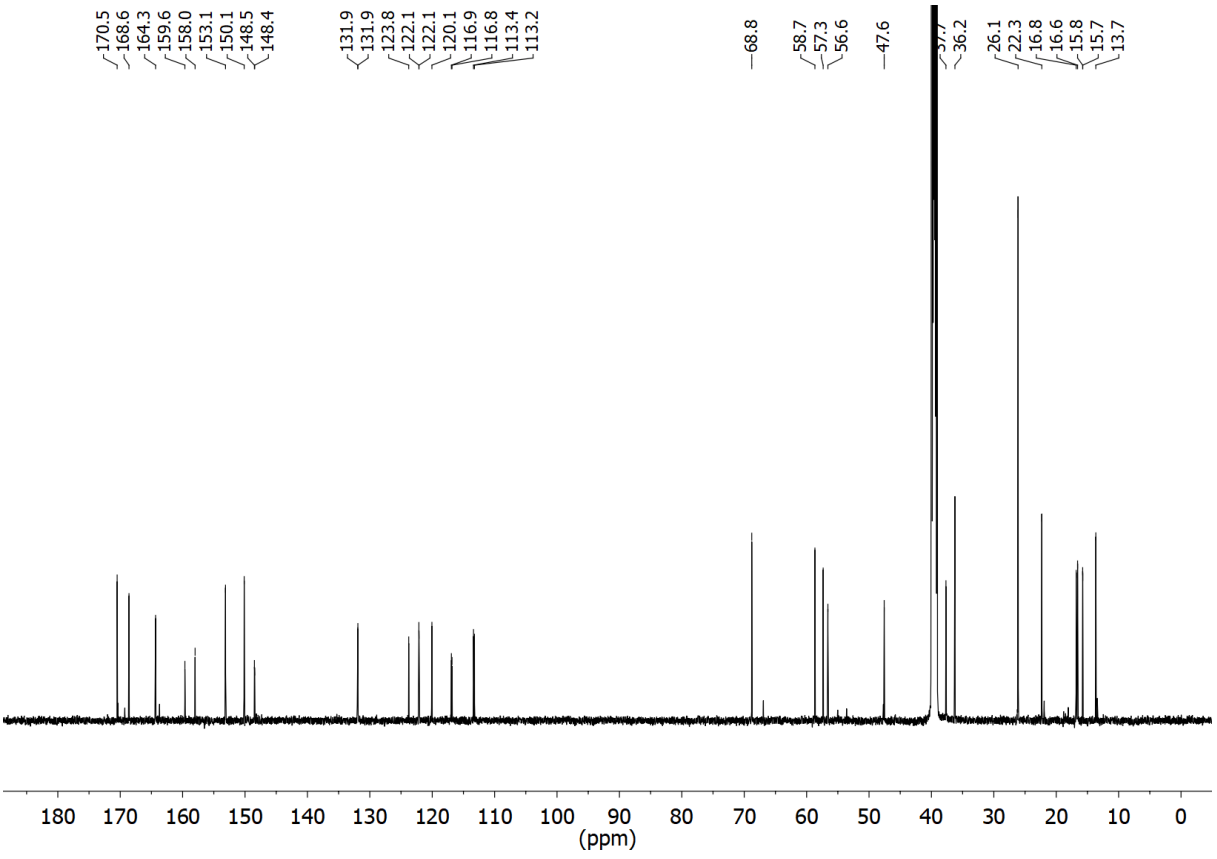

^{1}H and ^{13}C NMR spectra of compound **26**

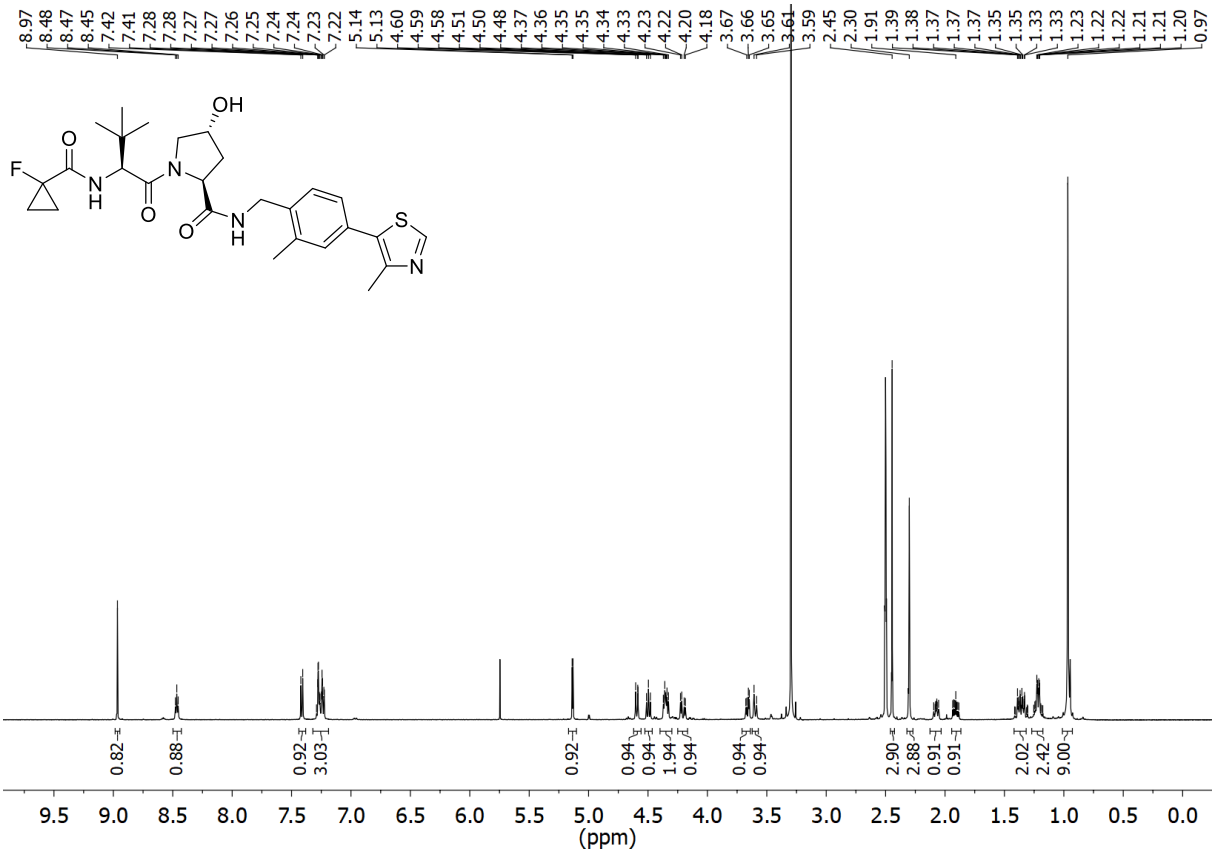

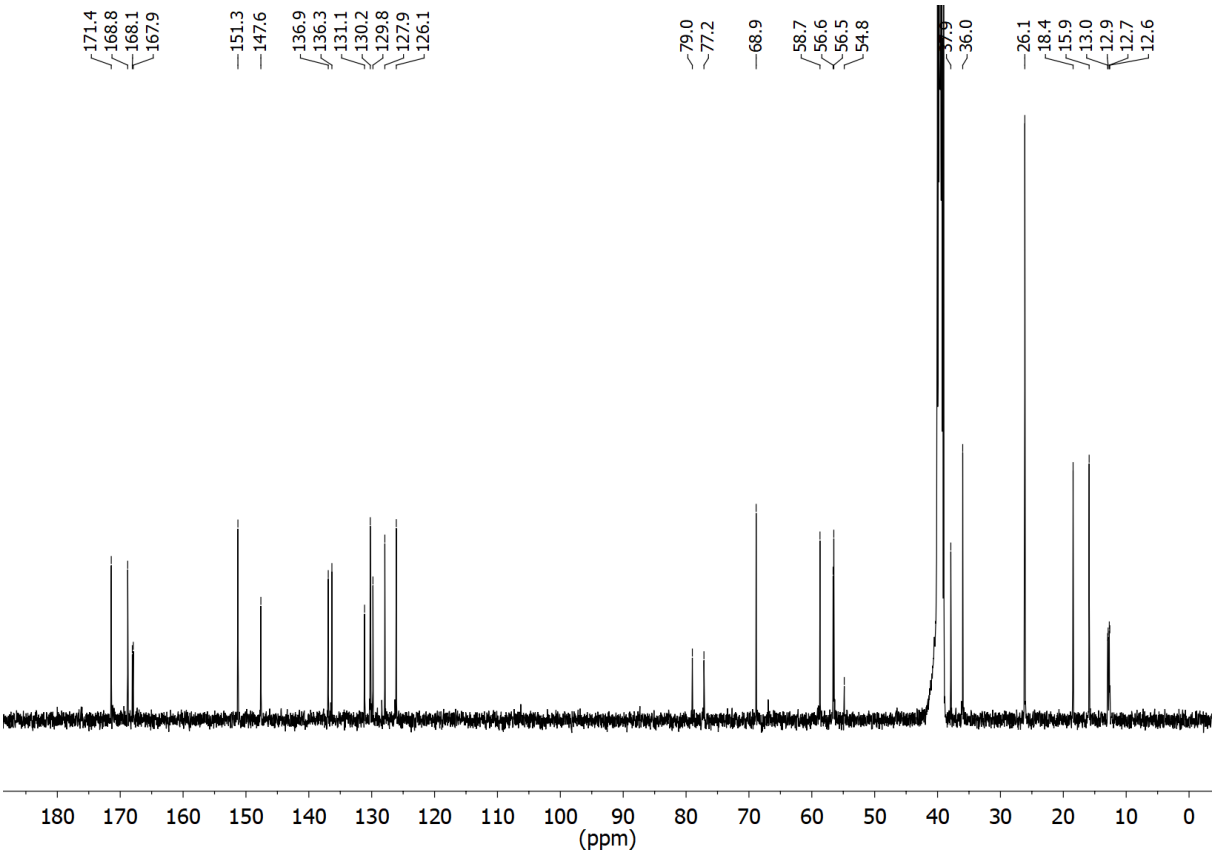

^{1}H and ^{13}C NMR spectra of compound **27**

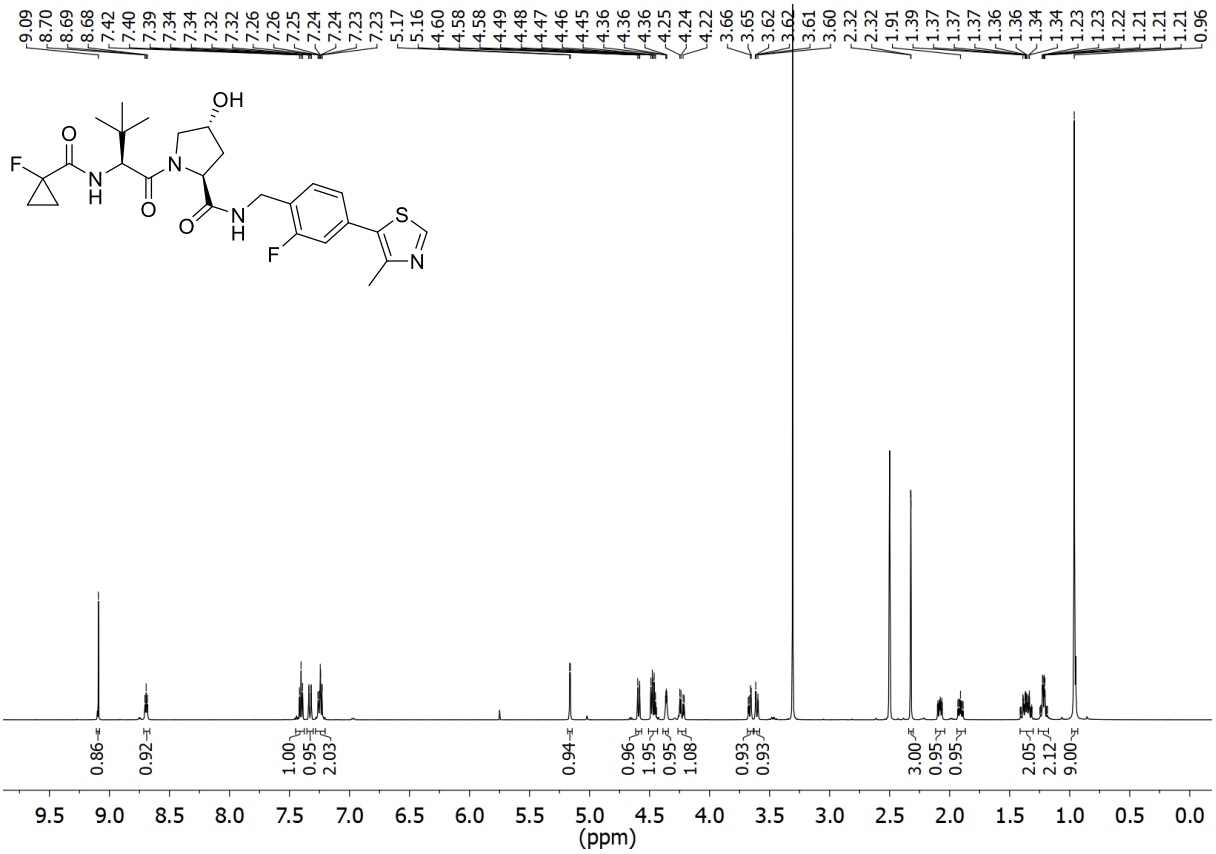

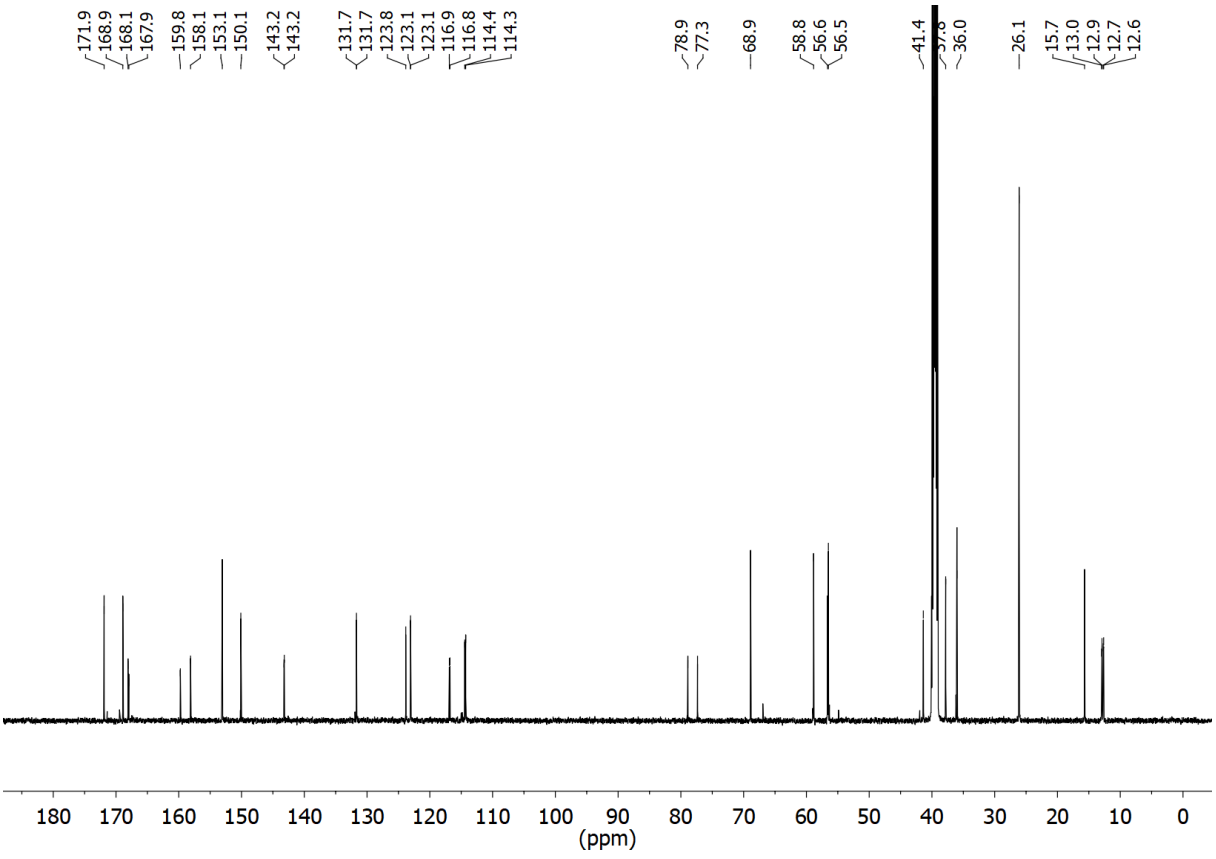

^{1}H and ^{13}C NMR spectra of compound **28**

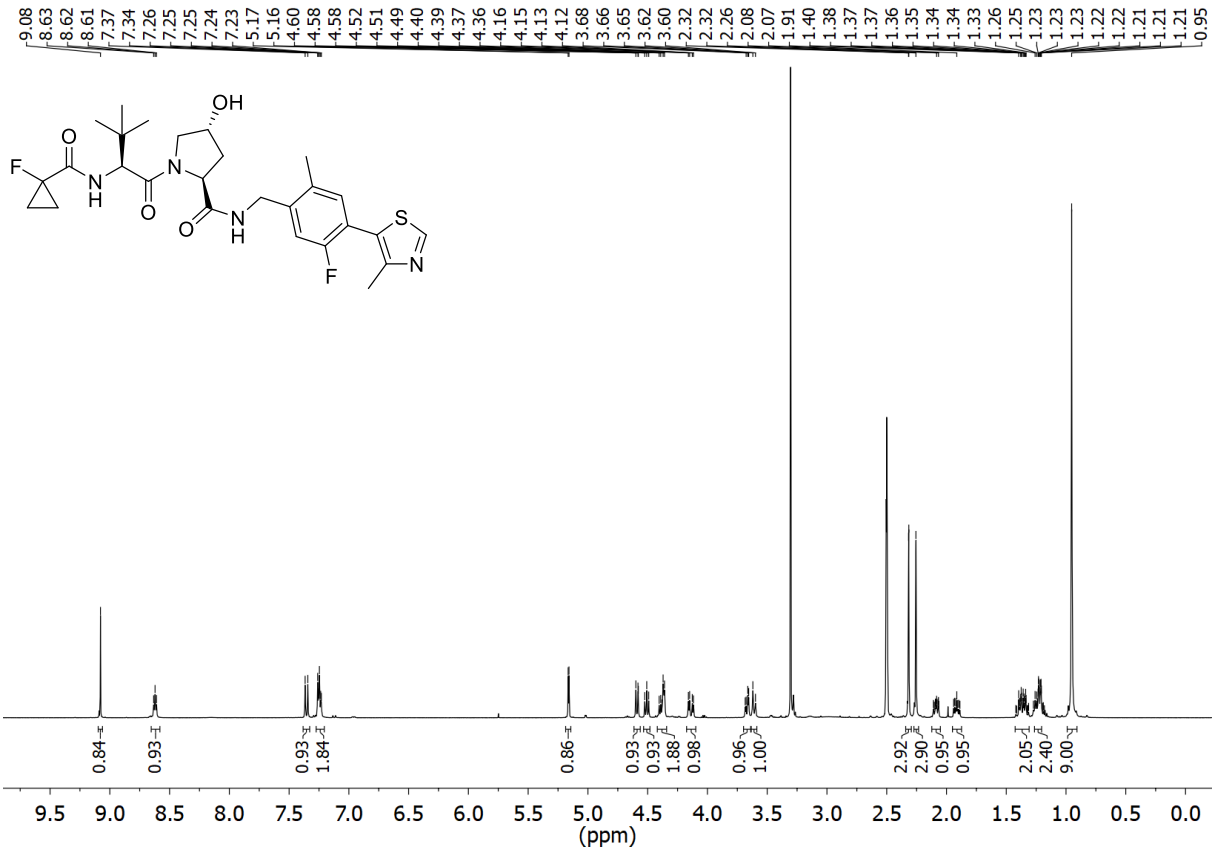

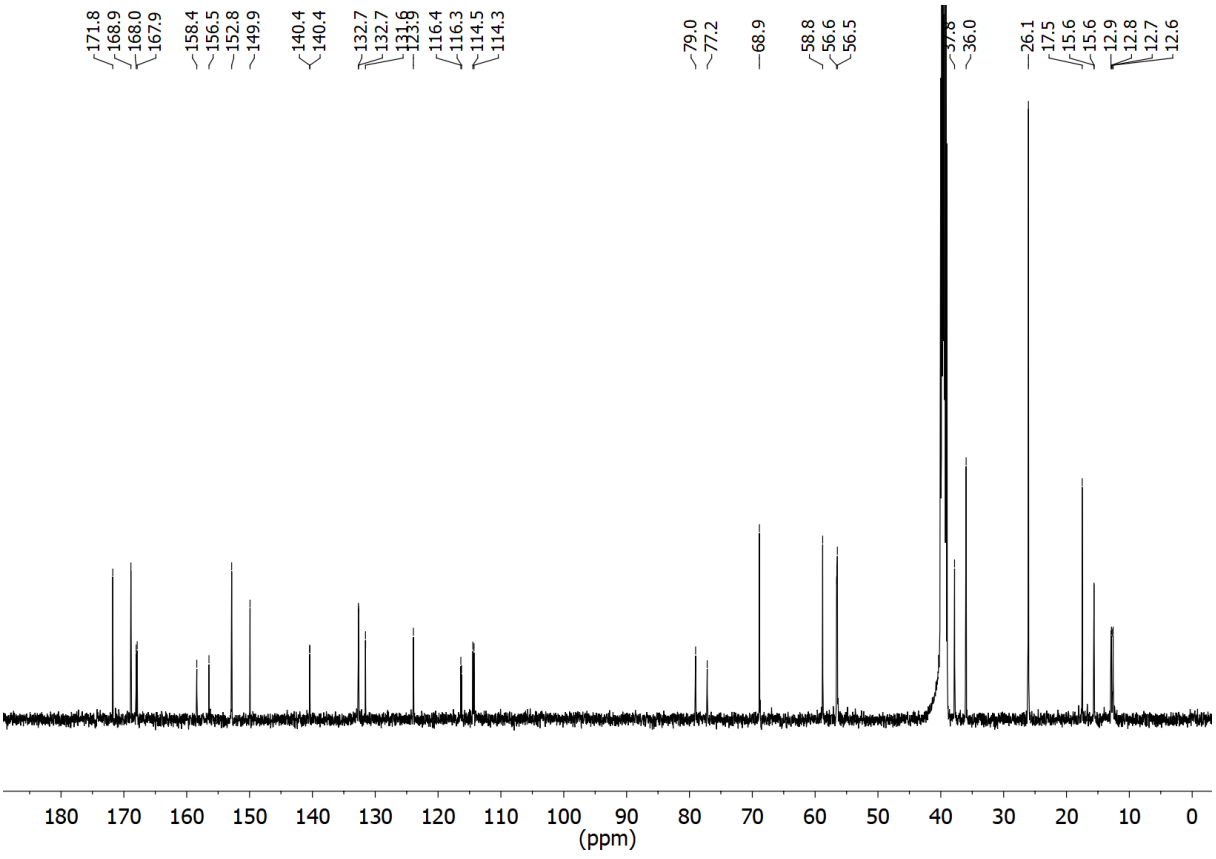

^{1}H and ^{13}C NMR spectra of compound **29**

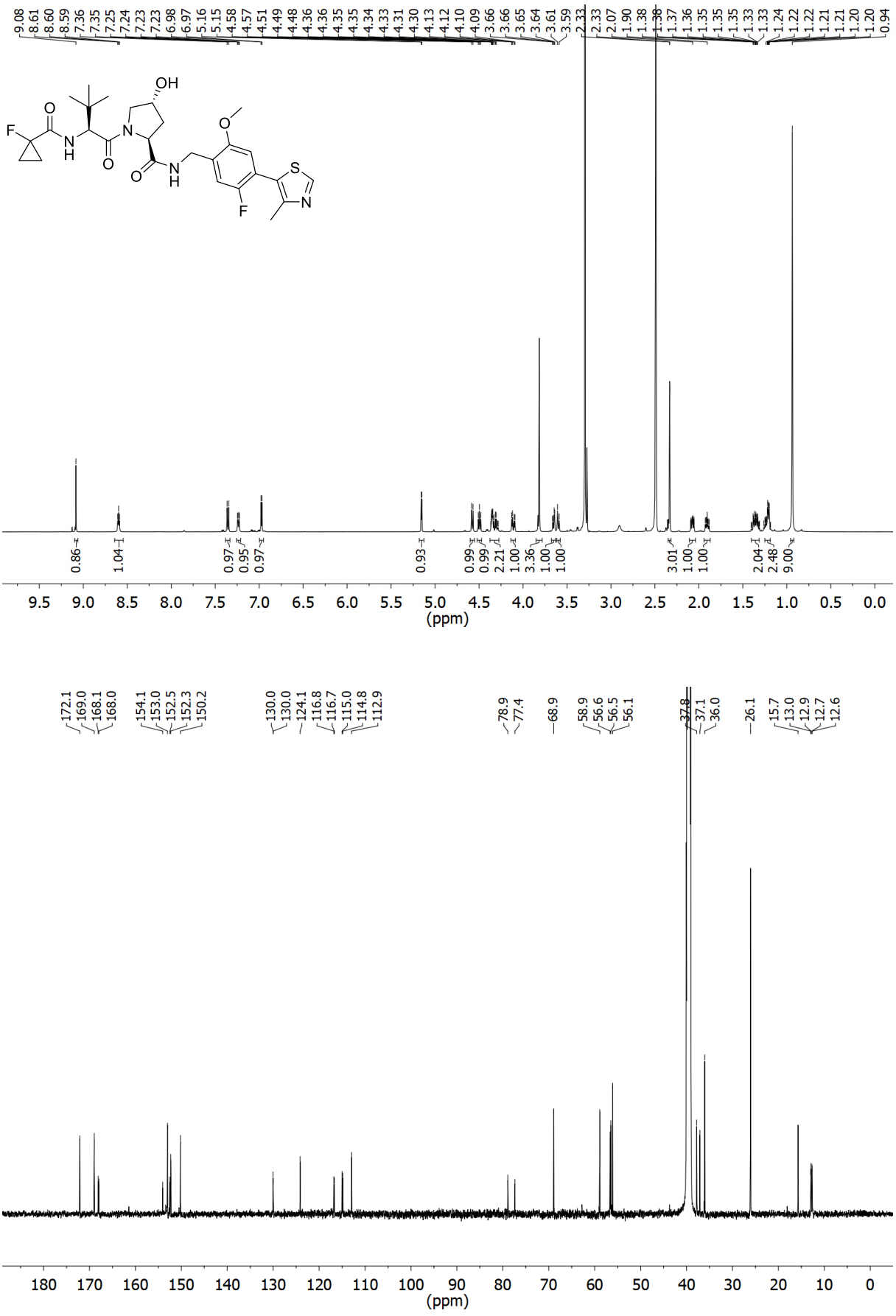

^{1}H and ^{13}C NMR spectra of compound **30**

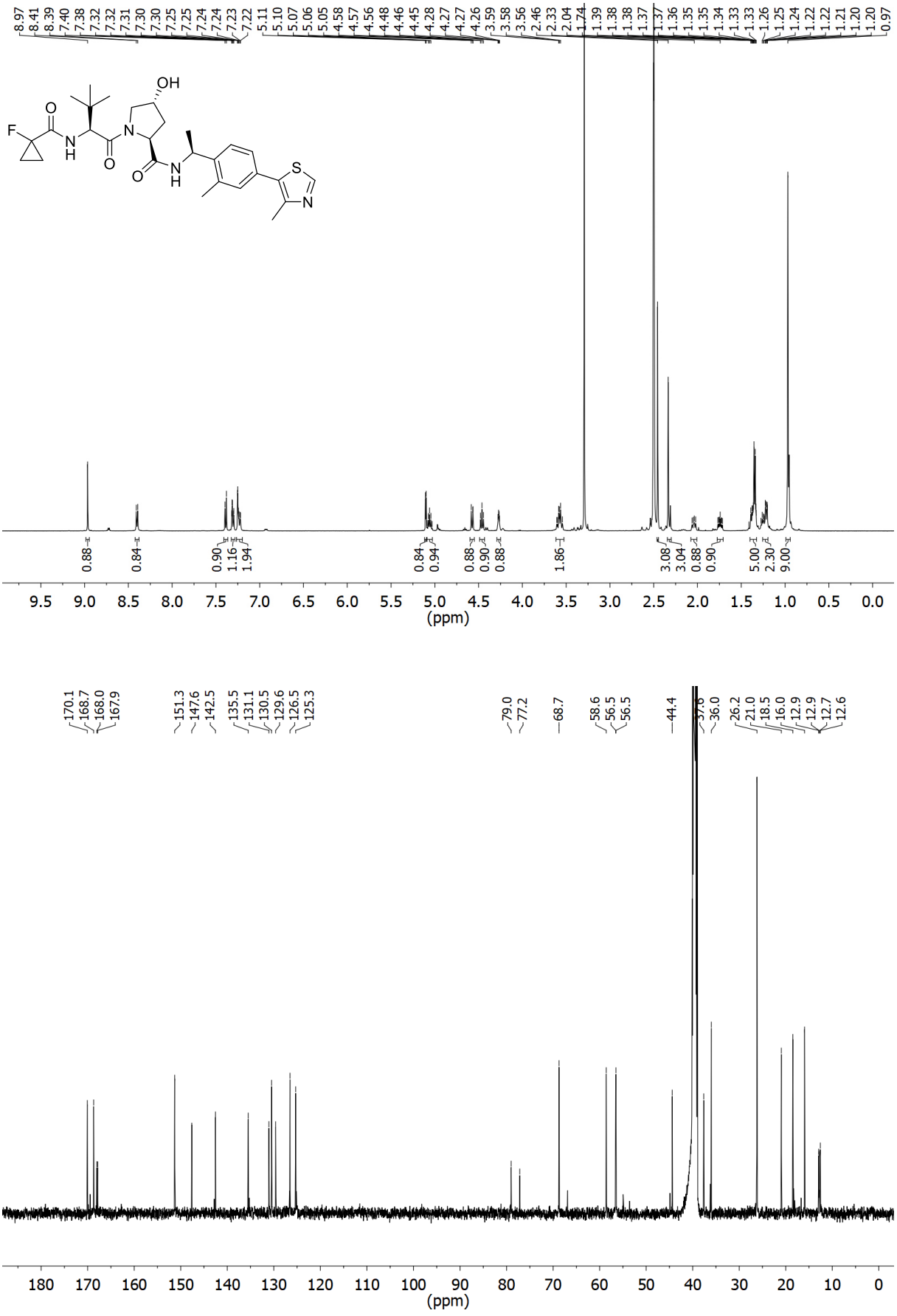

^{1}H and ^{13}C NMR spectra of compound **31**

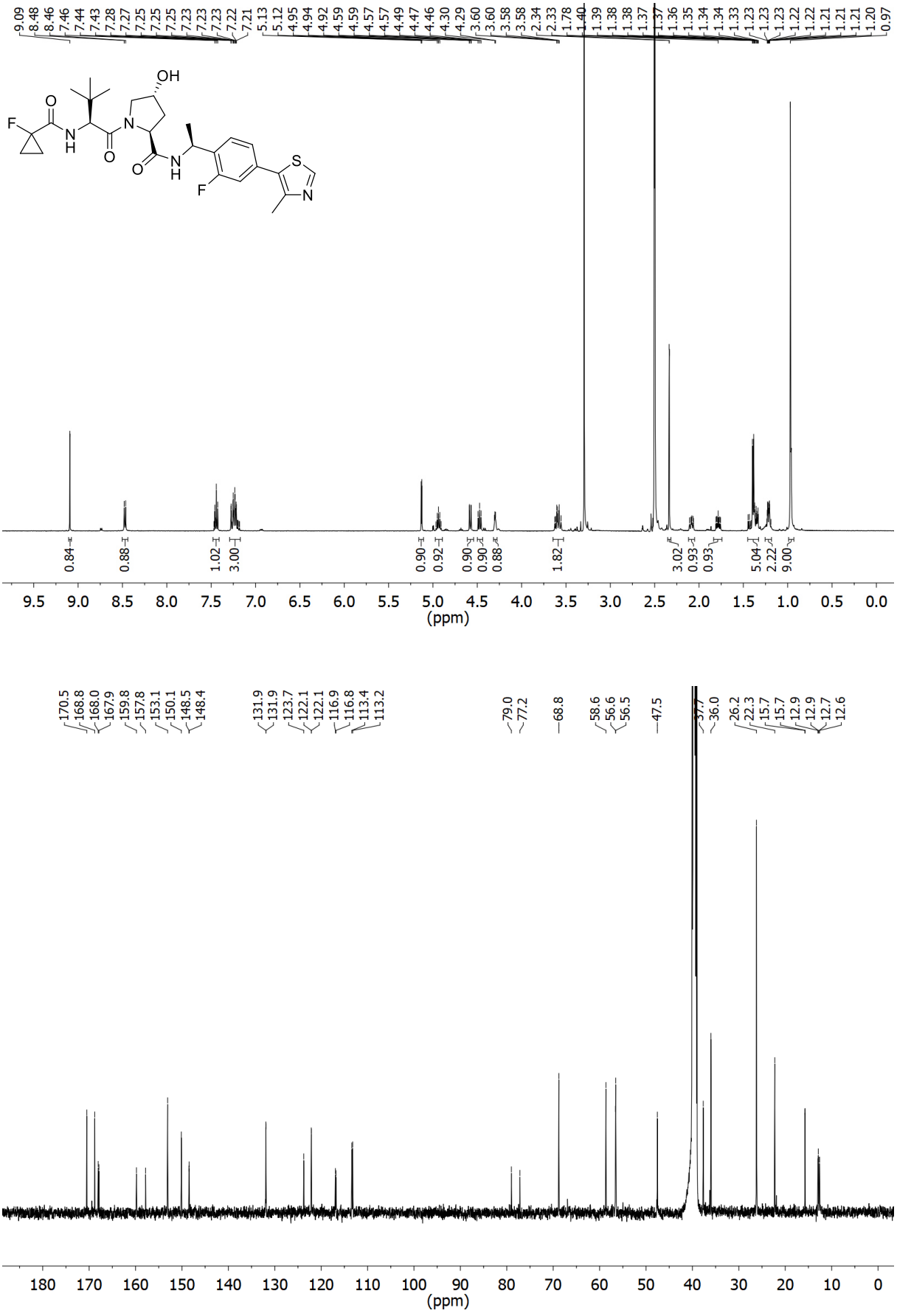

^{1}H and ^{13}C NMR spectra of compound **32**

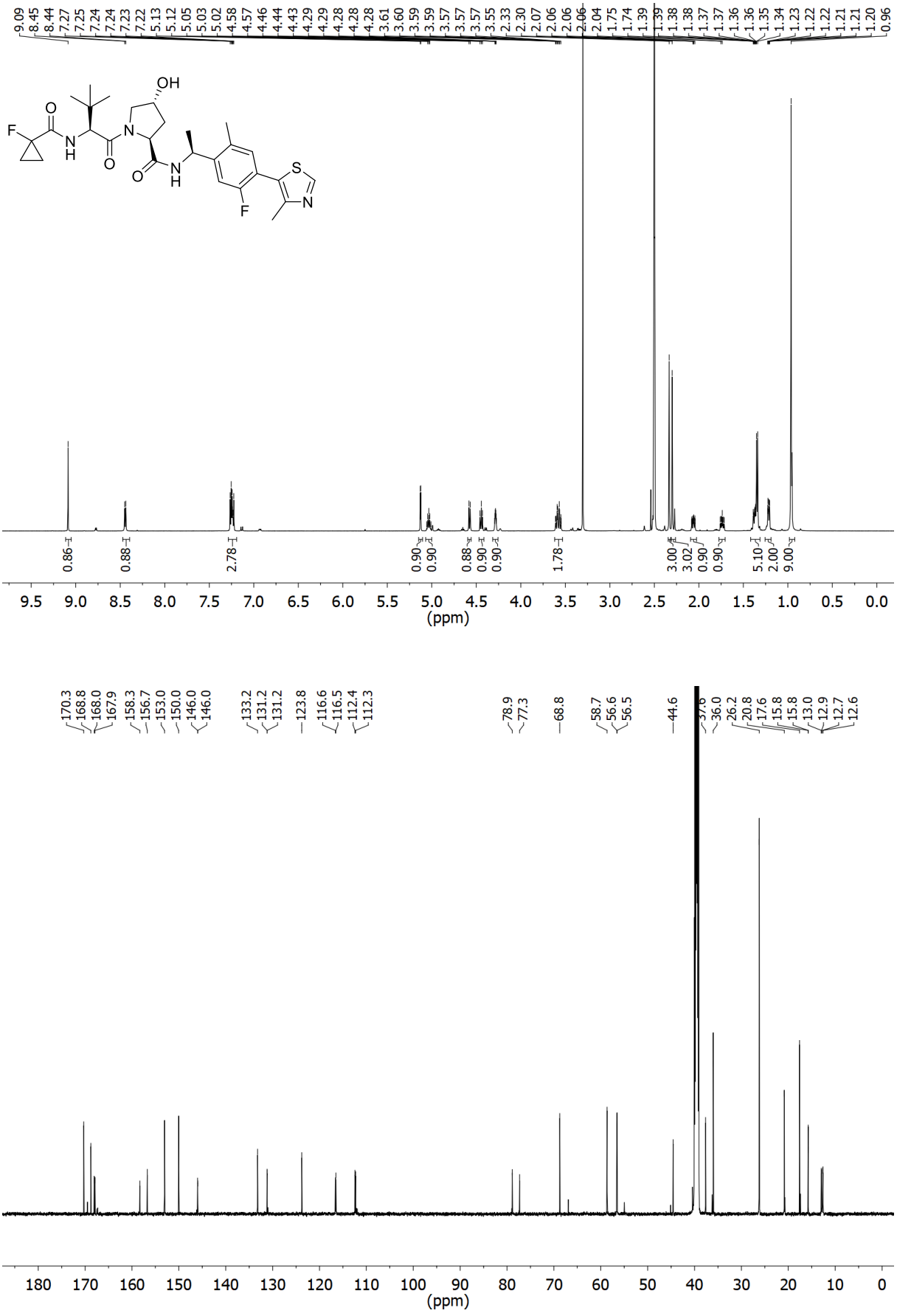

^{1}H and ^{13}C NMR spectra of compound **33**

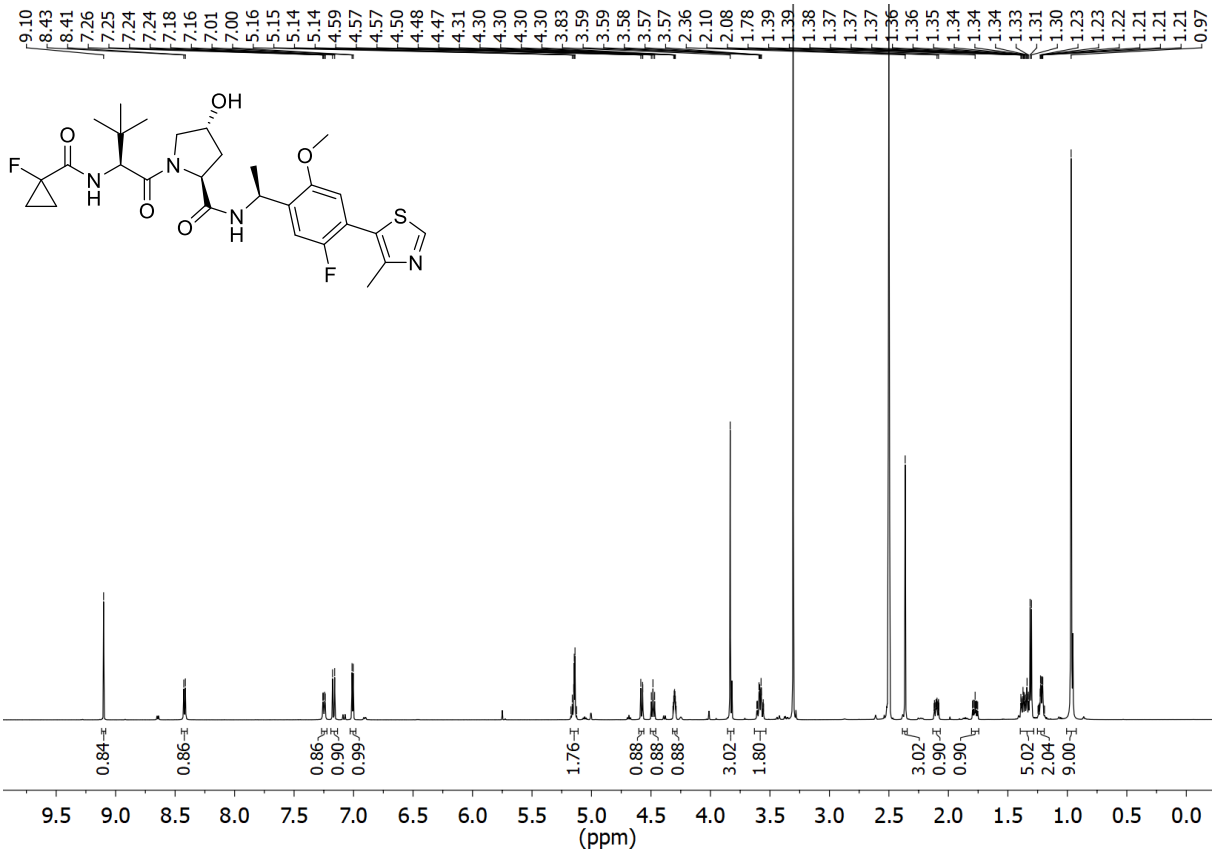

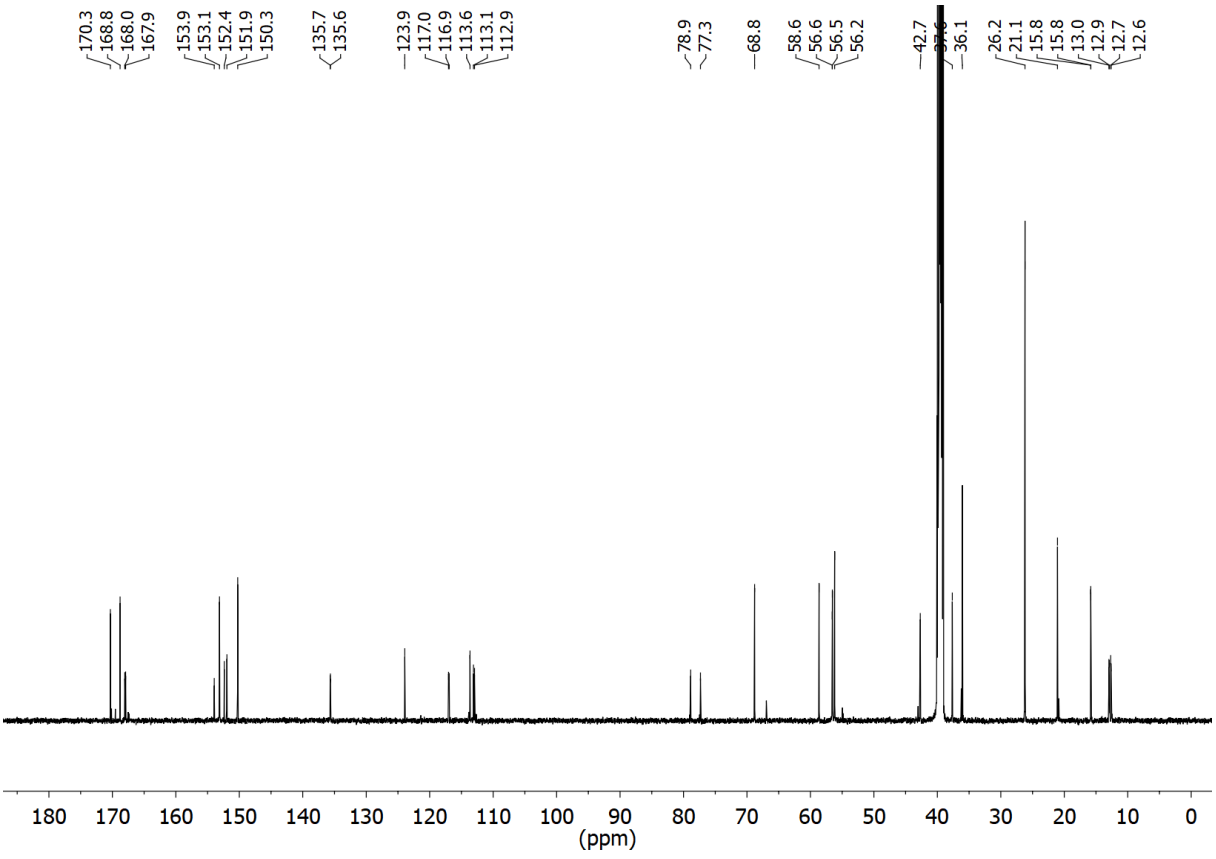

^{1}H and ^{13}C NMR spectra of compound **34**

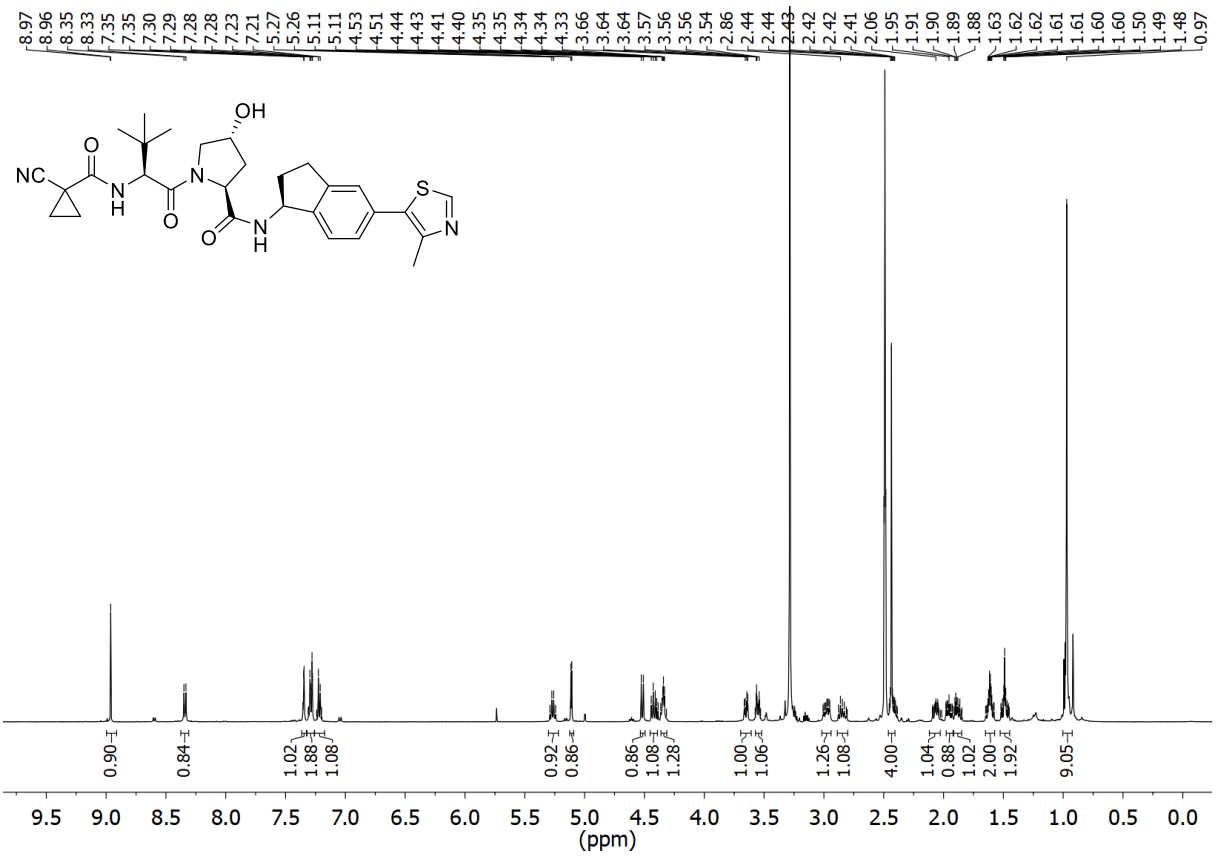

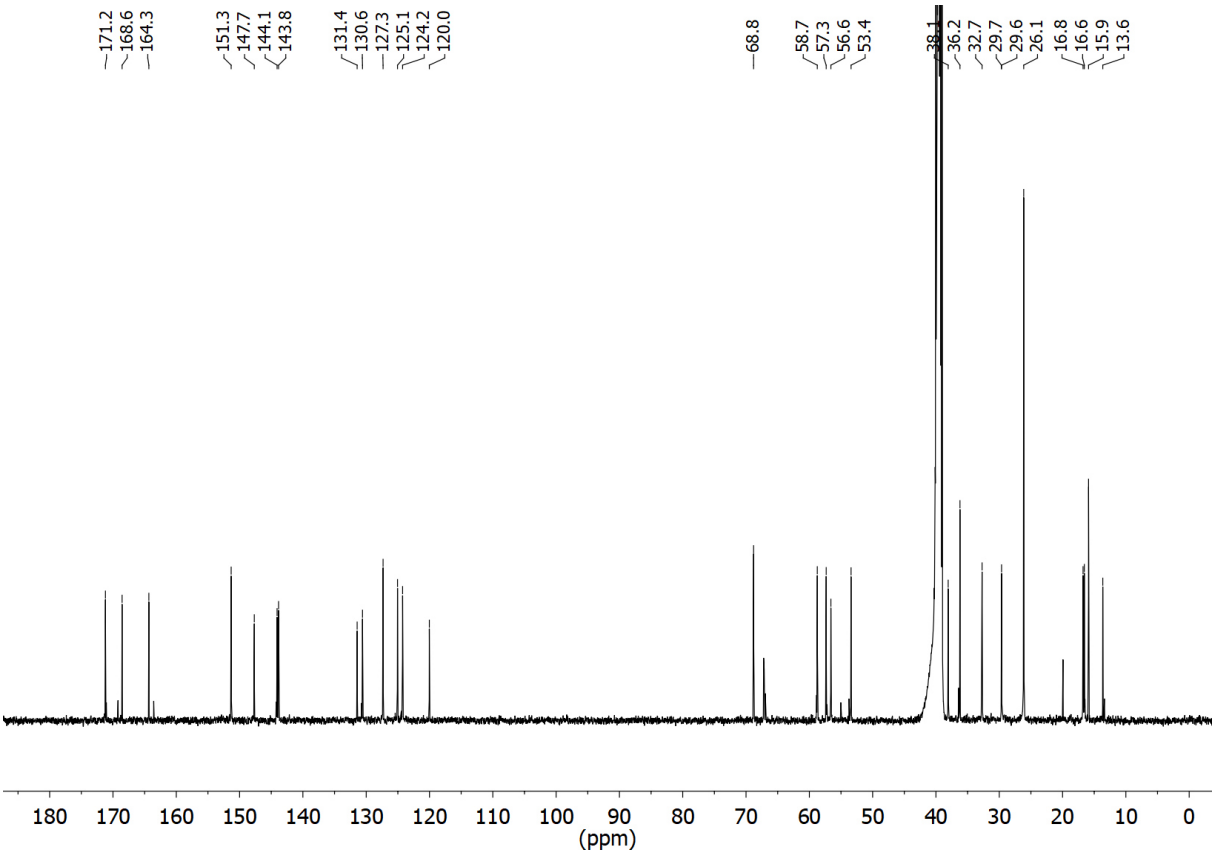

^{1}H and ^{13}C NMR spectra of compound **35**

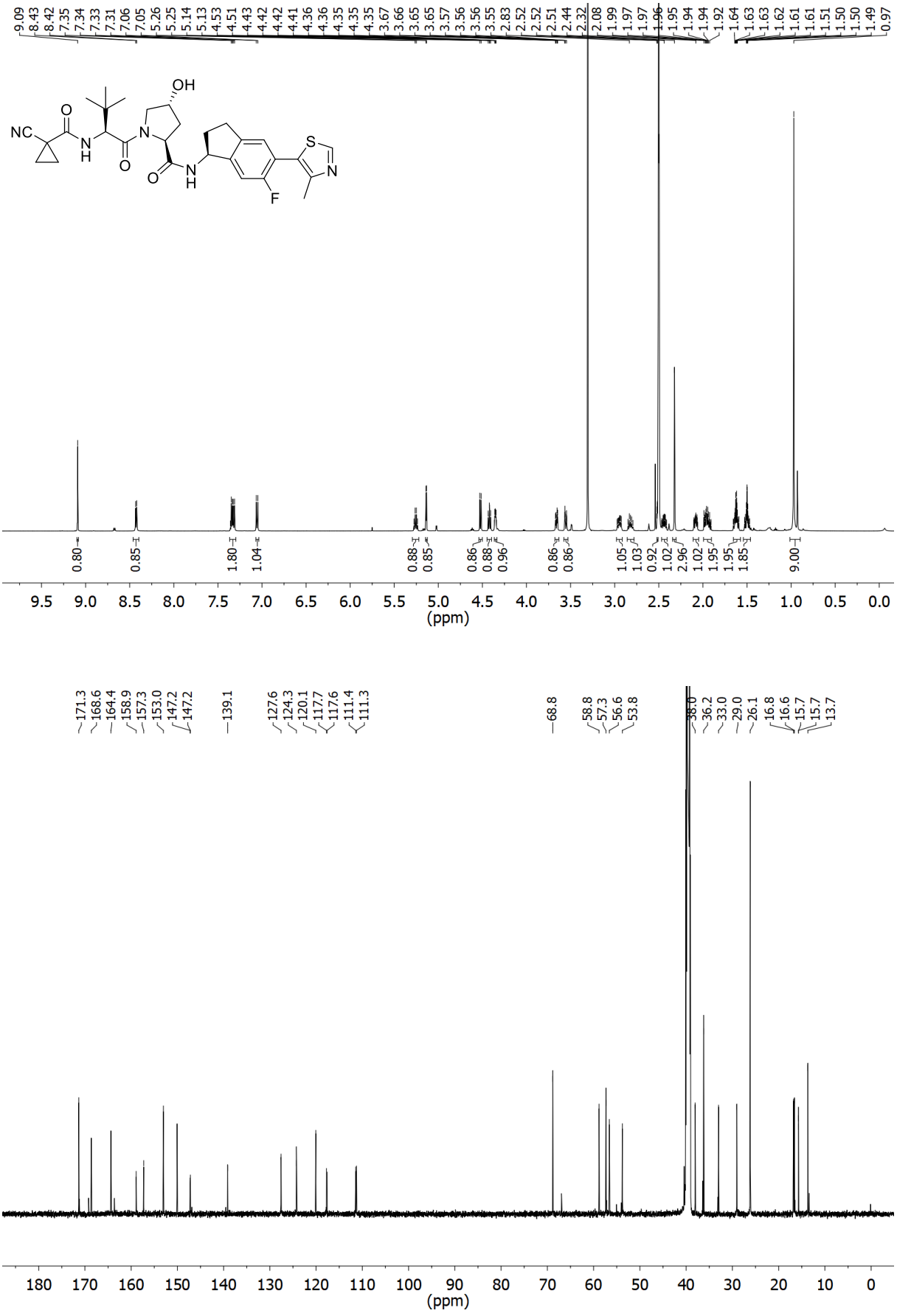

^{1}H and ^{13}C NMR spectra of compound **36**

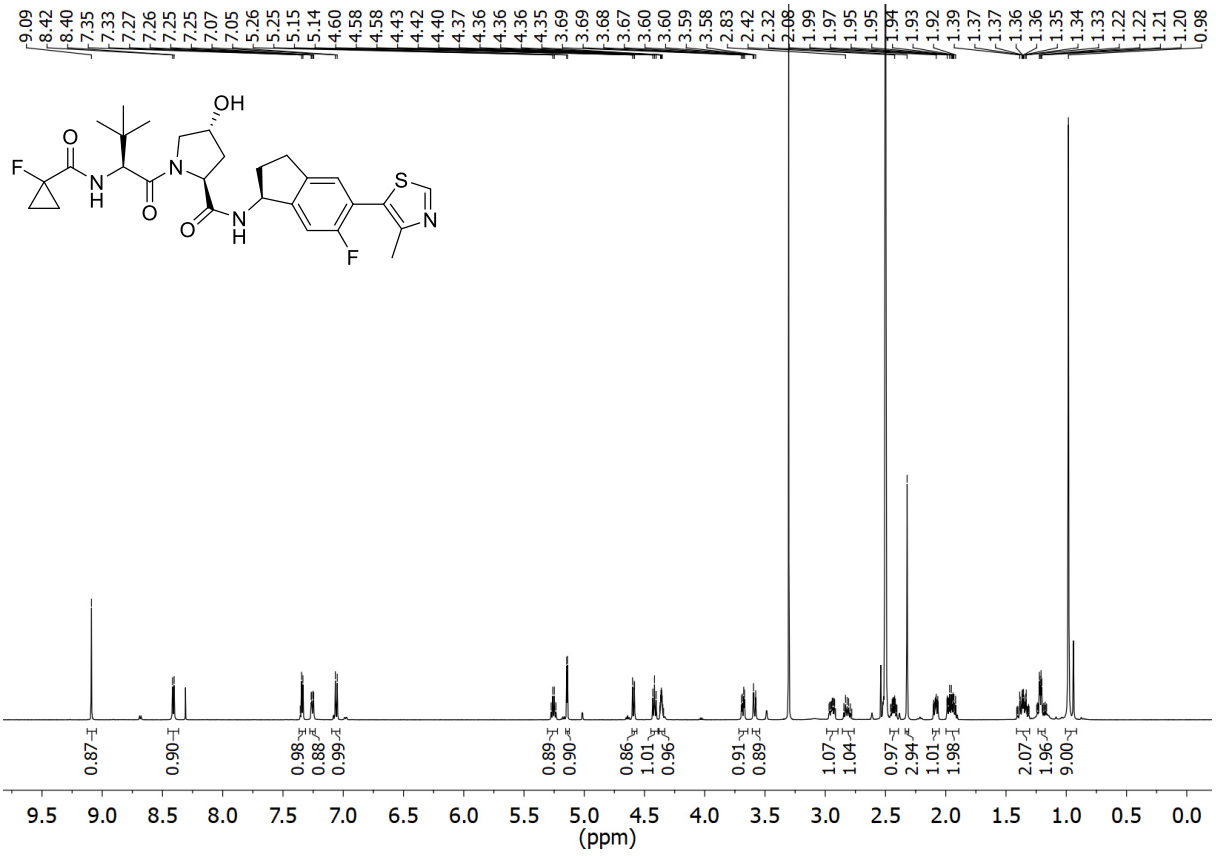

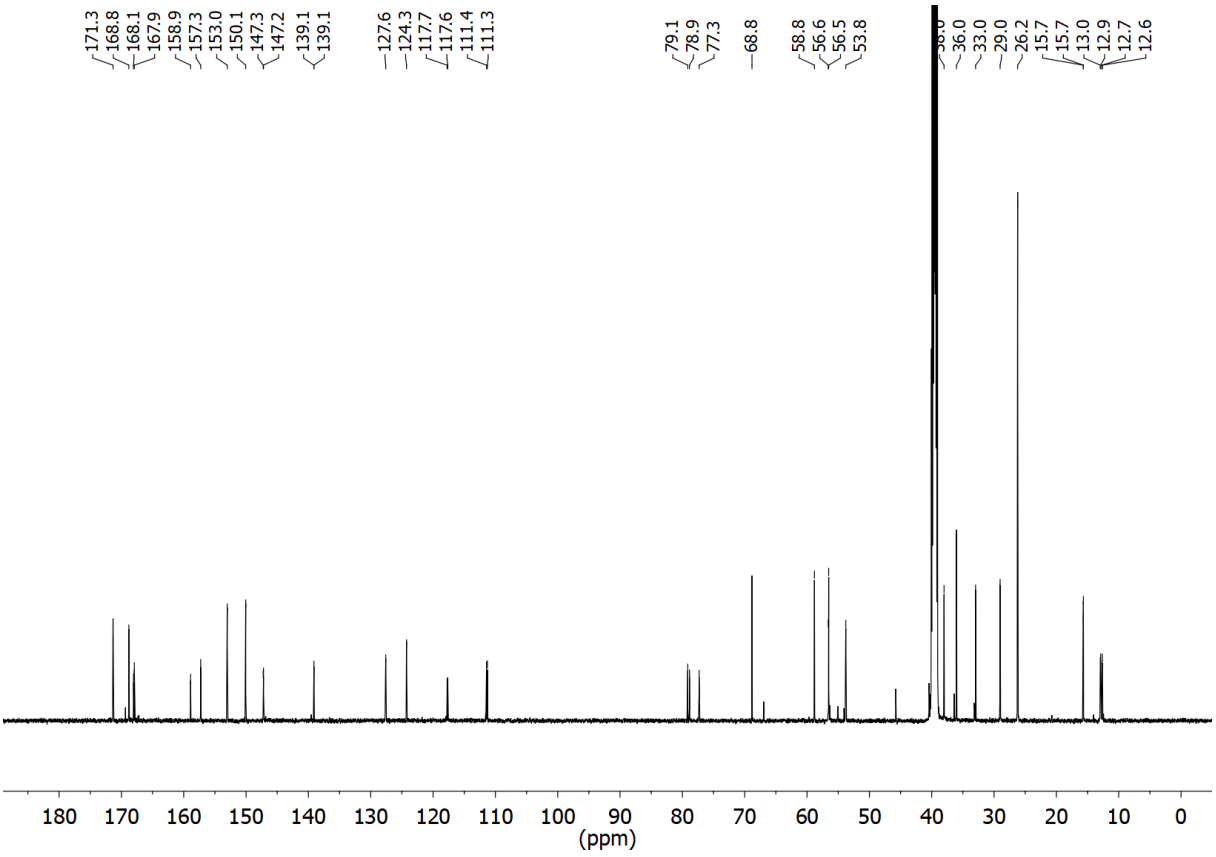

^{1}H and ^{13}C NMR spectra of compound **37**

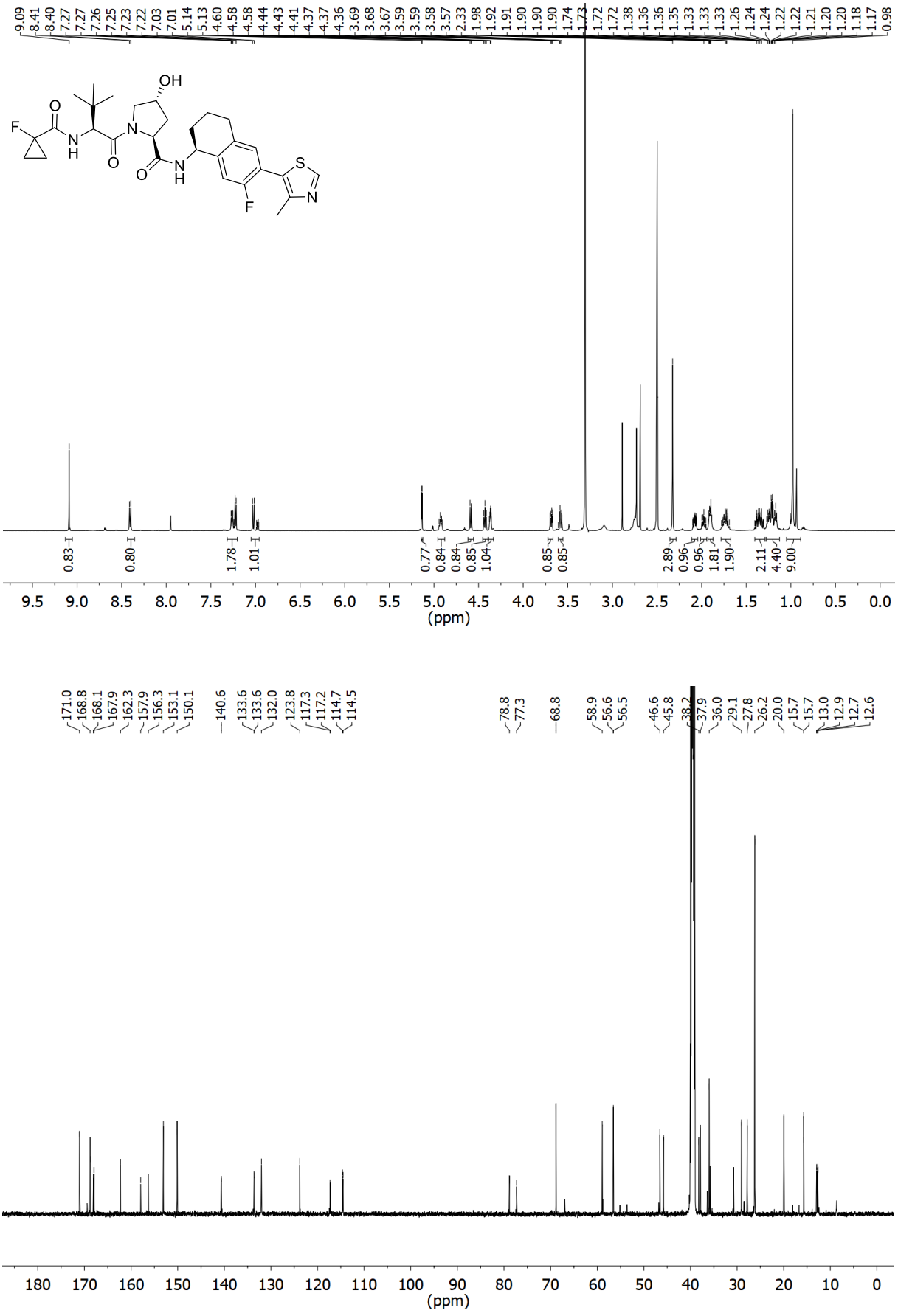

Appendix III. NMR Spectra of Compounds reported in Chapter 5

The following pages include ^{1}H and ^{13}C NMR spectra of compounds reported in chapter 5. Only spectra of final compounds are shown.

^{1}H and ^{13}C NMR spectra of compound **95**

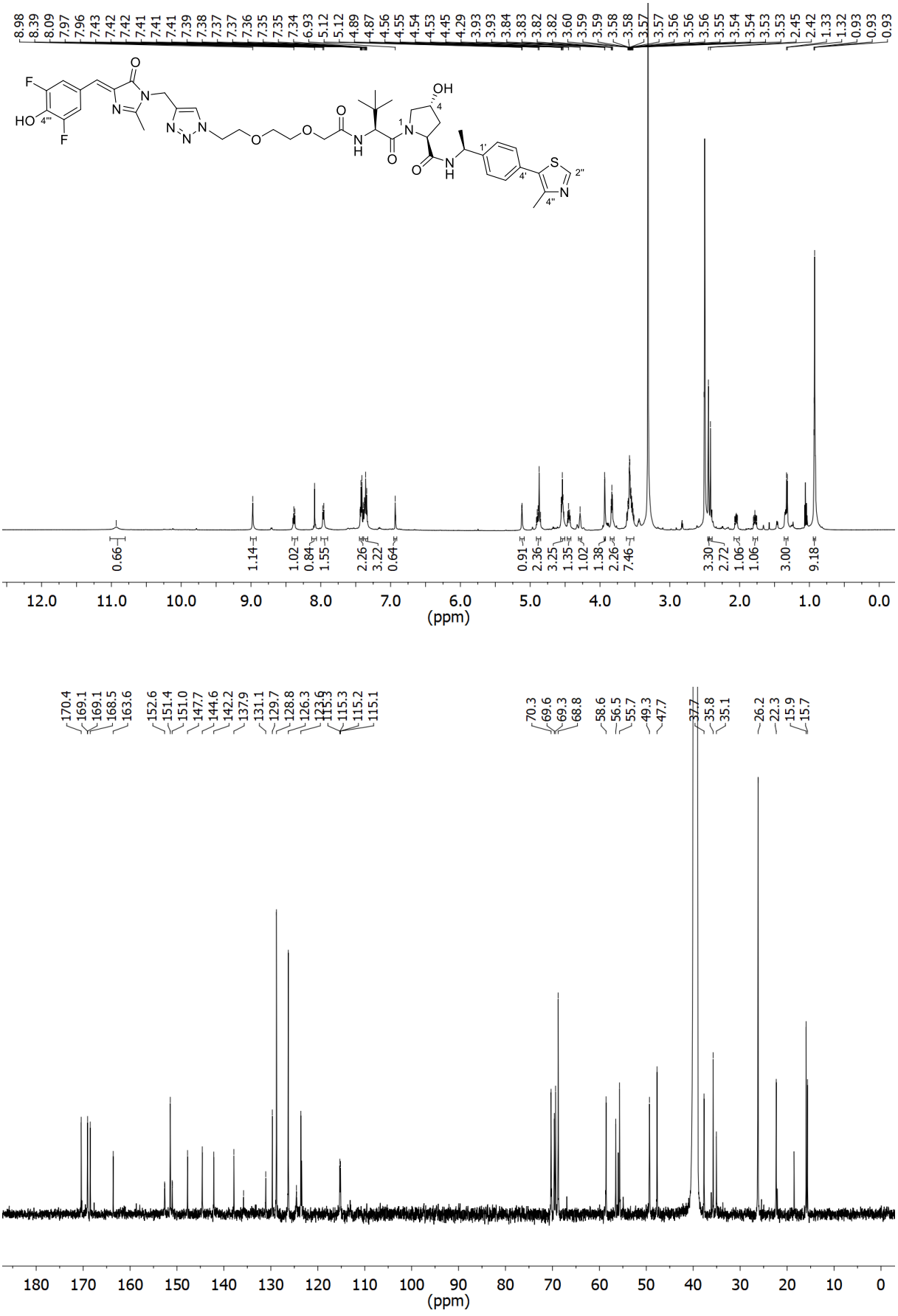

^{1}H and ^{13}C NMR spectra of compound **96**

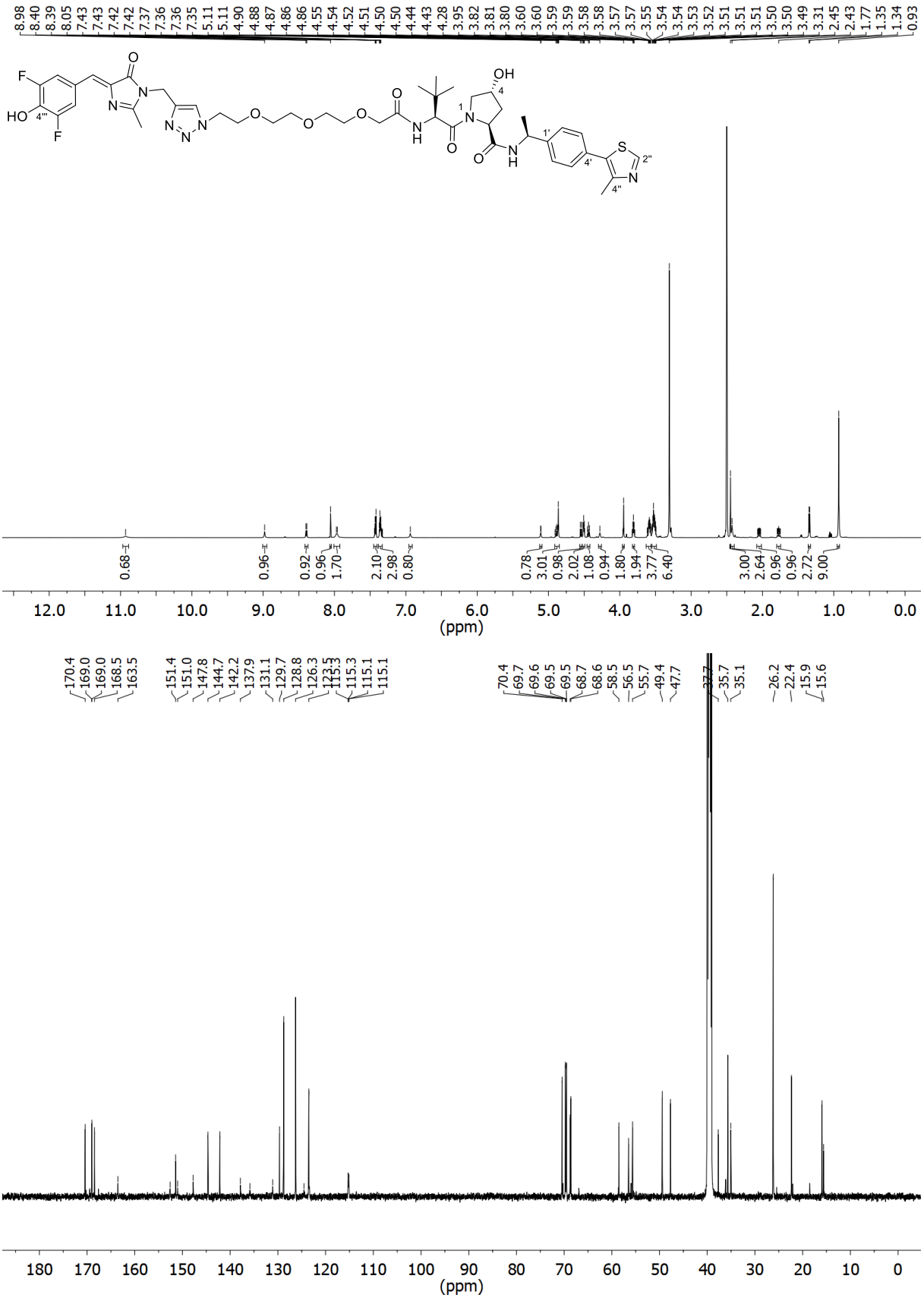

^{1}H and ^{13}C NMR spectra of compound **97**

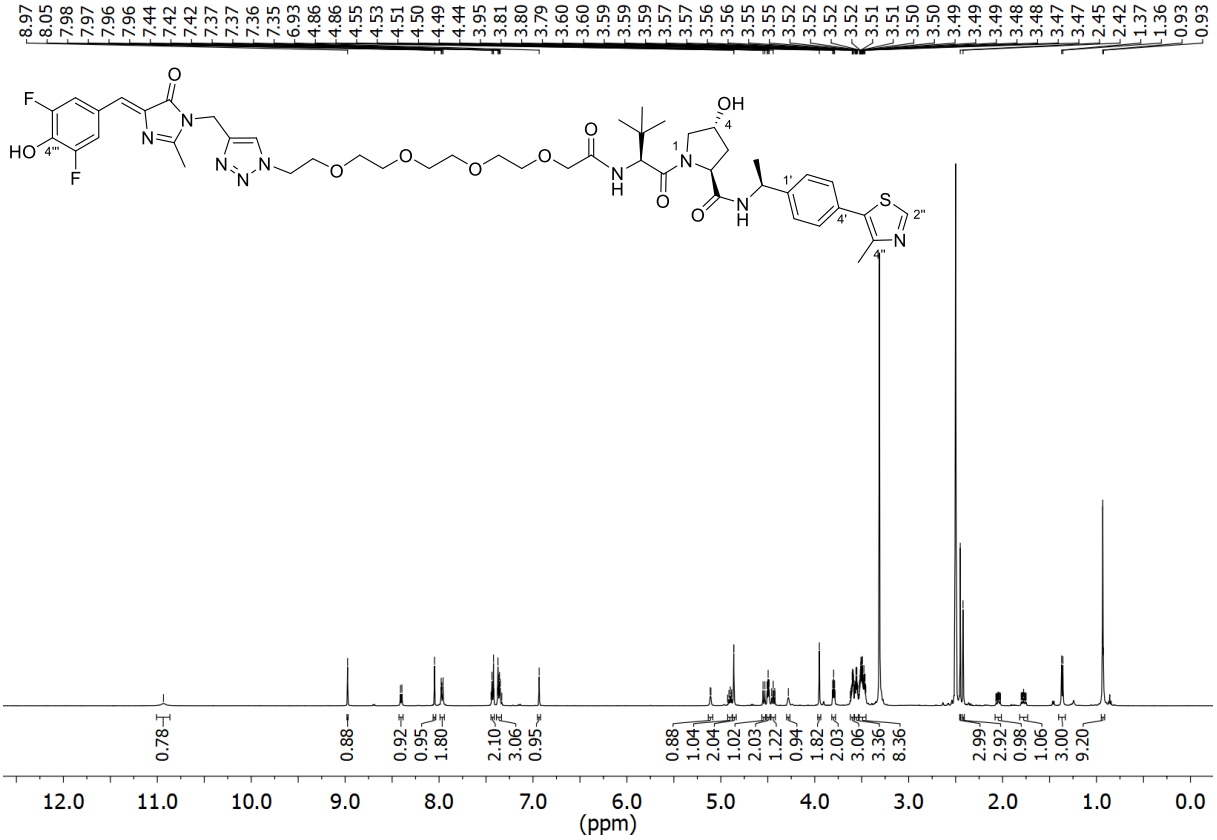

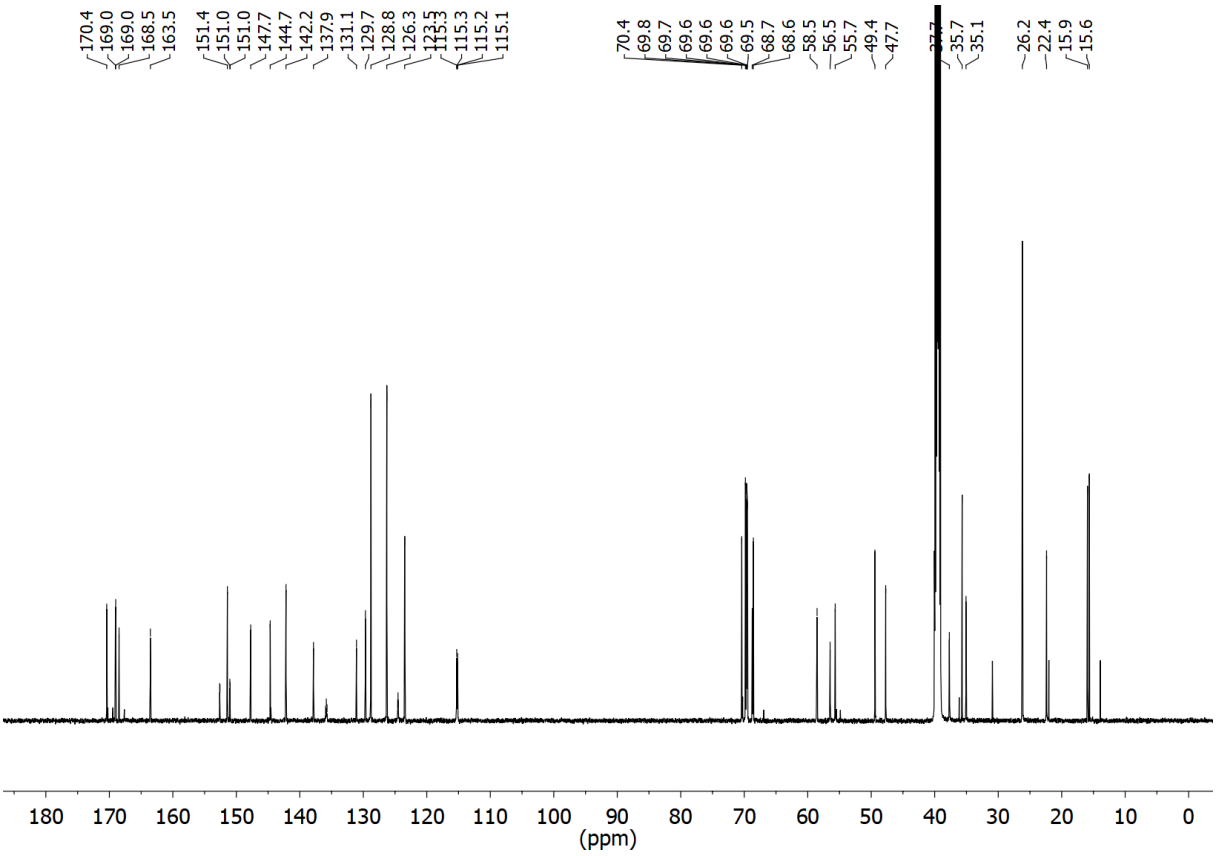

^{1}H and ^{13}C NMR spectra of compound **98**

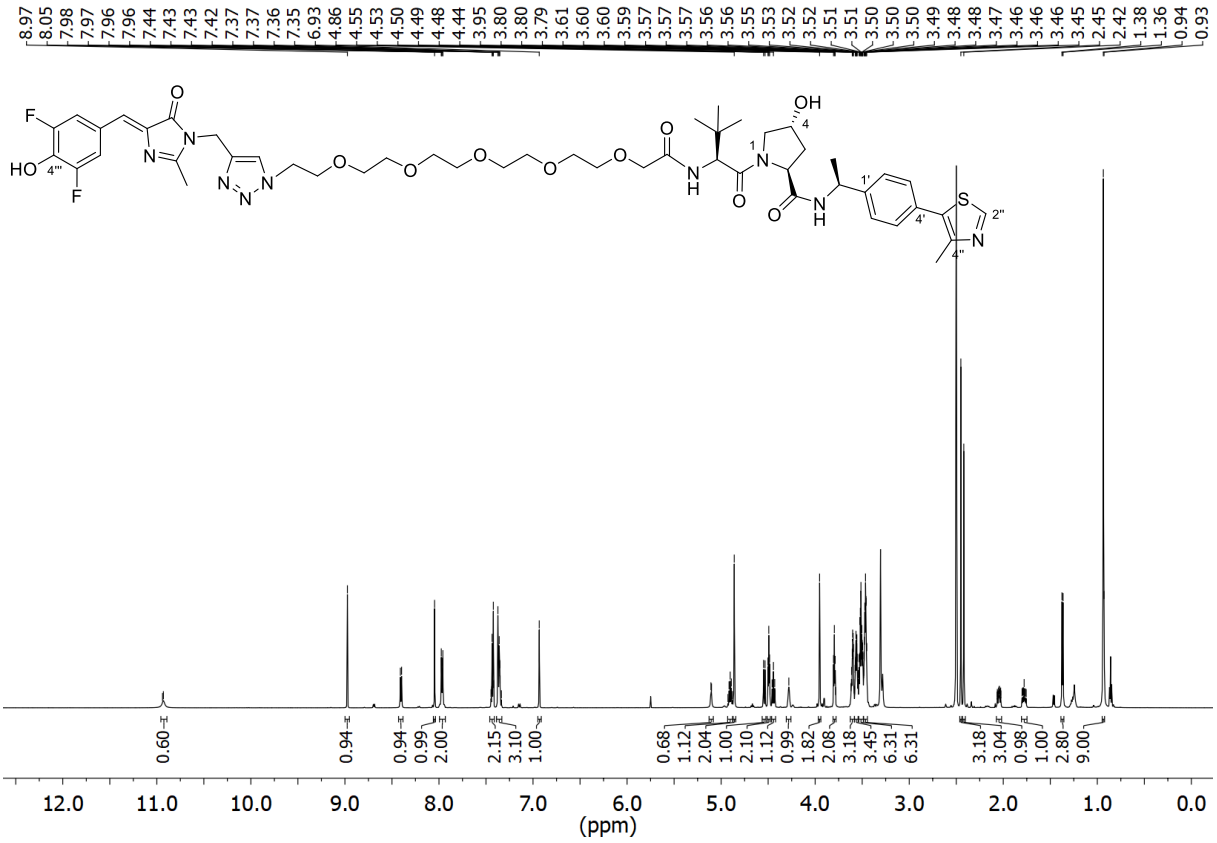

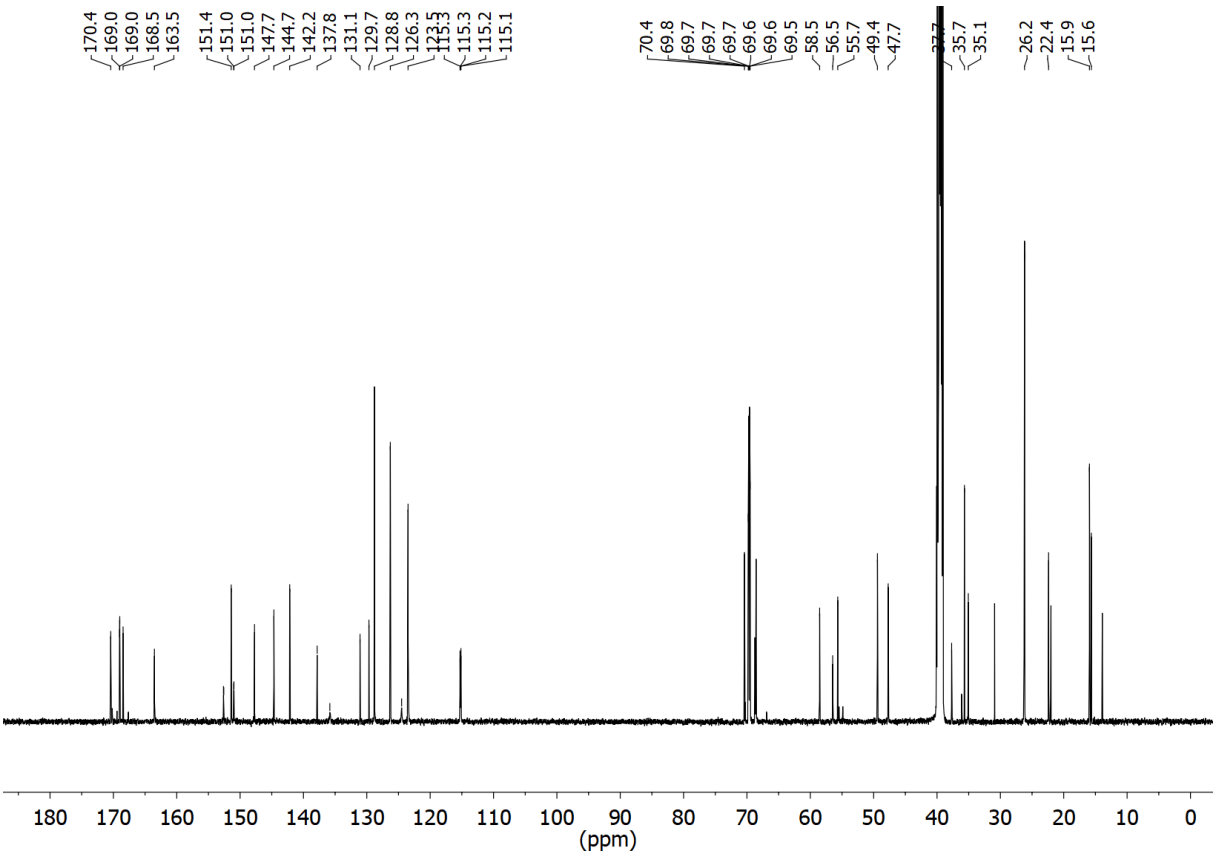

^{1}H and ^{13}C NMR spectra of compound **99**

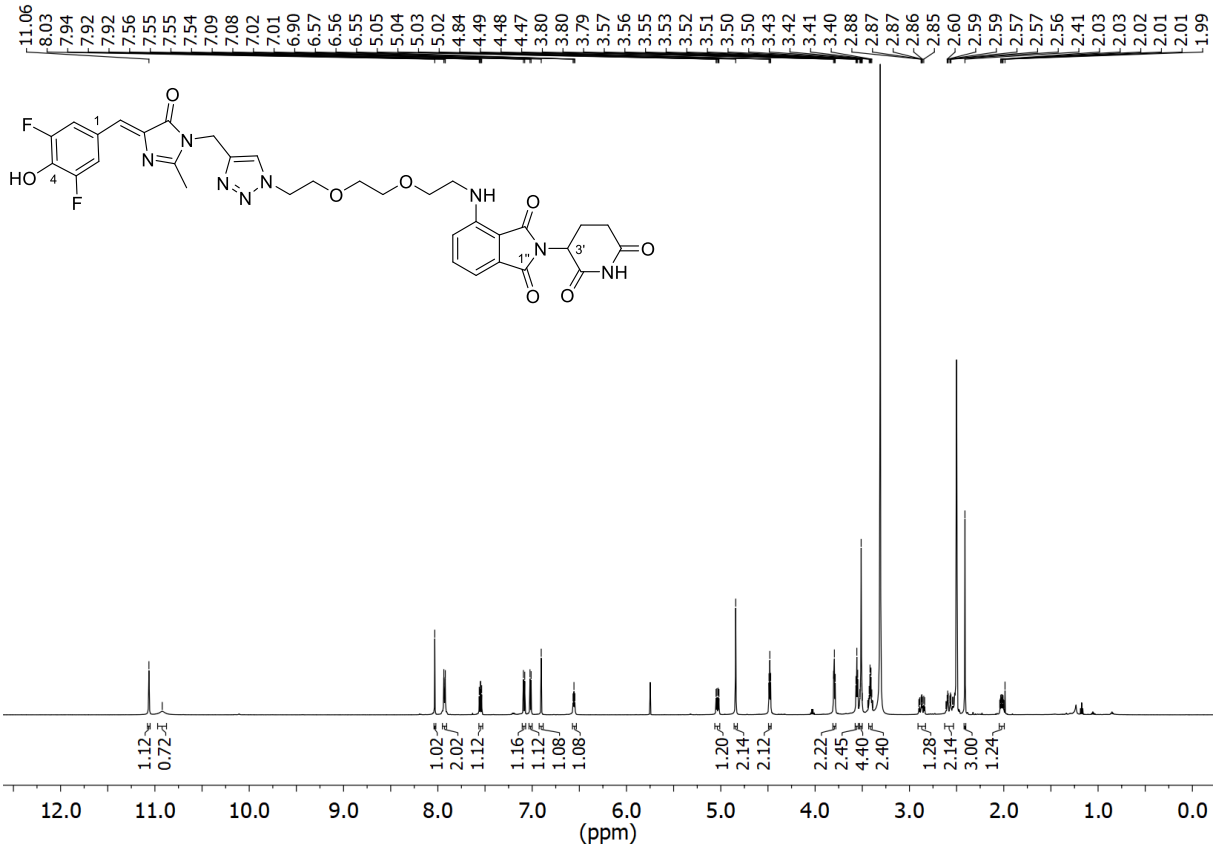

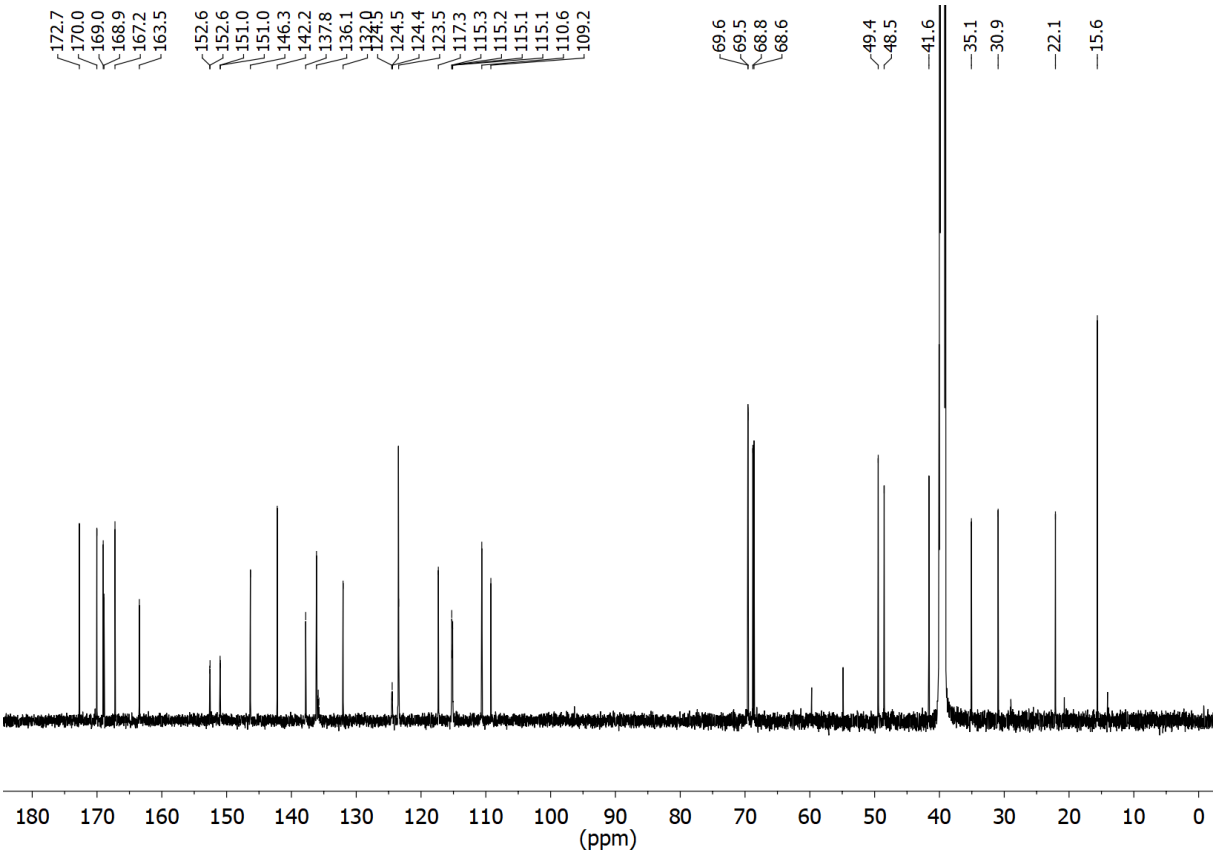

^{1}H and ^{13}C NMR spectra of compound **100**

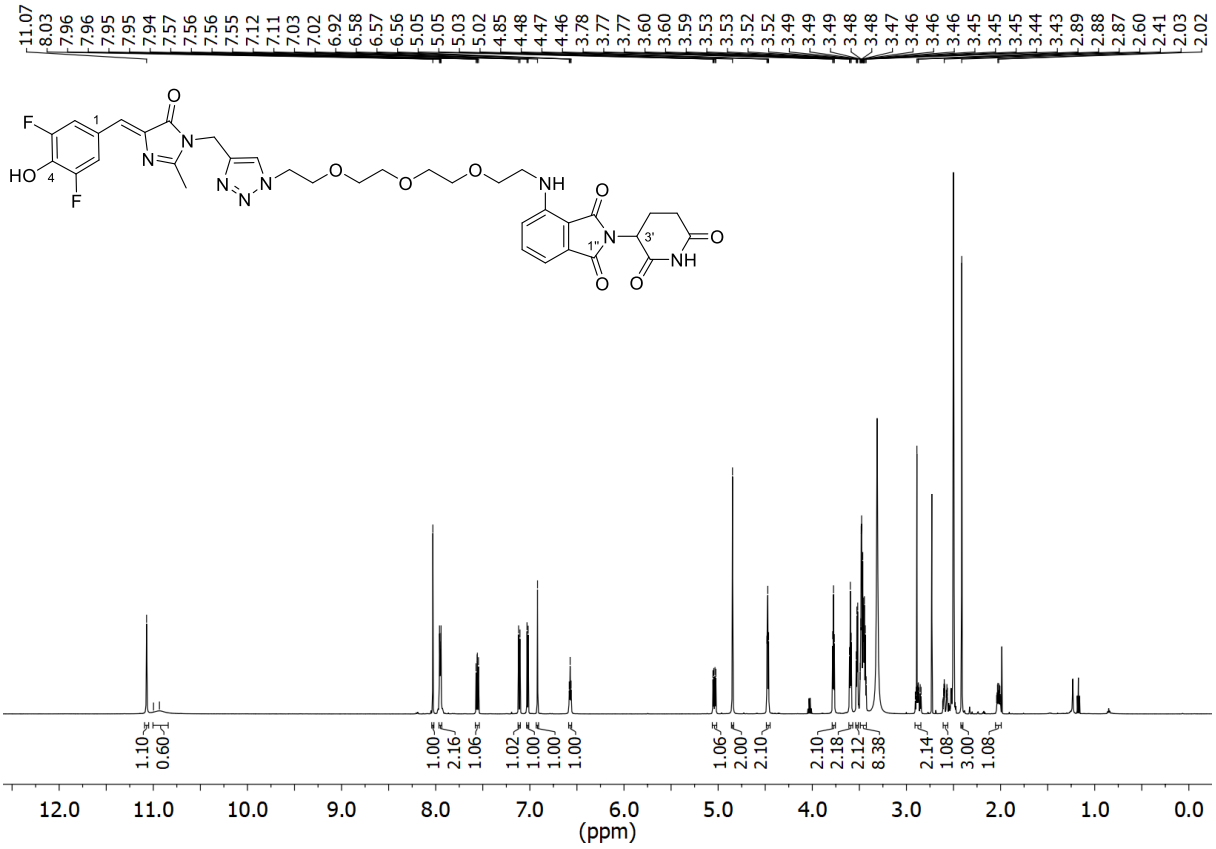

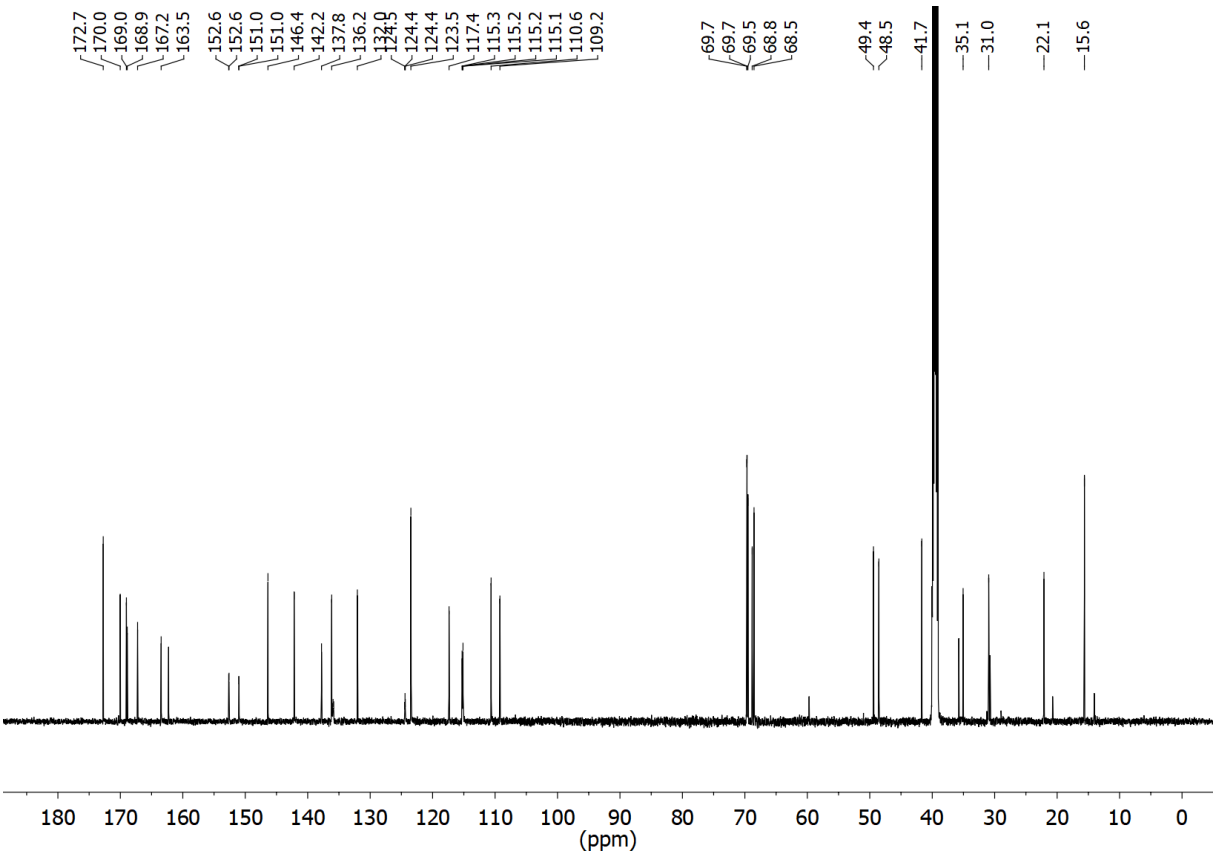

^{1}H and ^{13}C NMR spectra of compound **101**

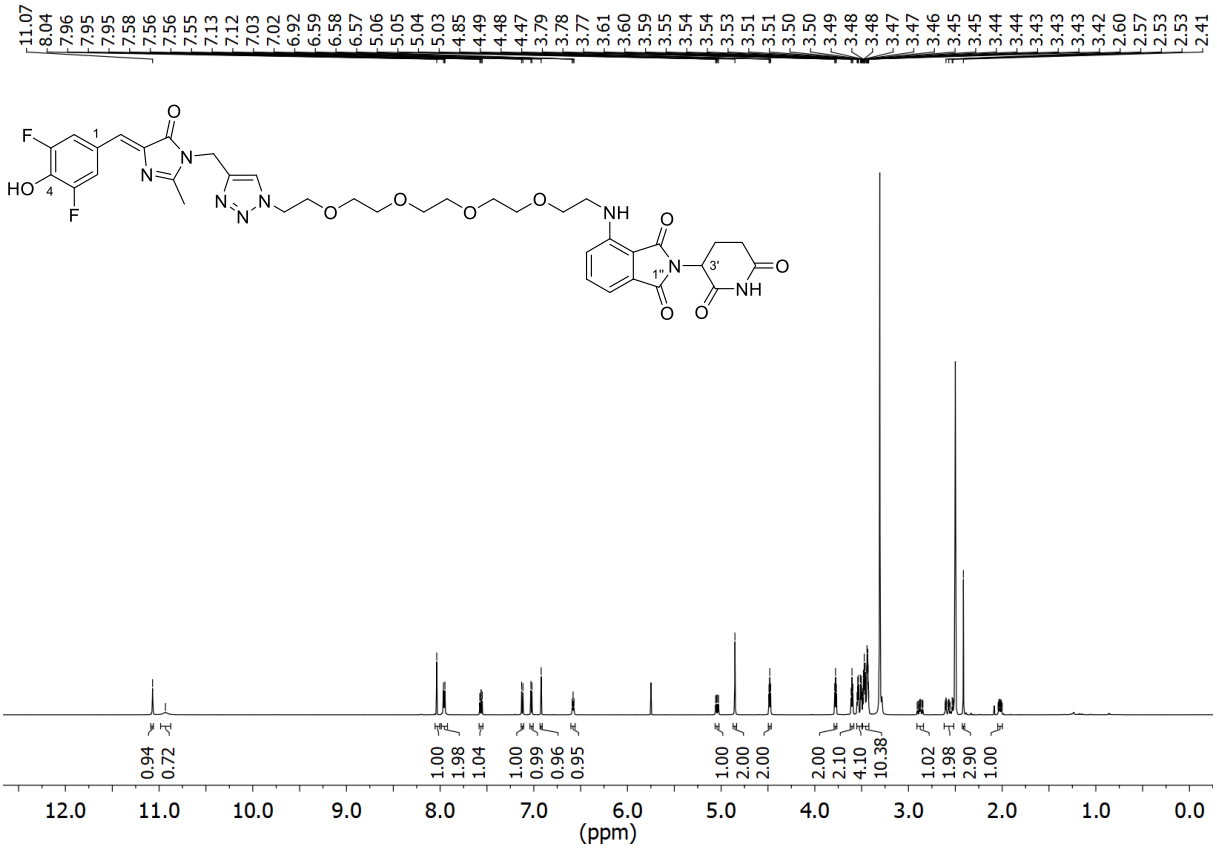

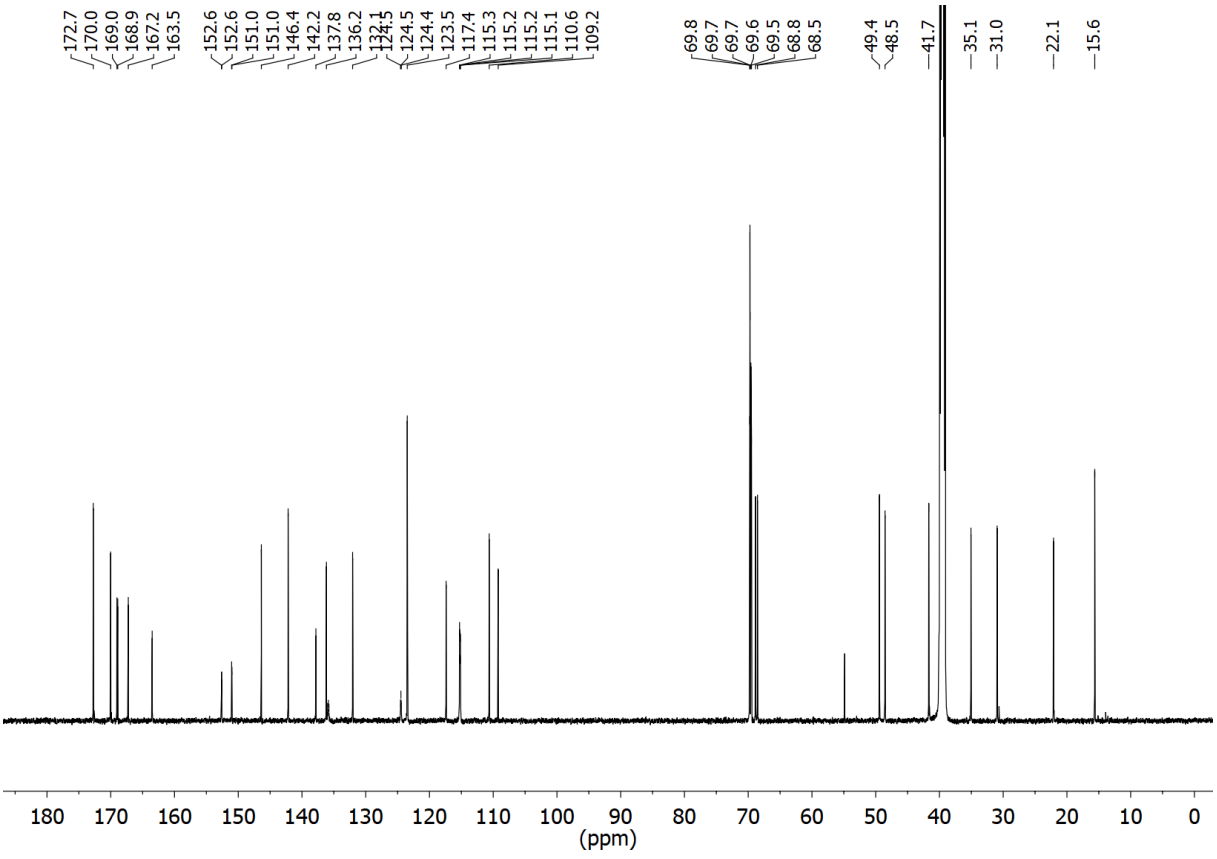

^{1}H and ^{13}C NMR spectra of compound **102**

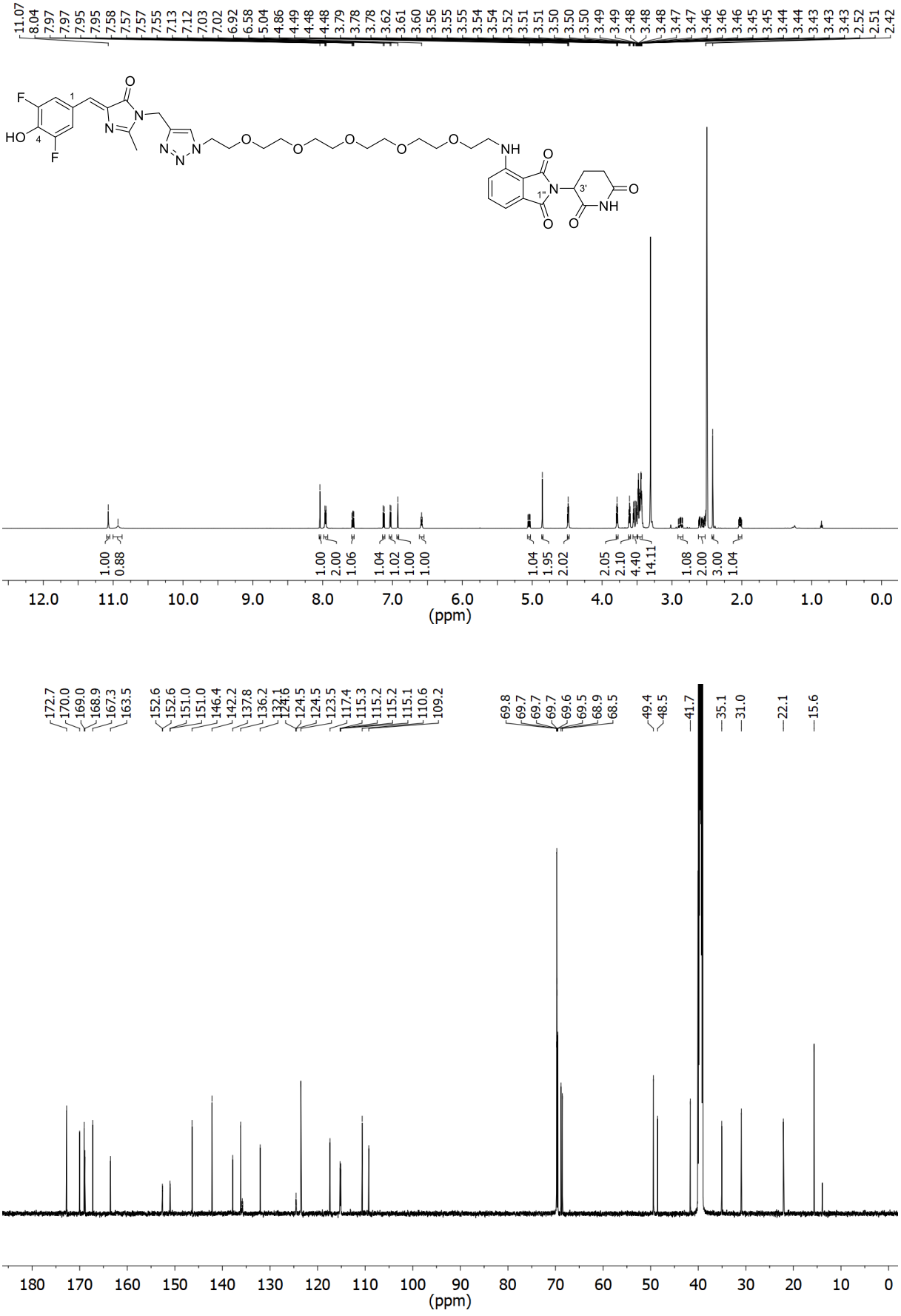

Danksagung

Meinen besonderen Dank möchte ich an allererster Stelle Herrn Prof. Dr. Michael Gütschow aussprechen. Dies gilt nicht nur für die Möglichkeit, meine Doktorarbeit in seinem Arbeitskreis anfertigen zu können, sondern auch für die sehr gute Betreuung, die wissenschaftlichen Ratschläge und Anregungen, die stetige Bereitschaft zur Diskussion sowie das mir entgegengebrachte Vertrauen.

Herrn Prof. Dr. Gerd Bendas möchte ich vielmals für die Anfertigung des Zweitgutachtens danken.

Ich bedanke mich außerdem bei Prof. Dr. Martin Baunach und Prof. Dr. Dirk Menche für die Mitwirkung in meiner Prüfungskommission.

Der Bonn International Graduate School of Drug Sciences (BIGS DrugS) danke ich für die finanzielle Unterstützung in Form von Reisestipendien für die Teilnahme an verschiedenen Konferenzen und für den Forschungsaufenthalt im Ausland.

Mein Dank gilt auch Herrn Prof. Dr. Alessio Ciulli für die Bereitschaft, mich zweimal in seinem Arbeitskreis willkommen zu heißen, und für seine Begeisterung und Ideen zum gemeinsamen Kollaborationsprojekt. Ebenso danke ich seinen Mitarbeiter*innen, Dr. Adam Bond, Dr. Ryan Casement und Dr. Claudia Diehl, für die gute Zusammenarbeit und Unterstützung im Labor sowie für die regelmäßigen After-Work Drinks während dieser Zeit.

Des Weiteren danke ich allen weiteren Koautor*innen, ohne die das Erscheinen mancher Publikationen nicht möglich gewesen wäre oder sein wird.

Besonders Assoc. Prof. Dr. Izidor Sosic, Aleša Bricelj, Nika Strašek und Assoc. Prof. Dr. Andrej Perdih danke ich herzlich für die gute Kollaboration, die bereitgestellten Substanzen und Daten und den fachlichen Austausch während der gemeinsamen Projekte.

Herrn Prof. Dr. Günter Mayer danke ich für die Initiierung des sehr interessanten Aptamer-Projektes, wodurch sich die Möglichkeit ergab, in dieser Kollaboration zusammenzuarbeiten.

Marion Schneider, Christiane Bous, Sabine Terhart-Krabbe, Annette Reiner danke ich für die Durchführung der LC/MS- und HRMS-Messungen sowie für die Aufnahme der NMR-Spektren.

Dr. Gregor Schnakenburg danke ich für die Röntgen-Kristallstrukturanalyse einiger Verbindungen.

Bei Dr. Christian Steinebach und Tim Keuler möchte ich mich für die Zurverfügungstellung von verschiedenen Verbindungen, die für gemeinsame Projekte benötigt wurden, bedanken.

Allen aktuellen und ehemaligen Kolleg*innen des Arbeitskreises, Dr. Christian Steinebach, Tim Keuler, Robert Kuchta, Julian Breidenbach, Rabea Voget, Sophie Wittenburg, Dr. Carina Wirtz, Dr. Martin Mangold, Dr. Jim Küppers, Dr. Christian Breuer, Dr. Erik Gilberg, danke ich nicht nur für die eine oder andere gute Zusammenarbeit, sondern auch herzlichst für die freundschaftliche Kollegialität, die gegenseitige Unterstützung, die zahlreichen und unterhaltsamen Kaffee- und Mittagspausen, und generell für die schöne gemeinsame Zeit in den vergangenen Jahren!

Meinen Bürokollegen Tim Keuler und Julian Breidenbach danke ich für die unzähligen Gespräche, die nicht nur das Fachliche betrafen, sondern auch oft darüber hinausgegangen sind. Danke euch für das offene Ohr bei jeglichen Problemen.

Ich möchte mich auch bei all meinen Praktikant*innen, Wahlpflichtfach- und Bachelorstudent*innen für ihre Unterstützung und Mitarbeit im Labor bedanken, vor allem bei meiner ersten Praktikantin Carolin Pikullik.

Dr. Marcus Hubert sowie allen aktuellen und ehemaligen Kolleg*innen des OC-Praktikums im 3. Semester Pharmazie möchte ich mich für die hervorragende Arbeitsatmosphäre bedanken.

Ich danke Dr. Marc Oeller für das Korrekturlesen von Teilen dieser Arbeit und auch für die Freundschaft seit Beginn unseres Studiums.

Ein ganz besonderer Dank geht an Marcel, meinen Freunden und meine Familie, die während des Studiums und der Promotion mir immer zur Seite standen und mich unterstützt haben.